TP XXXXXX

Assessment of Vessel Noise within the Southern Resident Killer Whale Critical Habitat

Final Report—Version 2.1

Prepared for:
Innovation Centre
Transport Canada / Government of Canada

By:
JASCO Applied Sciences (Canada) Ltd.

July 2018

JASCO
APPLIED SCIENCES

TP XXXXXX

Assessment of Vessel Noise within the Southern Resident Killer Whale Critical Habitat

Final Report
Version 2.1

By:

Marie-Noël R. Matthews
Zahraalsadat Alavizadeh
David E. Hannay
Loren Horwich
Héloïse Frouin-Mouy

JASCO Applied Sciences (Canada) Ltd

July 13, 2018

NOTICES

Disclaimer:

This report reflects the views of JASCO Applied Sciences and not necessarily those of the Innovation Centre, Transport Canada.

The results presented here could be misinterpreted if not considered in context of the acoustic sources and environments described in this report. Accordingly, if information from this report is used in documents released to regulatory bodies, such documents must clearly cite the original report, which shall be made readily available to the recipients in integral and unedited form.

Suggested citation:

Matthews, M.-N. R., Z. Alavizadeh, D.E. Hannay, L. Horwich, and H. Frouin-Mouy. 2018. *Assessment of Vessel Noise within the Southern Resident Killer Whale Critical Habitat: Final Report*. Document number 01618, Version 2.1. Technical report by JASCO Applied Sciences for the Innovation Centre, Transport Canada/Government of Canada.

© (2018) Transport Canada

EXECUTIVE SUMMARY

Purpose of this Study

The International Maritime Organization's (IMO) Marine Environment Protection Committee recognizes that underwater noise from commercial ships may have short- and long-term impacts on marine mammals (IMO 2014). Commercial shipping lanes leading to Canadian ports pass through important habitat of many species that could be affected by vessel noise. The Salish Sea is a particularly sensitive habitat, important to several marine mammal species including the endangered Southern Resident Killer Whale (SRKW; SARA 2002). Much of the SRKW population is often present near the shipping lanes, especially in summer and fall when they feed on Chinook salmon in the southern Salish Sea. This population experiences substantial levels of shipping noise that has the potential to disturb these animals and to mask important sounds such as communication calls and echolocation signals used for foraging. Masking of important sounds is likely to have negative effect on fitness and could hinder recovery of their population (DFO 2011). Shipping activity in the Salish Sea is expected to increase due to planned terminal expansion projects and increased oil tanker and associated tug transits. Strategic management of this additional traffic and the noise it produces will be necessary to ensure marine fauna are not exposed to increases in underwater noise. Transport Canada recognizes the need to assess existing and future underwater noise conditions in the Salish Sea, and to investigate options for managing and reducing noise exposures to SRKW. In light of these concerns, Transport Canada has commissioned this study to assess underwater shipping noise levels in the Salish Sea in key areas of critical habitat for SRKW, and to investigate the effectiveness of several potential noise mitigation approaches.

Study Approach

This study applied specialized computer models to examine shipping noise levels over four sub-regions of the southern Salish Sea in SRKW critical habitat that the major shipping lanes leading to Vancouver pass though: Strait of Georgia, Haro Strait, Juan de Fuca Strait, and Swiftsure Bank.

Baseline (present case) noise levels were established by modelling the noise emissions of existing shipping traffic, represented by all tracked vessel transits from July 2015. A future case scenario was developed to represent vessel traffic conditions in 2020 or later; it assumes that new oil tanker and tug traffic associated the expected expansion of the Trans Mountain Pipeline Project will increase the baseline traffic. The study also examines and compares noise levels of the future traffic under several possible vessel noise mitigation options. These mitigation options are:

- **Vessel speed reductions**: Noise emissions of most vessel classes are known to decrease with reduced speed, as has been confirmed recently by measurements performed under Vancouver Fraser Port Authority's ECHO program. A mitigation option was tested by slowing vessels to either 15 knots or 11 knots, depending on vessel class and location.
- **Grouping vessels into convoys**: This mitigation is intended to produce longer quiet times between vessel convoys, which could allow animals longer periods of quiet for more effective use of sound for echolocation foraging and communicating. Convoys spaced at 4 hours in Haro Strait and Juan de Fuca Strait, and an additional 2 hour spacing in Haro Strait were investigated.
- **Re-routing the traffic lanes away from SRKW habitat**: In one scenario, the traffic lanes in southern Haro Strait were moved west, away from known SRKW feeding grounds on Salmon Bank off San Juan Island. In a second scenario, large vessel traffic was shifted to the southern side of the outbound lane in Juan de Fuca Strait and tug traffic was moved to its centre, away from the higher SRKW density area along the southwestern coast of Vancouver Island.

- **Restricting traffic during a specific time of day (no-go period) in Haro Strait**: Vessel traffic was restricted from passing through the strait from 0:00 to 04:00 each day. The restricted vessels were distributed through other times of the day.
- **Replacing 10% of the noisiest vessels with quieter vessels**: The selection of the noisiest 10% of vessels was performed after ranking them using two approaches: first using unweighted noise emission levels and second, using SRKW audiogram-weighting to account for killer whales' more acute hearing sensitivity to high-frequency sounds. Results differed between these two approaches.
- **Reducing noise emissions (source levels) of specific vessel classes by 3 and 6 decibels**: This evaluation considered the outcomes of the method in terms of the change in noise levels in SRKW habitat, but it did not suggest how the reductions in noise emission levels would be achieved

The potential effectiveness of two additional noise mitigation options were examined using information published in other studies, rather than with models. These options are:

- Reducing noise and vibration generated by different vessel components (such as propellers and onboard machinery).
- Reducing noise exposures through modifying vessel operating approaches (such as slowing down in the presence of animals).

The noise models applied here were developed by JASCO Applied Sciences. They account for vessel type (class), position, and speed, as obtained from Automatic Identification System (AIS) broadcasts that are mandated for most commercial vessels. The models consider ocean and seabed properties and how those parameters affect vessel noise propagation in the ocean. The models calculate sound levels generated by the contributions of large numbers of ships in 1-minute time steps, to allow for an understanding of noise variability. These sound levels are also compiled as monthly averages that are presented as maps showing the geographic distribution of average noise levels from shipping. Temporal variations in noise levels are evaluated to calculate percentiles (e.g., the 50th percentile is the median sound level) at several fixed sample locations (also referred to as receiver sites) in each sub-region. These results are useful for interpreting the fraction of time that noise is likely to disturb SRKW, affect their communications, and reduce their echolocation foraging efficiency.

A large component of vessel noise occurs at low sound frequencies, below 1000 hertz. Vessel sounds also extend to many tens of kilohertz, albeit at lower levels. As killer whales are more sensitive to higher than to lower sound frequencies, it is important that their frequency-dependent hearing acuity be accounted for when assessing the importance of vessel noise. This study presents and interprets noise levels in two ways: unfiltered (or unweighted) results, which do not account for SRKW's frequency-dependent hearing sensitivity, and SRKW audiogram-weighted results, which do. While impacts to SRKW should be assessed primarily based on the weighted results, there is some evidence that high-amplitude, low-frequency sounds may be sensed through non-auditory means. The unfiltered results may be useful for assessing that type of effect, but the audiogram weighted levels should be given higher priority when considering masking-related effects. The unfiltered results are also relevant for assessing noise loudness for species that have better low-frequency hearing sensitivity, such as for pinnipeds, and particularly for the mysticetes, including humpback, blue, fin, sei, and minke whales, that visit the Salish Sea.

Key Findings

Slowing vessels: Vessel speed reductions were found to decrease noise levels at most receiver sites in Haro Strait, Juan de Fuca Strait, and Swiftsure Bank. Slowing vessels in Strait of Georgia did not produce substantial noise savings, largely because of the noise contributions of ferries and the higher densities of several other vessel classes that were exempted from slowing.

Reducing commercial vessel speeds in Haro Strait from their standard 13-20 knots to 11 knots led to lower noise levels relative to baseline levels at the 7 receiver sites closest to the slow-down zone, even with increased future vessel traffic. The receiver located farthest from the slow-down zone and outside the speed transition zone (where vessels slowed down and sped up) showed a slight increase by 0.4 dB. Most receivers experienced decreases of broadband noise levels, appropriate for assessing effects on baleen whales, seals and sea lions, and in SRKW audiogram-weighted levels. The reductions in audiogram-weighted levels were smaller, mainly because these were influenced more by the high-frequency components of ship noise that propagate a shorter distance than lower-frequency noise. An 11 knot speed limit in Haro Strait reduced SRKW-weighted noise levels by 1.3 to 1.9 dB for receivers near the shipping lane, and by 0 to 0.2 dB for more distant receivers. A speed limit much higher than 11 knots would likely be insufficient to balance the additional noise produced by Trans Mountain project traffic. Slow-down speeds of 10 and 7 knots were also investigated in Haro Strait. The slowest speed evaluated (7 knots) produced approximately twice the decibel reduction of the 11 knot speed limit. Slow-downs could, therefore, be beneficial to SRKW in areas near a prescribed slow-down zone in Haro Strait.

Two slow-down mitigation approaches were evaluated in the other sub-regions: Strait of Georgia, Juan de Fuca Strait, and Swiftsure Bank. Here tests were performed with an 11 knot speed limit and a dual-speed approach whereby slower commercial classes (Merchant, Tanker, and Tugs) were slowed to 11 knots, and higher speed commercial classes (Container, Cruise ship, and Vehicle carrier) were slowed to 15 knots.

As might be expected, the noise savings in Strait of Georgia were smaller than in Haro Strait due to the presence and noise contributions of ferry traffic and other traffic that was not slowed. Also, commercial vessels in Strait of Georgia already travel at relatively slow speeds, so the speed reductions were less than those in Haro Strait. Still, the mitigated SRKW audiogram-weighted levels were generally equal to baseline levels, indicating that slowing vessels in Strait of Georgia at least offset the added noise of increased tanker and tug traffic from Trans Mountain's project.

The slowdown results in Strait of Juan de Fuca were substantial: the 11 knot speed limit for all classes led to reductions of 0.2 to 1.8 dB for the mean unweighted sound levels, and 0 to 0.7 dB reductions in mean SRKW audiogram weighted levels, depending on the receiver site. Median sound level reductions (from the time-based noise assessment) were about twice that of the mean level reductions. The dual 11/15 knot speed limit resulted in reductions of 0.1 to 0.9 dB in mean unweighted levels and 0 to 0.2 dB in mean SRKW audiogram weighted levels.

The slow-down results for Swiftsure Bank were similar to those in Strait of Juan de Fuca on the north side of the shipping lanes, closer to the outbound lane which was slowed. However, receiver sites 6 and 7 in that sub-region are south of the inbound lane. Those receivers experienced increased noise levels because inbound vessel traffic, transiting on the American side of the border, was not slowed. All receivers between the lanes or north of the shipping lanes experienced noise level reductions relative to the baseline case. The 11 knot speed limit produced unweighted mean reductions of 0.5 to 2.1 dB and mean SRKW audiogram weighted reductions of 0 to 0.9 dB. The dual 11/15 knot limit produced reductions of 0.2 to 1.9 dB in mean unweighted levels, and reductions of 0.2 to 0.9 dB in mean SRKW audiogram weighted levels.

Overall, vessel speed reductions appear to be effective at reducing noise exposures at nearly all receiver sites in SRKW habitat in all study sub-regions except Strait of Georgia. This mitigation measure is likely one of the most straightforward to implement, but it does have impacts on vessel schedules and operating costs, and possibly on navigational safety that need to be considered.

Rerouting shipping lanes and traffic: The study tested a westward shift of the existing inbound and outbound shipping lanes in Haro Strait, and a southward movement of traffic in the existing outbound shipping lane from Juan de Fuca Strait to Swiftsure Bank. These changes produced noise savings at the receiver sites in the respective sub-regions.

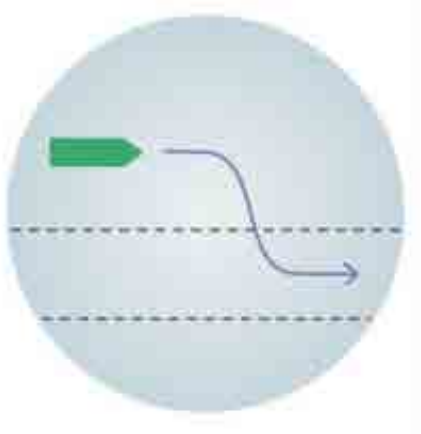

A shift of the shipping lanes westward in Haro Strait, away from the important SRKW foraging areas on the west side of San Juan Island, reduced the audiogram-weighted noise levels at receiver sites by 0.0 to 1.9 dB. The two stations adjacent to the original lanes experienced larger decreases of 2.5 and 7.0 dB. Generally, this mitigation approach was found to be relatively effective. It is important to note that the lane and traffic separation zone changes examined in Haro Strait were not vetted by the Coast Guard or the pilots' association. This option would require full coordination of those organizations to ensure any implemented route changes are feasible and safe. As this approach provides noise savings at key SRKW locations in Haro Strait, it warrants further consideration.

The examined traffic shift in Strait of Juan de Fuca involved changing the traffic patterns within the existing outbound lane only, with no change to the existing lane boundaries. Inbound traffic was not rerouted because the inbound lane lies mainly in American waters. Higher-speed vessels were moved to the southeastern side of the outbound lane and slower vessels, including tugs, were moved to its centre. As the lane is nominally just 1 nautical mile wide, the lateral displacement of vessels inside the lane were so small that the effect of those changes had little effect on noise levels at most receiver sites. However, because much of the present tug traffic transits substantially northeast of the lane, directly through the SRKW habitat closer to the shore of Vancouver Island, the lateral displacement of that tug traffic southwest into the lane produced important noise savings at most Juan de Fuca Strait receiver sites. That noise savings is substantial enough to warrant further consideration of this mitigation, primarily by moving the tug traffic into or adjacent to the existing shipping lane of Juan de Fuca Strait.

Outbound traffic over Swiftsure Bank was modified similarly to that of Juan de Fuca Strait, where faster vessels were moved to the south side of the outbound lane and slower traffic to its centre. Because most of the tug traffic that travelled northeast of the shipping lane in Juan de Fuca Strait continues up the coast of Vancouver Island and not along the shipping lane over Swiftsure Bank, the same noise savings from moving tug sail tracks did not occur. Most of the receiver locations on Swiftsure Bank showed a slight increase in noise levels with this approach, mainly due to the increased traffic from Trans Mountain. Therefore, this mitigation approach, as tested, does not appear to be valuable for Swiftsure Bank.

Overall, rerouting traffic appears to be a potentially effective approach to mitigate noise levels for key locations in the SRKW habitat along southeastern San Juan Island in Haro Strait, and along the southwestern coast of Vancouver Island in Juan de Fuca Strait. The primary benefit in Juan de Fuca Strait arises from moving tug traffic, which currently transits largely outside the shipping lanes, and, therefore, closer to important SRKW habitat, into or at least closer to the shipping lane. That change should be relatively simple to implement.

Vessel convoys: Grouping vessels in convoys increases the noise amplitude during each convoy pass, because multiple vessels are present, but it might allow for longer quiet periods between passes. An assessment of two alternatives for convoying vessels was performed, by modifying departure times of individual vessels so they converged into groups. This study assumed that only Containers, Merchant, Cruise ship, Vehicle carrier, Tanker, and Tugs associated with Trans Mountain operations, would be convoyed. Noise from all vessel classes that broadcast AIS was included in the assessment, but vessels in classes other than those convoyed remained on their usual schedules. One alternative simulated grouping vessels at the north and south boundaries of Haro Strait, depending on their sail directions. The convoy departures were simulated using 2-hour and 4-hour intervals. The second alternative implemented carefully-scheduled vessel departure times from their respective Canadian ports, so that they would arrive in groups spaced at 10-minute intervals at the Victoria Brotchie Pilot station every 4 hours. This led to the formation of convoys starting approximately from mid-Strait of Georgia to Boundary Pass, continuing together through Haro Strait, Juan de Fuca Strait, and across Swiftsure Bank.

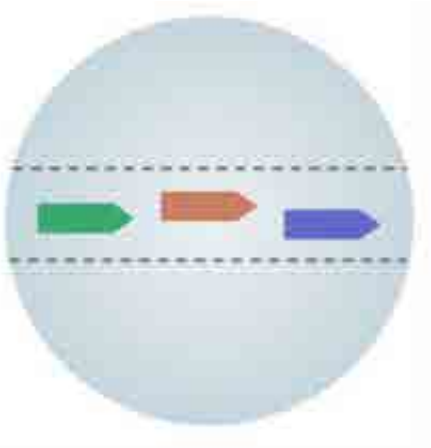

The Haro Strait convoy analysis (with 2 and 4 hour spacing) considered the magnitude and temporal distribution of noise levels at all 8 receiver sites in that sub-region. These results indicated that 2-hour convoys led to an increase in the median noise levels at most of the receiver sites. The 4-hour convoys produced slight reductions, but the changes in SRKW audiogram-weighted noise levels during the quiet times between vessel groups in the daytime were insignificant. The lack of noise improvements from implementing convoys was surprising and led to further investigation: the way the results have been plotted shows that the results improve when noise contributions of non-convoyed vessels are removed. The lack of benefit of this approach is attributed to noise from non-convoyed vessels filling in the quiet times between convoys. Further, the even spacing of convoys in time led to reductions in some of the naturally-larger intervals between vessel passes. Importantly, this study did not include noise from most whale watching vessels or other non-AIS vessels, that would further contribute noise received by SRKW in the times between convoy passes, thereby further reducing its effectiveness. Therefore, these results suggest that convoys in Haro Strait are not highly beneficial.

The larger-area analysis convoyed outbound traffic only, from Juan de Fuca Strait to Swiftsure Bank, in 4 hour intervals; the effect from this approach was assessed through all sub-regions from Strait of Georgia through Swiftsure Bank. Inbound traffic was omitted from this assessment as much of its route is through American waters (through Juan de Fuca Strait and Swiftsure Bank). This analysis found that both unweighted and SRKW audiogram-weighted noise levels at the receiver sites was not influenced significantly by convoys: in Strait of Georgia, noise from ferries and the non-convoyed classes (e.g. fishing vessels, tugs) dominated the received levels. In Juan de Fuca Strait and Swiftsure Bank, a large fraction of commercial vessels originates from ports in the American Puget Sound and that traffic was not included in the simulated convoys. As a result, vessel convoys, as defined here, had very little effect on noise at the receiver sites. Consequently, this study suggests that the convoys, as designed here, are not beneficial in Strait of Georgia, Juan de Fuca Strait, and Swiftsure Bank.

Restricting commercial vessel traffic at night: This scenario investigated the option of restricting commercial vessel traffic in Haro Strait from midnight to 04:00 (no-go period). As might be expected, this greatly decreased SRKW-weighted noise levels during the restricted period (by 1.0 to 12.8 dB depending on receiver site). However, the restricted nighttime traffic must be rescheduled for daytime transits, which increased daytime (04:00 through midnight) noise levels. Noise levels during the non-restricted period therefore increased at the receiver sites by 0.1 to 0.5 dB. It is noted that the observed decreases during the restricted time period appear larger (numerically) than the increases during the non-restricted period, but this is somewhat misleading because the decibel scale is logarithmic; the same change in acoustic energy leads to a larger decrease than increase in units of decibels. However, the most important reason is that commercial vessels contribute most to the noise throughout the region at night, whereas other vessel types contribute largely to daytime noise. Implementing a restricted night-time period therefore could create a very low-noise (quiet) situation for a few hours. Its benefit would depend on how marine fauna use their habitat during the hours of the vessel restriction; a related outstanding question is whether SRKW forage substantially at night. This approach could be fairly easy to implement and could provide substantial noise savings if implemented at night. It, therefore, warrants further consideration.

Replacing the top 10% of noisiest commercial vessels: The study investigated a reduction in noise levels produced by replacing the noisiest 10% of vessels in each commercial vessel class with the corresponding quietest 10%. Importantly, the findings vary depending on how the “noisiest” vessels were defined. When the vessels were ranked using unfiltered noise results, this method produced no reduction to the perceived loudness of sounds to SRKW. When the vessels were ranked using killer whale audiogram-weighted levels, the perceived loudness was reduced nominally by 1 dB. This result suggests that vessel noise emissions at low frequencies are not correlated well with their emissions at high frequencies. Consequently, it is very important to consider killer whale frequency-dependent hearing acuity when ranking the noise emissions of vessels. That is rarely done, but it is noted that the Vancouver Fraser Port Authority’s ECHO program vessel measurements and ranking system does implement killer whale weighting. The reduction of 10% of noisiest vessels potentially reduces noise levels throughout the entire study area and warrants consideration since it now is possible with systems such as the ECHO listening station to at least identify these vessels. They could, therefore, be selectively mitigated through some other means (such as targeted slowing).

Reducing vessel noise emission levels: When noise emission levels from commercial vessel were reduced in all frequency bands by a fixed amount, there was a corresponding but smaller reduction in shipping noise levels experienced at the receiver sites. The reduction in received levels was less than the specified reduction in commercial vessels noise emission because non-commercial vessels also contributed to the soundscape. When emission levels from Containers, Merchants, Cruise ships, Tankers, Tugs, and Vehicle carriers were reduced by 3 dB, the nominal levels at the receiver sites in Haro Strait were reduced by 1.2 to 2.5 dB. When these vessels' noise emission levels were reduced by 6 dB, the received noise reductions were 2.2 to 5.3 dB. While this may appear to be an effective noise mitigation approach, there are presently no known methods for reducing the noise emission levels of commercial vessels at all frequencies.

Other mitigations: This study reviewed literature about several other vessel noise mitigation approaches. The key methods investigated included:

- Technical solutions involving ship design and retrofitting vessels;
- Operational changes involving operator behaviour;
- Operational changes at the shipping industry level, involving loading plans and timing; and
- Operational changes at the traffic management level, involving dynamic speed limits, temporal and spatial area closures in response to real-time monitoring of whale presence, etc.

Ship design changes, vessel retrofitting, and regular ship maintenance should be long term goals to reduce noise in SRKW habitat. These actions would also benefit other oceanic habitats and result in a long-lasting change in underwater noise levels everywhere that these vessels operate. These mitigation actions are the responsibility of vessel owners, so will be driven largely by financial decisions. Incentive programs, such as the Port of Vancouver's discount for certified quiet vessels, could be used to encourage the implementation of quieting technologies.

Operator behaviour changes that reduce noise levels include avoiding sudden vessel accelerations, maintaining speed limits within critical habitat, and reducing speed to maintain appropriate distances from other vessels and whales. These changes can be achieved through better education, voluntary compliance, incentives for shipping companies, or by regulations such as setting maximum noise emission thresholds for vessels accessing sensitive habitats. Support for vessel operator education programs could be an effective way to encourage noise-reducing behaviours, which themselves can be quite effective.

Targeted regulation of commercial traffic within the SRKW habitat, such as dynamic speed limits or rerouting traffic based on real-time visual and acoustic detections of whales near shipping lanes, can be an effective way to implement mitigations with less impact on schedules and less cost to the shipping industry. The premise for dynamic mitigation is that it is applied only when animals are present at locations and times they could be impacted. Notifications of whale presence would also allow vessels to increase monitoring to avoid approaching too close to these animals, thus reducing the risk of vessel strikes. Real-time automated passive acoustic monitoring networks, such as the Port of Vancouver's underwater listening station, DFO's shore-cabled hydrophone stations, and others, have been shown to be highly effective at real-time monitoring for SRKW. These animals are known to vocalize frequently, and hence they are relatively more acoustically-detectable than other species. A network of such systems at locations where vessel traffic lanes intersect with key locations in the SRKW habitat could be highly effective. These systems can also be used to track vessel noise continuously and evaluate changes over longer time periods.

SOMMAIRE

[Sommaire en français.]

CONTENTS

FIGURES

TABLES

GLOSSARY

1/3 octave
One third of an octave. Note: A one-third octave is approximately equal to one decidecade (1/3 oct ≈ 1.003 ddec) (ISO 2017).

1/3-octave-band
Frequency band whose bandwidth is one one-third octave. Note: The bandwidth of a one-third octave band increases with increasing centre frequency.

absorption
The reduction of acoustic pressure amplitude due to conversion of acoustic particle motion energy to heat in the propagation medium.

AIS
Automated Identification System

ambient noise
All-encompassing sound at a given place, usually a composite of sound from many sources near and far (ANSI S1.1-1994 R2004), e.g., shipping vessels, seismic activity, precipitation, sea ice movement, wave action, and biological activity.

ANSI
American National Standard Institute

attenuation
The gradual loss of acoustic energy from absorption and scattering as sound propagates through a medium.

audiogram
A graph of hearing threshold level (sound pressure levels) as a function of frequency, which describes the hearing sensitivity of an animal over its hearing range.

audiogram weighting
The process of applying an animal's audiogram to sound pressure levels (SPL) to determine the sound level relative to the animal's hearing threshold (HT). Audiogram-weighted SPL have units of dB re HT.

broadband sound level
The total sound pressure level measured over a specified frequency range. If the frequency range is unspecified, it refers to the entire measured frequency range.

cavitation
A rapid formation and collapse of vapor cavities (i.e., bubbles or voids) in water, most often caused by a rapid change in pressure. Fast-spinning vessel propellers typically cause cavitation, which creates a lot of noise.

continuous sound
A sound whose sound pressure level remains above ambient sound during the observation period (ANSI/ASA S1.13-2005 R2010). A sound that gradually varies in intensity with time, for example, sound from a marine vessel.

CPA
closest point of approach

cumulative distribution function (CDF)
Probability that a variable presented on the *x* axis will be less than or equal to the associated value on the *y* axis. For this report, it is the percent of time that modelled received levels were below a specified value.

decade
Logarithmic frequency interval whose upper bound is ten times larger than its lower bound (ISO 2006).

decidecade
One tenth of a decade (ISO 2017). Note: An alternative name for decidecade (symbol ddec) is 'one-tenth decade'. A decidecade is approximately equal to one third of an octave (1 ddec ≈ 0.3322 oct) and for this reason is sometimes referred to as a "one-third octave".

decidecade band
Frequency band whose bandwidth is one decidecade. Note: The bandwidth of a decidecade band increases with increasing centre frequency.

decibel (dB)
One-tenth of a bel. Unit of level when the base of the logarithm is the tenth root of ten, and the quantities concerned are proportional to power (ANSI S1.1-1994 R2004).

DFO
Fisheries and Oceans Canada

ECHO
Enhancing Cetacean Habitat Observations

frequency
The rate of oscillation of a periodic function measured in cycles-per-unit-time. The reciprocal of the period. Unit: hertz (Hz). Symbol: *f*. 1 Hz is equal to 1 cycle per second.

geoacoustic
Relating to the acoustic properties of the seabed.

harmonic
A sinusoidal sound component that has a frequency that is an integer multiple of the frequency of a sound to which it is related. For example, the second harmonic of a sound has a frequency that is double the fundamental frequency of the sound.

hearing threshold
The sound pressure level for any frequency of the hearing range that is barely audible for a given individual in the absence of substantial background noise during a specific percentage of experimental trials.

hertz (Hz)
A unit of frequency defined as one cycle per second.

HT
Hearing Threshold

IMO
International Maritime Organization

intensity, acoustic
The amount of acoustic energy flowing through a unit area perpendicular to the direction of propagation, per unit time. Unit: W/m^2.

ISO
International Organization for Standardization

median
The 50th percentile of a statistical distribution.

MEOPAR
Marine Environmental Observation, Prediction and Response Network

MMO
Marine Mammal Observer

MONM
Marine Operations Noise Model

MSL
monopole source level

MSRS
Mandatory Ship Reporting System

NEB
National Energy Board

NEMES
Noise Exposure to the Marine Environment from Ships

NGDC
National Geophysical Data Centre

NOAA
National Oceanic and Atmospheric Administration

NRC
National Research Council

octave
logarithmic frequency interval whose upper bound is twice its lower bound (ISO 2006).

ONC
Ocean Networks Canada

parabolic equation method
A computationally-efficient solution to the acoustic wave equation that is used to model propagation loss. The parabolic equation approximation omits effects of back-scattered sound, simplifying the computation of propagation loss. The effect of back-scattered sound is negligible for most ocean-acoustic propagation problems.

power spectrum density
The acoustic signal power per unit frequency as measured at a single frequency. Unit: $\mu Pa^2/Hz$, or $\mu Pa^2 \cdot s$.

pressure, acoustic
The deviation from the ambient hydrostatic pressure caused by a sound wave. Also called overpressure. Unit: pascal (Pa). Symbol: *p*.

pressure, hydrostatic
The pressure at any given depth in a static liquid that is the result of the weight of the liquid acting on a unit area at that depth, plus any pressure acting on the surface of the liquid. Unit: pascal (Pa).

propagation loss (PL)
The decibel reduction in sound level between two stated points that results from sound spreading away from an acoustic source subject to the influence of the surrounding environment. Also referred as transmission loss.

RAM
Range-dependent Acoustic Model

received level (RL)
The sound level measured (or that would be measured) at a defined location.

rms
root-mean-square

Ro-ro
roll-on/roll-off

SARA
Species at Risk Act

signature
The specific temporal and frequency characteristics of a sound signal generated by a source.

sound
A time-varying pressure disturbance generated by mechanical vibration waves travelling through a fluid medium such as air or water.

sound exposure
Time integral of squared, instantaneous frequency-weighted sound pressure over a stated time interval or event. Unit: pascal-squared second ($Pa^2 \cdot s$) (ANSI S1.1-1994 R2004).

sound exposure level (SEL)
A cumulative measure related to the sound energy dose received over time.

sound field
Region containing sound waves (ANSI S1.1-1994 R2004).

sound pressure level (SPL)
The decibel ratio of the time-mean-square sound pressure, in a stated frequency band, to the square of the reference sound pressure (ANSI S1.1-1994 R2004).

For sound in water, the reference sound pressure is one micropascal (p_0 = 1 µPa) and the unit for SPL is dB re 1 µPa:

$$\mathrm{SPL} = 10\log_{10}\left(p^2 / p_0^2\right) = 20\log_{10}\left(p / p_0\right) .$$

Unless otherwise stated, SPL refers to the root-mean-square sound pressure level.

sound speed profile
The speed of sound in the water column as a function of depth below the water surface.

source level (SL)
The sound level measured in the far-field and scaled back to a standard reference distance of 1 metre from the acoustic centre of the source. Unit: dB re 1 µPa m (pressure level) or dB re 1 µPa^2·s m (exposure level).

spectrum
An acoustic signal represented in terms of its power (or energy) distribution in frequency.

SRKW
Southern Resident Killer Whale

thermocline
The depth interval near the ocean surface that experiences temperature gradients due to warming or cooling by heat conduction from the atmosphere and by warming from solar heating.

transmission loss (TL)
The decibel reduction in sound level between two stated points that results from sound spreading away from an acoustic source subject to the influence of the surrounding environment. Also referred as propagation loss.

ULS
Underwater Listening Station

UVic
University of Victoria

wavelength
Distance over which a wave completes one oscillation cycle. Unit: meter (m). Symbol: λ.

1. INTRODUCTION

The International Maritime Organization (IMO) recognizes that underwater noise from commercial ships may have short- and long-term negative consequences on marine life, especially for marine mammals that rely on the use of sound for many purposes. The Salish Sea is an important habitat for several marine mammal species, including the endangered Southern Resident Killer Whales (SRKW; SARA 2002). Much of the SRKW critical habitat lies within the Salish Sea near high-traffic shipping lanes. The SRKW population, therefore, experiences substantial levels of noise from commercial vessels. Expected increases in shipping activity in the Salish Sea could lead to further increases in these noise levels. Man-made noise, including vessel noise, has the potential to disturb or injure marine animals, and it has been identified as a factor that hinders recovery of the SRKW population (DFO 2011). Strategic management of future vessel traffic will be necessary to ensure marine animals in the region are not exposed to substantial increases in underwater noise. Transport Canada recognizes the need to examine existing and projected underwater noise conditions in the Salish Sea due to present and future increases in vessel traffic, and to investigate the effectiveness of options for reducing vessel noise exposures to marine animals. This report describes a study performed to quantify vessel noise in current and future conditions, with and without noise mitigation options.

1.1. Study Overview

JASCO's vessel noise model was used to examine the effectiveness of several potential mitigation approaches for reducing vessel noise exposures of SRKW habitat in the southern Salish Sea. The model was applied in four regions of interest within key SRKW areas, to calculate monthly averaged noise levels, as well as sound pressure levels (SPL) in 1-minute steps from which daily noise distributions could be obtained. Each model scenario represents either the current (baseline) vessel traffic, or a potential mitigation option affecting future vessel traffic and/or operating conditions. The model results of mitigation options are compared with baseline results and the relative effectiveness of these approaches is assessed quantitatively according to the estimated changes in noise levels. Some noise mitigation options, however, were assessed without modelling, based on previous studies and other information published about their effectiveness. These options were assessed here in a qualitative sense only, because their effectiveness varies with application and most have not been adequately characterized by measurements.

The vessel noise model requires several inputs, including the noise emission levels, traffic densities, and transit speeds for each vessel class. It also incorporates oceanographic data such as ocean temperature, salinity profiles, water depth variations, and seabed properties. Wind and ambient noise are also accounted for in the time-dependent scenarios. A large range of sound frequencies (from 10 Hz to 63 kHz) is examined. This frequency range covers most of the frequencies used by killer whales for communication and echolocation (although echolocation click frequency content can extend weakly to 100 kHz). It is important to assess the frequency-dependence of noise because noise emissions from ships vary substantially across this frequency range. Most vessel sound energy occurs below 1 kHz, whereas killer whale hearing sensitivity is best between 15–30 kHz (Branstetter et al. 2017). Nevertheless, vessel noise emissions extend to many tens of kHz, so can interfere with killer whales' use of sound.

For this study, noise emission levels of vessels were obtained from a database of measurements recorded at the Strait of Georgia Underwater Listening Station (ULS) by JASCO for the Enhancing Cetacean Habitat Observations (ECHO) program, in collaboration with Vancouver Fraser Port Authority and Ocean Networks Canada. Vessel density and speed information for multiple commercial, government, and recreational vessel classes in the Salish Sea, were derived from a high-resolution Automated Identification System (AIS) dataset that contains the location of many thousands of vessels (MarineTraffic 2017). This information was extracted for two one-month periods: January and July 2015, representing winter and summer baseline

conditions, respectively. Maps of baseline vessel densities and speed for different vessel classes were prepared, covering four regions of the southern Salish Sea: Strait of Georgia, Haro Strait, Juan de Fuca Strait, and Swiftsure Bank. These regions are referred to as Local Study Areas. Some scenarios were also evaluated over a larger region, with a coarser grid, covering the southern portion of the Salish Sea, from the Strait of Georgia to Swiftsure Bank. This area is referred to as the Regional Study Area. Vessel density and speed data for traffic from oil tankers and assisting tugs were also synthesized, based on Trans Mountain's forecast (NEB 2016) of vessel activity forecasted to start in the year 2020. The densities of future tanker and tug traffic were added to the baseline vessel densities to simulate the unmitigated future (i.e., projected) vessel density information.

Sound levels were modelled over relatively large regions and tabulated at fixed sample locations in the SRKW habitat to evaluate the change from baseline to mitigated future noise levels, and to quantify the effectiveness of the various mitigation approaches. For most scenarios, vessel noise was assessed as a monthly average. These results are presented as maps showing the spatial distribution of equivalent continuous underwater noise levels (L_{eq}). The monthly L_{eq} were calculated similar to the 8-hour L_{eq} used for human workplace noise assessments but using a much longer averaging time (1 month versus 8 hours). Since L_{eq} is a time average, it does not provide information about noise level variations over time within the averaging period. Time variability is important for certain analyzes, however, such as for estimating how often sound levels exceed marine mammal effects thresholds.

For scenarios that alter the schedule and speed of vessel passes, the model was applied in time-dependent mode. In this mode, the model produces a 4-D (3 spatial coordinates plus time) representation of the underwater noise field over a representative day, in time steps of 1 minute. Results from the time-dependent analysis are presented as SPL temporal variation plots and cumulative distribution functions at eight or nine sample locations of key importance for SRKW in each Local Study Area (or sub-region). These results provide information about the temporal distribution of noise exposures that cannot be obtained from longer-time averages. For example, this approach allows the determination of the median (or 50th percentile) sound level which is exceeded half of the time. Likewise, other percentiles can be directly determined. This information can be also be used to estimate the duration of quiet (at ambient level) and noisy (above ambient) periods, and to estimate if a mitigation approach is likely to increase or decrease the amount of quiet time.

This report is divided into three main sections. Section 2 presents an overview of the scenarios and methods; more detailed descriptions of the methods are provided in Appendices A–D. Section 3 present the results. Unmitigated modelled noise levels (baseline (current) and future) are first presented, followed by results for each mitigation approach. The modelled mitigated noise levels listed in Table 2 are compared to baseline noise levels; the results for other mitigation approaches (also listed in Table 2) are discussed in a qualitative manner. Results modelled over the Regional Study Area (Salish Sea) are presented in Appendix E. Section 4 discusses the study results: 1) in terms of the overall effectiveness of each mitigation approach, and 2) as the effectiveness of mitigations in each studied region.

2. METHODS

Cumulative noise modelling for all shipping traffic over specified time intervals was performed for the following scenarios, described in Section 2.2:

- Unmitigated baseline traffic,
- Unmitigated future traffic, and
- The following mitigation approaches on projected traffic:
    - Implementing a vessel slow-down zone,
    - Restricting traffic during a specific time of day (no-go period) in Haro Strait,
    - Replacing 10% of noisiest ships,
    - Reducing noise emission levels of specific vessel classes,
    - Adjusting the traffic routes in Haro Strait and Juan de Fuca Strait, and
    - Grouping vessel into convoys.

Cumulative noise levels are calculated over a common timeframe of 1 month for all scenarios, except convoying. These results provide one-month equivalent continuous underwater noise levels (L_{eq}), which reflect the average sound pressure level (SPL) that can be detected at anytime over the course of the month. For scenarios that alter the timing and speed of vessel passes, i.e. for the slow-down and convoying scenarios, the model calculated SPL in 1-minute steps over the course of about one day. These results provide information on the temporal variation of the noise levels associated with mitigated and non-mitigated vessel classes. The effectiveness of additional mitigation approaches, described in Section 2.6, are qualitatively assessed through a literature review.

To produce time-averaged or time-dependent acoustic field maps, the cumulative noise model requires three main input parameters, shown in Figure 1:

- A representation of the vessel traffic throughout a Local Study Area, including individual vessel types, sail tracks, vessel densities, and speeds by class (Vessel Traffic Data),
- A description of how sound propagates away from a vessel at any location in a Local Study Area (Sound Propagation Curves), and
- A description of the noise emitted by each vessel (Vessel Source Levels).

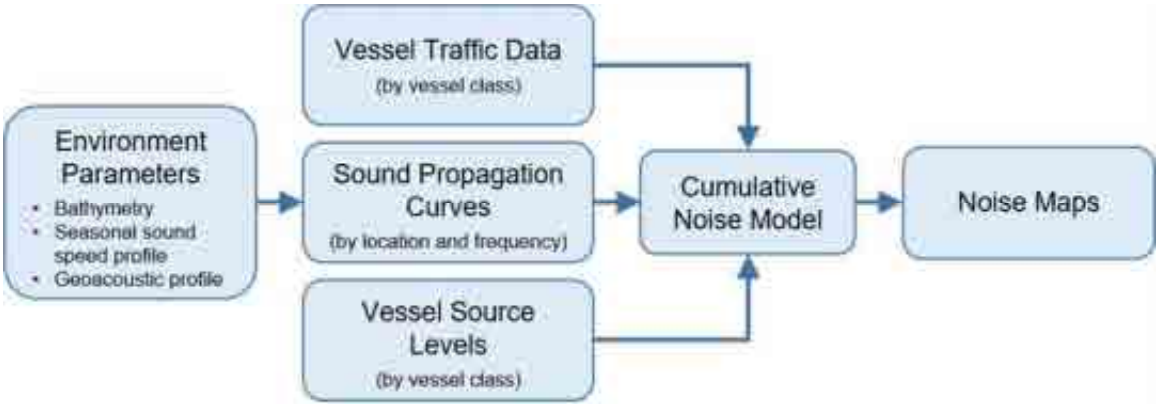

Figure 1. High-level flow chart of cumulative noise model inputs and outputs.

The sound propagation curves are computed by the noise model's internal algorithms. These calculations are independent of the modelled vessel scenarios. They account for the ocean environment at all locations in all study areas. Sections 2.3–2.3.1 detail the components of cumulative noise model flow chart presented in Figure 1.

Vessel traffic densities, speeds, and noise emission levels are adjusted based on the mitigation characteristics of each scenario. In all modelling scenarios, the following 12 vessel classes described in Appendix B were considered:

- Container,
- Cruise ship,
- Ferry (roll-on/roll-off (Ro-ro) passenger ferries, Ro-ro cargo ferries, and Clipper ferries),
- Fishing,
- Government,
- Merchant,
- Passenger,
- Recreational,
- Tanker,
- Tug,
- Vehicle carrier, and
- Other/miscellaneous.

Future unmitigated and mitigated scenarios are developed by increasing the vessel density of the tanker and tug classes to represent increases in the number of these vessels, as proposed by Trans Mountain's assessment (NEB 2016). The vessel classes complying to the mitigation approaches are:

- Container,
- Cruise ship,
- Merchant,
- Tanker,
- Tug, and
- Vehicle carrier.

One ferry vessel route is also included in the slow-down scenario in Haro Strait. The Washington State Ferries on this route are said to have participated in previous slow-down trials (Port of Vancouver 2018); their compliance with a full-time slow-down zone can be expected.

2.1. Study Area

This study focuses on the southern section of the Salish Sea, which includes critical habitat for SRKW. All modelled mitigation scenarios are analyzed over at least one of four Local Study Areas, with a grid resolution of 200 × 200 m. Some are also analyzed over the large Regional Study Area (208 × 184 km) covering the southeast portion of the Salish Sea, with a grid resolution of 800 × 800 m; these results are presented in Appendix E. The extent of each study area is present in Figure 2. The coloured dots in Figure 2 represent the locations where noise fields were sampled and further analyzed; as explained below, they were placed at key locations within the critical habitat for SRKW.

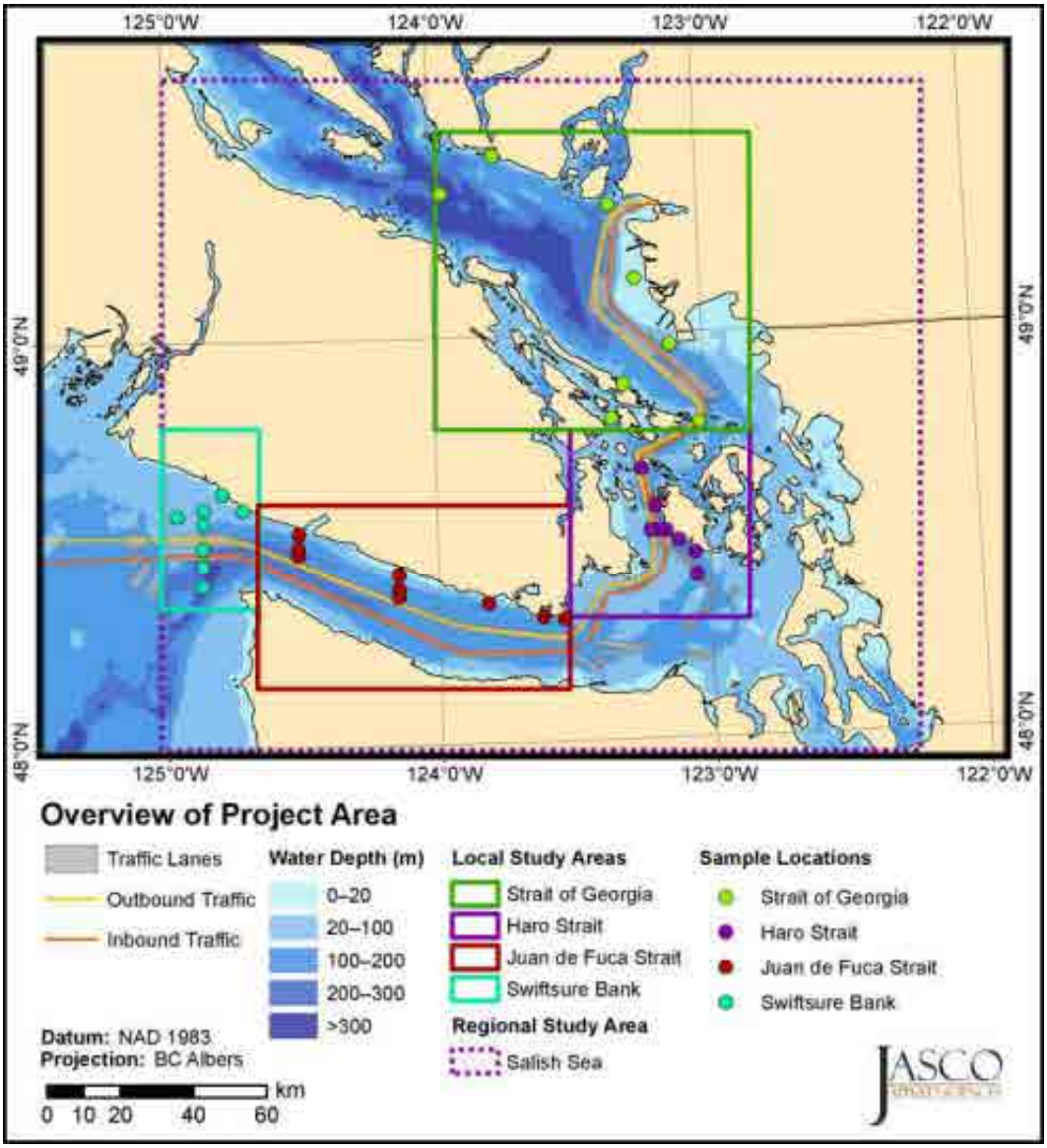

Figure 2. Extent of the model areas referenced as the Regional Study Area (dash line) and the four Local Study Areas (solid lines).

Figure 3 shows that the critical habitat for SRKW extends from Swiftsure Bank to the southeast region of the Strait of Georgia, and south into American waters off Washington State. All southern resident pod groups (J, K, and L) share a core region in Haro Strait, notably during spring, summer, and fall (Osborne 1999, Wiles 2004). In addition, J-pod inhabits northern Rosario Strait and areas near Active Pass, while the L-pod is often encountered in an area south of Vancouver Island in the Juan de Fuca Strait. The location of SRKW in winter is less understood, but the whales seem to visit the Salish Sea occasionally (DFO 2011). Figure 4 shows the summer density of SRKW within the critical habitat shown in Figure 3.

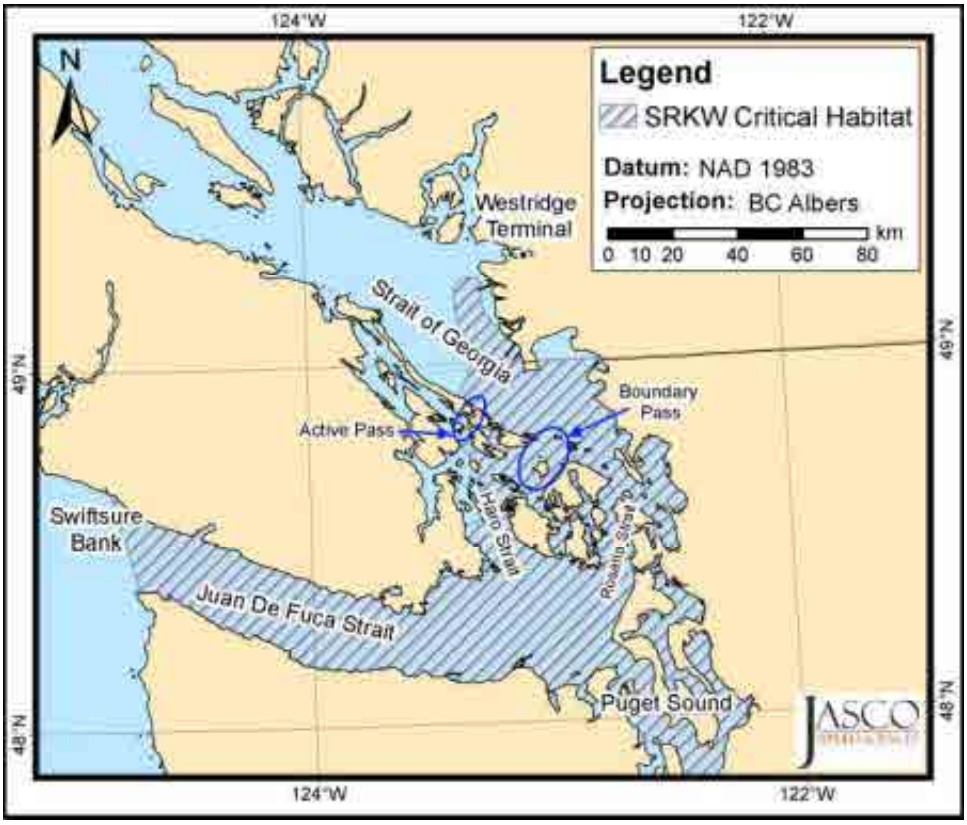

Figure 3. Overview of the SRKW critical habitat (DFO 2011).

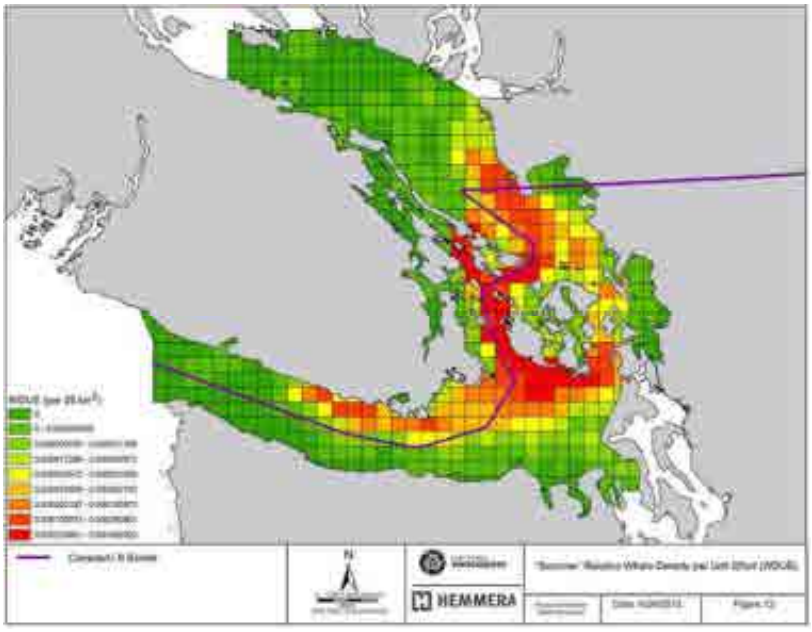

Figure 4. Relative summer killer whale density.[1] (Hemmera and SMRU 2014, Figure 12).

[1] Relative killer whale density per unit of effort per 25 km^2. This map does not include effort and related DFO sightings along the west coast of Vancouver Island and Brian Gisborne's Swiftsure sightings (Personal communication with Dr Dom Tollit; Hemmera and SMRU 2014).

In the Strait of Georgia model region, the noise fields were sampled at eight sites that are key locations within and north of the SRKW habitat. These sample locations are shown in Figure 5 and listed in Table 1. Sample locations 1–3 are the northernmost sample locations; SRKW are likely to travel through this region, to and from more southern foraging regions. Sample locations 4–5, located off Fraser Delta, are important feeding areas from June to October; the high SRKW density in this region is associated with the abundance of salmon (Hauser et al. 2007, Hanson et al. 2010). Sample locations 6, off Active Pass, and 8, off North Pender Island, are in areas where SKRW concentrate their activity during summer; these sites were selected based on their proximity to the ferry route. Sample location 7, off Boundary Pass, is a SRKW foraging area and is in the commercial shipping lane.

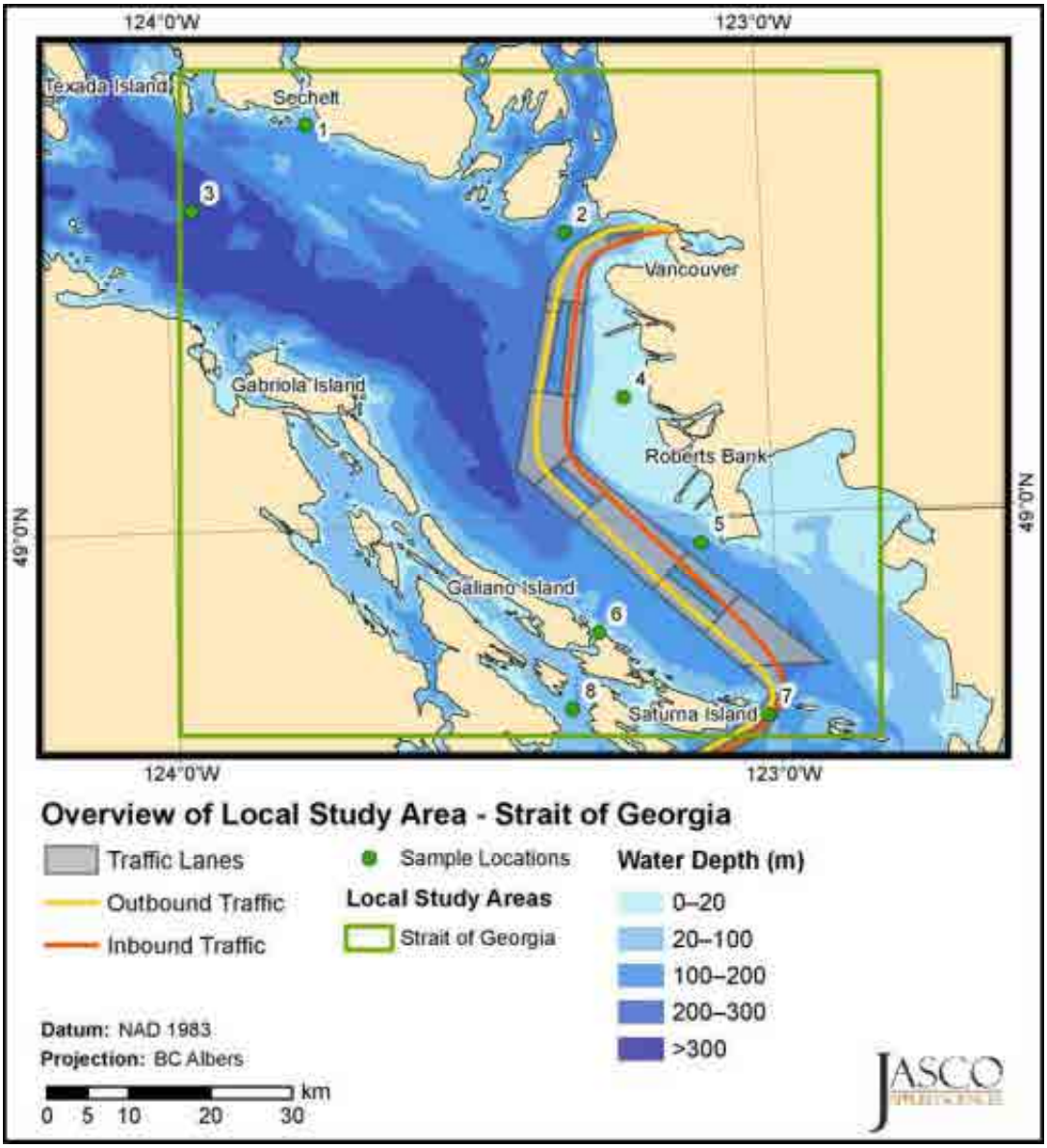

Figure 5. *Strait of Georgia*: Noise field sample locations based on the SRKW critical habitat, relative to shipping lanes.

In the Haro Strait model region, the noise fields were sampled at eight sites that are key locations within the SRKW habitat and in regions of high vessel density, close to the traffic lanes. These sample locations are shown in Figure 6 and listed in Table 1. Sample location 1 represents an important area where SRKW travel and forage before entering Haro Strait. Sample locations 2–5, located along the shore of San Juan Island, are within important feeding areas with high SRKW density in summer (Hauser et al. 2007). Sample location 6 is the northernmost sample location. SRKW are likely present there in summer and winter. Sample locations 6–8 are located within the shipping lanes. Results at these locations are relevant for assessing the temporal variation in noise levels, such as those presented for the convoying scenarios. The monthly-averaged results (for all other scenarios) at these locations are largely influenced by the exact transit of the simulated traffic; a slight change in the position of the simulated traffic could substantially affect the results because the locations are near the ship tracks. Thus, Sample locations 1–5 are best suited for assessing the effects of most mitigation approaches.

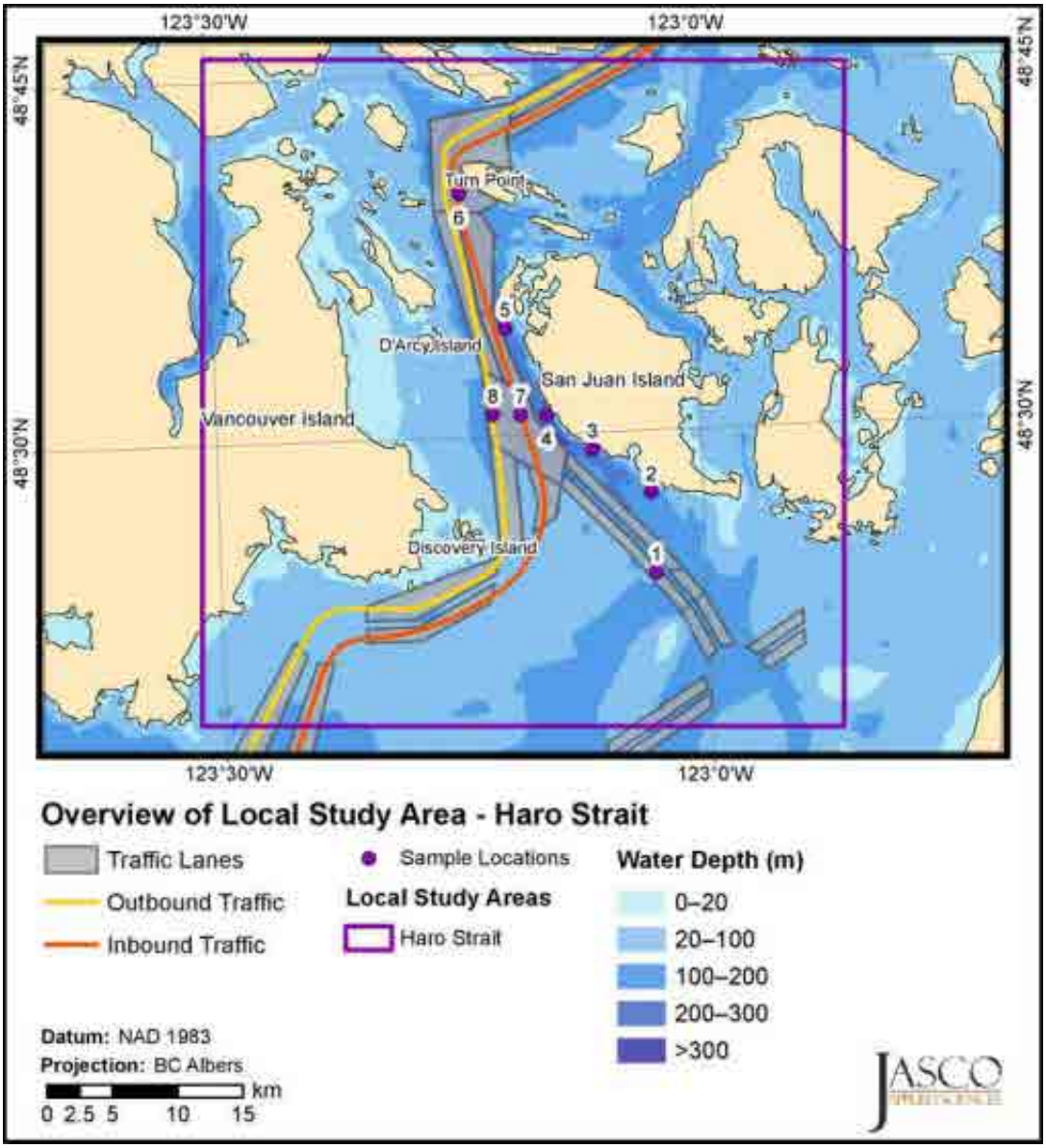

Figure 6. *Haro Strait*: Noise field sample locations based on the SRKW critical habitat, relative to shipping lanes.

In the Juan de Fuca Strait model region, the noise fields were sampled at nine sites that are key locations within SRKW habitat. These sample locations are shown in Figure 7 and listed in Table 1. Sample locations 1–3 represent hotspots where SRKW are frequently encountered transiting between Juan de Fuca Strait and San Juan Island (Ford et al. 2017) and where fishing occurs. Sample locations 4–6, located in central Juan de Fuca Strait, are foraging areas (Hanson et al. 2010). These sites are situated at three distances (2, 4, and 8 km) from the outbound shipping lane to sample the variation in noise levels moving away from the lanes, toward the shore. Sample locations 7–9, located northwest of the Strait, are in a foraging area off Port Renfrew (Hanson et al. 2010) where recreational fishing occurs. These sample locations were also placed at three distances (2, 4, and 8 km) from the outbound shipping lane to sample the variation in noise levels perpendicular to the lanes, toward the shore.

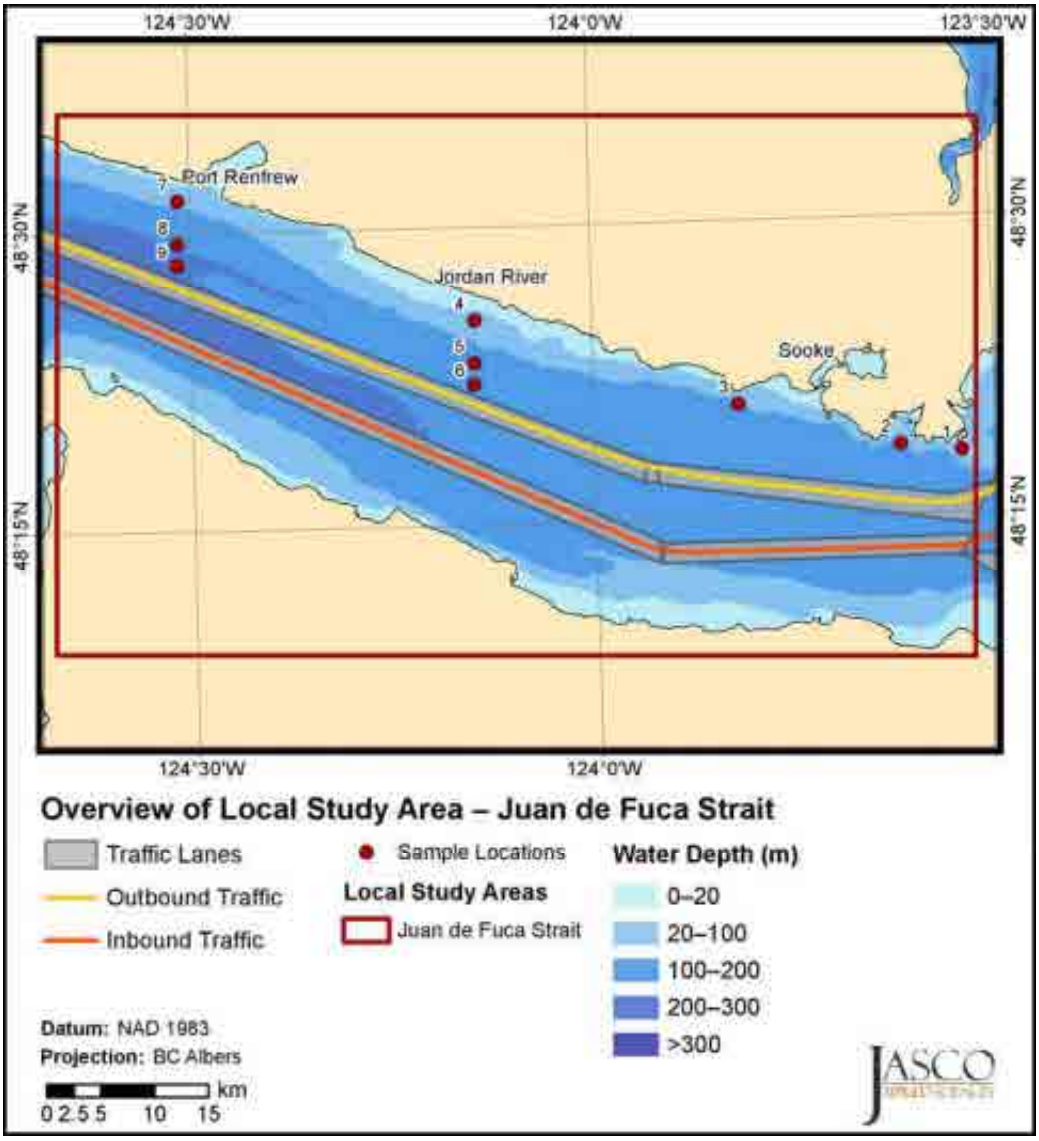

Figure 7. *Juan de Fuca Strait*: Noise field sample locations based on the SRKW critical habitat, relative to shipping lanes.

Finally in Swiftsure Bank, the noise fields were sampled at eight sites that are key locations within SRKW habitat. This area has recently been identified as of special importance to SRKW off Vancouver Island (Ford et al. 2017). Swiftsure Bank is among the most productive fishing areas for Chinook and other salmonids on the North American west coast (McFarlane et al. 1997). The sample locations are shown in Figure 8 and listed in Table 1. Sample locations 1–3 are located in a foraging area frequented by SRKW (Hanson et al. 2010, Ford et al. 2017). Sample locations 4–7 are located at multiple distances from the shipping lanes with varied depths on the Bank. Sample location 8 is near a DFO hydrophone, which frequently detects SRKW calls.

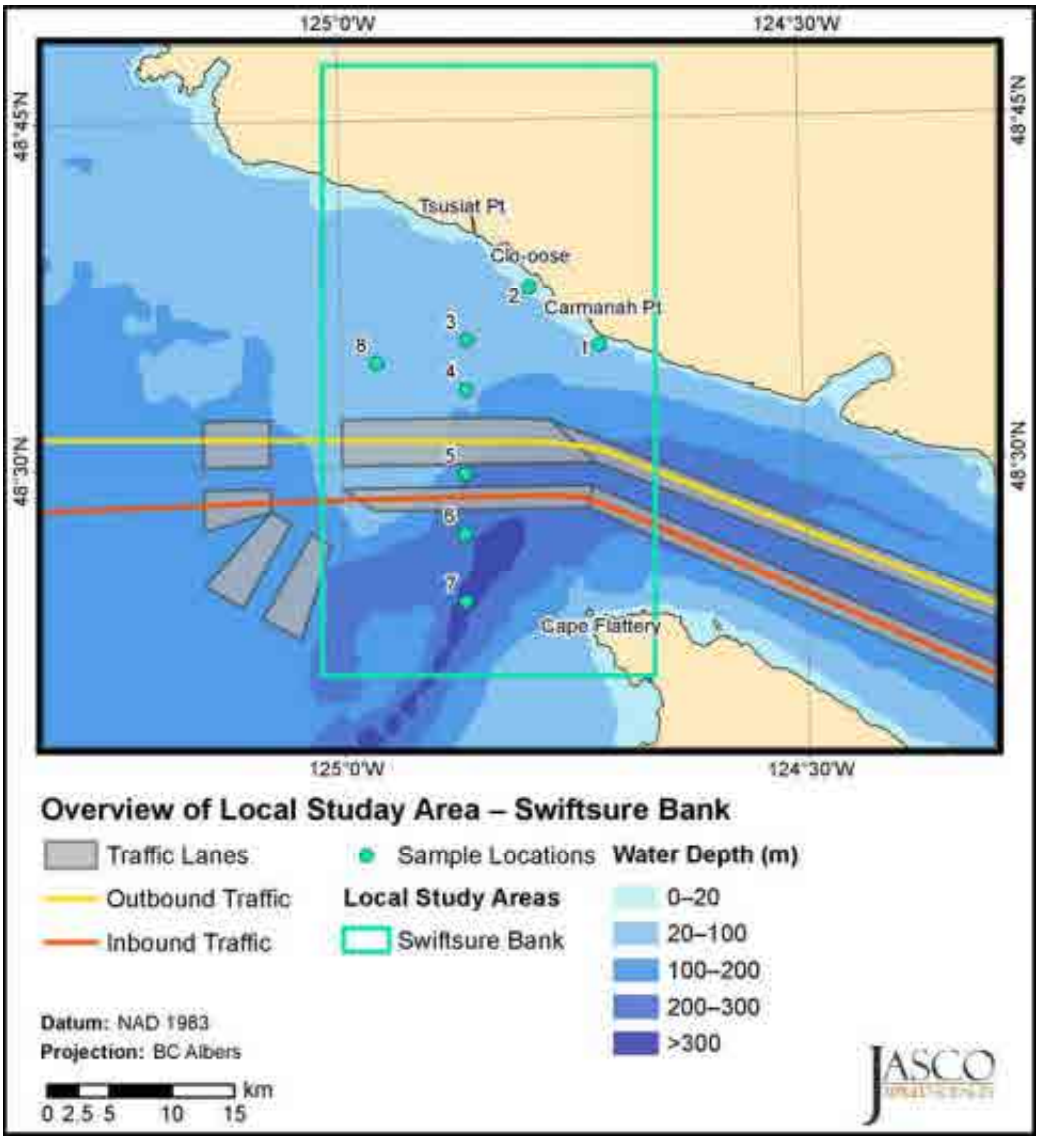

Figure 8. *Swiftsure Bank*: Noise field sample locations based on the SRKW critical habitat, relative to shipping lanes.

Table 1. Noise field sample locations in each Local Study Area.

Region	Sample location	Description	Easting/Northing (m), BC Albers Projection		Latitude	Longitude
Strait of Georgia	1	Sechelt	1162503 E	494981 N	49° 26' 52.8330" N	123° 45' 36.5344" W
	2	Howe Sound	1194156 E	481732 N	49° 19' 08.3646" N	123° 19' 52.0036" W
	3	South of Texada Island	1148575 E	484334 N	49° 21' 21.7615" N	123° 57' 22.4979" W
	4	Sandheads	1201414 E	461597 N	49° 08' 07.4208" N	123° 14' 31.9855" W
	5	Southern Strait	1210945 E	443697 N	48° 58' 15.4312" N	123° 07' 18.5579" W
	6	Mayne Island	1198458 E	432766 N	48° 52' 37.3099" N	123° 17' 51.7764" W
	7	Saturna Island	1219264 E	422666 N	48° 46' 43.0535" N	123° 01' 13.8709" W
	8	Swanson Channel	1195226 E	423272 N	48° 47' 33.6873" N	123° 20' 47.4900" W
Haro Strait	1	South Haro Strait/ Juan de Fuca	1218680 E	380765 N	48° 24' 06.0100" N	123° 03' 07.7198" W
	2	South San Juan	1218303 E	386920 N	48° 27' 26.0500" N	123° 03' 13.5601" W
	3	Central South San Juan	1213787 E	390220 N	48° 29' 19.0400" N	123° 06' 46.2100" W
	4	Central San Juan	1210304 E	392842 N	48° 30' 48.5900" N	123° 09' 30.2101" W
	5	North San Juan/ Henry Island	1207105 E	399437 N	48° 34' 26.4900" N	123° 11' 52.9901" W
	6	Stuart Island	1203577 E	409760 N	48° 40' 05.5200" N	123° 14' 25.0598" W
	7	Inbound Traffic Lane	1208303 E	392857 N	48° 30' 51.6626" N	123° 11' 07.4354" W
	8	Outbound Traffic Lane	1206185 E	392843 N	48° 30' 53.9157" N	123° 12' 50.3791" W
Juan de Fuca Strait	1	Race Rocks	1182671 E	368398 N	48° 18' 09.6267" N	123° 32' 34.4892" W
	2	East Sooke Park	1176989 E	368933 N	48° 18' 33.2573" N	123° 37' 08.5042" W
	3	Sooke	1161925 E	372540 N	48° 20' 46.0102" N	123° 49' 12.2199" W
	4	Jordan River 1	1137474 E	380295 N	48° 25' 20.1152" N	124° 08' 46.8220" W
	5	Jordan River 2	1137473 E	376304 N	48° 23' 10.6589" N	124° 08' 51.9185" W
	6	Jordan River 3	1137490 E	374308 N	48° 22' 05.9186" N	124° 08' 53.6153" W
	7	Port Renfrew 1	1109947 E	391307 N	48° 31' 38.3123" N	124° 30' 51.3554" W
	8	Port Renfrew 2	1109926 E	387315 N	48° 29' 28.8593" N	124° 30' 56.4624" W
	9	Port Renfrew 3	1109897 E	385319 N	48° 28' 24.1354" N	124° 30' 59.8667" W
Swiftsure Bank	1	Carmanah Point	1094661 E	397613 N	48° 35' 12.4831" N	124° 43' 09.2702" W
	2	Clo-oose	1089031 E	402133 N	48° 37' 42.2916" N	124° 47' 39.7011" W
	3	Tsusiat Point 1	1083968 E	397897 N	48° 35' 27.6325" N	124° 51' 49.7660" W
	4	Tsusiat Point 2	1083962 E	393905 N	48° 33' 18.1561" N	124° 51' 53.1752" W
	5	Tsusiat Point 3	1083922 E	387193 N	48° 29' 40.4776" N	124° 52' 00.3755" W
	6	Tsusiat Point 4	1083919 E	382352 N	48° 27' 03.4675" N	124° 52' 04.2659" W
	7	Tsusiat Point 5	1083980 E	376879 N	48° 24' 05.8850" N	124° 52' 05.5549" W
	8	Swiftsure Bank	1076791 E	396044 N	48° 34' 31.1123" N	124° 57' 40.6724" W

2.2. Modelled Underwater Noise Scenarios

Table 2 summarizes the baseline, future unmitigated, and future mitigated modelled scenarios, as well as the literature-based scenarios that will be presented in this report.

Table 2. List of scenarios, results type, and the study area.

Scenario	Description	Results type		Study area
Modelled Mitigation Options		Time-averaged (1 month)	Time-dependent (24 or 33 hours)	
Baseline	Current vessel traffic	✓	✓	All Local Study Areas Regional (Salish Sea)
Future unmitigated	Current vessel traffic+ projected increase in tanker and tug traffic due to the Trans Mountain project	✓		All Local Study Areas Regional (Salish Sea)
Implementing a slow-down zone	Implementing a speed limit(s)to commercial traffic within a prescribed zone.	✓	✓	All Local Study Areas
Implementing a no-go period	Restricting navigation of commercial traffic between midnight and 04:00 h within a prescribed zone	✓		Haro Strait
Replacing 10% of noisiest vessels	Replacing 10% of noisiest commercial vessels with quieter vessels of the same class	✓		All Local Study Areas Regional (Salish Sea)
Reducing noise emission levels	Reducing all commercial vessel noise levels by a fixed amount at all frequencies	✓		All Local Study Areas Regional (Salish Sea)
Adjusting traffic lanes	Adjusting a portion of the traffic lanes or the traffic density away from SRKW habitat	✓		Haro Strait Juan de Fuca Strait Swiftsure Bank
Convoying	Grouping commercial traffic into convoys with a set time interval for transiting within a prescribed zone		✓	All Local Study Areas
Other Mitigation Options				
Retrofitting vessels	Retrofitting vessels with technologies to reduce noise emissions	No modelling (literature review)		
Replacing tugs	Replacing Trans Mountain tugs with noise-reduced tugs			
Changing ship designs	Changing ship designs to reduce noise emission			
Changing maintenance	Changing ship maintenance cycled in areas relating to noise emission			
Changing operator behaviour	Changing operational behaviours such as reducing acceleration rate in sensitive area			
Changing shipping practices	Changing shipping practices such as the number of tugs required and the use of onboard machinery			
Applying real-time mitigation	Applying real-time mitigation such as whale avoidance and speed reduction in hot spot areas			
Adjusting traffic lanes	Applying possible changes in traffic lanes in areas other than Haro Strait and Juan de Fuca Strait			
Using larger vessels	Using larger vessels to reduce the number of transits required			

2.2.1. Baseline Noise Scenario

This scenario represents the current vessel noise conditions. It is used to calculated changes in noise levels associated with future increase in (unmitigated and mitigated) shipping traffic. The baseline vessel noise levels are modelled using AIS vessel data from 2015. Winter (January 2015) and summer (July 2015) levels were compared over the Regional Study Area. These results are presented in Section 3. Although winter conditions are more favourable to long-distance sound propagation, SRKW are present in larger number in the summer. Thus, only summer conditions were modelled for all other scenarios; these results, modelled over each Local Study Area, are presented in Section 3.1.

The daily average in vessel transits through each Local Study area are presented in Table 3 for both January and July 2015. Vessel traffic is generally higher in July than in January in Strait of Georgia and Haro Strait. The January and July traffic levels were used to represent general winter and summer traffic conditions, but it is acknowledged that there can be month-to-month variations even within winter and summer seasons that are not considered here. It is therefore possible that the density estimates used here may not accurately represent all months. However, most vessel traffic density errors would be common to both scenarios (Baseline and Future-case mitigated) as the future case is obtained simply by augmenting the baseline traffic. As the analysis of mitigation effectiveness is based on the differences in noise levels between baseline and future cases, any density errors will largely cancel in these differences. This would not be the case for months when the relative densities of mitigated to non-mitigated vessel classes are different, so some potential for density difference effects remains. Still, those relative differences are expected to be small and most monthly variability in density will not influence the results due to cancellation in the differences as described above.

Table 3. Daily (median) vessel transits in January and July 2015.

Vessel class	Strait of Georgia		Haro Strait		Juan de Fuca Strait		Swiftsure Bank	
	January	July	January	July	January	July	January	July
Container	5	6	5	6	5	6	5	5
Cruise ship	0	4	0	3	0	3	0	3
Ferry (Ro-ro Passenger)	197	248	113	151	0	0	0	0
Ferry (Ro-ro Cargo)	10	8	4	5	0	0	0	0
Ferry (Clipper)	0	0	2	9	0	0	0	0
Fishing	14	12	1	5	3	9	1	5
Government	14	29	9	17	1	2	0	1
Merchant	26	21	10	9	10	8	9	9
Other	47	44	16	27	1	1	1	1
Passenger (<100 m)	18	34	0	20	0	0	0	0
Recreational	32	126	17	177	0	11	0	5
Tanker	1	1	2	2	3	3	3	2
Tug	327	344	13	19	5	5	4	3
Vehicle carrier	2	1	1	1	2	3	2	2

2.2.2. Unmitigated Future Noise Scenario

This scenario assesses the increase in noise levels associated with the increase in vessel traffic for Trans Mountain's expanded shipping requirements, expected to begin in 2020. The modelled levels include all traffic from the baseline scenario plus tankers and tugs sailing along the inbound and outbound traffic lanes between Swiftsure Bank, off the mouth of Juan de Fuca Strait, and the Westridge Marine Terminal in Burrard Inlet. These locations are indicated in Figure 9. It is estimated that over 1 month, 29 new tankers will be required to assist with exporting petroleum products from the Westridge Terminal (NEB 2016). These new vessels will sail independently along the inbound route. One tug will escort each tanker along the outbound route. The 29 escort tugs will sail back to Westridge terminal along the inbound route. The position and speed of each vessel is simulated along the traffic lanes (inbound and outbound, as seen in Figure 9 and discussed in Section 2.3.2) and added to the baseline vessel density and speed data. The projected levels are modelled for July over all model areas presented in Figure 2.

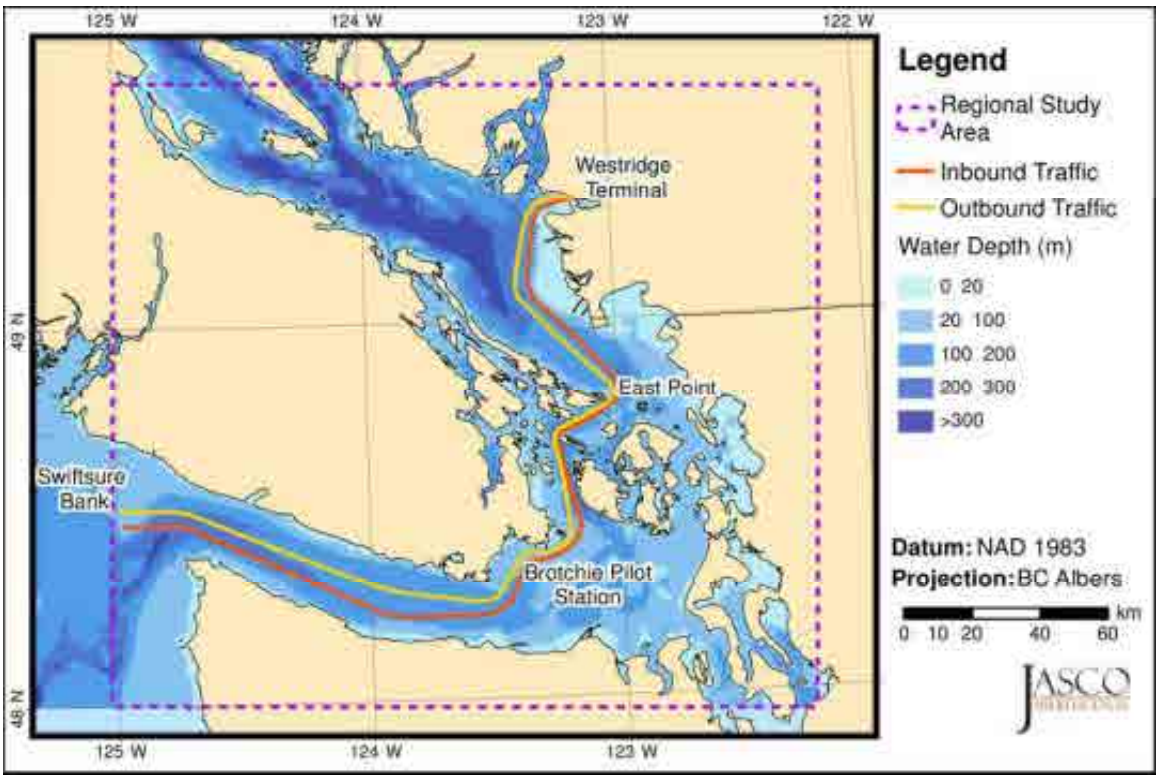

Figure 9. Traffic routes used to simulate marine traffic for Trans Mountain tankers and tugs.

2.2.3. Mitigated Future Noise Scenarios

2.2.3.1. Slowing Down Vessels

This mitigation scenario explores implementing 'slow-down zones' where ships are required to adhere to a speed limit within a prescribed zone. Two types of slow-down approaches are modelled. First, changes in sound levels are evaluated for maximum speeds of 11 knots, for all commercial classes. (Maximum speeds of 7 and 10 knots were also modelled for commercial classes transiting in Haro Strait.) Then, in the Strait of Georgia, Juan de Fuca Strait, and Swiftsure Bank, changes in sound levels are evaluated for maximum speeds of 11 knots for relatively slow commercial classes (Merchant, Tanker, and Tugs), and 15 knots for faster commercial classes (Container, Cruise ship, and Vehicle carrier).

Transition zones were used to model gradual changes in vessel speed as they approach and depart a slow-down zone. In a transition zone, vessels are assumed to travel at a speed that is half way between their unmitigated speed (based on average speeds used for baseline scenario) and the maximum speed in the slow-down zone. The simulated slow-down and transition zones in each Local Study Area are shown in Figure 10.

All vessel traffic included in the unmitigated future scenario (baseline vessel classes plus additional Trans Mountain tankers and tugs) is also included in this scenario. Only specific vessel classes would have to adhere to the slow-down limit: Container, Cruise ship, Merchant, Tanker, Tug, and Vehicle carrier. One ferry route (connecting Anacortes, WA, and Sydney, BC, via Haro Strait) was also included as a mitigated vessel. These vessels participated in the slow-down trial organized by the Port of Vancouver, which ran from 7 August to 6 October 2017 (Port of Vancouver 2018), and they are therefore expected to adhere to a slow-down limit.

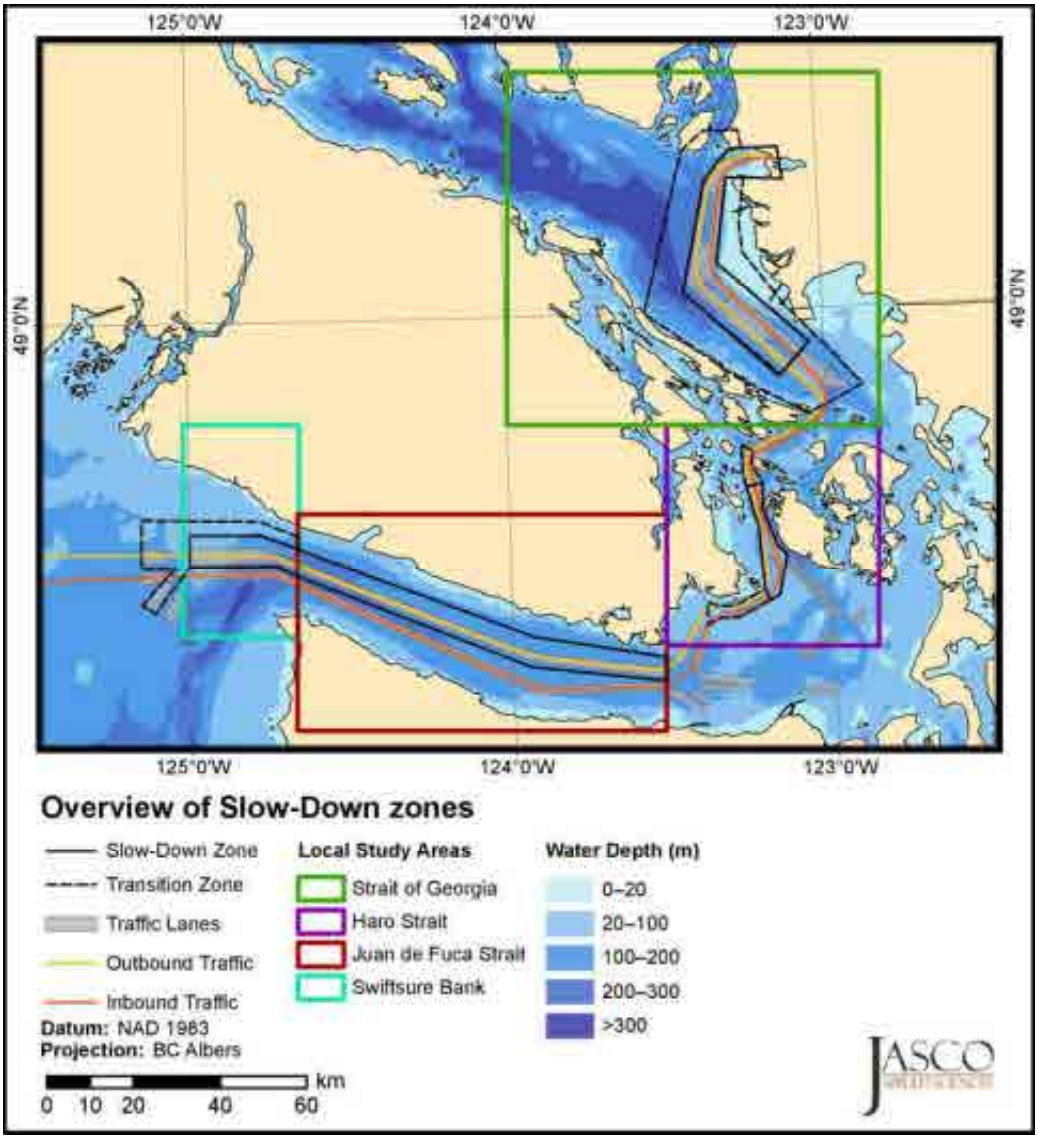

Figure 10. The modelled slow-down zones (solid black line) and speed transition zones (dash black lines).The transition region surrounds the slow-down zone but does not include it.

2.2.3.2. Implementing a No-Go Period

The no-go mitigation scenario is based on restricting commercial vessel traffic in Haro Strait from midnight to 04:00. The purpose of this mitigation approach is to create a quieter period that marine mammals can use for important activities such as foraging, communicating, and resting. The restricted vessel classes in the no-go periods are Container, Cruise ship, Merchant, Tanker, Tug, and Vehicle carrier. It is assumed that all vessels in these classes would delay their transit through Haro Strait to sail during unrestricted hours, as opposed to cancelling their transit. For this scenario, two time frames were modelled and two monthly average noise maps were produced:

- **Midnight to 04:00**: Only vessels in the unrestricted classes are present. Traffic density for these classes is proportional to that recorded in the AIS database during the restricted hours.
- **04:00 to midnight**: All vessel classes are present. Traffic density for the restricted classes is scaled up by the percentage of transits that were postponed. Traffic density for the unrestricted classes is proportional to that recorded in the AIS database during the unrestricted hours.

Percentages of vessels transiting during the restricted and unrestricted periods are listed in Table 4 for the baseline scenario (i.e., current conditions) and the no-go scenario. The no-go period only effects vessels transiting though Haro Strait; this scenario is only modelled in the Haro Strait Local Study Area.

Table 4. Percentage of traffic density applied to the restricted (midnight to 04:00) and unrestricted (04:00 to midnight) periods with and without no-go mitigation.

Vessel class	Baseline (Unmitigated current conditions)		Implementing a No-Go Period (Mitigated future conditions)	
	Restricted period (%)	Unrestricted period (%)	Restricted period (%)	Unrestricted period (%)
Container	20	80	0	100
Cruise ship	38	62	0	100
Ferry (Clipper)	0	100	0	100
Ferry (Ro-ro Cargo)	24	76	24	76
Ferry (Ro-ro Passenger)	0	100	0	100
Fishing	17	83	17	83
Government	11	89	11	89
Merchant	16	84	0	100
Other	8	92	8	92
Passenger (<100 m)	0	100	0	100
Recreational	0	100	0	100
Tanker	15	85	0	100
Tug	22	78	0	100
Vehicle carrier	20	80	0	100

2.2.3.3. Replacing 10% of Noisiest Ships

This mitigation scenario removes 10% of the noisiest vessels in specific vessel classes and replaces them with quieter vessels. The affected vessel classes are: Container, Cruise ship, Merchant, Tanker, Tug, and Vehicle carrier. For each affected vessel class, the mean source level spectrum (i.e., the mean noise emission levels as a function of frequency), based on JASCO and Port of Vancouver's proprietary database of vessel noise measurements, are computed by replacing the 10% of the measurements with the highest broadband noise emission level, with the 10% of the measurements with the lowest noise emission level. Noise levels are then modelled using the same traffic density and speed values as for the unmitigated future levels, but with the lower mean noise emission levels for the affected vessel classes.

For this mitigation approach, two approaches for selecting the 10% noisiest (and quietest) ships are used. These involve calculating unweighted and SKRW audiogram-weighted broadband noise emission levels (radiated noise levels) and then ranking ships within each class according to these metrics. Interestingly, the loudest vessels, as ranked by their unweighted levels, tend to be ranked as much quieter according to their SRKW audiogram-weighted levels. In other words, loudest vessels at low frequencies are quieter at high frequencies and vice versa. This difference can be seen in Figure 11, which compares derived average noise emission levels, as a function of frequency, for the 10% noisiest merchant vessels based on unweighted and SRKW audiogram-weighted noise emission level and for all measured merchant vessels. Appendix D provides more details on this subject.

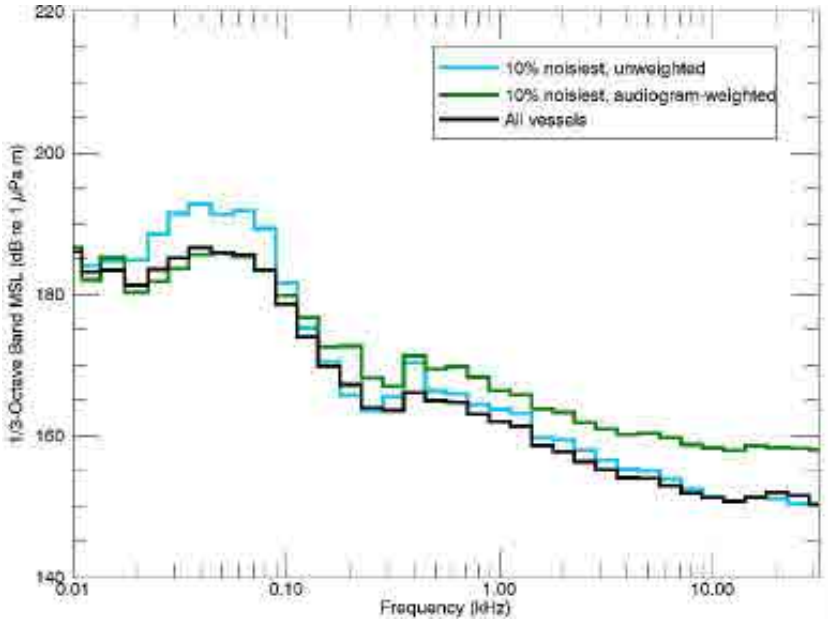

Figure 11. *Merchant vessels*: Average source level spectra for 10% (50 vessels) with the highest unweighted (blue) and SRKW audiogram-weighted (green) noise emission levels, compared to the average source level spectrum of all measured vessels in this class (black; 502 vessels).

2.2.3.4. Reducing Noise Emissions of Classes of Concern

This mitigation scenario reduces noise emission levels for commercial classes of concern by 3 and 6 dB. The affected vessel classes are: Container, Cruise ship, Merchant, Tanker, Tug, and Vehicle carrier. For each of these classes, mean source level spectrum (noise emission levels as a function of frequency), based on JASCO and Port of Vancouver's proprietary database of vessel noise measurements, are reduced by 3 and 6 dB across all modelled frequencies. Noise levels are modelled using the same traffic density and speed values as for the unmitigated future levels, but with the lower mean noise emission levels for affected vessel classes.

2.2.3.5. Shifting Vessel Traffic

This mitigation scenario first investigates the effect of rerouting the shipping lanes in southern Haro Strait, away from key SRKW habitat along the southwest coast of San Juan Island. The shoals northeast of Discovery Island, as shown in dashed area of Figure 12, constrain the possible lane adjustments in that area. The northbound (inbound) lane must be moved from the east side of the shoal to its west side, where the existing southbound (outbound) lane already passes. This move requires the traffic lanes to be narrowed so the south and north lanes can pass west of the shoals. This change may benefit commercial traffic because it shortens the total length of the inbound (northbound) shipping lane. The physical blocking of sound propagation by the shoal should also improve underwater noise conditions (reduced noise levels) for SRKW along the coast of San Juan Island.

To model rerouting of commercial traffic through the new shipping lanes, all transits that pass through Haro Strait are mitigated by either simulating the full track through the new lanes or by manually moving transit waypoints for a portion of the track. Tracks are simulated as if transiting between Juan de Fuca and Vancouver (inbound or outbound) and manually mitigated if taking a different route (e.g., to/from the USA or north through Vancouver Islands).

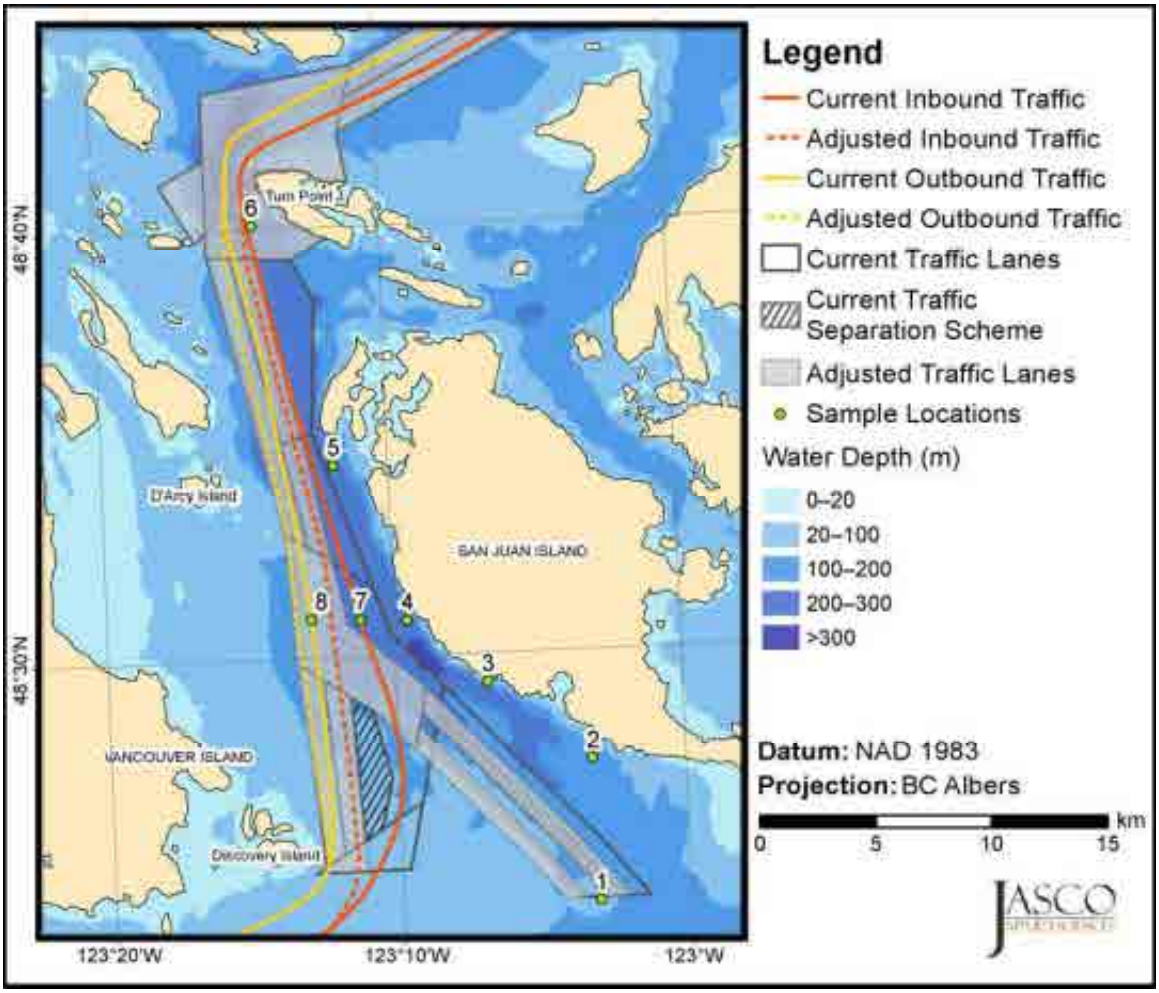

Figure 12. *Haro Strait*: Current and proposed (modelled) shipping routes.

This mitigation scenario also investigates the effect of rerouting the traffic within the outbound shipping lane from Juan de Fuca Strait to Swiftsure Bank, away from key SRKW habitat along the southern coast of Vancouver Island. Here, all mitigated traffic, except tugs, is simulated as transiting along the sound boundary of the current outbound shipping lane. Since tugs are usually slower than other commercial classes, they usually transit along the northern section or outside of the outbound traffic lane. Thus, for this mitigation scenario tugs are simulated as transiting at the centre of the current traffic lane, north of the rest of the commercial traffic. Figure 13 compares the current and simulated shipping routes in Juan de Fuca Strait and Swiftsure Bank.

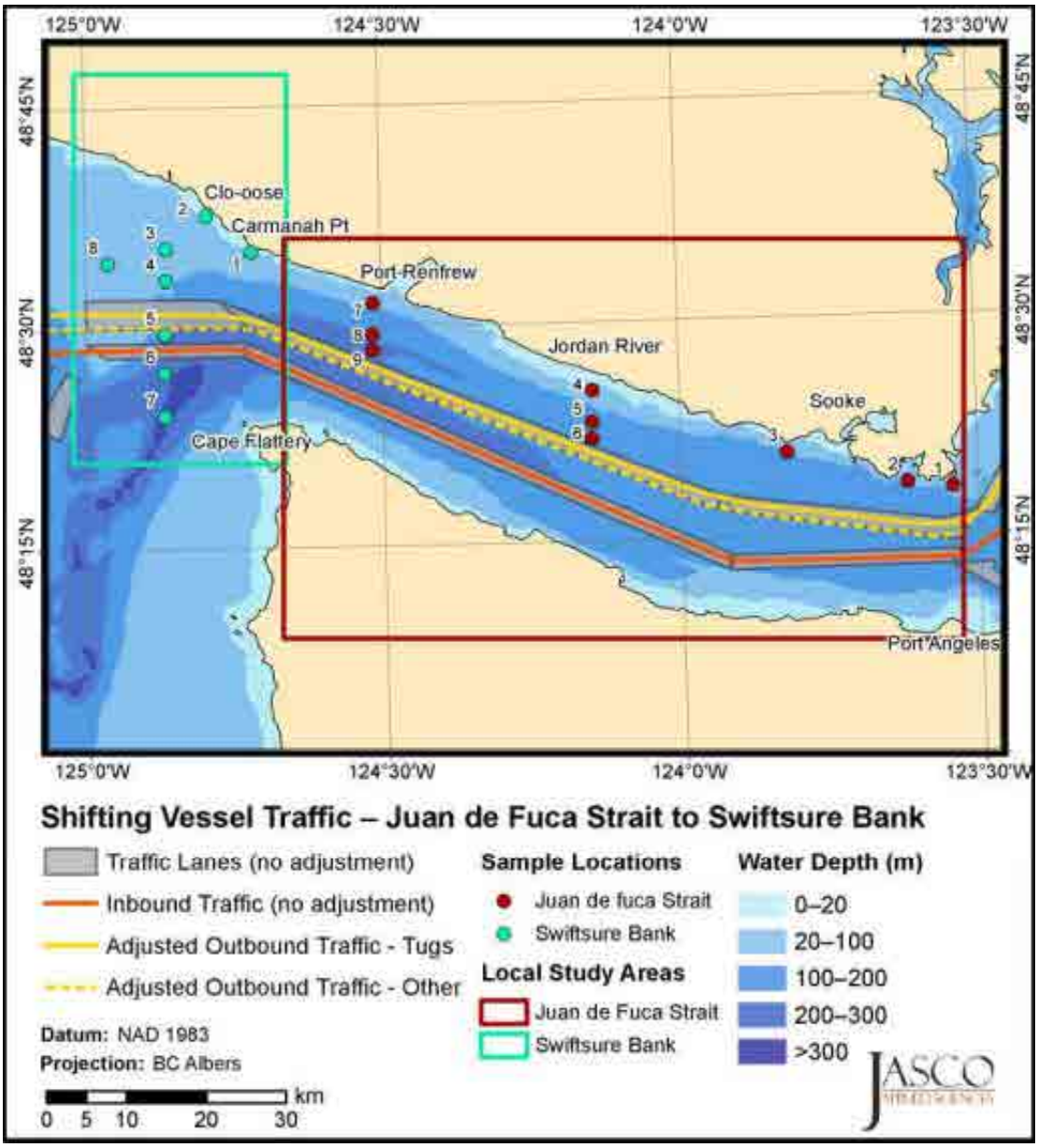

Figure 13. *Juan de Fuca Strait to Swiftsure Bank*: Current and proposed (modelled) shipping routes.

2.2.3.6. Implementing Vessel Convoys

This mitigation scenario changes the schedule of commercial vessels for transiting in groups (convoys) every few hours, instead of their present (somewhat random) schedules. This could create quiet periods between convoys when animals might be exposed to less vessel noise. This analysis was based on actual traffic on July 29, 2015, nominally a representative day for July, based on the number of vessels and class distributions in all Local Study Areas. Vessel classes included in convoys are Container, Cruise ship, Merchant, Vehicle carrier, Tanker, and Tugs.

Two alternatives are modelled: first, a convoy corridor in Haro Strait, where inbound and outbound traffic is regulated, and second, the convoying of outbound traffic from VH buoy (south of Victoria, BC) to Swiftsure Bank. In the first alternative, the convoy corridor lies between the north and south boundary of Haro Strait, as seen in Figure 14. Only one convoy at a time is present in the corridor (i.e., inbound and outbound convoys alternate their entrance in the corridor at a regular time interval). Intervals of 2 and 4 hours are modelled. The convoy speed is limited to 10 knots, in accordance with the speed of outbound Trans Mountain escorted tankers and to accommodate slower vessels. Vessels within a convoy transit in a single file, with a separation of 1000 m (from stern of the forward ship to bow of the following ship). The vessels included in each convoy were selected based on the time when they originally entered the convoy corridor; Tables 5 and 6 list the composition of each convoy for the first alternative, with 2 and 4 hour intervals.

Table 5. *Convoy Alternative 1 – 2 hour interval*: Convoy composition and timing. TM: Trans Mountain.

Convoy #	Direction	Speed (kn)	Vessel class	Time at the convoy corridor boundary	
				Original	Mitigated
1	Inbound	10	TM Tanker	n/a	29 Jul at 00:00 h
2	Outbound	10	Container	29 Jul at 00:23 h	29 Jul at 02:00 h
			Merchant	28 Jul at 23:02 h	29 Jul at 02:03 h
			Merchant	28 Jul at 23:06 h	29 Jul at 02:06 h
			Tanker	29 Jul at 02:37 h	29 Jul at 02:09 h
3	Inbound	10	TM Tug	n/a	29 Jul at 04:00 h
4	Outbound	10	Merchant	29 Jul at 04:36 h	29 Jul at 06:00 h
			Merchant	29 Jul at 04:57 h	29 Jul at 06:03 h
5	Inbound	10	Merchant	29 Jul at 07:52 h	29 Jul at 08:00 h
6	Outbound	10	TM Tanker	n/a	29 Jul at 10:00 h
			TM Tug	n/a	29 Jul at 10:00 h
7	Inbound	10	Container	29 Jul at 11:17 h	29 Jul at 12:00 h
8	Outbound	10	Container	29 Jul at 16:19 h	29 Jul at 14:00 h
9	Inbound	10	Merchant	29 Jul at 14:21 h	29 Jul at 16:00 h
			Merchant	29 Jul at 14:47 h	29 Jul at 16:03 h
			Merchant	29 Jul at 14:56 h	29 Jul at 16:06 h
10	Outbound	10	Container	29 Jul at 17:48 h	29 Jul at 18:00 h
			Tug	29 Jul at 17:05 h	29 Jul at 18:03 h
11	Inbound	10	Vehicle carrier	30 Jul at 00:30	29 Jul at 20:00 h
			Merchant	29 Jul at 23:10 h	29 Jul at 20:03 h
12	Outbound	10	Container	29 Jul at 21:37 h	29 Jul at 22:00 h

Table 6. *Convoy Alternative 1 – 4 hour interval*: Convoy composition and timing. TM: Trans Mountain.

Convoy #	Direction	Speed (kn)	Vessel class	Time at the convoy corridor boundary	
				Original	Mitigated
1	Inbound	10	TM Tanker	n/a	29 Jul at 00:00 h
2	Outbound	10	Container	29 Jul at 00:23 h	29 Jul at 04:00 h
			Merchant	28 Jul at 23:02 h	29 Jul at 04:03 h
			Merchant	28 Jul at 23:06 h	29 Jul at 04:06 h
			Tanker	29 Jul at 02:37 h	29 Jul at 04:09 h
3	Inbound	10	Merchant	29 Jul at 07:52 h	29 Jul at 08:00 h
			TM Tug	n/a	29 Jul at 08:03 h
4	Outbound	10	Merchant	29 Jul at 04:36 h	29 Jul at 12:00 h
			Merchant	29 Jul at 04:57 h	29 Jul at 12:03 h
			TM Tanker	n/a	29 Jul at 12:06 h
			TM Tug	n/a	29 Jul at 12:06 h
5	Inbound	10	Container	29 Jul at 11:17 h	29 Jul at 16:00 h
			Vehicle carrier	30 Jul at 00:30	29 Jul at 16:03 h
			Merchant	29 Jul at 14:21 h	29 Jul at 16:06 h
			Merchant	29 Jul at 14:47 h	29 Jul at 16:09 h
			Merchant	29 Jul at 14:56 h	29 Jul at 16:12 h
			Merchant	29 Jul at 23:10 h	29 Jul at 16:15 h
6	Outbound	10	Container	29 Jul at 16:19 h	29 Jul at 20:00 h
			Container	29 Jul at 17:48 h	29 Jul at 20:03 h
			Container	29 Jul at 21:37 h	29 Jul at 20:06 h
			Tug	29 Jul at 17:05 h	29 Jul at 20:09 h

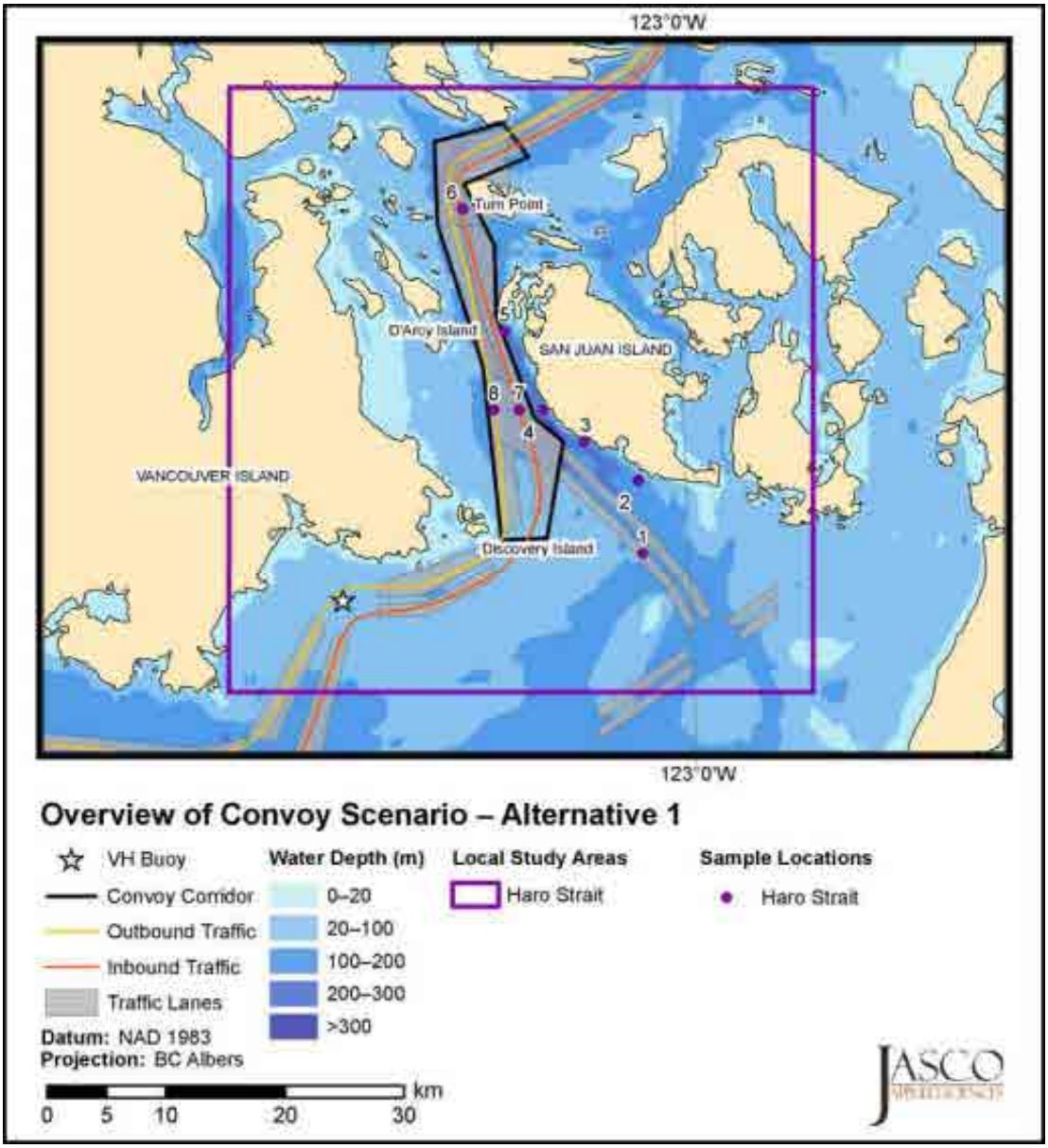

Figure 14. *Convoy Alternative 1* (*Convoying in Haro Strait)*: Boundaries of the convoy corridor.

In the second alternative, the convoy corridor, as seen in Figure 15, lies in Juan de Fuca Strait, between the VH buoy south of Victoria, and the Pacific Ocean west of Swiftsure Bank. Only outbound commercial traffic passing by the VH buoy, often slowing down to disembark a pilot, is required to be part of the convoy. An interval of 4 hours between convoys is modelled. The convoy speed depends on the classes in the convoy: convoys with Container, Cruise ship, and Vehicle carrier are limited to 16.5 knots, convoys with Merchant, Tanker, and Tug are limited to 12 knots. The speeds are in accordance with the baseline average speed of the convoyed classes in Juan de Fuca Strait, and to accommodate slower vessels. Vessels within a convoy transit in a single file; their separation is based on the interval (10 min) between their arrival time at the VH buoy. The vessels included in each convoy were selected based on the time when they originally passed VH buoy; Table 7 lists the composition of each convoy for this second alternative.

Table 7. *Convoy Alternative 2*: Convoy composition and timing. TM: Trans Mountain.

Convoy #	Direction	Speed (kn)	Vessel class	Time at the convoy corridor boundary	
				Original	Mitigated
1	Outbound	16.5	Container	28 Jul at 23:04 h	29 Jul at 00:00 h
		16.5	Vehicle carrier	28 Jul at 20:29 h†	29 Jul at 00:10 h†
		12	Merchant	29 Jul at 00:25 h‡	29 Jul at 00:20 h‡
		12	Merchant	29 Jul at 01:25 h†	29 Jul at 00:20 h†
2	Outbound	16.5	Container	29 Jul at 02:02 h†	29 Jul at 04:00 h†
		12	Merchant	29 Jul at 03:17 h	29 Jul at 04:10 h
		12	Tanker	29 Jul at 04:46 h	29 Jul at 04:20 h
		12	Tug	n/a	29 Jul at 04:20 h
3	Outbound	12	Merchant	29 Jul at 06:43 h	29 Jul at 08:00 h
		12	Merchant	29 Jul at 07:15 h	29 Jul at 08:10 h
4	Outbound	12	Merchant	29 Jul at 11:43 h	29 Jul at 12:00 h
		12	TM Tanker	n/a	29 Jul at 12:10 h
		12	TM Tug	n/a	29 Jul at 12:10 h
5	Outbound	16.5	Cruise ship	29 Jul at 14:38 h*	29 Jul at 16:00 h*
6	Outbound	12	Tug	29 Jul at 19:31 h	29 Jul at 20:00 h

† Leaving from Roberts Bank
‡ Leaving from Nanaimo
* Leaving from Victoria

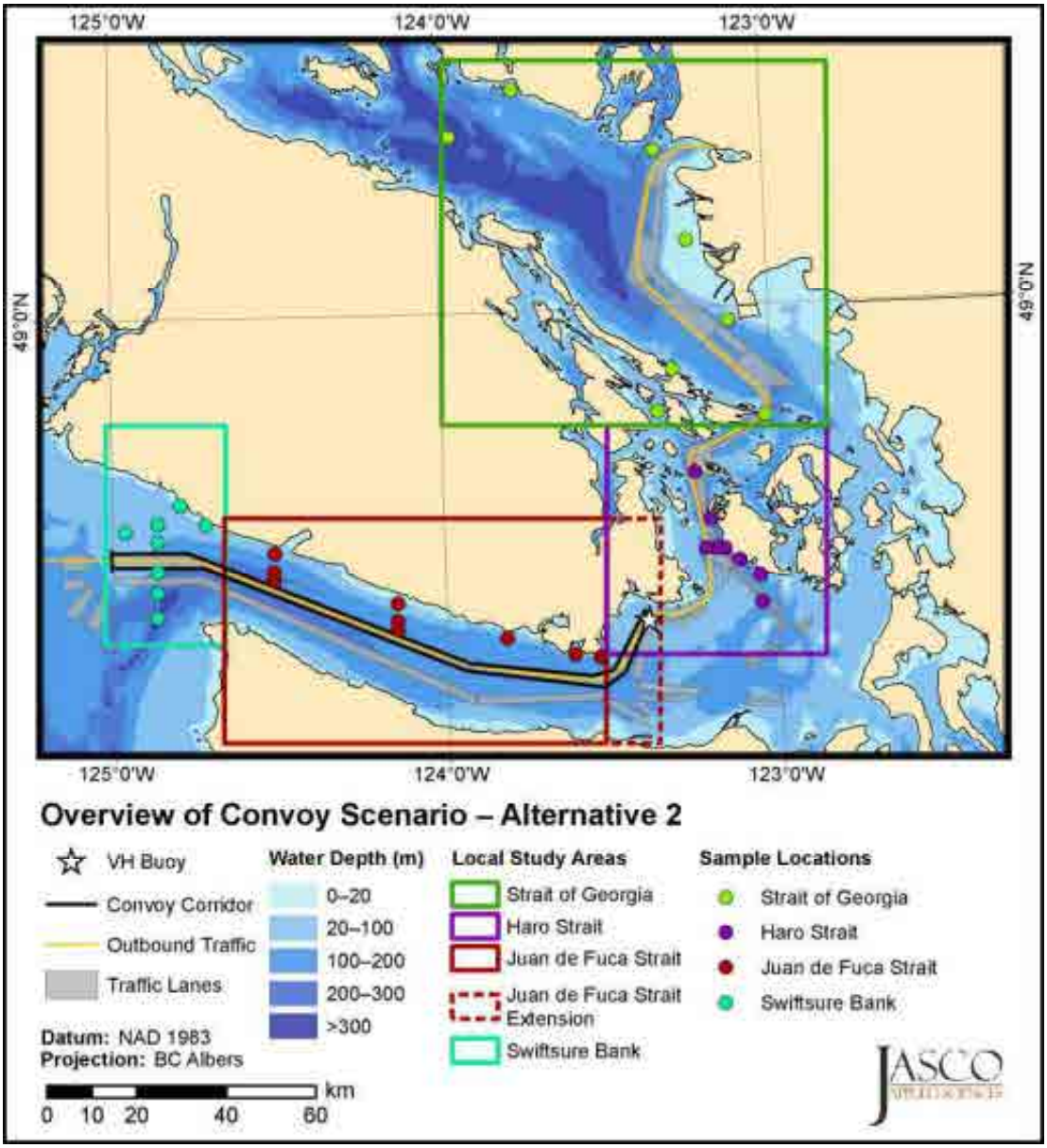

Figure 15. *Convoy Alternative 2 (Convoying in Juan de Fuca Strait)*: Boundaries of the convoy corridor.

2.3. Cumulative Noise Model Input

To produce time-averaged or time-dependent acoustic field maps, the cumulative noise model requires the main input parameters shown in Figure 1. This section summarizes these parameters for the current study; more details are provided in Appendices A–C.

2.3.1. Environmental Parameters and Sound Propagation

Sound propagation through the ocean depends on the environmental parameters of a region, such as temperature, salinity, and water depth, as well as geological properties of the seabed, such as sediment type (e.g., sand, silt, and bedrock) and layer thickness. Once a region's environmental parameters are characterized, models are used to calculate how sound travels through the water away from a sound source. Details about the environmental parameters used in this study are provided in Appendix A.4.

Acoustic propagation loss is the decrease in intensity of a sound as it travels away from its source through an environment. JASCO's Marine Operations Noise Model (MONM) is used to calculate the regional propagation loss. MONM uses the environmental parameters mentioned in Section 2.3.1 to compute the decrease in sound levels with distance for each frequency band, out to a maximum of 75 km from the sound source. Past measurements from a propagation loss study (JASCO 2015) are used to validate MONM predictions within each study area.

In this study, the Regional Study Area is divided into 20 zones, based on four unique geoacoustic regions and five water depth ranges. Propagation loss is modelled for each zone using the mean sound speed profile for the appropriate month and six source depths (1 to 6 m, every one 1 m), representing the nominal acoustic emission centres of modelled vessel classes. More details are provided in Appendices A.4 and A.5.1.

2.3.2. Vessel Traffic Data

To assess the effect of each mitigation approach, noise levels are first calculated for historical shipping traffic density to get a baseline understanding of the shipping noise in the studied regions. These baseline noise levels are calculated from the AIS dataset for January and July 2015, which represent the extremes for sound propagation based on seasonal environmental changes. The regional noise levels from all other months are assumed to be contained within the levels for July (lowest) and January (highest).

The vessels in the AIS dataset are divided into the same class set as the noise emission levels, described in Section 2.3.3. The study area is divided in grid cells, within which per-class vessel densities and average speeds are calculated. Each vessel contributes to the vessel density in the map grid cells through which they pass. The time each vessel spends within a map grid cell is accumulated, and its speed recorded to calculate the class' average over that cell. Density and speed grids are produced this way for each vessel class.

By the end of the year 2020, the Trans Mountain shipping requirements are expected to increase from the current levels (5 outbound tankers per month) to projected levels (34 outbound tankers per month). The future unmitigated and mitigated scenarios represent levels occurring after this projected increase in Trans Mountain traffic. The resulting levels are only modelled for July because this month corresponds to the time of year when SRKW are most present in the region.

For the future scenarios, traffic data is simulated for the extra tankers and tugs associated with the increased shipping requirements for Trans Mountain. Vessel movement is randomized using a normal (Gaussian) distribution of vessel position, centred along the current traffic routes. The speed of the tankers and tug escorts along the outbound route is limited to 5.144 m/s (10 knots) between East Point (northern limit of Haro Strait; as seen in Figure 9) and the Brotchie Pilot Station (at the VH buoy, south of Victoria; as seen in Figure 9). Their speed is limited to the

expected maximum speed of tugs at 7.2 m/s (14 knots) north of East Point and west of Brotchie Pilot Station. The simulated speed of each vessel along the inbound route is equal to that of the current average speed for its class, based on the 2015 AIS data.

For the slow-down mitigation scenario, vessel speeds are reduced in the slow-down and transition zones. For the no-go mitigation scenario, the vessel density is modified to simulate reduced traffic for certain vessel classes during the "no-go" times and higher traffic concentration during the "go" times. For the mitigation scenario of replacing 10% of the noisiest ships, the vessel densities and speeds are unchanged (from the future unmitigated scenario), but the vessel noise emission levels are modified according to a specialized analysis of vessel emission level distribution. For the adjusted traffic lanes mitigation scenario, vessel speeds are unchanged, but adjusted densities are calculated using simulated vessel tracks along the new routes.

To produce time-dependent noise levels, time-stamped vessel tracks over a relatively short period (24 to 33 hours) are used, as opposed to monthly density and speed grids. One day is selected (here, July 29) to extract AIS data representative of the average traffic density in that month. Unmodified tracks make up the baseline scenario. For future mitigated scenarios (i.e., convoy and slow-down scenarios), new tracks are simulated for the additional tankers and tugs associated with the Trans Mountain increased shipping, and tracks of individual vessels are modified according to the modelled mitigation approach.

Table 8 presents the number of transits for July 29 compared to the median across all days in July, through Haro Strait. The classes affected for each mitigated scenario are: Container, Cruise ship, Merchant, Tanker, Tug, and Vehicle carrier. Not all individual vessel tracks within a mitigated class are modified; only the tracks crossing a specified zone are modified.

Table 8. The July daily median compared to the numer of vessel transits for July 29.

Vessel class	Strait of Georgia		Haro Strait		Juan de Fuca Strait		Swiftsure Bank	
	July daily median	July 29	July daily median	July 29	July daily median	July 29	July daily median	July 29
Container	6	4	6	5	6	7	5	7
Cruise ship	4	4	3	2	3	2	3	2
Ferry (Ro-ro Passenger)	248	248	151	153	0	0	0	0
Ferry (Ro-ro Cargo)	8	11	5	6	0	0	0	0
Ferry (Clipper)	0	0	9	7	0	0	0	0
Fishing	12	9	5	4	9	1	5	2
Government	29	43	17	17	2	3	1	0
Merchant	21	10	9	10	8	12	9	13
Other	44	49	27	23	1	1	1	1
Passenger (<100 m)	34	37	20	26	0	0	0	0
Recreational	126	128	177	177	11	15	5	5
Tanker	1	0	2	3	3	5	2	4
Tug	344	338	19	16	5	5	3	5
Vehicle carrier	1	0	1	1	3	2	2	1

2.3.3. Vessel Noise Emission Levels

Propeller cavitation and hull vibration caused by internal machinery are the main sources of underwater noise from vessels. Different types of vessels have characteristic source level spectra (i.e., variations of sound emission levels with sound frequency) because of their specific design and operating conditions. For the purpose of modelling noise from hundreds of vessels over a large area and long durations, omnidirectional source level spectrum representative of the mean levels for each vessel class are used (NRC 2003).

For this study, noise emission level (i.e., source level) derived from measurements from the ECHO program ULS, described in Appendix A.3.3, are assigned to ten different classes, according to vessel class information embedded in the AIS logs. Source levels for four additional vessel classes not covered by the ULS data (Passenger (<100 m), Clipper Ferry, Recreational, and Other) were obtained from other sources (MacGillivray et al. 2014, Veirs et al. 2016).

Figure 16 shows the frequency-dependent source levels, compiled in 1/3-octave bands from 10 Hz to 63.1 kHz, that are used to represent noise emissions of corresponding vessels in the cumulative noise model.

Vessel noise emissions generally increase with speed through water, due to speed-related increases in machinery vibration and propeller cavitation. Vessel source levels in the cumulative noise model are scaled according to speed using a well-established power-law model (Ross 1976). For each vessel class, a unique speed scaling parameter is calculated from ULS data, based on a multivariate analysis accounting for the effect of speed, vessel length, and measurement closest point of approach, as described in Appendix C. A default scaling parameter of 6 is used for categories with insufficient or missing data.

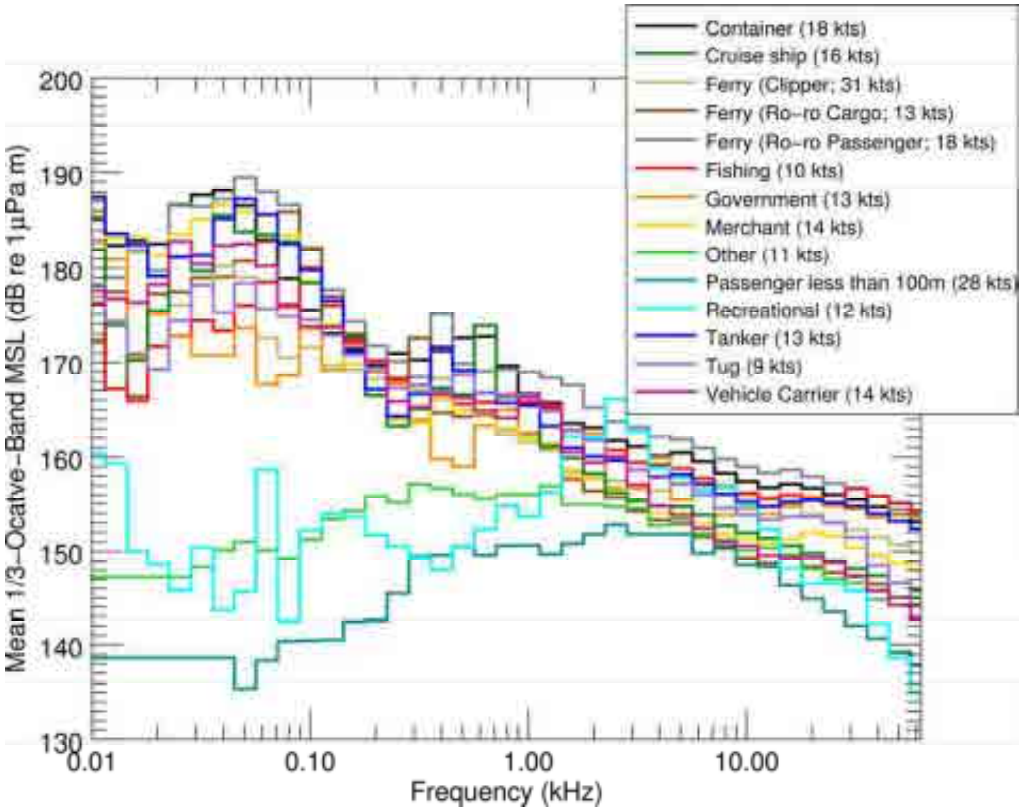

Figure 16. Frequency-dependent source levels by vessel class in 1/3-octave bands. The reference speed (average transit speed, in knots) for each class is indicated in the legend. ULS source levels are extrapolated above 31 kHz based on the terminal slope of the 1/3-octave-band level curves.

2.4. Cumulative Noise Model

The Cumulative Vessel Noise Model can be run as a time-averaged density model or a time-dependent track model. The time-averaged version of the model is used for baseline, future unmitigated, and all future mitigated scenarios except convoying. It accepts monthly averaged density and speed data over the model grid, as described in Section 2.3.2. Results are presented as equivalent continuous noise levels[2] (L_{eq}) to the cumulative (total) noise level from all vessel classes, averaged over the month. The time-dependent version of the model is used for convoying and slow-down scenarios. It accepts time-dependent vessel track data, as described in Section 2.3.2. Because this type of modelling is more computationally expensive, these time-dependent results are calculated over a relatively short period (24 to 33 hours, in the present study). Results are presented as sound pressure levels (SPL) over the model grid for each minute of the day.

The Cumulative Noise Model combines the modelled regional propagation losses described in Appendix A.5.1 with the vessel source level data for each vessel class described in Section 2.3.3. The model is based on a grid representing a region divided into equally sized square cells. For each vessel class, the vessel density or track data and average speed is assigned to each cell; the associated noise level is propagated outwards into neighbouring cells, out to a range of 75 km.

2.4.1. Cumulative Spatial Noise Assessment

Results for the time-averaged scenarios are presented as maps of equivalent continuous noise level (L_{eq}). L_{eq} is calculated by dividing the cumulative sound exposure level (SEL), which is modelled, by the averaging time in seconds. The L_{eq} metric is useful for presenting geographic distributions of mean noise levels. In the present study, L_{eq} is calculated over 1 month. Thus, in this report, L_{eq} represents the mean noise level that marine animals are expected to be exposed to at any time in July.

2.4.2. Temporal Noise Assessment

Vessel convoy scenarios are evaluated using the acoustic model's time-dependent calculation mode. In this mode, the model tracks the noise field from every vessel individually, in 1-minute steps, as they move through a study area. It sums those fields across all vessels to compute a composite time-varying noise field (essentially a snapshot of the overall noise every minute). To investigate the noise characteristics of convoys, vessel movement scenarios are developed based on maintaining the same number of ships as non-convoy scenarios but adjusting their transit times so these ships sailed in groups through the convoy corridor. Vessel speeds in the corridor are also adjusted to a standard speed to maintain the integrity of the convoys. To investigate the noise characteristics of slow-down scenarios, vessel movements are also based on maintaining the same number of ships as non-mitigated scenarios but adjusting their transit time and speed, so these ships adhere to a speed limit within a prescribed zone.

Results from the time-dependent analysis are presented as temporal variation plots and cumulative distribution functions (CFDs) at each sample location. These result formats provide information about the fraction of time animals are likely to be exposed to sound from commercial and/or non-commercial traffic. This information can be used to estimate the duration of quiet (at ambient level) and noisy (above ambient) periods, and the effectiveness of a mitigation approach in increasing the amount of quiet time.

[2] Refer to Appendix A.1 for a description of acoustic metrics.

2.5. Audiogram Weighting

When assessing the effectiveness of each mitigation approach, the frequencies contained in ship noise must be considered in association with the ability of killer whales and other marine animals to detect those sounds. It is less likely that man-made noise will affect a marine animal if the animal cannot perceive the sound well, with an exception for sound pressures high enough to cause physical injury. For noise levels that are below physical injury thresholds, frequency weighting based on audiograms can be applied to weight the importance of noise levels at particular frequencies in a manner reflective of an animal's sensitivity to those frequencies (Nedwell and Turnpenny 1998, Nedwell et al. 2007).

Audiogram-weighted levels represent sound levels above an animal's hearing threshold (dB re HT), and they cannot be directly compared with unweighted levels, nor compared to any impact threshold levels mentioned in the current literature. It is not fully understood what dB re HT levels signify the onset of behavioural disturbance in killer whales, but Williams et al. (2014) suggested that responses can start between 56 and 64 dB re HT.

In this study, results are presented based on unweighted and SRKW audiogram-weighted noise levels; SRKW audiogram weighting, seen in Figure A-10, is applied to sound levels generated by the cumulative noise model. In this report, audiogram-weighted equivalent continuous noise level (L_{eq}) represents the mean noise level perceived by a SRKW at any time in July.

2.6. Other Noise Mitigation Options

Nine mitigation approaches are assessed in a qualitative sense, because of the variety of ways they can reduce noise. These approaches use emerging technologies to address key noise-generating aspects of vessels. These literature-based mitigation assessments focus on the primary causes of hydroacoustic noise radiating from commercial vessels, which are:

- **In-water propulsion mechanisms,** such as propellers and thrusters, which primarily create underwater noise through cavitation[3], as discussed in Appendix A.3.1, and
- **Shipboard machinery**, such as engines and generators, which create underwater noise through hull-borne vibration, as discussed in Appendix A.3.2.

If the noise from one component is more than 10 dB above other noise components in the same frequency bands, then the other components are largely irrelevant (McCauley et al. 1996). When cavitation occurs, sound from the propeller rotation is generally the dominant underwater noise source (Ross 1976), and shipboard machinery becomes irrelevant. Leaper and Renilson (2012) and Renilson et al. (2012) recently demonstrated that there is considerable difference in the noise propagated by the noisiest and the quietest conventional commercial vessels, and that excessive cavitation is the dominant sound source of the noisiest ones.

Secondary causes of underwater noise include acoustic vibrations within compartments below the waterline and hydrodynamic noise created by flow interaction with hull features. However, the greatest gains in controlling underwater noise emissions from vessels are generally achieved by treating the primary sources.

2.6.1. Retrofitting Ships

This component of the literature review focuses on identifying possible technologies that can be fitted to the current commercial fleet to reduce underwater noise emissions. One focus of the literature-based assessment is the possible reduction of broadband noise levels associated with controlling cavitation with new propulsion systems, and with controlling internal machinery noise. This qualitative assessment is presented in Section 3.9.

[3] Cavitation refers to streams of vapour bubbles that form on the surface of marine propellers when a vessel is moving quickly.

2.6.2. Replacing Trans Mountain Tugs with Specialized Tugs

This component of the literature review focuses on using electric or hybrid-electric/diesel tugs instead of diesel tugs to reduce broadband sound levels associated with the Trans Mountain tug fleet. These tugs would escort tankers from Westridge Terminal to Swiftsure Bank, for an expected total of 68 transits per month (34 outbound, 34 inbound). Diesel-electric propulsion systems are found in vessels that have strict requirements for low onboard noise and vibration, as well as low underwater noise emissions (e.g., cruise ships and research vessels, Baudin and Mumm 2015). This qualitative assessment is presented in Section 3.10.

2.6.3. Changing Ship Designs

This component of the literature review focuses on possible reductions in broadband sound levels associated with changing propeller and hull designs of commercial vessels. Newly built vessels could incorporate these designs in the future. This qualitative assessment is presented in Section 3.11.

2.6.4. Changing Maintenance of Ships

This component of the literature review estimates the possible reduction in broadband sound levels associated with changing current maintenance practices, such as those relating to cleaning hulls and maintaining propellers. This qualitative assessment is presented in Section 3.12.

2.6.5. Changing Operator Behaviour

This component of the literature review investigates the effect of operators piloting vessels with a focus on decreasing noise generation. For example, reducing acceleration rates could reduce vessel noise in sensitive areas. This qualitative assessment is presented in Section 3.13.

2.6.6. Changing Shipping Practices

This component of the literature review investigates the effect of changing shipping practices, including station keeping versus anchoring, and reducing the number of handling tugs. This qualitative assessment is presented in Section 3.14.

2.6.7. Applying Real-time Mitigation in Hot Spots

This component of the literature review investigates the effect of applying real-time mitigation in areas when key species (e.g., whales) have been detected. Ships avoidance practices and voluntary speed limits are already in use to reduce the number of ship strikes. These methods may also be effective in mitigating noise levels. This qualitative assessment is presented in Section 3.15.

2.6.8. Using Larger Vessels

This component of the literature review investigates the effect of using larger vessels to reduce number of vessel transits required. This qualitative assessment is presented in Section 3.16.

3. RESULTS

In this section, all results are present with and without SRKW audiogram-weighting applied. The two types of results are easily identified by the different colour scale used in mapping equivalent continuous noise levels (L_{eq}).

Baseline levels include noise from all vessels in the July 2015 AIS data. Maps of L_{eq} for the baseline scenarios are presented in Figures 17–20 in Section 3.1. Future unmitigated and mitigated noise levels include noise from vessels associated with the Trans Mountain Project expansion as described in Section 2.2.2, in addition to the noise from all vessels in the 2015 AIS data.

For each monthly-average scenario, maps of L_{eq} and changes in L_{eq} relative to the baseline are presented. These one-month average levels were sampled at the key locations in each Local Study Area shown in Figures 5–8. These results are also summarized in Tables 71–72 in Section 4.1, using a spatial analysis of the differences between baseline and future mitigated levels.

The time-dependent results for the slow-down and convoy mitigation scenarios are presented as temporal variations over a 24- or 33-hour period at the same key locations in each Local Study Area. These results are first presented as plots of unweighted and audiogram-weighted noise levels as a function of time. They compare the levels from all traffic (and ambient noise) to the levels from only the mitigated commercial traffic. In each plot, the top graph shows results for the baseline (2015 unmitigated traffic) and bottom graph(s) show results for the future mitigated scenario.

To interpret the time-varying model outputs, a simple temporal analysis was applied to the sampled received levels. Percentiles and mean values of the temporal variation in received noise levels (SPL) are presented at each sample location, for the baseline and future mitigated scenarios. These results are presented in two formats: 1) tables listing absolute values and their difference relative to baseline levels, and 2) bar plots to help visualize the difference between the baseline to the mitigated levels.

The time-dependent received noise levels were also used to generate cumulative distribution functions (CDFs) at each sample location. These functions show the percent of time that modelled received levels were below a specified value. As an example, the CDF curves can be interpreted as follows: for an arbitrary sample location, the SPL was 100 dB at the 40th percentile level for the baseline scenario and at the 50th percentile level for the future mitigated scenario. This means that baseline noise levels at this location were at or below 100 dB 40% of the time, and the mitigated noise levels were at or below 100 dB 50% of the time. Thus, at this location, noise levels lower than 100 dB would occur more often (50% as opposed to 40% of the time) if this mitigation approach is applied.

3.1. Baseline Noise Levels

Figures 17–20 show maps of unweighted and audiogram-weighted equivalent noise levels (L_{eq}) for July 2015 for Strait of Georgia, Haro Strait, Juan de Fuca Strait, and Swiftsure Bank. The maps represent summer baseline levels over the fine-scale (200 × 200 m map grid cell resolution) Local Study Areas. Tables 9–12 present the unweighted and audiogram-weighted noise levels sampled at the key locations in the SRKW critical habitat in each region. The sample locations are listed in Table 1 and shown as green dots in each map below.

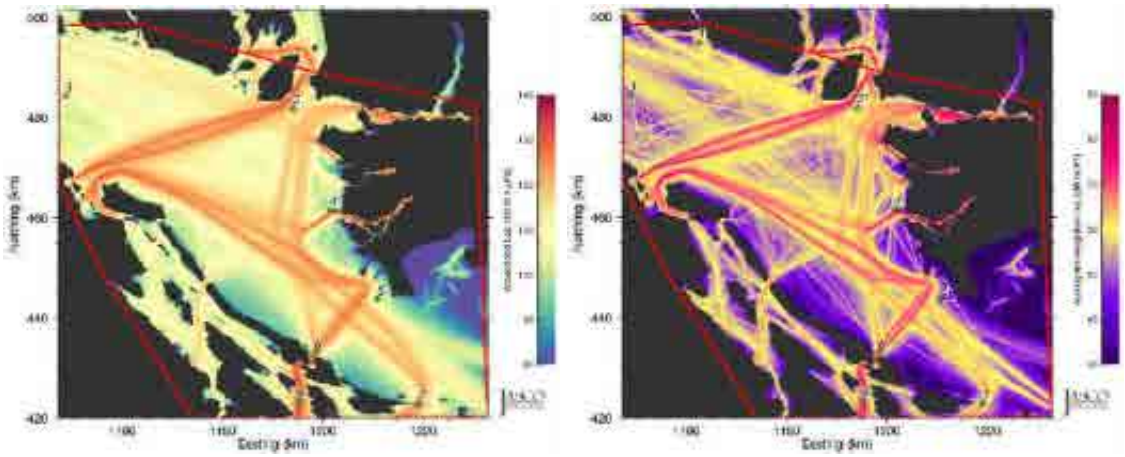

Figure 17. *Strait of Georgia – Baseline*: Unweighted (left) and audiogram-weighted (right) equivalent continuous noise levels (L_{eq}) over the Local Study Area. Grid resolution is 200 × 200 m. The green dots are the sample locations in the SRKW critical habitat. The red line shows the boundary of the area where statistical values (percentiles and mean) were derived.

Table 9. *Strait of Georgia – Baseline*: Unweighted (dB re 1 µPa) and audiogram-weighted received levels (dB re HT) at the sample locations in the SRKW critical habitat.

Sample location	Unweighted (dB re 1 µPa)	Audiogram-weighted (dB re HT)
1	113.0	59.5
2	118.2	63.5
3	106.4	53.9
4	113.0	64.7
5	107.8	53.8
6	129.8	74.9
7	125.3	66.0
8	130.9	72.9

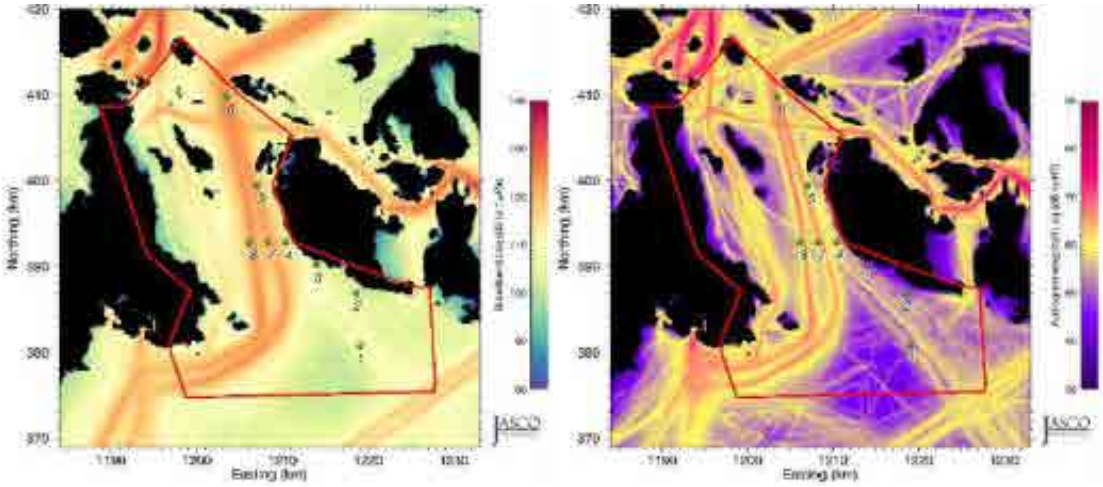

Figure 18. *Haro Strait – Baseline*: Unweighted (left) and audiogram-weighted (right) equivalent continuous noise levels (*Leq*) over the Local Study Area. Grid resolution is 200 × 200 m. The green dots are the sample locations in the SRKW critical habitat. The red line shows the boundary of the area where statistical values (percentiles and mean) were derived.

Table 10. *Haro Strait – Baseline*: Unweighted (dB re 1 µPa) and audiogram-weighted received levels (dB re HT) at the sample locations in the SRKW critical habitat.

Sample location	Unweighted (dB re 1 µPa)	Audiogram-weighted (dB re HT)
1	109.2	56.2
2	103.9	51.6
3	106.5	46.9
4	114.3	56.3
5	119.0	60.8
6	123.4	64.6
7	122.9	65.2
8	123.5	66.2

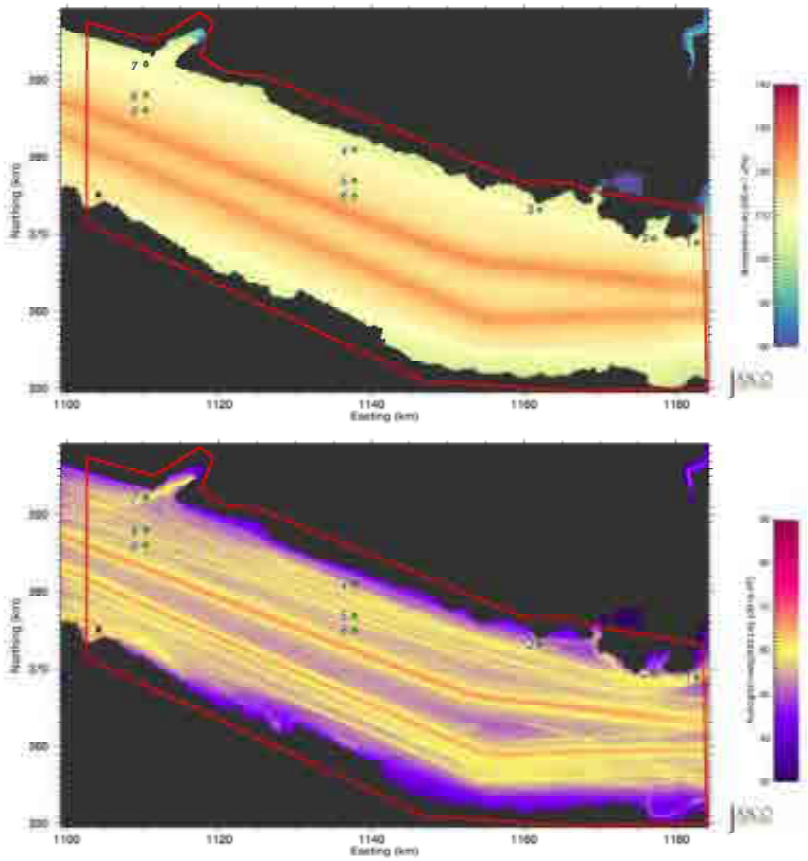

Figure 19. *Juan de Fuca Strait – Baseline*: Unweighted (top) and audiogram-weighted (bottom) equivalent continuous noise levels (L_{eq}) over the Local Study Area. Grid resolution is 200 × 200 m. The green dots are the sample locations in the SRKW critical habitat. The red line shows the boundary of the area where statistical values (percentiles and mean) were derived.

Table 11. *Juan de Fuca Strait – Baseline*: Unweighted (dB re 1 µPa) and audiogram-weighted received levels (dB re HT) at the sample locations in the SRKW critical habitat.

Sample location	Unweighted (dB re 1 µPa)	Audiogram-weighted (dB re HT)
1	111.4	59.1
2	111.6	56.9
3	110.2	55.4
4	109.9	56.6
5	113.8	55.6
6	117.5	56.3
7	109.6	55.0
8	114.0	55.9
9	117.5	55.9

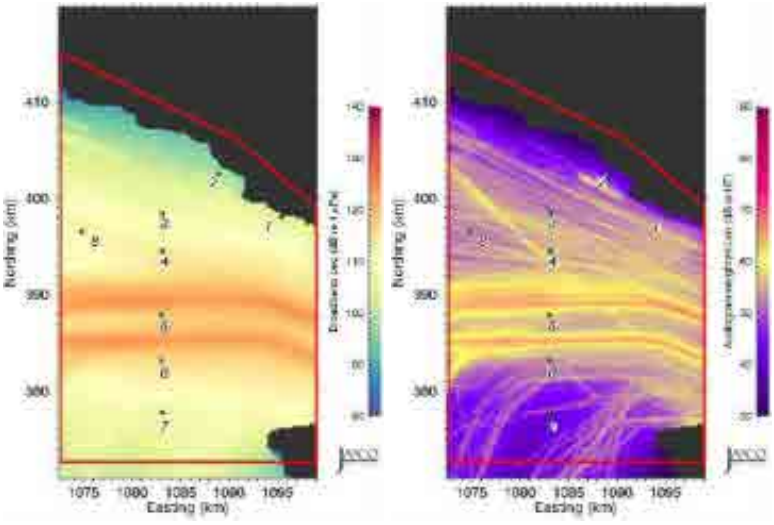

Figure 20. *Swiftsure Bank – Baseline*: Unweighted (left) and audiogram-weighted (right) equivalent continuous noise levels (L_{eq}) over the Local Study Area. Grid resolution is 200 × 200 m. The green dots are the sample locations in the SRKW critical habitat. The red line shows the boundary of the area where statistical values (percentiles and mean) were derived.

Table 12. *Swiftsure Bank – Baseline*: Unweighted (dB re 1 µPa) and audiogram-weighted received levels (dB re HT) at the sample locations in the SRKW critical habitat.

Sample location	Unweighted (dB re 1 µPa)	Audiogram-weighted (dB re HT)
1	105.9	52.3
2	99.1	43.1
3	107.4	52.3
4	114.3	55.8
5	118.3	55.2
6	114.8	52.3
7	106.8	41.4
8	112.0	53.2

3.2. Future Unmitigated Noise Levels

Figures 21–28 (left/top) present maps of projected (i.e., future) unmitigated equivalent noise levels (L_{eq}, unweighted and audiogram-weighted, respectively) for July. The maps represent the future noise levels due to expected increase in vessel traffic associated with the Trans Mountain requirements over the Local Study Areas. Figures 21–28 (right/bottom) present maps of the increase in equivalent noise levels (unweighted and audiogram-weighted, respectively) relative to the 2015 baseline levels over the same area. Tables 13–20 compare unweighted and audiogram-weighted noise levels for the baseline and future unmitigated scenarios at the sample locations in the SRKW critical habitat. The sample locations are listed in Table 1 and shown as green dots in each map below.

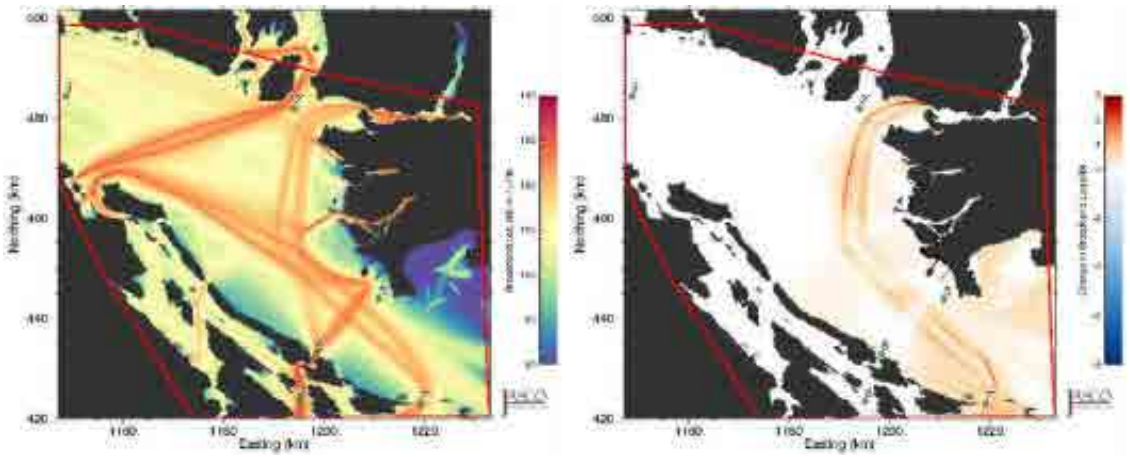

Figure 21. *Strait of Georgia – Future Unmitigated*: Unweighted equivalent continuous noise levels (L_{eq}; left) and change in L_{eq} (right) relative to July 2015 baseline levels. Grid resolution is 200 × 200 m. The green dots are the sample locations in the SRKW critical habitat. The red line shows the boundary of the area where statistical values (percentiles and mean) were derived.

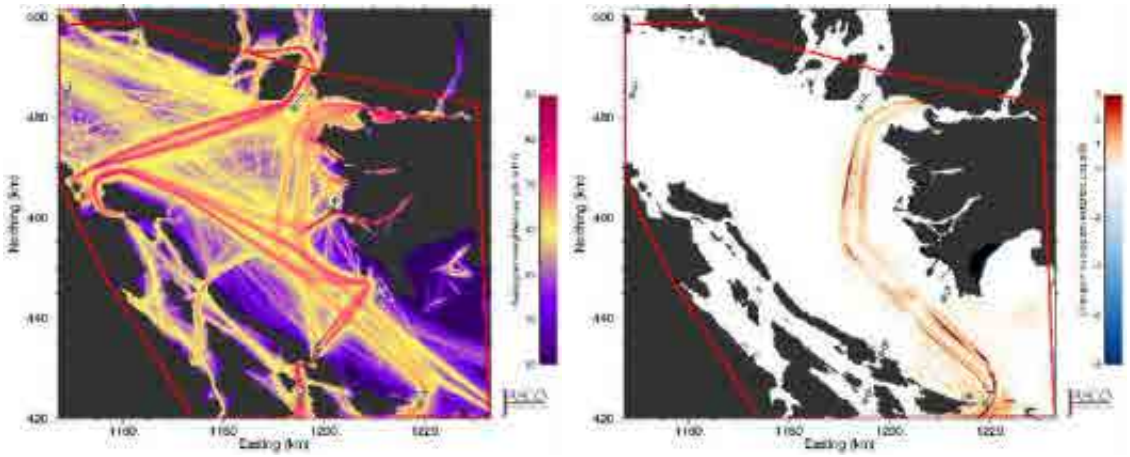

Figure 22. *Strait of Georgia – Future Unmitigated*: Audiogram-weighted equivalent continuous noise levels (L_{eq}; left) and change in L_{eq} (right) relative to July 2015 baseline levels. Grid resolution is 200 × 200 m. The green dots are the sample locations in the SRKW critical habitat. The red line shows the boundary of the area where statistical values (percentiles and mean) were derived.

Table 13. *Strait of Georgia – Baseline* vs. *Future Unmitigated*: Unweighted received levels (dB re 1 µPa), changes in received levels (dB), and changes in acoustic intensity (%) at the sample locations in the SRKW critical habitat shown in Figure 5.

Sample location	Baseline (dB re 1 µPa)	Future unmitigated (dB re 1 µPa)	Change	
			dB	%
1	113.0	113.0	0.0	0.0
2	118.2	118.2	0.0	0.0
3	106.4	106.4	0.0	0.0
4	113.0	113.0	0.0	0.0
5	107.8	107.9	+0.1	+2.3
6	129.8	129.8	0.0	0.0
7	125.3	125.7	+0.4	+9.6
8	130.9	130.9	0.0	0.0

Table 14. *Strait of Georgia – Baseline* vs. *Future Unmitigated*: Audiogram-weighted received levels (dB re HT), changes in received levels (dB), and changes in acoustic intensity (%) at the sample locations in the SRKW critical habitat shown in Figure 5.

Sample location	Baseline (dB re HT)	Future unmitigated (dB re HT)	Change	
			dB	%
1	59.5	59.5	0.0	0.0
2	63.5	63.5	0.0	0.0
3	53.9	53.9	0.0	0.0
4	64.7	64.7	0.0	0.0
5	53.8	53.9	+0.1	+2.3
6	74.9	74.9	0.0	0.0
7	66.0	66.4	+0.4	+9.6
8	72.9	72.9	0.0	0.0

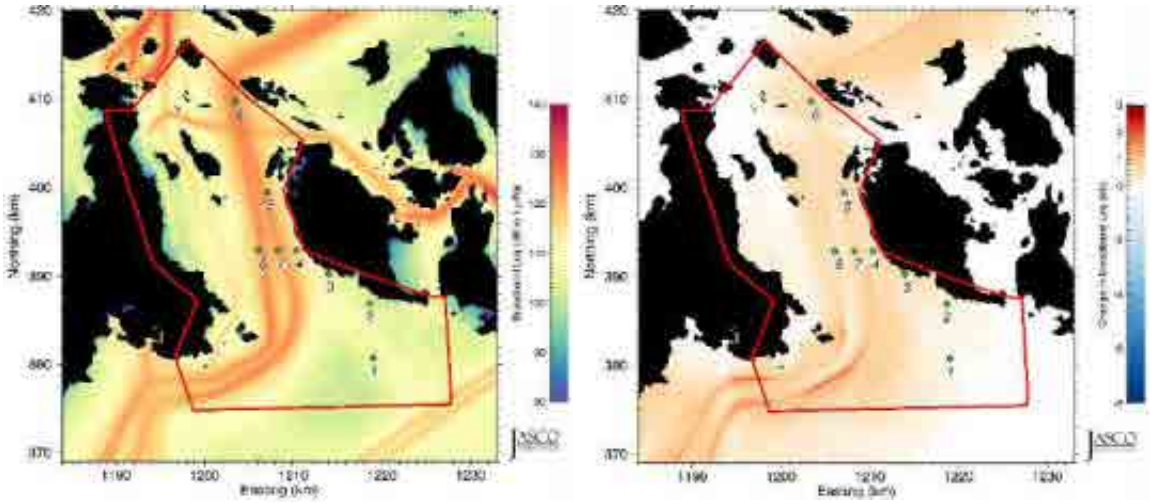

Figure 23. *Haro Strait – Future Unmitigated*: Unweighted equivalent continuous noise levels (L_{eq}; left) and change in L_{eq} (right) relative to July 2015 baseline levels. Grid resolution is 200 × 200 m. The green dots are the sample locations in the SRKW critical habitat. The red line shows the boundary of the area where statistical values (percentiles and mean) were derived.

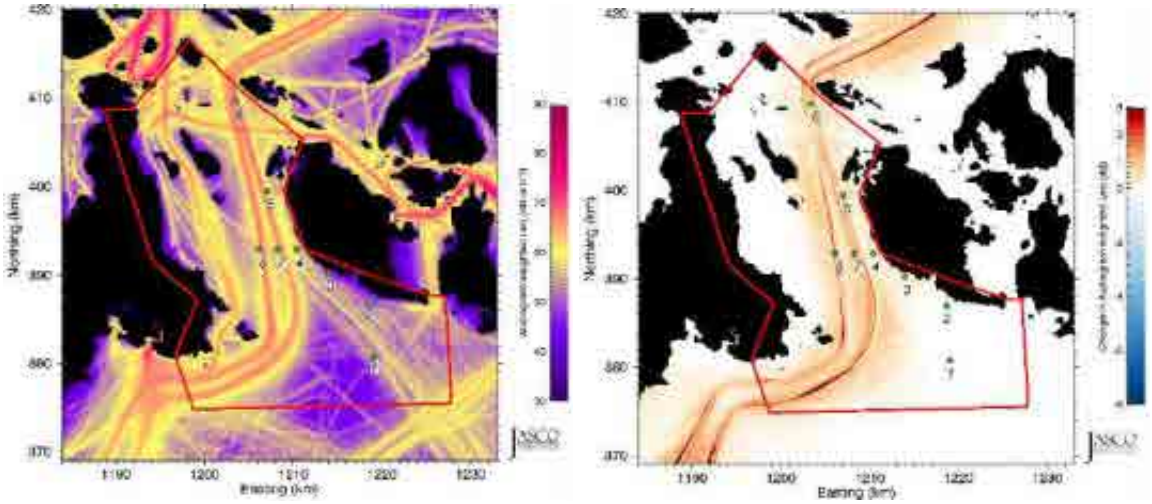

Figure 24. *Haro Strait – Future Unmitigated*: Audiogram-weighted equivalent continuous noise levels (L_{eq}; left) and change in L_{eq} (right) relative to July 2015 baseline levels. Grid resolution is 200 × 200 m. The green dots are the sample locations in the SRKW critical habitat. The red line shows the boundary of the area where statistical values (percentiles and mean) were derived.

Table 15. *Haro Strait – Baseline* vs. *Future Unmitigated*: Unweighted received levels (dB re 1 µPa), changes in received levels (dB), and changes in acoustic intensity (%) at the sample locations in the SRKW critical habitat shown in Figure 6.

Sample location	Baseline (dB re 1 µPa)	Future unmitigated (dB re 1 µPa)	Change	
			dB	%
1	109.2	109.3	+0.1	+2.3
2	103.9	104.1	+0.2	+4.7
3	106.5	107.1	+0.6	+14.8
4	114.3	114.9	+0.6	+14.8
5	119.0	119.6	+0.6	+14.8
6	123.4	124.1	+0.7	+17.5
7	122.9	123.5	+0.6	+14.8
8	123.5	124.0	+0.5	+12.2

Table 16. *Haro Strait – Baseline* vs. *Future Unmitigated*: Audiogram-weighted received levels (dB re HT), changes in received levels (dB), and changes in acoustic intensity (%) at the sample locations in the SRKW critical habitat shown in Figure 6.

Sample location	Baseline (dB re HT)	Future unmitigated (dB re HT)	Change	
			dB	%
1	59.5	59.5	0.0	0.0
2	62.9	62.9	0.0	0.0
3	53.8	53.8	0.0	0.0
4	64.7	64.7	0.0	0.0
5	53.5	53.6	+0.1	+2.3
6	62.7	62.7	0.0	0.0
7	66.0	66.4	+0.4	+9.6
8	64.3	64.3	0.0	0.0

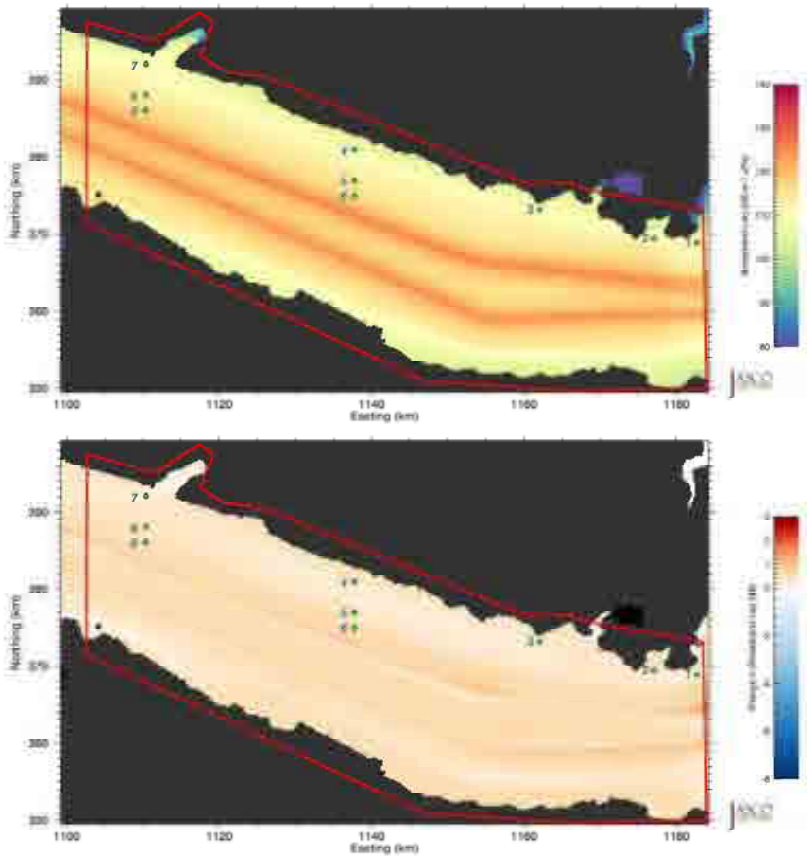

Figure 25. *Juan de Fuca Strait – Future Unmitigated*: Unweighted equivalent continuous noise levels (L_{eq}; top) and change in L_{eq} (bottom) relative to July 2015 baseline levels. Grid resolution is 200 × 200 m. The green dots are the sample locations in the SRKW critical habitat. The red line shows the boundary of the area where statistical values (percentiles and mean) were derived.

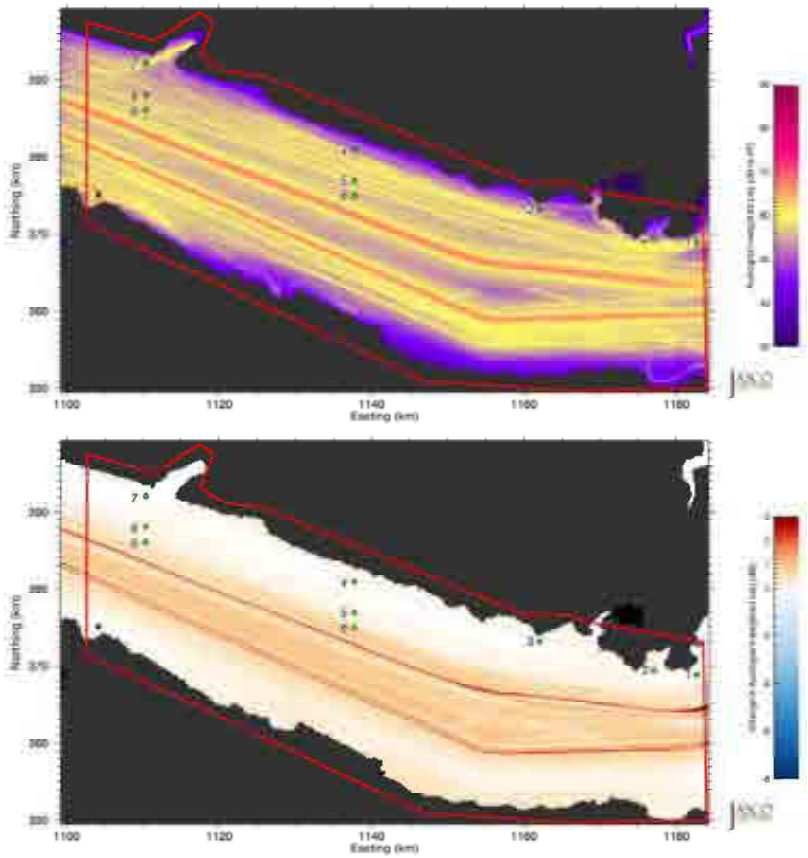

Figure 26. *Juan de Fuca Strait – Future Unmitigated*: Audiogram-weighted equivalent continuous noise levels (L_{eq}; top) and change in L_{eq} (bottom) relative to July 2015 baseline levels. Grid resolution is 200 × 200 m. The green dots are the sample locations in the SRKW critical habitat. The red line shows the boundary of the area where statistical values (percentiles and mean) were derived.

Table 17. *Juan de Fuca Strait – Baseline* vs. *Future Unmitigated*: Unweighted received levels (dB re 1 µPa), changes in received levels (dB), and changes in acoustic intensity (%) at the sample locations in the SRKW critical habitat shown in Figure 7.

Sample location	Baseline (dB re 1 µPa)	Future unmitigated (dB re 1 µPa)	Change	
			dB	%
1	111.4	111.5	+0.1	+2.3
2	111.6	111.9	+0.3	+7.2
3	110.2	110.5	+0.3	+7.2
4	109.9	110.2	+0.3	+7.2
5	113.8	114.3	+0.5	+12.2
6	117.5	118.2	+0.7	+17.5
7	109.6	110.0	+0.4	+9.6
8	114.0	114.5	+0.5	+12.2
9	117.5	118.1	+0.6	+14.8

Table 18. *Juan de Fuca Strait – Baseline* vs. *Future Unmitigated*: Audiogram-weighted received levels (dB re HT), changes in received levels (dB), and changes in acoustic intensity (%) at the sample locations in the SRKW critical habitat shown in Figure 7

Sample location	Baseline (dB re HT)	Future unmitigated (dB re HT)	Change	
			dB	%
1	59.1	59.1	0.0	0.0
2	56.9	57.0	+0.1	+2.3
3	55.4	55.4	0.0	0.0
4	56.6	56.6	0.0	0.0
5	55.6	55.7	+0.1	+2.3
6	56.3	57.0	+0.7	+17.5
7	55.0	55.0	0.0	0.0
8	55.9	56.1	+0.2	+4.7
9	55.9	56.4	+0.5	+12.2

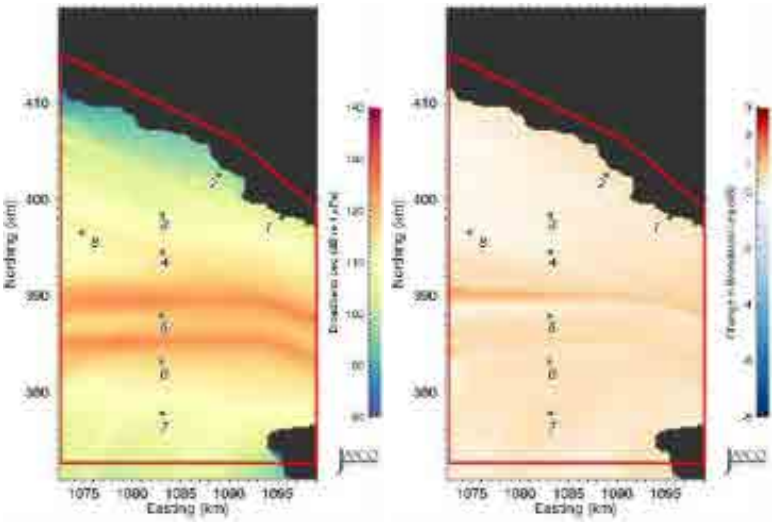

Figure 27. *Swiftsure Bank – Future Unmitigated*: Unweighted equivalent continuous noise levels (L_{eq}; left) and change in L_{eq} (right) relative to July 2015 baseline levels. Grid resolution is 200 × 200 m. The green dots are the sample locations in the SRKW critical habitat. The red line shows the boundary of the area where statistical values (percentiles and mean) were derived.

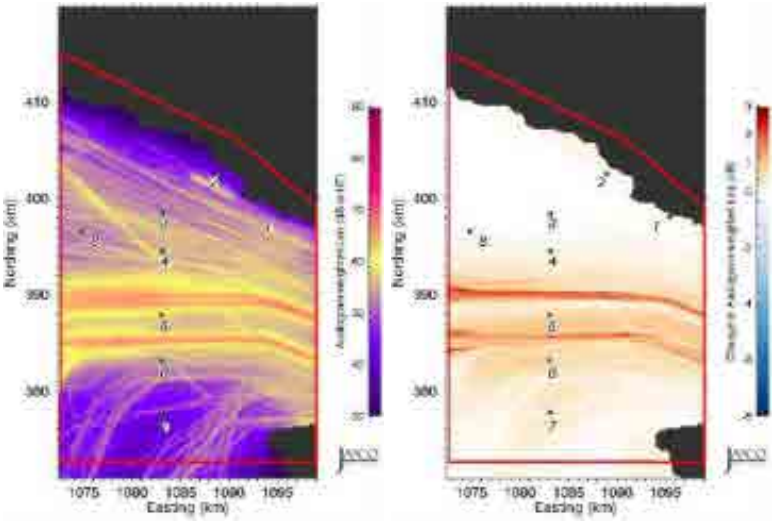

Figure 28. *Swiftsure Bank – Future Unmitigated*: Audiogram-weighted equivalent continuous noise levels (L_{eq}; left) and change in L_{eq} (right) relative to July 2015 baseline levels. Grid resolution is 200 × 200 m. The green dots are the sample locations in the SRKW critical habitat. The red line shows the boundary of the area where statistical values (percentiles and mean) were derived.

Table 19. Swiftsure Bank – *Baseline* vs. *Future Unmitigated*: Unweighted received levels (dB re 1 µPa), changes in received levels (dB), and changes in acoustic intensity (%) at the sample locations in the SRKW critical habitat shown in Figure 8.

Sample location	Baseline (dB re 1 µPa)	Future unmitigated (dB re 1 µPa)	Change	
			dB	%
1	105.9	106.30	+0.4	+9.6
2	99.1	99.60	+0.5	+12.2
3	107.4	107.70	+0.3	+7.2
4	114.3	114.50	+0.2	+4.7
5	118.3	118.80	+0.5	+12.2
6	114.8	115.30	+0.5	+12.2
7	106.8	107.40	+0.6	+14.8
8	112.0	112.10	+0.1	+2.3

Table 20. *Swiftsure Bank – Baseline* vs. *Future Unmitigated*: Audiogram-weighted received levels (dB re HT), changes in received levels (dB), and changes in acoustic intensity (%) at the sample locations in the SRKW critical habitat shown in Figure 8.

Sample location	Baseline (dB re HT)	Future unmitigated (dB re HT)	Change	
			dB	%
1	52.3	52.3	0.0	0.0
2	43.1	43.1	0.0	0.0
3	52.3	52.3	0.0	0.0
4	55.8	55.9	+0.1	+2.3
5	55.2	56.1	+0.9	+23.0
6	52.3	52.9	+0.6	+14.8
7	41.4	41.7	+0.3	+7.2
8	53.2	53.3	+0.1	+2.3

3.3. Future Mitigated Noise Levels–Slowing Down Vessels

This section presents equivalent noise levels (L_{eq}, unweighted and audiogram-weighted) over the four Local Study Areas. The mitigated results represent the expected increase in vessel traffic associated with the Trans Mountain project and implementing a slow-down zone for commercial vessel classes.

Time-averaged equivalent noise levels (L_{eq}) for multiple alternatives are presented for the Local Study Areas. In each area, a speed limit of 11 knots was first imposed on all commercial traffic in the prescribed zones. In Haro Strait, speed limits of 10 and 7 knots were also applied to all commercial traffic within the area. In the Strait of Georgia and Juan de Fuca Strait, dual-speed limits of 11 and 15 knots were applied for slow and fast commercial vessels, as described in Section 2.2.3.1.

Time-dependent noise levels (SPL) are presented for one alternative, common to all Local Study Areas, where a speed limit of 11 knots was imposed on all commercial traffic in the prescribed zones. The modelled received levels at the key locations in the SRKW critical habitat were sampled every 1 minute over the 33-hour period. The SPL “snapshots” from the model simulations were rendered as animations to show the time evolution of the vessel traffic noise in the Local Study Area. Examples of the snapshots are presented in Figures 33, 52, 69, and 87.

Plots of unweighted and audiogram-weighted noise levels as a function of time, at each sample location, are presented for each Local Study Area in Figures 34–41, 53–60, 70–78, and 88–95. These plots compare the noise levels from all traffic (and ambient noise) to noise from only the commercial traffic. In each plot, the top and bottom graph shows results for the baseline (2015 unmitigated traffic) and future mitigated (slow-down) scenarios. Percentile and mean values of the temporal variation in received noise levels (SPL) are presented at each sample location in Tables 23–24, 27–28, 31–32, and 35–36, for the baseline and slow-down scenarios, and as bar plots in Figures 42–43, 61–62, 79–80, and 96–97. The received levels were also used to generate cumulative distribution functions (CDFs) at each sample location; they are presented in Figures 44–45, 63–64, 81–82, and 98–99.

3.3.1. Strait of Georgia

Time-averaged results for two speed limit alternatives (a maximum speed of 11 knots and a dual maximum speed of 11 or 15 knots, through the Strait of Georgia shipping lanes) are presented in Figures 29–32 and Tables 21–22. In Figures 29–32, the maps on the left present the L_{eq} and the maps on the right present the change in L_{eq} with respect to baseline levels for July, seen in Figure 17. Tables 21 and 22 compare baseline and mitigated L_{eq} for the two alternatives at eight sample locations in the SRKW critical habitat. The sample locations are shown as green dots in Figures 29–32.

Figures 33–45 and Tables 23–24 present the time-dependent results for a maximum speed of 11 knots for all commercial traffic though the Strait of Georgia shipping lanes.

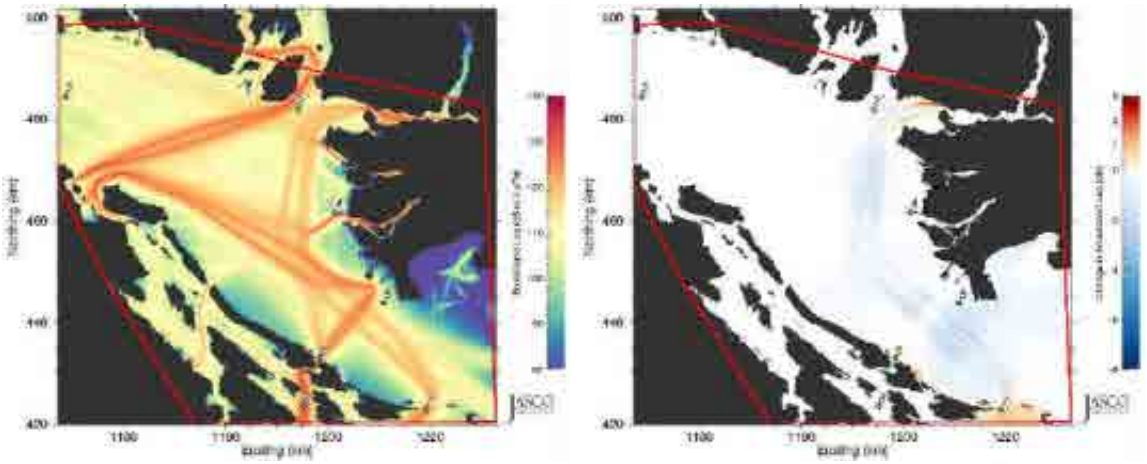

Figure 29. *Strait of Georgia – Slow-Down, 11-knot speed limit*: Unweighted equivalent continuous noise levels (L_{eq}; left) and change in L_{eq} (right) relative to July 2015 baseline levels. Grid resolution is 200 × 200 m. The green dots are the sample locations in the SRKW critical habitat. The red line shows the boundary of the area where statistical values (percentiles and mean) were derived.

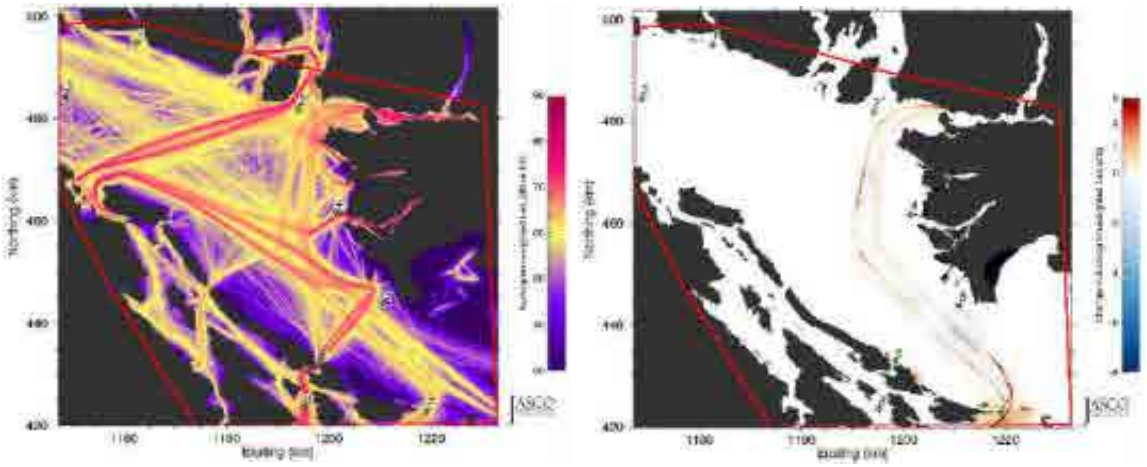

Figure 30. *Strait of Georgia – Slow-Down, 11-knot speed limit*: Audiogram-weighted equivalent continuous noise levels (L_{eq}; left) and change in L_{eq} (right) relative to July 2015 baseline levels. Grid resolution is 200 × 200 m. The green dots are the sample locations in the SRKW critical habitat. The red line shows the boundary of the area where statistical values (percentiles and mean) were derived.

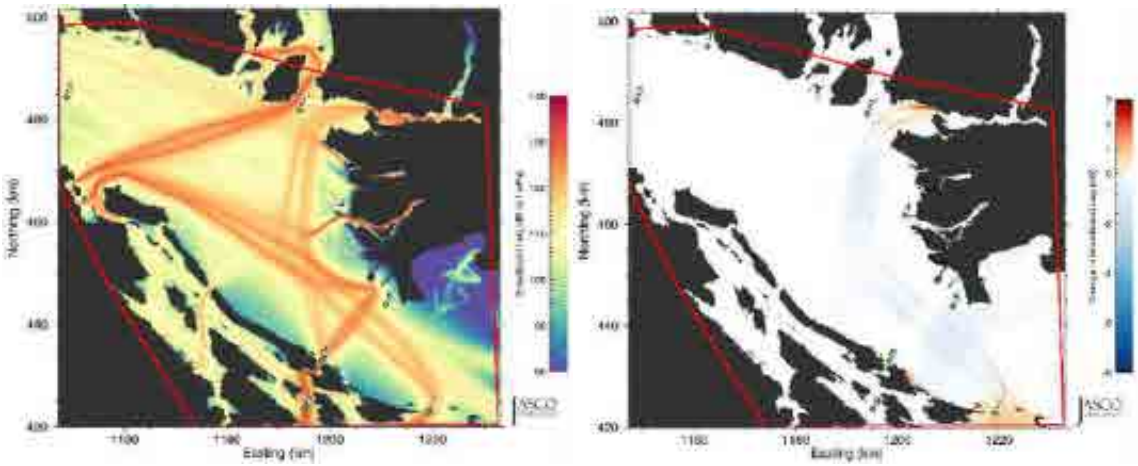

Figure 31. *Strait of Georgia – Slow-Down, 11- and 15-knot speed limits*: Unweighted equivalent continuous noise levels (L_{eq}; left) and change in L_{eq} (right) relative to July 2015 baseline levels. Grid resolution is 200 × 200 m. The green dots are the sample locations in the SRKW critical habitat. The red line shows the boundary of the area where statistical values (percentiles and mean) were derived.

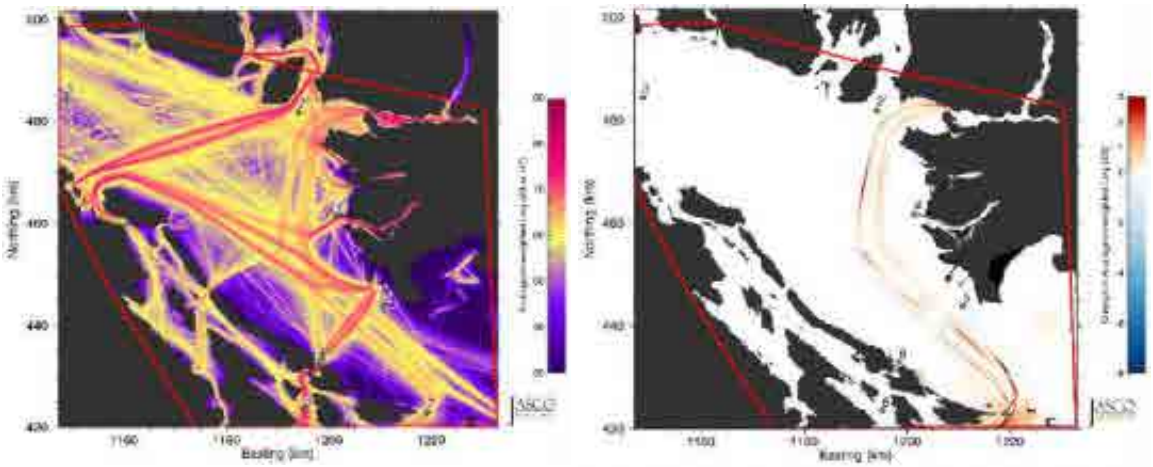

Figure 32. *Strait of Georgia – Slow-Down, 11- and 15-knot speed limits*: Audiogram-weighted equivalent continuous noise levels (L_{eq}; left) and change in L_{eq} (right) relative to July 2015 baseline levels. Grid resolution is 200 × 200 m. The green dots are the sample locations in the SRKW critical habitat. The red line shows the boundary of the area where statistical values (percentiles and mean) were derived.

Table 21. *Strait of Georgia – Baseline* vs. *Slow-Down*: Unweighted received levels (dB re 1 µPa), changes in received levels (dB), and changes in acoustic intensity (%) at the sample locations in the SRKW critical habitat shown in Figure 5.

Sample location	Baseline (dB re 1 µPa)	11 knots			11 and 15 knots		
		Mitigated (dB re 1 µPa)	Change		Mitigated (dB re 1 µPa)	Change	
			dB	%		dB	%
1	113.0	113.0	0.0	0.0	113.0	0.0	0.0
2	118.2	117.5	−0.7	−14.9	117.9	−0.3	−6.7
3	106.4	106.4	+0.0	0.0	106.4	0.0	0.0
4	113.0	113	+0.0	0.0	113	0.0	0.0
5	107.8	106.9	−0.9	−18.7	107.5	−0.3	−6.7
6	129.8	129.8	0.0	0.0	129.8	0.0	0.0
7	125.3	125.7	+0.4	+9.6	125.7	+0.4	+9.6
8	130.9	130.9	0.0	0.0	130.9	0.0	0.0

Table 22. *Strait of Georgia – Baseline* vs. *Slow-Down*: Audiogram-weighted received levels (dB re HT), changes in received levels (dB), and changes in acoustic intensity (%) at the sample locations in the SRKW critical habitat shown in Figure 5.

Sample location	Baseline (dB re HT)	11 knots			11 and 15 knots		
		Mitigated (dB re HT)	Change		Mitigated (dB re HT)	Change	
			dB	%		dB	%
1	59.5	59.5	0.0	0.0	59.5	0.0	0.0
2	63.5	63.3	−0.2	−4.5	63.4	−0.1	−2.3
3	53.9	53.9	0.0	0.0	53.9	0.0	0.0
4	64.7	64.7	0.0	0.0	64.7	0.0	0.0
5	53.8	53.7	−0.1	−2.3	53.8	0.0	0.0
6	74.9	74.9	0.0	0.0	74.9	0.0	0.0
7	66.0	66.4	0.4	+9.6	66.4	+0.4	+9.6
8	72.9	72.9	0.0	0.0	72.9	0.0	0.0

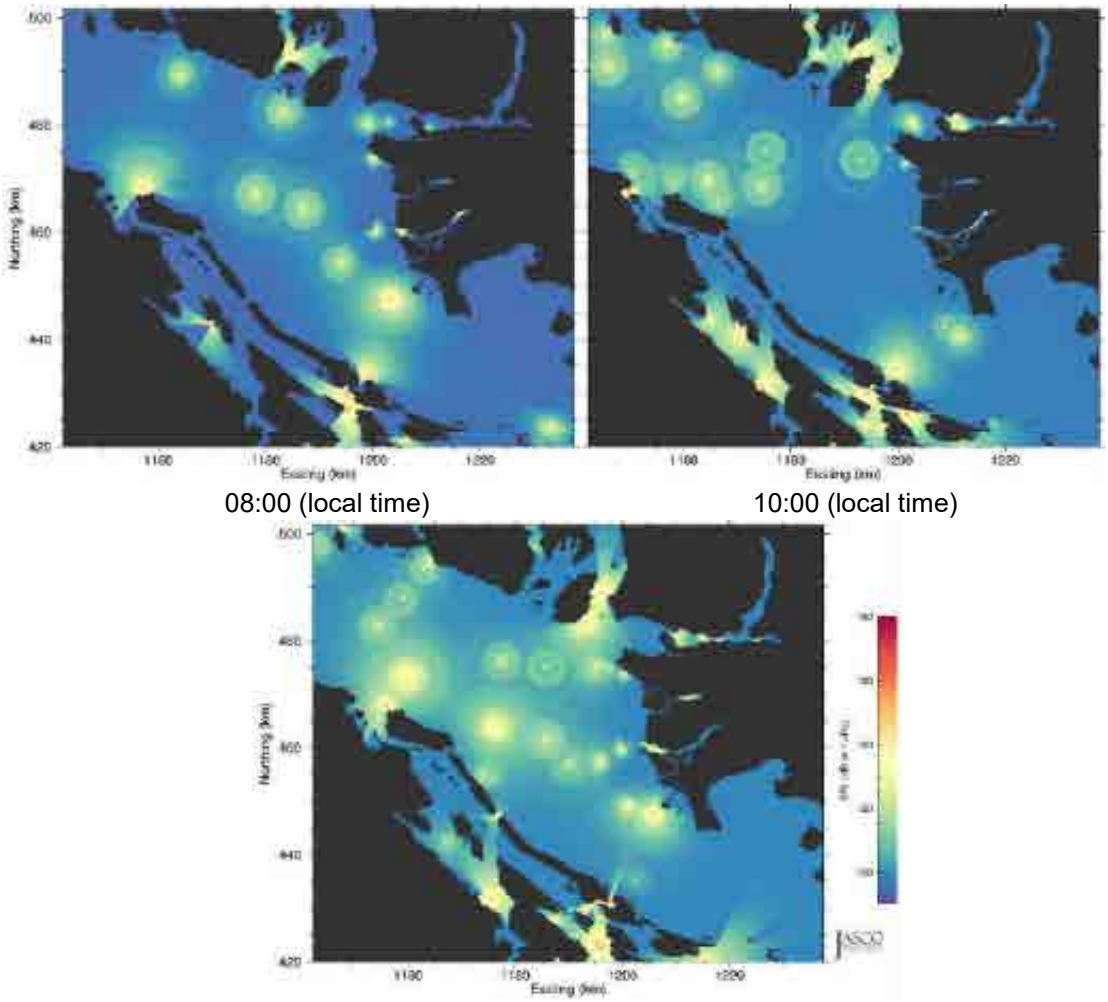

Figure 33. *Strait of Georgia – Slow*-Down *(11-knot speed limit):* Example time snapshots of future mitigated SPL (unweighted with ambient, 10 Hz to 50 kHz) from 08:00 to 12:00 (local time) in 2-hour increments. Easting and northing are BC Albers projected coordinates.

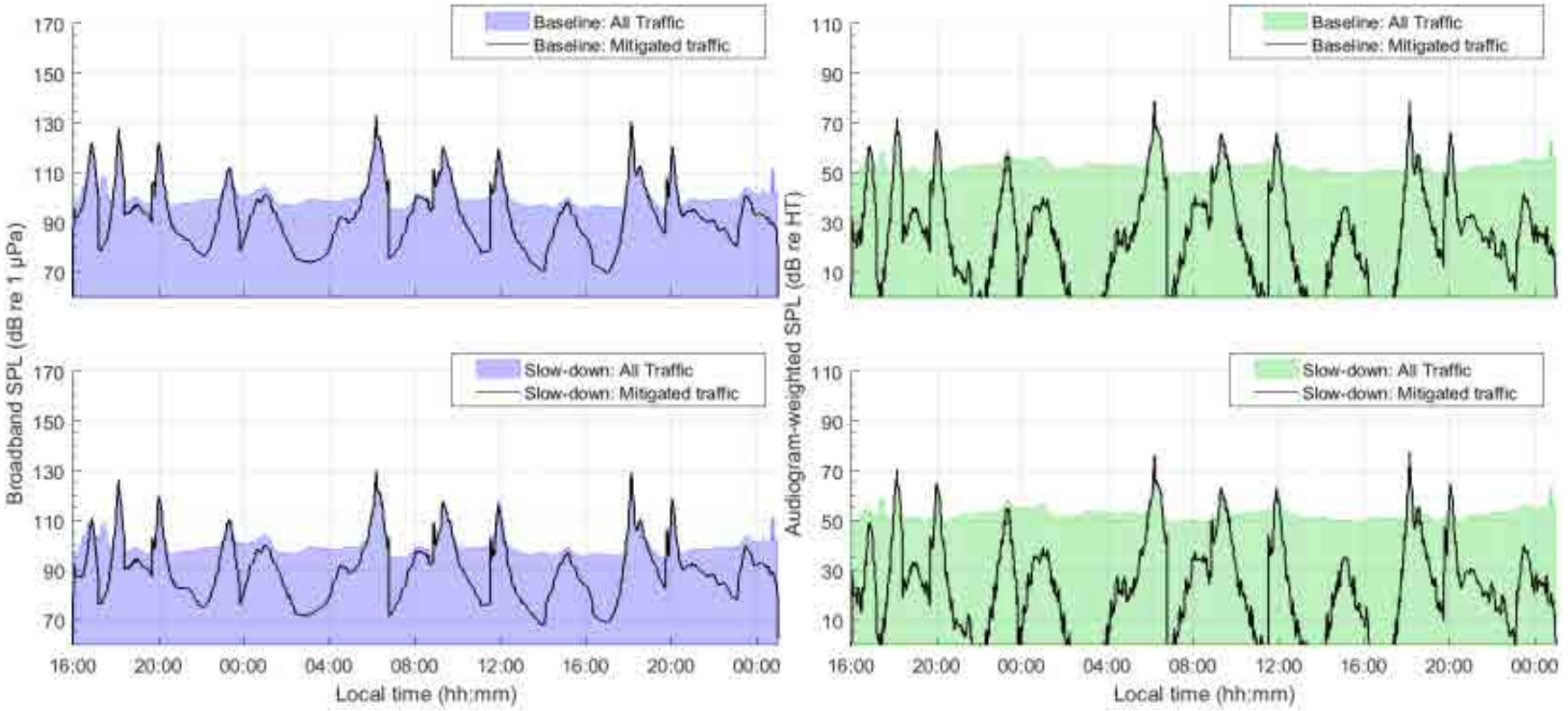

Figure 34. *Strait of Georgia – Baseline vs Slow-Down (11-knot speed limit), Sample location 1*: Temporal variability of unweighted (left) and audiogram-weighted (right) received levels for (top) baseline (no slow-down) and (bottom) slow-down scenarios. The blue and green lines above the shaded area show received levels caused by all traffic and ambient noise. The black lines show received levels caused by commercial traffic only. The receiver location is shown in Figure 5.

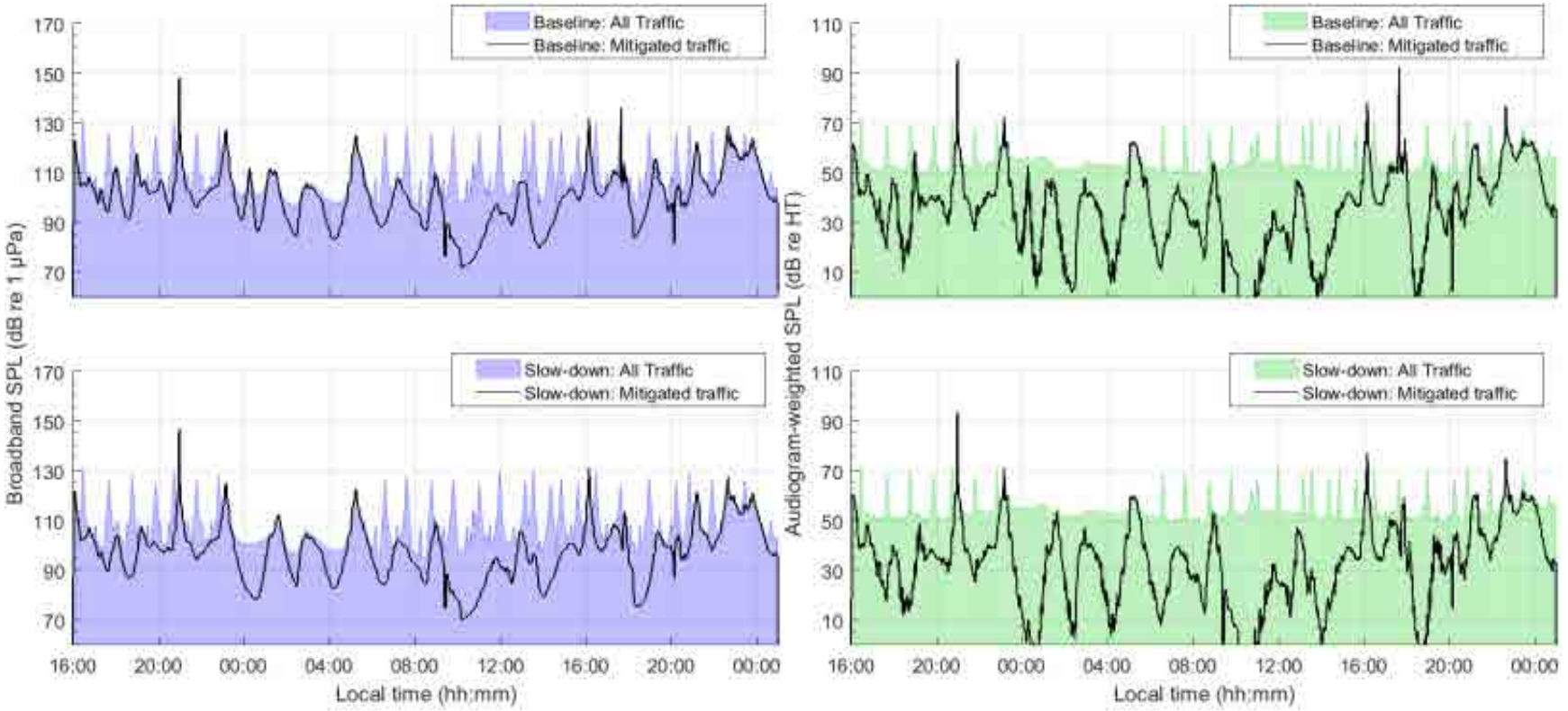

Figure 35. *Strait of Georgia – Baseline vs Slow-Down (11-knot speed limit), Sample location 2*: Temporal variability of unweighted (left) and audiogram-weighted (right) received levels for (top) baseline (no slow-down) and (bottom) slow-down scenarios. The blue and green lines above the shaded area show received levels caused by all traffic and ambient noise. The black lines show received levels caused by commercial traffic only. The receiver location is shown in Figure 5.

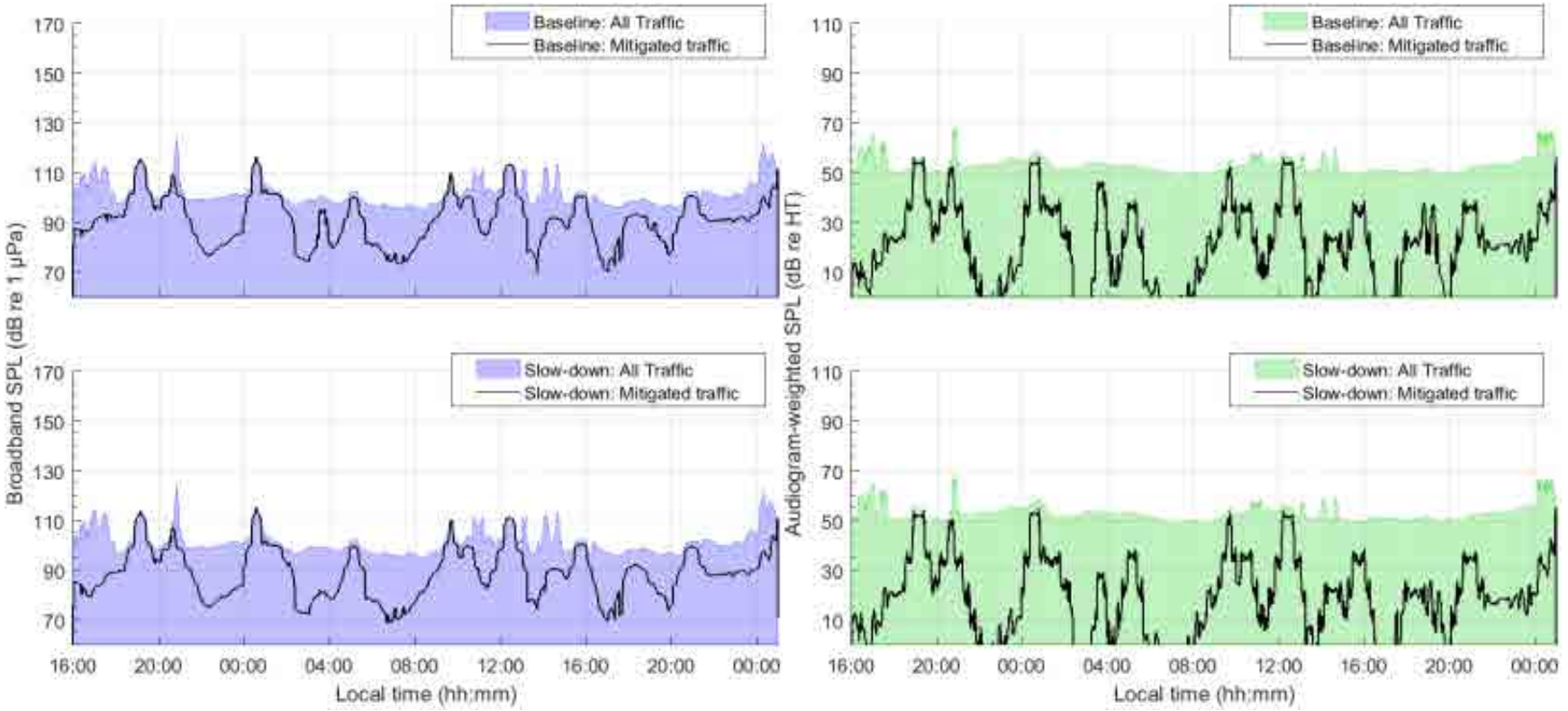

Figure 36. *Strait of Georgia – Baseline vs Slow-Down (11-knot speed limit), Sample location 3*: Temporal variability of unweighted (left) and audiogram-weighted (right) received levels for (top) baseline (no slow-down) and (bottom) slow-down scenarios. The blue and green lines above the shaded area show received levels caused by all traffic and ambient noise. The black lines show received levels caused by commercial traffic only. The receiver location is shown in Figure 5.

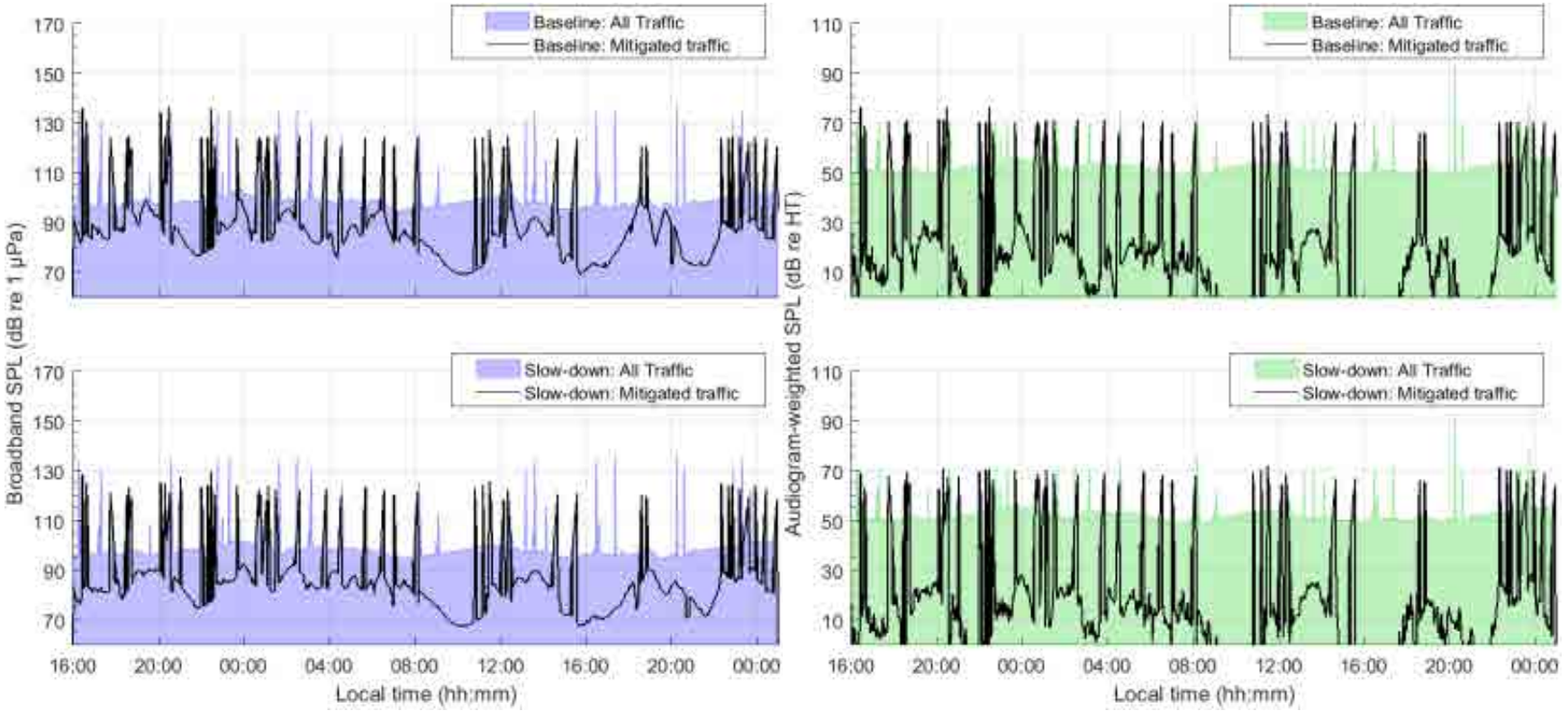

Figure 37. *Strait of Georgia – Baseline vs Slow-Down (11-knot speed limit), Sample location 4*: Temporal variability of unweighted (left) and audiogram-weighted (right) received levels for (top) baseline (no slow-down) and (bottom) slow-down scenarios. The blue and green lines above the shaded area show received levels caused by all traffic and ambient noise. The black lines show received levels caused by commercial traffic only. The receiver location is shown in Figure 5.

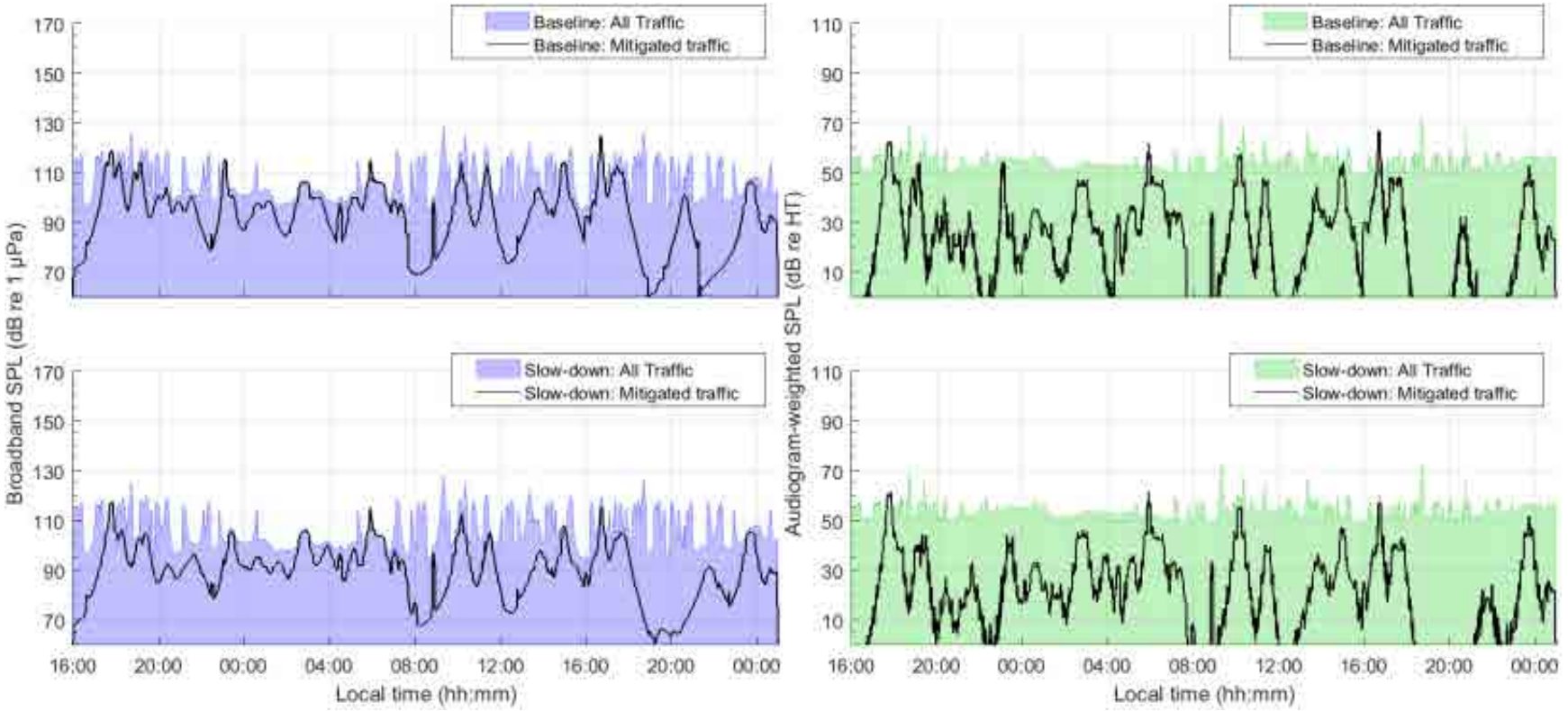

Figure 38. *Strait of Georgia – Baseline vs Slow-Down (11-knot speed limit), Sample location 5*: Temporal variability of unweighted (left) and audiogram-weighted (right) received levels for (top) baseline (no slow-down) and (bottom) slow-down scenarios. The blue and green lines above the shaded area show received levels caused by all traffic and ambient noise. The black lines show received levels caused by commercial traffic only. The receiver location is shown in Figure 5.

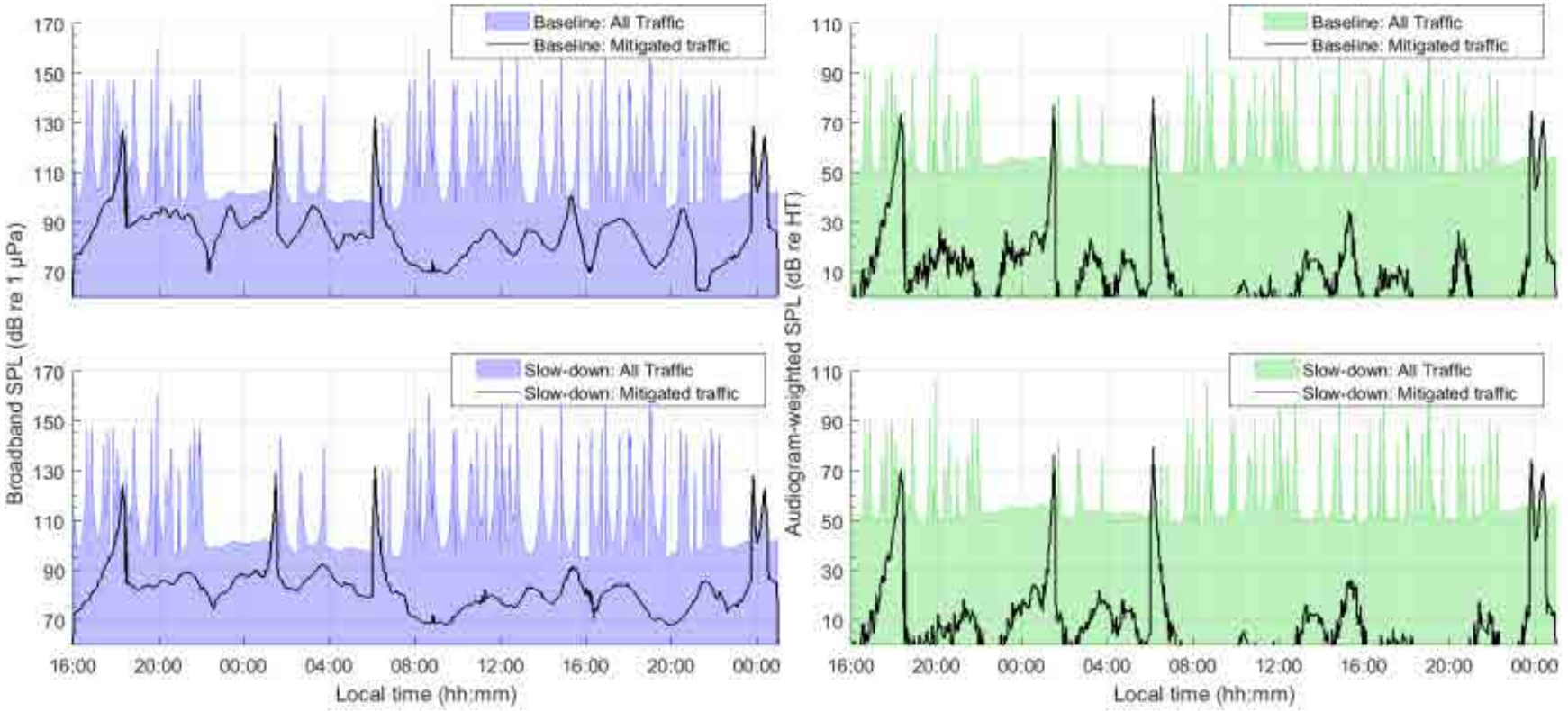

Figure 39. *Strait of Georgia – Baseline vs Slow-Down (11-knot speed limit), Sample location 6*: Temporal variability of unweighted (left) and audiogram-weighted (right) received levels for (top) baseline (no slow-down) and (bottom) slow-down scenarios. The blue and green lines above the shaded area show received levels caused by all traffic and ambient noise. The black lines show received levels caused by commercial traffic only. The receiver location is shown in Figure 5.

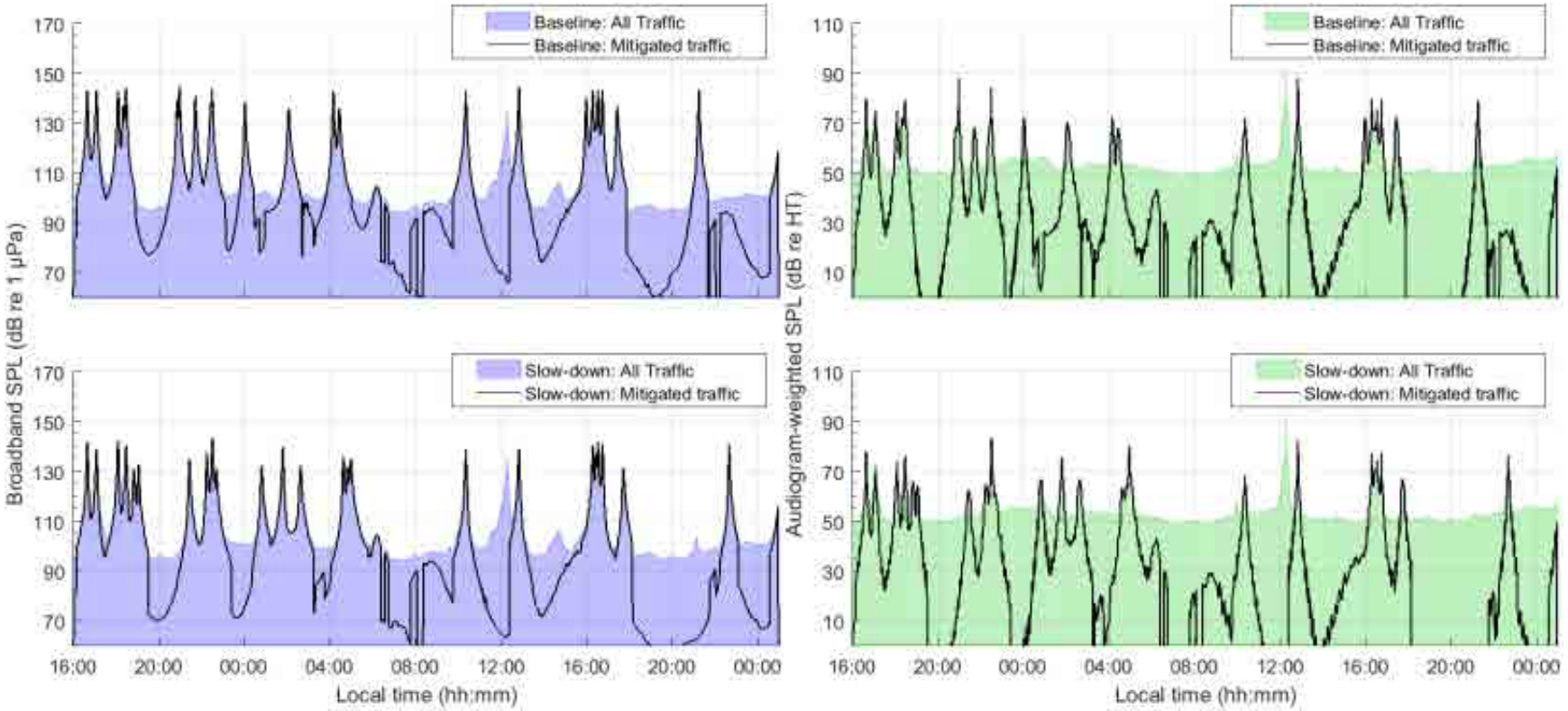

Figure 40. *Strait of Georgia – Baseline vs Slow-Down (11-knot speed limit), Sample location 7*: Temporal variability of unweighted (left) and audiogram-weighted (right) received levels for (top) baseline (no slow-down) and (bottom) slow-down scenarios. The blue and green lines above the shaded area show received levels caused by all traffic and ambient noise. The black lines show received levels caused by commercial traffic only. The receiver location is shown in Figure 5.

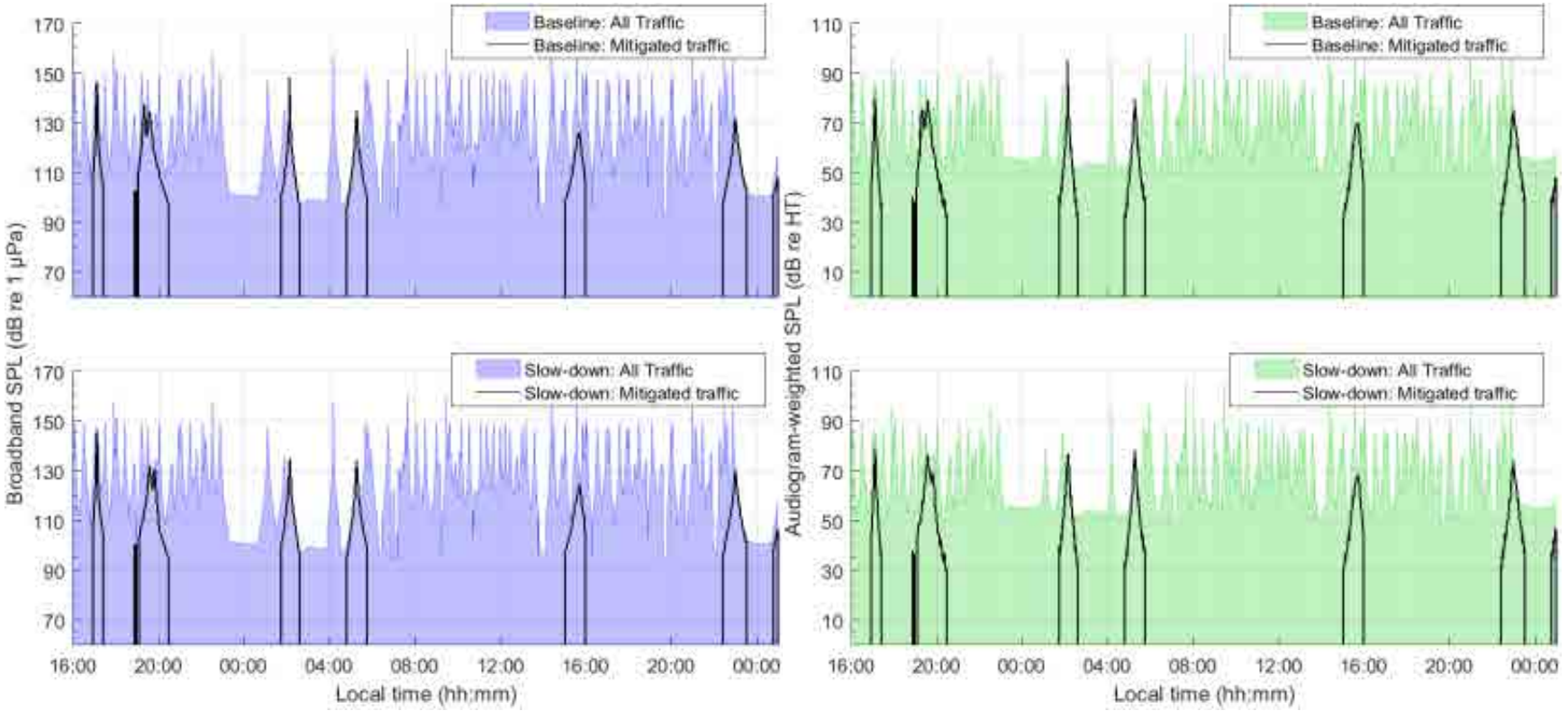

Figure 41. *Strait of Georgia – Baseline vs Slow-Down (11-knot speed limit), Sample location 8*: Temporal variability of unweighted (left) and audiogram-weighted (right) received levels for (top) baseline (no slow-down) and (bottom) slow-down scenarios. The blue and green lines above the shaded area show received levels caused by all traffic and ambient noise. The black lines show received levels caused by commercial traffic only. The receiver location is shown in Figure 5.

Table 23. *Strait of Georgia – Baseline vs Slow-Down (11-knot speed limit):* Temporal analysis of unweighted received noise levels (dB re 1 µPa), difference in received noise levels (dB), and difference acoustic intensity (%). The values indicate the percentile or mean calculated over a 33-hour period without (Baseline) and with mitigation (Slow-down), at the sample locations within the SRKW critical habitat shown in Figure 5.

Sample location	Scenario	Temporal analysis of noise level (dB re 1 µPa), difference in noise levels (dB), and difference in acoustic intensity (%)			
		5th	50th	95th	Mean
1	Baseline	96.0	99.3	117.4	101.7 ±6.4
	Slow-down	95.9	99.0	114.1	100.9 ±5.6
	Difference	**−0.1 (−2.3%)**	**−0.3 (−6.7%)**	**−3.3 (−53.2%)**	**−0.8 (−16.5%)**
2	Baseline	98.2	107.9	124.8	109.2 ±8.1
	Slow-down	98.0	106.8	124.2	108.3 ±8.0
	Difference	**−0.2 (−4.5%)**	**−1.1 (−22.4%)**	**−0.6 (−12.9%)**	**−0.9 (−18.7%)**
3	Baseline	96.2	100.5	113.5	101.9 ±5.3
	Slow-down	96.1	100.3	112.4	101.6 ±5.1
	Difference	**−0.1 (−2.3%)**	**−0.2 (−4.5%)**	**−1.1 (−22.4%)**	**−0.3 (−7.1%)**
4	Baseline	95.5	98.9	123.3	102.3 ±8.7
	Slow-down	95.3	98.6	121.0	101.8 ±8.3
	Difference	**−0.2 (−4.5%)**	**−0.3 (−6.7%)**	**−2.3 (−41.1%)**	**−0.5 (−10.6%)**
5	Baseline	97.4	106.2	118.4	107.0 ±7.3
	Slow-down	97.3	104.6	118.0	106.4 ±7.2
	Difference	**−0.1 (−2.3%)**	**−1.6 (−30.8%)**	**−0.4 (−8.8%)**	**−0.7 (−14.1%)**
6	Baseline	96.7	103.5	139.0	109.7 ±13.6
	Slow-down	96.4	103.4	139.0	109.5 ±13.6
	Difference	**−0.3 (−6.7%)**	**−0.1 (−2.3%)**	**0.0 (0.0%)**	**−0.2 (−4.5%)**
7	Baseline	95.0	101.6	134.0	106.6 ±11.9
	Slow-down	95.0	101.8	130.7	106.0 ±11.2
	Difference	**0.0 (0.0%)**	**+0.2 (+4.7%)**	**−3.3 (−53.2%)**	**−0.5 (−11.6%)**
8	Baseline	98.6	123.5	146.6	122.4 ±14.7
	Slow-down	98.6	123.5	146.6	122.4 ±14.7
	Difference	**0.0 (0.0%)**	**0.0 (0.0%)**	**0.0 (0.0%)**	**0.0 (0.0%)**

Table 24. *Strait of Georgia – Baseline vs Slow-Down (11-knot speed limit):* Temporal analysis of SRKW audiogram-weighted received noise levels (dB re HT), difference in received noise levels (dB), and difference acoustic intensity (%). The values indicate the percentile or mean calculated over a 33-hour period without (Baseline) and with mitigation (Slow-down), at the sample locations within the SRKW critical habitat shown in Figure 5.

Sample location	Scenario	Temporal analysis of noise level (dB re HT), difference in noise levels (dB), and difference in acoustic intensity (%)			
		5th	50th	95th	Mean
1	Baseline	49.5	52.7	61.8	53.4 ±3.9
	Slow-down	49.5	52.5	60.2	53.1 ±3.4
	Difference	**0.0 (0.0%)**	**−0.2 (−4.5%)**	**−1.6 (−30.8%)**	**−0.3 (−6.7%)**
2	Baseline	50.2	53.6	66.2	55.4 ±5.2
	Slow-down	50.1	53.5	66.1	55.1 ±5.0
	Difference	**−0.1 (−2.3%)**	**−0.1 (−2.3%)**	**−0.1 (−2.3%)**	**−0.3 (−6.7%)**
3	Baseline	49.5	52.4	59.6	53.2 ±3.4
	Slow-down	49.5	52.4	59.6	53.1 ±3.4
	Difference	**0.0 (0.0%)**	**0.0 (0.0%)**	**0.0 (0.0%)**	**−0.1 (−2.3%)**
4	Baseline	49.5	52.5	67.0	54.4 ±5.6
	Slow-down	49.5	52.4	66.4	54.1 ±5.2
	Difference	**0.0 (0.0%)**	**−0.1 (−2.3%)**	**−0.6 (−12.9%)**	**−0.3 (−6.7%)**
5	Baseline	49.9	53.7	59.2	54.3 ±3.3
	Slow-down	49.9	53.6	59.1	54.2 ±3.2
	Difference	**0.0 (0.0%)**	**−0.1 (−2.3%)**	**−0.1 (−2.3%)**	**−0.1 (−2.3%)**
6	Baseline	49.9	53.7	79.8	58.1 ±10.1
	Slow-down	49.9	53.7	79.8	58.1 ±10.1
	Difference	**0.0 (0.0%)**	**0.0 (0.0%)**	**0.0 (0.0%)**	**0.0 (0.0%)**
7	Baseline	49.6	53.2	69.2	54.8 ±6.1
	Slow-down	49.6	52.9	66.8	54.5 ±5.6
	Difference	**0.0 (0.0%)**	**−0.3 (−6.7%)**	**−2.4 (−42.5%)**	**−0.3 (−6.7%)**
8	Baseline	52.1	65.0	85.0	66.5 ±11.3
	Slow-down	52.1	65.0	84.7	66.4 ±11.3
	Difference	**0.0 (0.0%)**	**0.0 (0.0%)**	**−0.3 (−6.7%)**	**−0.1 (−2.3%)**

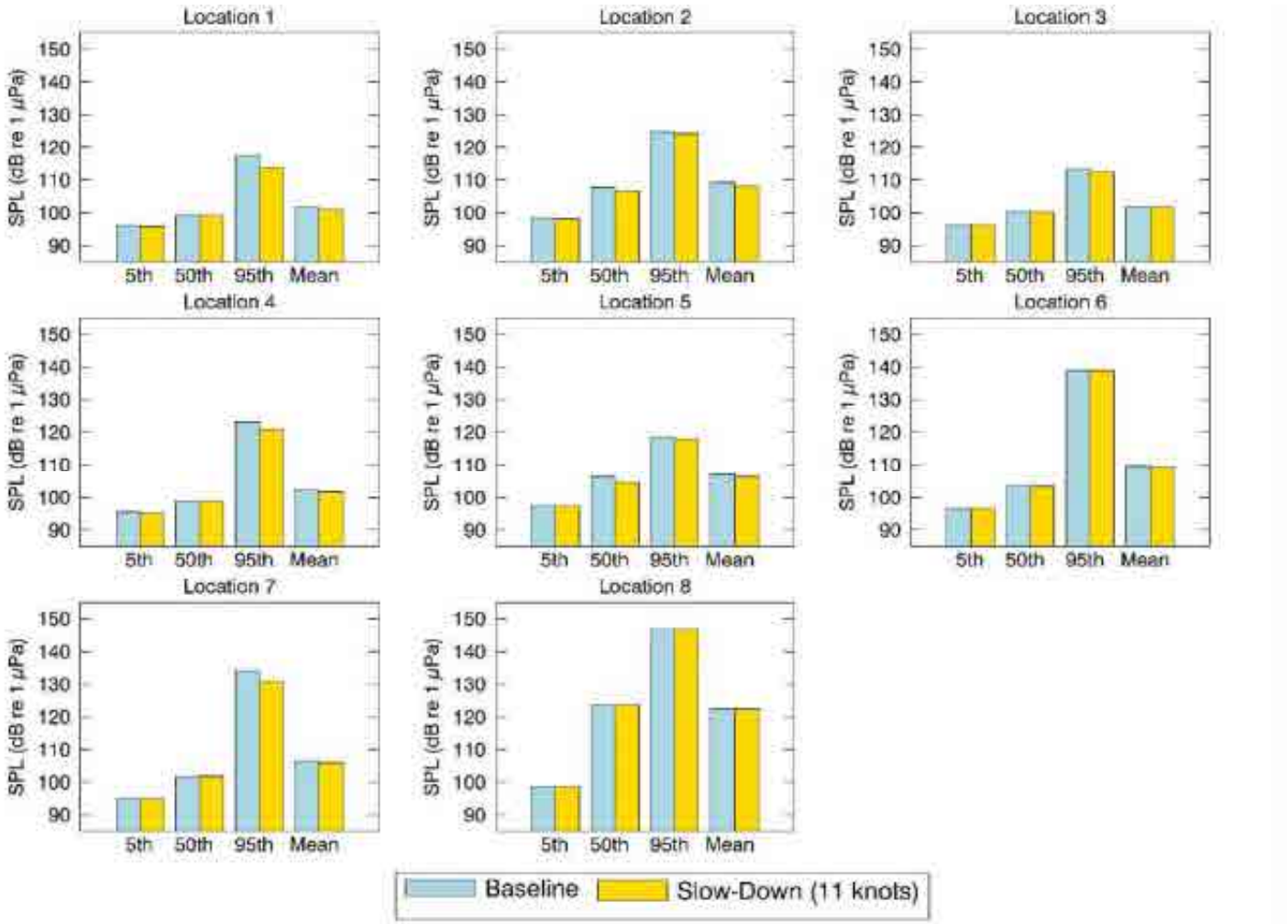

Figure 42. *Strait of Georgia – Baseline vs Slow-Down (11-knot speed limit)*: Histogram representation of the temporal analysis of unweighted received noise levels (dB re 1 µPa). The vertical bars indicate the percentile or mean calculated over a 33-hour period without (baseline) and with mitigation, at the sample locations within the SRKW critical habitat shown in Figure 5.

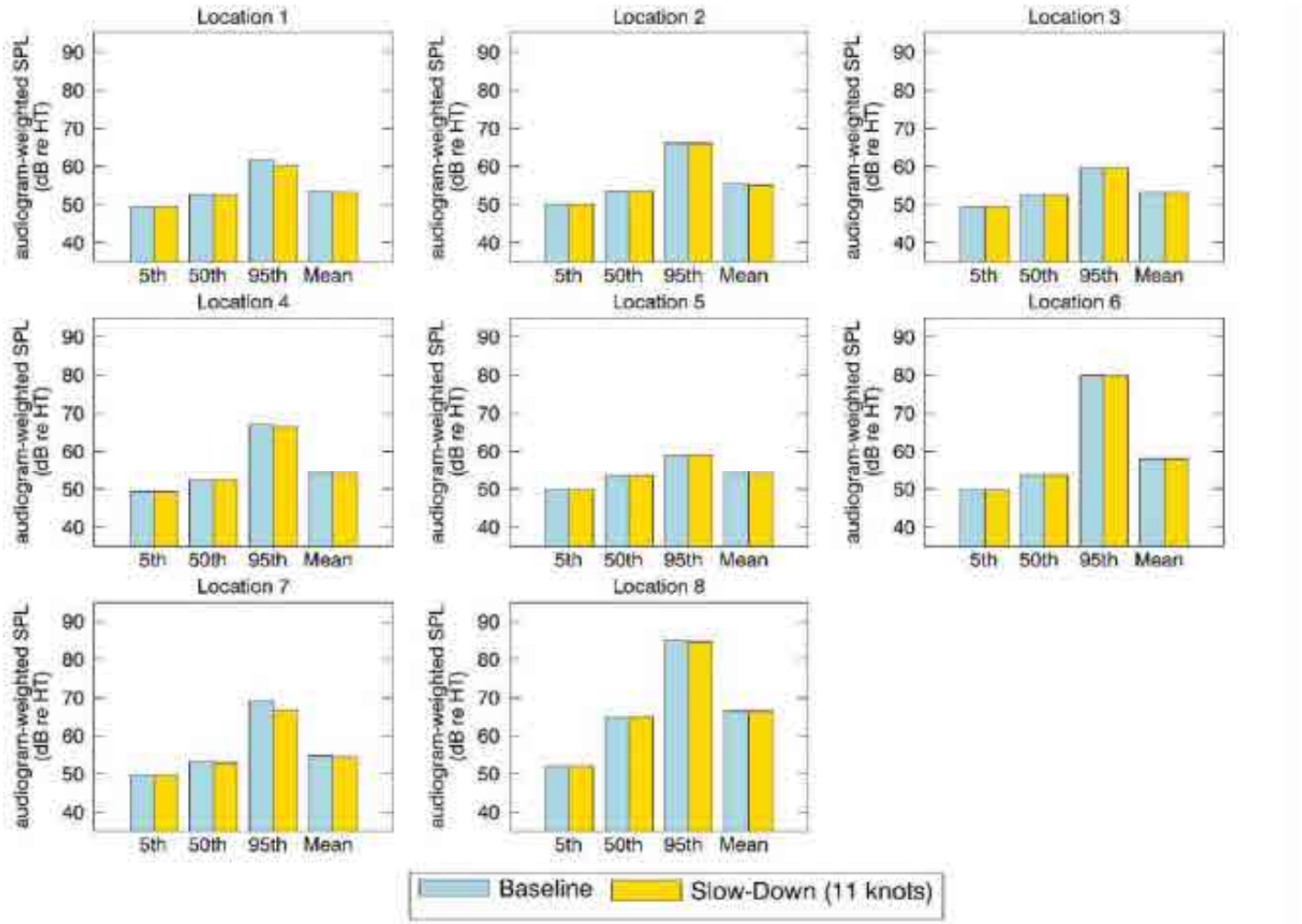

Figure 43. *Strait of Georgia – Baseline vs Slow-Down (11-knot speed limit)*: Histogram representation of the temporal analysis of SRKW audiogram-weighted received noise levels (dB re HT). The vertical bars indicate the percentile or mean calculated over a 33-hour period without (baseline) and with mitigation, at the sample locations within the SRKW critical habitat shown in Figure 5.

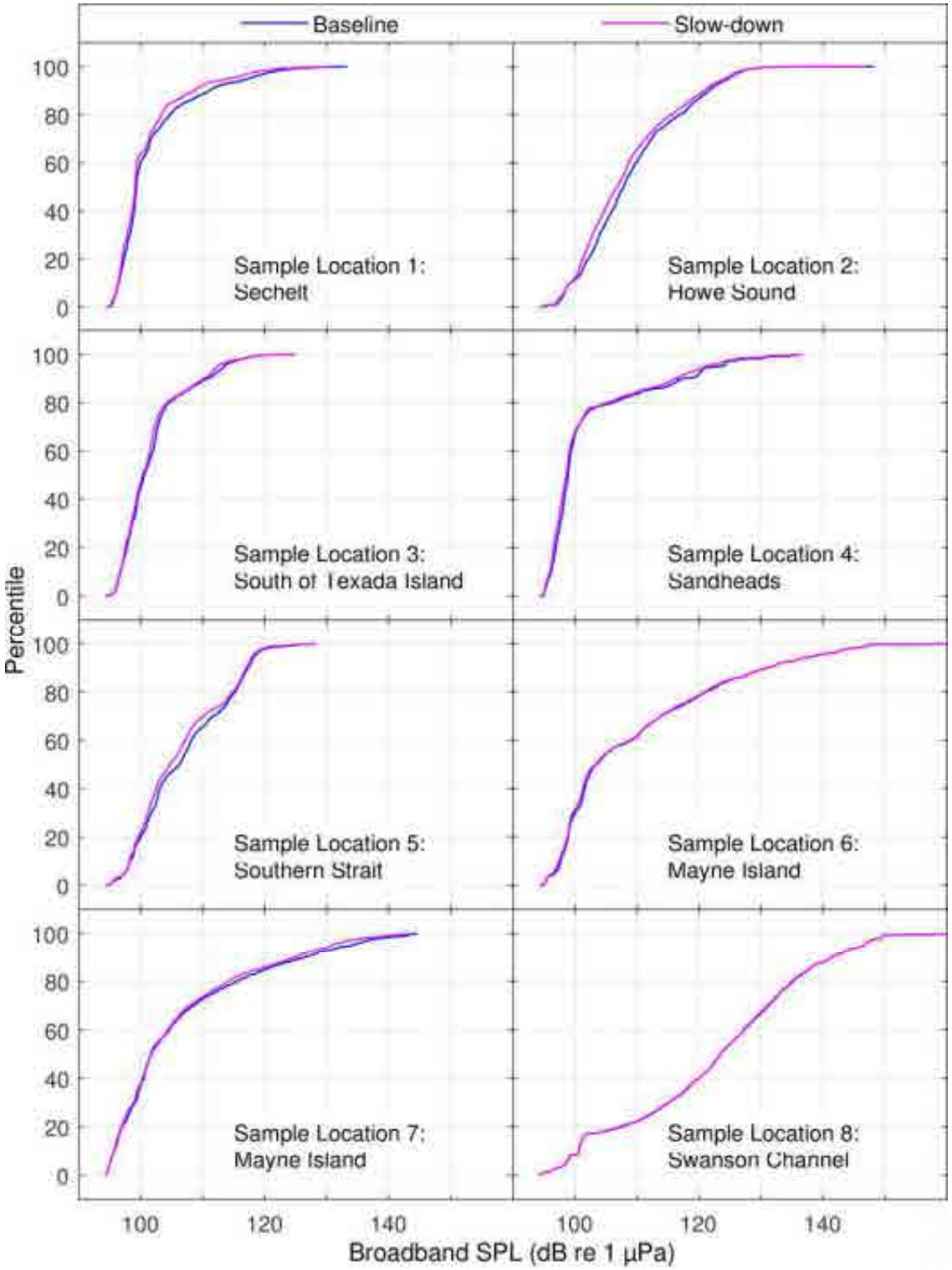

Figure 44. *Strait of Georgia – Baseline vs Slow-Down (11-knot speed limit):* CDF curves of time-dependent unweighted SPL for baseline and mitigated scenarios at the sample locations shown in Figure 5.

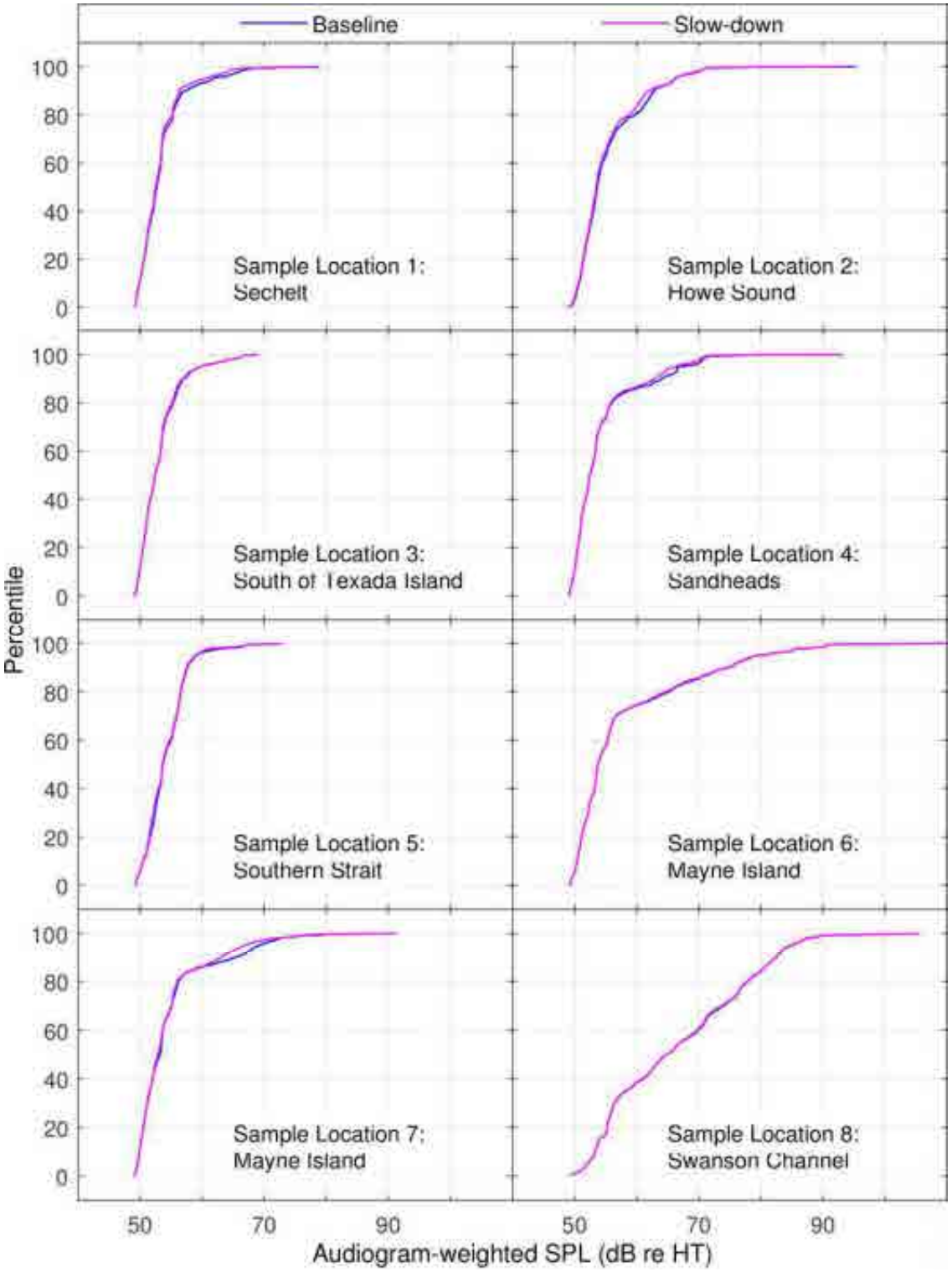

Figure 45. *Strait of Georgia – Baseline vs Slow-Down (11-knot speed limit):* CDF curves of time-dependent audiogram-weighted SPL for baseline and mitigated scenarios at the sample locations shown in Figure 5.

3.3.2. Haro Strait

Time-averaged results for three speed limit alternatives (a maximum speed of 11, 10, and 7 knots through the Haro Strait shipping lanes) are presented in Figures 46–51 and Tables 25–26. In Figures 46–51, the maps on the left present the L_{eq} and the maps on the right present the change in L_{eq} with respect to baseline levels for July, seen in Figure 18. Tables 25 and 26 compare baseline and mitigated L_{eq} for the three speed limits at eight sample locations in the SRKW critical habitat. The sample locations are shown as green dots in Figures 46–51.

Figures 52–64 and Tables 27–28 present the time-dependent results for a maximum speed of 11 knots for all commercial traffic though the Haro Strait shipping lanes.

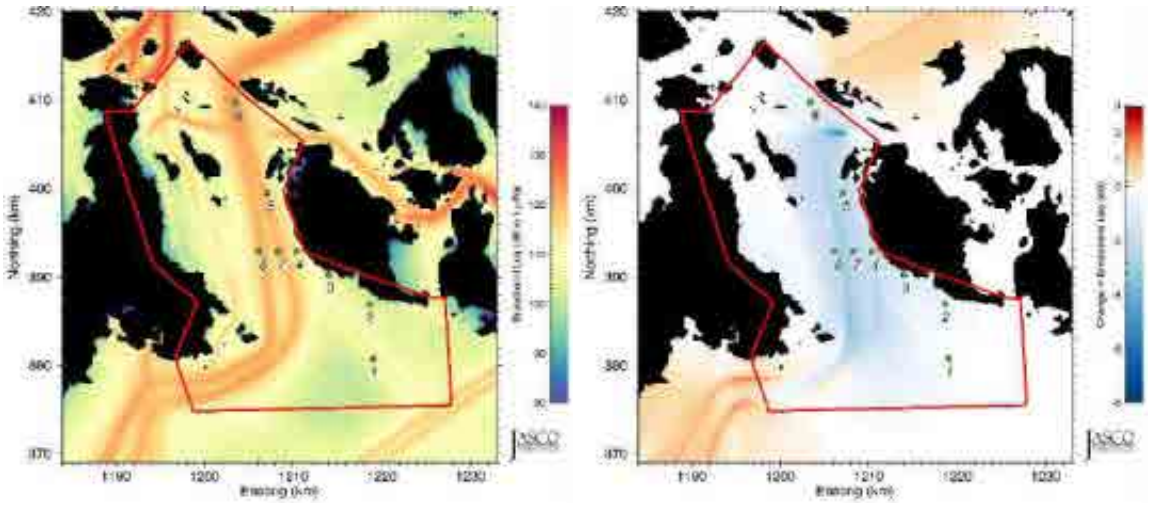

Figure 46. *Haro Strait – Slow-Down, 11-knot speed limit*: Unweighted equivalent continuous noise levels (L_{eq}; left) and change in L_{eq} (right) relative to July 2015 baseline levels. Grid resolution is 200 × 200 m. The green dots are the sample locations in the SRKW critical habitat. The red line shows the boundary of the area where statistical values (percentiles and mean) were derived.

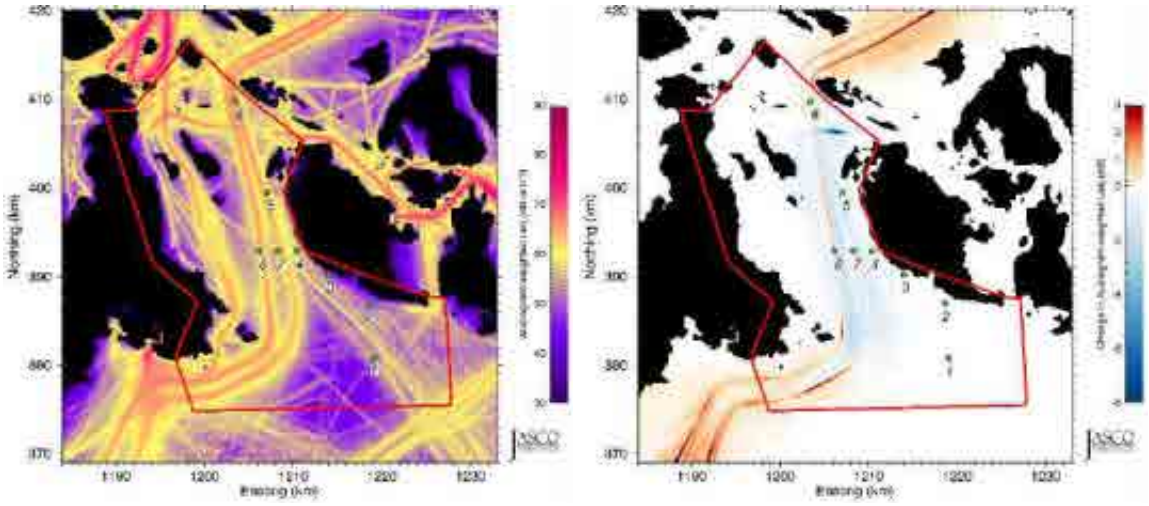

Figure 47. *Haro Strait – Slow-Down, 11-knot speed limit*: Audiogram-weighted equivalent continuous noise levels (L_{eq}; left) and change in L_{eq} (right) relative to July 2015 baseline levels. Grid resolution is 200 × 200 m. The green dots are the sample locations in the SRKW critical habitat. The red line shows the boundary of the area where statistical values (percentiles and mean) were derived.

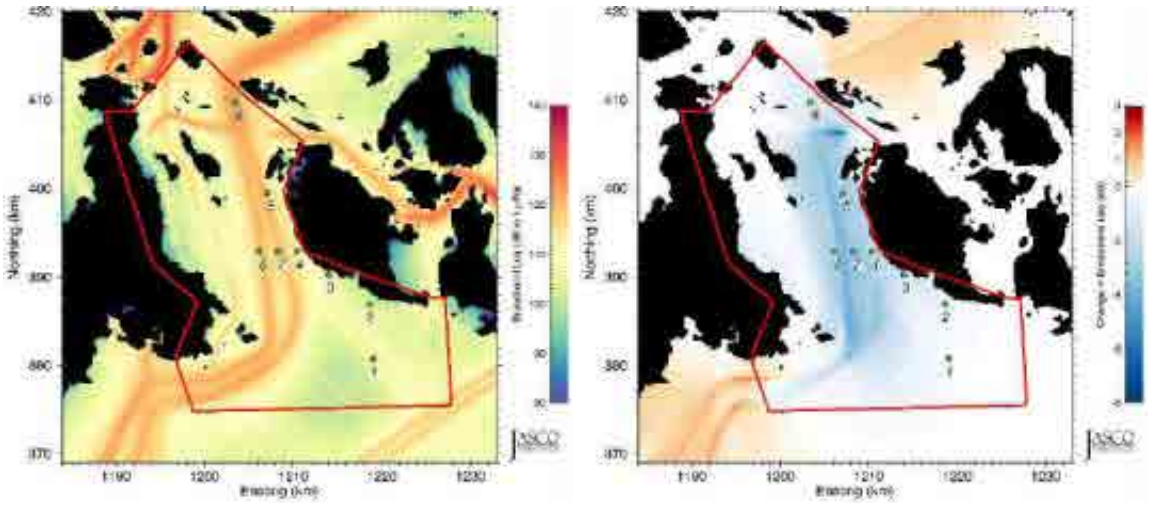

Figure 48. *Haro Strait – Slow-Down, 10-knot speed limit*: Unweighted equivalent continuous noise levels (L_{eq}; left) and change in L_{eq} (right) relative to July 2015 baseline levels. Grid resolution is 200 × 200 m. The green dots are the sample locations in the SRKW critical habitat. The red line shows the boundary of the area where statistical values (percentiles and mean) were derived.

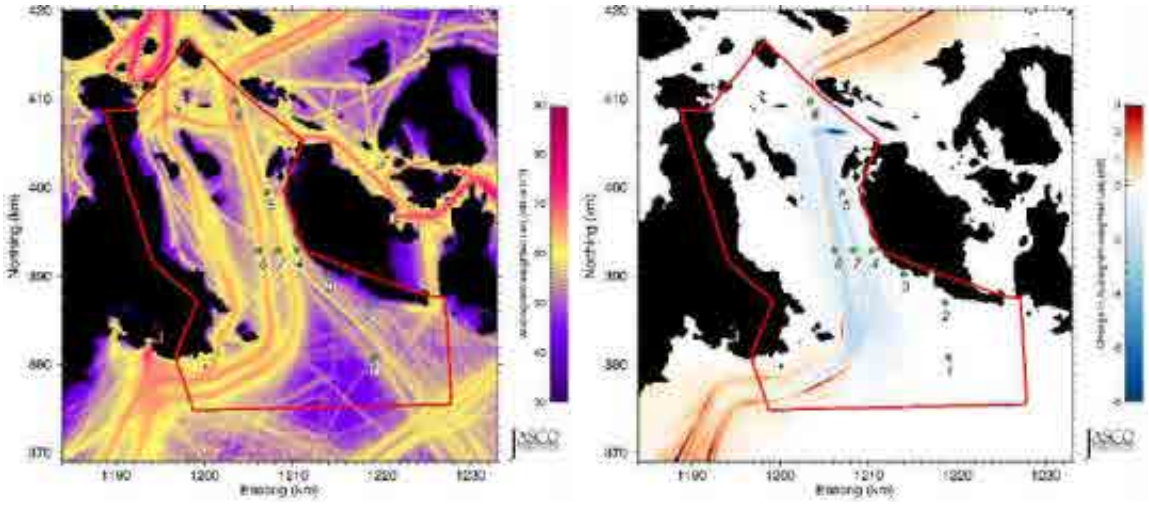

Figure 49. *Haro Strait – Slow-Down, 10-knot speed limit*: Audiogram-weighted equivalent continuous noise levels (L_{eq}; left) and change in L_{eq} (right) relative to July 2015 baseline levels. Grid resolution is 200 × 200 m. The green dots are the sample locations in the SRKW critical habitat. The red line shows the boundary of the area where statistical values (percentiles and mean) were derived.

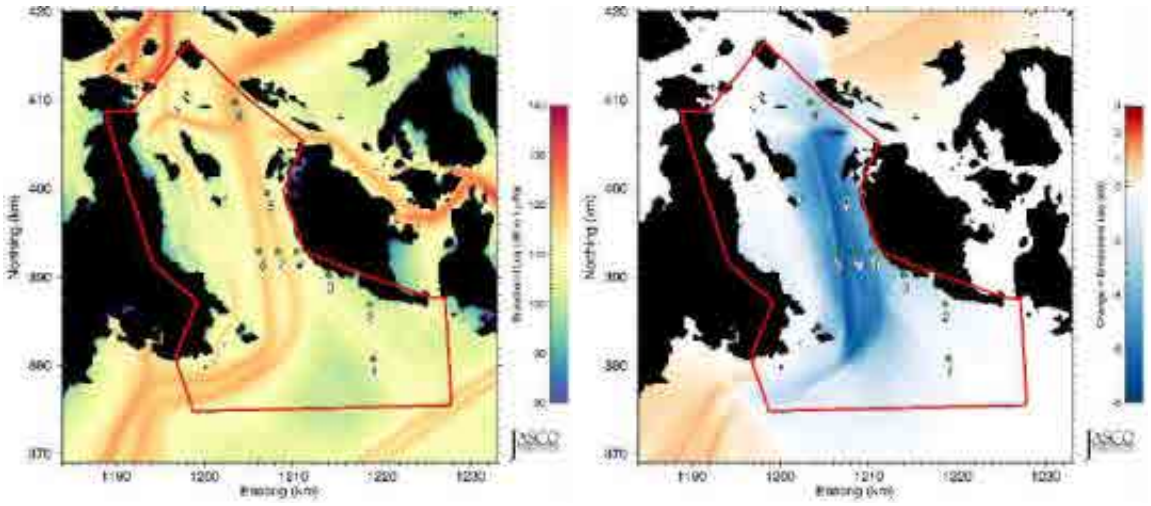

Figure 50. *Haro Strait – Slow-Down, 7-knot speed limit*: Unweighted equivalent continuous noise levels (L_{eq}; left) and change in L_{eq} (right) relative to July 2015 baseline levels. Grid resolution is 200 × 200 m. The green dots are the sample locations in the SRKW critical habitat. The red line shows the boundary of the area where statistical values (percentiles and mean) were derived.

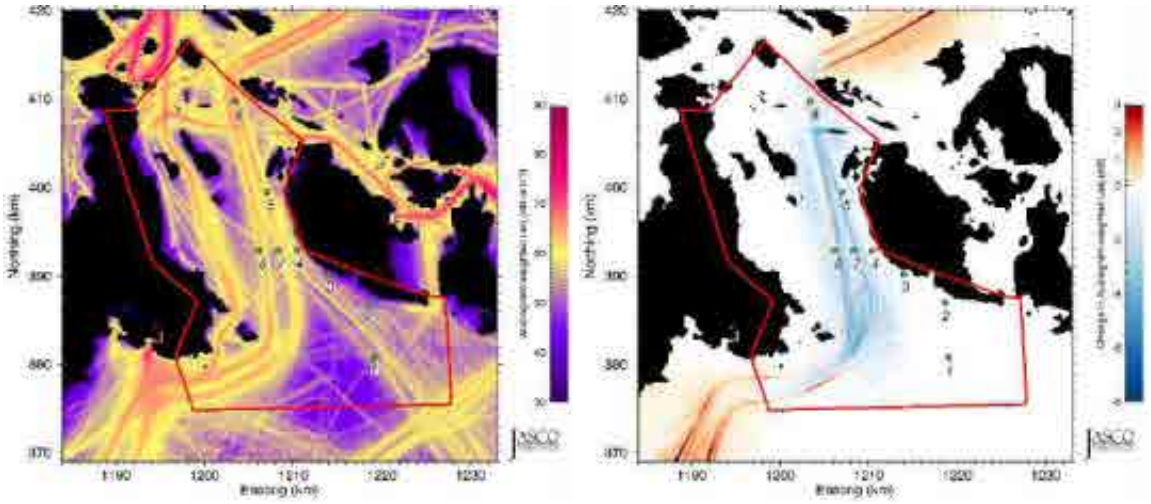

Figure 51. *Haro Strait – Slow-Down, 7-knot speed limit*: Audiogram-weighted equivalent continuous noise levels (L_{eq}; left) and change in L_{eq} (right) relative to July 2015 baseline levels. Grid resolution is 200 × 200 m. The green dots are the sample locations in the SRKW critical habitat. The red line shows the boundary of the area where statistical values (percentiles and mean) were derived.

Table 25. *Haro Strait – Baseline* vs. *Slow-Down*: Unweighted received levels (dB re 1 µPa), changes in received levels (dB), and changes in acoustic intensity (%) at the sample locations in the SRKW critical habitat shown in Figure 6.

Sample location	Baseline (dB re 1 µPa)	11 knots			10 knots			7 knots		
		Mitigated (dB re 1 µPa)	Change		Mitigated (dB re 1 µPa)	Change		Mitigated (dB re 1 µPa)	Change	
			dB	%		dB	%		dB	%
1	109.2	109.2	0.0	0.0	109.2	0.0	0.0	109.2	0.0	0.0
2	103.9	103.5	−0.4	−8.8	103.3	−0.6	−12.9	103.0	−0.9	−18.7
3	106.5	105.1	−1.4	−27.6	104.7	−1.8	−33.9	103.5	−3.0	−49.9
4	114.3	112.5	−1.8	−33.9	111.9	−2.4	−42.5	110.0	−4.3	−62.8
5	119.0	117.0	−2.0	−36.9	116.3	−2.7	−46.3	114.0	−5.0	−68.4
6	123.4	122.8	−0.6	−12.9	122.4	−1.0	−20.6	121.1	−2.3	−41.1
7	122.9	120.5	−2.4	−42.5	119.6	−3.3	−53.2	116.6	−6.3	−76.6
8	123.5	121.0	−2.5	−43.8	120.3	−3.2	−52.1	117.6	−5.9	−74.3

Table 26. *Haro Strait – Baseline* vs. *Slow-Down*: Audiogram-weighted received levels (dB re HT), changes in received levels (dB), and changes in acoustic intensity (%) at the sample locations in the SRKW critical habitat shown in Figure 6.

Sample location	Baseline (dB re HT)	11 knots			10 knots			7 knots		
		Mitigated (dB re HT)	Change		Mitigated (dB re HT)	Change		Mitigated (dB re HT)	Change	
			dB	%		dB	%		dB	%
1	56.2	56.2	0.0	0.0	56.2	0.0	0.0	56.2	0.0	0.0
2	51.6	51.6	0.0	0.0	51.6	0.0	0.0	51.5	−0.1	−2.3
3	46.9	46.7	−0.2	−4.5	46.6	−0.3	−6.7	46.5	−0.4	−8.8
4	56.3	56.1	−0.2	−4.5	56.0	−0.3	−6.7	55.9	−0.4	−8.8
5	60.8	60.7	−0.1	−2.3	60.6	−0.2	−4.5	60.5	−0.3	−6.7
6	64.6	65.0	+0.4	+9.6	64.8	+0.2	+4.7	64.2	−0.4	−8.8
7	65.2	63.3	−1.9	−35.4	62.8	−2.4	−42.5	61.2	−4.0	−60.2
8	66.2	64.9	−1.3	−25.9	64.6	−1.6	−30.8	63.6	−2.6	−45.0

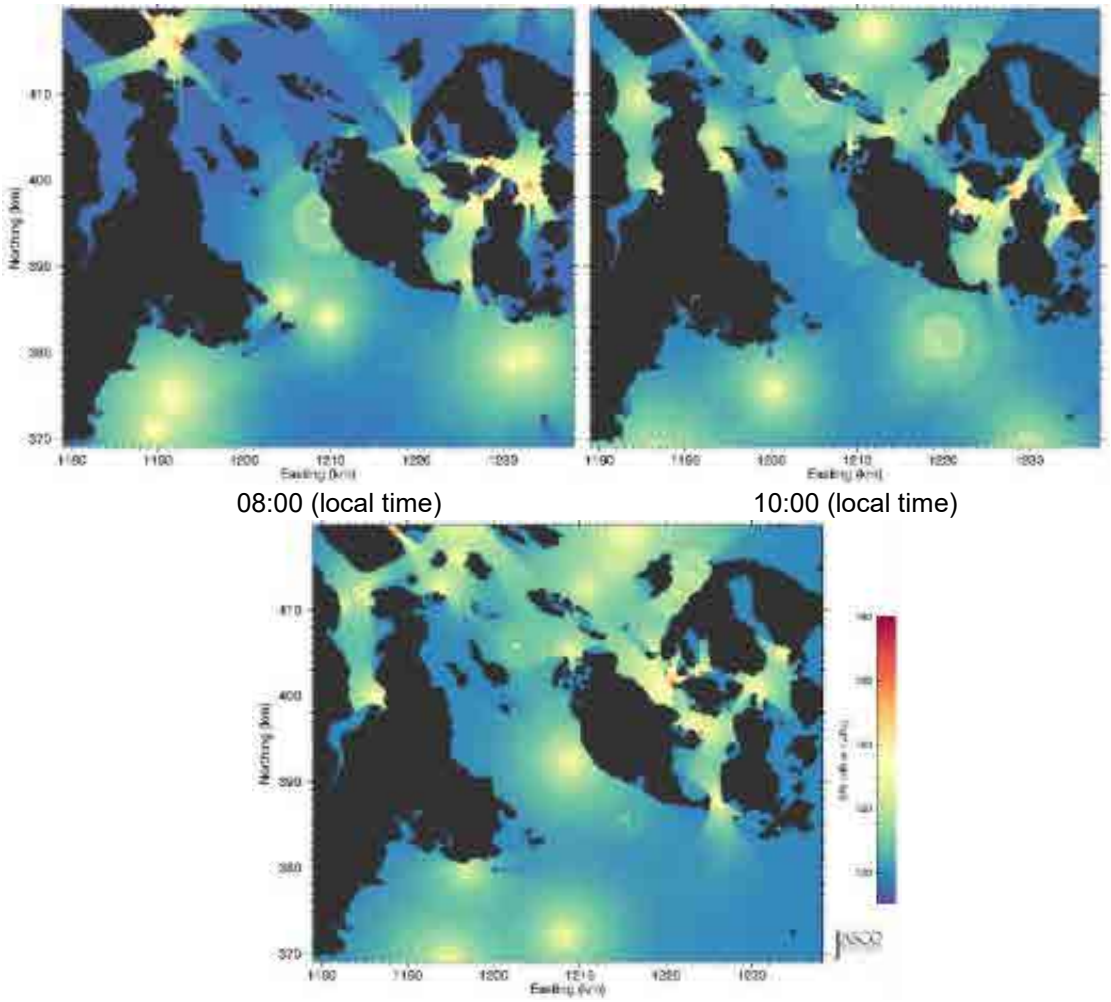

Figure 52. *Haro Strait – Slow-Down (11-knot speed limit):* Example time snapshots of future mitigated SPL (unweighted with ambient, 10 Hz to 50 kHz) from 08:00 to 12:00 (local time) in 2-hour increments. Easting and northing are BC Albers projected coordinates.

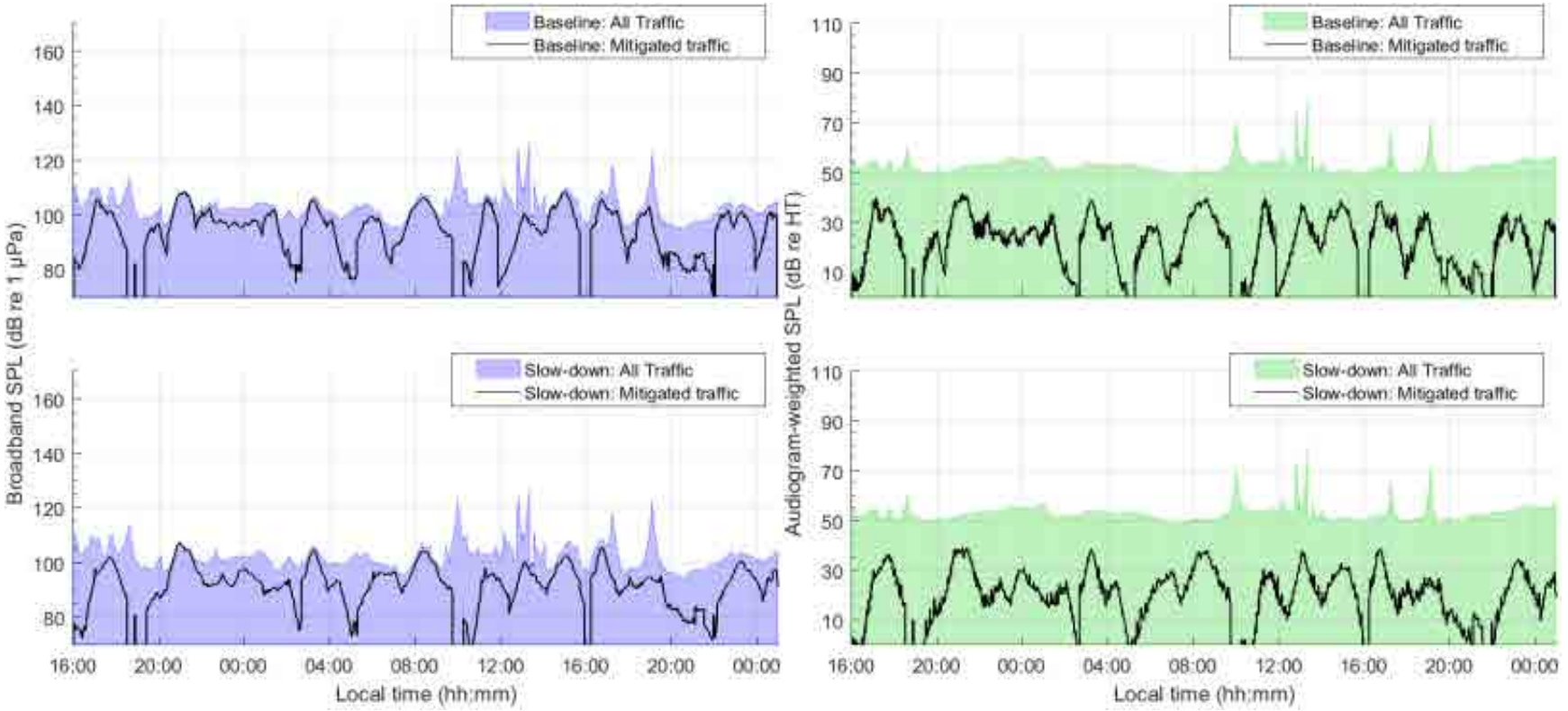

Figure 53. *Haro Strait – Baseline vs Slow-Down (11-knot speed limit), Sample location 1*: Temporal variability of unweighted (left) and audiogram-weighted (right) received levels for (top) baseline (no slow-down) and (bottom) slow-down scenarios. The blue and green lines above the shaded area show received levels caused by all traffic and ambient noise. The black lines show received levels caused by commercial traffic only. The receiver location is shown in Figure 6.

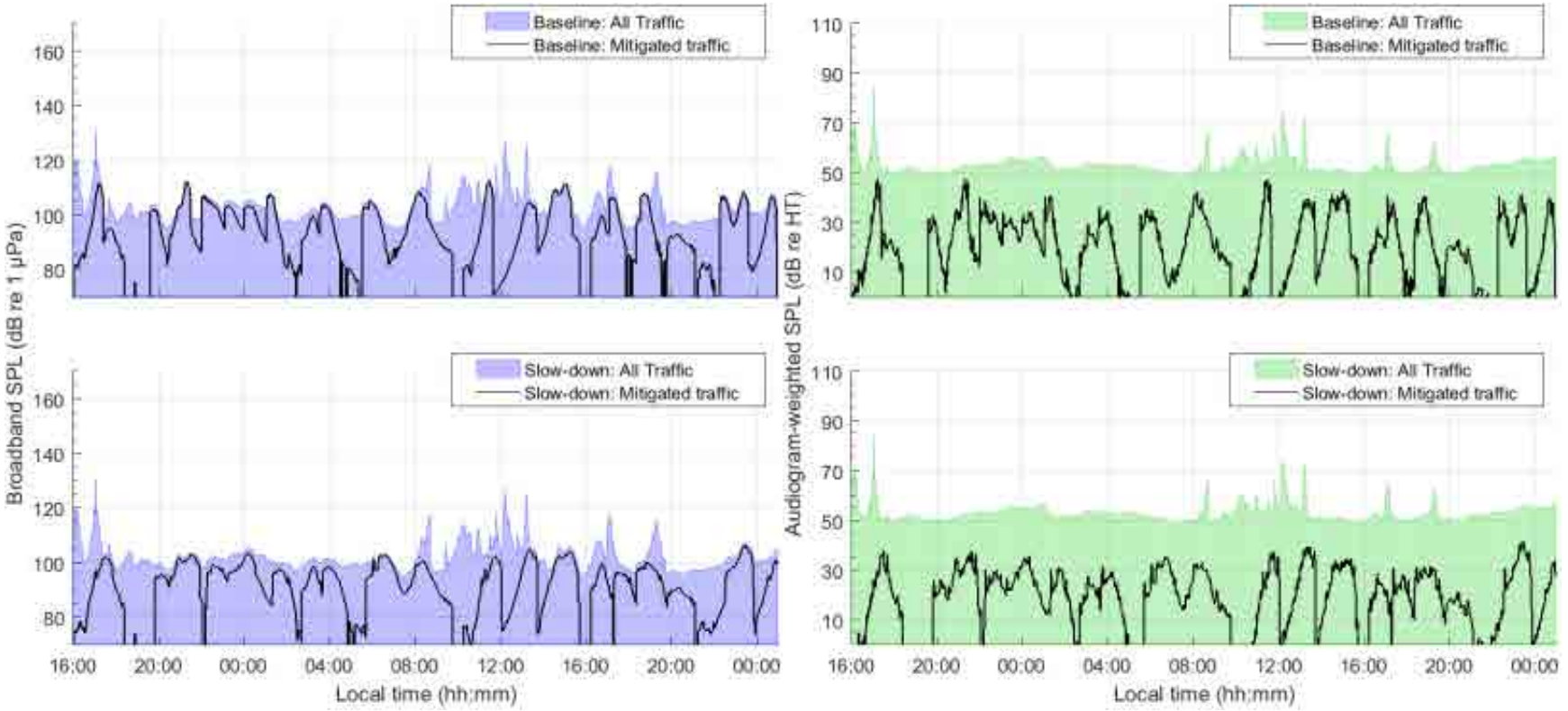

Figure 54. *Haro Strait – Baseline vs Slow-Down (11-knot speed limit), Sample location 2*: Temporal variability of unweighted (left) and audiogram-weighted (right) received levels for (top) baseline (no slow-down) and (bottom) slow-down scenarios. The blue and green lines above the shaded area show received levels caused by all traffic and ambient noise. The black lines show received levels caused by commercial traffic only. The receiver location is shown in Figure 6.

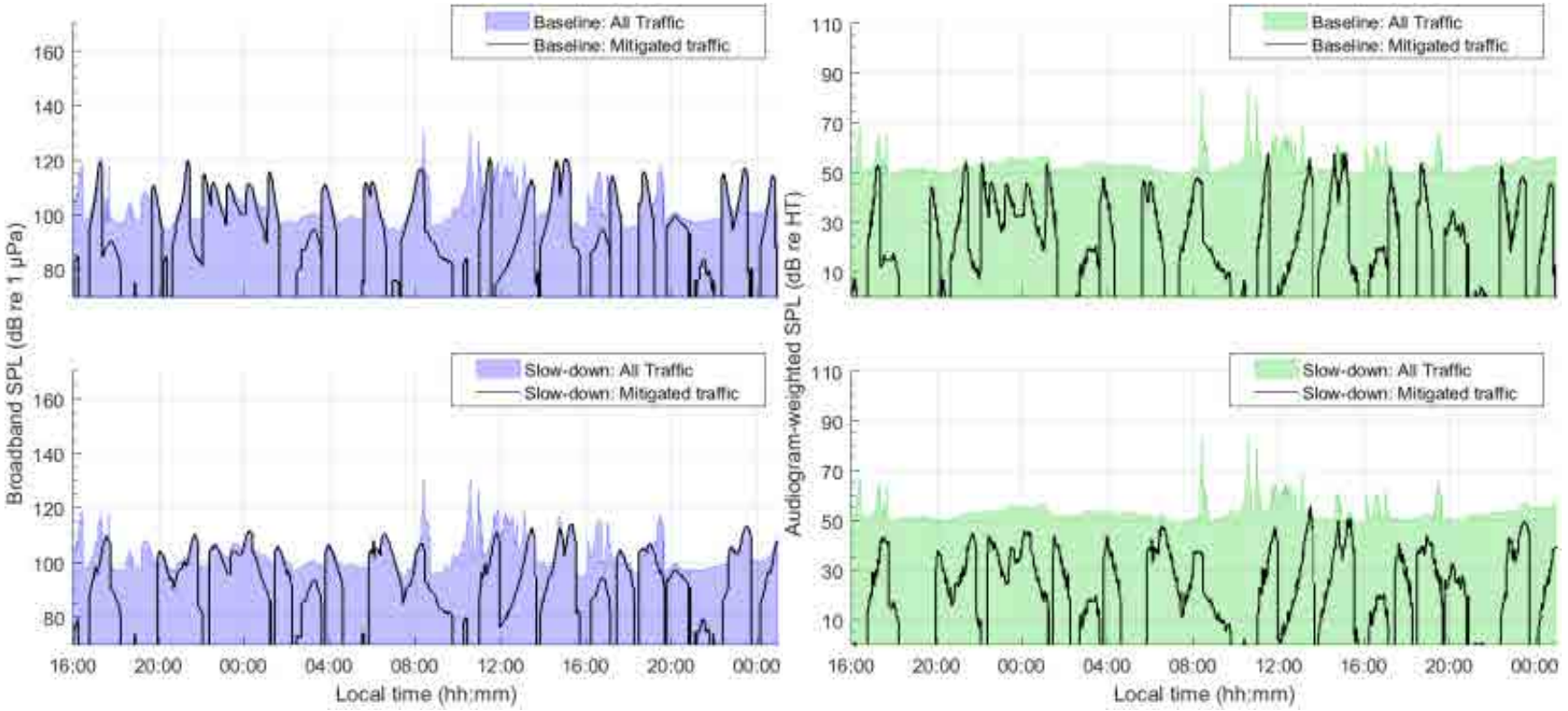

Figure 55. *Haro Strait – Baseline vs Slow-Down (11-knot speed limit), Sample location 3*: Temporal variability of unweighted (left) and audiogram-weighted (right) received levels for (top) baseline (no slow-down) and (bottom) slow-down scenarios. The blue and green lines above the shaded area show received levels caused by all traffic and ambient noise. The black lines show received levels caused by commercial traffic only. The receiver location is shown in Figure 6.

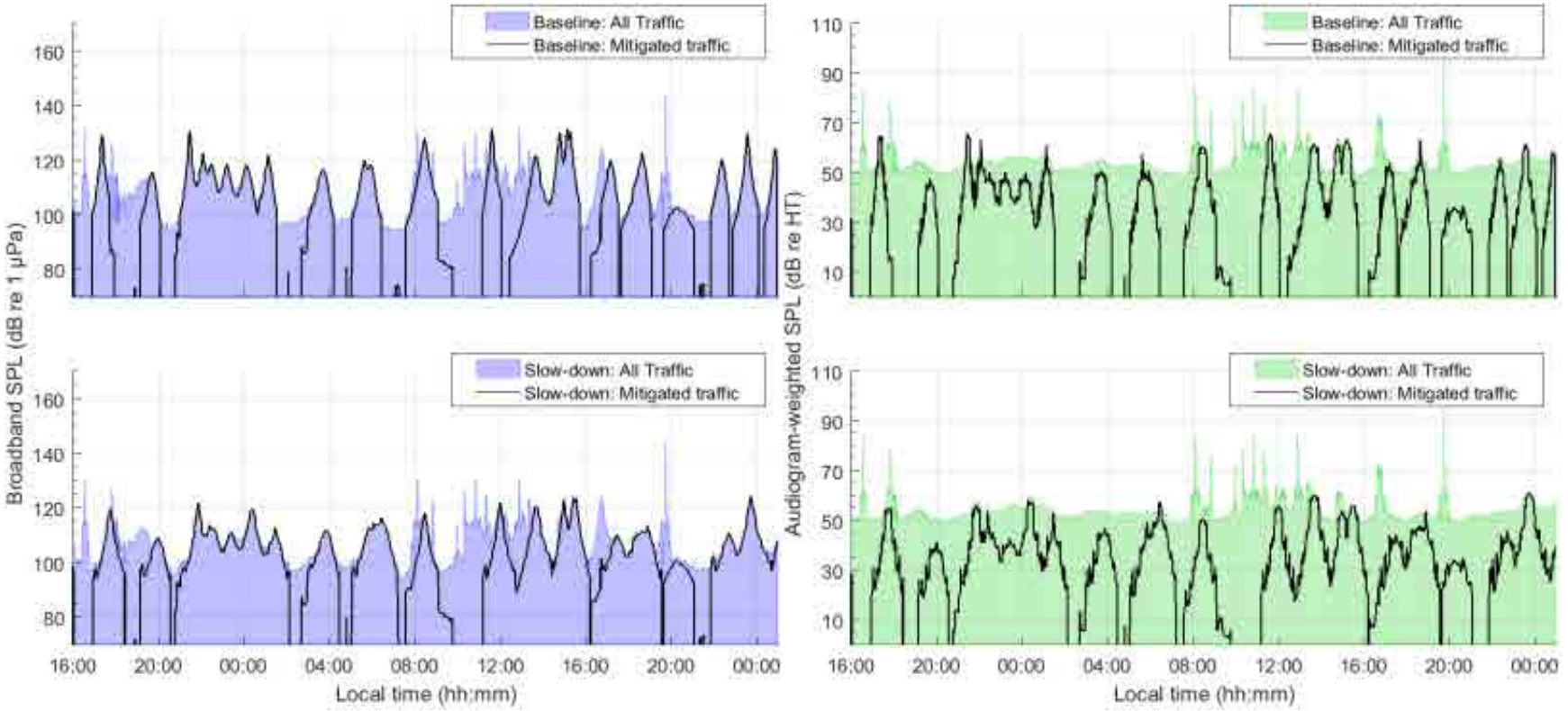

Figure 56. *Haro Strait – Baseline vs Slow-Down (11-knot speed limit), Sample location 4*: Temporal variability of unweighted (left) and audiogram-weighted (right) received levels for (top) baseline (no slow-down) and (bottom) slow-down scenarios. The blue and green lines above the shaded area show received levels caused by all traffic and ambient noise. The black lines show received levels caused by commercial traffic only. The receiver location is shown in Figure 6.

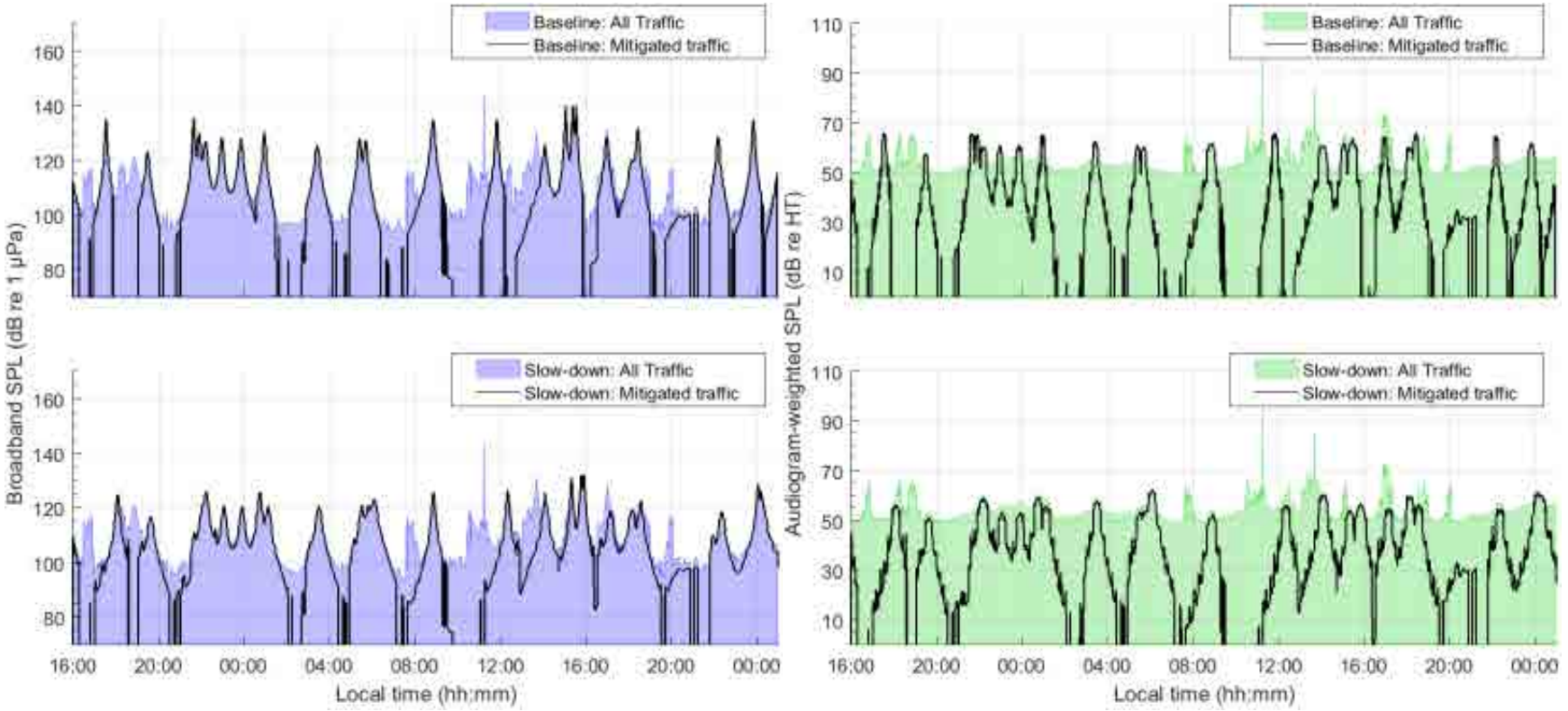

Figure 57. *Haro Strait – Baseline vs Slow-Down (11-knot speed limit), Sample location 5*: Temporal variability of unweighted (left) and audiogram-weighted (right) received levels for (top) baseline (no slow-down) and (bottom) slow-down scenarios. The blue and green lines above the shaded area show received levels caused by all traffic and ambient noise. The black lines show received levels caused by commercial traffic only. The receiver location is shown in Figure 6.

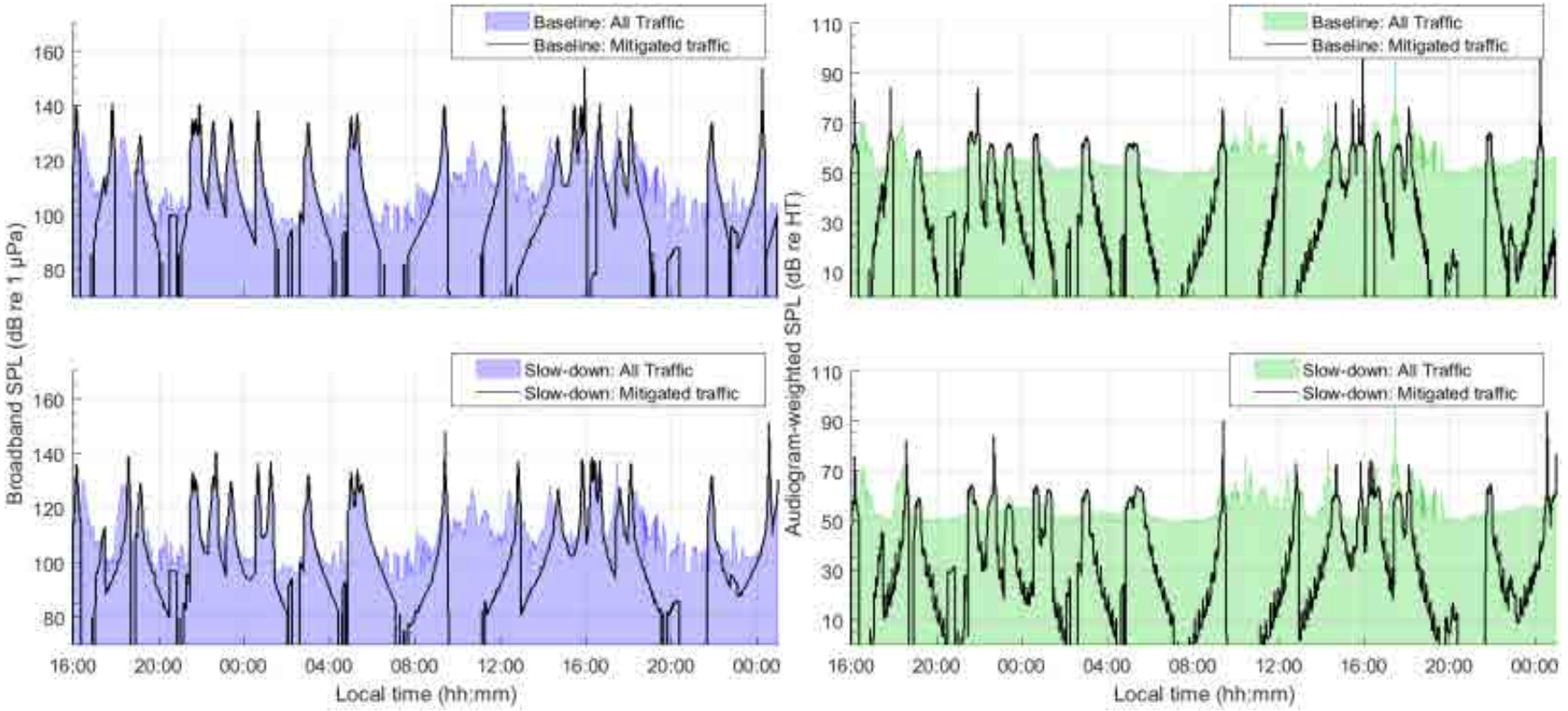

Figure 58. *Haro Strait – Baseline vs Slow-Down (11-knot speed limit), Sample location 6*: Temporal variability of unweighted (left) and audiogram-weighted (right) received levels for (top) baseline (no slow-down) and (bottom) slow-down scenarios. The blue and green lines above the shaded area show received levels caused by all traffic and ambient noise. The black lines show received levels caused by commercial traffic only. The receiver location is shown in Figure 6.

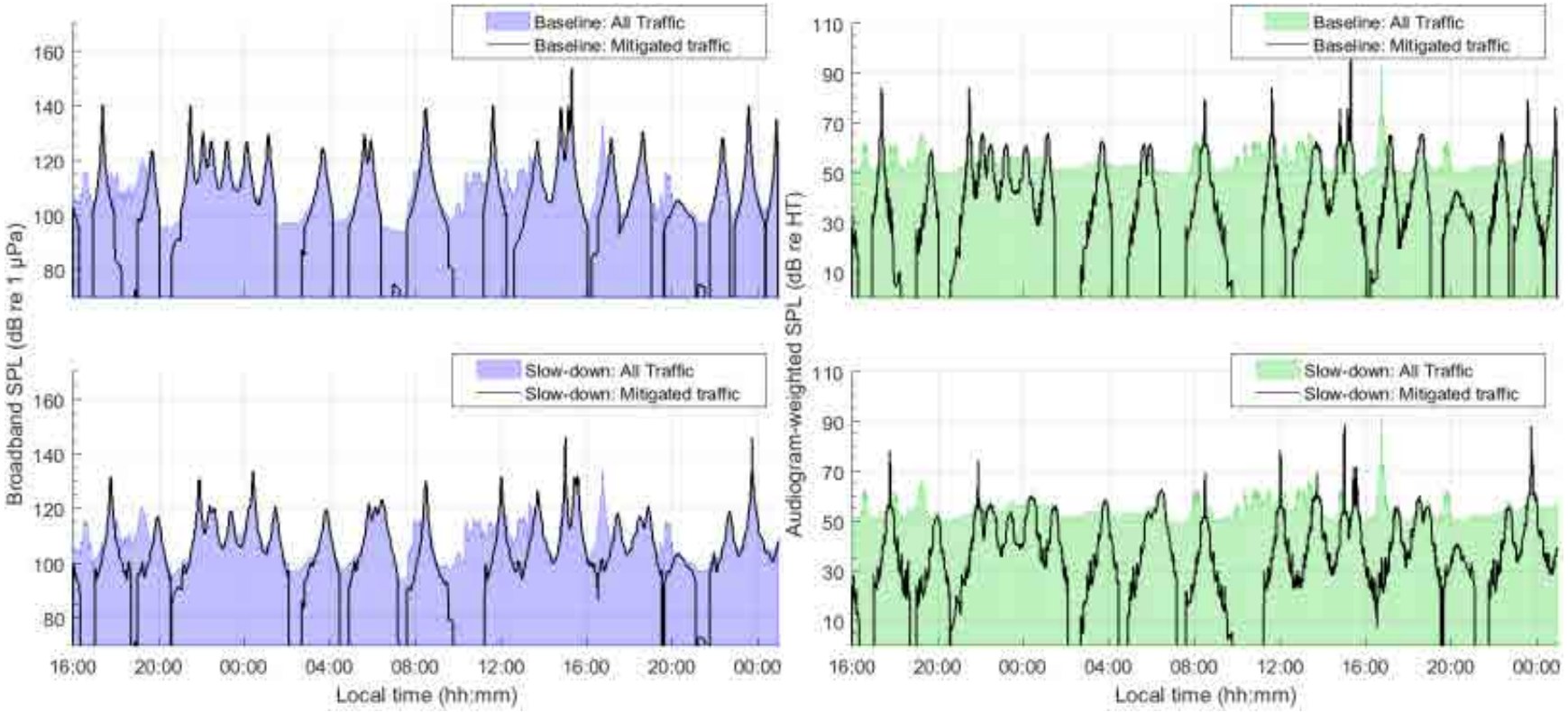

Figure 59. *Haro Strait – Baseline vs Slow-Down (11-knot speed limit), Sample location 7*: Temporal variability of unweighted (left) and audiogram-weighted (right) received levels for (top) baseline (no slow-down) and (bottom) slow-down scenarios. The blue and green lines above the shaded area show received levels caused by all traffic and ambient noise. The black lines show received levels caused by commercial traffic only. The receiver location is shown in Figure 6.

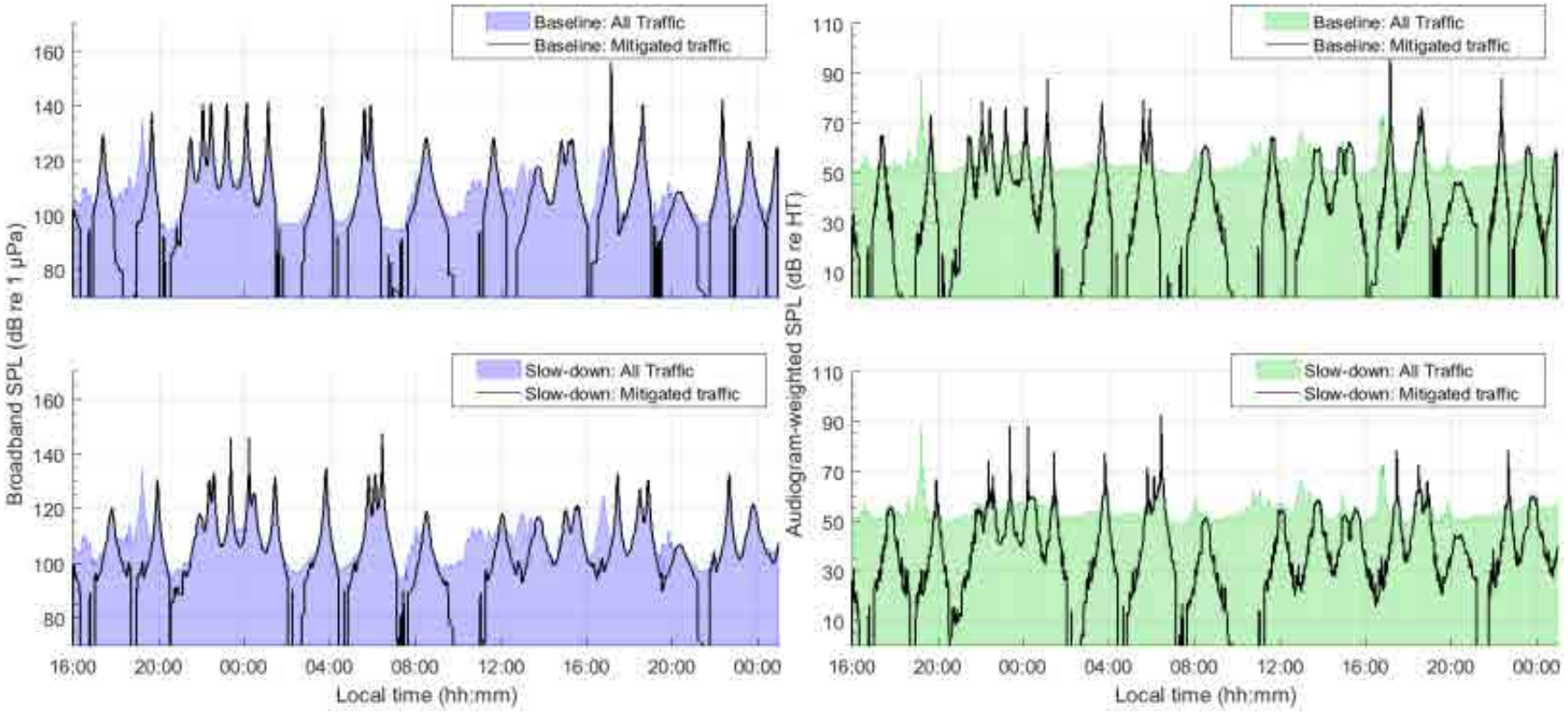

Figure 60. *Haro Strait – Baseline vs Slow-Down (11-knot speed limit), Sample location 8*: Temporal variability of unweighted (left) and audiogram-weighted (right) received levels for (top) baseline (no slow-down) and (bottom) slow-down scenarios. The blue and green lines above the shaded area show received levels caused by all traffic and ambient noise. The black lines show received levels caused by commercial traffic only. The receiver location is shown in Figure 6.

Table 27. *Haro Strait – Baseline vs Slow-Down (11-knot speed limit):* Temporal analysis of unweighted received noise levels (dB re 1 µPa), difference in received noise levels (dB), and difference acoustic intensity (%). The values indicate the percentile or mean calculated over a 33-hour period without (Baseline) and with mitigation (Slow-down), at the sample locations within the SRKW critical habitat shown in Figure 6.

Sample location	Scenario	Temporal analysis of noise level (dB re 1 µPa), difference in noise levels (dB), and difference in acoustic intensity (%)			
		5th	50th	95th	Mean
1	Baseline	96.2	103.0	110.4	103.1 ±4.7
	Slow-down	96.8	102.1	110.4	102.5 ±4.6
	Difference	**+0.6 (+14.8%)**	**−0.9 (−18.7%)**	**0.0 (0.0%)**	**−0.6 (−12.9%)**
2	Baseline	96.0	102.4	113.5	103.2 ±5.5
	Slow-down	96.6	101.3	113.1	102.3 ±4.9
	Difference	**+0.6 (+14.8%)**	**−1.1 (−22.4%)**	**−0.4 (−8.8%)**	**−0.9 (−18.7%)**
3	Baseline	95.5	102.4	117.7	104.4 ±7.2
	Slow-down	96.6	102.4	115.3	103.6 ±5.9
	Difference	**+1.1 (+28.8%)**	**0.0 (0.0%)**	**−2.4 (−42.5%)**	**−0.8 (−16.8%)**
4	Baseline	95.6	108.7	124.2	108.8 ±9.0
	Slow-down	97.5	107.9	119.8	107.7 ±7.0
	Difference	**+1.9 (+54.9%)**	**−0.8 (−16.8%)**	**−4.4 (−63.7%)**	**−1.1 (−22.4%)**
5	Baseline	96.1	109.7	128.1	110.0 ±10.3
	Slow-down	97.1	108.7	123.6	109.2 ±8.6
	Difference	**+1.0 (+25.9%)**	**−1.0 (−20.6%)**	**−4.5 (−64.5%)**	**−0.8 (−16.8%)**
6	Baseline	96.6	110.5	132.8	112.0 ±11.2
	Slow-down	96.8	109.4	130.5	111.3 ±10.6
	Difference	**+0.2 (+4.7%)**	**−1.1 (−22.4%)**	**−2.3 (−41.1%)**	**−0.7 (−14.9%)**
7	Baseline	96.0	109.5	128.3	110.4 ±10.3
	Slow-down	97.5	109.1	123.5	109.6 ±8.3
	Difference	**+1.5 (+41.3%)**	**−0.4 (−8.8%)**	**−4.8 (−66.9%)**	**−0.8 (−16.8%)**
8	Baseline	96.0	108.7	128.6	110.1 ±10.4
	Slow-down	97.5	108.6	125.8	109.5 ±8.7
	Difference	**+1.5 (+41.3%)**	**−0.1 (−2.3%)**	**−2.8 (−47.5%)**	**−0.6 (−12.9%)**

Table 28. *Haro Strait – Baseline vs Slow-Down (11-knot speed limit):* Temporal analysis of SRKW audiogram-weighted received noise levels (dB re HT), difference in received noise levels (dB), and difference acoustic intensity (%). The values indicate the percentile or mean calculated over a 33-hour period without (Baseline) and with mitigation (Slow-down), at the sample locations within the SRKW critical habitat shown in Figure 6.

Sample location	Scenario	Temporal analysis of noise level (dB re HT), difference in noise levels (dB), and difference in acoustic intensity (%)			
		5th	50th	95th	Mean
1	Baseline	49.7	52.5	56.6	52.9 ±3.0
	Slow-down	49.7	52.5	56.6	52.9 ±3.0
	Difference	**0.0 (0.0%)**	**0.0 (0.0%)**	**0.0 (0.0%)**	**0.0 (0.0%)**
2	Baseline	49.6	52.4	59.5	53.1 ±3.5
	Slow-down	49.6	52.3	59.4	53.1 ±3.5
	Difference	**0.0 (0.0%)**	**−0.1 (−2.3%)**	**−0.1 (−2.3%)**	**0.0 (0.0%)**
3	Baseline	49.6	52.7	61.6	53.6 ±3.8
	Slow-down	49.7	52.4	61.6	53.4 ±3.8
	Difference	**+0.1 (+2.3%)**	**−0.3 (−6.7%)**	**0.0 (0.0%)**	**−0.2 (−4.5%)**
4	Baseline	49.8	53.5	63.5	54.8 ±4.8
	Slow-down	49.9	53.3	61.8	54.4 ±4.5
	Difference	**+0.1 (+2.3%)**	**−0.2 (−4.5%)**	**−1.7 (−32.4%)**	**−0.4 (−8.8%)**
5	Baseline	49.8	53.6	65.2	55.4 ±5.1
	Slow-down	49.8	53.6	64.0	54.9 ±4.5
	Difference	**0.0 (0.0%)**	**0.0 (0.0%)**	**−1.2 (−24.1%)**	**−0.5 (−10.9%)**
6	Baseline	50.0	54.6	66.7	56.4 ±6.0
	Slow-down	49.9	54.4	66.0	56.0 ±5.7
	Difference	**−0.1 (−2.3%)**	**−0.2 (−4.5%)**	**−0.7 (−14.9%)**	**−0.4 (−8.8%)**
7	Baseline	49.8	53.9	64.8	55.6 ±5.3
	Slow-down	50.0	53.9	62.6	55.1 ±4.5
	Difference	**+0.2 (+4.7%)**	**0.0 (0.0%)**	**−2.2 (−39.7%)**	**−0.5 (−10.9%)**
8	Baseline	49.9	53.7	66.3	55.4 ±5.5
	Slow-down	50.2	53.7	63.3	55.0 ±4.8
	Difference	**+0.3 (+7.2%)**	**0.0 (0.0%)**	**−3.0 (−49.9%)**	**−0.4 (−8.8%)**

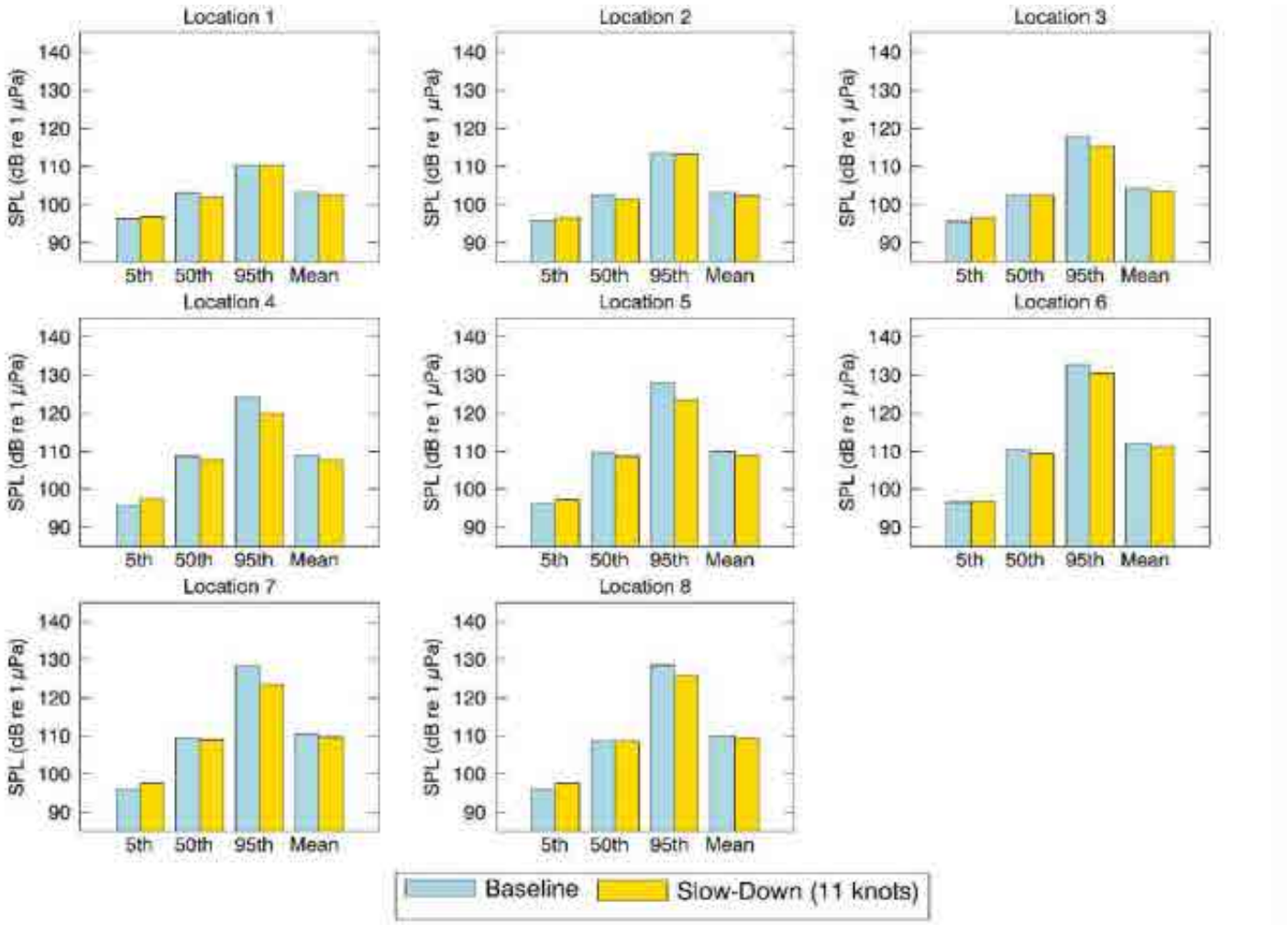

Figure 61. *Haro Strait – Baseline vs Slow-Down (11-knot speed limit)*: Histogram representation of the temporal analysis of unweighted received noise levels (dB re 1 µPa). The vertical bars indicate the percentile or mean calculated over a 33-hour period without (baseline) and with mitigation, at the sample locations within the SRKW critical habitat shown in Figure 6.

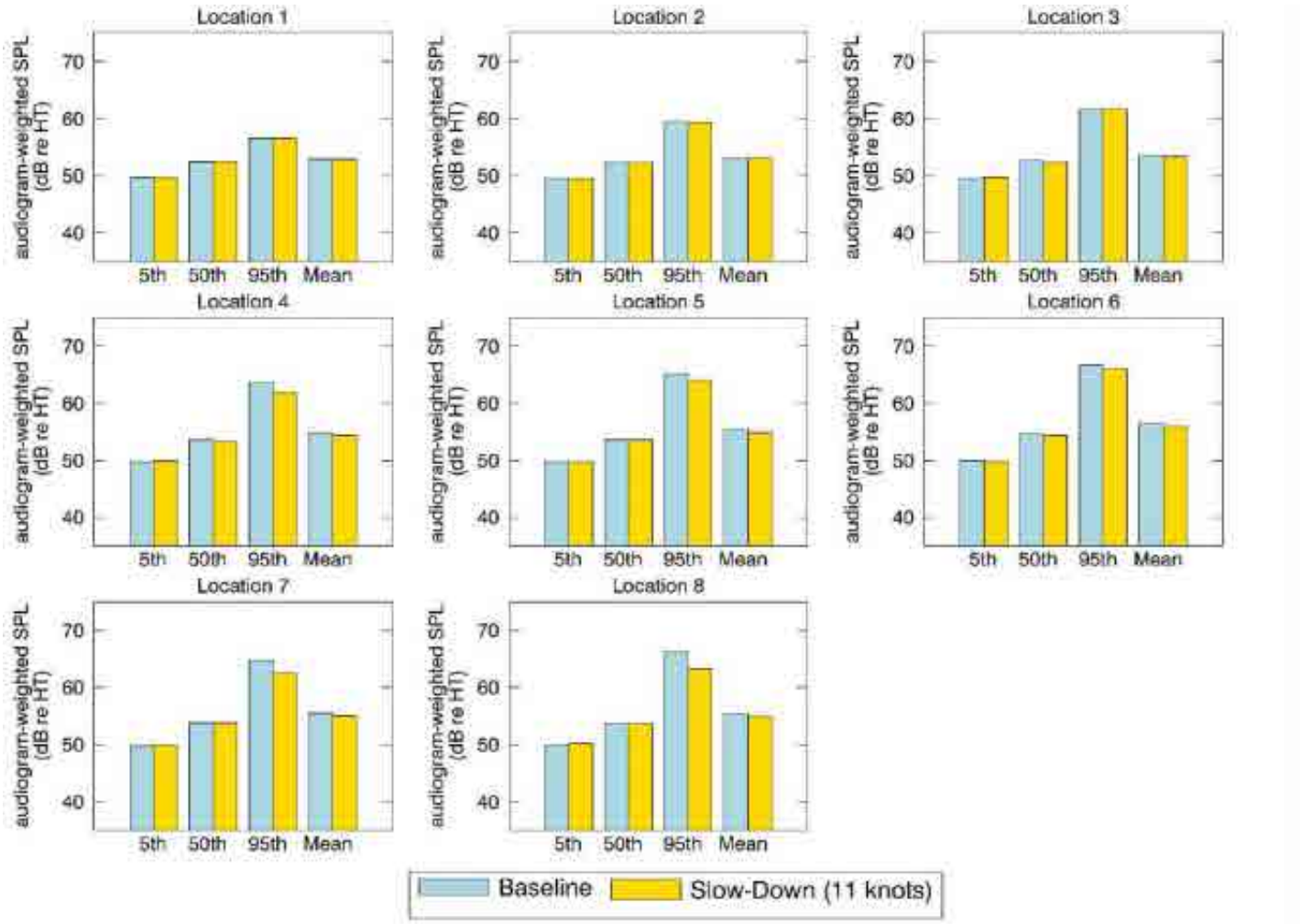

Figure 62. *Haro Strait – Baseline vs Slow-Down (11-knot speed limit):* Histogram representation of the temporal analysis of SRKW audiogram-weighted received noise levels (dB re HT). The vertical bars indicate the percentile or mean calculated over a 33-hour period without (baseline) and with mitigation, at the sample locations within the SRKW critical habitat shown in Figure 6.

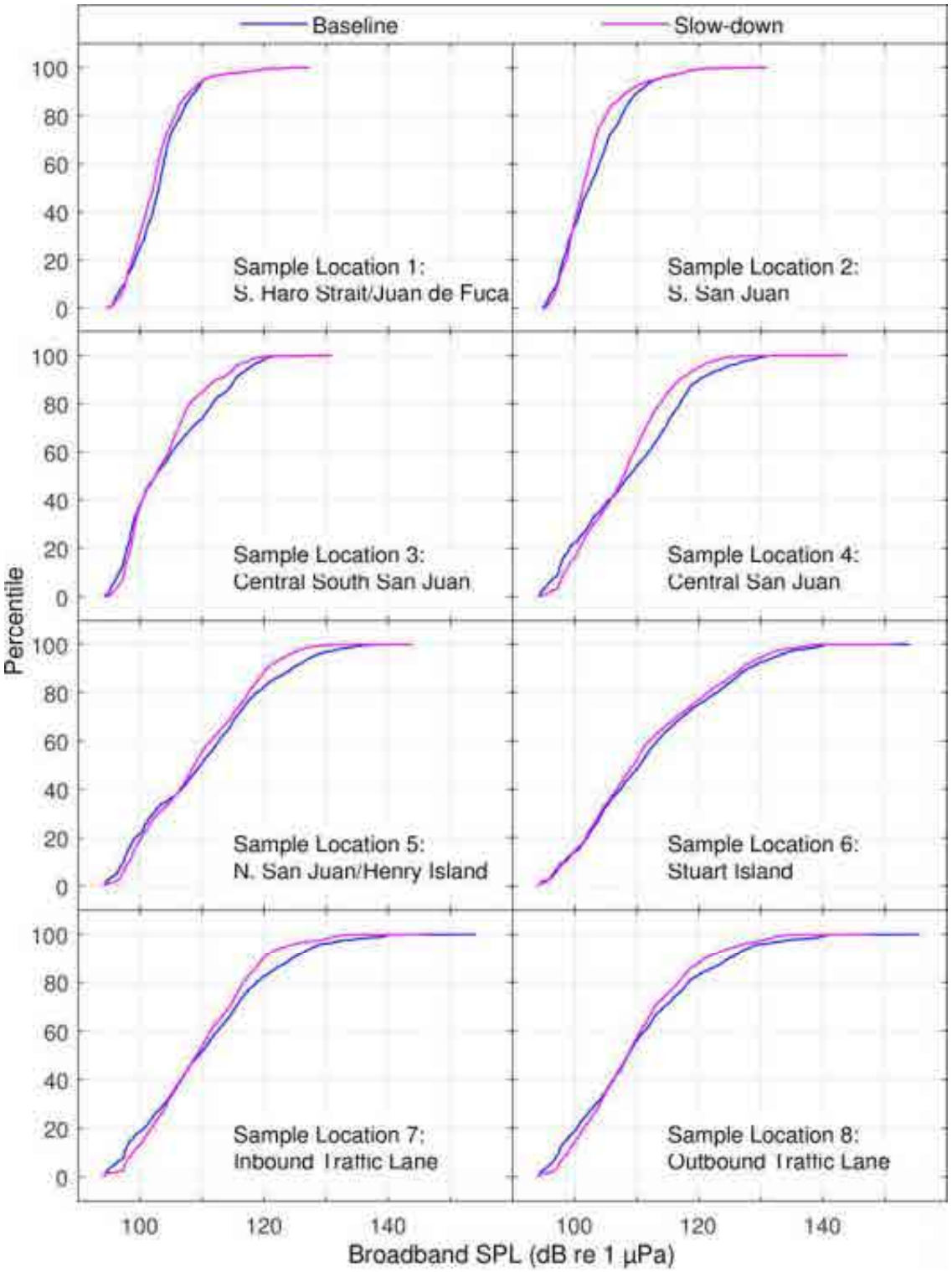

Figure 63. *Haro Strait – Baseline vs Slow-Down (11-knot speed limit):* CDF curves of time-dependent unweighted SPL for baseline and mitigated scenarios at the sample locations shown in Figure 6.

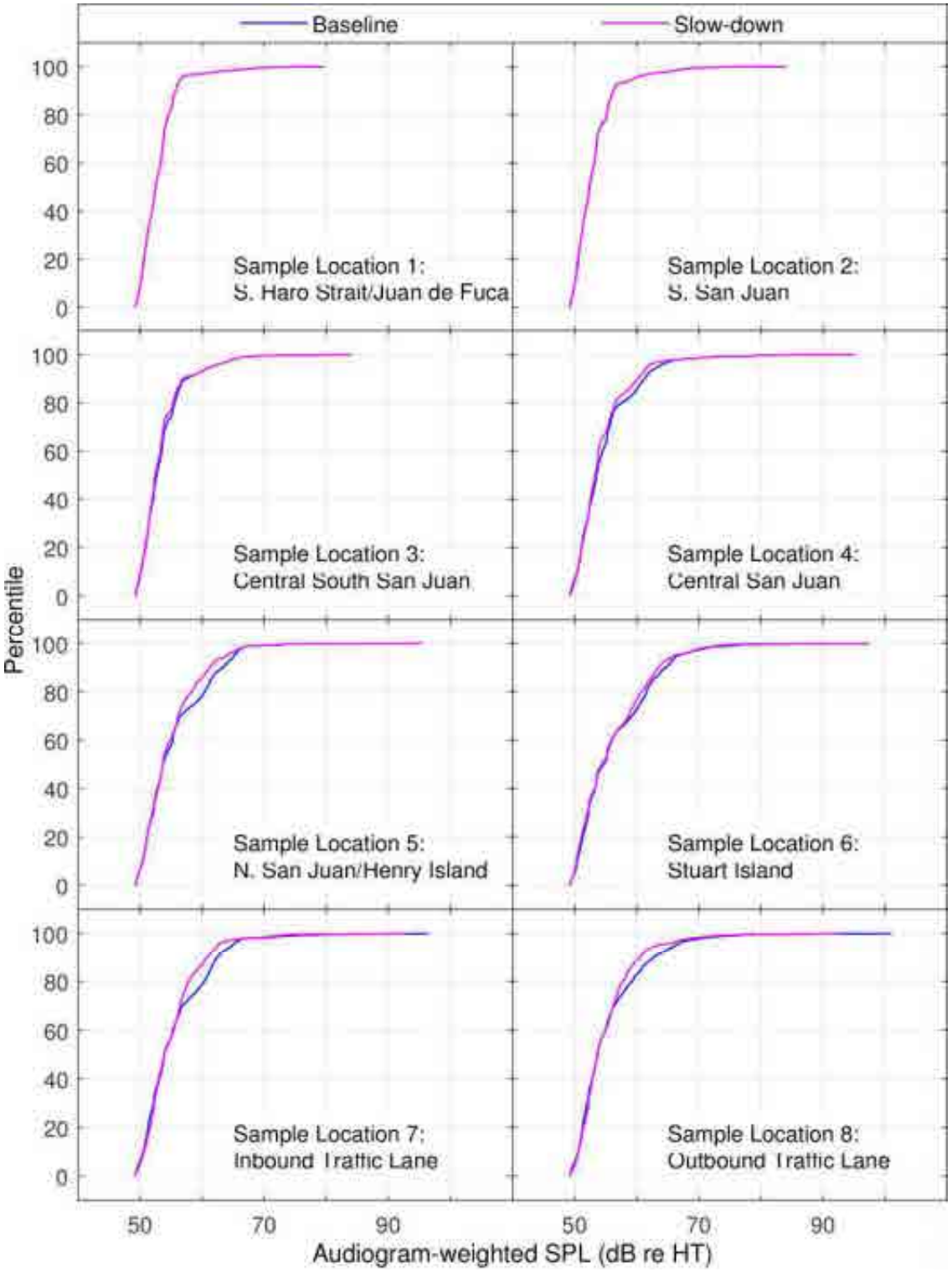

Figure 64. *Haro Strait – Baseline vs Slow-Down (11-knot speed limit):* CDF curves of time-dependent audiogram-weighted SPL for baseline and mitigated scenarios at the sample locations shown in Figure 6.

3.3.3. Juan de Fuca Strait

Time-averaged results for two speed limit alternatives (a maximum speed of 11 knots and a dual maximum speed of 11 or 15 knots, through the Juan de Fuca Strait shipping lanes) are presented in Figures 65–68 and Tables 29–30. In Figures 65–68, the maps on the top present the L_{eq} and the maps on the bottom present the change in L_{eq} with respect to baseline levels for July, seen in Figure 19. Tables 29 and 30 compare baseline and mitigated L_{eq} with three speed limits at nine sample locations in the SRKW critical habitat. The sample locations are shown as green dots in Figures 65–68.

Figures 69–82 and Tables 31–32 present the time-dependent results for a maximum speed of 11 knots for all commercial traffic though the Juan de Fuca Strait shipping lanes.

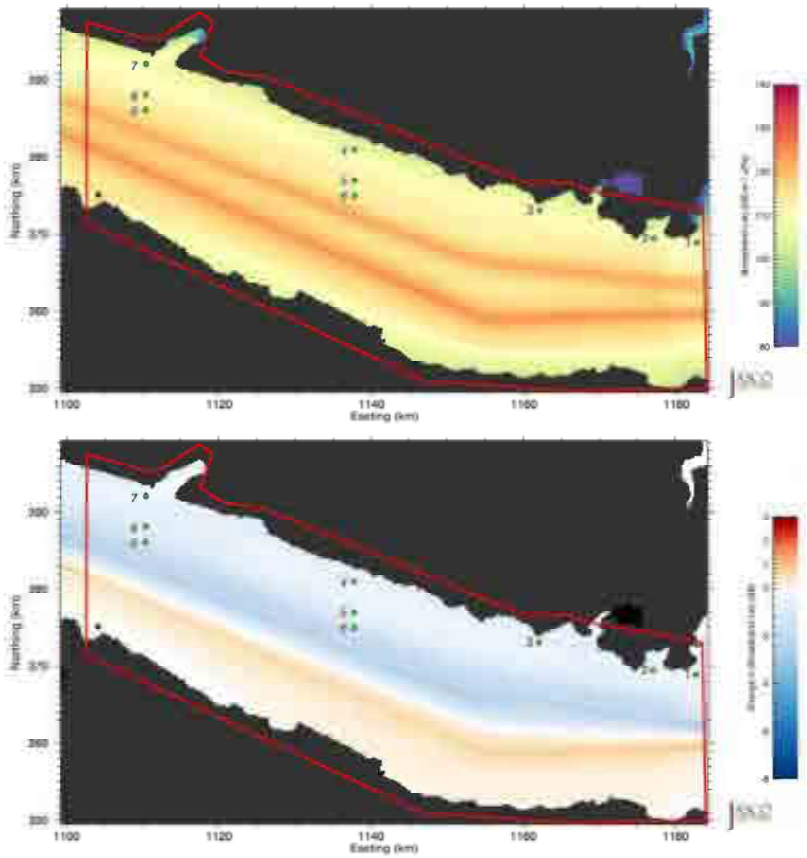

Figure 65. *Juan de Fuca Strait – Slow-Down, 11-knot speed limit*: Unweighted equivalent continuous noise levels (L_{eq}; top) and change in L_{eq} (bottom) relative to July 2015 baseline levels. Grid resolution is 200 × 200 m. The green dots are the sample locations in the SRKW critical habitat. The red line shows the boundary of the area where statistical values (percentiles and mean) were derived.

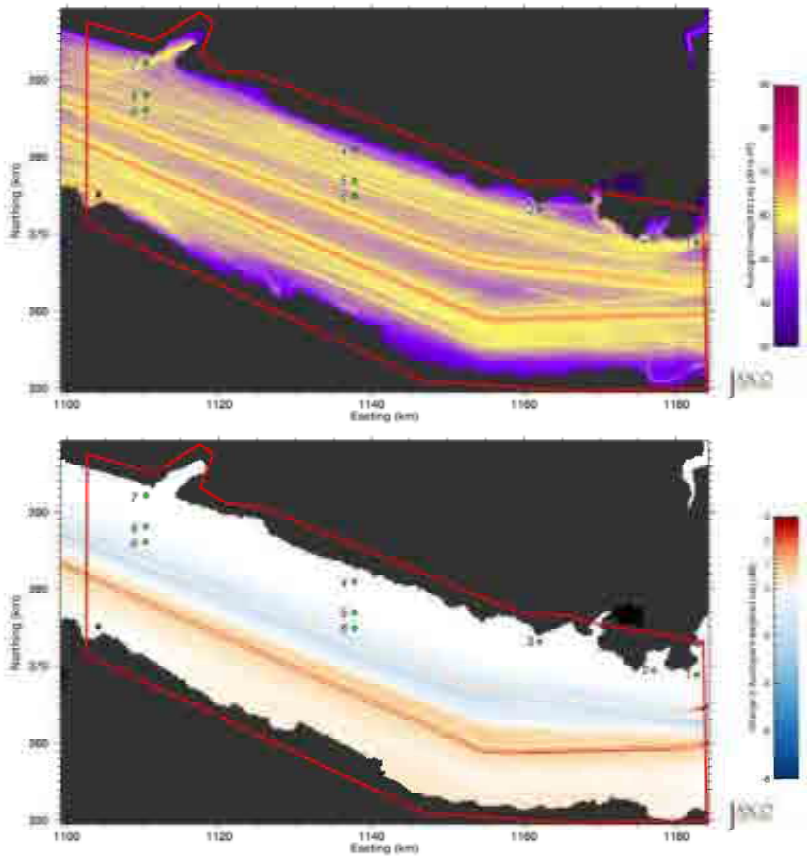

Figure 66. *Juan de Fuca Strait – Slow-Down, 11-knot speed limit*: Audiogram-weighted equivalent continuous noise levels (L_{eq}; top) and change in L_{eq} (bottom) relative to July 2015 baseline levels. Grid resolution is 200 × 200 m. The green dots are the sample locations in the SRKW critical habitat. The red line shows the boundary of the area where statistical values (percentiles and mean) were derived.

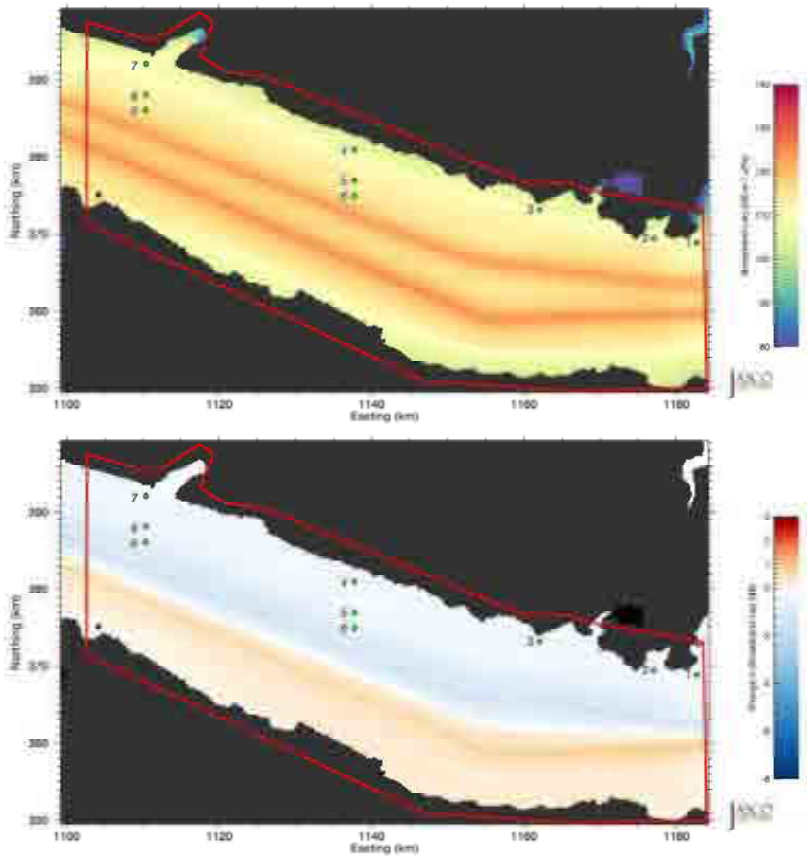

Figure 67. *Juan de Fuca Strait – Slow-Down, 11- and 15-knot speed limits*: Unweighted equivalent continuous noise levels (L_{eq}; top) and change in L_{eq} (bottom) relative to July 2015 baseline levels. Grid resolution is 200 × 200 m. The green dots are the sample locations in the SRKW critical habitat. The red line shows the boundary of the area where statistical values (percentiles and mean) were derived.

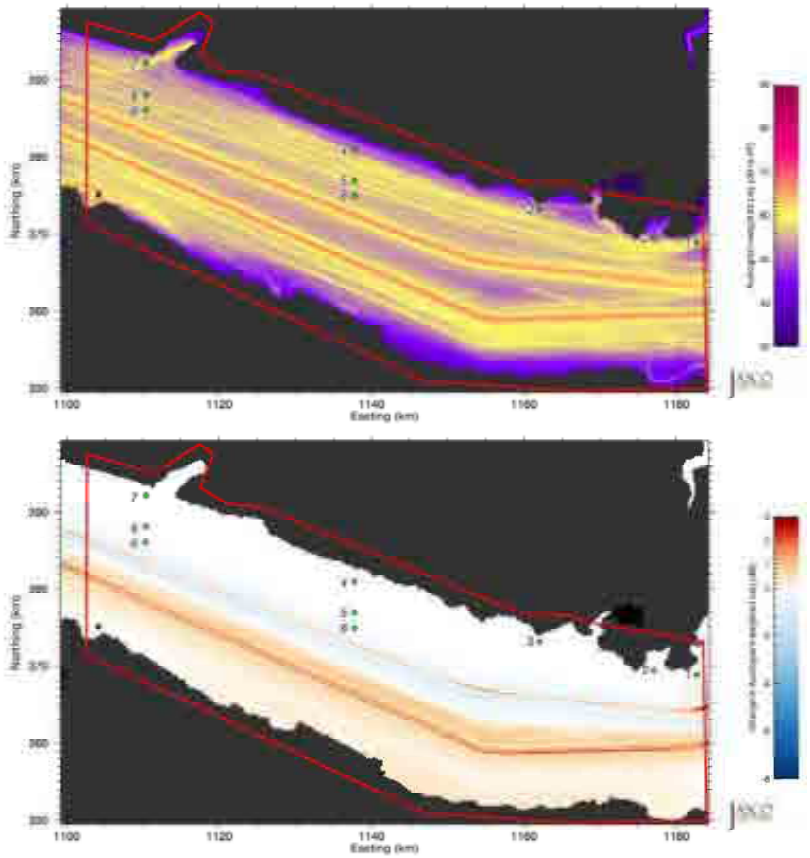

Figure 68. *Juan de Fuca Strait – Slow-Down, 11- and 15-knot speed limits*: Audiogram-weighted equivalent continuous noise levels (L_{eq}; top) and change in L_{eq} (bottom) relative to July 2015 baseline levels. Grid resolution is 200 × 200 m. The green dots are the sample locations in the SRKW critical habitat. The red line shows the boundary of the area where statistical values (percentiles and mean) were derived.

Table 29. *Juan de Fuca Strait – Baseline* vs. *Slow-Down*: Unweighted received levels (dB re 1 µPa), changes in received levels (dB), and changes in acoustic intensity (%) at the sample locations in the SRKW critical habitat shown in Figure 7.

Sample location	Baseline (dB re 1 µPa)	11 knots			11 and 15 knots		
		Mitigated (dB re 1 µPa)	Change		Mitigated (dB re 1 µPa)	Change	
			dB	%		dB	%
1	111.4	111.2	−0.2	−4.5	111.3	−0.1	−2.3
2	111.6	111	−0.6	−12.9	111.3	−0.3	−6.7
3	110.2	109.6	−0.6	−12.9	109.9	−0.3	−6.7
4	109.9	109.4	−0.5	−10.9	109.7	−0.2	−4.5
5	113.8	112.8	−1.0	−20.6	113.3	−0.5	−10.9
6	117.5	115.7	−1.8	−33.9	116.6	−0.9	−18.7
7	109.6	109.1	−0.5	−10.9	109.4	−0.2	−4.5
8	114	112.8	−1.2	−24.1	113.4	−0.6	−12.9
9	117.5	115.7	−1.8	−33.9	116.6	−0.9	−18.7

Table 30. *Juan de Fuca Strait – Baseline* vs. *Slow-Down*: Audiogram-weighted received levels (dB re HT), changes in received levels (dB), and changes in acoustic intensity (%) at the sample locations in the SRKW critical habitat shown in Figure 7.

Sample location	Baseline (dB re HT)	11 knots			11 and 15 knots		
		Mitigated (dB re HT)	Change		Mitigated (dB re HT)	Change	
			dB	%		dB	%
1	59.1	59.1	0.0	0.0	59.1	0.0	0.0
2	56.9	56.9	0.0	0.0	56.9	0.0	0.0
3	55.4	55.4	0.0	0.0	55.4	0.0	0.0
4	56.6	56.6	0.0	0.0	56.6	0.0	0.0
5	55.6	55.5	−0.1	−2.3	55.5	−0.1	−2.3
6	56.3	55.6	−0.7	−14.9	56.1	−0.2	−4.5
7	55	55	0.0	0.0	55	0.0	0.0
8	55.9	55.8	−0.1	−2.3	55.9	0.0	0.0
9	55.9	55.4	−0.5	−10.9	55.8	−0.1	−2.3

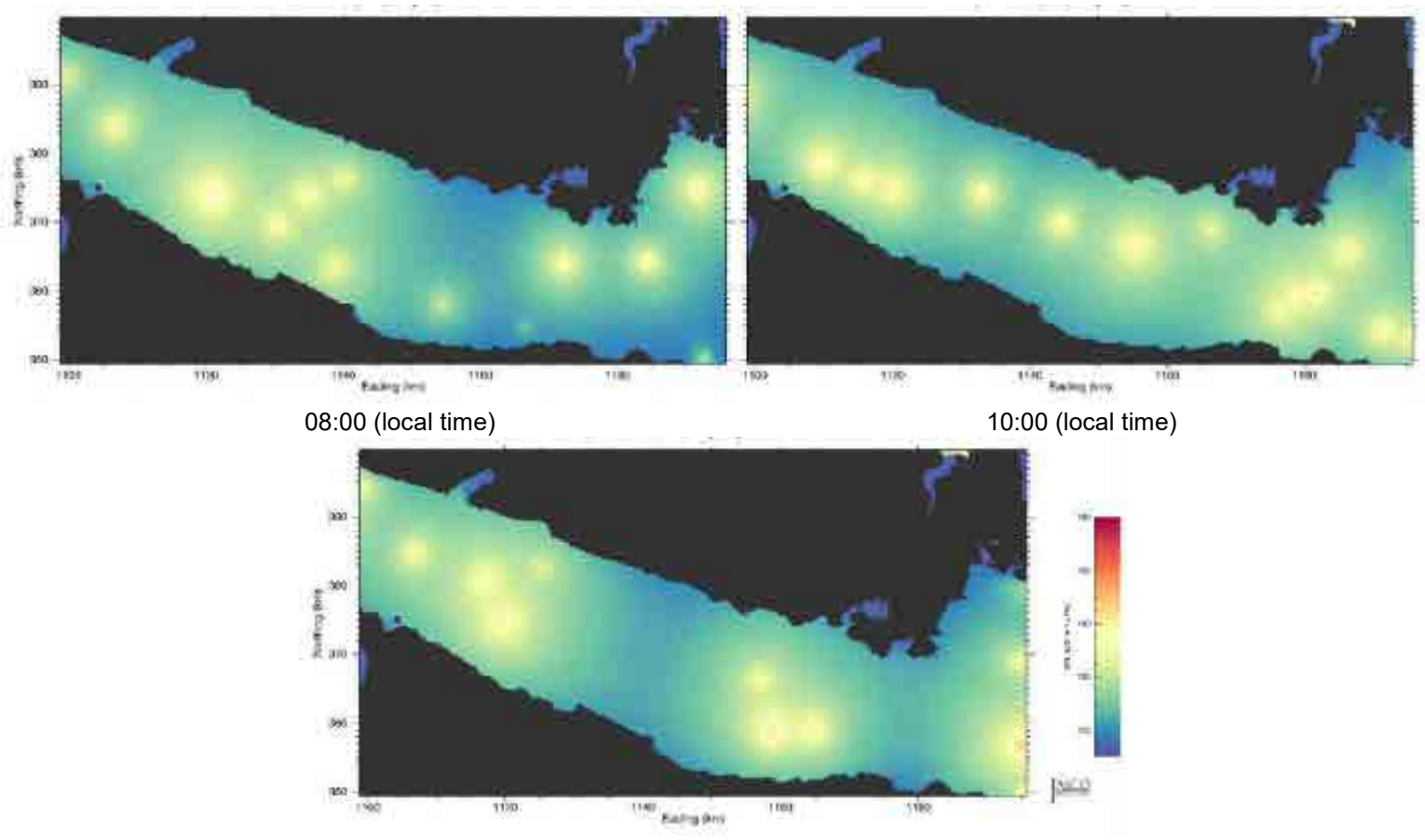

Figure 69. *Juan de Fuca Strait – Slow-Down (11-knot speed limit):* Example time snapshots of future mitigated SPL (unweighted with ambient, 10 Hz to 50 kHz) from 08:00 to 12:00 (local time) in 2-hour increments. Easting and northing are BC Albers projected coordinates.

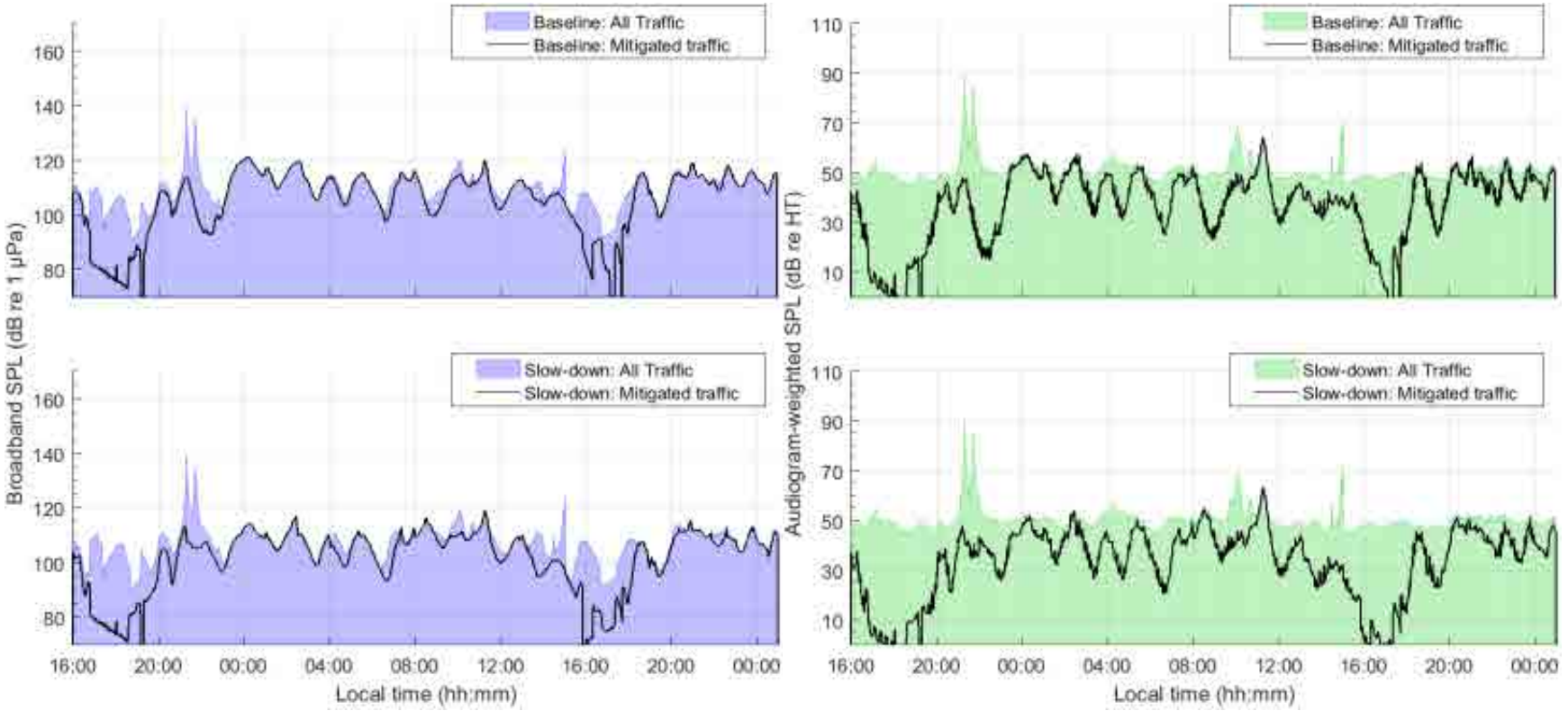

Figure 70. *Juan de Fuca Strait – Baseline vs Slow-Down (11-knot speed limit), Sample location 1*: Temporal variability of unweighted (left) and audiogram-weighted (right) received levels for (top) baseline (no slow-down) and (bottom) slow-down scenarios. The blue and green lines above the shaded area show received levels caused by all traffic and ambient noise. The black lines show received levels caused by commercial traffic only. The receiver location is shown in Figure 7.

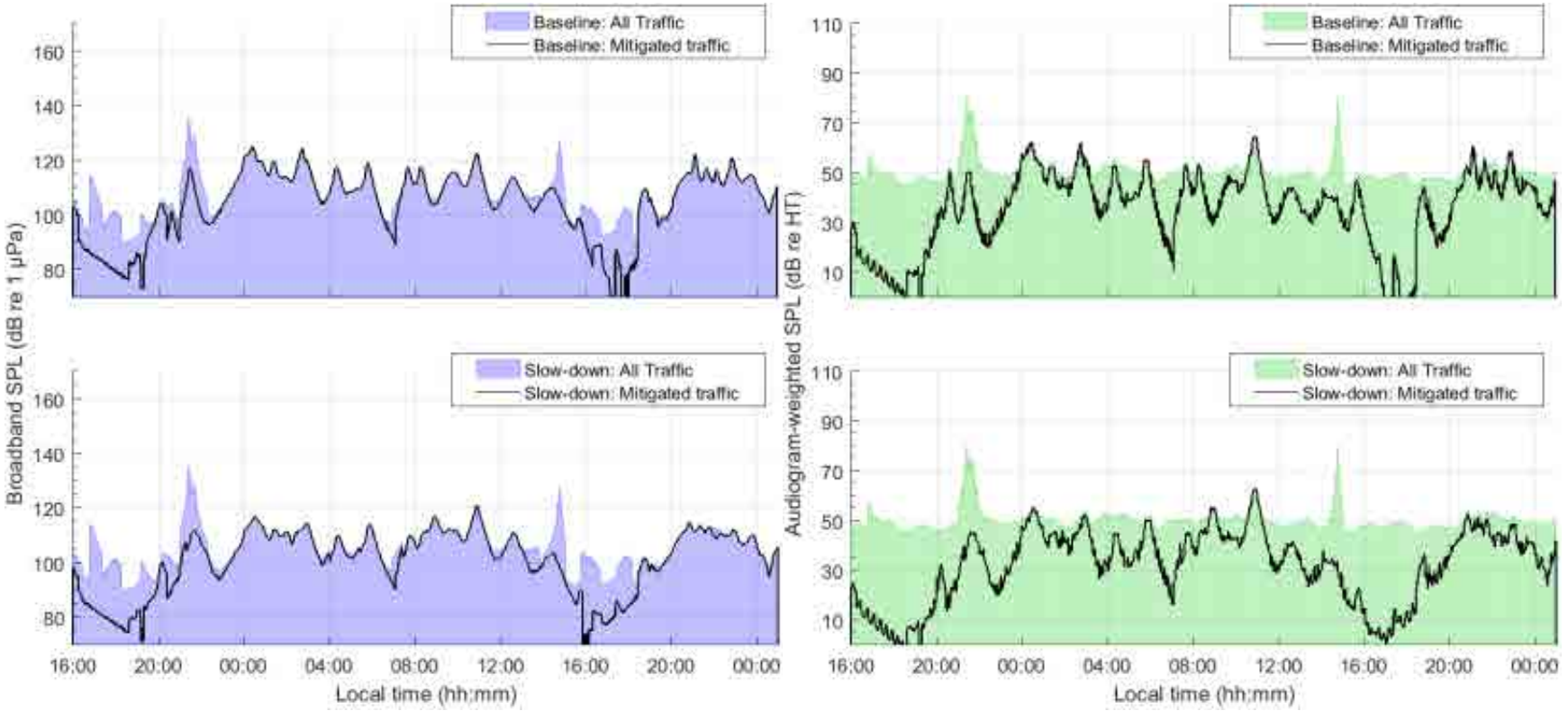

Figure 71. *Juan de Fuca Strait – Baseline vs Slow-Down (11-knot speed limit), Sample location 2*: Temporal variability of unweighted (left) and audiogram-weighted (right) received levels for (top) baseline (no slow-down) and (bottom) slow-down scenarios. The blue and green lines above the shaded area show received levels caused by all traffic and ambient noise. The black lines show received levels caused by commercial traffic only. The receiver location is shown in Figure 7.

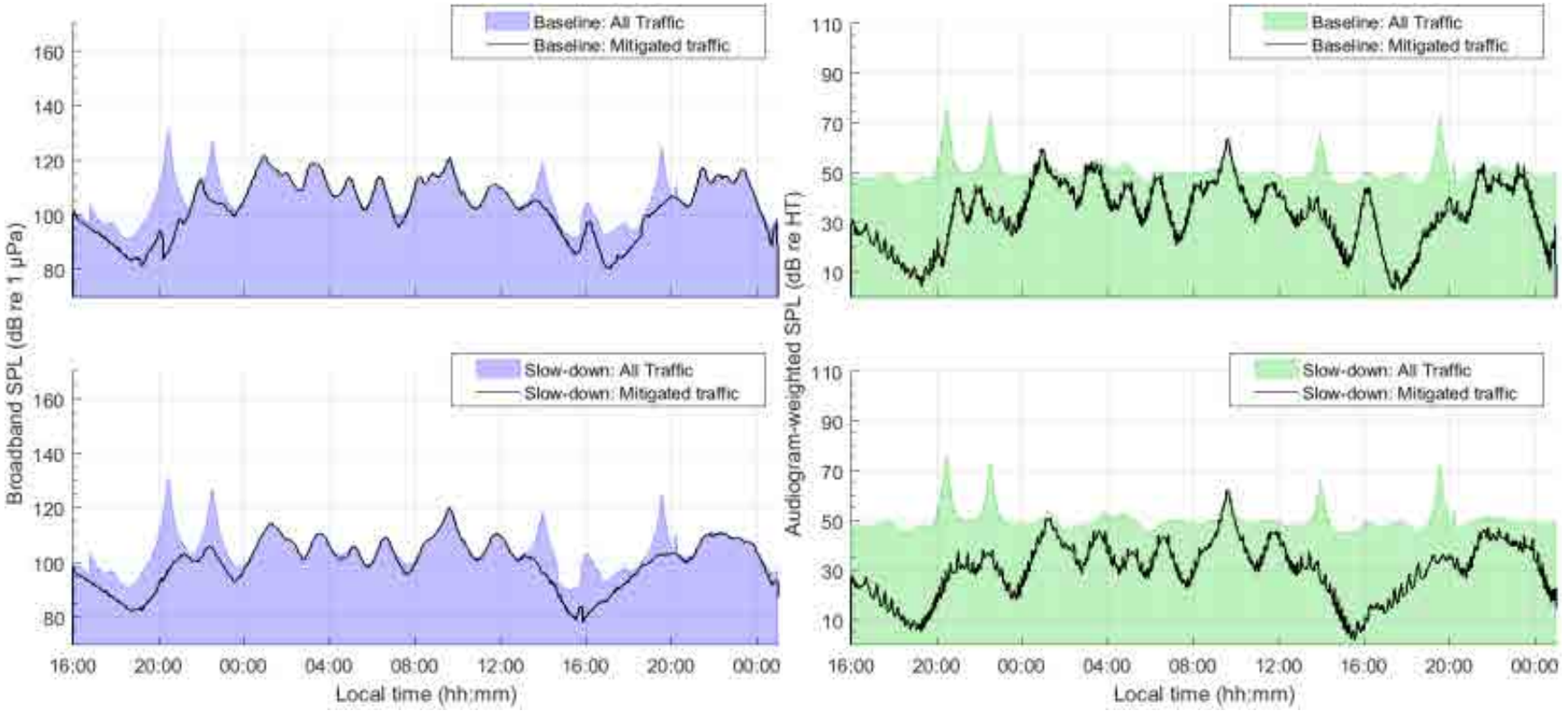

Figure 72. *Juan de Fuca Strait – Baseline vs Slow-Down (11-knot speed limit), Sample location 3*: Temporal variability of unweighted (left) and audiogram-weighted (right) received levels for (top) baseline (no slow-down) and (bottom) slow-down scenarios. The blue and green lines above the shaded area show received levels caused by all traffic and ambient noise. The black lines show received levels caused by commercial traffic only. The receiver location is shown in Figure 7.

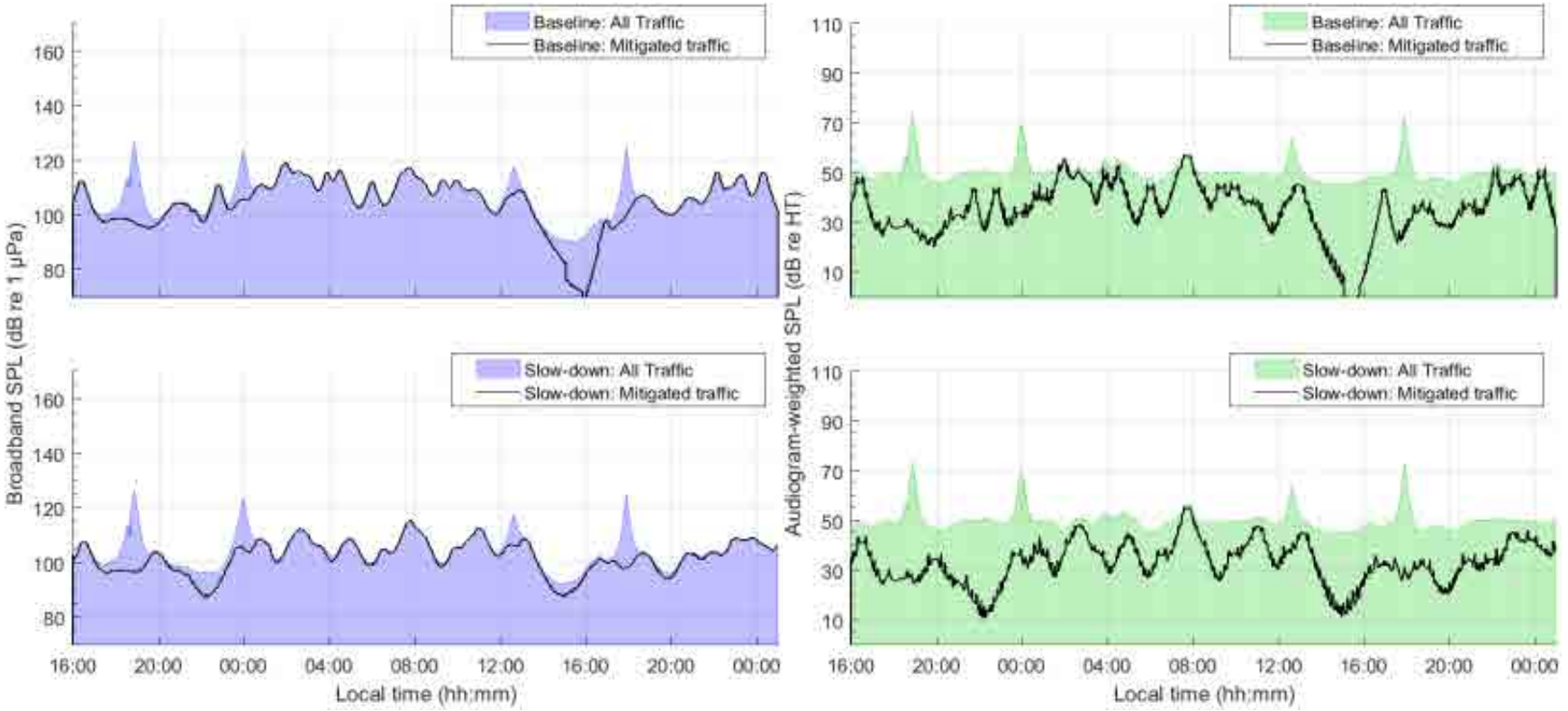

Figure 73. *Juan de Fuca Strait – Baseline vs Slow-Down (11-knot speed limit), Sample location 4*: Temporal variability of unweighted (left) and audiogram-weighted (right) received levels for (top) baseline (no slow-down) and (bottom) slow-down scenarios. The blue and green lines above the shaded area show received levels caused by all traffic and ambient noise. The black lines show received levels caused by commercial traffic only. The receiver location is shown in Figure 7.

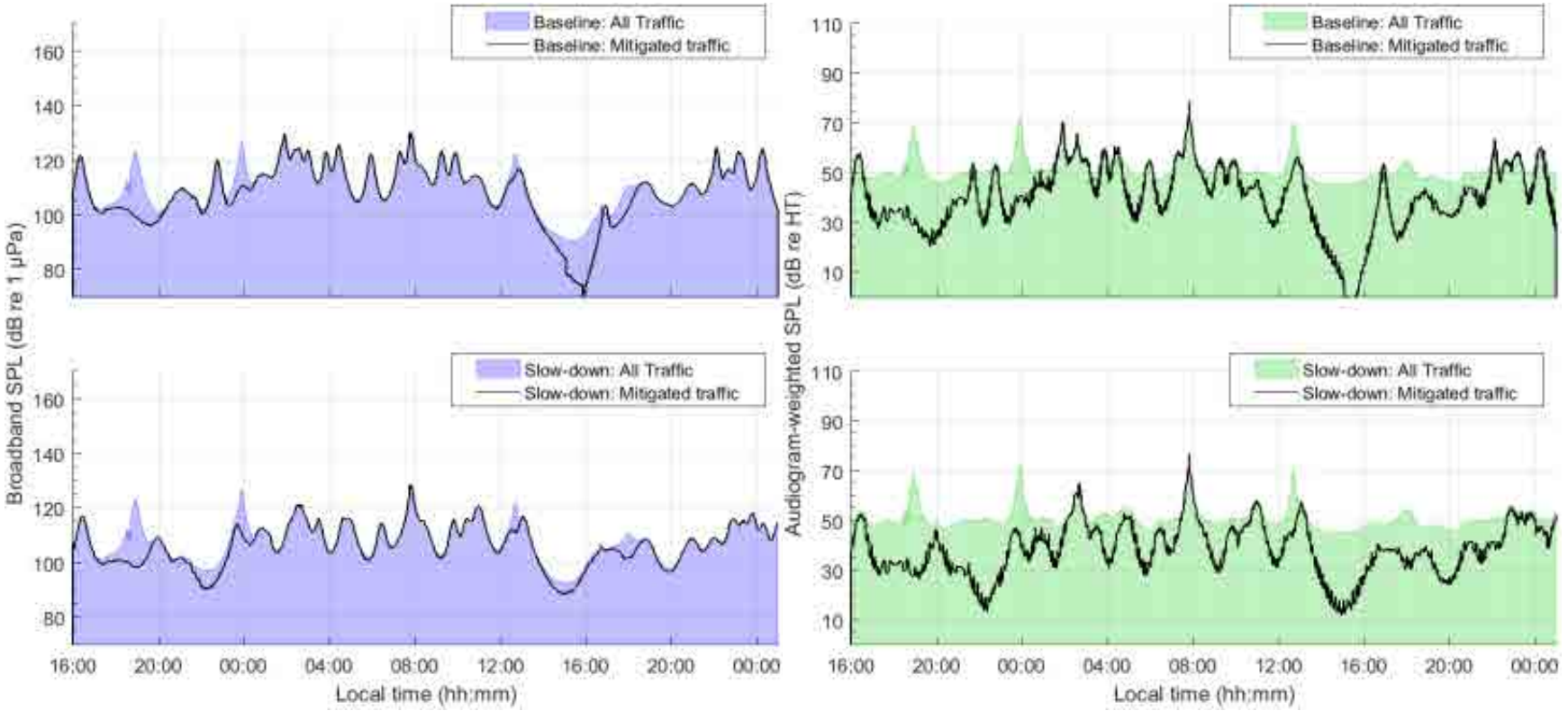

Figure 74. *Juan de Fuca Strait – Baseline vs Slow-Down (11-knot speed limit), Sample location 5*: Temporal variability of unweighted (left) and audiogram-weighted (right) received levels for (top) baseline (no slow-down) and (bottom) slow-down scenarios. The blue and green lines above the shaded area show received levels caused by all traffic and ambient noise. The black lines show received levels caused by commercial traffic only. The receiver location is shown in Figure 7.

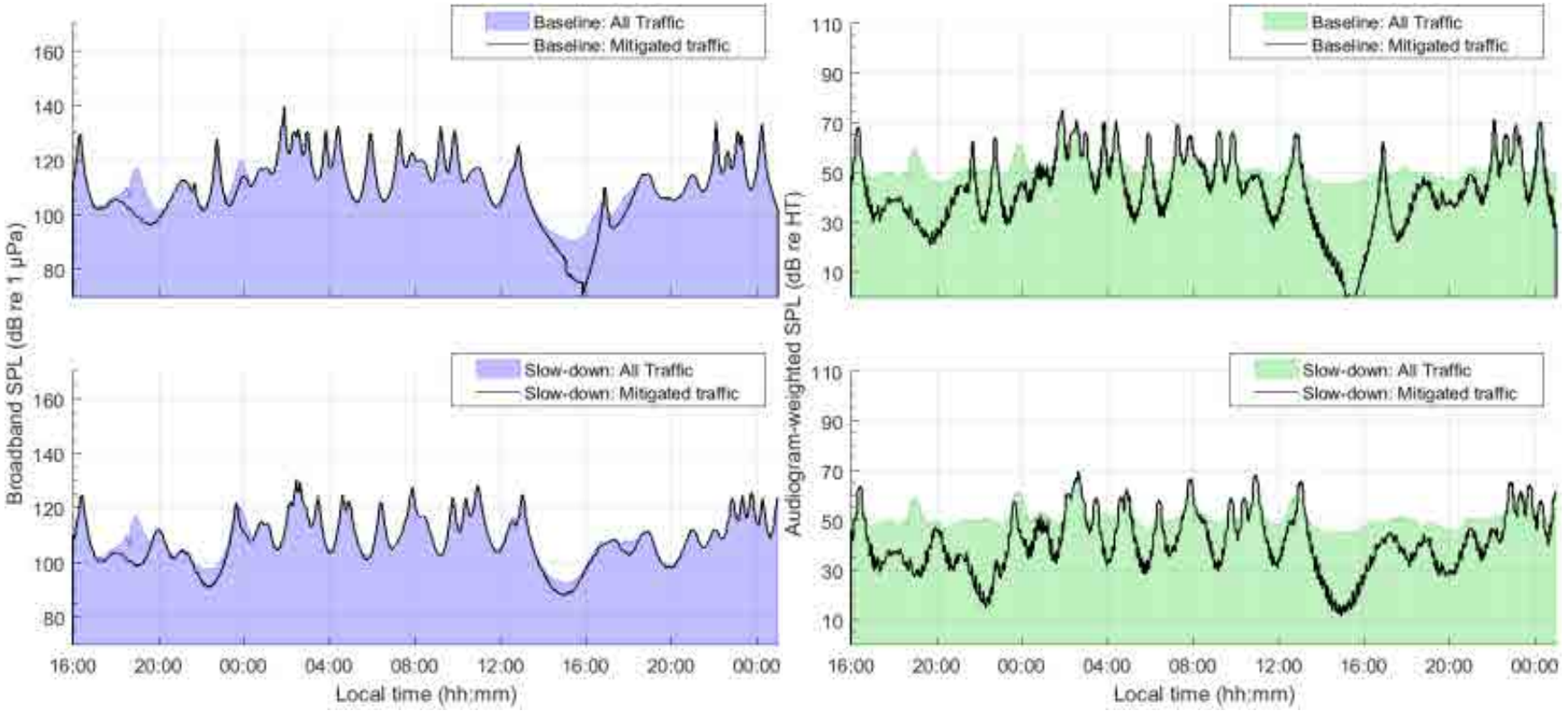

Figure 75. *Juan de Fuca Strait – Baseline vs Slow-Down (11-knot speed limit), Sample location 6*: Temporal variability of unweighted (left) and audiogram-weighted (right) received levels for (top) baseline (no slow-down) and (bottom) slow-down scenarios. The blue and green lines above the shaded area show received levels caused by all traffic and ambient noise. The black lines show received levels caused by commercial traffic only. The receiver location is shown in Figure 7.

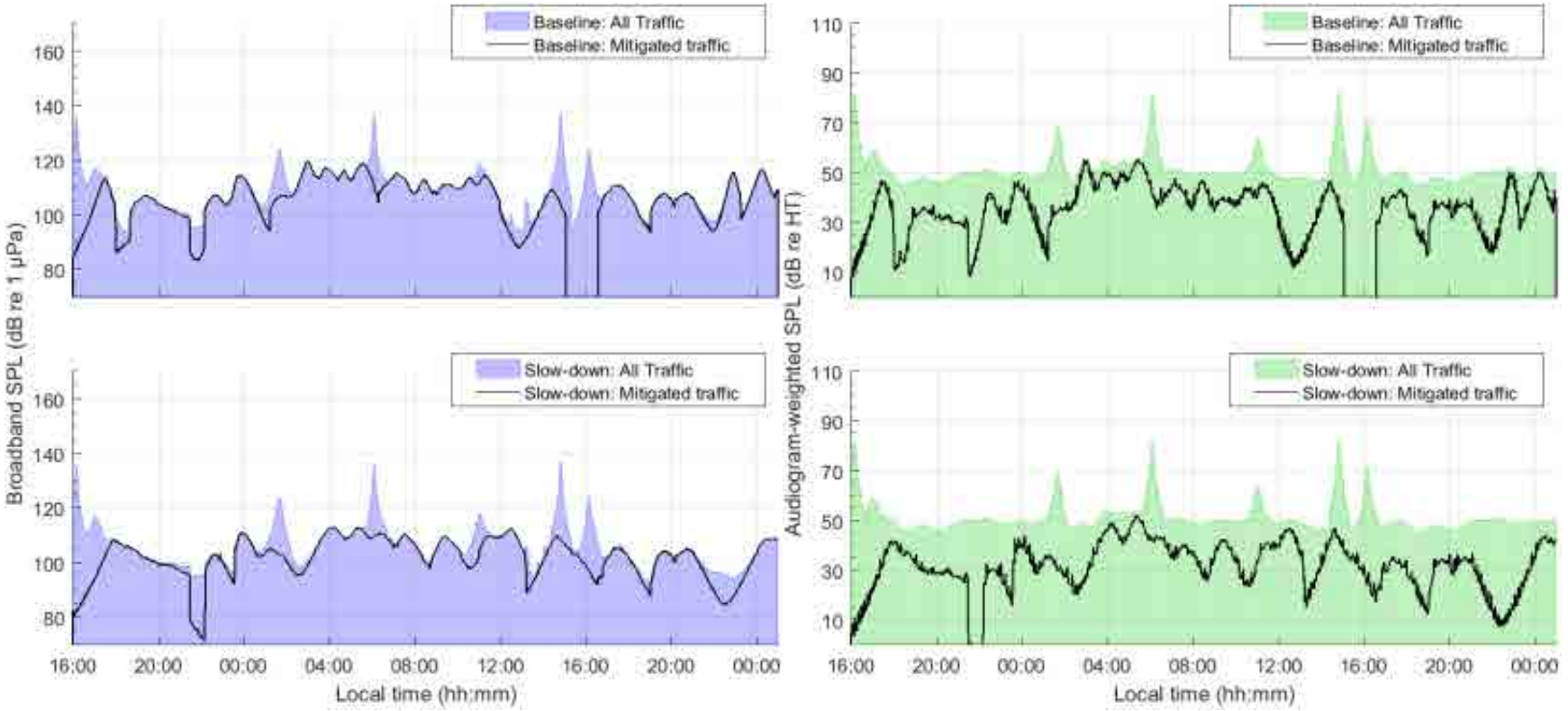

Figure 76. *Juan de Fuca Strait – Baseline vs Slow-Down (11-knot speed limit), Sample location 7*: Temporal variability of unweighted (left) and audiogram-weighted (right) received levels for (top) baseline (no slow-down) and (bottom) slow-down scenarios. The blue and green lines above the shaded area show received levels caused by all traffic and ambient noise. The black lines show received levels caused by commercial traffic only. The receiver location is shown in Figure 7.

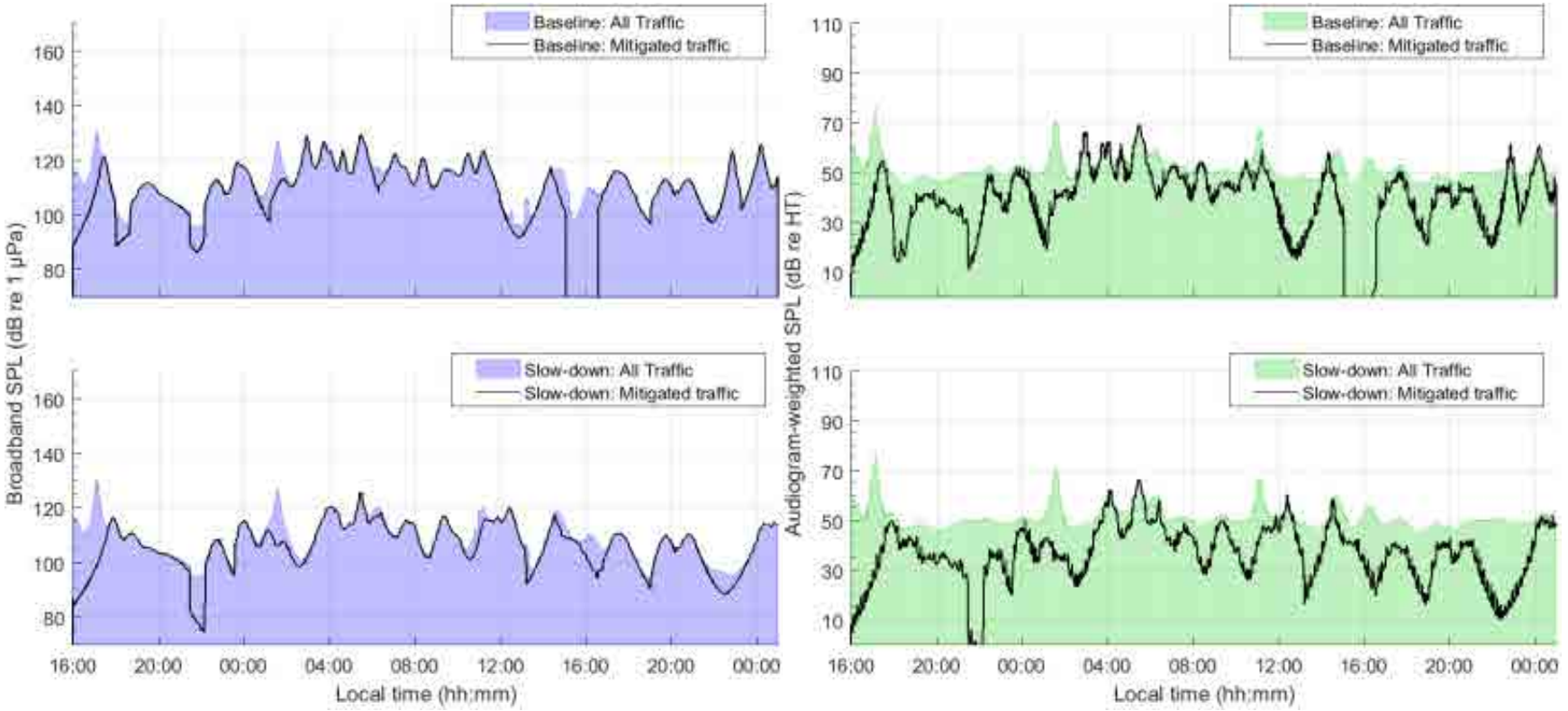

Figure 77. *Juan de Fuca Strait – Baseline vs Slow-Down (11-knot speed limit), Sample location 8*: Temporal variability of unweighted (left) and audiogram-weighted (right) received levels for (top) baseline (no slow-down) and (bottom) slow-down scenarios. The blue and green lines above the shaded area show received levels caused by all traffic and ambient noise. The black lines show received levels caused by commercial traffic only. The receiver location is shown in Figure 7.

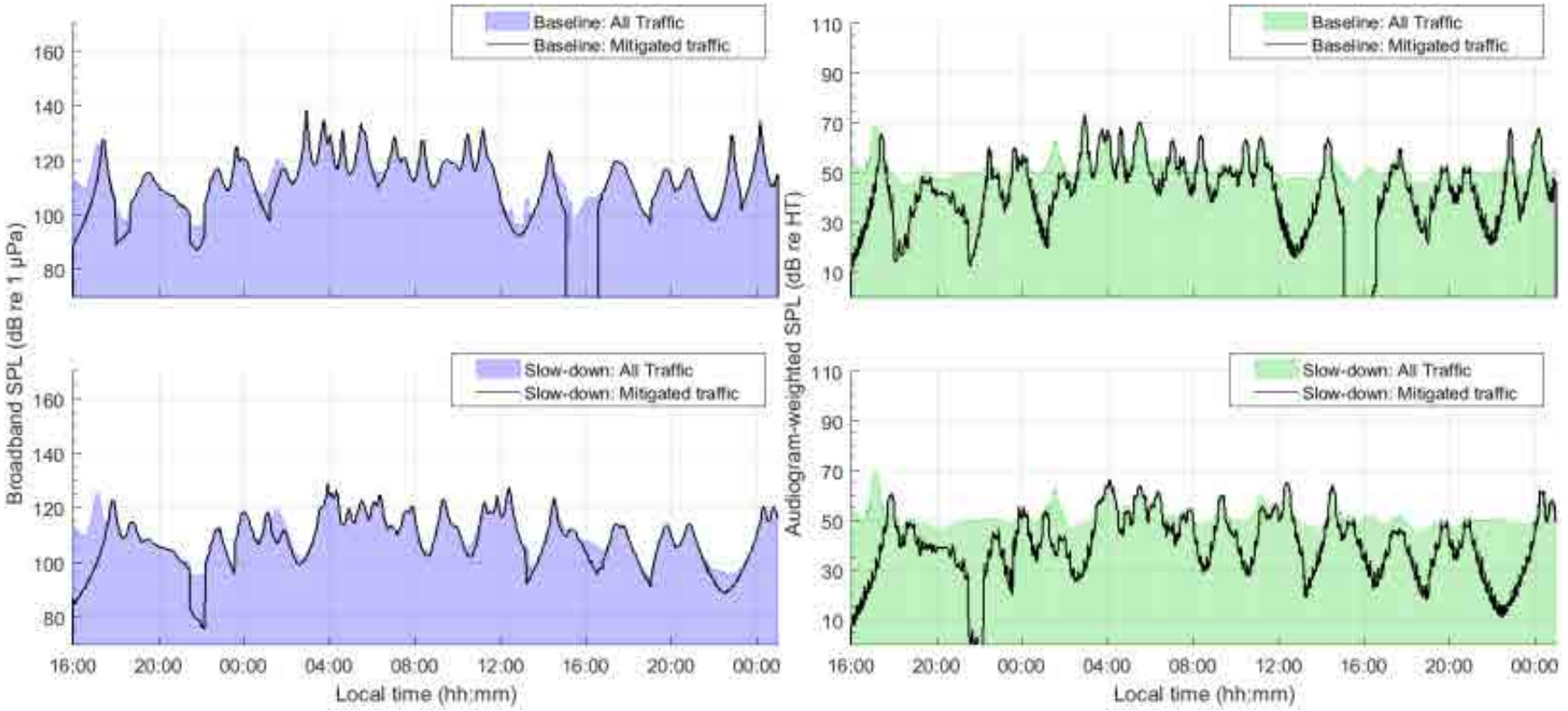

Figure 78. *Juan de Fuca Strait – Baseline vs Slow-Down (11-knot speed limit), Sample location 9*: Temporal variability of unweighted (left) and audiogram-weighted (right) received levels for (top) baseline (no slow-down) and (bottom) slow-down scenarios. The blue and green lines above the shaded area show received levels caused by all traffic and ambient noise. The black lines show received levels caused by commercial traffic only. The receiver location is shown in Figure 7.

Table 31. *Juan de Fuca Strait – Baseline vs Slow-Down (11-knot speed limit):* Temporal analysis of unweighted received noise levels (dB re 1 µPa), difference in received noise levels (dB), and difference acoustic intensity (%). The values indicate the percentile or mean calculated over a 33-hour period without (Baseline) and with mitigation (Slow-down), at the sample locations within the SRKW critical habitat shown in Figure 7.

Sample location	Scenario	Temporal analysis of noise level (dB re 1 µPa), difference in noise levels (dB), and difference in acoustic intensity (%)			
		5th	50th	95th	Mean
1	Baseline	98.9	110.6	119.3	109.9 ±6.5
	Slow-down	95.8	108.0	115.7	107.4 ±6.1
	Difference	**−3.1 (−51.0%)**	**−2.6 (−45.0%)**	**−3.6 (−56.3%)**	**−2.5 (−43.8%)**
2	Baseline	93.6	108.8	121.6	108.3 ±8.3
	Slow-down	92.6	105.6	116.7	105.7 ±7.5
	Difference	**−1.0 (−20.6%)**	**−3.2 (−52.1%)**	**−4.9 (−67.6%)**	**−2.6 (−45.0%)**
3	Baseline	93.0	107.3	118.9	107.0 ±8.2
	Slow-down	92.2	104.1	117.4	104.7 ±7.2
	Difference	**−0.8 (−16.8%)**	**−3.2 (−52.1%)**	**−1.5 (−29.2%)**	**−2.3 (−41.1%)**
4	Baseline	93.0	107.6	116.9	107.1 ±7.0
	Slow-down	95.6	104.3	114.9	104.7 ±6.0
	Difference	**+2.6 (+82.0%)**	**−3.3 (−53.2%)**	**−2.0 (−36.9%)**	**−2.4 (−42.5%)**
5	Baseline	93.9	110.9	123.4	110.7 ±8.4
	Slow-down	96.4	108.2	119.9	108.2 ±7.1
	Difference	**+2.5 (+77.8%)**	**−2.7 (−46.3%)**	**−3.5 (−55.3%)**	**−2.5 (−43.8%)**
6	Baseline	93.8	112.1	129.4	112.1 ±9.4
	Slow-down	96.3	109.1	123.1	109.8 ±8.0
	Difference	**+2.5 (+77.8%)**	**−3.0 (−49.9%)**	**−6.3 (−76.6%)**	**−2.3 (−41.1%)**
7	Baseline	95.9	108.7	119.6	108.9 ±7.4
	Slow-down	95.5	105.6	119.1	106.2 ±7.3
	Difference	**−0.4 (−8.8%)**	**−3.1 (−51.0%)**	**−0.5 (−10.9%)**	**−2.7 (−46.3%)**
8	Baseline	97.3	112.1	123.9	111.8 ±7.7
	Slow-down	96.3	109.3	119.9	109.1 ±7.1
	Difference	**−1.0 (−20.6%)**	**−2.8 (−47.5%)**	**−4.0 (−60.2%)**	**−2.7 (−46.3%)**
9	Baseline	97.8	113.5	128.1	113.2 ±8.7
	Slow-down	96.6	110.9	122.8	110.6 ±7.8
	Difference	**−1.2 (−24.1%)**	**−2.6 (−45.0%)**	**−5.3 (−70.5%)**	**−2.6 (−45.0%)**

Table 32. *Juan de Fuca Strait – Baseline vs Slow-Down (11-knot speed limit):* Temporal analysis of SRKW audiogram-weighted received noise levels (dB re HT), difference in received noise levels (dB), and difference acoustic intensity (%). The values indicate the percentile or mean calculated over a 33-hour period without (Baseline) and with mitigation (Slow-down), at the sample locations within the SRKW critical habitat shown in Figure 7.

Sample location	Scenario	Temporal analysis of noise level (dB re HT), difference in noise levels (dB), and difference in acoustic intensity (%)			
		5th	50th	95th	Mean
1	Baseline	46.8	50.0	58.7	51.3 ±4.7
	Slow-down	46.4	49.7	58.5	50.6 ±4.6
	Difference	**−0.4 (−8.8%)**	**−0.3 (−6.7%)**	**−0.2 (−4.5%)**	**−0.7 (−14.9%)**
2	Baseline	46.3	49.6	60.1	51.1 ±4.9
	Slow-down	46.1	49.4	57.0	50.4 ±4.5
	Difference	**−0.2 (−4.5%)**	**−0.2 (−4.5%)**	**−3.1 (−51.0%)**	**−0.7 (−14.9%)**
3	Baseline	45.9	49.6	60.1	50.8 ±4.7
	Slow-down	45.8	49.3	60.0	50.3 ±4.6
	Difference	**−0.1 (−2.3%)**	**−0.3 (−6.7%)**	**−0.1 (−2.3%)**	**−0.5 (−10.9%)**
4	Baseline	46.1	49.7	58.4	50.5 ±4.2
	Slow-down	45.9	49.4	58.4	50.1 ±4.2
	Difference	**−0.2 (−4.5%)**	**−0.3 (−6.7%)**	**0.0 (0.0%)**	**−0.4 (−8.8%)**
5	Baseline	46.1	50.4	62.3	52.0 ±5.1
	Slow-down	46.0	50.1	60.6	51.1 ±4.5
	Difference	**−0.1 (−2.3%)**	**−0.3 (−6.7%)**	**−1.7 (−32.4%)**	**−0.9 (−18.7%)**
6	Baseline	46.1	50.8	66.6	53.0 ±6.2
	Slow-down	46.1	50.3	63.1	51.9 ±5.0
	Difference	**0.0 (0.0%)**	**−0.5 (−10.9%)**	**−3.5 (−55.3%)**	**−1.1 (−22.4%)**
7	Baseline	46.3	49.9	64.5	51.6 ±6.0
	Slow-down	46.3	49.5	64.5	51.3 ±6.0
	Difference	**0.0 (0.0%)**	**−0.4 (−8.8%)**	**0.0 (0.0%)**	**−0.3 (−6.7%)**
8	Baseline	46.5	50.5	62.9	52.1 ±5.0
	Slow-down	46.7	50.1	60.9	51.4 ±4.7
	Difference	**+0.2 (+4.7%)**	**−0.4 (−8.8%)**	**−2.0 (−36.9%)**	**−0.7 (−14.9%)**
9	Baseline	46.7	51.0	65.7	52.9 ±5.6
	Slow-down	46.9	50.4	62.0	52.0 ±4.7
	Difference	**+0.2 (+4.7%)**	**−0.6 (−12.9%)**	**−3.7 (−57.3%)**	**−0.9 (−18.7%)**

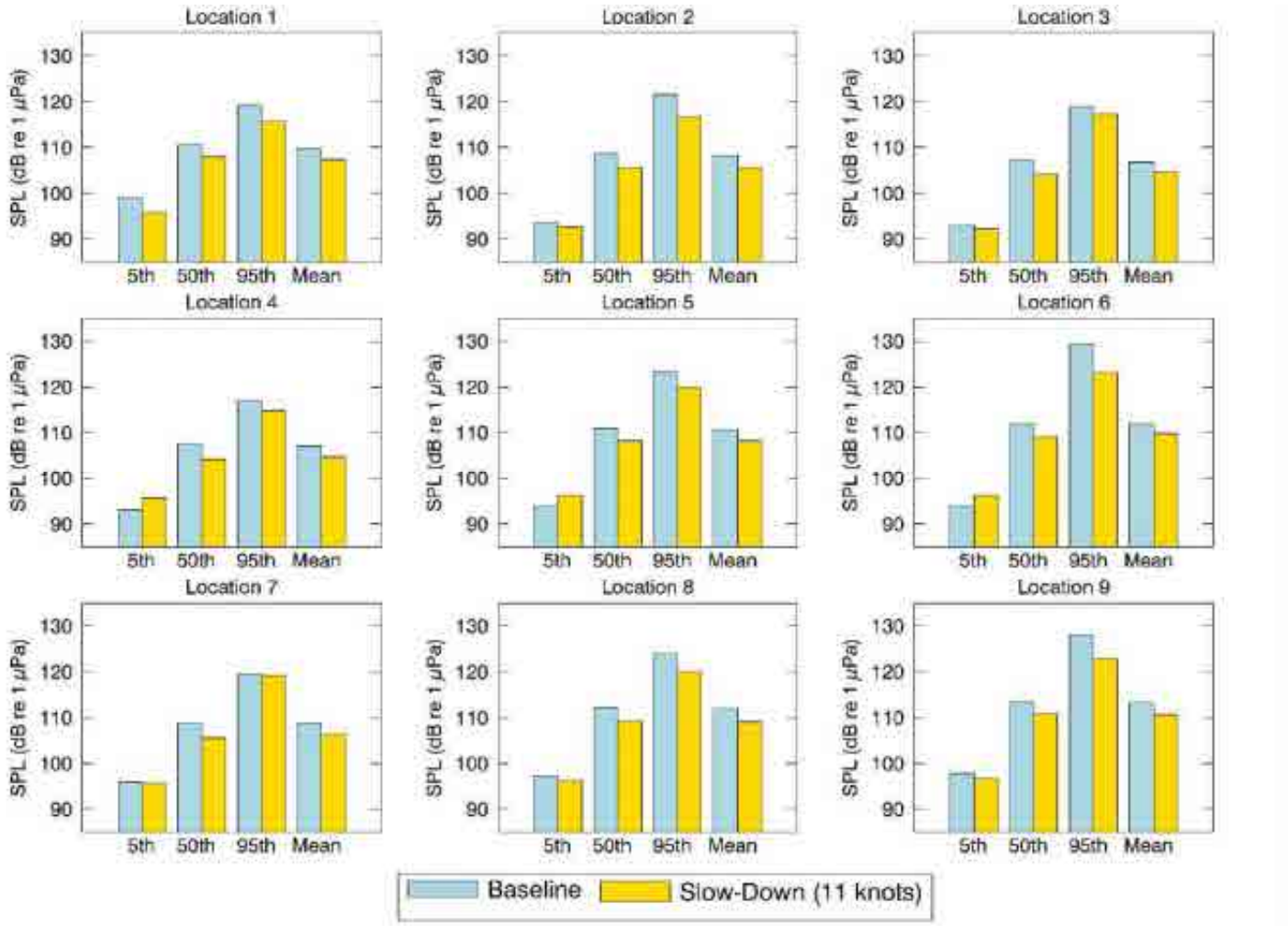

Figure 79. *Juan de Fuca Strait – Baseline vs Slow-Down (11-knot speed limit)*: Histogram representation of the temporal analysis of unweighted received noise levels (dB re 1 µPa). The vertical bars indicate the percentile or mean calculated over a 33-hour period without (baseline) and with mitigation, at the sample locations within the SRKW critical habitat shown in Figure 7.

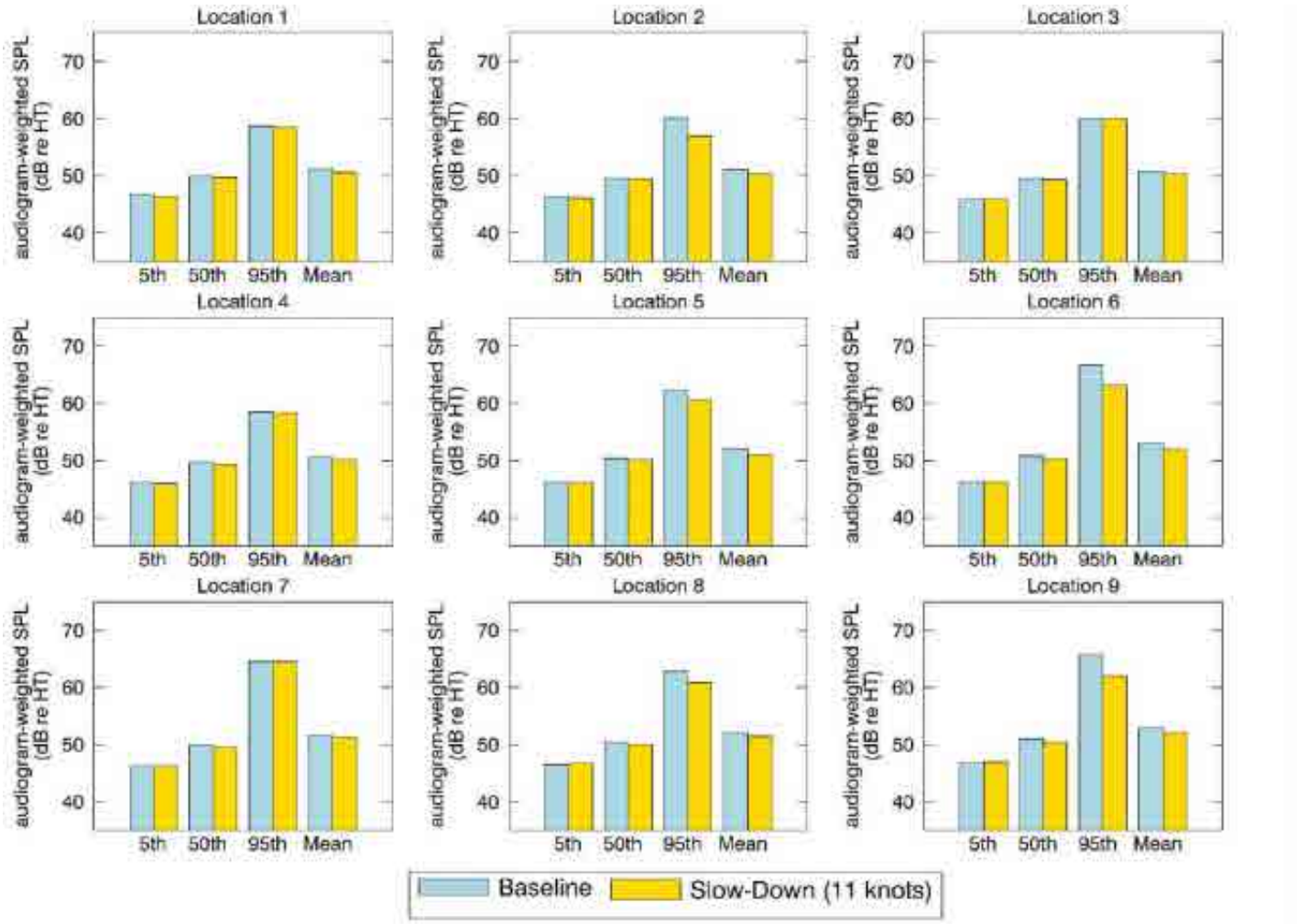

Figure 80. *Juan de Fuca Strait – Baseline vs Slow-Down (11-knot speed limit):* Histogram representation of the temporal analysis of SRKW audiogram-weighted received noise levels (dB re HT). The vertical bars indicate the percentile or mean calculated over a 33-hour period without (baseline) and with mitigation, at the sample locations within the SRKW critical habitat shown in Figure 7.

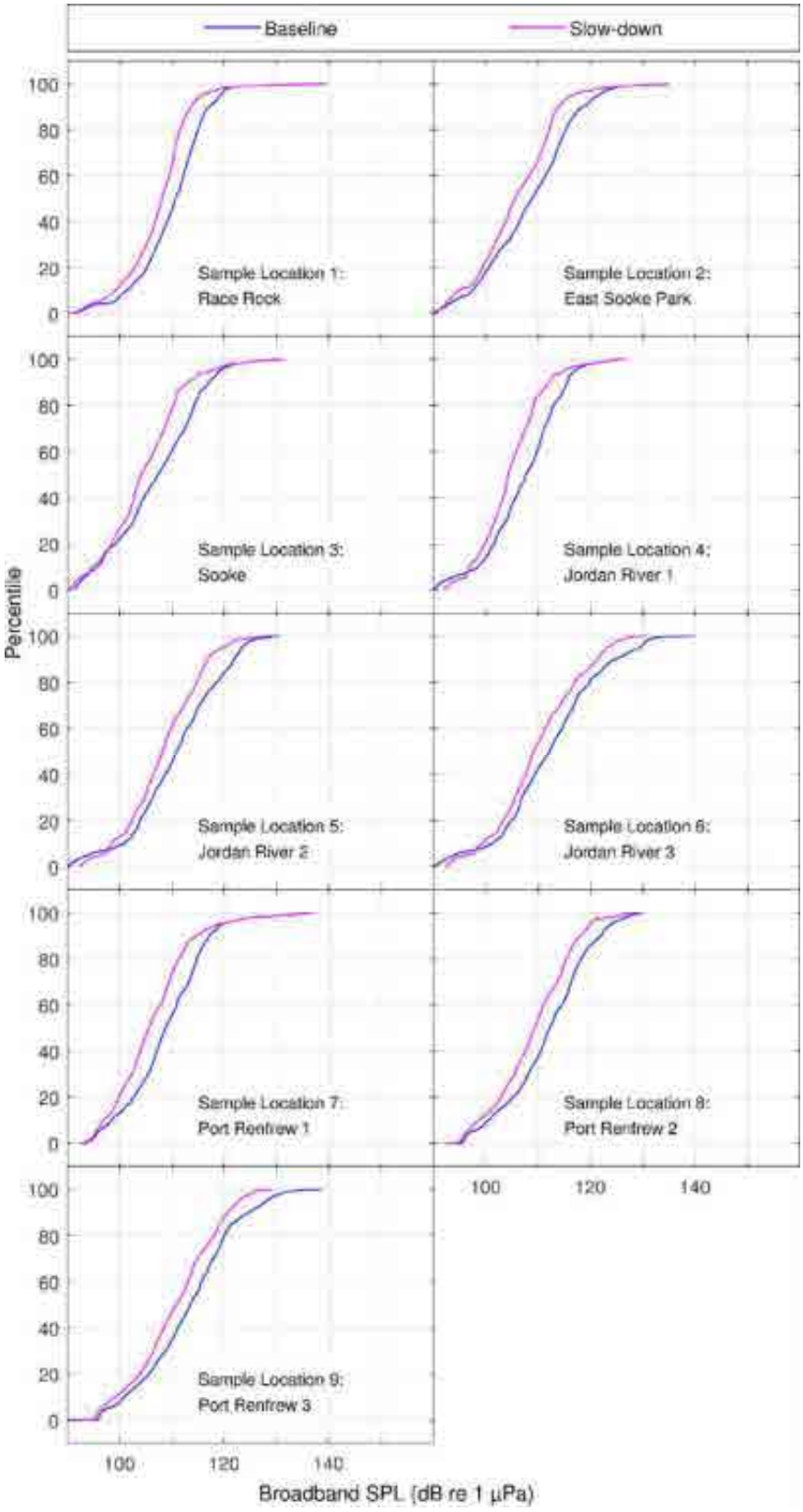

Figure 81. *Juan de* Fuca *Strait – Baseline vs Slow-Down (11-knot speed limit):* CDF curves of time-dependent unweighted SPL for baseline and mitigated scenarios at the sample locations shown in Figure 7.

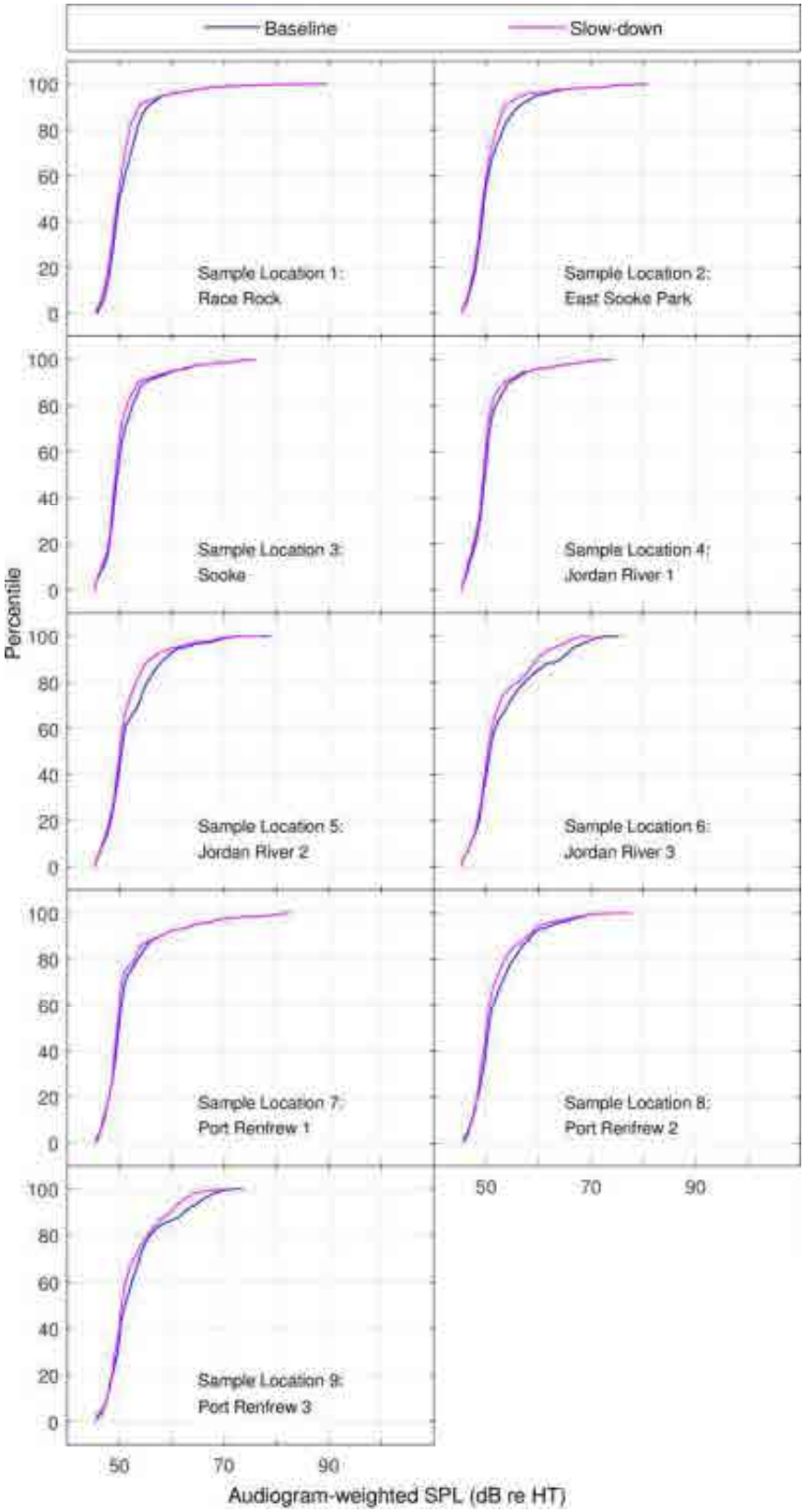

Figure 82. *Juan de Fuca Strait – Baseline vs Slow-Down (11-knot speed limit):* CDF curves of time-dependent audiogram-weighted SPL for baseline and mitigated scenarios at the sample locations shown in Figure 7.

3.3.4. Swiftsure Bank

Time-averaged results for two speed limit alternatives (a maximum speed of 11 knots and a dual maximum speed of 11 or 15 knots, through the shipping lanes in Swiftsure Bank) are presented in Figures 83–86 and Tables 33–34. In Figures 83–86, the maps on the left present the L_{eq} and the maps on the right present the change in L_{eq} with respect to baseline levels for July, seen in Figure 20. Tables 33 and 34 compare baseline and mitigated L_{eq} for the three speed limits at eight sample locations in the SRKW critical habitat. The sample locations are shown as green dots in Figures 83–86.

Figures 87–99 and Tables 35–36 present the time-dependent results for a maximum speed of 11 knots for all commercial traffic though the Swiftsure Bank area.

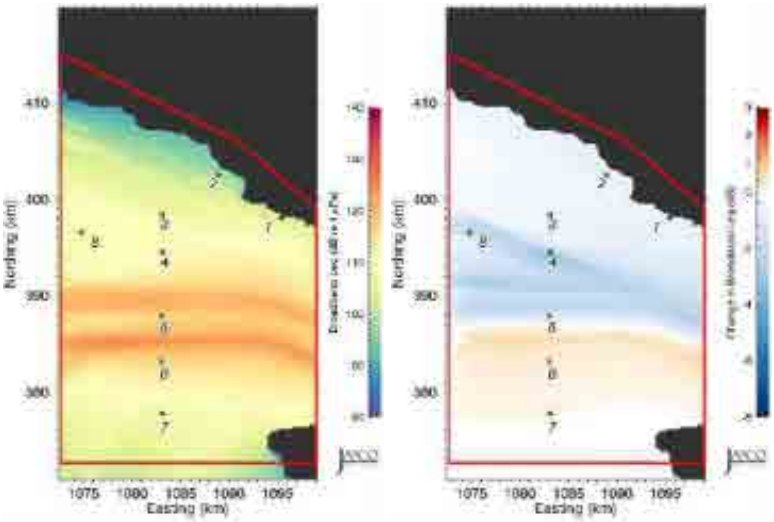

Figure 83. *Swiftsure Bank – Slow-Down, 11-knot speed limit*: Unweighted equivalent continuous noise levels (L_{eq}; left) and change in L_{eq} (right) relative to July 2015 baseline levels. Grid resolution is 200 × 200 m. The green dots are the sample locations in the SRKW critical habitat. The red line shows the boundary of the area where statistical values (percentiles and mean) were derived.

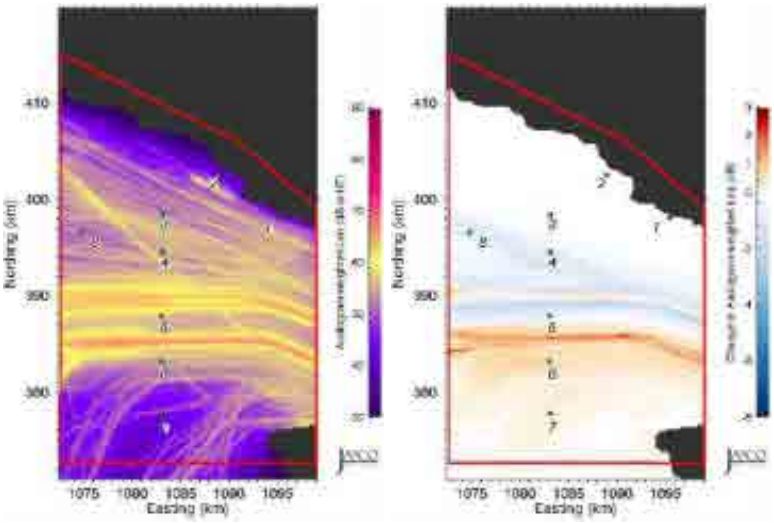

Figure 84. *Swiftsure Bank – Slow-Down, 11-knot speed limit*: Audiogram-weighted equivalent continuous noise levels (L_{eq}; left) and change in L_{eq} (right) relative to July 2015 baseline levels. Grid resolution is 200 × 200 m. The green dots are the sample locations in the SRKW critical habitat. The red line shows the boundary of the area where statistical values (percentiles and mean) were derived.

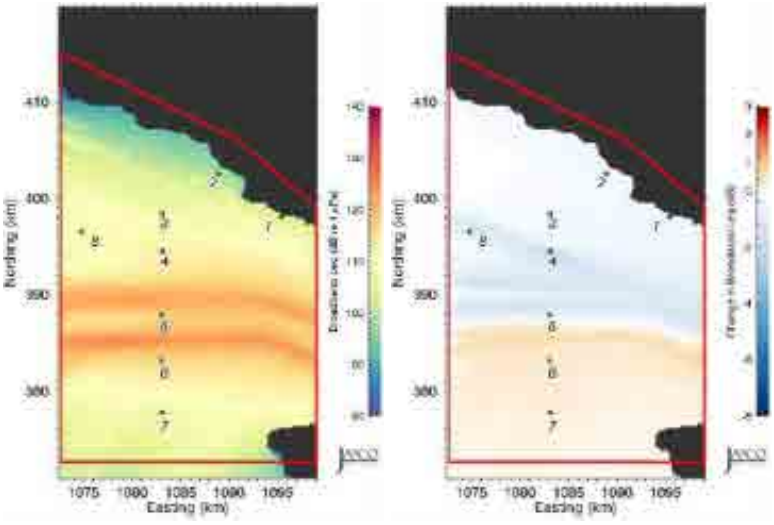

Figure 85. *Swiftsure Bank – Slow-Down, 11- and 15-knot speed limits*: Unweighted equivalent continuous noise levels (L_{eq}; left) and change in L_{eq} (right) relative to July 2015 baseline levels. Grid resolution is 200 × 200 m. The green dots are the sample locations in the SRKW critical habitat. The red line shows the boundary of the area where statistical values (percentiles and mean) were derived.

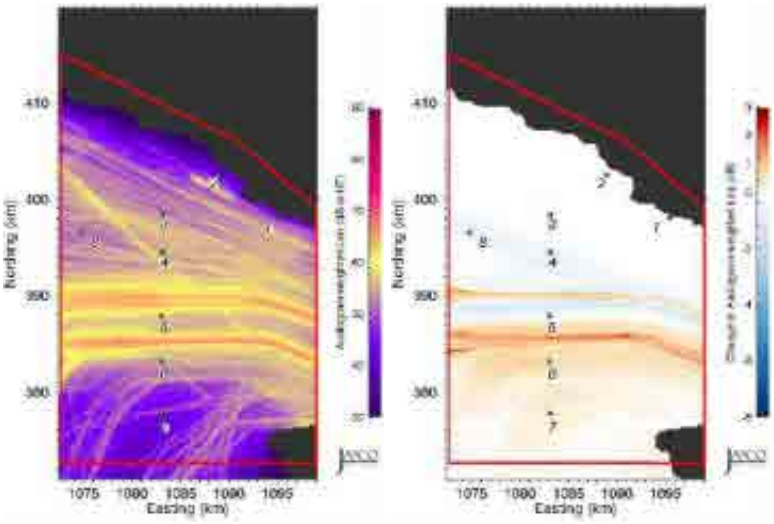

Figure 86. *Swiftsure Bank – Slow-Down, 11- and 15-knot speed limits*: Audiogram-weighted equivalent continuous noise levels (L_{eq}; left) and change in L_{eq} (right) relative to July 2015 baseline levels. Grid resolution is 200 × 200 m. The green dots are the sample locations in the SRKW critical habitat. The red line shows the boundary of the area where statistical values (percentiles and mean) were derived.

Table 33. *Swiftsure Bank – Baseline* vs. *Slow-Down*: Unweighted received levels (dB re 1 µPa), changes in received levels (dB), and changes in acoustic intensity (%) at the sample locations in the SRKW critical habitat shown in Figure 8.

Sample location	Baseline (dB re 1 µPa)	11 knots			11 and 15 knots		
		Mitigated (dB re 1 µPa)	Change		Mitigated (dB re 1 µPa)	Change	
			dB	%		dB	%
1	105.9	105.30	−0.6	−12.9	105.60	−0.3	−6.7
2	99.1	98.40	−0.7	−14.9	98.80	−0.3	−6.7
3	107.4	106.90	−0.5	−10.9	107.20	−0.2	−4.5
4	114.3	111.00	−3.3	−53.2	112.40	−1.9	−35.4
5	118.3	117.80	−0.5	−10.9	118.10	−0.2	−4.5
6	114.8	115.10	+0.3	+7.2	115.20	+0.4	+9.6
7	106.8	106.90	+0.1	+2.3	107.00	+0.2	+4.7
8	112.0	109.90	−2.1	−38.3	111.00	−1.0	−20.6

Table 34. *Swiftsure Bank – Baseline* vs. *Slow-Down*: Audiogram-weighted received levels (dB re HT), changes in received levels (dB), and changes in acoustic intensity (%) at the sample locations in the SRKW critical habitat shown in Figure 8.

Sample location	Baseline (dB re HT)	11 knots			11 and 15 knots		
		Mitigated (dB re HT)	Change		Mitigated (dB re HT)	Change	
			dB	%		dB	%
1	52.3	52.2	−0.1	−2.3	52.2	−0.1	−2.3
2	43.1	43.1	0.0	0.0	43.1	0.0	0.0
3	52.3	52.3	0.0	0.0	52.3	0.0	0.0
4	55.8	54.3	−1.5	−29.2	54.9	−0.9	−18.7
5	55.2	55.1	−0.1	−2.3	55.4	+0.2	+4.7
6	52.3	52.8	+0.5	+12.2	52.9	+0.6	+14.8
7	41.4	41.6	+0.2	+4.7	41.6	+0.2	+4.7
8	53.2	52.3	−0.9	−18.7	52.8	−0.4	−8.8

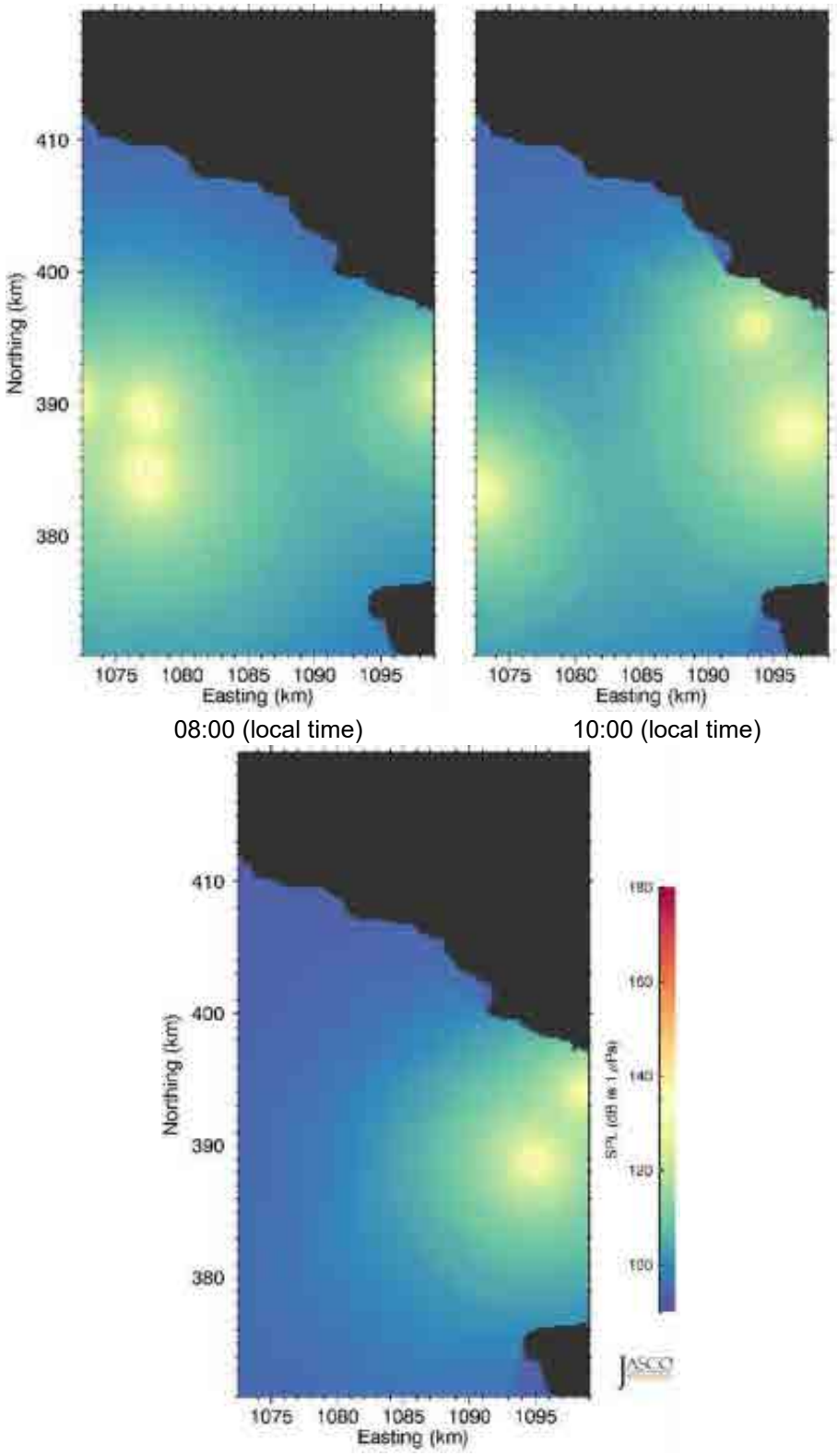

Figure 87. *Swiftsure Bank – Slow-Down (11-knot speed limit)*: Example time snapshots of future mitigated SPL (unweighted with ambient, 10 Hz to 50 kHz) from 08:00 to 12:00 (local time) in 2-hour increments. Easting and northing are BC Albers projected coordinates..

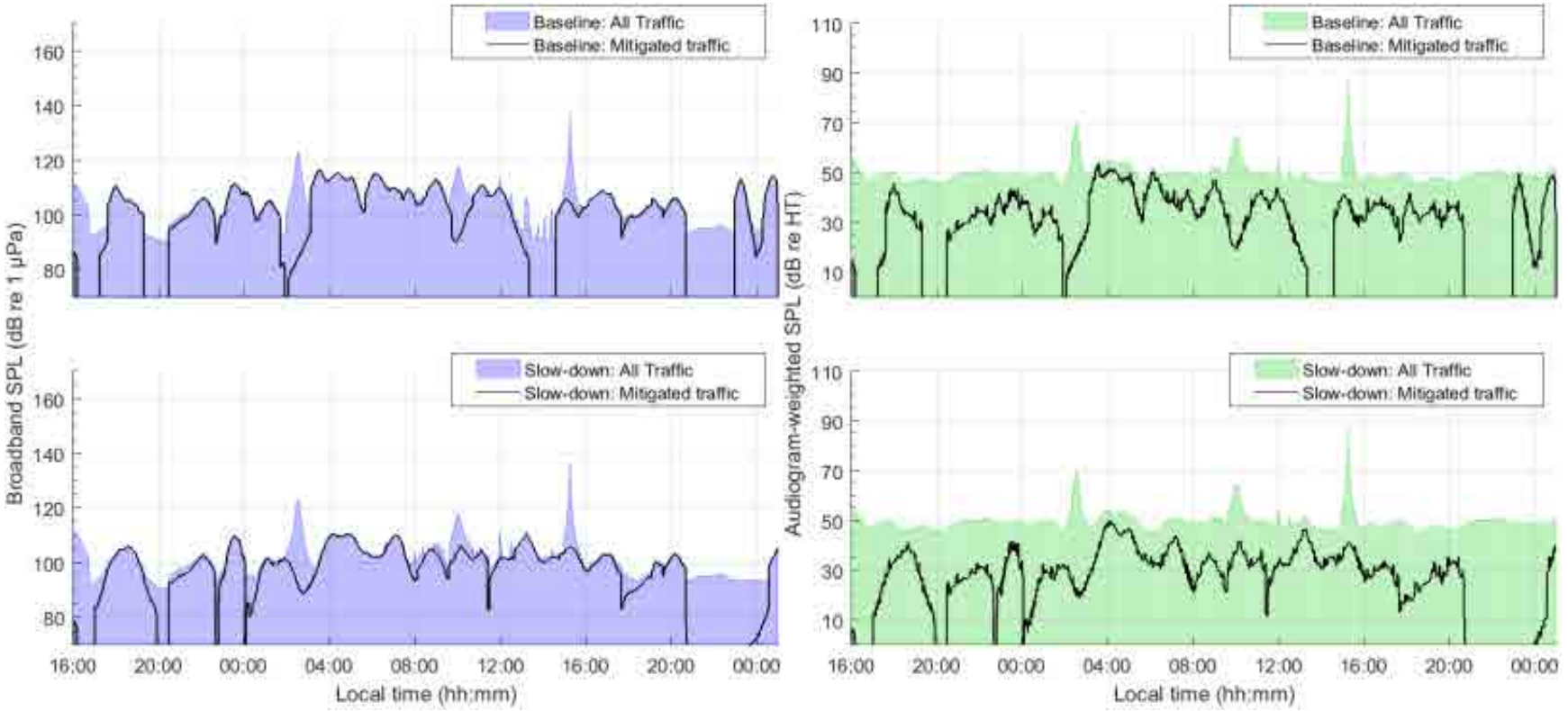

Figure 88. *Swiftsure Bank – Baseline vs Slow-Down (11-knot speed limit), Sample location 1*: Temporal variability of unweighted (left) and audiogram-weighted (right) received levels for (top) baseline (no slow-down) and (bottom) slow-down scenarios. The blue and green lines above the shaded area show received levels caused by all traffic and ambient noise. The black lines show received levels caused by commercial traffic only. The receiver location is shown in Figure 8.

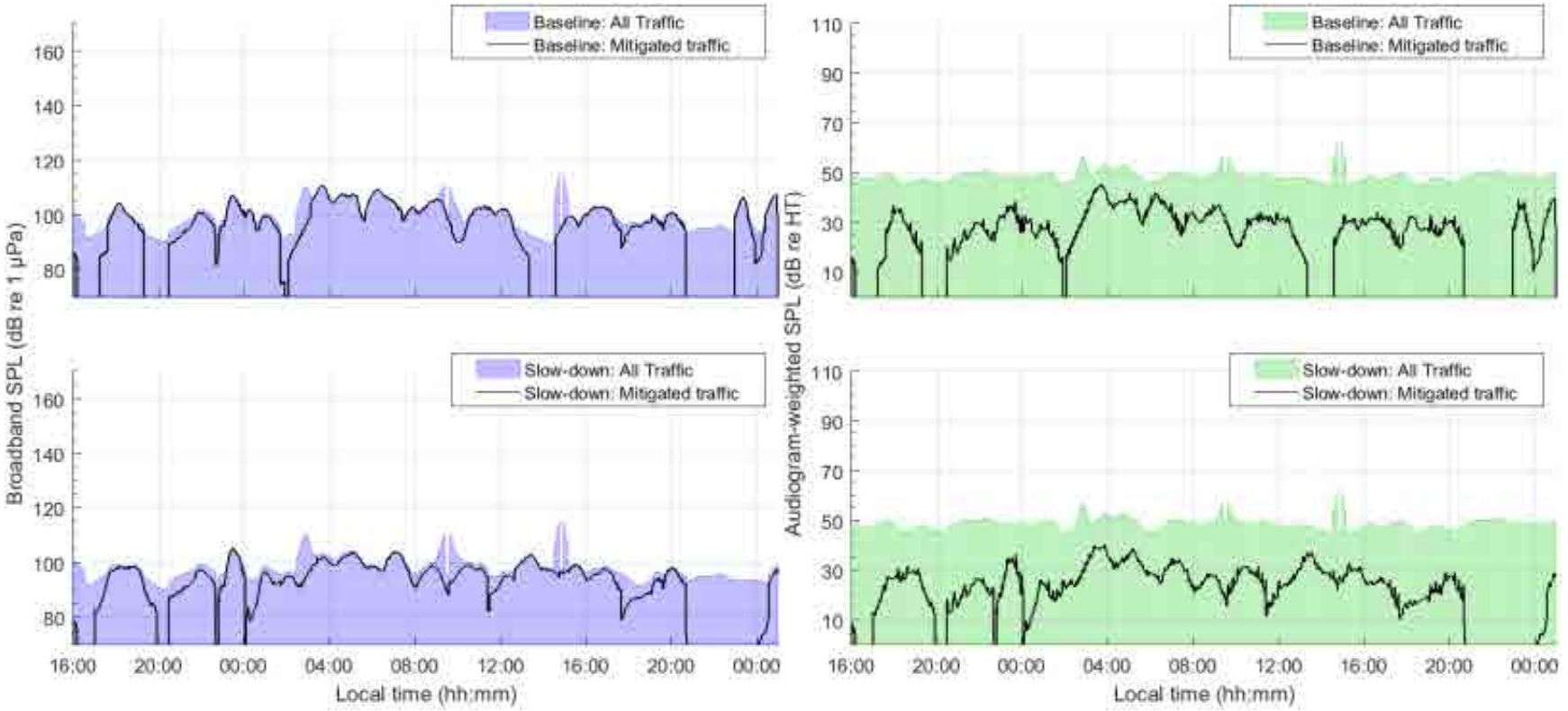

Figure 89. *Swiftsure Bank – Baseline vs Slow-Down (11-knot speed limit), Sample location 2*: Temporal variability of unweighted (left) and audiogram-weighted (right) received levels for (top) baseline (no slow-down) and (bottom) slow-down scenarios. The blue and green lines above the shaded area show received levels caused by all traffic and ambient noise. The black lines show received levels caused by commercial traffic only. The receiver location is shown in Figure 8.

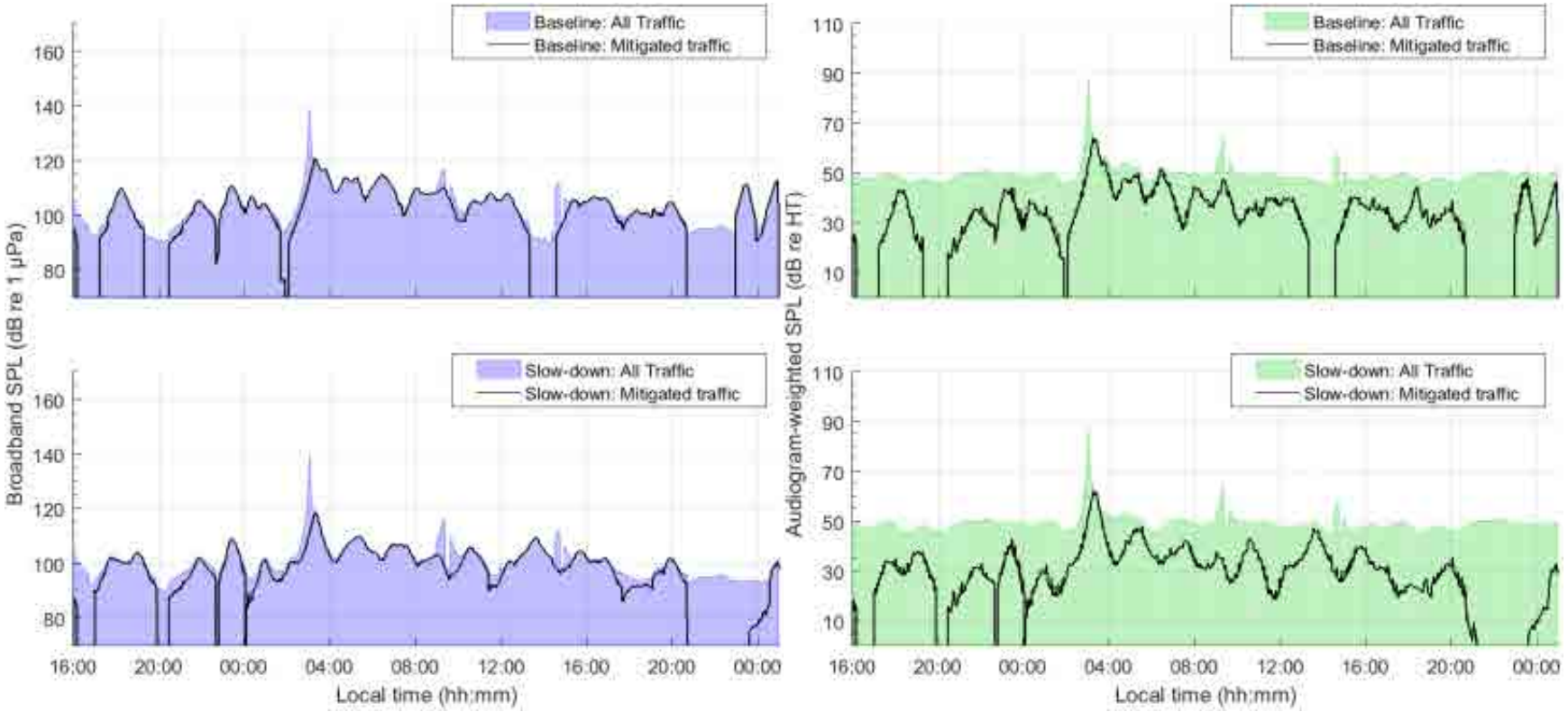

Figure 90. *Swiftsure Bank – Baseline vs Slow-Down (11-knot speed limit), Sample location 3*: Temporal variability of unweighted (left) and audiogram-weighted (right) received levels for (top) baseline (no slow-down) and (bottom) slow-down scenarios. The blue and green lines above the shaded area show received levels caused by all traffic and ambient noise. The black lines show received levels caused by commercial traffic only. The receiver location is shown in Figure 8.

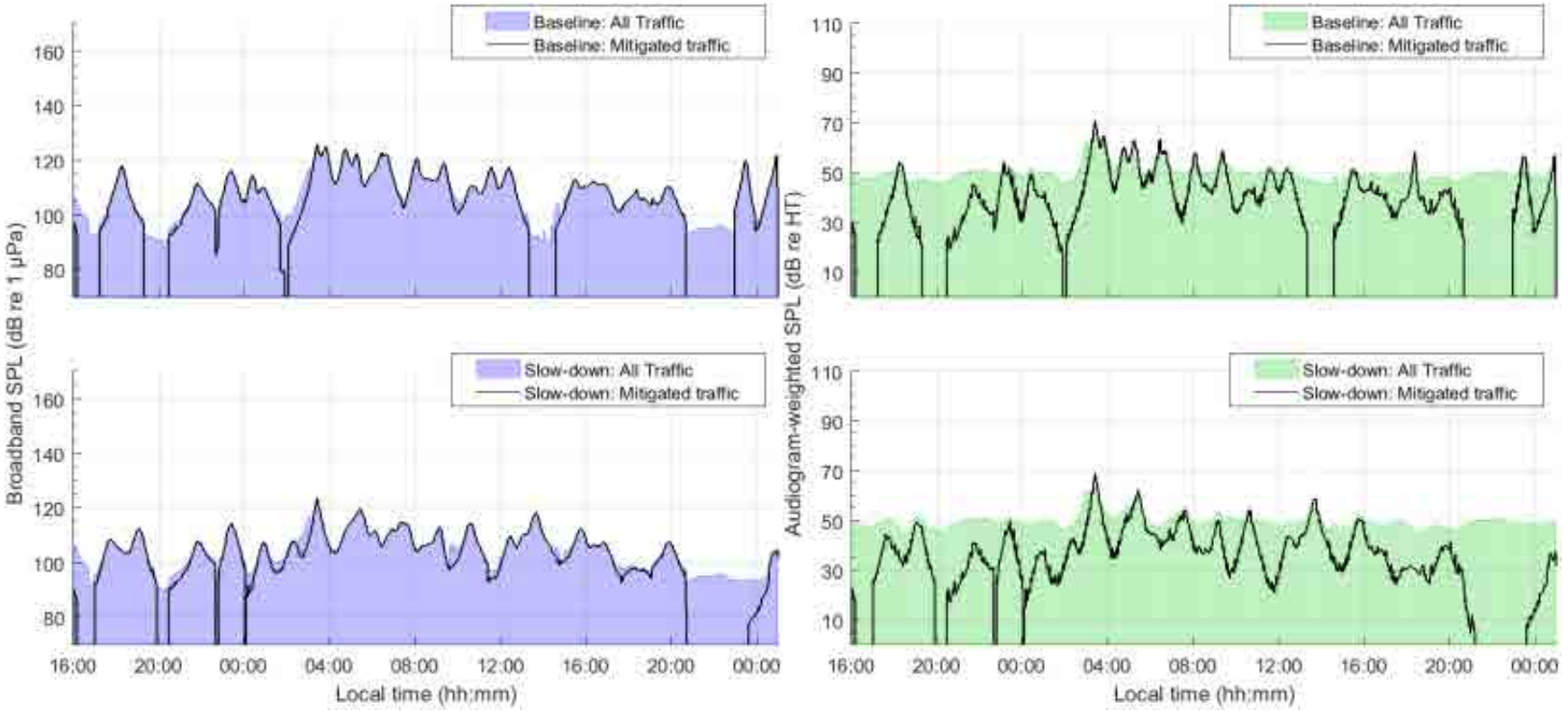

Figure 91. *Swiftsure Bank – Baseline vs Slow-Down (11-knot speed limit), Sample location 4*: Temporal variability of unweighted (left) and audiogram-weighted (right) received levels for (top) baseline (no slow-down) and (bottom) slow-down scenarios. The blue and green lines above the shaded area show received levels caused by all traffic and ambient noise. The black lines show received levels caused by commercial traffic only. The receiver location is shown in Figure 8.

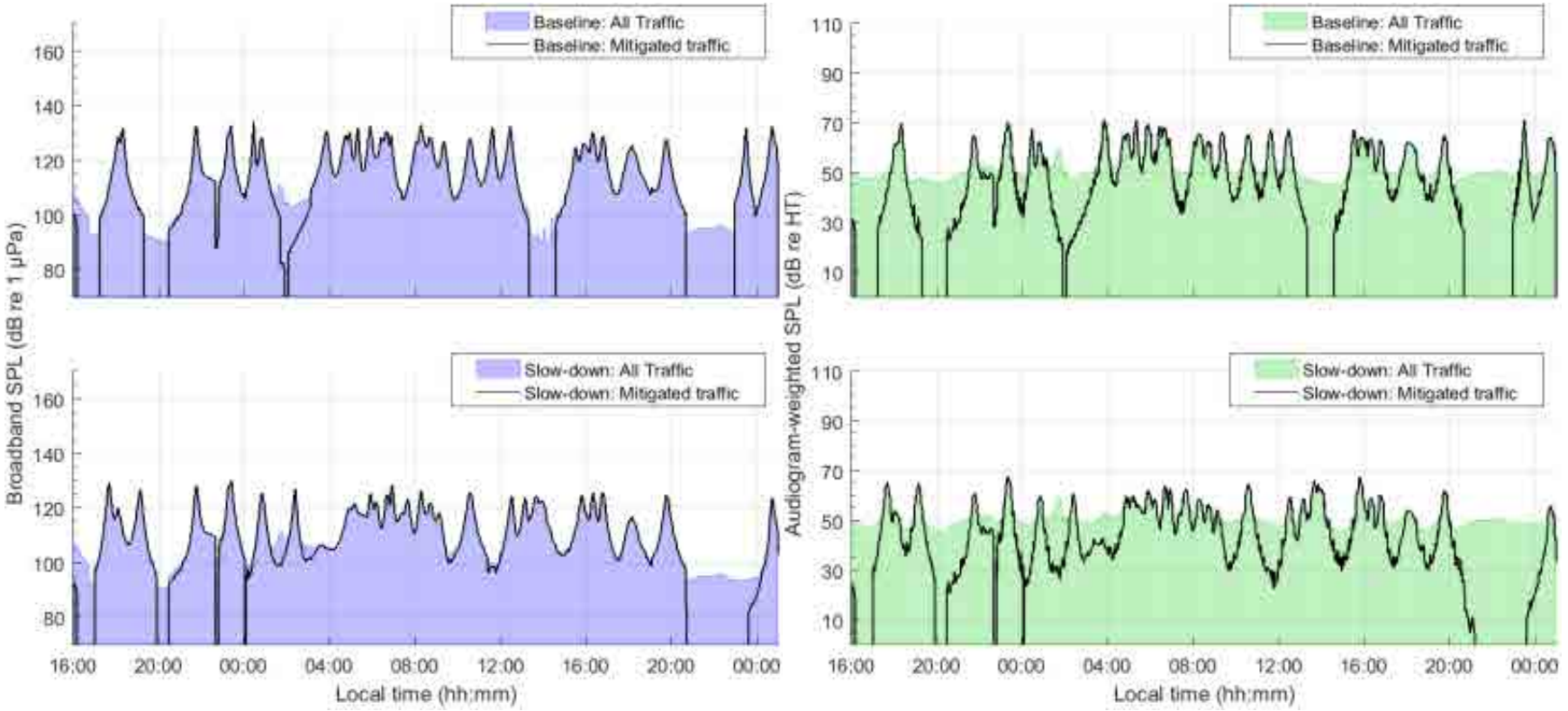

Figure 92. *Swiftsure Bank – Baseline vs Slow-Down (11-knot speed limit), Sample location 5*: Temporal variability of unweighted (left) and audiogram-weighted (right) received levels for (top) baseline (no slow-down) and (bottom) slow-down scenarios. The blue and green lines above the shaded area show received levels caused by all traffic and ambient noise. The black lines show received levels caused by commercial traffic only. The receiver location is shown in Figure 8.

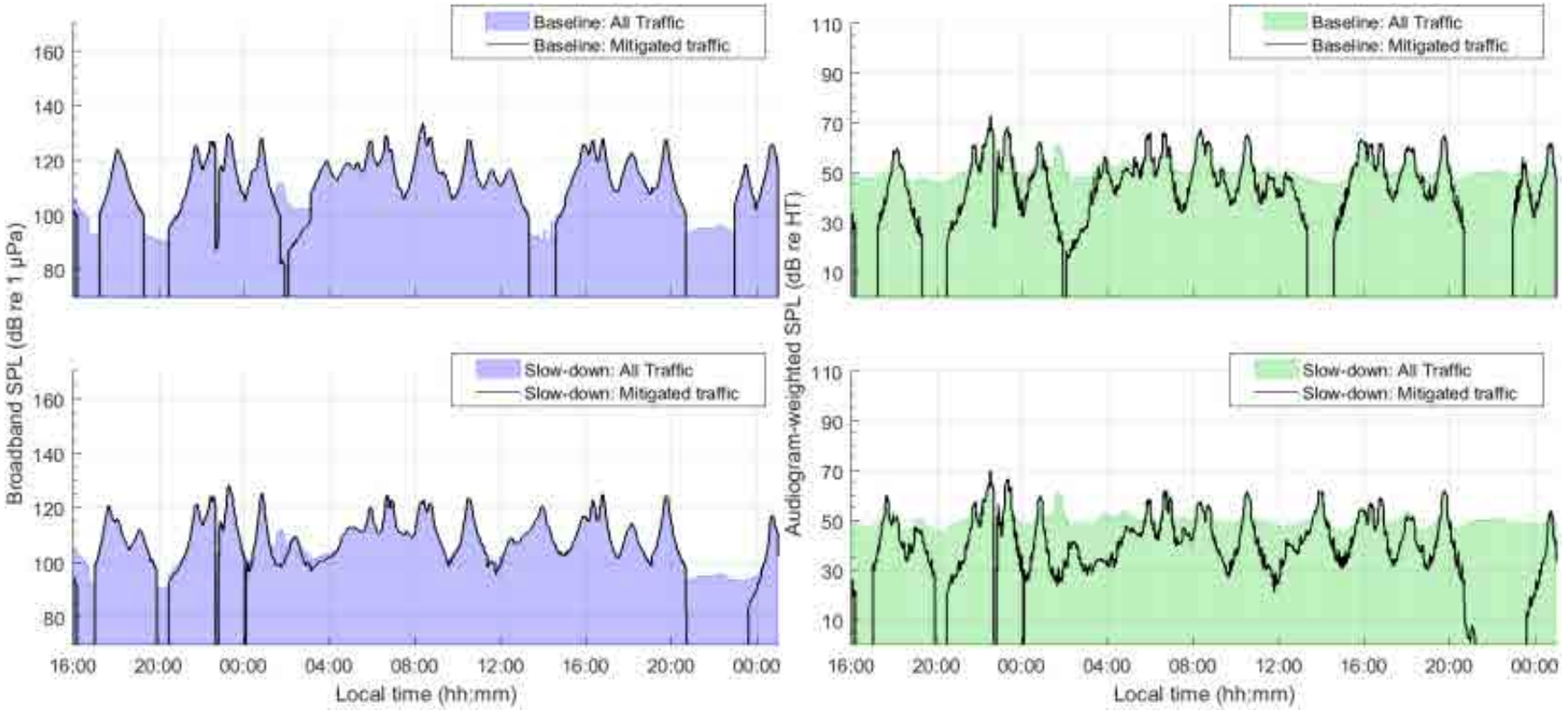

Figure 93. *Swiftsure Bank – Baseline vs Slow-Down (11-knot speed limit), Sample location 6*: Temporal variability of unweighted (left) and audiogram-weighted (right) received levels for (top) baseline (no slow-down) and (bottom) slow-down scenarios. The blue and green lines above the shaded area show received levels caused by all traffic and ambient noise. The black lines show received levels caused by commercial traffic only. The receiver location is shown in Figure 8.

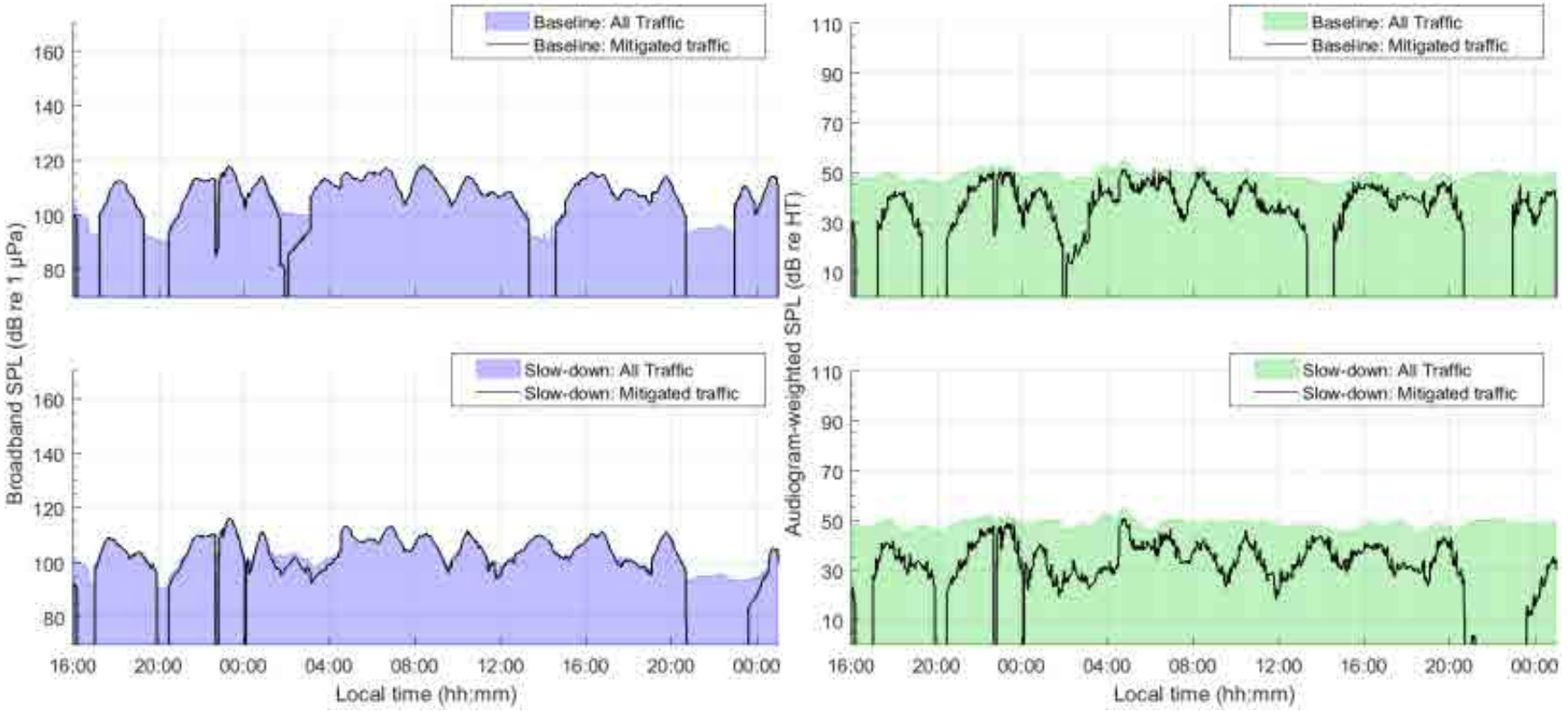

Figure 94. *Swiftsure Bank – Baseline vs Slow-Down (11-knot speed limit), Sample location 7*: Temporal variability of unweighted (left) and audiogram-weighted (right) received levels for (top) baseline (no slow-down) and (bottom) slow-down scenarios. The blue and green lines above the shaded area show received levels caused by all traffic and ambient noise. The black lines show received levels caused by commercial traffic only. The receiver location is shown in Figure 8.

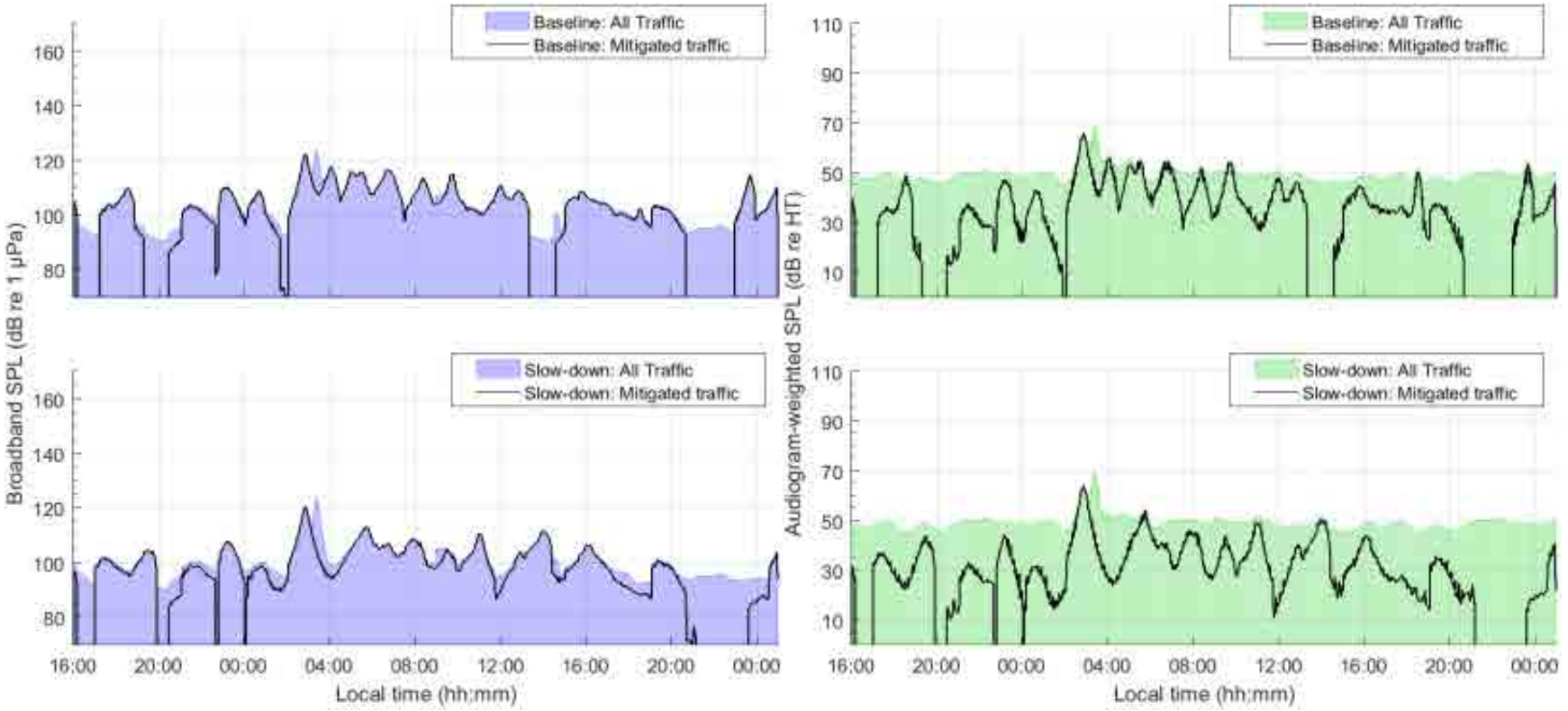

Figure 95. *Swiftsure Bank – Baseline vs Slow-Down (11-knot speed limit), Sample location 8*: Temporal variability of unweighted (left) and audiogram-weighted (right) received levels for (top) baseline (no slow-down) and (bottom) slow-down scenarios. The blue and green lines above the shaded area show received levels caused by all traffic and ambient noise. The black lines show received levels caused by commercial traffic only. The receiver location is shown in Figure 8.

Table 35. *Swiftsure Bank – Baseline vs Slow-Down (11-knot speed limit):* Temporal analysis of unweighted received noise levels (dB re 1 µPa), difference in received noise levels (dB), and difference acoustic intensity (%). The values indicate the percentile or mean calculated over a 33-hour period without (Baseline) and with mitigation (Slow-down), at the sample locations within the SRKW critical habitat shown in Figure 8.

Sample location	Scenario	Temporal analysis of noise level (dB re 1 µPa), difference in noise levels (dB), and difference in acoustic intensity (%)			
		5th	50th	95th	Mean
1	Baseline	92.2	105.2	115.0	104.4 ±7.2
	Slow-down	93.4	101.9	111.1	101.8 ±6.2
	Difference	**+1.2 (+31.8%)**	**−3.3 (−53.2%)**	**−3.9 (−59.3%)**	**−2.6 (−45.0%)**
2	Baseline	91.8	100.0	108.5	100.0 ±5.1
	Slow-down	92.6	97.8	104.7	98.1 ±4.0
	Difference	**+0.8 (+20.2%)**	**−2.2 (−39.7%)**	**−3.8 (−58.3%)**	**−1.9 (−35.4%)**
3	Baseline	92.0	103.6	114.1	103.2 ±7.0
	Slow-down	93.7	101.0	110.0	101.0 ±5.9
	Difference	**+1.7 (+47.9%)**	**−2.6 (−45.0%)**	**−4.1 (−61.1%)**	**−2.2 (−39.7%)**
4	Baseline	92.1	107.2	120.9	106.7 ±8.4
	Slow-down	93.8	104.9	115.6	104.2 ±6.9
	Difference	**+1.7 (+47.9%)**	**−2.3 (−41.1%)**	**−5.3 (−70.5%)**	**−2.5 (−43.8%)**
5	Baseline	92.1	112.7	129.2	112.1 ±11.7
	Slow-down	93.8	109.2	124.5	109.5 ±9.7
	Difference	**+1.7 (+47.9%)**	**−3.5 (−55.3%)**	**−4.7 (−66.1%)**	**−2.6 (−45.0%)**
6	Baseline	92.1	111.9	126.9	110.8 ±10.5
	Slow-down	93.8	107.8	122.3	107.9 ±8.5
	Difference	**+1.7 (+47.9%)**	**−4.1 (−61.1%)**	**−4.6 (−65.3%)**	**−2.9 (−48.7%)**
7	Baseline	92.0	108.1	115.8	106.5 ±7.5
	Slow-down	93.8	103.6	111.6	103.6 ±5.6
	Difference	**+1.8 (+51.4%)**	**−4.5 (−64.5%)**	**−4.2 (−62.0%)**	**−2.9 (−48.7%)**
8	Baseline	91.8	103.4	115.7	103.4 ±7.2
	Slow-down	93.1	99.9	111.3	100.7 ±5.9
	Difference	**+1.3 (+34.9%)**	**−3.5 (−55.3%)**	**−4.4 (−63.7%)**	**−2.7 (−46.3%)**

Table 36. *Swiftsure Bank – Baseline vs Slow-Down (11-knot speed limit):* Temporal analysis of SRKW audiogram-weighted received noise levels (dB re HT), difference in received noise levels (dB), and difference acoustic intensity (%). The values indicate the percentile or mean calculated over a 33-hour period without (Baseline) and with mitigation (Slow-down), at the sample locations within the SRKW critical habitat shown in Figure 8.

Sample location	Scenario	Temporal analysis of noise level (dB re HT), difference in noise levels (dB), and difference in acoustic intensity (%)			
		5th	50th	95th	Mean
1	Baseline	46.0	49.3	55.0	49.9 ±3.8
	Slow-down	46.0	48.9	54.8	49.6 ±3.8
	Difference	**0.0 (0.0%)**	**−0.4 (−8.8%)**	**−0.2 (−4.5%)**	**−0.3 (−6.7%)**
2	Baseline	45.8	48.9	52.7	48.8 ±2.1
	Slow-down	45.7	48.8	52.6	48.8 ±2.1
	Difference	**−0.1 (−2.3%)**	**−0.1 (−2.3%)**	**−0.1 (−2.3%)**	**0.0 (0.0%)**
3	Baseline	46.1	49.0	55.0	49.6 ±3.7
	Slow-down	45.9	48.9	53.7	49.3 ±3.6
	Difference	**−0.2 (−4.5%)**	**−0.1 (−2.3%)**	**−1.3 (−25.9%)**	**−0.3 (−6.7%)**
4	Baseline	46.4	49.8	59.1	50.6 ±3.8
	Slow-down	46.2	49.2	55.8	49.8 ±3.1
	Difference	**−0.2 (−4.5%)**	**−0.6 (−12.9%)**	**−3.3 (−53.2%)**	**−0.8 (−16.8%)**
5	Baseline	46.4	51.0	66.2	53.8 ±6.4
	Slow-down	46.5	50.6	62.4	52.3 ±4.8
	Difference	**+0.1 (+2.3%)**	**−0.4 (−8.8%)**	**−3.8 (−58.3%)**	**−1.5 (−29.2%)**
6	Baseline	46.4	50.4	63.6	52.3 ±5.2
	Slow-down	46.3	49.8	60.2	51.0 ±4.0
	Difference	**−0.1 (−2.3%)**	**−0.6 (−12.9%)**	**−3.4 (−54.3%)**	**−1.3 (−25.9%)**
7	Baseline	46.2	49.2	52.4	49.2 ±1.8
	Slow-down	45.9	48.8	51.7	48.8 ±1.7
	Difference	**−0.3 (−6.7%)**	**−0.4 (−8.8%)**	**−0.7 (−14.9%)**	**−0.4 (−8.8%)**
8	Baseline	46.2	49.2	55.3	49.7 ±3.2
	Slow-down	45.8	49.0	53.0	49.3 ±2.9
	Difference	**−0.4 (−8.8%)**	**−0.2 (−4.5%)**	**−2.3 (−41.1%)**	**−0.4 (−8.8%)**

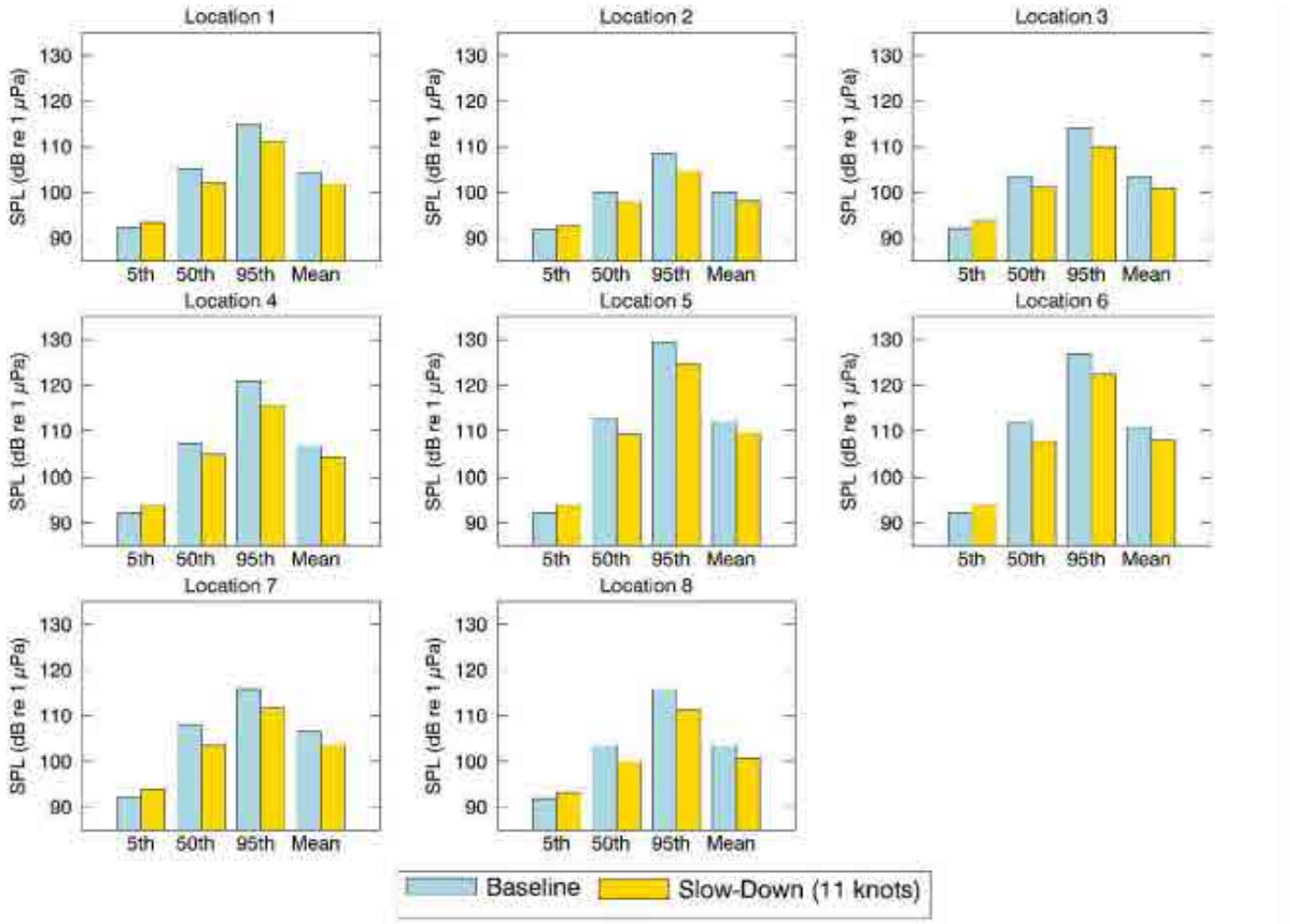

Figure 96. *Swiftsure Bank – Baseline vs Slow-Down (11-knot speed limit)*: Histogram representation of the temporal analysis of unweighted received noise levels (dB re 1 µPa). The vertical bars indicate the percentile or mean calculated over a 33-hour period without (baseline) and with mitigation, at the sample locations within the SRKW critical habitat shown in Figure 8.

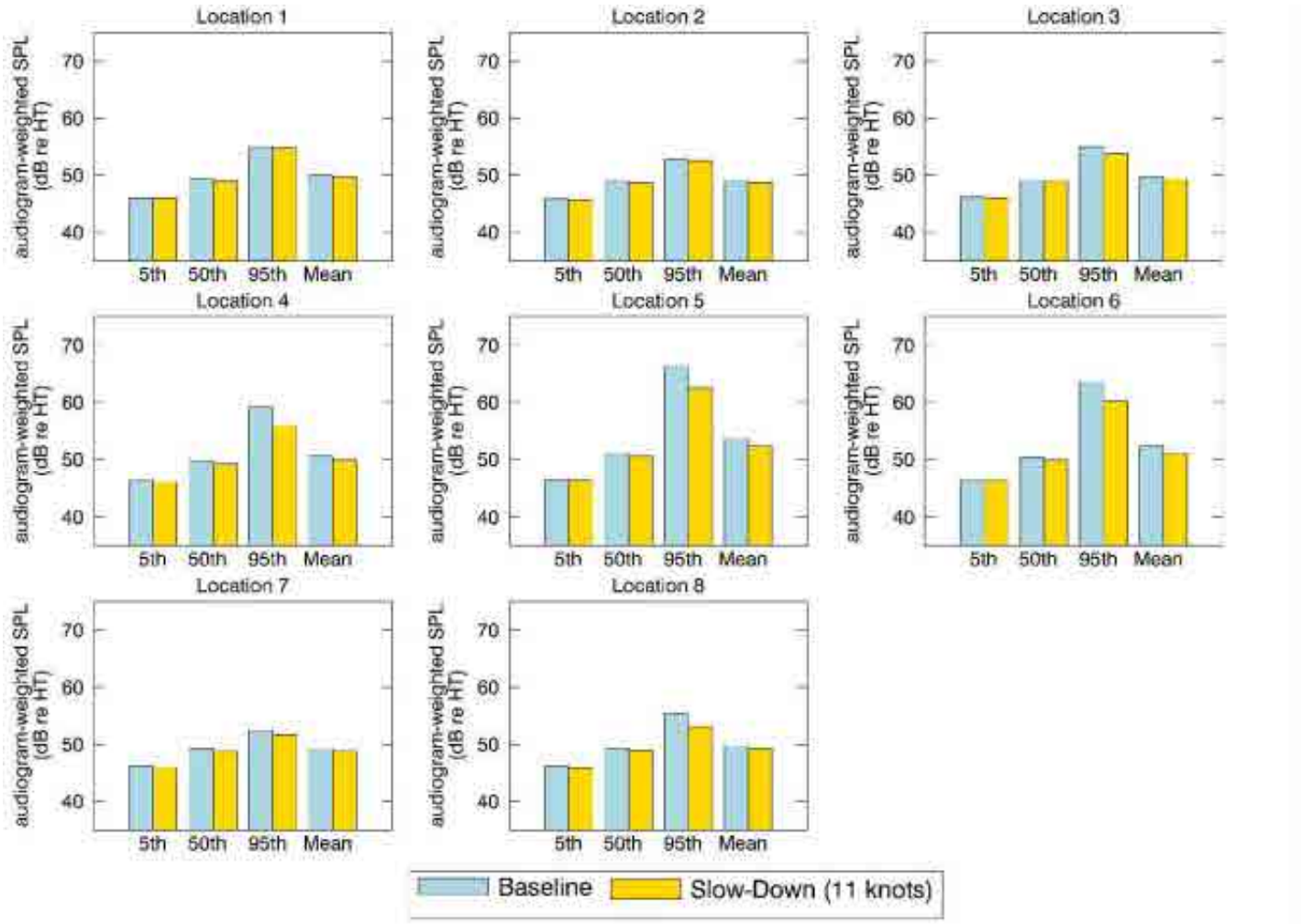

Figure 97. *Swiftsure Bank – Baseline vs Slow-Down (11-knot speed limit):* Histogram representation of the temporal analysis of SRKW audiogram-weighted received noise levels (dB re HT). The vertical bars indicate the percentile or mean calculated over a 33-hour period without (baseline) and with mitigation, at the sample locations within the SRKW critical habitat shown in Figure 8.

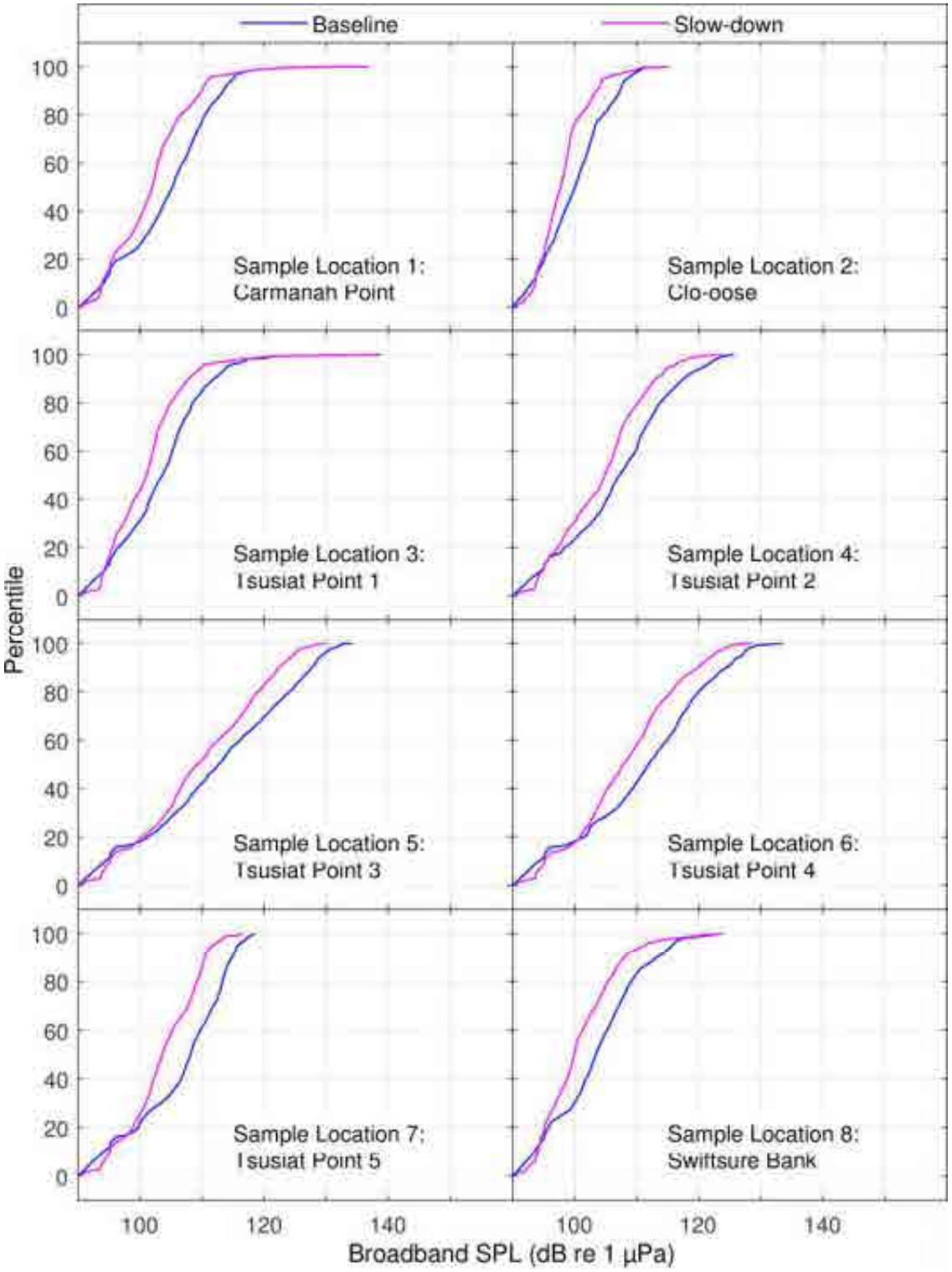

Figure 98. *Swiftsure Bank – Baseline vs Slow-Down (11-knot speed limit):* CDF curves of time-dependent unweighted SPL for baseline and mitigated scenarios at the sample locations shown in Figure 8.

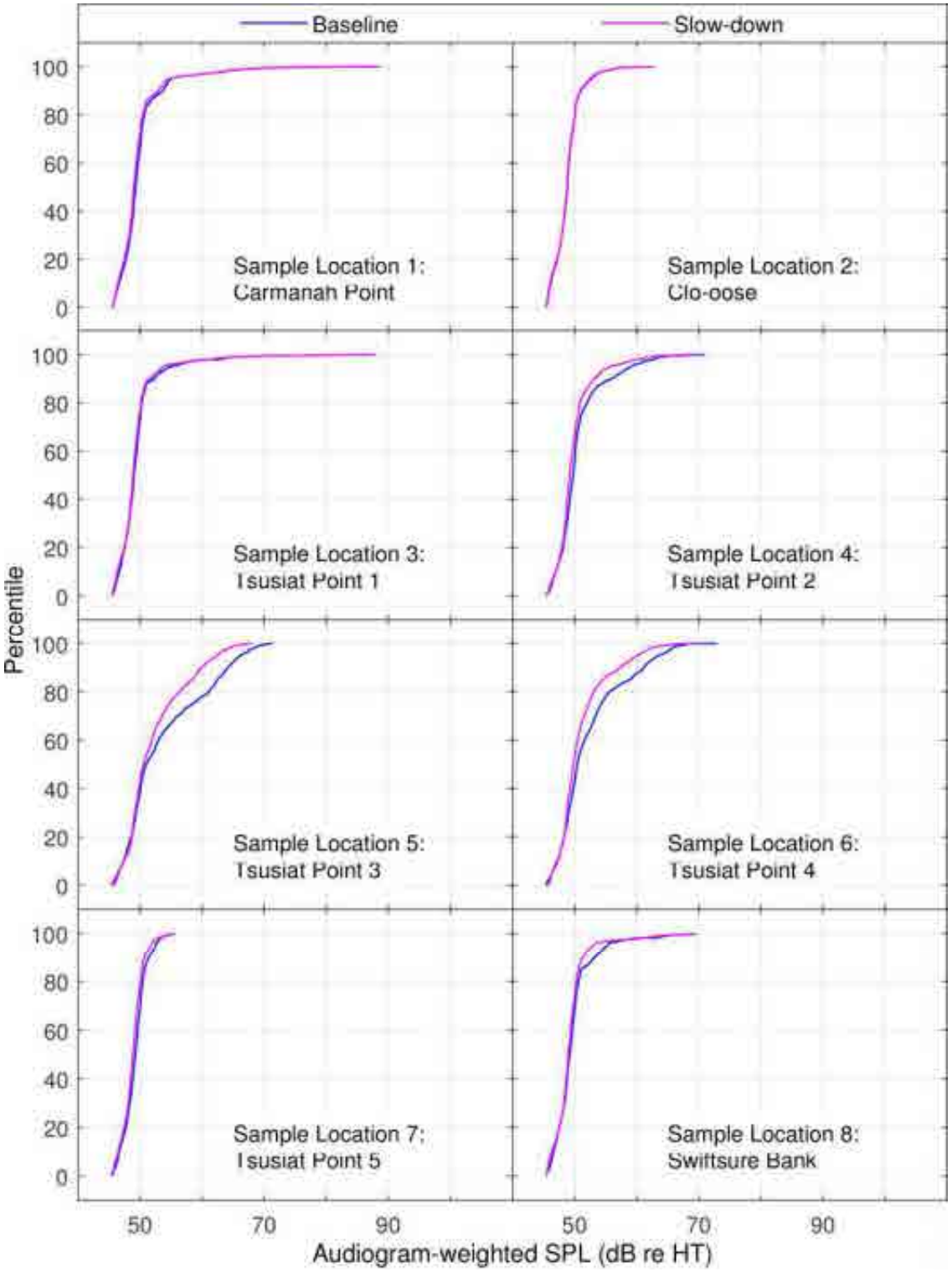

Figure 99. *Swiftsure Bank – Baseline vs Slow-Down (11-knot speed limit):* CDF curves of time-dependent audiogram-weighted SPL for baseline and mitigated scenarios at the sample locations shown in Figure 8.

3.4. Future Mitigated Noise Levels–Implementing a No-Go Period

This section presents equivalent noise levels (L_{eq}, unweighted and audiogram-weighted) for July, over the Haro Strait Local Study Area. The mitigated results represent the expected increase in vessel traffic associated with the Trans Mountain requirements and implementing daily no-go periods for commercial vessel classes for the hours of midnight to 04:00, as described in Section 2.2.3.2. Figures 100 and 101 present maps of the L_{eq} over the hours of midnight to 04:00, for baseline (top left) and mitigated (top right) scenarios, and change in L_{eq} with respect to baseline (bottom). Figures 102 and 103 present similar maps for L_{eq} over the hours of 04:00 to midnight (unrestricted period). Tables 37 and 38 present the L_{eq} for the baseline and mitigated scenarios at eight sample locations in the SRKW critical habitat. The sample locations are listed in Table 1 and shown as green dots in Figures 100–103.

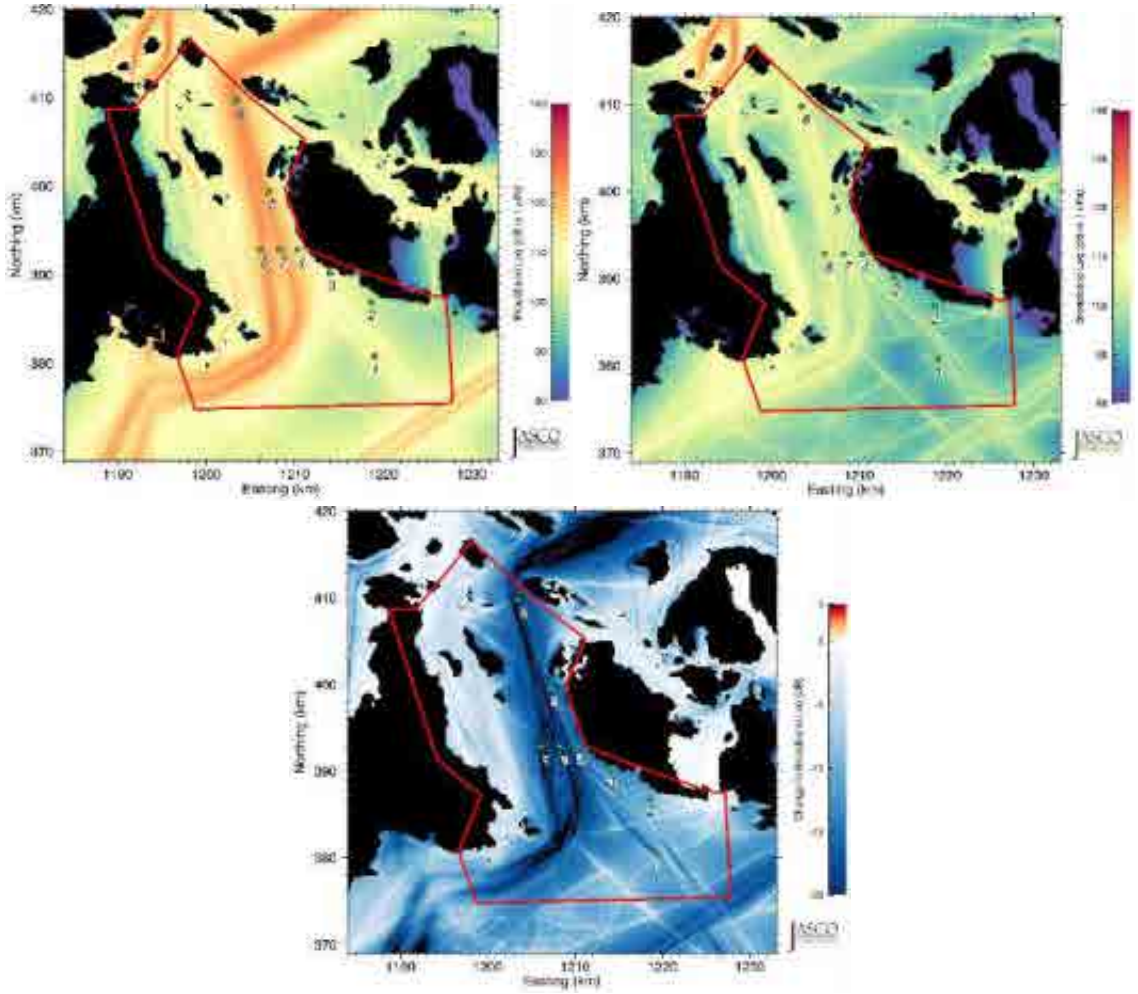

Figure 100. *Haro Strait – Restricted period (Midnight to 04:00):* Unweighted equivalent continuous noise levels (L_{eq}; top right) and change in L_{eq} (bottom) relative to July 2015 baseline levels (top left). Grid resolution is 200 × 200 m. The green dots are the sample locations in the SRKW critical habitat. The red line shows the Haro Strait regional boundaries.

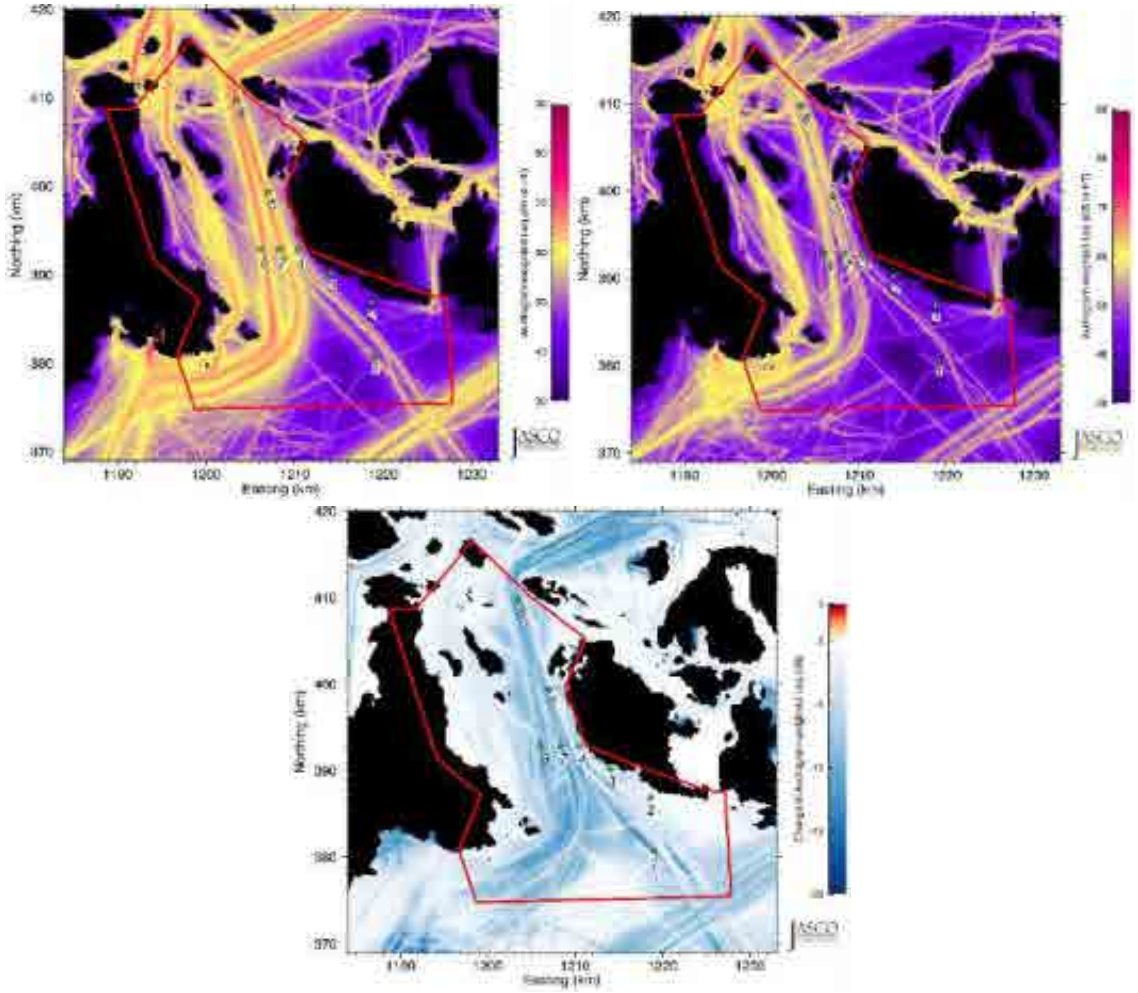

Figure 101. *Haro Strait – Restricted period (Midnight to 04:00):* Audiogram-weighted equivalent continuous noise levels (L_{eq}; top right) and change in L_{eq} (bottom) relative to July 2015 baseline levels (top left) in the Local Study Area. Grid resolution is 200 × 200 m. The green dots are the sample locations in the SRKW critical habitat. The red line shows the Haro Strait regional boundaries.

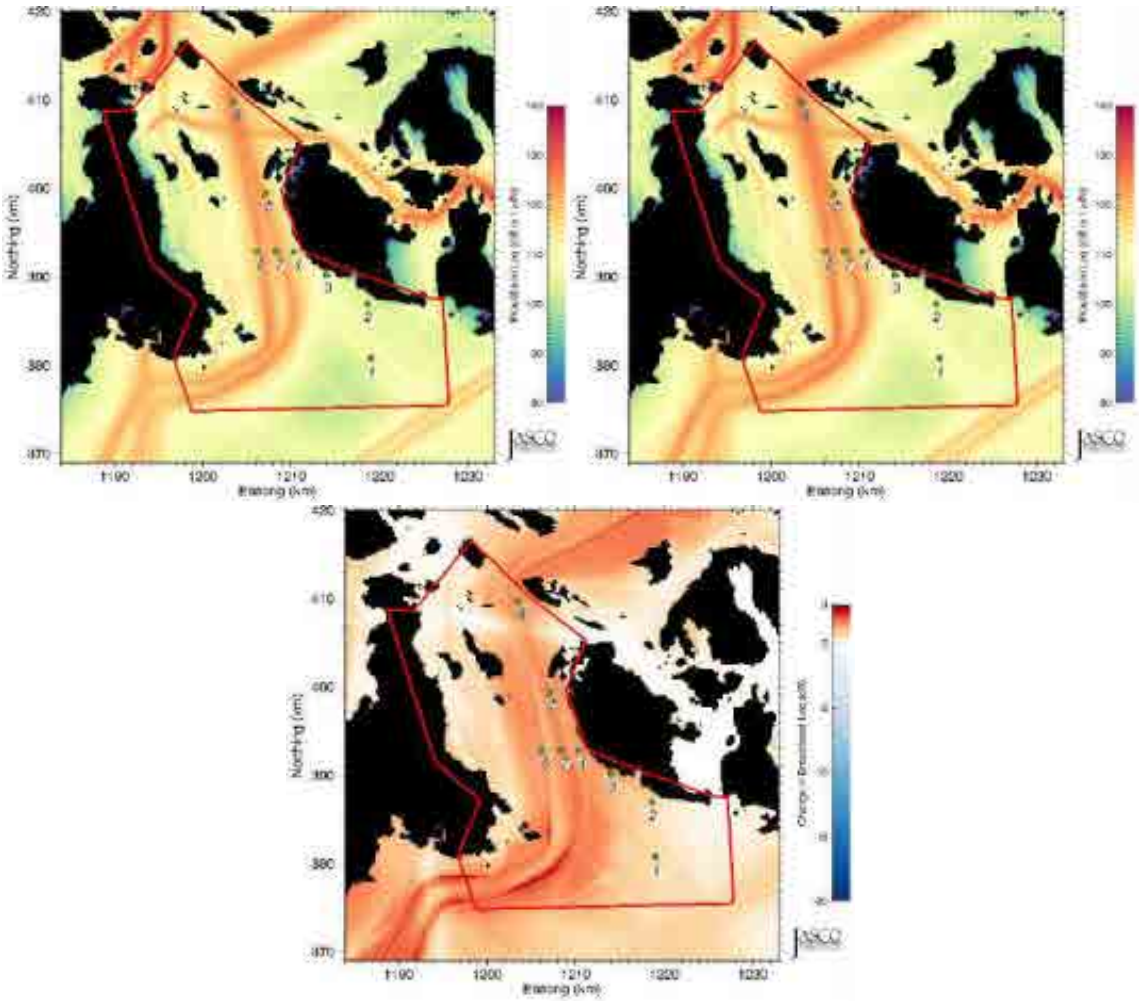

Figure 102. *Haro Strait – Unrestricted period (04:00 to Midnight):* Unweighted equivalent continuous noise levels (L_{eq}; top right) and change in L_{eq} (bottom) relative to July 2015 baseline levels (top left) in the Local Study Area. Grid resolution is 200 × 200 m. The green dots are the sample locations in the SRKW critical habitat. The red line shows the Haro Strait regional boundaries.

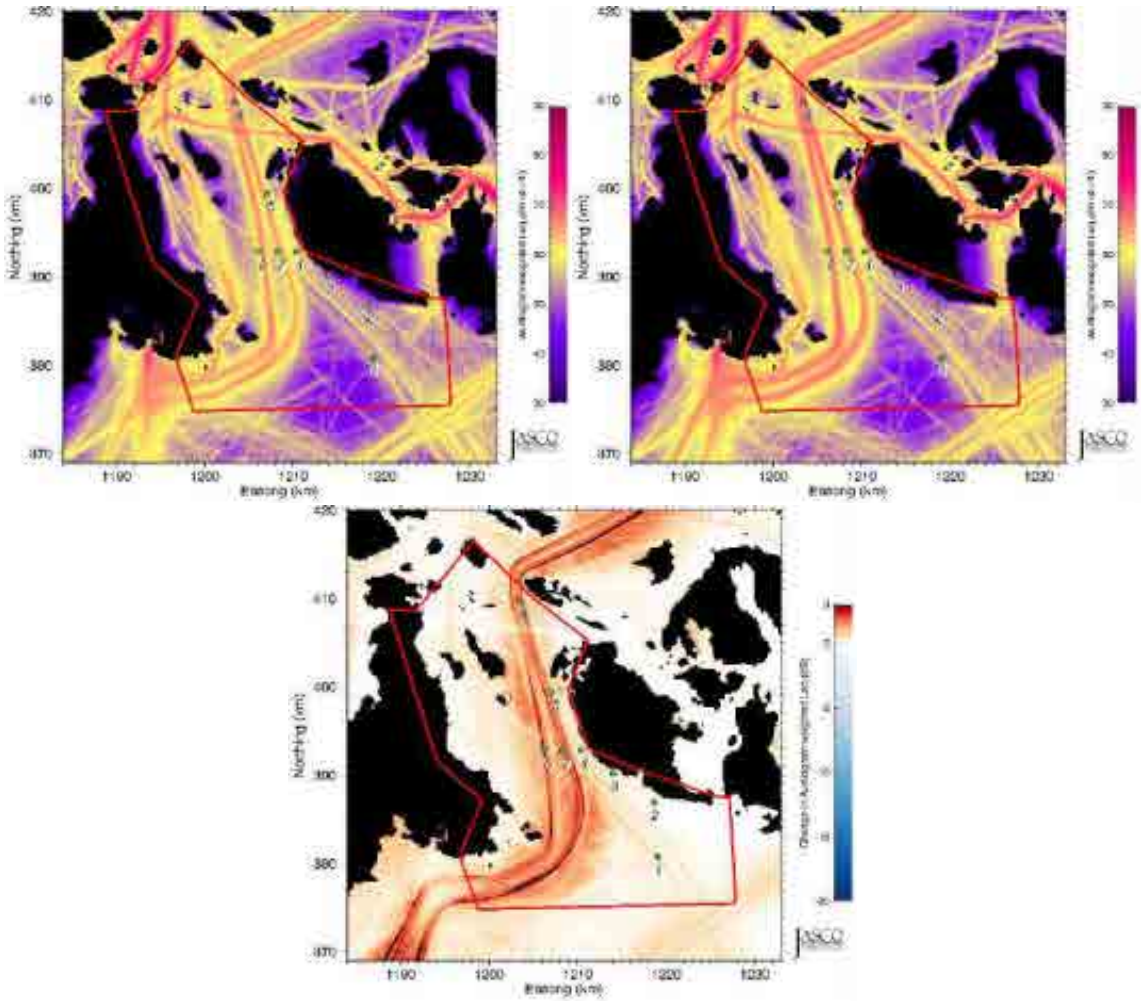

Figure 103. *Haro Strait – Unrestricted period (04:00 to Midnight):* Audiogram-weighted equivalent continuous noise levels (L_{eq}; top right) and change in L_{eq} (bottom) relative to July 2015 baseline levels (top left). Grid resolution is 200 × 200 m. The green dots are the sample locations in the SRKW critical habitat. The red line shows the Haro Strait regional boundaries.

Table 37. *Haro Strait – Baseline* vs. *No-Go Period*: Unweighted received levels (dB re 1 µPa), changes in received levels (dB), and changes in acoustic intensity (%) at the sample locations in the SRKW critical habitat shown in Figure 6.

Sample location	Restricted period (Midnight to 04:00)				Unrestricted period (04:00 to midnight)			
	Baseline (dB re 1 µPa)	Mitigated (dB re 1 µPa)	Change		Baseline (dB re 1 µPa)	Mitigated (dB re 1 µPa)	Change	
			dB	%			dB	%
1	109.1	93.8	−15.3	−97.0	109.3	110.0	+0.7	+17.5
2	101.5	92.0	−9.5	−88.8	104.2	104.9	+0.7	+17.5
3	106.5	93.1	−13.4	−95.4	106.5	107.8	+1.3	+34.9
4	114.3	98.6	−15.7	−97.3	114.2	115.6	+1.4	+38.0
5	119.2	106.3	−12.9	−94.9	118.9	120.3	+1.4	+38.0
6	123.5	106.4	−17.1	−98.1	123.4	124.9	+1.5	+41.3
7	123.2	103.5	−19.7	−98.9	122.9	124.3	+1.4	+38.0
8	123.8	105.5	−18.3	−98.5	123.5	124.8	+1.3	+34.9

Table 38. *Haro Strait – Baseline* vs. *No-Go Period*: Audiogram-weighted received levels (dB re HT), changes in received levels (dB), and changes in acoustic intensity (%) at the sample locations in the SRKW critical habitat shown in Figure 6.

Sample location	Restricted period (Midnight to 04:00)				Unrestricted period (04:00 to midnight)			
	Baseline (dB re HT)	Mitigated (dB re HT)	Change		Baseline (dB re HT)	Mitigated (dB re HT)	Change	
			dB	%			dB	%
1	54.8	42.0	−12.8	−94.8	56.5	57.0	+0.5	+12.2
2	44.3	43.3	−1.0	−20.6	52.2	52.3	+0.1	+2.3
3	44.0	37.8	−6.2	−76.0	47.3	47.8	+0.5	+12.2
4	52.5	47.6	−4.9	−67.6	56.8	57.2	+0.4	+9.6
5	59.4	58.2	−1.2	−24.1	61.0	61.3	+0.3	+7.2
6	64.6	58.1	−6.5	−77.6	64.6	66.4	+1.8	+51.4
7	65.4	55.2	−10.2	−90.5	65.1	66.5	+1.4	+38.0
8	66.2	58.1	−8.1	−84.5	66.2	67.5	+1.3	+34.9

3.5. Future Mitigated Noise Levels–Replacing 10% of Noisiest Ships

This section presents equivalent noise levels (L_{eq}, unweighted and audiogram-weighted) for July, over the four Local Study Areas. The mitigated results represent the expected increase in vessel traffic associated with the Trans Mountain requirements and replacing 10% of the noisiest vessels by the same amount of the least noisy vessels of that class, as described in Section 2.2.3.3. Two sets of results are present:

- 10% of noisiest vessel selected based on unweighted broadband source levels, and
- 10% of noisiest vessel selected based on audiogram-weighted broadband source levels.

Figures 104–119 present maps of (left/top) L_{eq} and (right/bottom) change in L_{eq} with respect to baseline levels for July, seen in Figures 17–20. Tables 39–46 present L_{eq} for the baseline and mitigated scenarios at the sample locations in the SRKW critical habitat. The sample locations are listed in Table 1 and shown in Figures 104–119.

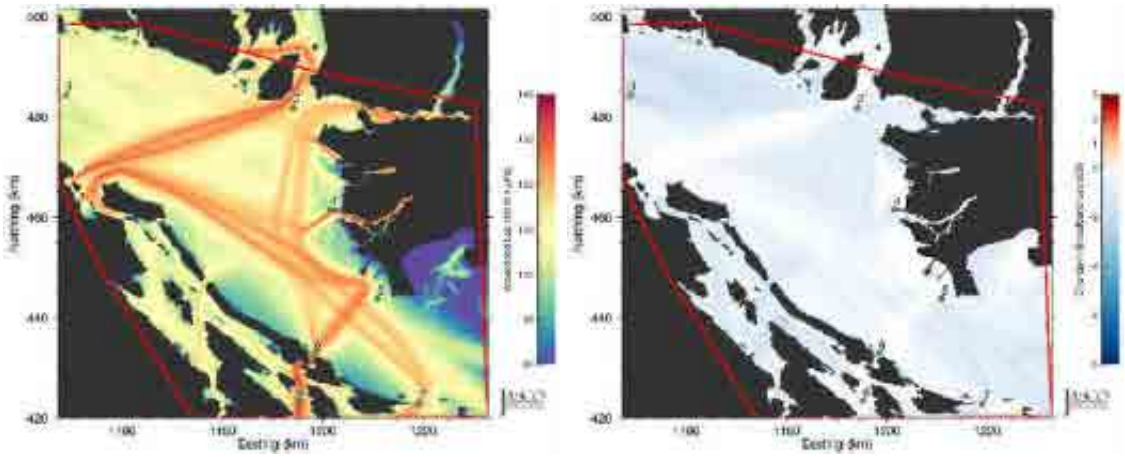

Figure 104. *Strait of Georgia – Replacing 10% of ships with highest unweighted broadband source levels*: Unweighted equivalent continuous noise levels (L_{eq}; left) and change in L_{eq} (right) relative to July 2015 baseline levels. Grid resolution is 200 × 200 m. The green dots are the sample locations in the SRKW critical habitat. The red line shows the boundary of the area where statistical values (percentiles and mean) were derived.

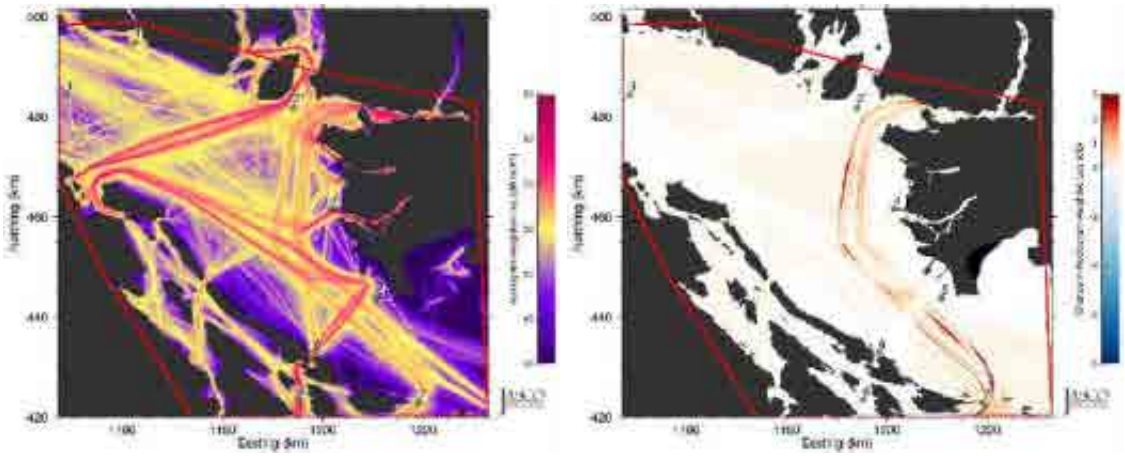

Figure 105. *Strait of Georgia – Replacing 10% of ships with highest unweighted broadband source levels*: Audiogram-weighted equivalent continuous noise levels (L_{eq}; left) and change in L_{eq} (right) relative to July 2015 baseline levels. Grid resolution is 200 × 200 m. The green dots are the sample locations in the SRKW critical habitat. The red line shows the boundary of the area where statistical values (percentiles and mean) were derived.

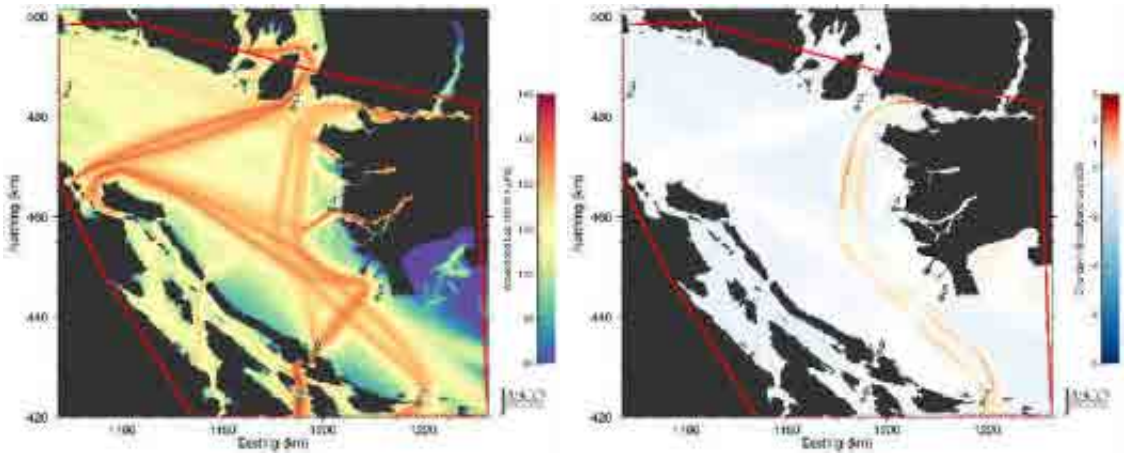

Figure 106. *Strait of Georgia – Replacing 10% of ships with highest audiogram-weighted broadband source levels*: Unweighted equivalent continuous noise levels (L_{eq}; left) and change in L_{eq} (right) relative to July 2015 baseline levels. Grid resolution is 200 × 200 m. The green dots are the sample locations in the SRKW critical habitat. The red line shows the boundary of the area where statistical values (percentiles and mean) were derived.

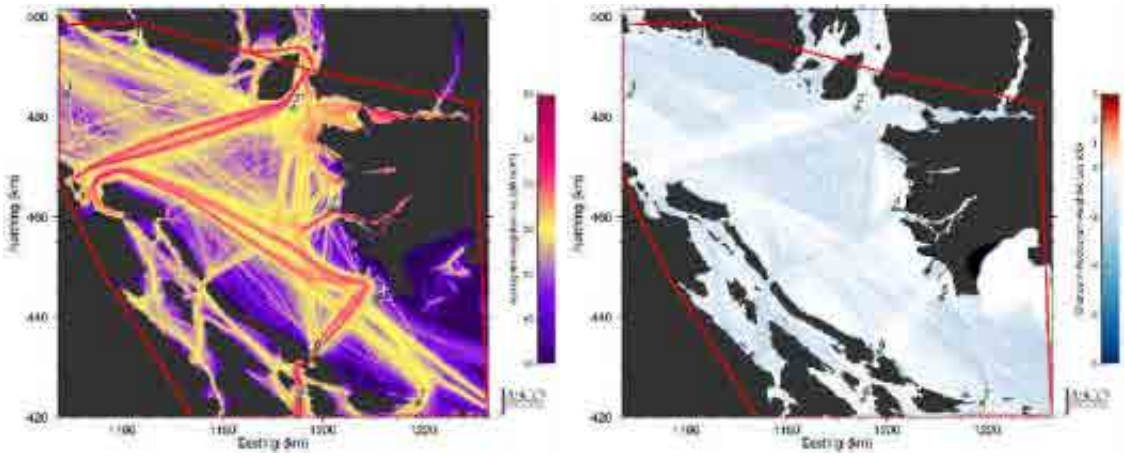

Figure 107. *Strait of Georgia – Replacing 10% of ships with highest audiogram-weighted broadband source levels*: Audiogram-weighted equivalent continuous noise levels (L_{eq}; left) and change in L_{eq} (right) relative to July 2015 baseline levels. Grid resolution is 200 × 200 m. The green dots are the sample locations in the SRKW critical habitat. The red line shows the boundary of the area where statistical values (percentiles and mean) were derived.

Table 39. *Strait of Georgia – Baseline* vs. *replacing 10% of ships with highest source levels*: Unweighted received levels (dB re 1 µPa), changes in received levels (dB), and changes in acoustic intensity (%) at the sample locations in the SRKW critical habitat shown in Figure 5.

Sample location	Baseline (dB re 1 µPa)	Selected based on unweighted broadband source levels			Selected based on audiogram-weighted broadband source levels		
		Mitigated (dB re 1 µPa)	Change		Mitigated (dB re 1 µPa)	Change	
			dB	%		dB	%
1	113.0	111.9	−1.1	−22.4	112.4	−0.6	−12.9
2	118.2	117	−1.2	−24.1	117.9	−0.3	−6.7
3	106.4	104.2	−2.2	−39.7	106.1	−0.3	−6.7
4	113.0	112.5	−0.5	−10.9	112.8	−0.2	−4.5
5	107.8	107	−0.8	−16.8	107.5	−0.3	−6.7
6	129.8	129.7	−0.1	−2.3	129.8	0.0	0.0
7	125.3	123.9	−1.4	−27.6	125.3	0.0	0.0
8	130.9	130.8	−0.1	−2.3	130.9	0.0	0.0

Table 40. *Strait of Georgia – Baseline* vs. *replacing 10% of ships with highest source levels*: Audiogram-weighted received levels (dB re HT), changes in received levels (dB), and changes in acoustic intensity (%) at the sample locations in the SRKW critical habitat shown in Figure 5.

Sample location	Baseline (dB re HT)	Selected based on unweighted broadband source levels			Selected based on audiogram-weighted broadband source levels		
		Mitigated (dB re HT)	Change		Mitigated (dB re HT)	Change	
			dB	%		dB	%
1	59.5	59.6	+0.1	+2.3	57.6	−1.9	−35.4
2	63.5	63.5	0.0	0.0	62.5	−1.0	−20.6
3	53.9	53.9	0.0	0.0	53.7	−0.2	−4.5
4	64.7	64.7	0.0	0.0	64.6	−0.1	−2.3
5	53.8	53.8	0.0	0.0	53.5	−0.3	−6.7
6	74.9	74.9	0.0	0.0	74.8	−0.1	−2.3
7	66.0	65.8	−0.2	−4.5	63.5	−2.5	−43.8
8	72.9	72.9	0.0	0.0	72.8	−0.1	−2.3

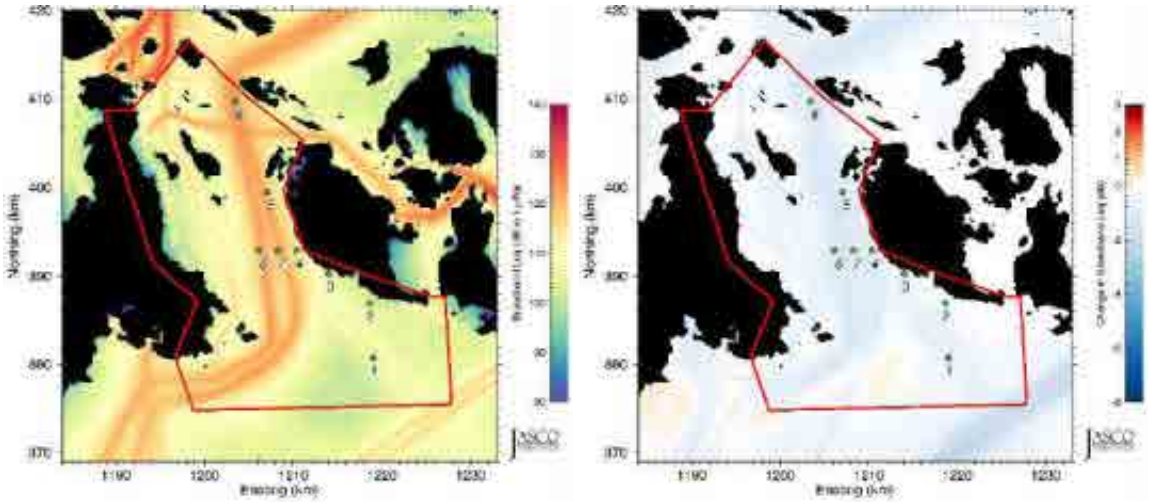

Figure 108. *Haro Strait – Replacing 10% of ships with highest unweighted broadband source levels*: Unweighted equivalent continuous noise levels (L_{eq}; left) and change in L_{eq} (right) relative to July 2015 baseline levels. Grid resolution is 200 × 200 m. The green dots are the sample locations in the SRKW critical habitat. The red line shows the boundary of the area where statistical values (percentiles and mean) were derived.

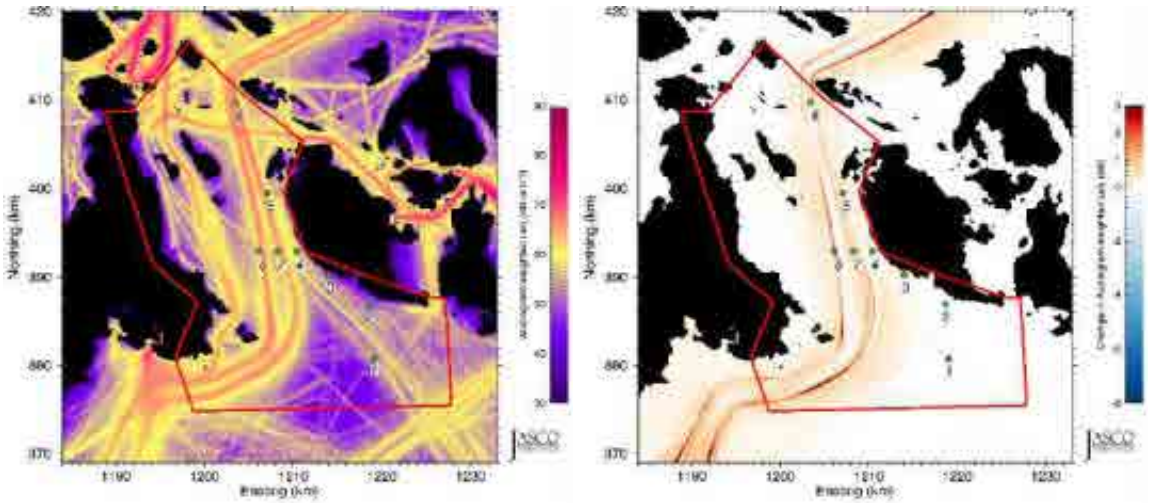

Figure 109. *Haro Strait – Replacing 10% of ships with highest unweighted broadband source levels*: Audiogram-weighted equivalent continuous noise levels (L_{eq}; left) and change in L_{eq} (right) relative to July 2015 baseline levels. Grid resolution is 200 × 200 m. The green dots are the sample locations in the SRKW critical habitat. The red line shows the boundary of the area where statistical values (percentiles and mean) were derived.

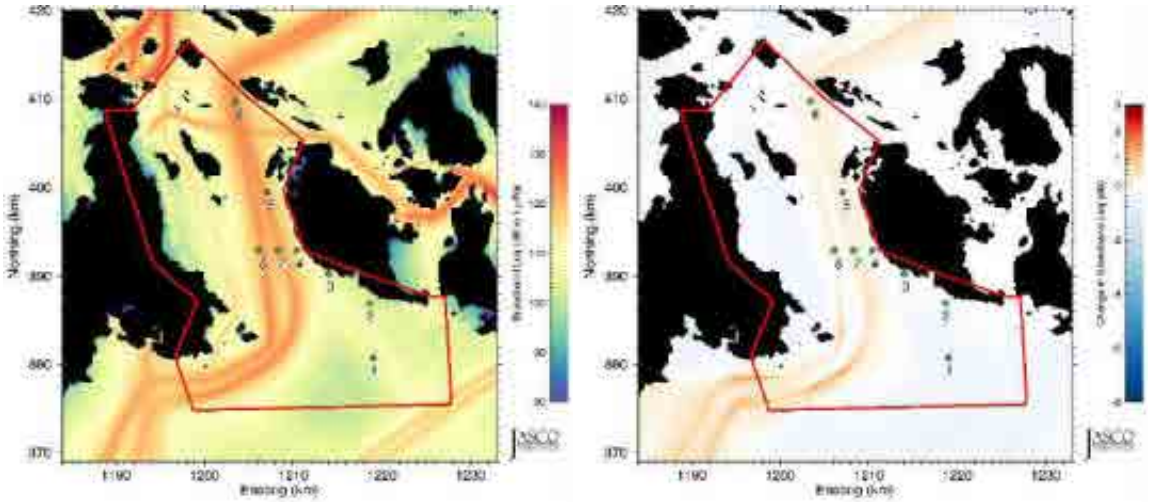

Figure 110. *Haro Strait – Replacing 10% of ships with highest audiogram-weighted broadband source levels*: Unweighted equivalent continuous noise levels (L_{eq}; left) and change in L_{eq} (right) relative to July 2015 baseline levels. Grid resolution is 200 × 200 m. The green dots are the sample locations in the SRKW critical habitat. The red line shows the boundary of the area where statistical values (percentiles and mean) were derived.

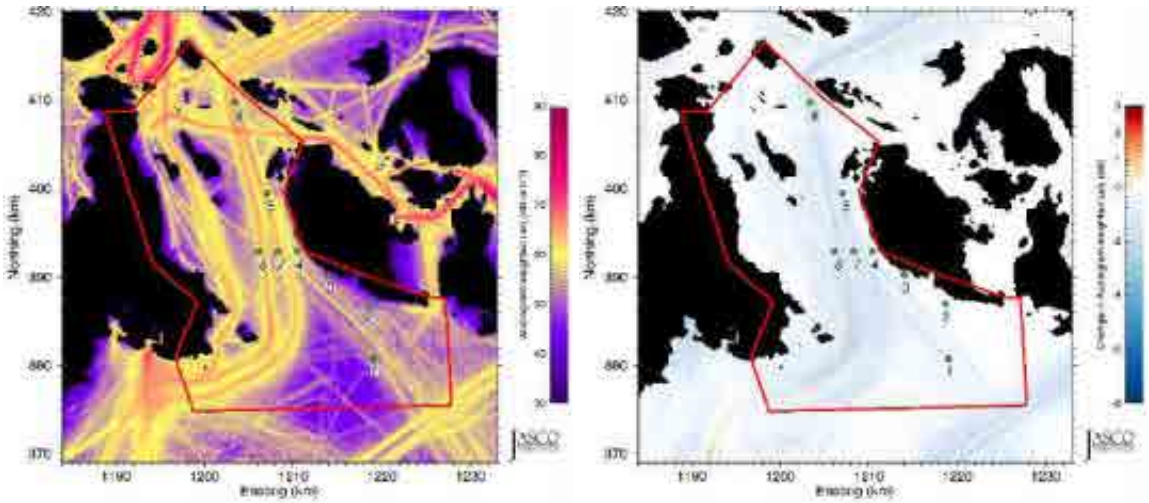

Figure 111. *Haro Strait – Replacing 10% of ships with highest audiogram-weighted broadband source levels*: Audiogram-weighted equivalent continuous noise levels (L_{eq}; left) and change in L_{eq} (right) relative to July 2015 baseline levels. Grid resolution is 200 × 200 m. The green dots are the sample locations in the SRKW critical habitat. The red line shows the boundary of the area where statistical values (percentiles and mean) were derived.

Table 41. *Haro Strait – Baseline* vs. *replacing 10% of ships with highest source levels*: Unweighted received levels (dB re 1 µPa), changes in received levels (dB), and changes in acoustic intensity (%) at the sample locations in the SRKW critical habitat shown in Figure 6.

Sample location	Baseline (dB re 1 µPa)	Selected based on unweighted broadband source levels			Selected based on audiogram-weighted broadband source levels		
		Mitigated (dB re 1 µPa)	Change		Mitigated (dB re 1 µPa)	Change	
			dB	%		dB	%
1	109.2	108.5	−0.7	−14.9	108.8	−0.4	−8.8
2	103.9	103.8	−0.1	−2.3	103.8	−0.1	−2.3
3	106.5	106.1	−0.4	−8.8	106.4	−0.1	−2.3
4	114.3	113.5	−0.8	−16.8	114.3	0.0	0.0
5	119.0	117.9	−1.1	−22.4	119.2	+0.2	+4.7
6	123.4	122.4	−1.0	−20.6	123.7	+0.3	+7.2
7	122.9	121.8	−1.1	−22.4	123.0	+0.1	+2.3
8	123.5	122.4	−1.1	−22.4	123.5	0.0	0.0

Table 42. *Haro Strait – Baseline* vs. *replacing 10% of ships with highest source levels*: Audiogram-weighted received levels (dB re HT), changes in received levels (dB), and changes in acoustic intensity (%) at the sample locations in the SRKW critical habitat shown in Figure 6.

Sample location	Baseline (dB re HT)	Selected based on unweighted broadband source levels			Selected based on audiogram-weighted broadband source levels		
		Mitigated (dB re HT)	Change		Mitigated (dB re HT)	Change	
			dB	%		dB	%
1	56.2	56.3	+0.1	+2.3	55.3	−0.9	−18.7
2	51.6	51.6	0.0	0.0	51.5	−0.1	−2.3
3	46.9	47.0	+0.1	+2.3	46.4	−0.5	−10.9
4	56.3	56.4	+0.1	+2.3	55.9	−0.4	−8.8
5	60.8	60.9	+0.1	+2.3	60.5	−0.3	−6.7
6	64.6	65.5	+0.9	+23.0	63.7	−0.9	−18.7
7	65.2	65.1	−0.1	−2.3	63.2	−2.0	−36.9
8	66.2	66.3	+0.1	+2.3	64.7	−1.5	−29.2

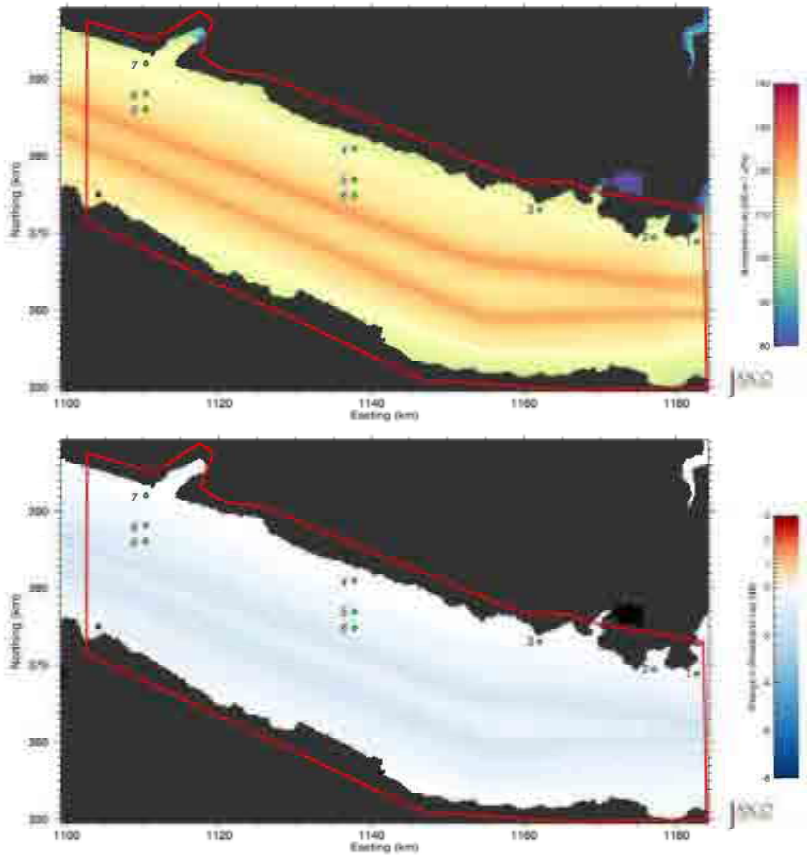

Figure 112. *Juan de Fuca Strait – Replacing 10% of ships with highest unweighted broadband source levels*: Unweighted equivalent continuous noise levels (L_{eq}; top) and change in L_{eq} (bottom) relative to July 2015 baseline levels. Grid resolution is 200 × 200 m. The green dots are the sample locations in the SRKW critical habitat. The red line shows the boundary of the area where statistical values (percentiles and mean) were derived.

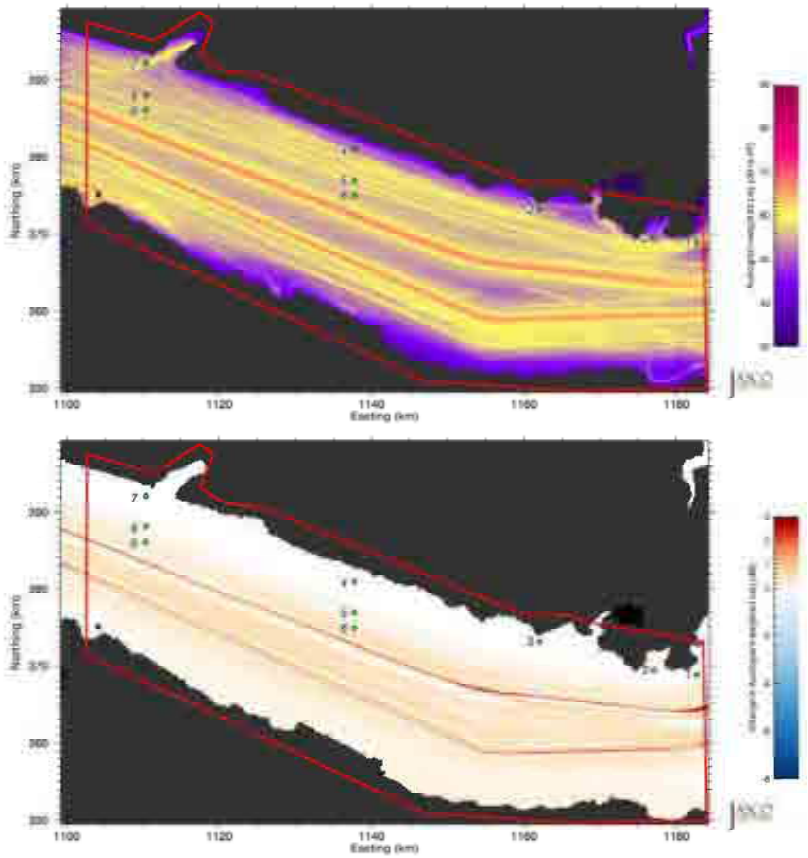

Figure 113. *Juan de Fuca Strait – Replacing 10% of ships with highest unweighted broadband source levels*: Audiogram-weighted equivalent continuous noise levels (L_{eq}; top) and change in L_{eq} (bottom) relative to July 2015 baseline levels. Grid resolution is 200 × 200 m. The green dots are the sample locations in the SRKW critical habitat. The red line shows the boundary of the area where statistical values (percentiles and mean) were derived.

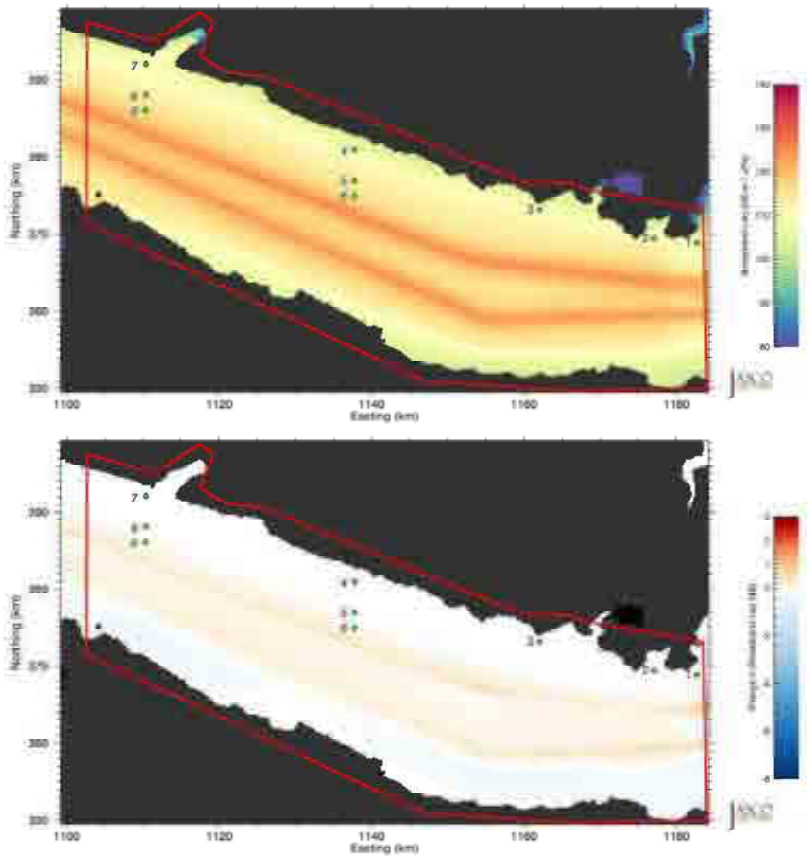

Figure 114. *Juan de Fuca Strait – Replacing 10% of ships with highest audiogram-weighted broadband source levels*: Unweighted equivalent continuous noise levels (L_{eq}; top) and change in L_{eq} (bottom) relative to July 2015 baseline levels. Grid resolution is 200 × 200 m. The green dots are the sample locations in the SRKW critical habitat. The red line shows the boundary of the area where statistical values (percentiles and mean) were derived.

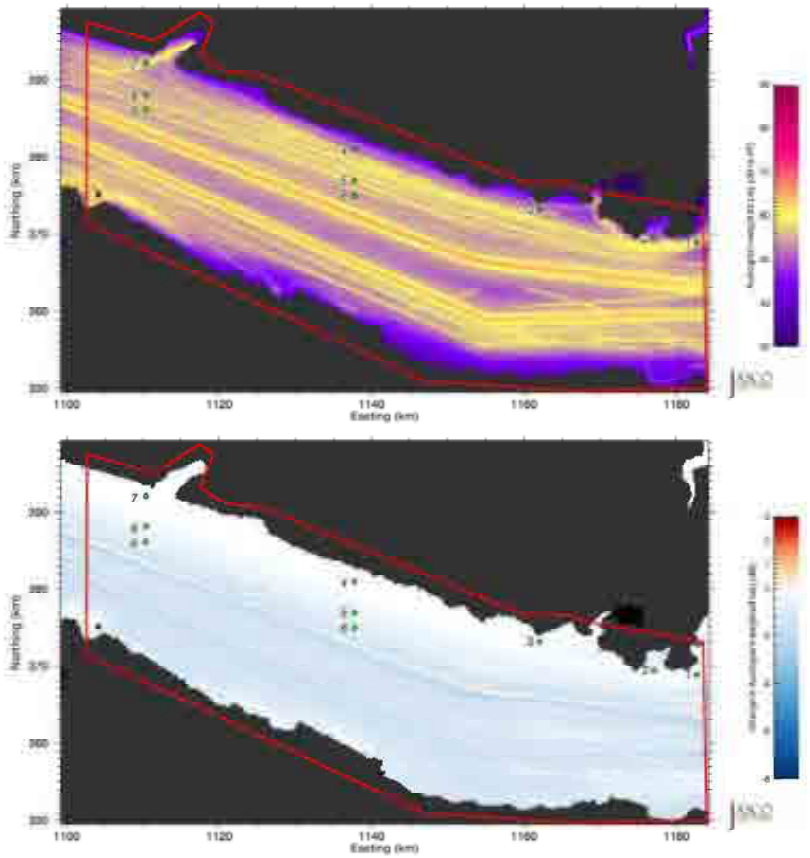

Figure 115. *Juan de Fuca Strait – Replacing 10% of ships with highest audiogram-weighted broadband source levels*: Audiogram-weighted equivalent continuous noise levels (L_{eq}; top) and change in L_{eq} (bottom) relative to July 2015 baseline levels. Grid resolution is 200 × 200 m. The green dots are the sample locations in the SRKW critical habitat. The red line shows the boundary of the area where statistical values (percentiles and mean) were derived.

Table 43. *Juan de Fuca Strait – Baseline* vs. *replacing 10% of ships with highest source levels*: Unweighted received levels (dB re 1 µPa), changes in received levels (dB), and changes in acoustic intensity (%) at the sample locations in the SRKW critical habitat shown in Figure 7.

Sample location	Baseline (dB re 1 µPa)	Selected based on unweighted broadband source levels			Selected based on audiogram-weighted broadband source levels		
		Mitigated (dB re 1 µPa)	Change		Mitigated (dB re 1 µPa)	Change	
			dB	%		dB	%
1	111.4	111.1	−0.3	−6.7	111.2	−0.2	−4.5
2	111.6	111.4	−0.2	−4.5	111.5	−0.1	−2.3
3	110.2	110.1	−0.1	−2.3	110.1	−0.1	−2.3
4	109.9	109.8	−0.1	−2.3	109.8	−0.1	−2.3
5	113.8	113.3	−0.5	−10.9	113.8	0.0	0.0
6	117.5	116.7	−0.8	−16.8	117.7	+0.2	+4.7
7	109.6	109.6	0.0	0.0	109.6	0.0	0.0
8	114.0	113.5	−0.5	−10.9	114.0	0.0	0.0
9	117.5	116.7	−0.8	−16.8	117.6	+0.1	+2.3

Table 44. *Juan de Fuca Strait – Baseline* vs. *replacing 10% of ships with highest source levels*: Audiogram-weighted received levels (dB re HT), changes in received levels (dB), and changes in acoustic intensity (%) at the sample locations in the SRKW critical habitat shown in Figure 7.

Sample location	Baseline (dB re HT)	Selected based on unweighted broadband source levels			Selected based on audiogram-weighted broadband source levels		
		Mitigated (dB re HT)	Change		Mitigated (dB re HT)	Change	
			dB	%		dB	%
1	59.1	59.1	0.0	0.0	58.8	−0.3	−6.7
2	56.9	57.0	+0.1	+2.3	56.8	−0.1	−2.3
3	55.4	55.4	0.0	0.0	55.3	−0.1	−2.3
4	56.6	56.6	0.0	0.0	56.6	0.0	0.0
5	55.6	55.7	+0.1	+2.3	54.8	−0.8	−16.8
6	56.3	56.7	+0.4	+9.6	55.2	−1.1	−22.4
7	55.0	55.0	0.0	0.0	54.9	−0.1	−2.3
8	55.9	56.0	+0.1	+2.3	55.4	−0.5	−10.9
9	55.9	56.2	+0.3	+7.2	54.6	−1.3	−25.9

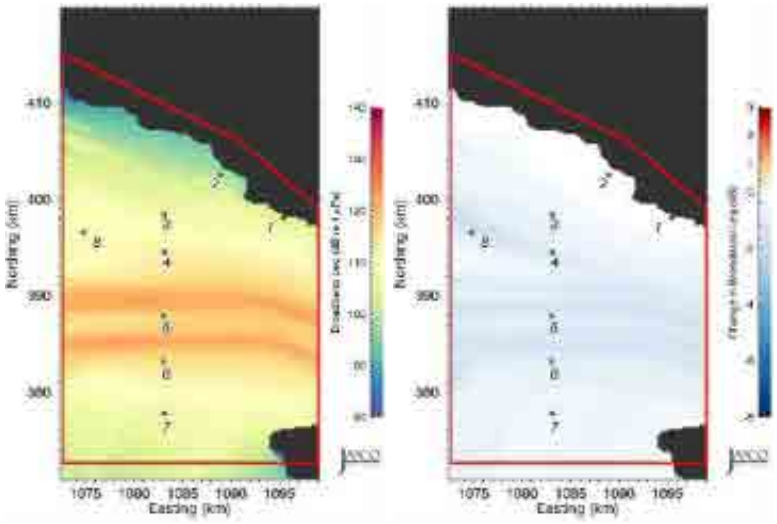

Figure 116. *Swiftsure Bank – Replacing 10% of ships with highest unweighted broadband source levels*: Unweighted equivalent continuous noise levels (L_{eq}; left) and change in L_{eq} (right) relative to July 2015 baseline levels. Grid resolution is 200 × 200 m. The green dots are the sample locations in the SRKW critical habitat. The red line shows the boundary of the area where statistical values (percentiles and mean) were derived.

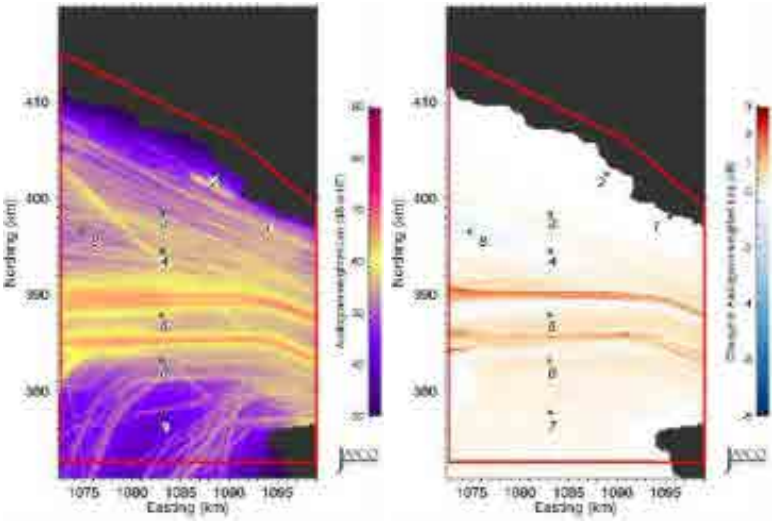

Figure 117. *Swiftsure Bank – Replacing 10% of ships with highest unweighted broadband source levels*: Audiogram-weighted equivalent continuous noise levels (L_{eq}; left) and change in L_{eq} (right) relative to July 2015 baseline levels. Grid resolution is 200 × 200 m. The green dots are the sample locations in the SRKW critical habitat. The red line shows the boundary of the area where statistical values (percentiles and mean) were derived.

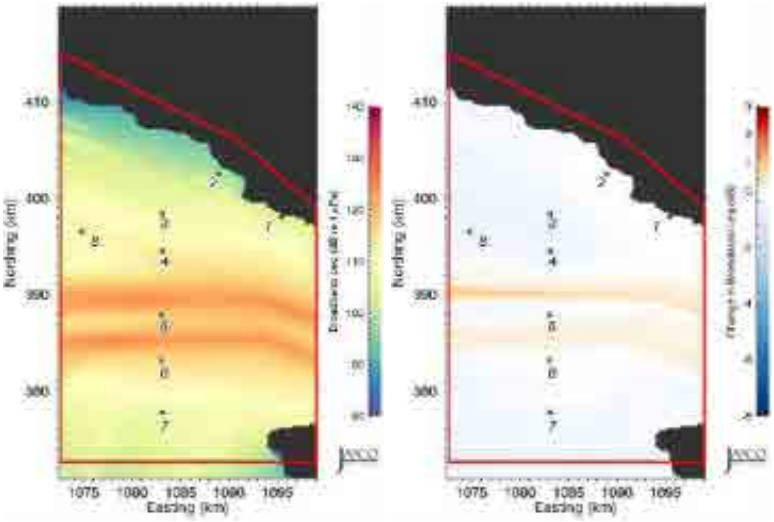

Figure 118. *Swiftsure Bank – Replacing 10% of ships with highest audiogram-weighted broadband source levels*: Unweighted equivalent continuous noise levels (L_{eq}; left) and change in L_{eq} (right) relative to July 2015 baseline levels. Grid resolution is 200 × 200 m. The green dots are the sample locations in the SRKW critical habitat. The red line shows the boundary of the area where statistical values (percentiles and mean) were derived.

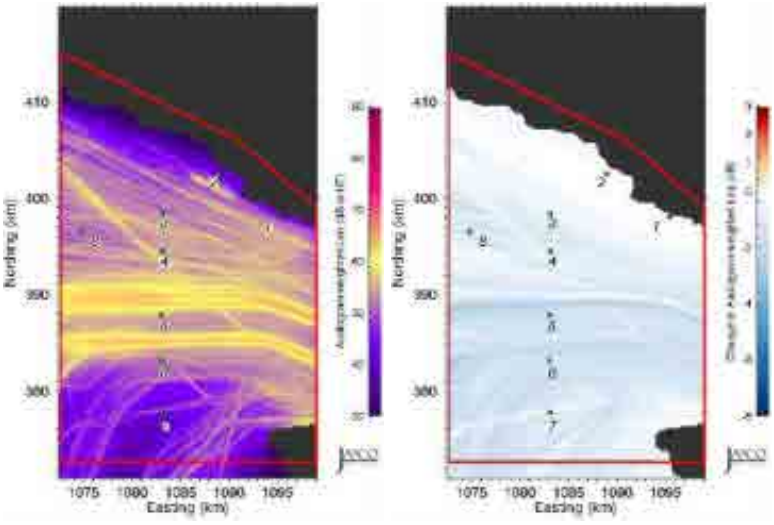

Figure 119. *Swiftsure Bank – Replacing 10% of ships with highest audiogram-weighted broadband source levels*: Audiogram-weighted equivalent continuous noise levels (L_{eq}; left) and change in L_{eq} (right) relative to July 2015 baseline levels. Grid resolution is 200 × 200 m. The green dots are the sample locations in the SRKW critical habitat. The red line shows the boundary of the area where statistical values (percentiles and mean) were derived.

Table 45. *Swiftsure Bank – Baseline* vs. *replacing 10% of ships with highest source levels*: Unweighted received levels (dB re 1 µPa), changes in received levels (dB), and changes in acoustic intensity (%) at the sample locations in the SRKW critical habitat shown in Figure 8.

Sample location	Baseline (dB re 1 µPa)	Selected based on unweighted broadband source levels			Selected based on audiogram-weighted broadband source levels		
		Mitigated (dB re 1 µPa)	Change		Mitigated (dB re 1 µPa)	Change	
			dB	%		dB	%
1	105.9	105.90	0.0	0.0	105.90	0.0	0.0
2	99.1	99.10	0.0	0.0	99.00	−0.1	−2.3
3	107.4	107.10	−0.3	−6.7	107.20	−0.2	−4.5
4	114.3	113.10	−1.2	−24.1	114.10	−0.2	−4.5
5	118.3	117.30	−1.0	−20.6	118.30	0.0	0.0
6	114.8	114.00	−0.8	−16.8	114.80	0.0	0.0
7	106.8	106.50	−0.3	−6.7	106.70	−0.1	−2.3
8	112.0	110.50	−1.5	−29.2	111.70	−0.3	−6.7

Table 46. *Swiftsure Bank – Baseline* vs. *replacing 10% of ships with highest source levels*: Audiogram-weighted received levels (dB re HT), changes in received levels (dB), and changes in acoustic intensity (%) at the sample locations in the SRKW critical habitat shown in Figure 8.

Sample location	Baseline (dB re HT)	Selected based on unweighted broadband source levels			Selected based on audiogram-weighted broadband source levels		
		Mitigated (dB re HT)	Change		Mitigated (dB re HT)	Change	
			dB	%		dB	%
1	52.3	52.3	0.0	0.0	52.2	−0.1	−2.3
2	43.1	43.1	0.0	0.0	43	−0.1	−2.3
3	52.3	52.3	0.0	0.0	51.8	−0.5	−10.9
4	55.8	55.6	−0.2	−4.5	54.8	−1.0	−20.6
5	55.2	55.6	+0.4	+9.6	53.6	−1.6	−30.8
6	52.3	52.6	+0.3	+7.2	50.7	−1.6	−30.8
7	41.4	41.5	+0.1	+2.3	40.3	−1.1	−22.4
8	53.2	53.1	−0.1	−2.3	52.3	−0.9	−18.7

3.6. Future Mitigated Noise Levels–Reducing Noise Emissions of Classes of Concern

This section presents equivalent noise levels (L_{eq}, unweighted and audiogram-weighted) for July over the four Local Study Areas. The mitigated results represent the expected increase in vessel traffic associated with the Trans Mountain requirements and reducing the source levels of classes of concern by 3 and 6 dB, as described in Section 2.2.3.4. In Figures 120–135, the maps on the left/top present the L_{eq} and the maps on the right/bottom present the change in L_{eq} with respect to baseline levels for July, shown in Figures 17–20. Figures 120–121, 124–125, 128–129, and 132–133 show the mitigated levels with a source level reduction of 3 dB for the four Local Study Areas. Figures 122–123, 126–127, 130–131, and 134–135 show the mitigated levels with a source level reduction of 6 dB. Tables 47–54 present the L_{eq} for the baseline and mitigated scenarios at the sample locations in the SRKW critical habitat. The sample locations are listed in Table 1 and shown as green dots in Figures 120–135.

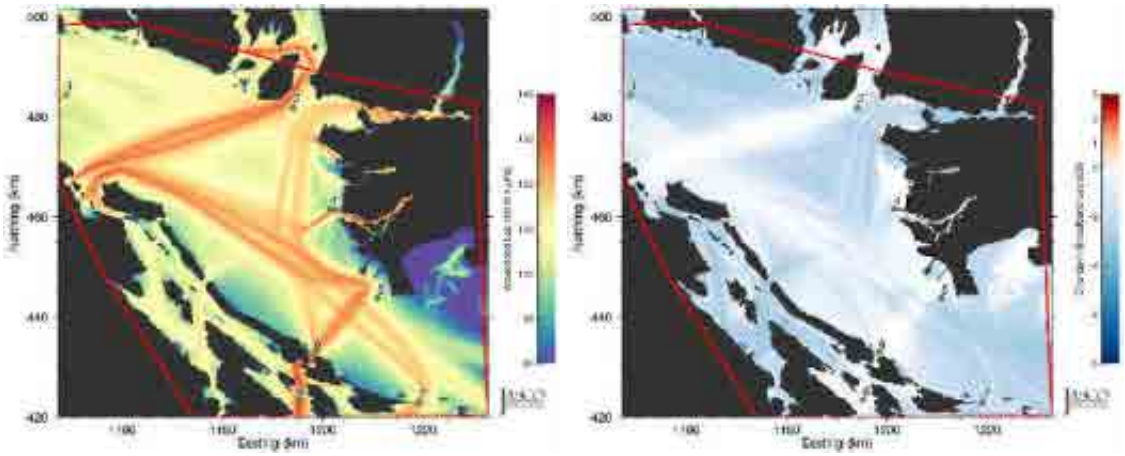

Figure 120. *Strait of Georgia – Reducing spectral source levels by 3 dB*: Unweighted equivalent continuous noise levels (L_{eq}; left) and change in L_{eq} (right) relative to July 2015 baseline levels. Grid resolution is 200 × 200 m. The green dots are the sample locations in the SRKW critical habitat. The red line shows the boundary of the area where statistical values (percentiles and mean) were derived.

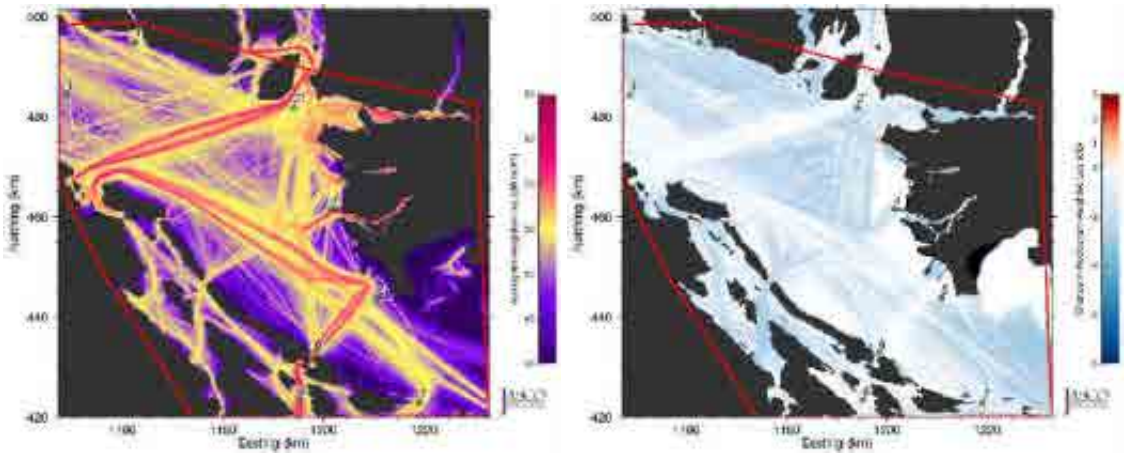

Figure 121. *Strait of Georgia – Reducing spectral source levels by 3 dB*: Audiogram-weighted equivalent continuous noise levels (L_{eq}; left) and change in L_{eq} (right) relative to July 2015 baseline levels. Grid resolution is 200 × 200 m. The green dots are the sample locations in the SRKW critical habitat. The red line shows the boundary of the area where statistical values (percentiles and mean) were derived.

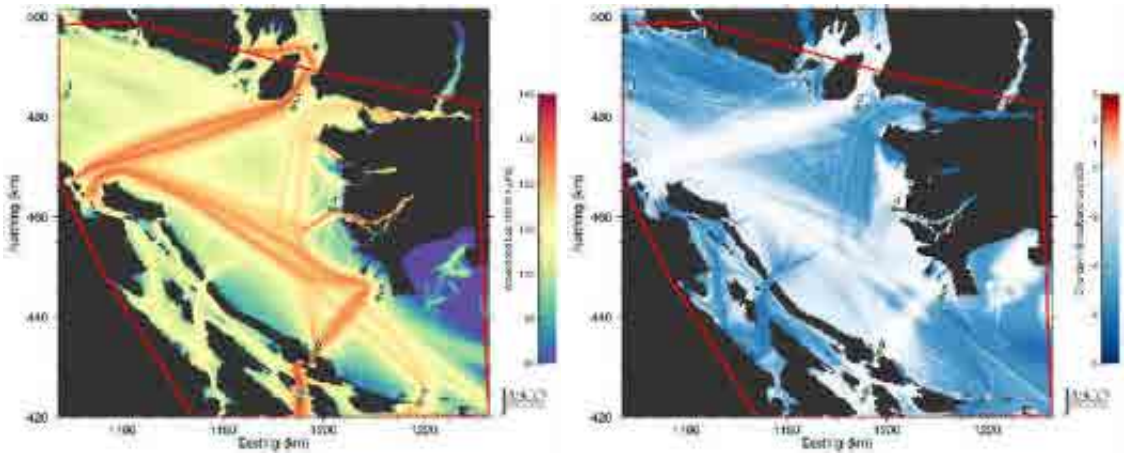

Figure 122. *Strait of Georgia – Reducing spectral source levels by 6 dB*: Unweighted equivalent continuous noise levels (L_{eq}; left) and change in L_{eq} (right) relative to July 2015 baseline levels. Grid resolution is 200 × 200 m. The green dots are the sample locations in the SRKW critical habitat. The red line shows the boundary of the area where statistical values (percentiles and mean) were derived.

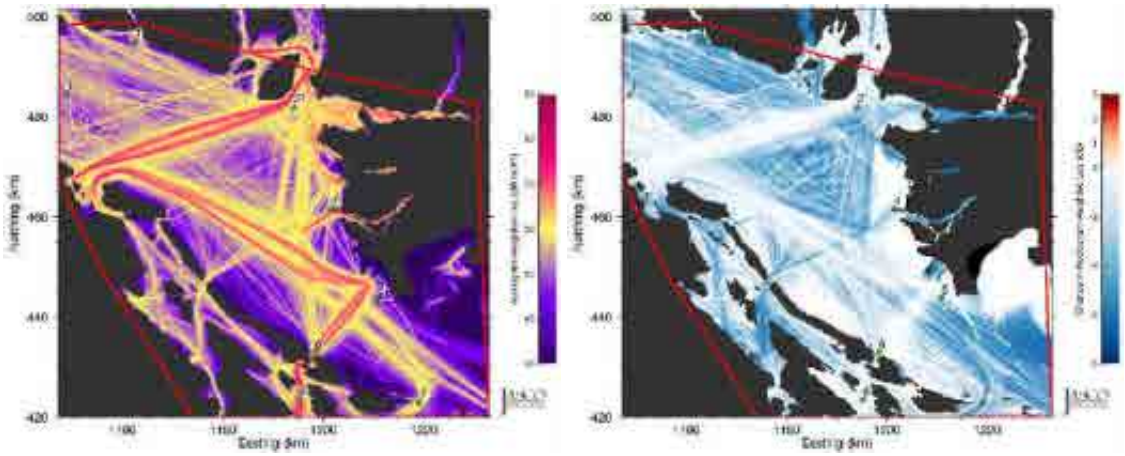

Figure 123. *Strait of Georgia – Reducing spectral source levels by 6 dB*: Audiogram-weighted equivalent continuous noise levels (L_{eq}; left) and change in L_{eq} (right) relative to July 2015 baseline levels. Grid resolution is 200 × 200 m. The green dots are the sample locations in the SRKW critical habitat. The red line shows the boundary of the area where statistical values (percentiles and mean) were derived.

Table 47. *Strait of Georgia – Baseline* vs. *reducing spectral source levels by 3 dB and 6 dB*: Unweighted received levels (dB re 1 µPa), changes in received levels (dB), and changes in acoustic intensity (%) at the sample locations in the SRKW critical habitat shown in Figure 5.

Sample location	Baseline (dB re 1 µPa)	3 dB			6 dB		
		Mitigated (dB re 1 µPa)	Change		Mitigated (dB re 1 µPa)	Change	
			dB	%		dB	%
1	113.0	110.2	−2.8	−47.5	107.4	−5.6	−72.5
2	118.2	116.4	−1.8	−33.9	115	−3.2	−52.1
3	106.4	104.4	−2.0	−36.9	102.9	−3.5	−55.3
4	113.0	112.2	−0.8	−16.8	111.7	−1.3	−25.9
5	107.8	106.2	−1.6	−30.8	105.1	−2.7	−46.3
6	129.8	129.7	−0.1	−2.3	129.7	−0.1	−2.3
7	125.3	122.7	−2.6	−45.0	119.8	−5.5	−71.8
8	130.9	130.8	−0.1	−2.3	130.8	−0.1	−2.3

Table 48. *Strait of Georgia – Baseline* vs. *reducing spectral source levels by 3 dB and 6 dB*: Audiogram-weighted received levels (dB re HT), changes in received levels (dB), and changes in acoustic intensity (%) at the sample locations in the SRKW critical habitat shown in Figure 5.

Sample location	Baseline (dB re HT)	3 dB			6 dB		
		Mitigated (dB re HT)	Change		Mitigated (dB re HT)	Change	
			dB	%		dB	%
1	59.5	56.9	−2.6	−45.0	54.5	−5.0	−68.4
2	63.5	62.1	−1.4	−27.6	61.2	−2.3	−41.1
3	53.9	53.7	−0.2	−4.5	53.6	−0.3	−6.7
4	64.7	64.5	−0.2	−4.5	64.4	−0.3	−6.7
5	53.8	53.5	−0.3	−6.7	53.3	−0.5	−10.9
6	74.9	74.8	−0.1	−2.3	74.7	−0.2	−4.5
7	66.0	63.6	−2.4	−42.5	60.9	−5.1	−69.1
8	72.9	72.8	−0.1	−2.3	72.7	−0.2	−4.5

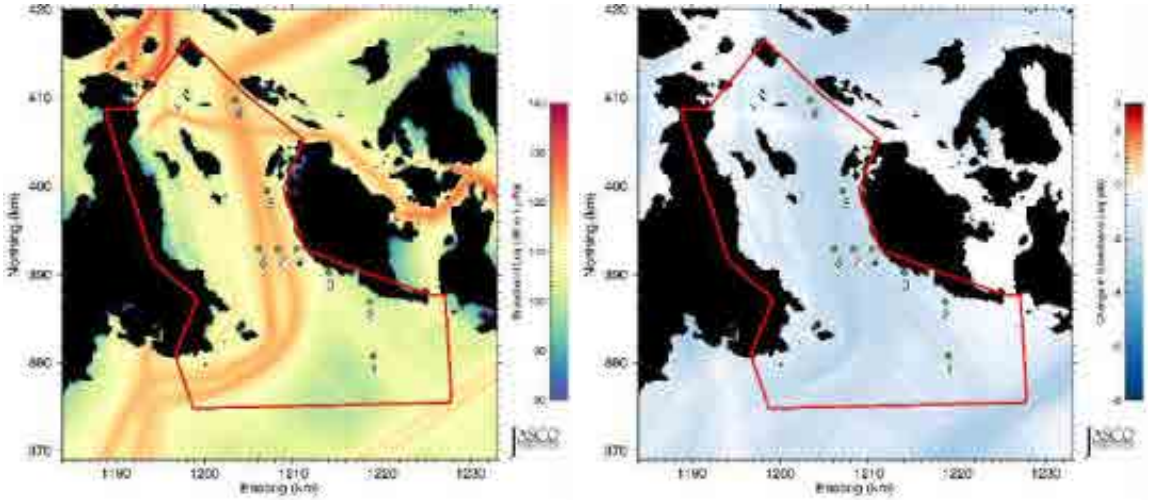

Figure 124. *Haro Strait – Reducing spectral source levels by 3 dB*: Unweighted equivalent continuous noise levels (L_{eq}; left) and change in L_{eq} (right) relative to July 2015 baseline levels. Grid resolution is 200 × 200 m. The green dots are the sample locations in the SRKW critical habitat. The red line shows the boundary of the area where statistical values (percentiles and mean) were derived.

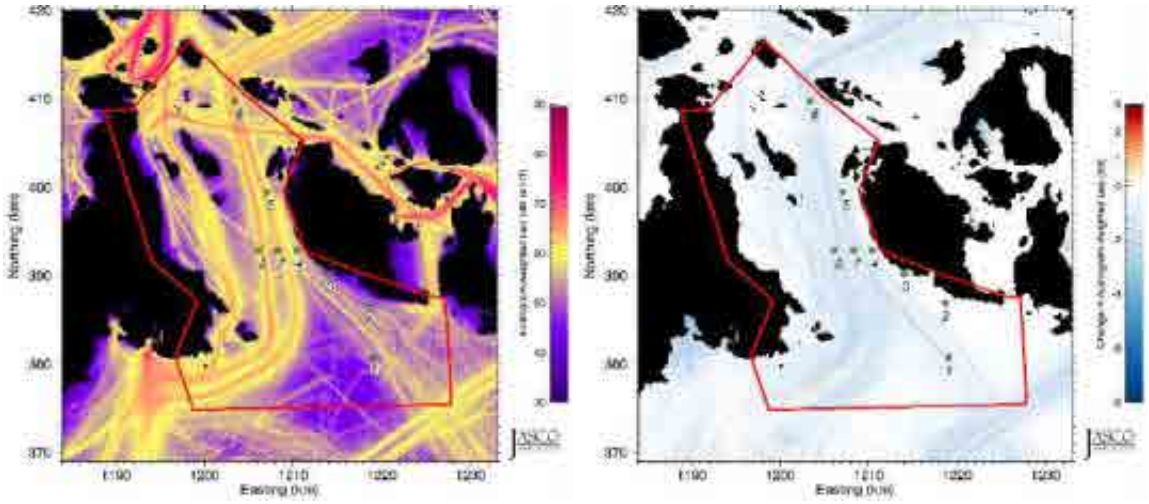

Figure 125. *Haro Strait – Reducing spectral source levels by 3 dB*: Audiogram-weighted equivalent continuous noise levels (L_{eq}; left) and change in L_{eq} (right) relative to July 2015 baseline levels. Grid resolution is 200 × 200 m. The green dots are the sample locations in the SRKW critical habitat. The red line shows the boundary of the area where statistical values (percentiles and mean) were derived.

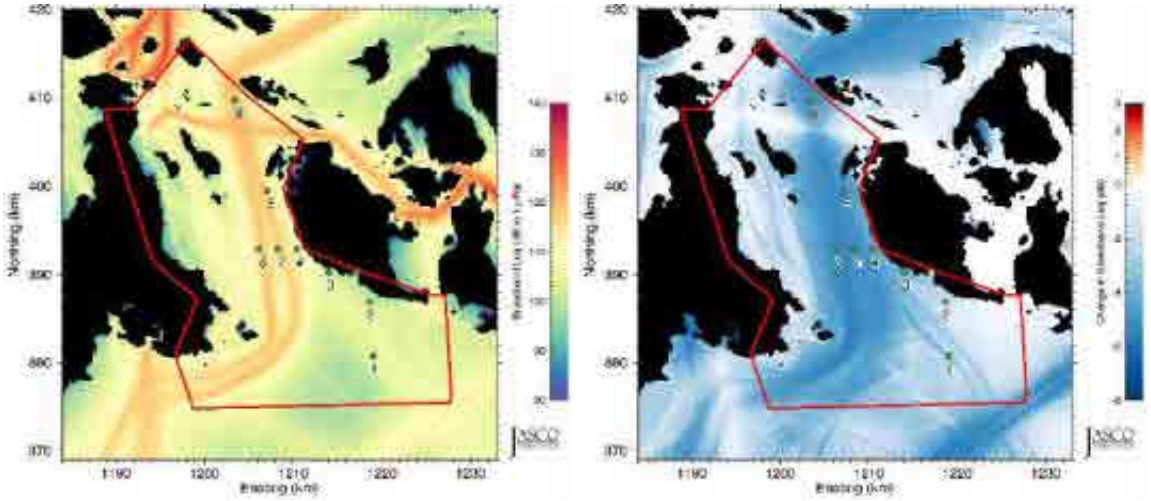

Figure 126. *Haro Strait – Reducing spectral source levels by 6 dB*: Unweighted equivalent continuous noise levels (L_{eq}; left) and change in L_{eq} (right) relative to July 2015 baseline levels. Grid resolution is 200 × 200 m. The green dots are the sample locations in the SRKW critical habitat. The red line shows the boundary of the area where statistical values (percentiles and mean) were derived.

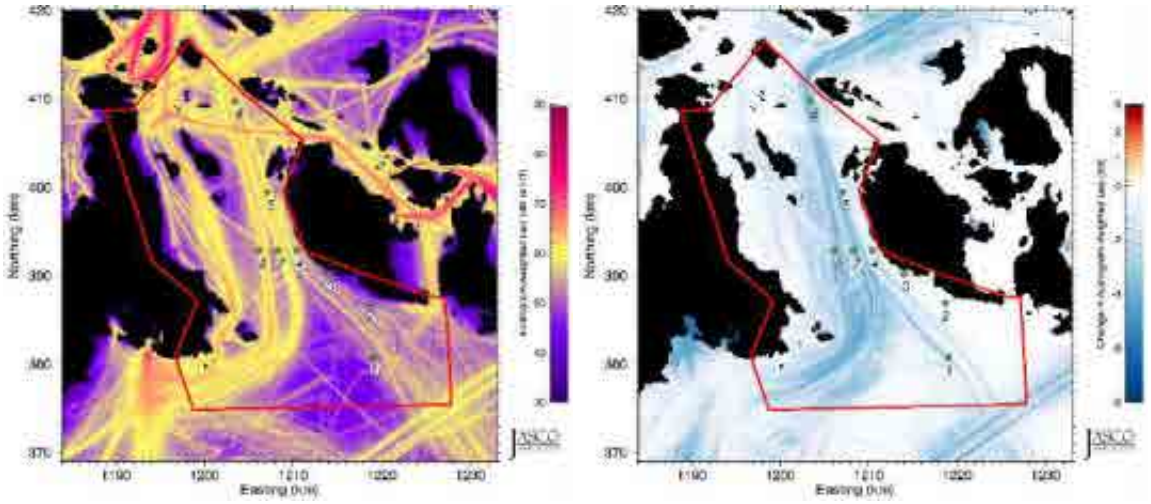

Figure 127. *Haro Strait – Reducing spectral source levels by 6 dB*: Audiogram-weighted equivalent continuous noise levels (L_{eq}; left) and change in L_{eq} (right) relative to July 2015 baseline levels. Grid resolution is 200 × 200 m. The green dots are the sample locations in the SRKW critical habitat. The red line shows the boundary of the area where statistical values (percentiles and mean) were derived.

Table 49. *Haro Strait – Baseline* vs. *reducing spectral source levels by 3 dB and 6 dB*: Unweighted received levels (dB re 1 µPa), changes in received levels (dB), and changes in acoustic intensity (%) at the sample locations in the SRKW critical habitat shown in Figure 6.

Sample location	Baseline (dB re 1 µPa)	3 dB			6 dB		
		Mitigated (dB re 1 µPa)	Change		Mitigated (dB re 1 µPa)	Change	
			dB	%		dB	%
1	109.2	107.3	−1.9	−35.4	105.9	−3.3	−53.2
2	103.9	103.0	−0.9	−18.7	102.3	−1.6	−30.8
3	106.5	104.6	−1.9	−35.4	102.5	−4.0	−60.2
4	114.3	112.2	−2.1	−38.3	109.9	−4.4	−63.7
5	119.0	116.9	−2.1	−38.3	114.4	−4.6	−65.3
6	123.4	121.3	−2.1	−38.3	118.5	−4.9	−67.6
7	122.9	120.6	−2.3	−41.1	117.7	−5.2	−69.8
8	123.5	121.1	−2.4	−42.5	118.3	−5.2	−69.8

Table 50. *Haro Strait – Baseline* vs. *reducing spectral source levels by 3 dB and 6 dB*: Audiogram-weighted received levels (dB re HT), changes in received levels (dB), and changes in acoustic intensity (%) at the sample locations in the SRKW critical habitat shown in Figure 6.

Sample location	Baseline (dB re HT)	3 dB			6 dB		
		Mitigated (dB re HT)	Change		Mitigated (dB re HT)	Change	
			dB	%		dB	%
1	56.2	55.0	−1.2	−24.1	54.1	−2.1	−38.3
2	51.6	51.5	−0.1	−2.3	51.5	−0.1	−2.3
3	46.9	46.3	−0.6	−12.9	45.8	−1.1	−22.4
4	56.3	55.9	−0.4	−8.8	55.5	−0.8	−16.8
5	60.8	60.5	−0.3	−6.7	60.3	−0.5	−10.9
6	64.6	63.7	−0.9	−18.7	62.1	−2.5	−43.8
7	65.2	63.3	−1.9	−35.4	61.2	−4.0	−60.2
8	66.2	64.7	−1.5	−29.2	63.0	−3.2	−52.1

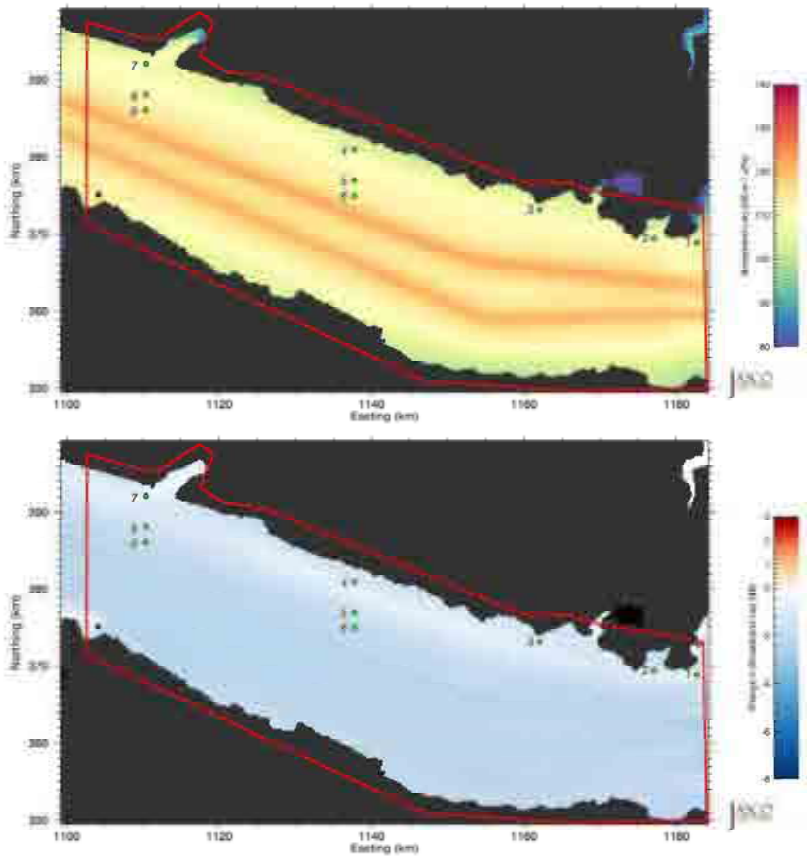

Figure 128. *Juan de Fuca Strait – Reducing spectral source levels by 3 dB*: Unweighted equivalent continuous noise levels (L_{eq}; top) and change in L_{eq} (bottom) relative to July 2015 baseline levels. Grid resolution is 200 × 200 m. The green dots are the sample locations in the SRKW critical habitat. The red line shows the boundary of the area where statistical values (percentiles and mean) were derived.

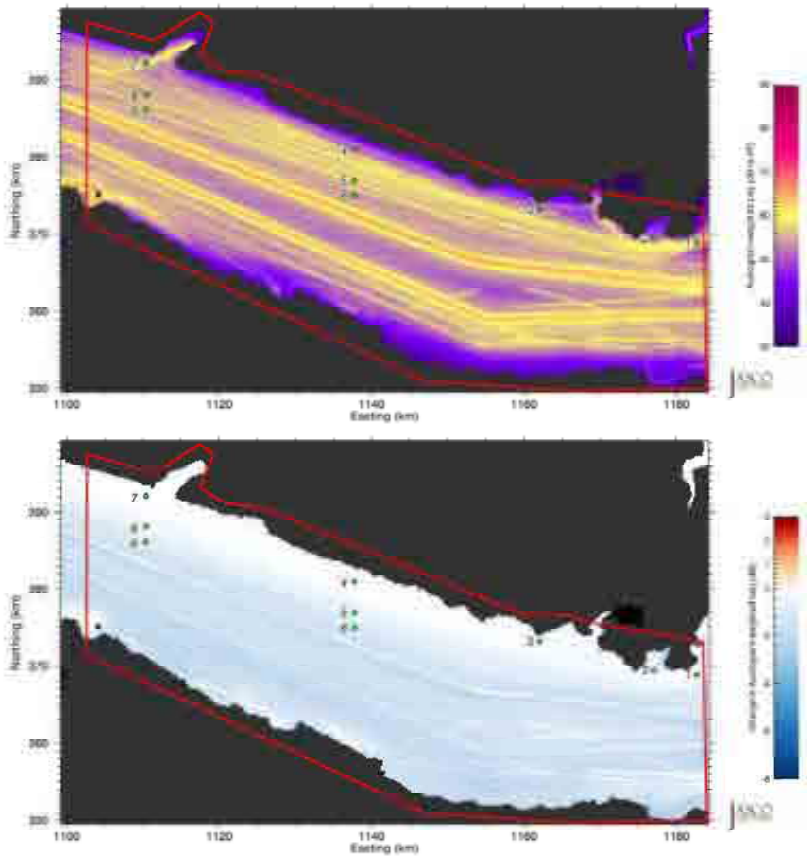

Figure 129. *Juan de Fuca Strait – Reducing spectral source levels by 3 dB*: Audiogram-weighted equivalent continuous noise levels (L_{eq}; top) and change in L_{eq} (bottom) relative to July 2015 baseline levels. Grid resolution is 200 × 200 m. The green dots are the sample locations in the SRKW critical habitat. The red line shows the boundary of the area where statistical values (percentiles and mean) were derived.

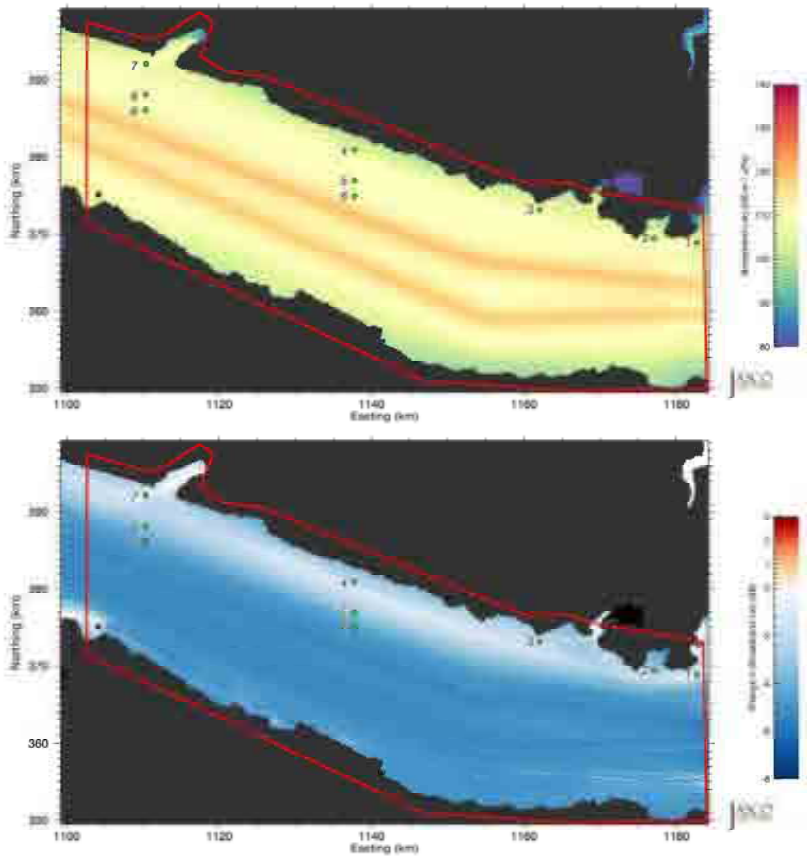

Figure 130. *Juan de Fuca Strait – Reducing spectral source levels by 6 dB*: Unweighted equivalent continuous noise levels (L_{eq}; top) and change in L_{eq} (bottom) relative to July 2015 baseline levels. Grid resolution is 200 × 200 m. The green dots are the sample locations in the SRKW critical habitat. The red line shows the boundary of the area where statistical values (percentiles and mean) were derived.

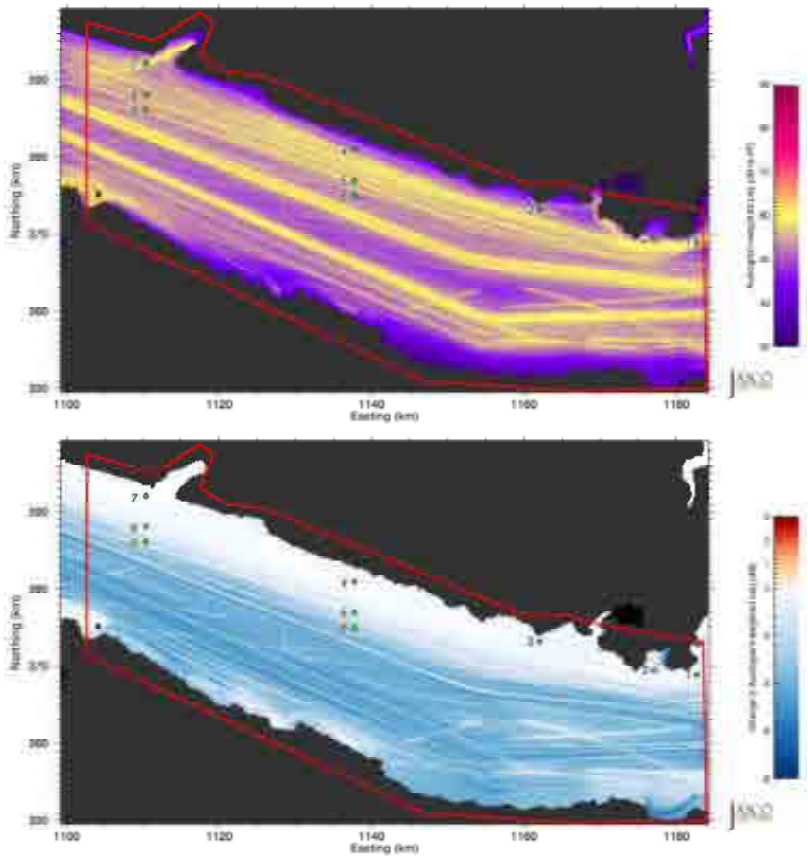

Figure 131. *Juan de Fuca Strait – Reducing spectral source levels by 6 dB*: Audiogram-weighted equivalent continuous noise levels (L_{eq}; top) and change in L_{eq} (bottom) relative to July 2015 baseline levels. Grid resolution is 200 × 200 m. The green dots are the sample locations in the SRKW critical habitat. The red line shows the boundary of the area where statistical values (percentiles and mean) were derived.

Table 51. *Juan de Fuca Strait – Baseline* vs. *reducing spectral source levels by 3 dB and 6 dB*: Unweighted received levels (dB re 1 µPa), changes in received levels (dB), and changes in acoustic intensity (%) at the sample locations in the SRKW critical habitat shown in Figure 7.

Sample location	Baseline (dB re 1 µPa)	3 dB			6 dB		
		Mitigated (dB re 1 µPa)	Change		Mitigated (dB re 1 µPa)	Change	
			dB	%		dB	%
1	111.4	110.3	−1.1	−22.4	109.6	−1.8	−33.9
2	111.6	110.4	−1.2	−24.1	109.4	−2.2	−39.7
3	110.2	109.2	−1.0	−20.6	108.3	−1.9	−35.4
4	109.9	109.0	−0.9	−18.7	108.3	−1.6	−30.8
5	113.8	111.9	−1.9	−35.4	109.9	−3.9	−59.3
6	117.5	115.4	−2.1	−38.3	112.7	−4.8	−66.9
7	109.6	108.7	−0.9	−18.7	107.8	−1.8	−33.9
8	114.0	112.1	−1.9	−35.4	110.1	−3.9	−59.3
9	117.5	115.3	−2.2	−39.7	112.7	−4.8	−66.9

Table 52. *Juan de Fuca Strait – Baseline* vs. *reducing spectral source levels by 3 dB and 6 dB*: Audiogram-weighted received levels (dB re HT), changes in received levels (dB), and changes in acoustic intensity (%) at the sample locations in the SRKW critical habitat shown in Figure 7.

Sample location	Baseline (dB re HT)	3 dB			6 dB		
		Mitigated (dB re HT)	Change		Mitigated (dB re HT)	Change	
			dB	%		dB	%
1	59.1	58.7	−0.4	−8.8	58.5	−0.6	−12.9
2	56.9	56.8	−0.1	−2.3	56.7	−0.2	−4.5
3	55.4	55.3	−0.1	−2.3	55.2	−0.2	−4.5
4	56.6	56.6	0.0	0.0	56.5	−0.1	−2.3
5	55.6	54.5	−1.1	−22.4	53.7	−1.9	−35.4
6	56.3	55.0	−1.3	−25.9	53.6	−2.7	−46.3
7	55.0	54.9	−0.1	−2.3	54.9	−0.1	−2.3
8	55.9	55.2	−0.7	−14.9	54.7	−1.2	−24.1
9	55.9	54.3	−1.6	−30.8	52.6	−3.3	−53.2

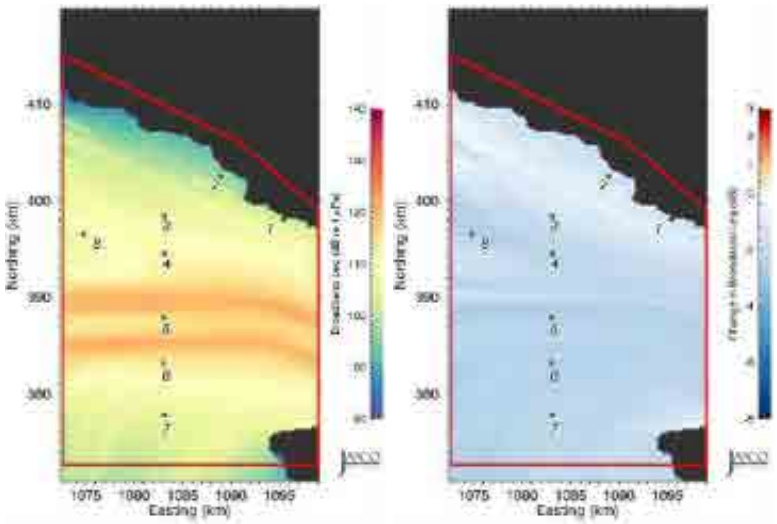

Figure 132. *Swiftsure Bank – Reducing spectral source levels by 3 dB*: Unweighted equivalent continuous noise levels (L_{eq}; left) and change in L_{eq} (right) relative to July 2015 baseline levels. Grid resolution is 200 × 200 m. The green dots are the sample locations in the SRKW critical habitat. The red line shows the boundary of the area where statistical values (percentiles and mean) were derived.

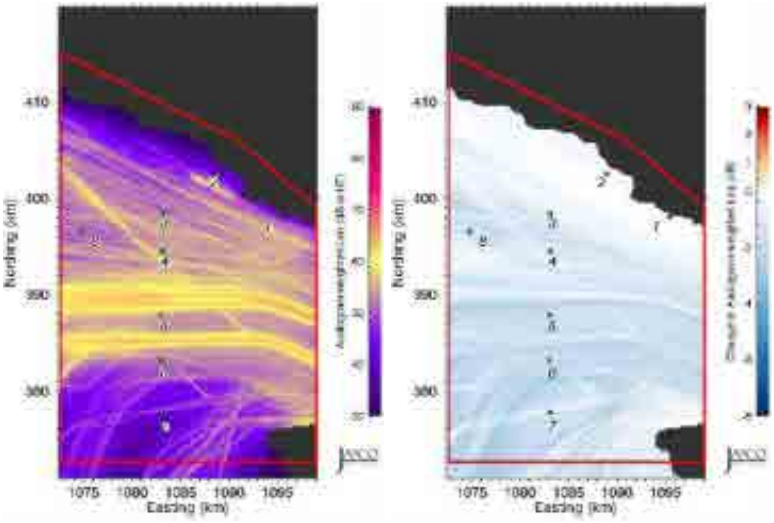

Figure 133. *Swiftsure Bank – Reducing spectral source levels by 3 dB*: Audiogram-weighted equivalent continuous noise levels (L_{eq}; left) and change in L_{eq} (right) relative to July 2015 baseline levels. Grid resolution is 200 × 200 m. The green dots are the sample locations in the SRKW critical habitat. The red line shows the boundary of the area where statistical values (percentiles and mean) were derived.

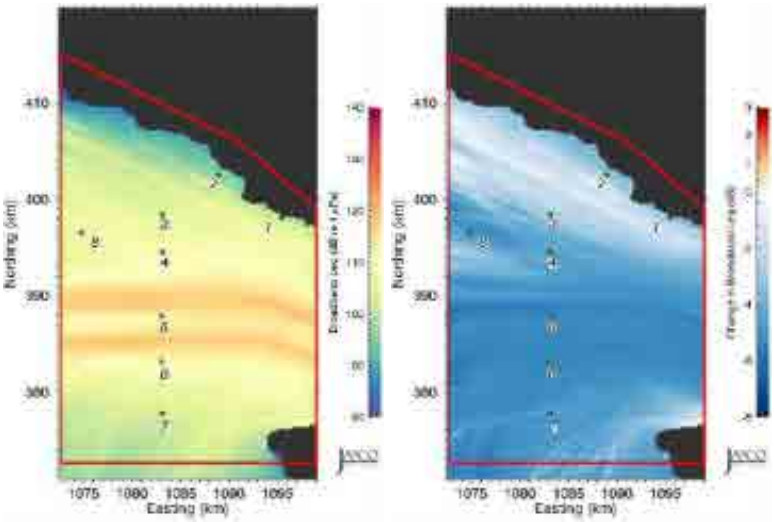

Figure 134. *Swiftsure Bank – Reducing spectral source levels by 6 dB*: Unweighted equivalent continuous noise levels (L_{eq}; left) and change in L_{eq} (right) relative to July 2015 baseline levels. Grid resolution is 200 × 200 m. The green dots are the sample locations in the SRKW critical habitat. The red line shows the boundary of the area where statistical values (percentiles and mean) were derived.

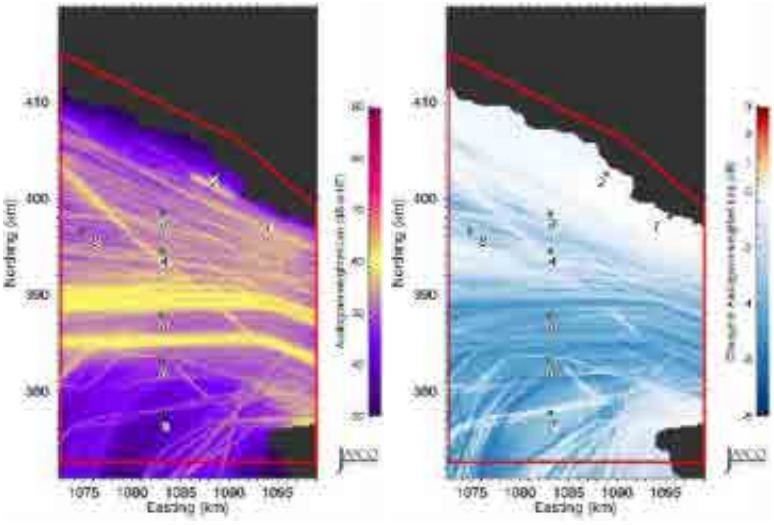

Figure 135. *Swiftsure Bank – Reducing spectral source levels by 6 dB*: Audiogram-weighted equivalent continuous noise levels (L_{eq}; left) and change in L_{eq} (right) relative to July 2015 baseline levels. Grid resolution is 200 × 200 m. The green dots are the sample locations in the SRKW critical habitat. The red line shows the boundary of the area where statistical values (percentiles and mean) were derived.

Table 53. *Swiftsure Bank – Baseline* vs. *reducing spectral source levels by 3 dB and 6 dB*: Unweighted received levels (dB re 1 µPa), changes in received levels (dB), and changes in acoustic intensity (%) at the sample locations in the SRKW critical habitat shown in Figure 8.

Sample location	Baseline (dB re 1 µPa)	3 dB			6 dB		
		Mitigated (dB re 1 µPa)	Change		Mitigated (dB re 1 µPa)	Change	
			dB	%		dB	%
1	105.9	104.80	−1.1	−22.4	103.80	−2.1	−38.3
2	99.1	97.60	−1.5	−29.2	96.10	−3.0	−49.9
3	107.4	105.90	−1.5	−29.2	104.70	−2.7	−46.3
4	114.3	111.90	−2.4	−42.5	109.60	−4.7	−66.1
5	118.3	115.90	−2.4	−42.5	113.00	−5.3	−70.5
6	114.8	112.40	−2.4	−42.5	109.60	−5.2	−69.8
7	106.8	104.60	−2.2	−39.7	102.00	−4.8	−66.9
8	112.0	109.40	−2.6	−45.0	107.00	−5.0	−68.4

Table 54. *Swiftsure Bank – Baseline* vs. *reducing spectral source levels by 3 dB and 6 dB*: Audiogram-weighted received levels (dB re HT), changes in received levels (dB), and changes in acoustic intensity (%) at the sample locations in the SRKW critical habitat shown in Figure 8.

Sample location	Baseline (dB re HT)	3 dB			6 dB		
		Mitigated (dB re HT)	Change		Mitigated (dB re HT)	Change	
			dB	%		dB	%
1	52.3	52.2	−0.1	−2.3	52.2	−0.1	−2.3
2	43.1	43.0	−0.1	−2.3	43.0	−0.1	−2.3
3	52.3	51.7	−0.6	−12.9	51.3	−1.0	−20.6
4	55.8	54.5	−1.3	−25.9	53.6	−2.2	−39.7
5	55.2	53.4	−1.8	−33.9	50.9	−4.3	−62.8
6	52.3	50.2	−2.1	−38.3	47.6	−4.7	−66.1
7	41.4	39.8	−1.6	−30.8	38.4	−3.0	−49.9
8	53.2	51.9	−1.3	−25.9	51.0	−2.2	−39.7

3.7. Future Mitigated Noise Levels–Shifting Vessel Traffic

This section presents equivalent noise levels (L_{eq}, unweighted and audiogram-weighted) for July over the Haro Strait, Juan de Fuca Strait, and Swiftsure Bank Local Study Areas. The mitigated results represent the expected increase in vessel traffic associated with the Trans Mountain requirements and rerouting the traffic lanes within Juan de Fuca Strait. Figures 136–141 present maps of the mitigated L_{eq} (left/top) and changes in L_{eq} (right/bottom) with respect to baseline levels for July, seen in Figures 17–20. Tables 55–60 present L_{eq} for the baseline and mitigated scenarios at the sample locations in the SRKW critical habitat. The sample locations are listed in Table 1 and shown as green dots in Figures 136–141.

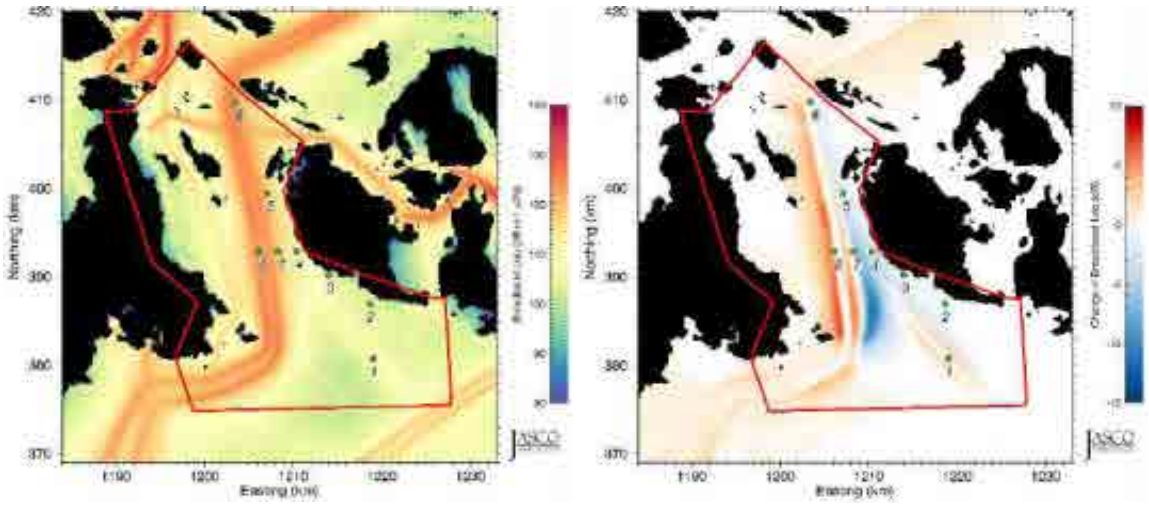

Figure 136. *Haro Strait – Shifting Vessel Traffic*: Unweighted equivalent continuous noise levels (L_{eq}; left) and change in L_{eq} (right) relative to July 2015 baseline levels. Grid resolution is 200 × 200 m. The green dots are the sample locations in the SRKW critical habitat. The red line shows the boundary of the area where statistical values (percentiles and mean) were derived.

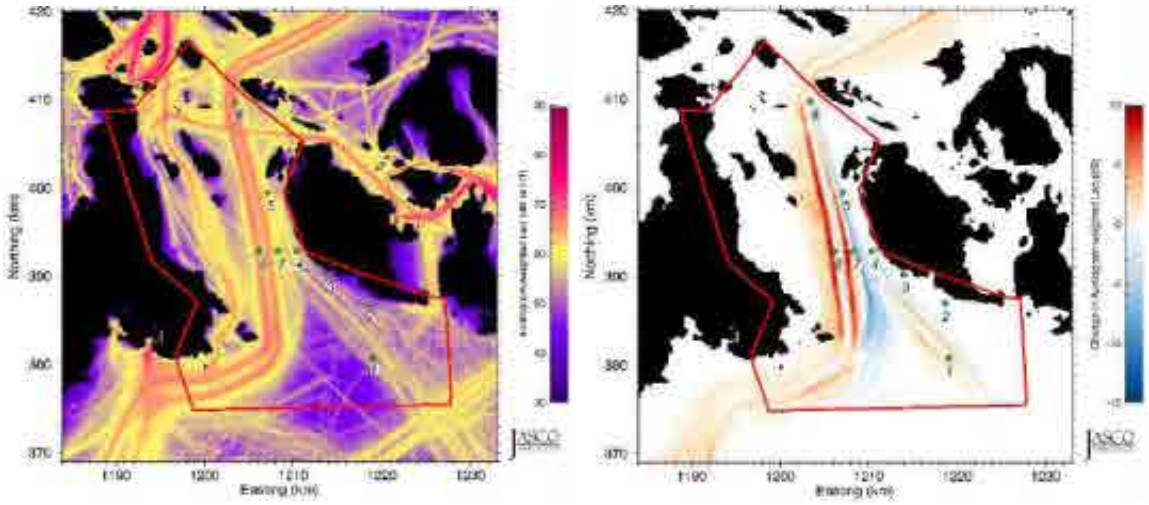

Figure 137. *Haro Strait – Shifting Vessel Traffic*: Audiogram-weighted equivalent continuous noise levels (L_{eq}; left) and change in L_{eq} (right) relative to July 2015 baseline levels. Grid resolution is 200 × 200 m. The green dots are the sample locations in the SRKW critical habitat. The red line shows the boundary of the area where statistical values (percentiles and mean) were derived.

Table 55. *Haro Strait – Baseline vs. Shifting Vessel Traffic*: Unweighted received levels (dB re 1 µPa), changes in received levels (dB), and changes in acoustic intensity (%) at the sample locations in the SRKW critical habitat shown in Figure 6.

Sample location	Baseline received level (dB re 1 µPa)	Mitigated received level (dB re 1 µPa)	Change	
			dB	%
1	109.2	107.5	−1.7	−32.4
2	103.9	103.5	−0.4	−8.8
3	106.5	105.0	−1.5	−29.2
4	114.3	111.6	−2.7	−46.3
5	119.0	117.4	−1.6	−30.8
6	123.4	122.8	−0.6	−12.9
7	122.9	117.1	−5.8	−73.7
8	123.5	123.0	−0.5	−10.9

Table 56. *Haro Strait – Baseline vs. Shifting Vessel Traffic*: Audiogram-weighted received levels (dB re HT), changes in received levels (dB), and changes in acoustic intensity (%) at the sample locations in the SRKW critical habitat shown in Figure 6.

Sample location	Baseline received level (dB re HT)	Mitigated received level (dB re HT)	Change	
			dB	%
1	56.2	54.3	−1.9	−35.4
2	51.6	51.5	−0.1	−2.3
3	46.9	46.2	−0.7	−14.9
4	56.3	55.8	−0.5	−10.9
5	60.8	60.8	0.0	0.0
6	64.6	63.6	−1.0	−20.6
7	65.2	58.2	−7.0	−80.0
8	66.2	63.7	−2.5	−43.8

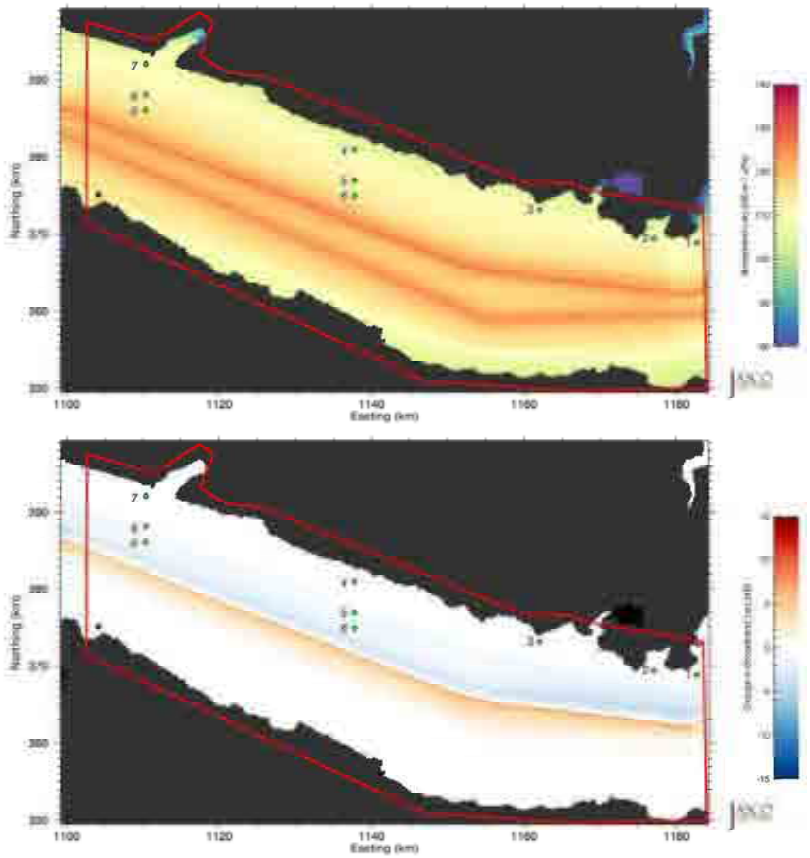

Figure 138. *Juan de Fuca Strait – Shifting Vessel Traffic*: Unweighted equivalent continuous noise levels (L_{eq}; top) and change in L_{eq} (bottom) relative to July 2015 baseline levels. Grid resolution is 200 × 200 m. The green dots are the sample locations in the SRKW critical habitat. The red line shows the boundary of the area where statistical values (percentiles and mean) were derived.

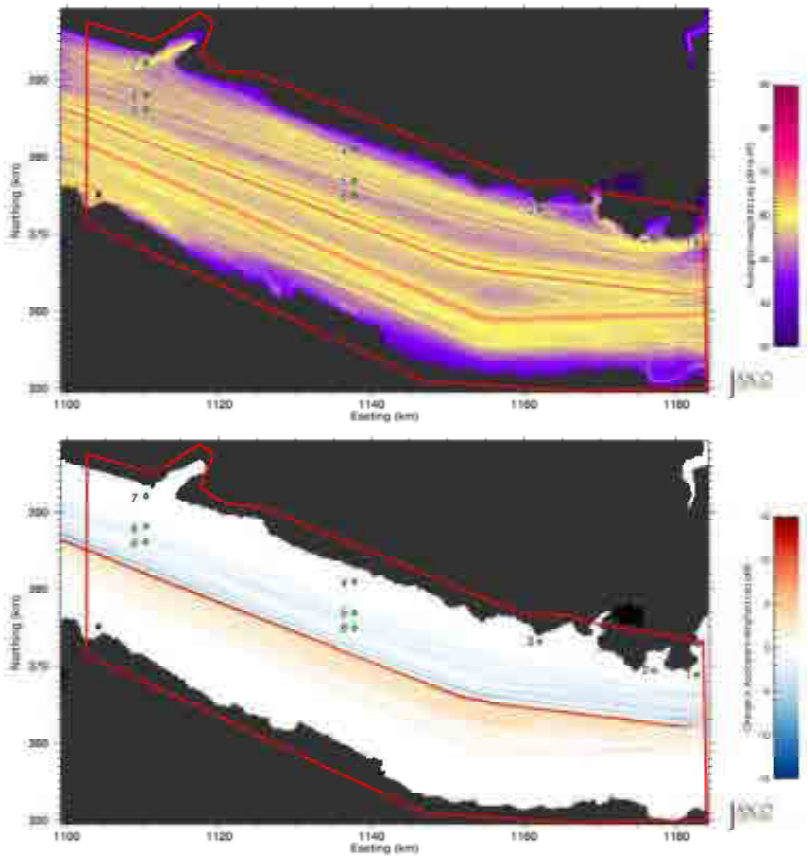

Figure 139. *Juan de Fuca Strait – Shifting Vessel Traffic*: Audiogram-weighted equivalent continuous noise levels (L_{eq}; top) and change in L_{eq} (bottom) relative to July 2015 baseline levels. Grid resolution is 200 × 200 m. The green dots are the sample locations in the SRKW critical habitat. The red line shows the boundary of the area where statistical values (percentiles and mean) were derived.

Table 57. *Juan de Fuca Strait – Baseline vs. Shifting Vessel Traffic*: Unweighted received levels (dB re 1 µPa), changes in received levels (dB), and changes in acoustic intensity (%) at the sample locations in the SRKW critical habitat shown in Figure 7.

Sample location	Baseline received level (dB re 1 µPa)	Mitigated received level (dB re 1 µPa)	Change	
			dB	%
1	111.4	110.3	−1.1	−22.4
2	111.6	110.9	−0.7	−14.9
3	110.2	109.8	−0.4	−8.8
4	109.9	109.8	−0.1	−2.3
5	113.8	112.7	−1.1	−22.4
6	117.5	116.0	−1.5	−29.2
7	109.6	109.5	−0.1	−2.3
8	114.0	113.0	−1.0	−20.6
9	117.5	116.1	−1.4	−27.6

Table 58. *Juan de Fuca Strait – Baseline vs. Shifting Vessel Traffic*: Audiogram-weighted received levels (dB re HT), changes in received levels (dB), and changes in acoustic intensity (%) at the sample locations in the SRKW critical habitat shown in Figure 7.

Sample location	Baseline received level (dB re HT)	Mitigated received level (dB re HT)	Change	
			dB	%
1	59.1	58.4	−0.7	−14.9
2	56.9	56.7	−0.2	−4.5
3	55.4	55.3	−0.1	−2.3
4	56.6	56.6	0.0	0.0
5	55.6	53.7	−1.9	−35.4
6	56.3	55.8	−0.5	−10.9
7	55.0	54.9	−0.1	−2.3
8	55.9	54.7	−1.2	−24.1
9	55.9	54.2	−1.7	−32.4

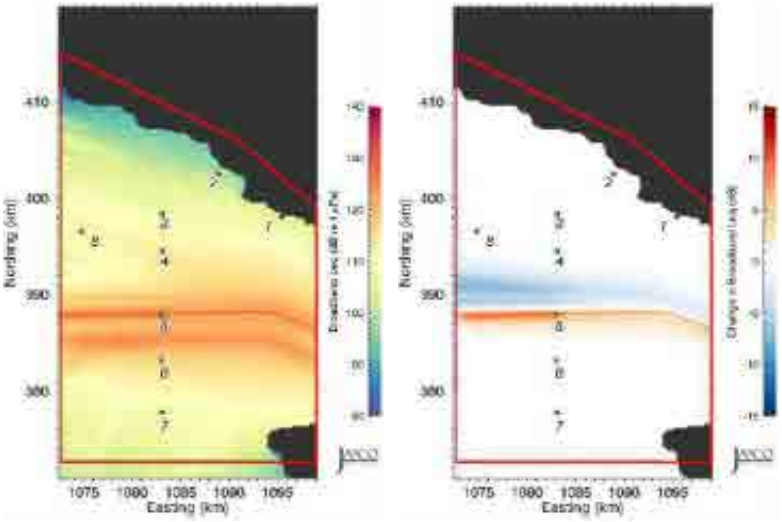

Figure 140. *Swiftsure Bank – Shifting Vessel Traffic*: Unweighted equivalent continuous noise levels (L_{eq}; left) and change in L_{eq} (right) relative to July 2015 baseline levels. Grid resolution is 200 × 200 m. The green dots are the sample locations in the SRKW critical habitat. The red line shows the boundary of the area where statistical values (percentiles and mean) were derived.

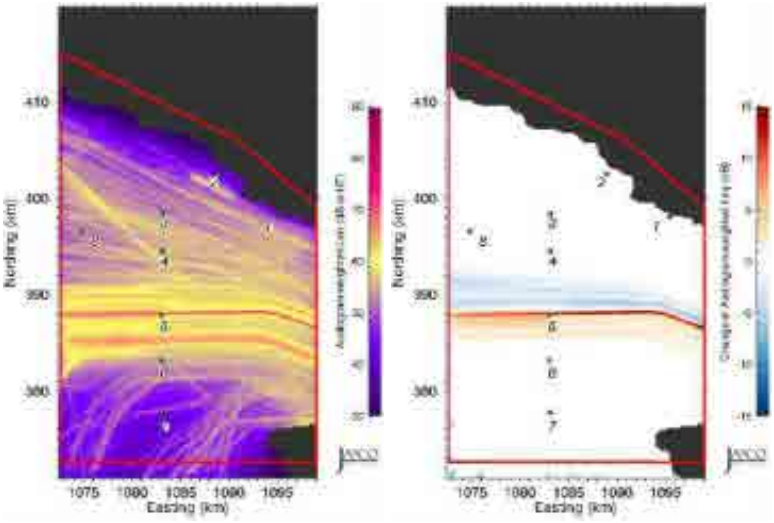

Figure 141. *Swiftsure Bank – Shifting Vessel Traffic*: Audiogram-weighted equivalent continuous noise levels (L_{eq}; left) and change in L_{eq} (right) relative to July 2015 baseline levels. Grid resolution is 200 × 200 m. The green dots are the sample locations in the SRKW critical habitat. The red line shows the boundary of the area where statistical values (percentiles and mean) were derived.

Table 59. *Swiftsure Bank – Baseline vs. Shifting Vessel Traffic*: Unweighted received levels (dB re 1 µPa), changes in received levels (dB), and changes in acoustic intensity (%) at the sample locations in the SRKW critical habitat shown in Figure 7.

Sample location	Baseline received level (dB re 1 µPa)	Mitigated received level (dB re 1 µPa)	Change	
			dB	%
1	105.9	106	+0.1	+2.3%
2	99.1	99.3	+0.2	+4.7%
3	107.4	107.4	0.0	0.0%
4	114.3	114.0	−0.3	−6.7%
5	118.3	122.3	+4.0	+151.2%
6	114.8	115.6	+0.8	+20.2%
7	106.8	107.6	+0.8	+20.2%
8	112.0	111.9	−0.1	−2.3%

Table 60. *Swiftsure Bank – Baseline vs. Shifting Vessel Traffic*: Audiogram-weighted received levels (dB re HT), changes in received levels (dB), and changes in acoustic intensity (%) at the sample locations in the SRKW critical habitat shown in Figure 7.

Sample location	Baseline received level (dB re HT)	Mitigated received level (dB re HT)	Change	
			dB	%
1	52.3	52.2	−0.1	−2.3%
2	43.1	43.1	0.0	0.0%
3	52.3	52.3	0.0	0.0%
4	55.8	55.7	−0.1	−2.3%
5	55.2	58.1	+2.9	+95.0%
6	52.3	53.0	+0.7	+17.5%
7	41.4	41.9	+0.5	+12.2%
8	53.2	53.2	0.0	0.0%

3.8. Future Mitigated Noise Levels–Implementing Vessel Convoys

3.8.1. Alternative 1: Convoying in Haro Strait

This section presents the temporal distribution of received noise levels, representing future mitigated levels with the expected increase in vessel traffic associated with the Trans Mountain requirements and implementing commercial vessel convoys in Haro Strait, as described in Section 2.2.3.6. The convoying occurs between points east of Discovery Island and north of Turn Point, as seen in Figure 14. Results are presented for the unmitigated baseline scenario (no convoy, no Trans Mountain vessel traffic), as well as for 2- and 4-hour convoy interval scenarios (which include Trans Mountain vessel traffic).

The modelled received levels at eight locations in the SRKW critical habitat were sampled every 1-minute over a 24-hour period. The sample locations are listed in Table 1 and shown in Figure 6. The sound field snapshots from the model simulations were rendered as animations to show the time evolution of the vessel traffic noise over Haro Strait. Examples of the snapshots are presented in Figure 142. Figures 143–150 present plots of unweighted (left) and audiogram-weighted (right) received levels as a function of time, at each sample location. These plots compare the levels from all traffic (and ambient noise) to that from only the mitigated commercial traffic. In each plot, the top, middle, and bottom graph shows results for the baseline (2015 traffic, no convoys), 2-hour convoy interval, and 4-hour convoy interval scenarios, respectively.

Tables 61 and 62 present the percentile and mean values of the temporal variation in received noise levels (SPL) at each sample location, for the baseline and the two convoy scenarios; Figures 151 and 152 present the percentile and mean values as bar plots. The received levels were also used to generate cumulative distribution functions (CDFs) at each sample location. These functions, presented in Figures 153–154, show the percent of time that modelled received levels were below a specified value.

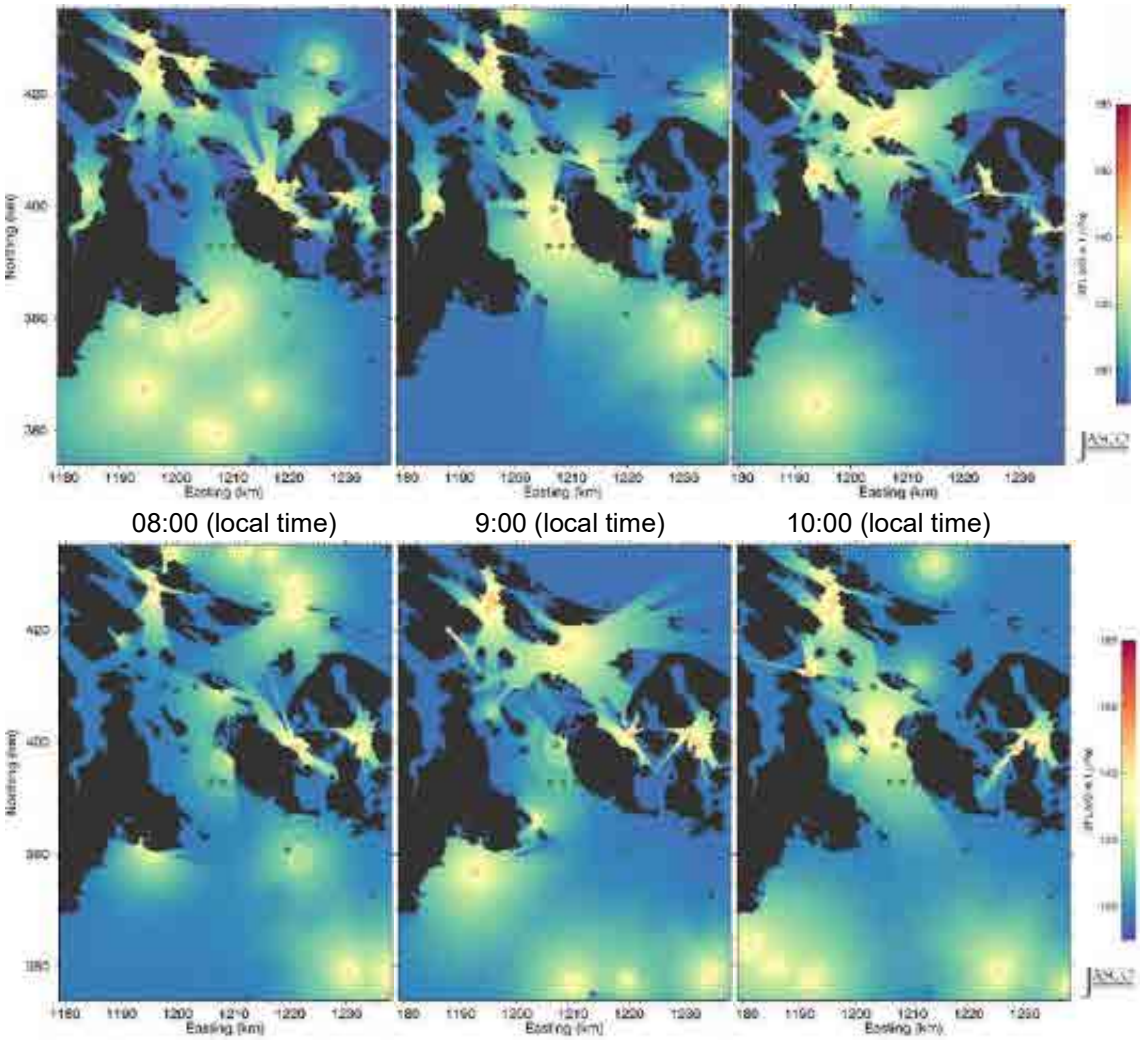

Figure 142. *Convoy Alternative 1, Haro Strait:* Example time snapshots of Future Mitigated SPL (unweighted with ambient, 10 Hz to 50 kHz) from 08:00 to 13:00 (local time) in 1-hour increments. Easting and northing are BC Albers projected coordinates.

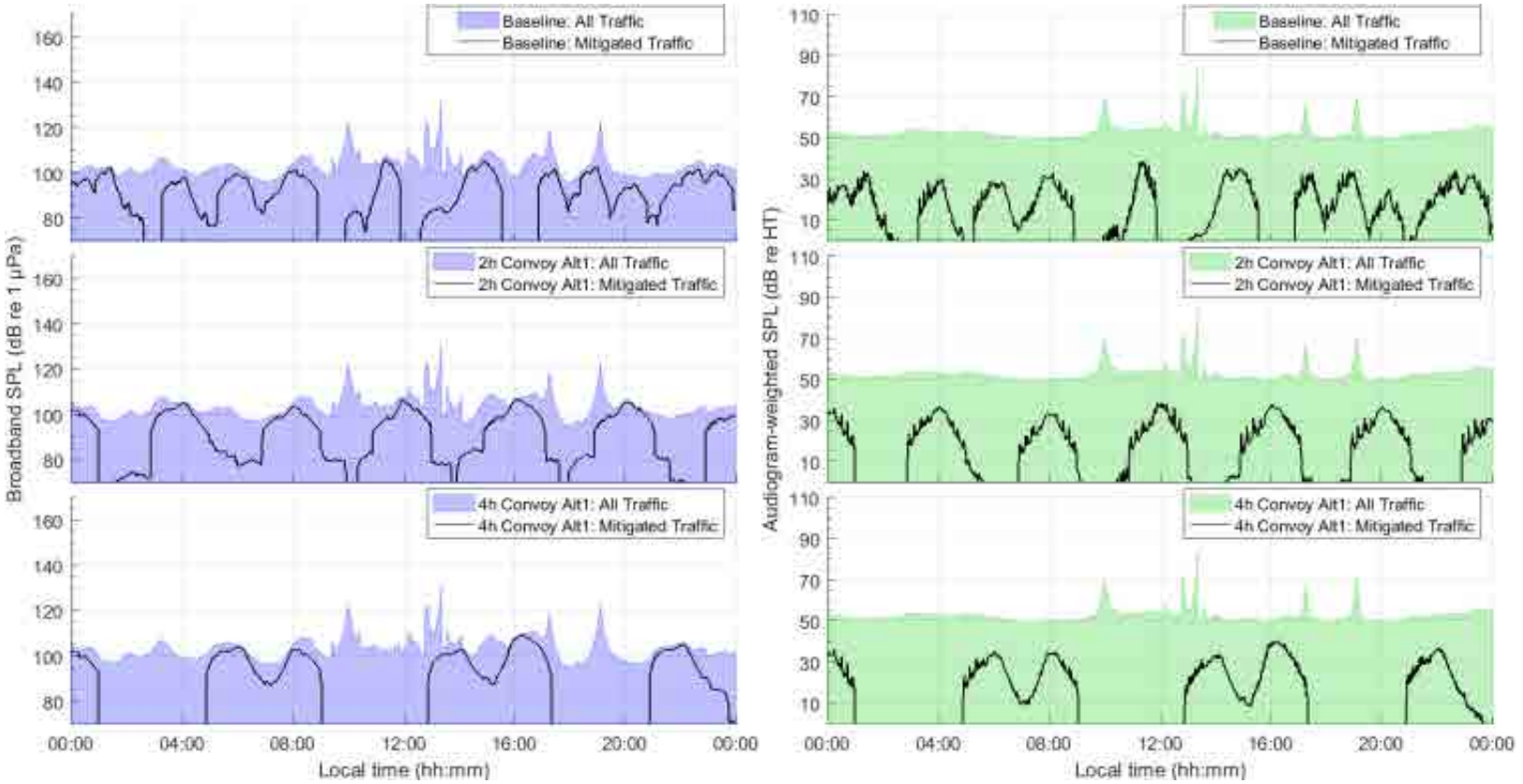

Figure 143. *Convoy Alternative 1, Haro Strait, Sample location 1*: Temporal variability of unweighted (left) and audiogram-weighted (right) received levels for (top) baseline (no convoy), (middle) 2-hour convoy, and (bottom) 4-hour convoy scenarios. The blue and green lines above the shaded area show received levels caused by all traffic and ambient noise. The black lines show received levels caused by commercial traffic only. The sample location is shown in Figure 6.

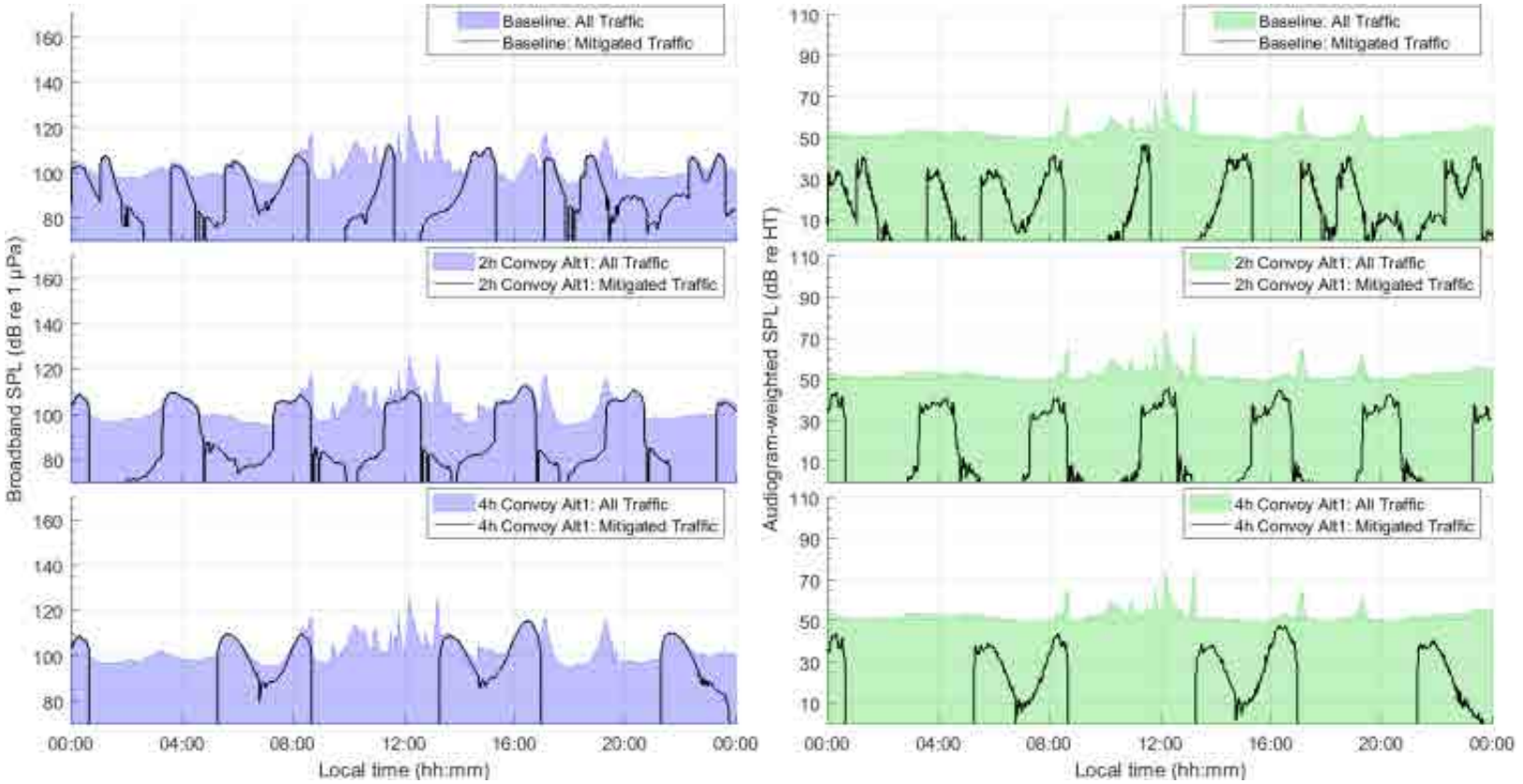

Figure 144. *Convoy Alternative 1, Haro Strait, Sample location 2*: Temporal variability of unweighted (left) and audiogram-weighted (right) received levels for (top) baseline (no convoy), (middle) 2-hour convoy, and (bottom) 4-hour convoy scenarios. The blue and green lines above the shaded area show received levels caused by all traffic and ambient noise. The black lines show received levels caused by commercial traffic only. The sample location is shown in Figure 6.

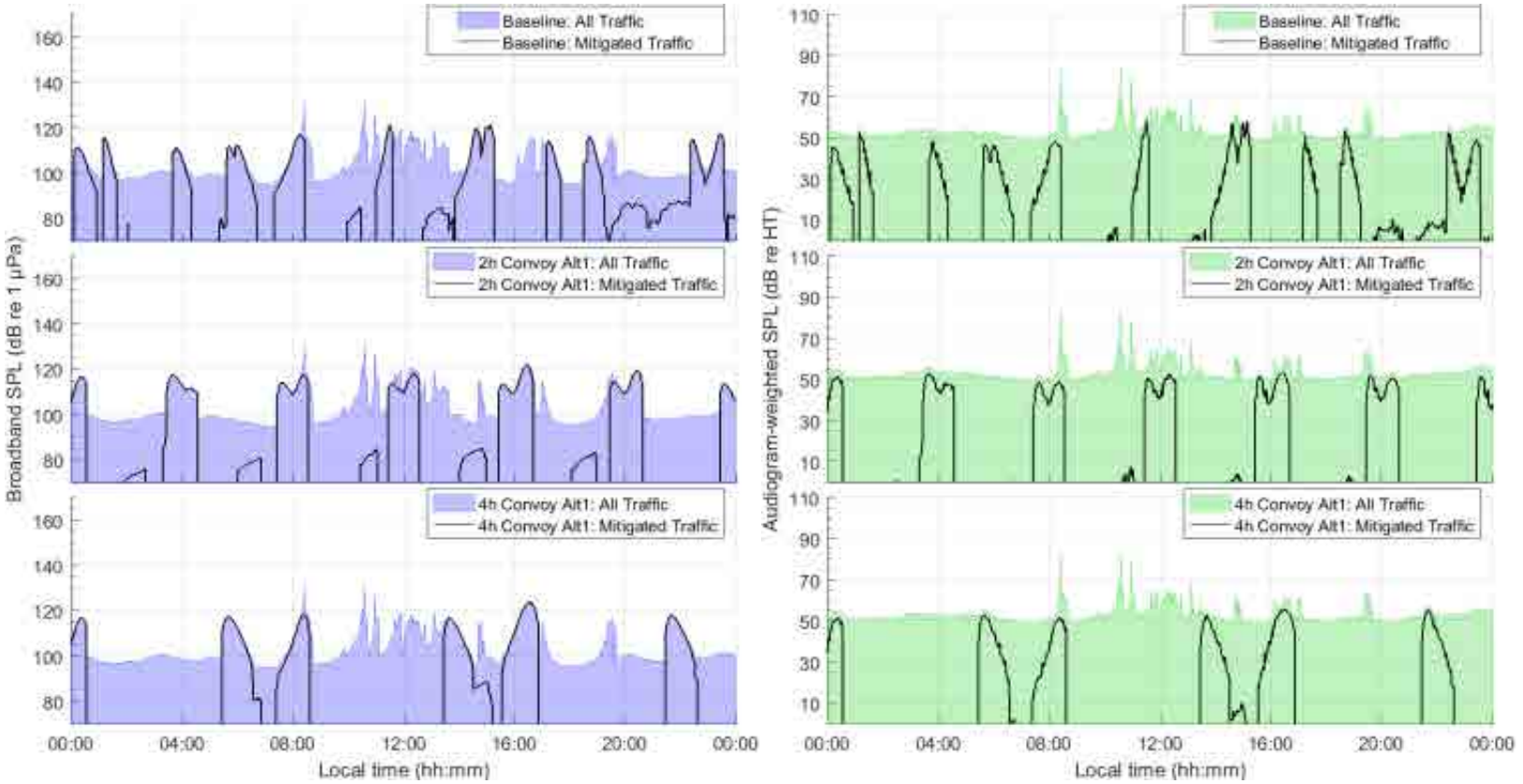

Figure 145. *Convoy Alternative 1, Haro Strait, Sample location 3*: Temporal variability of unweighted (left) and audiogram-weighted (right) received levels for (top) baseline (no convoy), (middle) 2-hour convoy, and (bottom) 4-hour convoy scenarios. The blue and green lines above the shaded area show received levels caused by all traffic and ambient noise. The black lines show received levels caused by commercial traffic only. The sample location is shown in Figure 6.

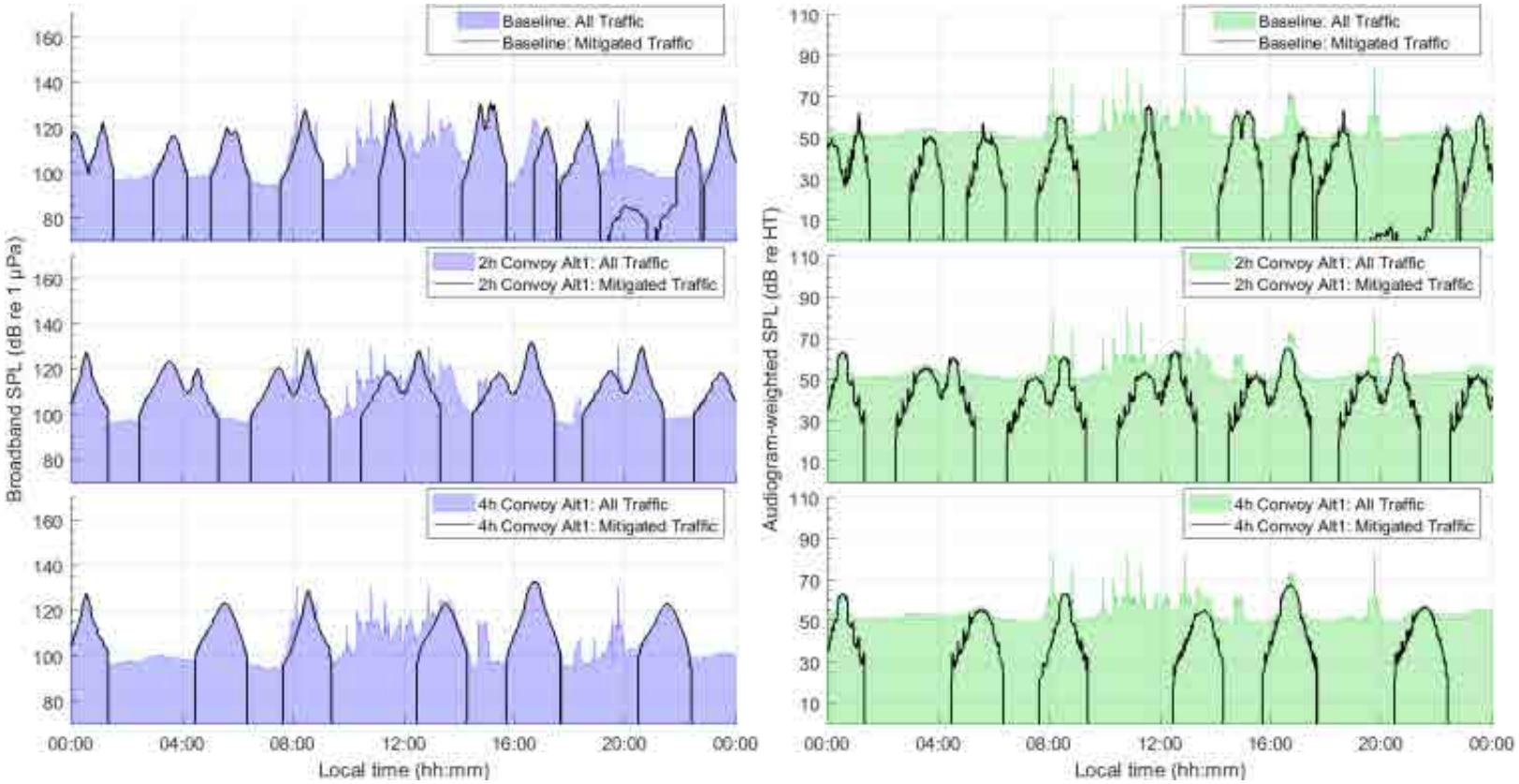

Figure 146. *Convoy Alternative 1, Haro Strait, Sample location 4*: Temporal variability of unweighted (left) and audiogram-weighted (right) received levels for (top) baseline (no convoy), (middle) 2-hour convoy, and (bottom) 4-hour convoy scenarios. The blue and green lines above the shaded area show received levels caused by all traffic and ambient noise. The black lines show received levels caused by commercial traffic only. The sample location is shown in Figure 6.

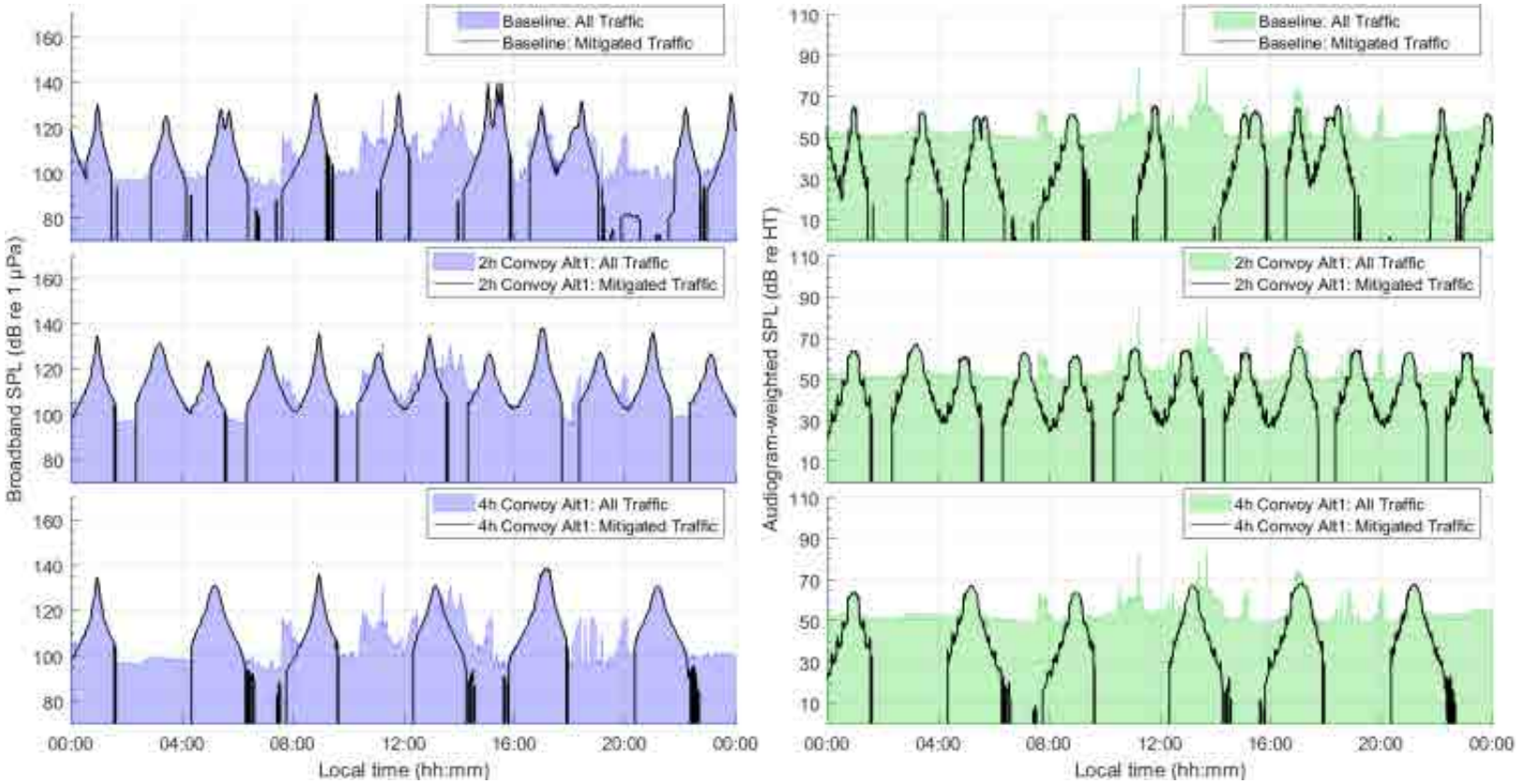

Figure 147. *Convoy Alternative 1, Haro Strait, Sample location 5*: Temporal variability of unweighted (left) and audiogram-weighted (right) received levels for (top) baseline (no convoy), (middle) 2-hour convoy, and (bottom) 4-hour convoy scenarios. The blue and green lines above the shaded area show received levels caused by all traffic and ambient noise. The black lines show received levels caused by commercial traffic only. The sample location is shown in Figure 6.

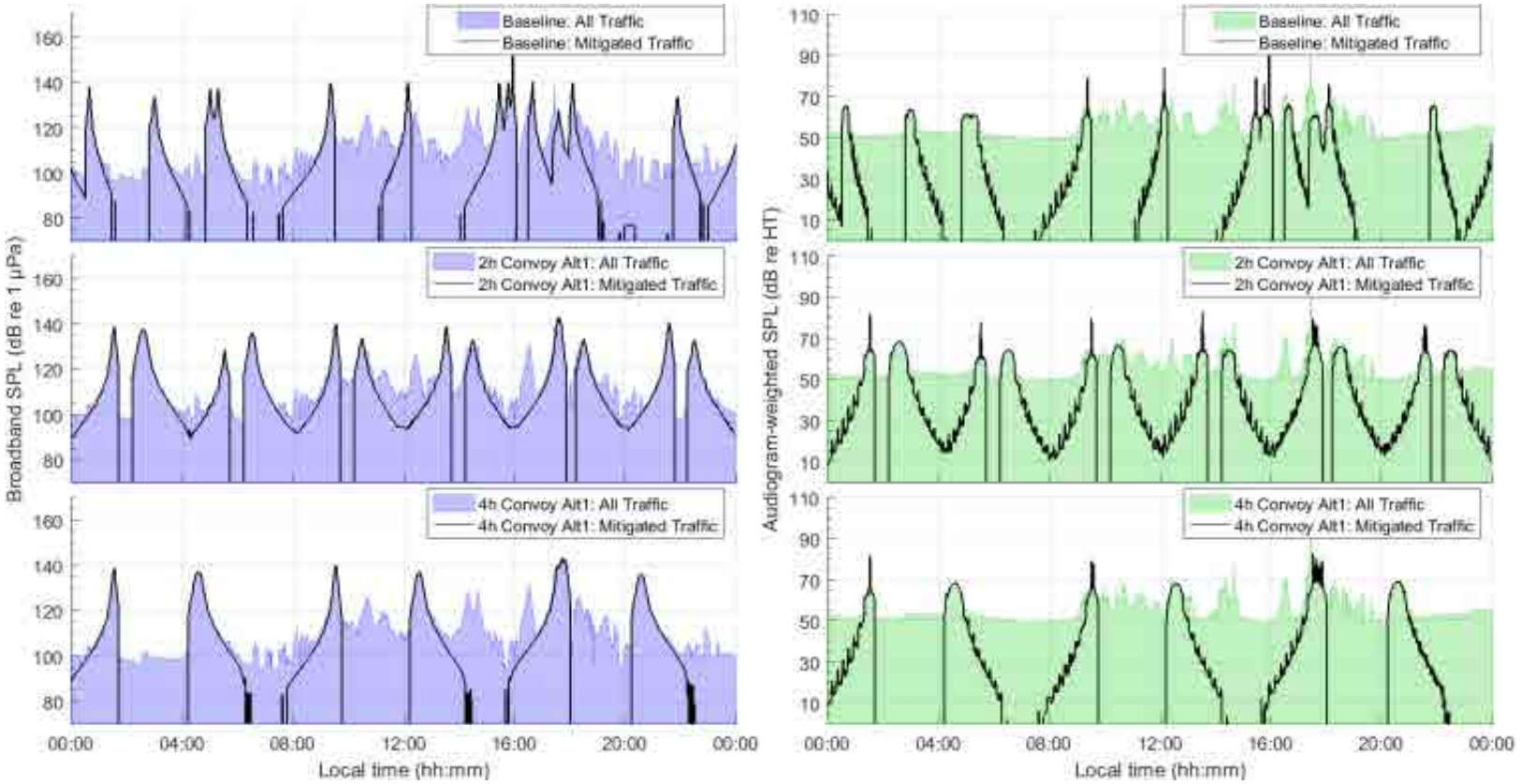

Figure 148. *Convoy Alternative 1, Haro Strait, Sample location 6*: Temporal variability of unweighted (left) and audiogram-weighted (right) received levels for (top) baseline (no convoy), (middle) 2-hour convoy, and (bottom) 4-hour convoy scenarios. The blue and green lines above the shaded area show received levels caused by all traffic and ambient noise. The black lines show received levels caused by commercial traffic only. The sample location is shown in Figure 6.

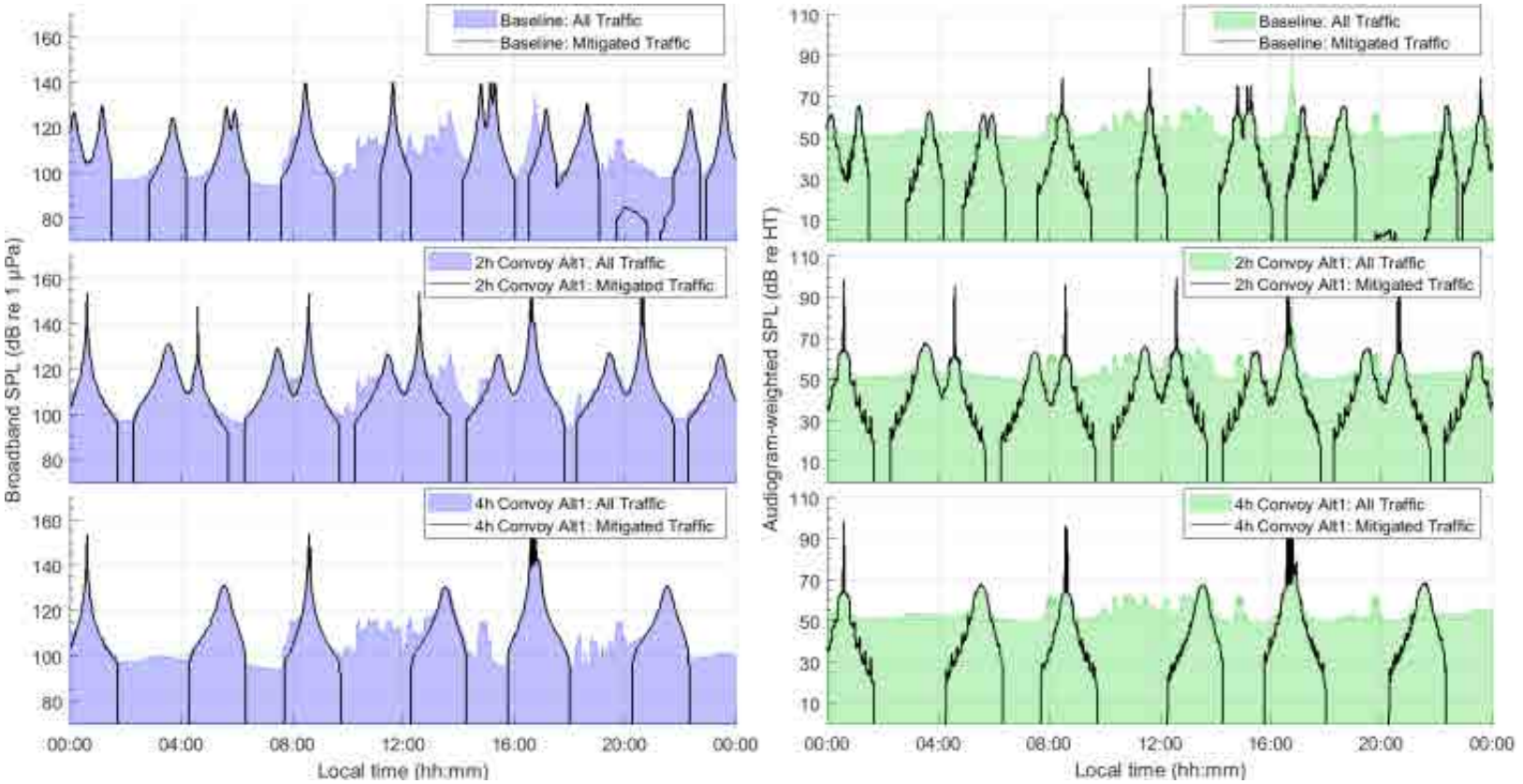

Figure 149. *Convoy Alternative 1, Haro Strait, Sample location 7*: Temporal variability of unweighted (left) and audiogram-weighted (right) received levels for (top) baseline (no convoy), (middle) 2-hour convoy, and (bottom) 4-hour convoy scenarios. The blue and green lines above the shaded area show received levels caused by all traffic and ambient noise. The black lines show received levels caused by commercial traffic only. The sample location is shown in Figure 6.

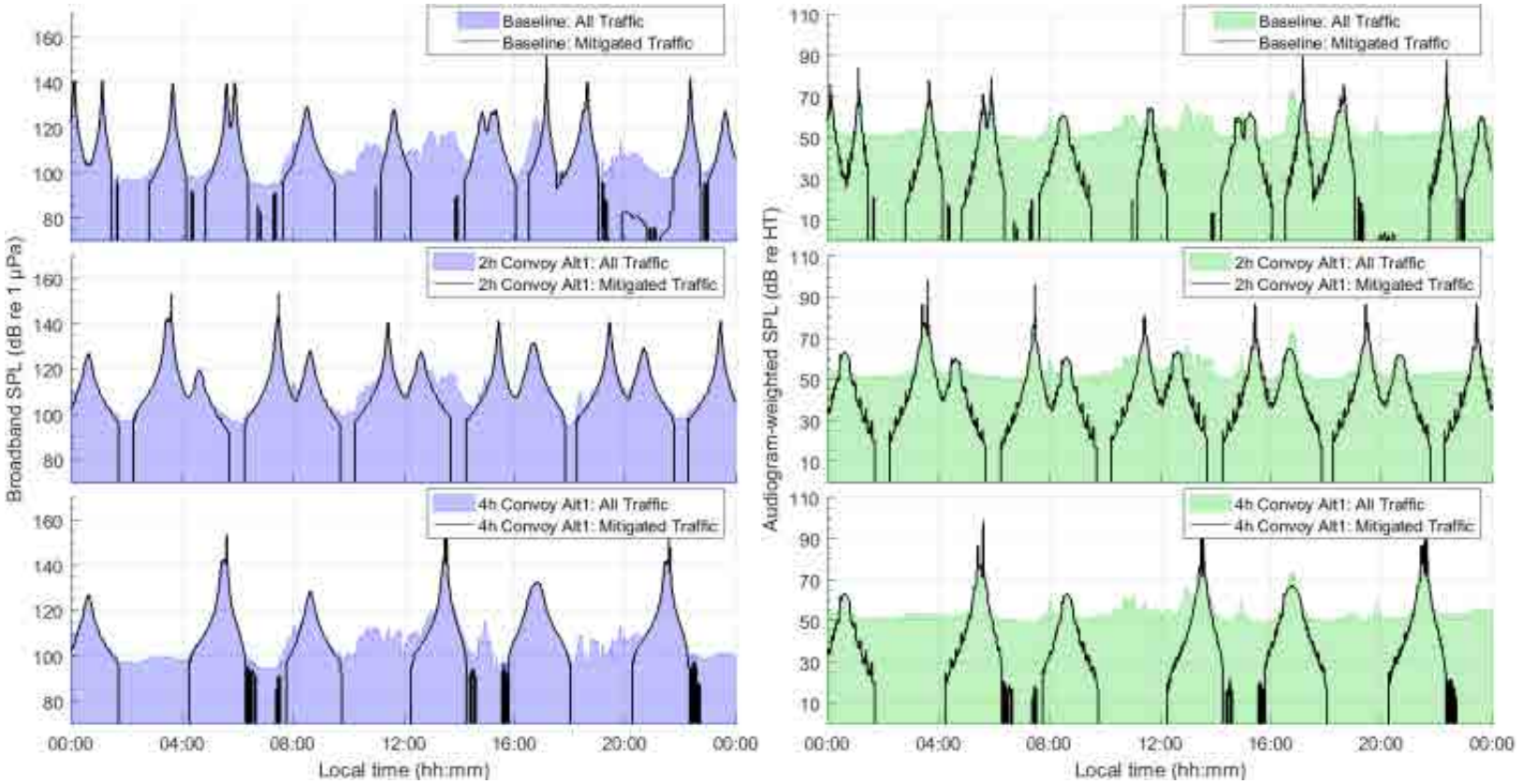

Figure 150. *Convoy Alternative 1, Haro Strait, Sample location 8*: Temporal variability of unweighted (left) and audiogram-weighted (right) received levels for (top) baseline (no convoy), (middle) 2-hour convoy, and (bottom) 4-hour convoy scenarios. The blue and green lines above the shaded area show received levels caused by all traffic and ambient noise. The black lines show received levels caused by commercial traffic only. The sample location is shown in Figure 6.

Table 61. *Convoy Alternative 1, Haro Strait:* Temporal analysis of unweighted received noise levels (dB re 1 µPa), difference in received noise levels (dB), and difference acoustic intensity (%). The values indicate the percentile or mean calculated over a 24-hour period without (baseline) and with mitigation, at the sample locations within the SRKW critical habitat shown in Figure 6.

Sample location	Scenario	Temporal analysis of noise level (dB re 1 µPa), difference in noise levels (dB), and difference in acoustic intensity (%)			
		5th	50th	95th	Mean
1	Baseline	97.5	102.6	111.3	103.3±4.7
	2-hour convoy	97.3	103.2	111.4	103.6±4.8
	Difference	**−0.2 (−4.5%)**	**+0.6 (+14.8%)**	**+0.1 (+2.3%)**	**+0.3 (+7.2%)**
	4-hour convoy	96.8	103.2	111.4	103.4±4.9
	Difference	**−0.7 (−14.9%)**	**+0.6 (+14.8%)**	**+0.1 (+2.3%)**	**+0.1 (+2.3%)**
2	Baseline	96.3	101.6	112.7	103.0±5.4
	2-hour convoy	96.1	102.5	113.3	103.4±5.8
	Difference	**−0.2 (−4.5%)**	**+0.9 (+23.0%)**	**+0.6 (+14.8%)**	**+0.4 (+9.6%)**
	4-hour convoy	96.1	101.4	114.3	103.1±5.9
	Difference	**−0.2 (−4.5%)**	**−0.2 (−4.5%)**	**+1.6 (+44.5%)**	**+0.1 (+2.3%)**
3	Baseline	95.7	101.4	117.4	104.5±7.4
	2-hour convoy	95.7	99.9	118.6	104.5±8.1
	Difference	**0.0 (0.0%)**	**−1.5 (−29.2%)**	**+1.2 (+31.8%)**	**0.0 (0.0%)**
	4-hour convoy	95.7	100.5	118.0	104.0±7.8
	Difference	**0.0 (0.0%)**	**−0.9 (−18.7%)**	**+0.6 (+14.8%)**	**−0.5 (−10.9%)**
4	Baseline	95.9	107.7	124.5	108.5±9.3
	2-hour convoy	96.5	111.7	125.8	110.9±9.2
	Difference	**+0.6 (+14.8%)**	**+4.0 (+151.2%)**	**+1.3 (+34.9%)**	**+2.4 (+73.8%)**
	4-hour convoy	95.6	106.6	125.0	107.8±9.9
	Difference	**−0.3 (−6.7%)**	**−1.1 (−22.4%)**	**+0.5 (+12.2%)**	**−0.7 (−14.9%)**
5	Baseline	95.8	108.6	128.5	109.4±10.5
	2-hour convoy	97.3	112.5	130.3	113.2±9.7
	Difference	**+1.5 (+41.3%)**	**+3.9 (+145.5%)**	**+1.8 (+51.4%)**	**+3.8 (+139.9%)**
	4-hour convoy	95.5	107.5	130.5	109.2±11.0
	Difference	**−0.3 (−6.7%)**	**−1.1 (−22.4%)**	**+2.0 (+58.5%)**	**−0.2 (−4.5%)**
6	Baseline	96.2	109.9	131.8	111.1±11.0
	2-hour convoy	98.6	112.1	134.2	113.8±11.1
	Difference	**+2.4 (+73.8%)**	**+2.2 (+66.0%)**	**+2.4 (+73.8%)**	**+2.7 (+86.2%)**
	4-hour convoy	96.5	109.2	135.4	111.3±11.6
	Difference	**+0.3 (+7.2%)**	**−0.7 (−14.9%)**	**+3.6 (+129.1%)**	**+0.2 (+4.7%)**
7	Baseline	96.2	108.2	128.6	109.9±10.5
	2-hour convoy	97.5	112.4	130.8	113.0±10.5
	Difference	**+1.3 (+34.9%)**	**+4.2 (+163.0%)**	**+2.2 (+66.0%)**	**+3.1 (+104.2%)**
	4-hour convoy	95.4	107.3	130.5	109.1±11.2
	Difference	**−0.8 (−16.8%)**	**−0.9 (−18.7%)**	**+1.9 (+54.9%)**	**−0.8 (−16.8%)**
8	Baseline	96.3	108.0	128.1	109.4±10.4
	2-hour convoy	97.4	111.5	132.0	112.6±10.5
	Difference	**+1.1 (+28.8%)**	**+3.5 (+123.9%)**	**+3.9 (+145.5%)**	**+3.2 (+108.9%)**
	4-hour convoy	95.5	107.1	131.9	108.7±11.2
	Difference	**−0.8 (−16.8%)**	**−0.9 (−18.7%)**	**+3.8 (+139.9%)**	**−0.7 (−14.9%)**

Table 62. *Convoy Alternative 1, Haro Strait:* Temporal analysis of SRKW audiogram-weighted received noise levels (dB re HT), difference in received noise levels (dB), and difference acoustic intensity (%). The values indicate the percentile or mean calculated over a 24-hour period without (baseline) and with mitigation, at the sample locations within the SRKW critical habitat shown in Figure 6.

Sample location	Scenario	Temporal analysis of noise level (dB re HT), difference in noise levels (dB), and difference in acoustic intensity (%)			
		5th	50th	95th	Mean
1	Baseline	49.6	52.2	57.0	52.7±3.3
	2-hour convoy	49.7	52.2	57.0	52.8±3.3
	Difference	**+0.1 (+2.3%)**	**0.0 (0.0%)**	**0.0 (0.0%)**	**+0.1 (+2.3%)**
	4-hour convoy	49.7	52.2	57.0	52.8±3.3
	Difference	**+0.1 (+2.3%)**	**0.0 (0.0%)**	**0.0 (0.0%)**	**+0.1 (+2.3%)**
2	Baseline	49.5	52.2	59.1	52.8±3.2
	2-hour convoy	49.6	52.2	59.1	52.8±3.2
	Difference	**+0.1 (+2.3%)**	**0.0 (0.0%)**	**0.0 (0.0%)**	**0.0 (0.0%)**
	4-hour convoy	49.6	52.2	59.1	52.8±3.2
	Difference	**+0.1 (+2.3%)**	**0.0 (0.0%)**	**0.0 (0.0%)**	**0.0 (0.0%)**
3	Baseline	49.5	52.5	61.9	53.5±3.9
	2-hour convoy	49.9	52.5	61.9	53.5±3.9
	Difference	**+0.4 (+9.6%)**	**0.0 (0.0%)**	**0.0 (0.0%)**	**0.0 (0.0%)**
	4-hour convoy	49.5	52.6	61.9	53.5±4.0
	Difference	**0.0 (0.0%)**	**+0.1 (+2.3%)**	**0.0 (0.0%)**	**0.0 (0.0%)**
4	Baseline	49.6	53.3	63.5	54.8±5.1
	2-hour convoy	50.3	53.4	63.7	55.3±5.1
	Difference	**+0.7 (+17.5%)**	**+0.1 (+2.3%)**	**+0.2 (+4.7%)**	**+0.5 (+12.2%)**
	4-hour convoy	49.5	53.4	63.8	54.8±5.2
	Difference	**−0.1 (−2.3%)**	**+0.1 (+2.3%)**	**+0.3 (+7.2%)**	**0.0 (0.0%)**
5	Baseline	49.6	53.3	65.4	55.3±5.3
	2-hour convoy	50.0	53.5	65.8	56.0±5.6
	Difference	**+0.4 (+9.6%)**	**+0.2 (+4.7%)**	**+0.4 (+9.6%)**	**+0.7 (+17.5%)**
	4-hour convoy	49.5	53.4	67.1	55.3±5.7
	Difference	**−0.1 (−2.3%)**	**+0.1 (+2.3%)**	**+1.7 (+47.9%)**	**0.0 (0.0%)**
6	Baseline	49.9	53.5	66.5	56.1±6.1
	2-hour convoy	49.6	54.5	68.4	56.9±6.5
	Difference	**−0.3 (−6.7%)**	**+1.0 (+25.9%)**	**+1.9 (+54.9%)**	**+0.8 (+20.2%)**
	4-hour convoy	49.6	53.6	68.8	56.4±6.4
	Difference	**−0.3 (−6.7%)**	**+0.1 (+2.3%)**	**+2.3 (+69.8%)**	**+0.3 (+7.2%)**
7	Baseline	49.6	53.5	64.7	55.4±5.4
	2-hour convoy	50.4	53.7	65.5	56.4±6.4
	Difference	**+0.8 (+20.2%)**	**+0.2 (+4.7%)**	**+0.8 (+20.2%)**	**+1.0 (+25.9%)**
	4-hour convoy	49.5	53.5	67.0	55.4±6.4
	Difference	**−0.1 (−2.3%)**	**0.0 (0.0%)**	**+2.3 (+69.8%)**	**0.0 (0.0%)**
8	Baseline	49.7	53.3	66.2	55.1±5.4
	2-hour convoy	50.4	53.6	69.0	56.2±6.5
	Difference	**+0.7 (+17.5%)**	**+0.3 (+7.2%)**	**+2.8 (+90.5%)**	**+1.1 (+28.8%)**
	4-hour convoy	49.6	53.4	69.2	55.2±6.6
	Difference	**−0.1 (−2.3%)**	**+0.1 (+2.3%)**	**+3.0 (+99.5%)**	**+0.1 (+2.3%)**

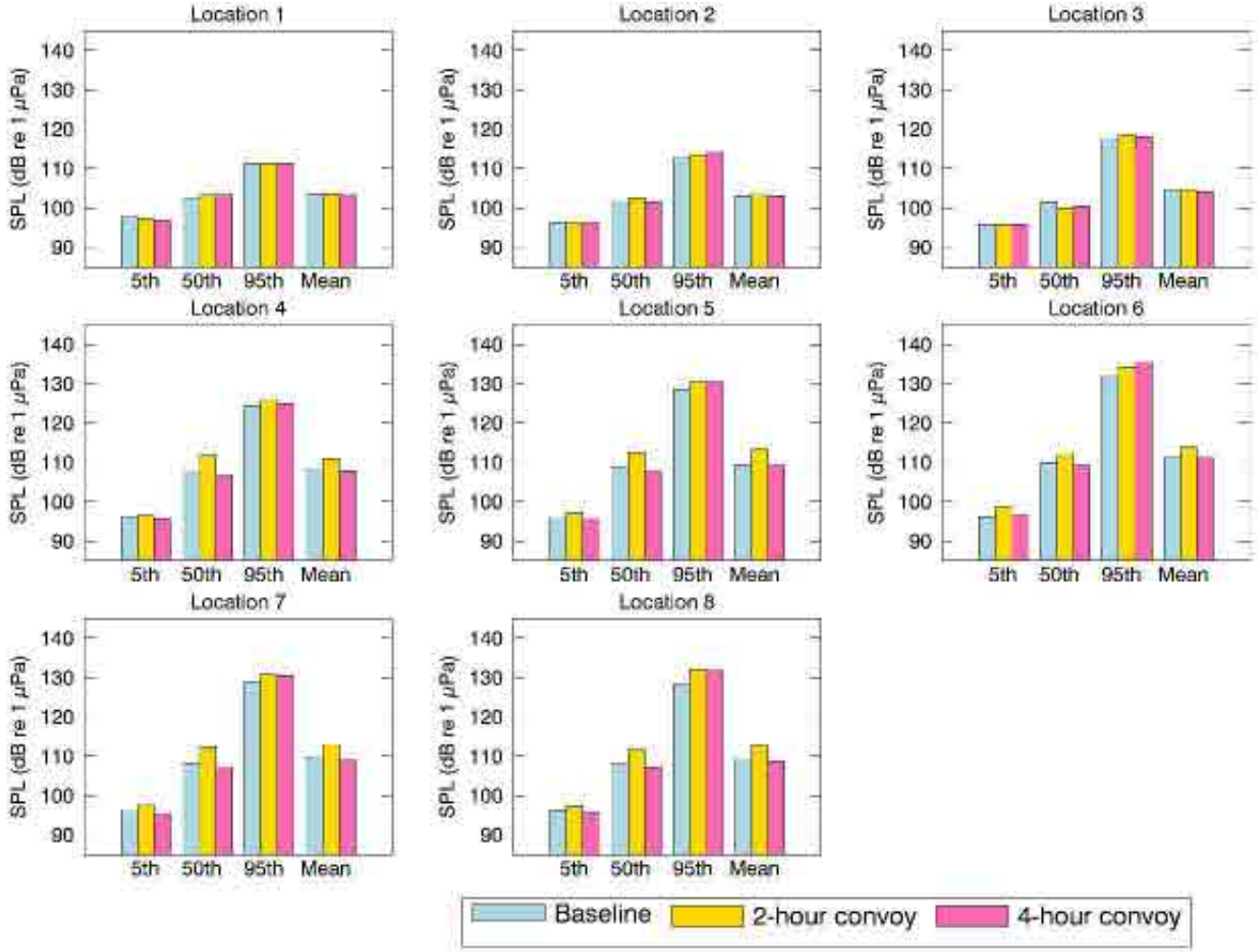

Figure 151. *Convoy Alternative 1, Haro Strait:* Histogram representation of the temporal analysis of unweighted received noise levels (dB re 1 µPa). The vertical bars indicate the percentile or mean calculated over a 24-hour period without (baseline) and with mitigation, at the sample locations within the SRKW critical habitat shown in Figure 6.

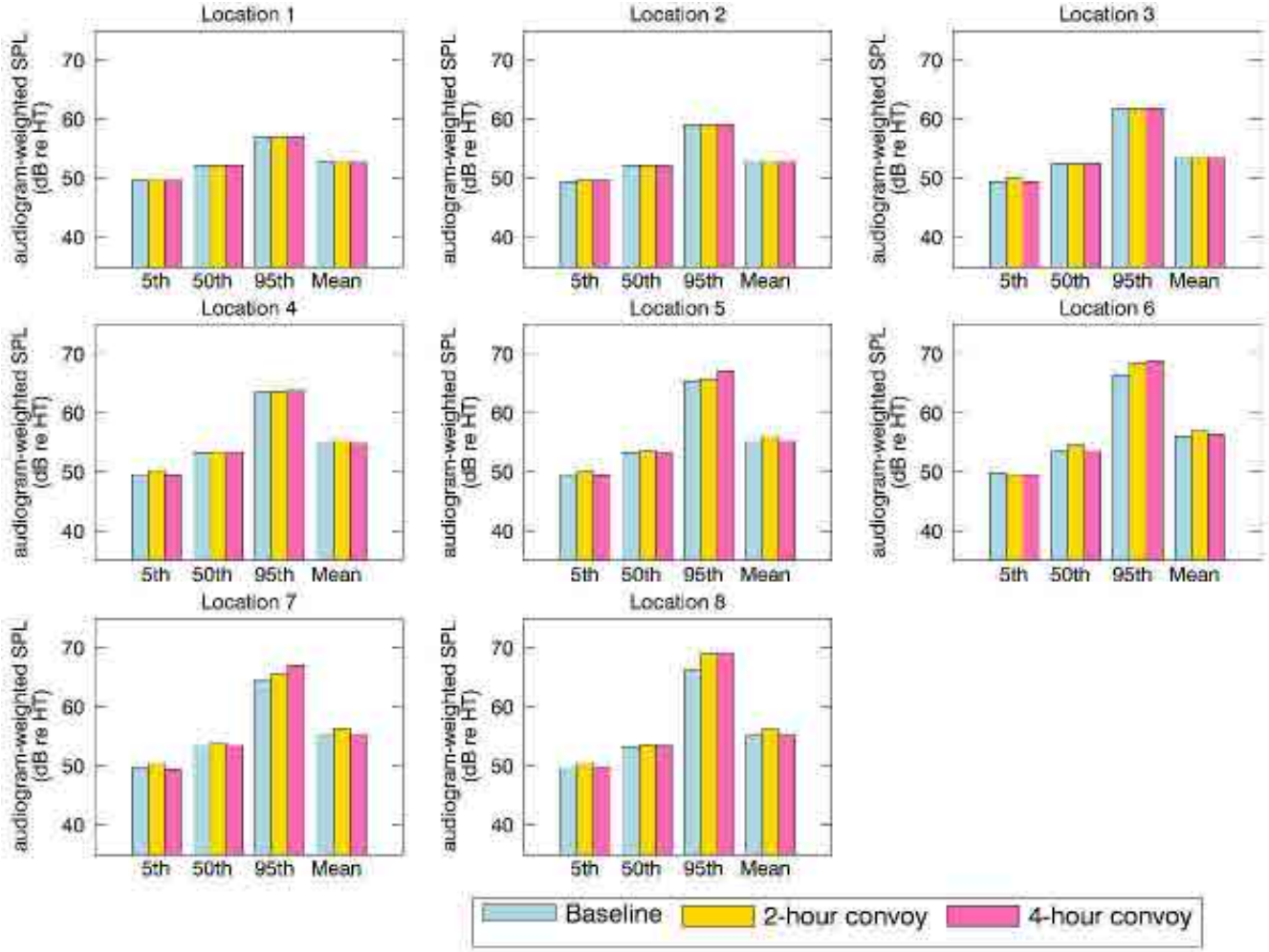

Figure 152. *Convoy Alternative 1, Haro Strait:* Histogram representation of the temporal analysis of SRKW audiogram-weighted received noise levels (dB re 1 µPa). The vertical bars indicate the percentile or mean calculated over a 24-hour period without (baseline) and with mitigation, at the sample locations within the SRKW critical habitat shown in Figure 6.

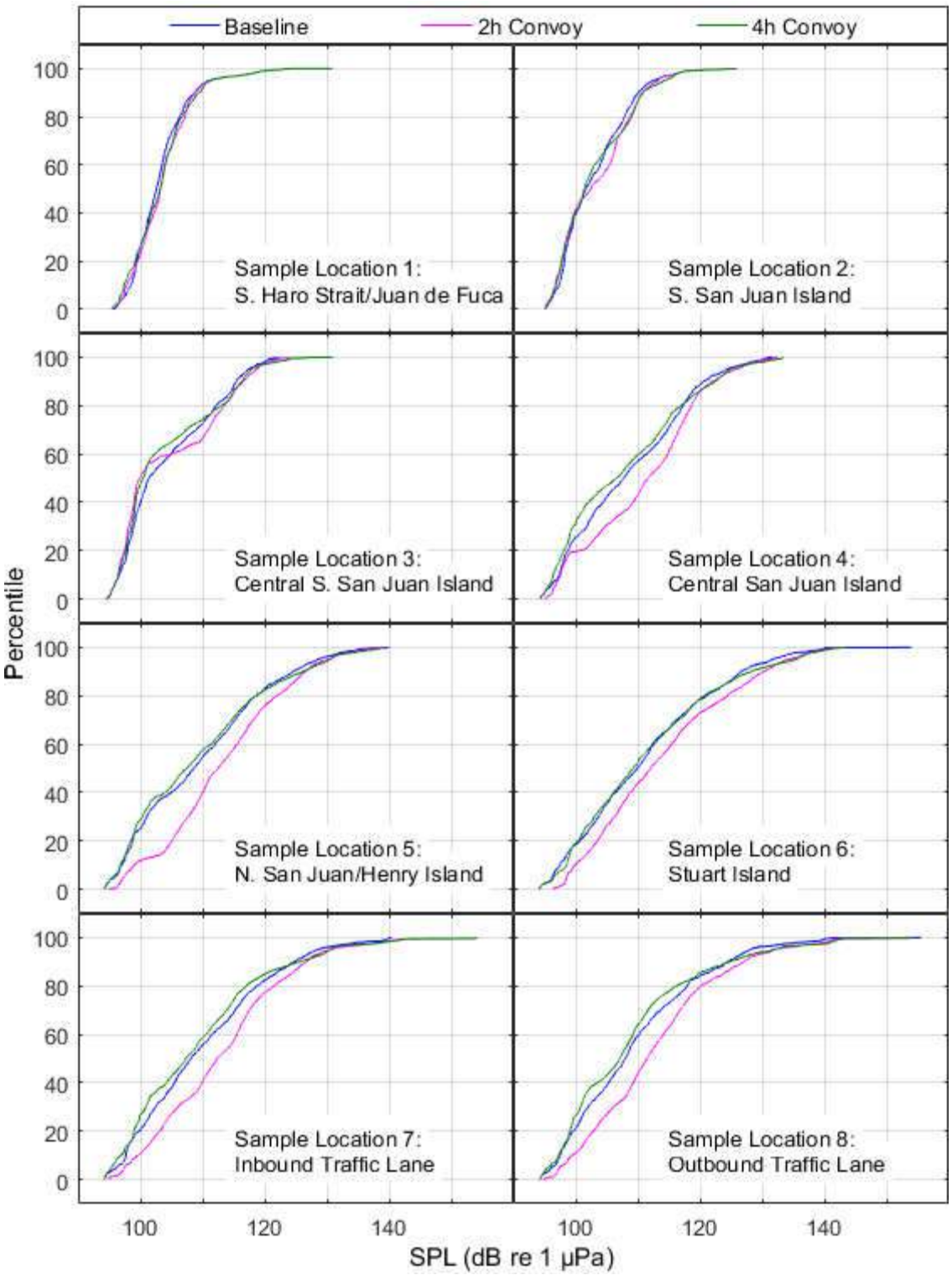

Figure 153. *Convoy Alternative 1, Haro Strait:* CDF curves of time-dependent unweighted SPL for baseline and mitigated scenarios at the sample locations shown in Figure 6.

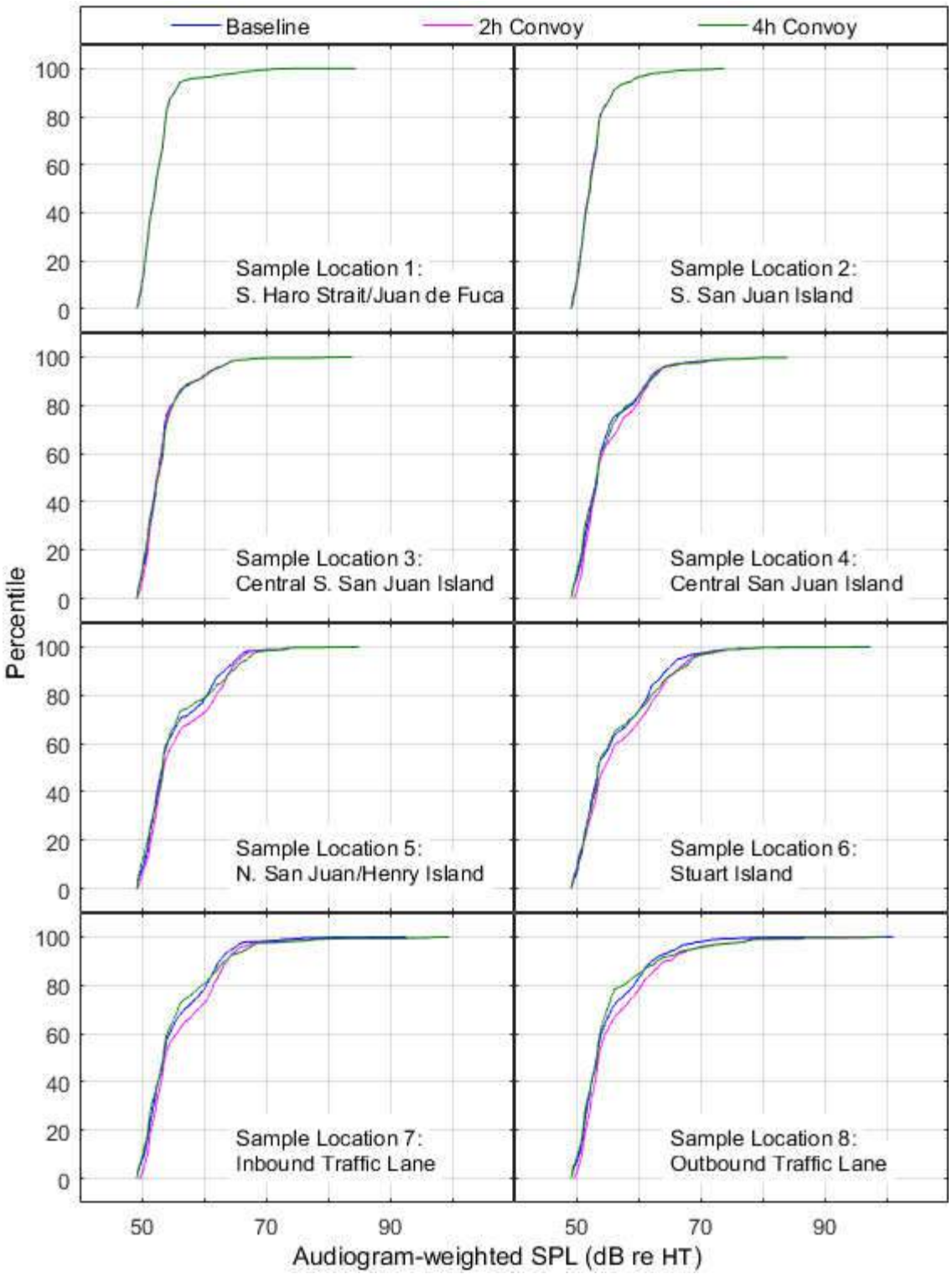

Figure 154. *Convoy Alternative 1, Haro Strait:* CDF curves of time-dependent audiogram-weighted SPL for baseline and mitigated scenarios at the sample locations shown in Figure 6.

3.8.2. Alternative 2: Convoying in Juan de Fuca Strait

This section presents the temporal distribution of received noise levels, representing future mitigated levels with the expected increase in vessel traffic associated with the Trans Mountain requirements and implementing commercial vessel convoys in Juan de Fuca Strait, as described in Section 2.2.3.6. The convoying occurs between the VH buoy south of Victoria and the Pacific Ocean west of Juan de Fuca Strait, as seen in Figure 15. Results are presented for the unmitigated baseline scenario (no convoy, no Trans Mountain vessel traffic), as well as for a 4-hour convoy interval scenario (which includes Trans Mountain traffic).

Because convoying in Juan de Fuca Strait will affect the noise levels in all Local Study Areas, the modelled received levels at the sample locations in the SRKW critical habitat were sampled every 1-minute over the 33-hour period, in each area. The sample locations are listed in Table 1 and shown in Figures 5–8. The sound field snapshots from the model simulations were rendered as animations to show the time evolution of the vessel traffic noise in the Local Study Areas. Examples of the snapshots are presented in Figures 155, 168, 181, and 195.

The same type of results as for Alternative 1 are presented for Alternative 2: (1) unweighted and audiogram-weighted received noise levels (SPL) as a function of time, (2) percentile and mean values of the temporal variation, and (3) cumulative distribution functions (CDFs) at each sample location. The results are presented for each Local Study Area in Sections 3.8.2.1–3.8.2.4. In the Strait of Georgia, SRKW audiogram-weighted levels from the mitigated vessel did not reach Sample locations 1 and 3; thus, the black line cannot be seen on the right-side graphs in Figures 156 and 158.

3.8.2.1. Strait of Georgia

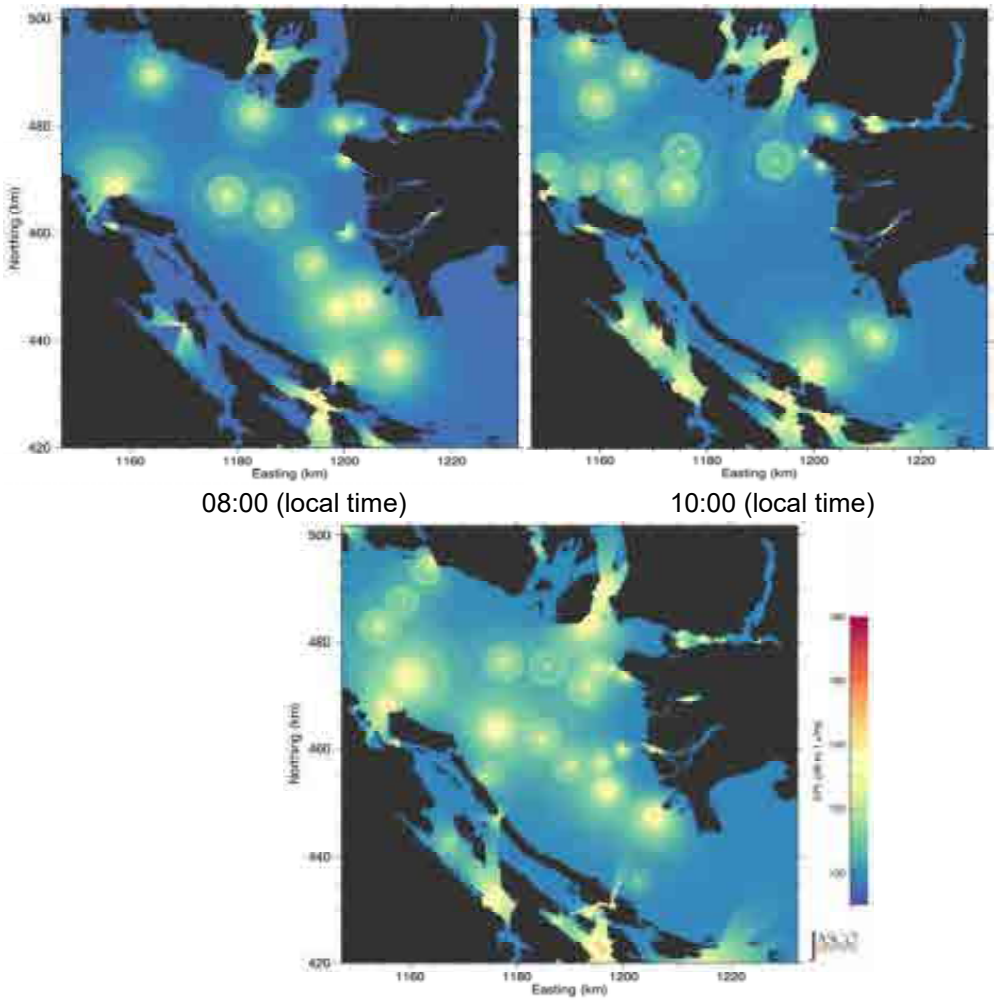

Figure 155. *Convoy Alternative 2, Strait of Georgia:* Example time snapshots of future mitigated SPL (unweighted with ambient, 10 Hz to 50 kHz) from 08:00 to 12:00 (local time) in 2-hour increments. Easting and northing are BC Albers projected coordinates.

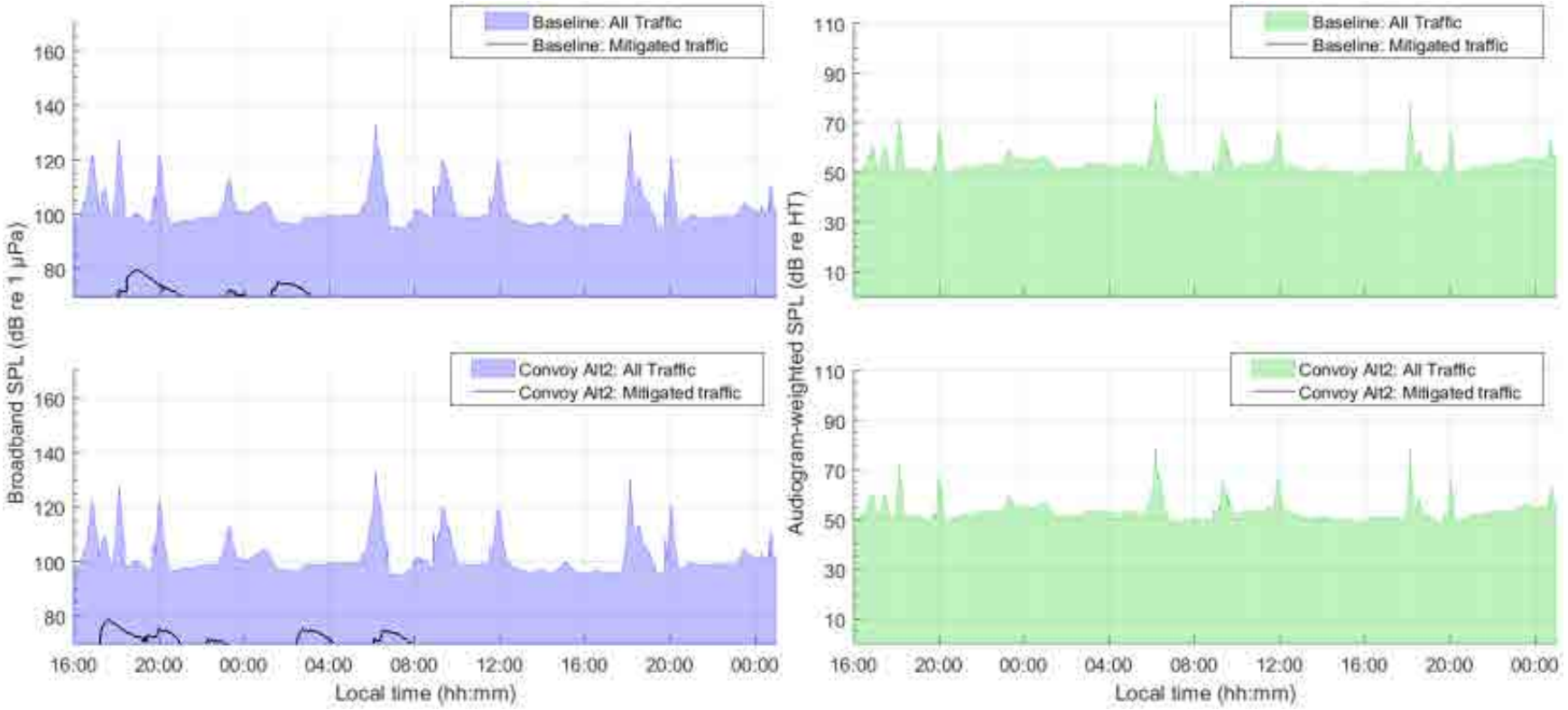

Figure 156. *Convoy Alternative 2, Strait of Georgia, Sample location 1*: Temporal variability of unweighted (left) and audiogram-weighted (right) received levels for (top) baseline (no convoy) and (bottom) convoy scenarios. The blue and green lines above the shaded area show received levels caused by all traffic and ambient noise. The black lines show received levels caused by commercial traffic only. The receiver location is shown in Figure 5. SRKW audiogram-weighted levels from the mitigated vessel did not reach Sample location 1; thus, the black line cannot be seen on the right-side graphs.

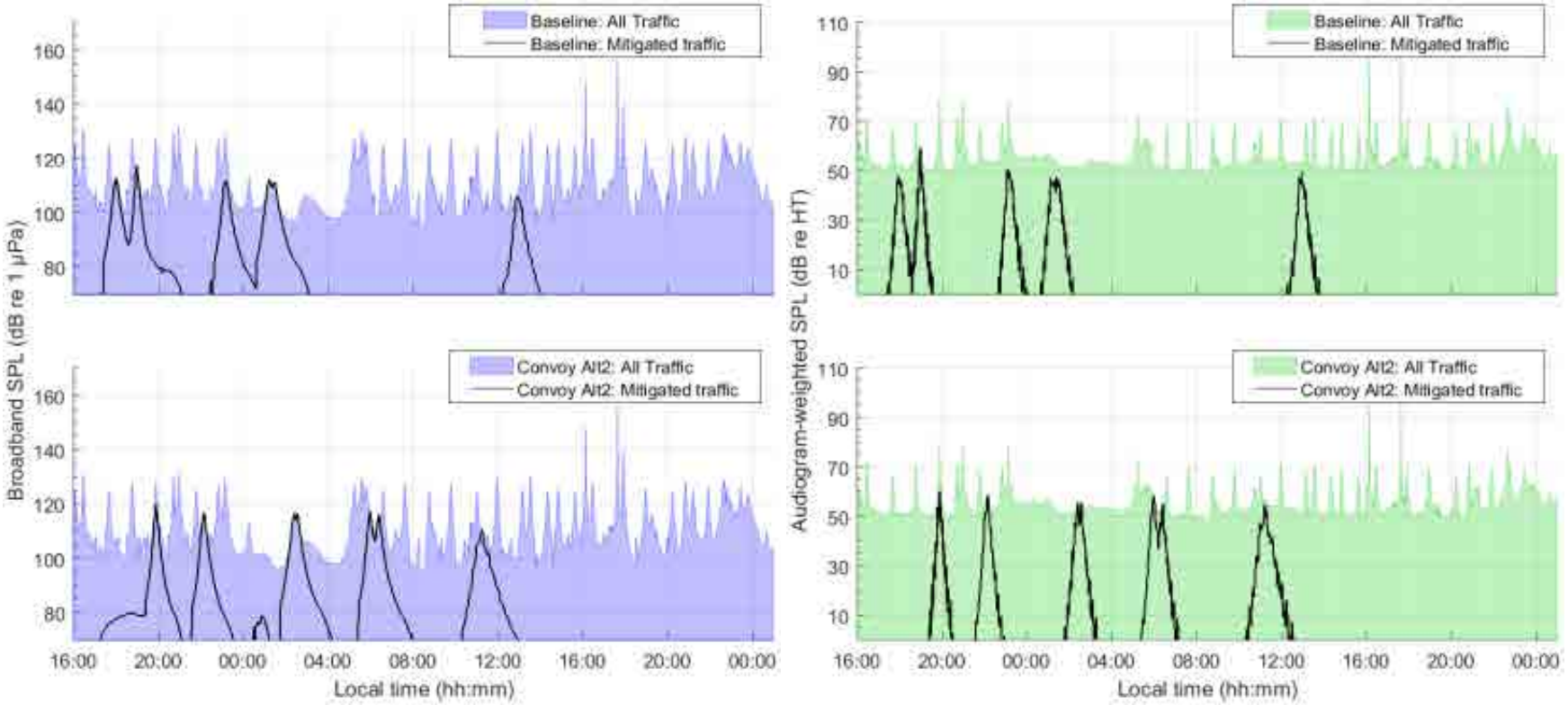

Figure 157. *Convoy Alternative 2, Strait of Georgia, Sample location 2*: Temporal variability of unweighted (left) and audiogram-weighted (right) received levels for (top) baseline (no convoy) and (bottom) convoy scenarios. The blue and green lines above the shaded area show received levels caused by all traffic and ambient noise. The black lines show received levels caused by commercial traffic only. The receiver location is shown in Figure 5.

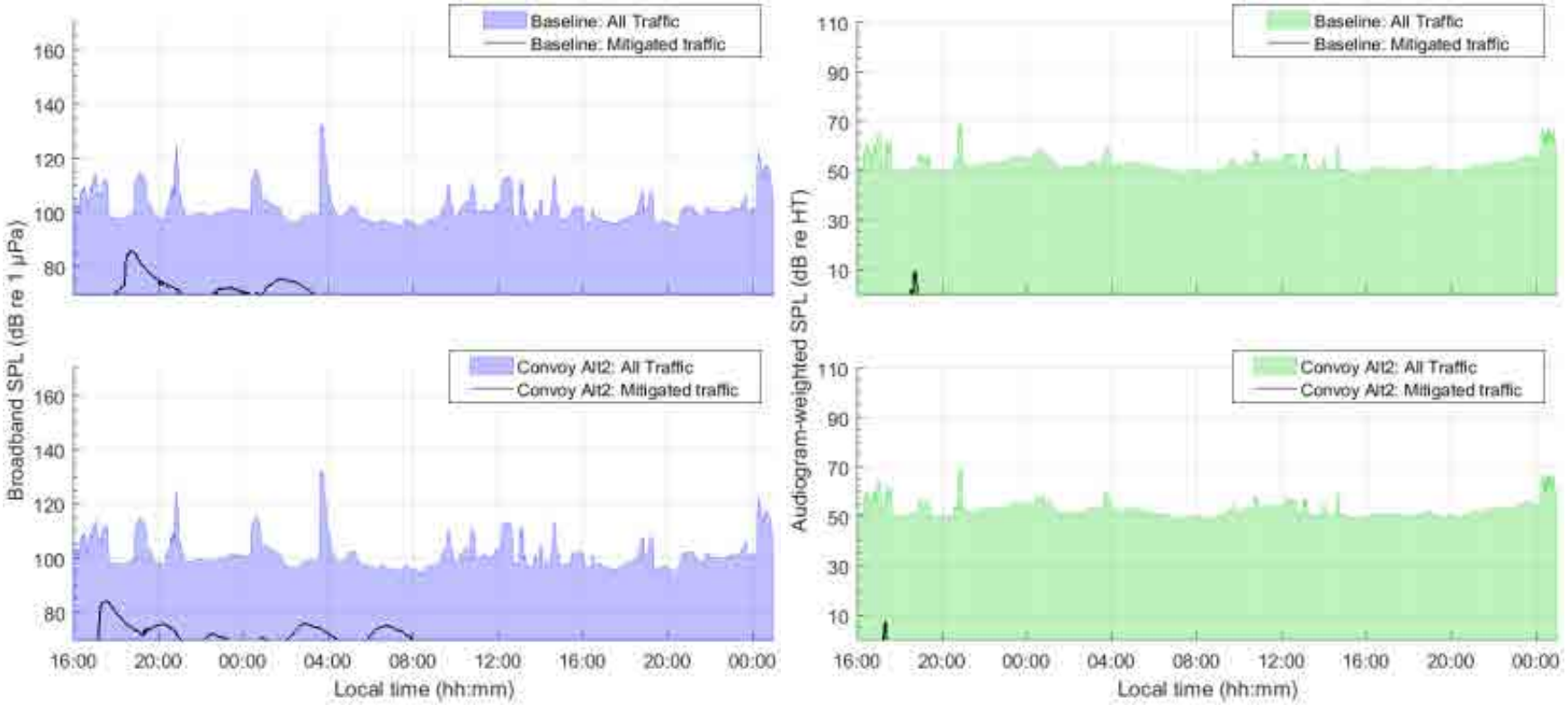

Figure 158. *Convoy Alternative 2, Strait of Georgia, Sample location 3*: Temporal variability of unweighted (left) and audiogram-weighted (right) received levels for (top) baseline (no convoy) and (bottom) convoy scenarios. The blue and green lines above the shaded area show received levels caused by all traffic and ambient noise. The black lines show received levels caused by commercial traffic only. The receiver location is shown in Figure 5. SRKW audiogram-weighted levels from the mitigated vessel did not reach Sample location 3; thus, the black line cannot be seen on some of the right-side graphs.

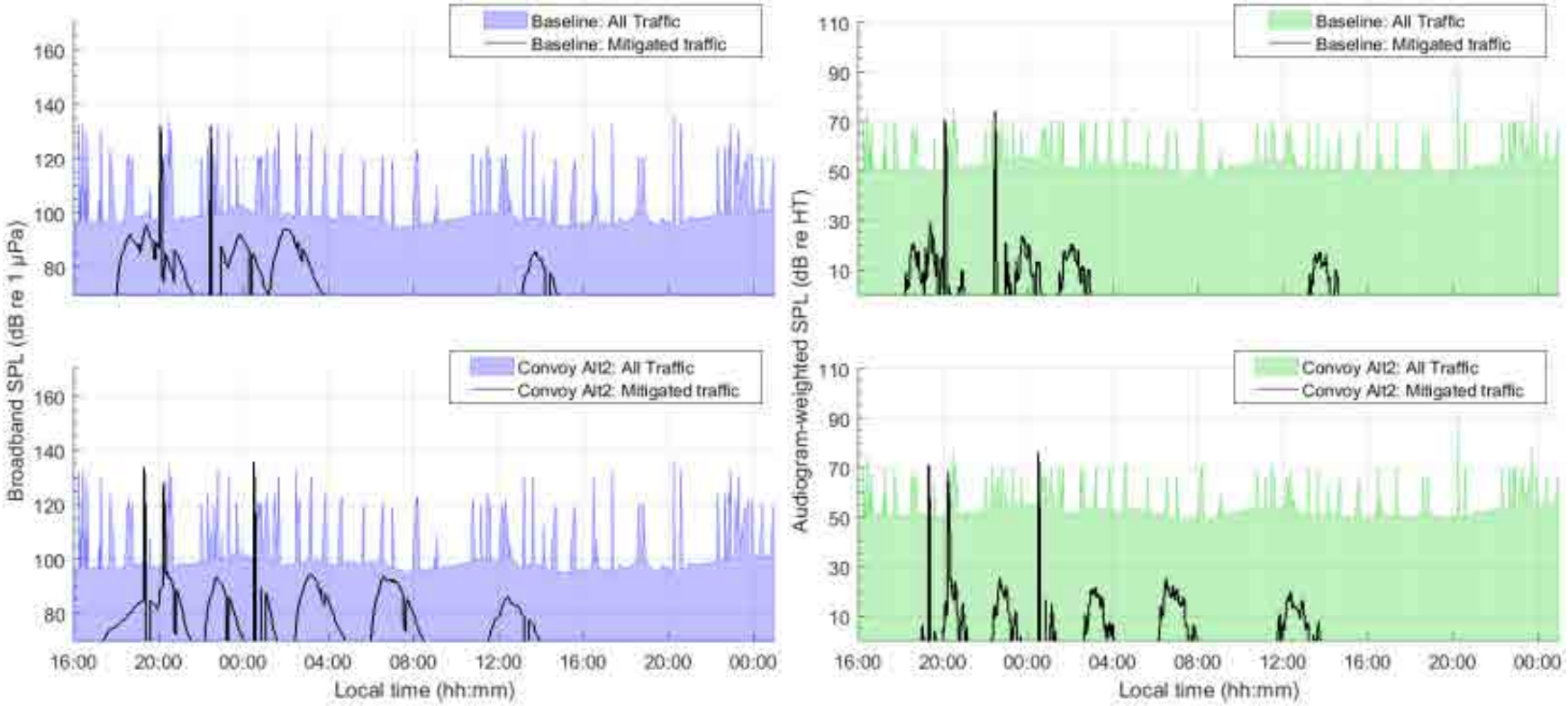

Figure 159. *Convoy Alternative 2, Strait of Georgia, Sample location 4*: Temporal variability of unweighted (left) and audiogram-weighted (right) received levels for (top) baseline (no convoy) and (bottom) convoy scenarios. The blue and green lines above the shaded area show received levels caused by all traffic and ambient noise. The black lines show received levels caused by commercial traffic only. The receiver location is shown in Figure 5.

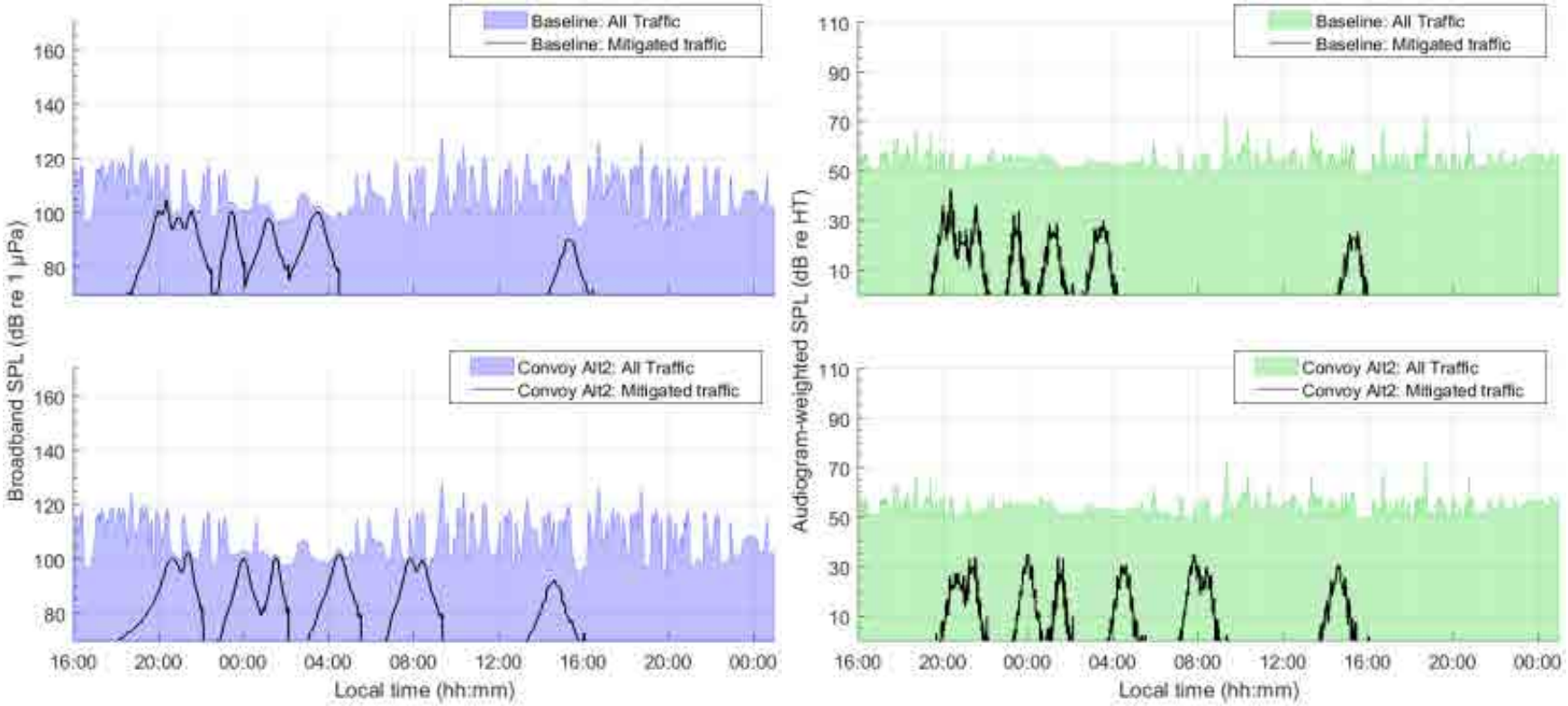

Figure 160. *Convoy Alternative 2, Strait of Georgia, Sample location 5*: Temporal variability of unweighted (left) and audiogram-weighted (right) received levels for (top) baseline (no convoy) and (bottom) convoy scenarios. The blue and green lines above the shaded area show received levels caused by all traffic and ambient noise. The black lines show received levels caused by commercial traffic only. The receiver location is shown in Figure 5.

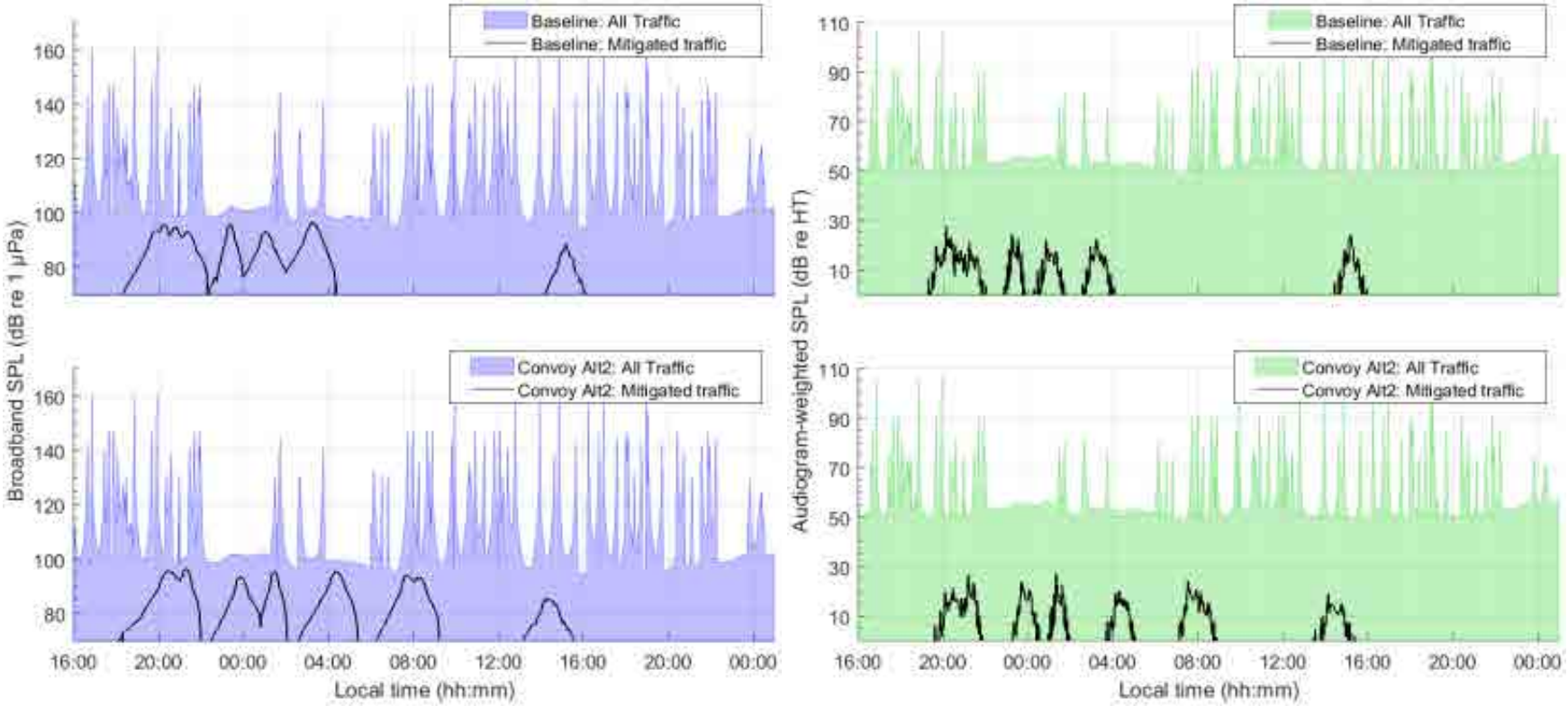

Figure 161. *Convoy Alternative 2, Strait of Georgia, Sample location 6*: Temporal variability of unweighted (left) and audiogram-weighted (right) received levels for (top) baseline (no convoy) and (bottom) convoy scenarios. The blue and green lines above the shaded area show received levels caused by all traffic and ambient noise. The black lines show received levels caused by commercial traffic only. The receiver location is shown in Figure 5.

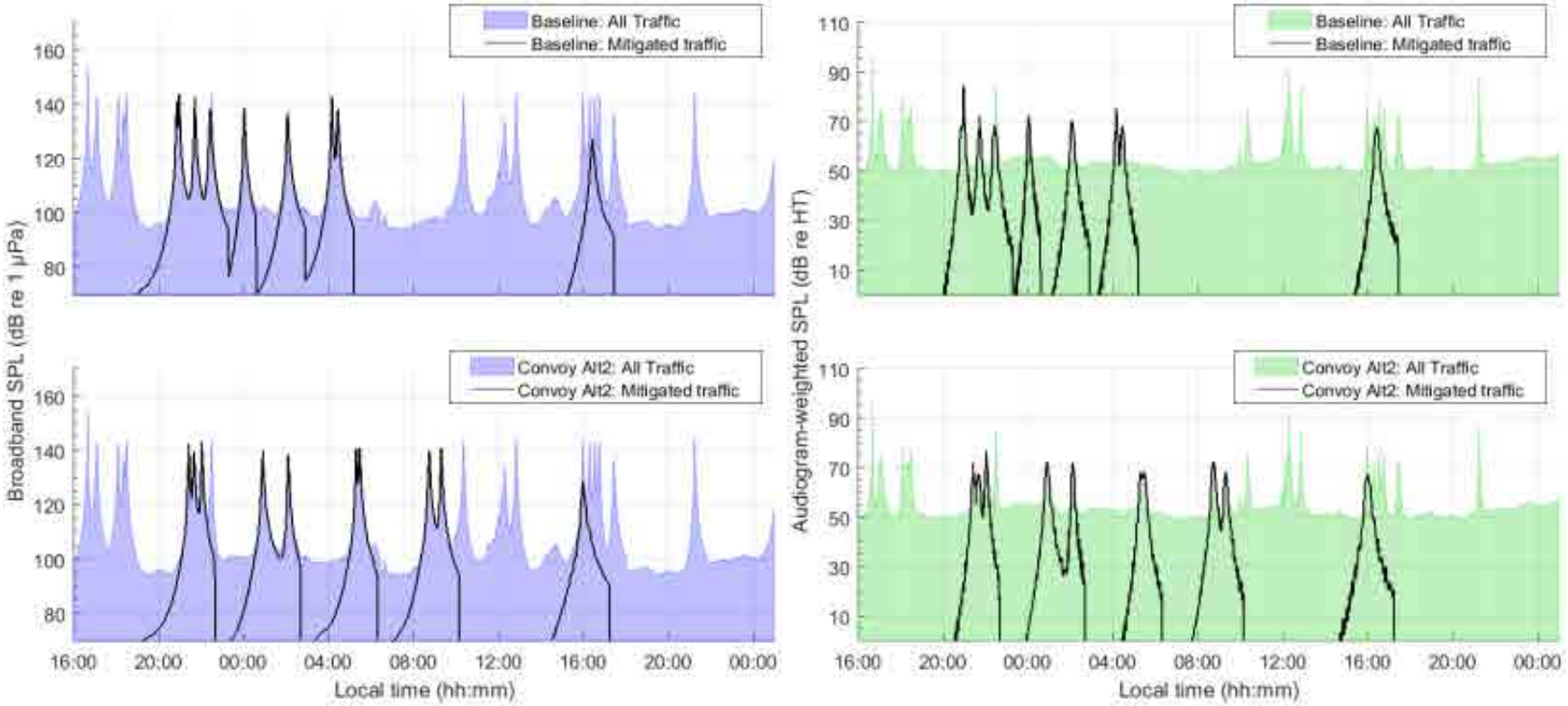

Figure 162. *Convoy Alternative 2, Strait of Georgia, Sample location 7*: Temporal variability of unweighted (left) and audiogram-weighted (right) received levels for (top) baseline (no convoy) and (bottom) convoy scenarios. The blue and green lines above the shaded area show received levels caused by all traffic and ambient noise. The black lines show received levels caused by commercial traffic only. The receiver location is shown in Figure 5.

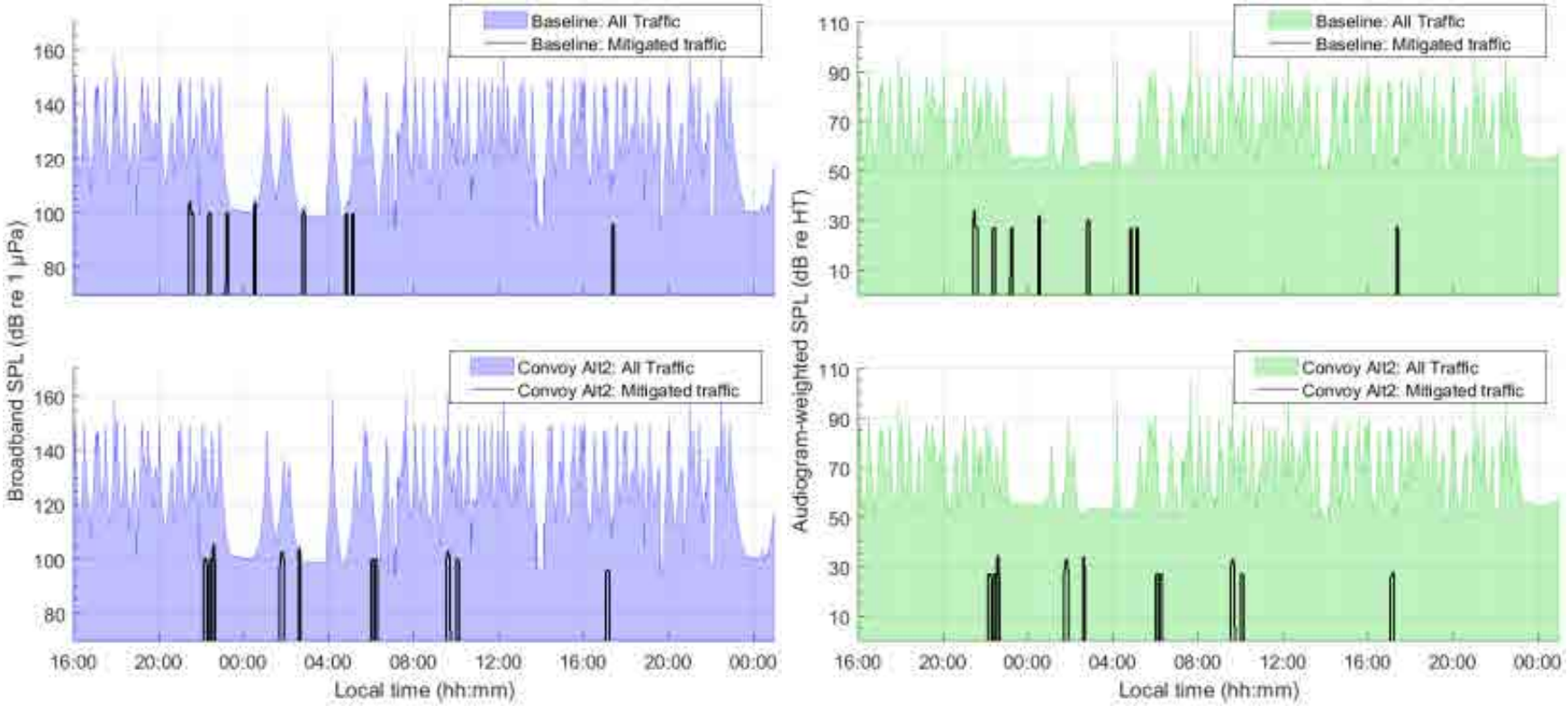

Figure 163. *Convoy Alternative 2, Strait of Georgia, Sample location 8*: Temporal variability of unweighted (left) and audiogram-weighted (right) received levels for (top) baseline (no convoy) and (bottom) convoy scenarios. The blue and green lines above the shaded area show received levels caused by all traffic and ambient noise. The black lines show received levels caused by commercial traffic only. The receiver location is shown in Figure 5.

Table 63. *Convoy Alternative 2, Strait of Georgia*: Temporal analysis of unweighted received noise levels (dB re 1 µPa), difference in received noise levels (dB), and difference acoustic intensity (%). The values indicate the percentile or mean calculated over a 33-hour period without (Baseline) and with mitigation (Convoy), at the sample locations within the SRKW critical habitat shown in Figure 5.

Sample location	Scenario	Temporal analysis of noise level (dB re 1 µPa), difference in noise levels (dB), and difference in acoustic intensity (%)			
		5th	50th	95th	Mean
1	Baseline	96.0	99.4	117.5	101.8 ±6.4
	Convoy	96.0	99.4	117.5	101.8 ±6.4
	Difference	**0.0 (0.0%)**	**0.0 (0.0%)**	**0.0 (0.0%)**	**0.0 (0.0%)**
2	Baseline	98.3	108.1	125.4	109.8 ±8.4
	Convoy	98.3	108.4	125.4	109.9 ±8.5
	Difference	**0.0 (0.0%)**	**+0.2 (+5.0%)**	**0.0 (0.0%)**	**+0.2 (+4.4%)**
3	Baseline	96.2	100.2	113.6	101.8 ±5.7
	Convoy	96.2	100.2	113.5	101.8 ±5.7
	Difference	**0.0 (0.0%)**	**0.0 (0.0%)**	**0.0 (0.0%)**	**0.0 (0.0%)**
4	Baseline	95.5	99.0	122.3	103.0 ±9.1
	Convoy	95.7	98.9	122.3	103.1 ±9.2
	Difference	**+0.2 (+5.3%)**	**−0.1 (−2.5%)**	**0.0 (0.0%)**	**0.0 (0.0%)**
5	Baseline	97.4	106.3	118.4	107.0 ±7.2
	Convoy	97.9	106.2	118.4	107.1 ±7.1
	Difference	**+0.6 (+13.8%)**	**0.0 (0.0%)**	**0.0 (0.0%)**	**+0.1 (+2.7%)**
6	Baseline	96.8	103.6	138.2	109.8 ±13.5
	Convoy	96.9	103.6	138.2	109.8 ±13.5
	Difference	**+0.1 (+3.5%)**	**0.0 (0.0%)**	**0.0 (0.0%)**	**0.0 (0.0%)**
7	Baseline	95.0	101.9	133.7	106.7 ±11.9
	Convoy	95.0	102.3	134.3	107.4 ±12.2
	Difference	**0.0 (0.0%)**	**+0.4 (+10.0%)**	**+0.6 (+14.9%)**	**+0.7 (+17.9%)**
8	Baseline	98.9	123.5	146.6	122.5 ±14.4
	Convoy	98.9	123.5	146.6	122.5 ±14.5
	Difference	**0.0 (0.0%)**	**0.0 (0.0%)**	**0.0 (0.0%)**	**0.0 (0.0%)**

Table 64. *Convoy Alternative 2, Strait of Georgia*: *:*Temporal analysis of SRKW audiogram-weighted received noise levels (dB re HT), difference in received noise levels (dB), and difference acoustic intensity (%). The values indicate the percentile or mean calculated over a 33-hour period without (Baseline) and with mitigation (Convoy), at the sample locations within the SRKW critical habitat shown in Figure 5.

Sample location	Scenario	Temporal analysis of noise level (dB re HT), difference in noise levels (dB), and difference in acoustic intensity (%)			
		5th	50th	95th	Mean
1	Baseline	49.5	52.7	61.8	53.5 ±3.9
	Convoy	49.5	52.7	61.8	53.5 ±3.9
	Difference	**0.0 (0.0%)**	**0.0 (0.0%)**	**0.0 (0.0%)**	**0.0 (0.0%)**
2	Baseline	50.2	53.7	66.4	55.6 ±5.4
	Convoy	50.2	53.8	66.4	55.7 ±5.4
	Difference	**0.0 (0.0%)**	**+0.1 (+2.7%)**	**0.0 (0.0%)**	**0.0 (0.0%)**
3	Baseline	49.5	52.3	59.3	53.0 ±3.3
	Convoy	49.5	52.3	59.3	53.0 ±3.3
	Difference	**0.0 (0.0%)**	**0.0 (0.0%)**	**0.0 (0.0%)**	**0.0 (0.0%)**
4	Baseline	49.5	52.7	66.7	54.8 ±5.8
	Convoy	49.5	52.7	66.8	54.8 ±5.8
	Difference	**0.0 (0.0%)**	**0.0 (0.0%)**	**+0.1 (+2.8%)**	**0.0 (0.0%)**
5	Baseline	49.9	53.7	59.0	54.3 ±3.2
	Convoy	49.9	53.7	59.0	54.3 ±3.2
	Difference	**0.0 (0.0%)**	**0.0 (0.0%)**	**0.0 (0.0%)**	**0.0 (0.0%)**
6	Baseline	49.9	53.8	79.9	58.2 ±10.1
	Convoy	49.9	53.8	79.9	58.2 ±10.1
	Difference	**0.0 (0.0%)**	**0.0 (0.0%)**	**0.0 (0.0%)**	**0.0 (0.0%)**
7	Baseline	49.6	53.2	68.9	54.8 ±6.2
	Convoy	49.7	53.3	69.5	55.1 ±6.3
	Difference	**+0.1 (+2.4%)**	**+0.1 (+2.8%)**	**+0.6 (+15.2%)**	**+0.3 (+7.9%)**
8	Baseline	52.2	64.8	84.7	66.4 ±11.2
	Convoy	52.2	64.8	84.7	66.4 ±11.2
	Difference	**0.0 (0.0%)**	**0.0 (0.0%)**	**0.0 (0.0%)**	**0.0 (0.0%)**

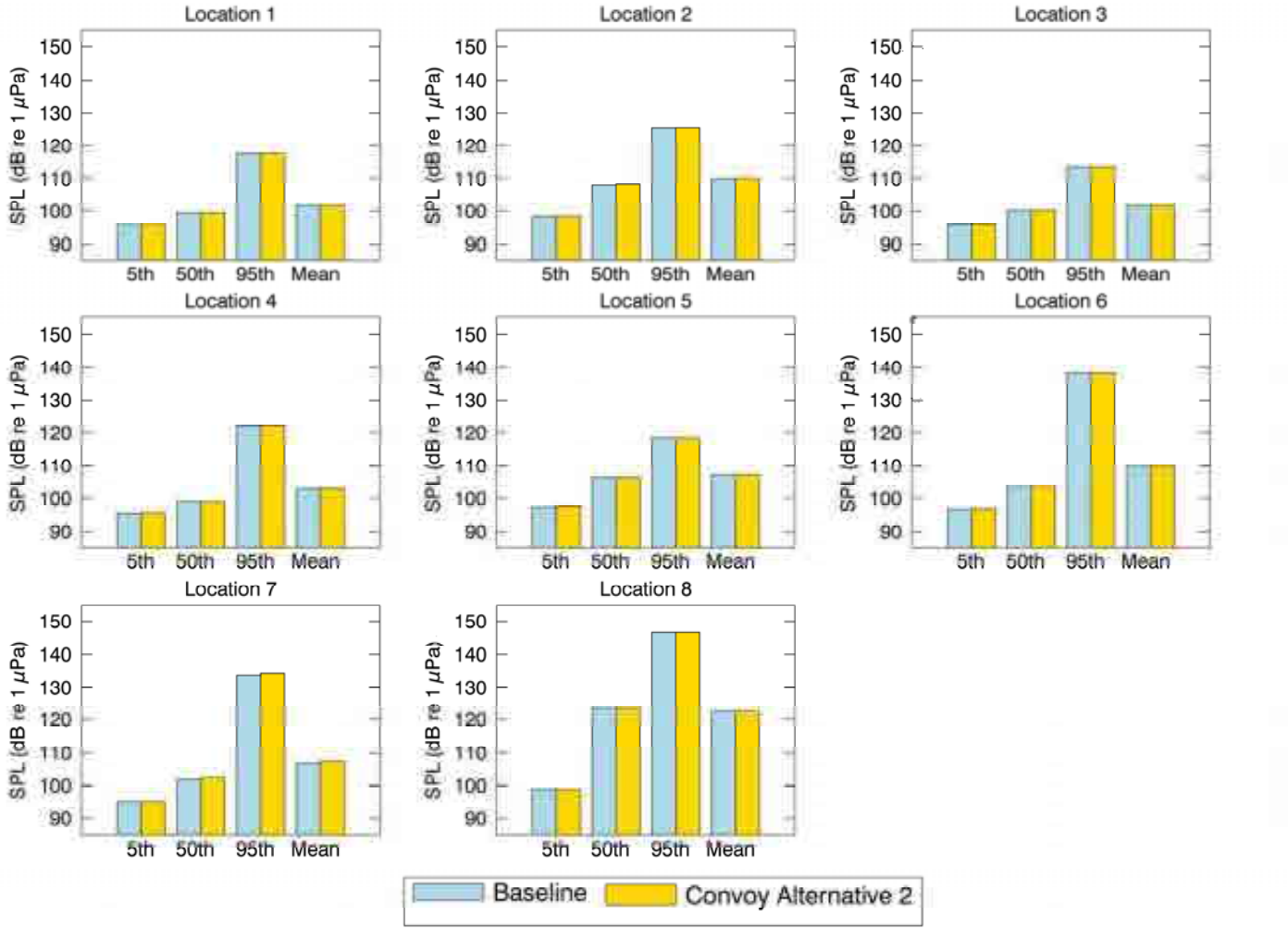

Figure 164. *Convoy Alternative 2, Strait of Georgia*: Histogram representation of the temporal analysis of unweighted received noise levels (dB re 1 µPa). The vertical bars indicate the percentile or mean calculated over a 33-hour period without (baseline) and with mitigation, at the sample locations within the SRKW critical habitat shown in Figure 5.

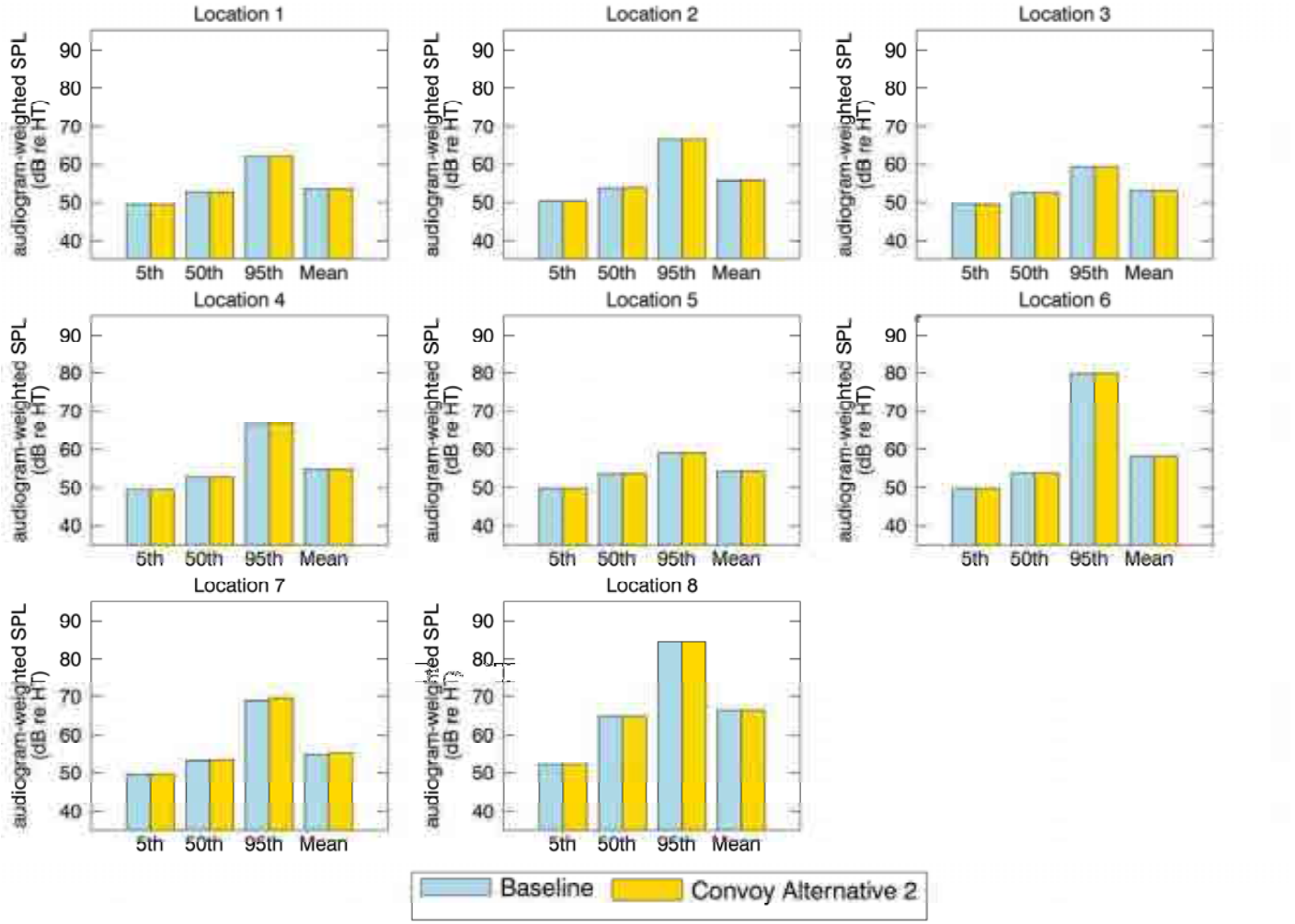

Figure 165. *Convoy Alternative 2, Strait of Georgia*: Histogram representation of the temporal analysis of SRKW audiogram-weighted received noise levels (dB re HT). The vertical bars indicate the percentile or mean calculated over a 33-hour period without (baseline) and with mitigation, at the sample locations within the SRKW critical habitat shown in Figure 5.

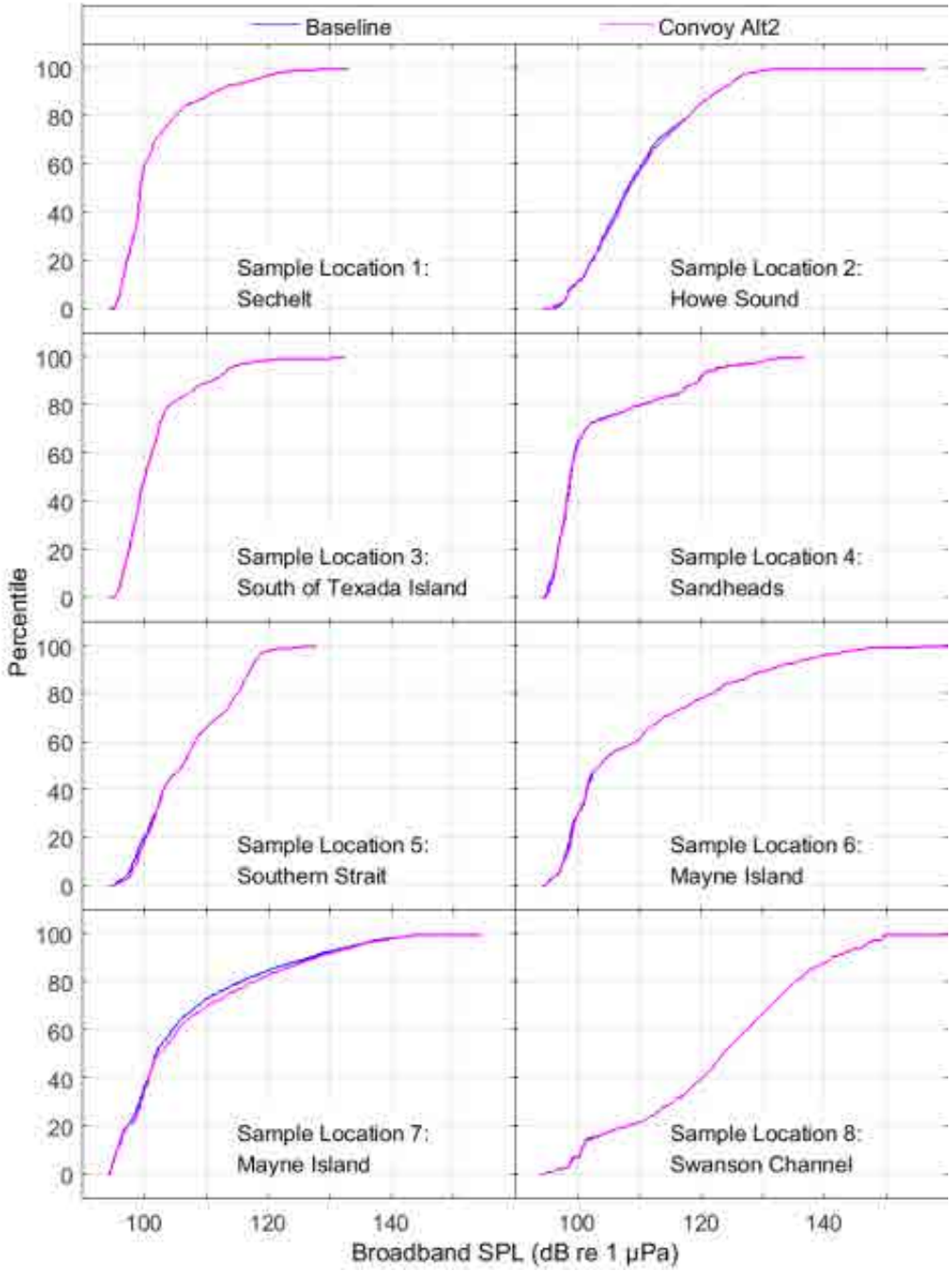

Figure 166. *Convoy Alternative 2, Strait of Georgia:* CDF curves of time-dependent unweighted SPL for baseline and mitigated scenarios at the sample locations shown in Figure 5.

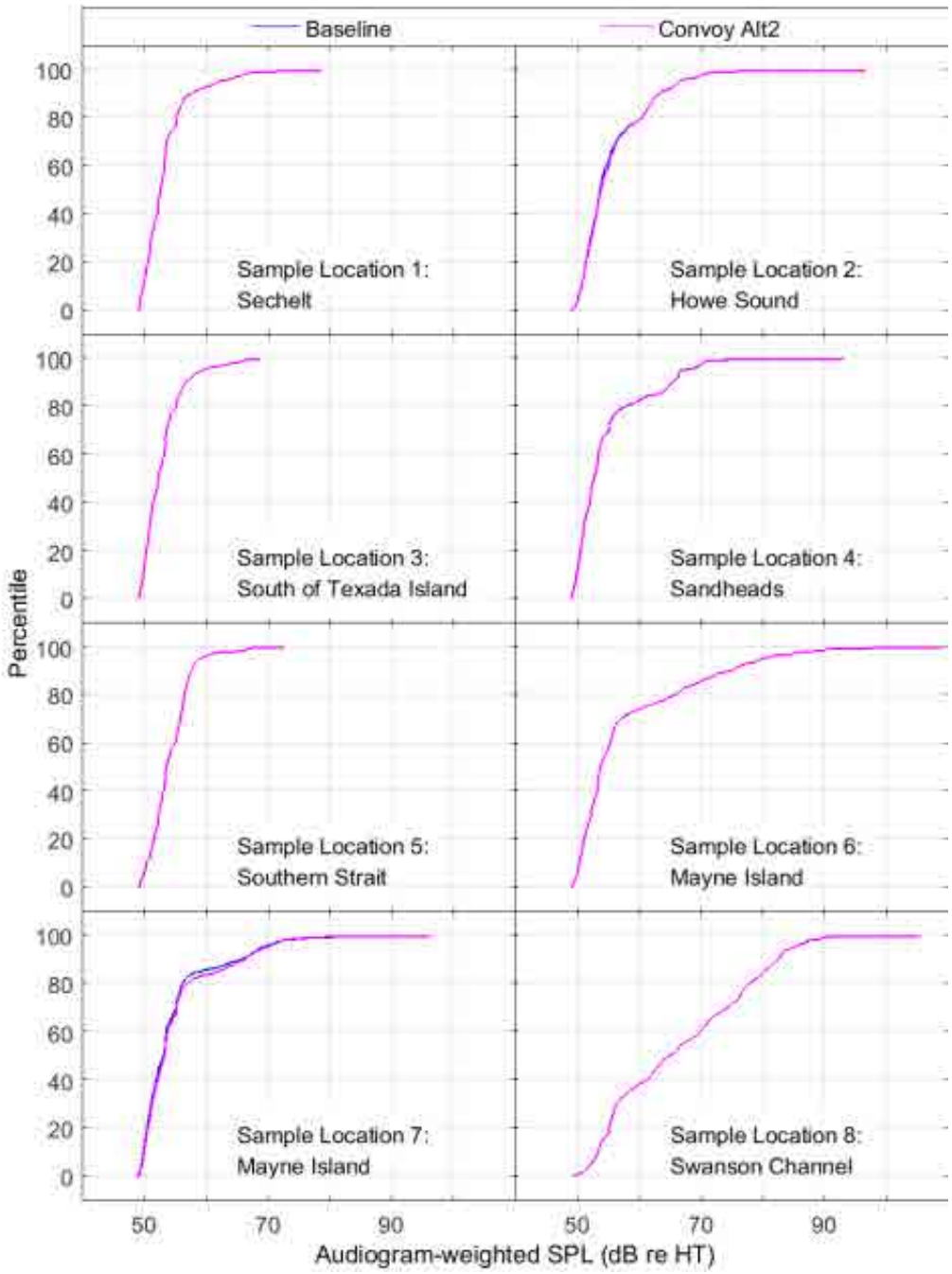

Figure 167. *Convoy Alternative 2, Strait of Georgia:* CDF curves of time-dependent audiogram-weighted SPL for baseline and mitigated scenarios at the sample locations shown in Figure 5.

3.8.2.2. Haro Strait

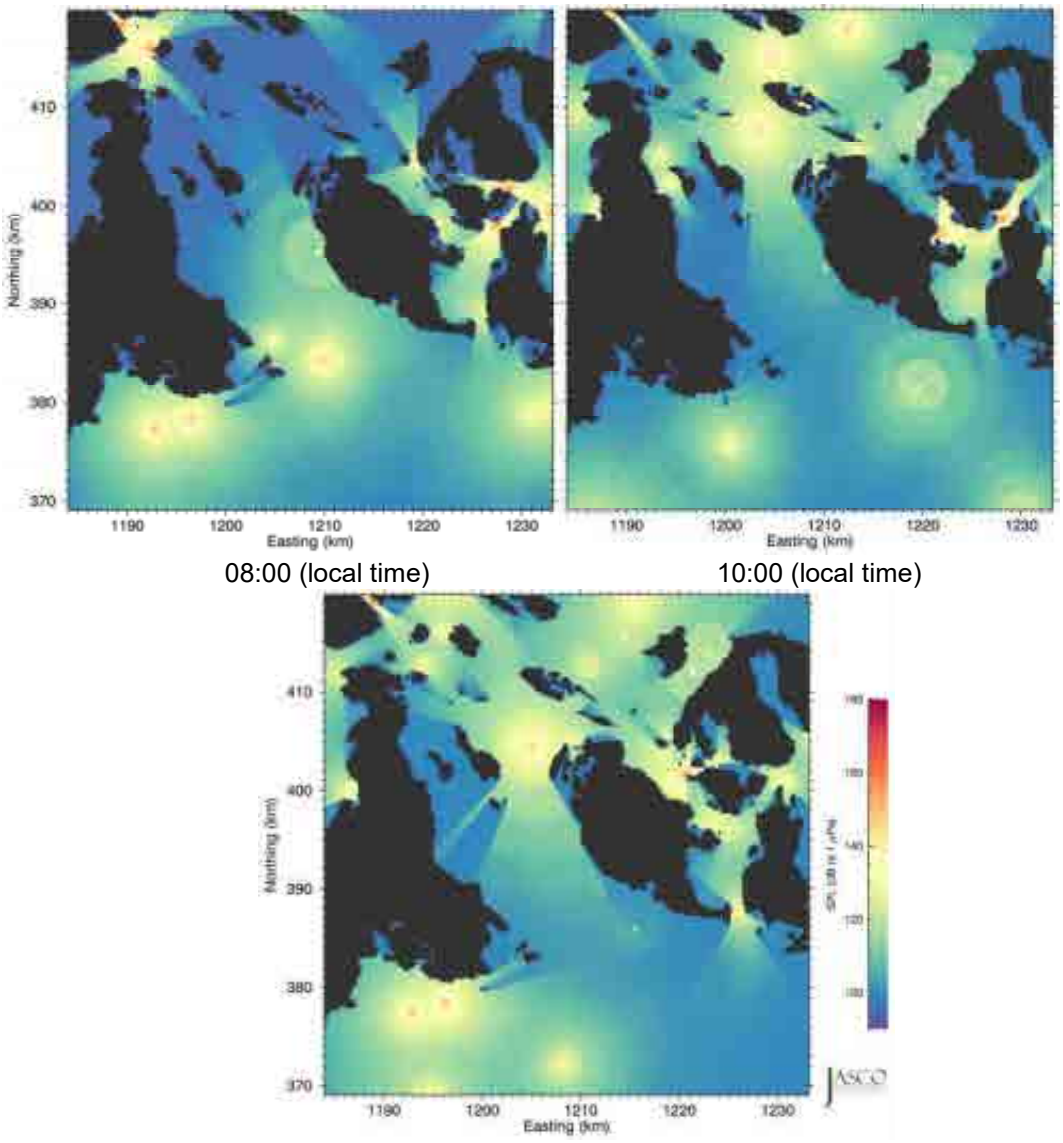

Figure 168. *Convoy Alternative 2, Haro Strait:* Example time snapshots of future mitigated SPL (unweighted with ambient, 10 Hz to 50 kHz) from 08:00 to 12:00 (local time) in 2-hour increments. Easting and northing are BC Albers projected coordinates.

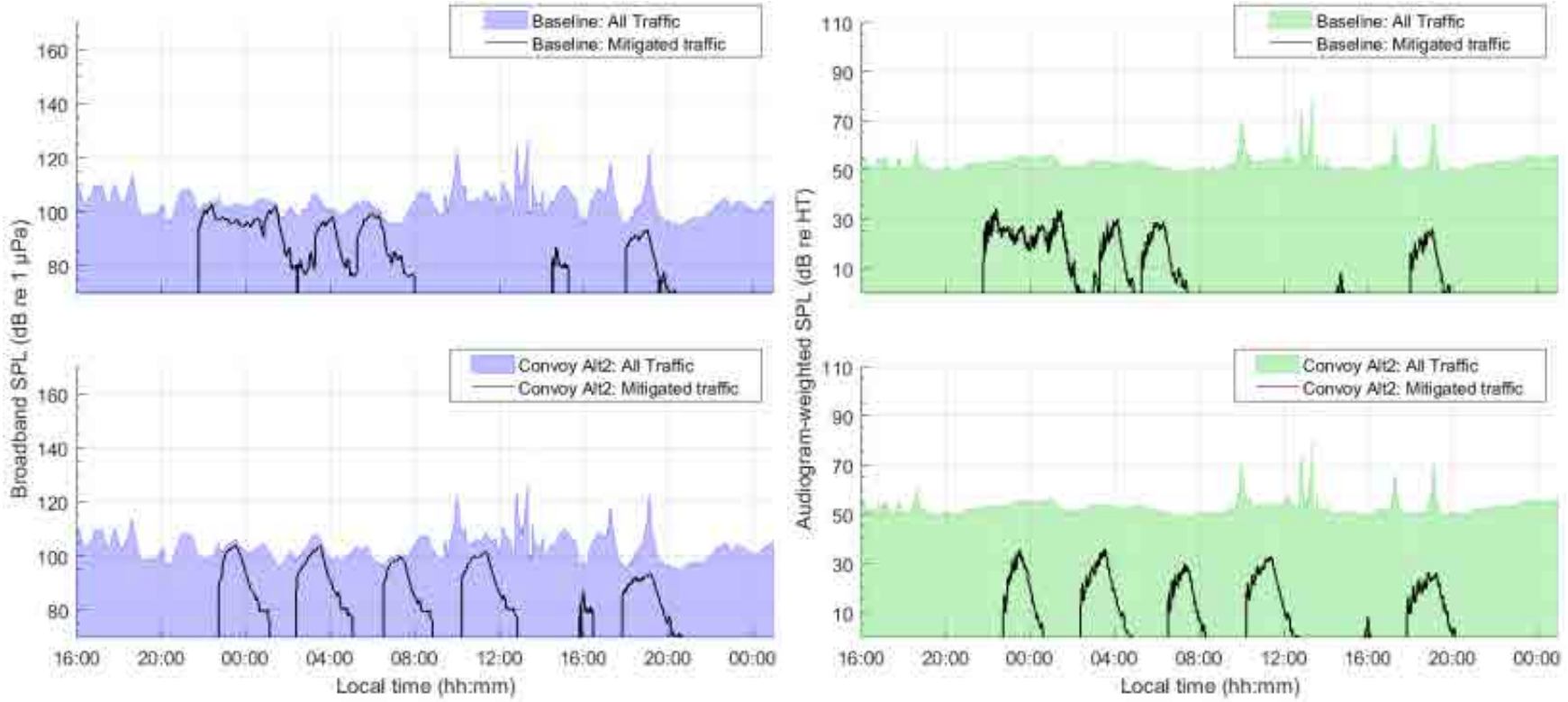

Figure 169. *Convoy Alternative 2, Haro Strait, Sample location 1*: Temporal variability of unweighted (left) and audiogram-weighted (right) received levels for (top) baseline (no convoy) and (bottom) convoy scenarios. The blue and green lines above the shaded area show received levels caused by all traffic and ambient noise. The black lines show received levels caused by commercial traffic only. The receiver location is shown in Figure 6.

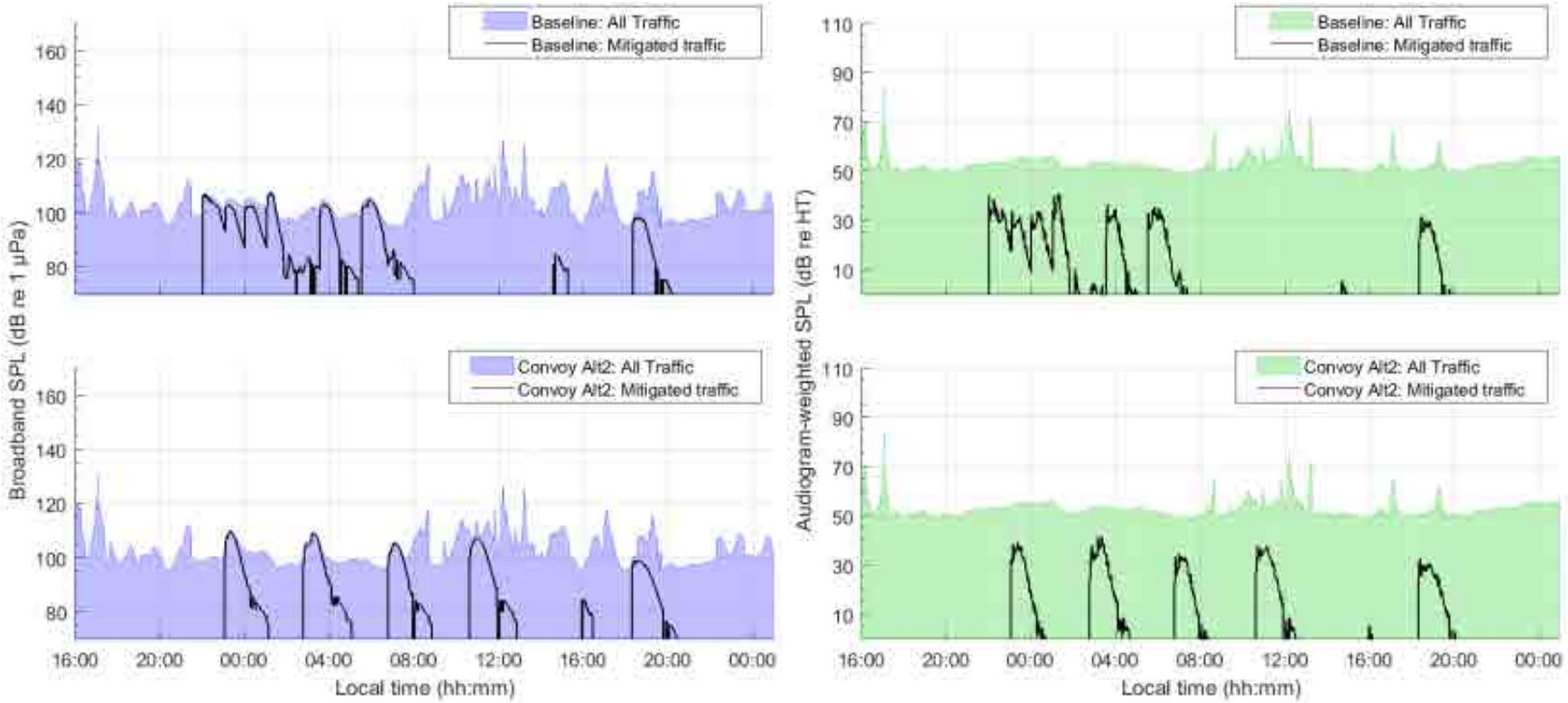

Figure 170. *Convoy Alternative 2, Haro Strait, Sample location 2*: Temporal variability of unweighted (left) and audiogram-weighted (right) received levels for (top) baseline (no convoy) and (bottom) convoy scenarios. The blue and green lines above the shaded area show received levels caused by all traffic and ambient noise. The black lines show received levels caused by commercial traffic only. The receiver location is shown in Figure 6.

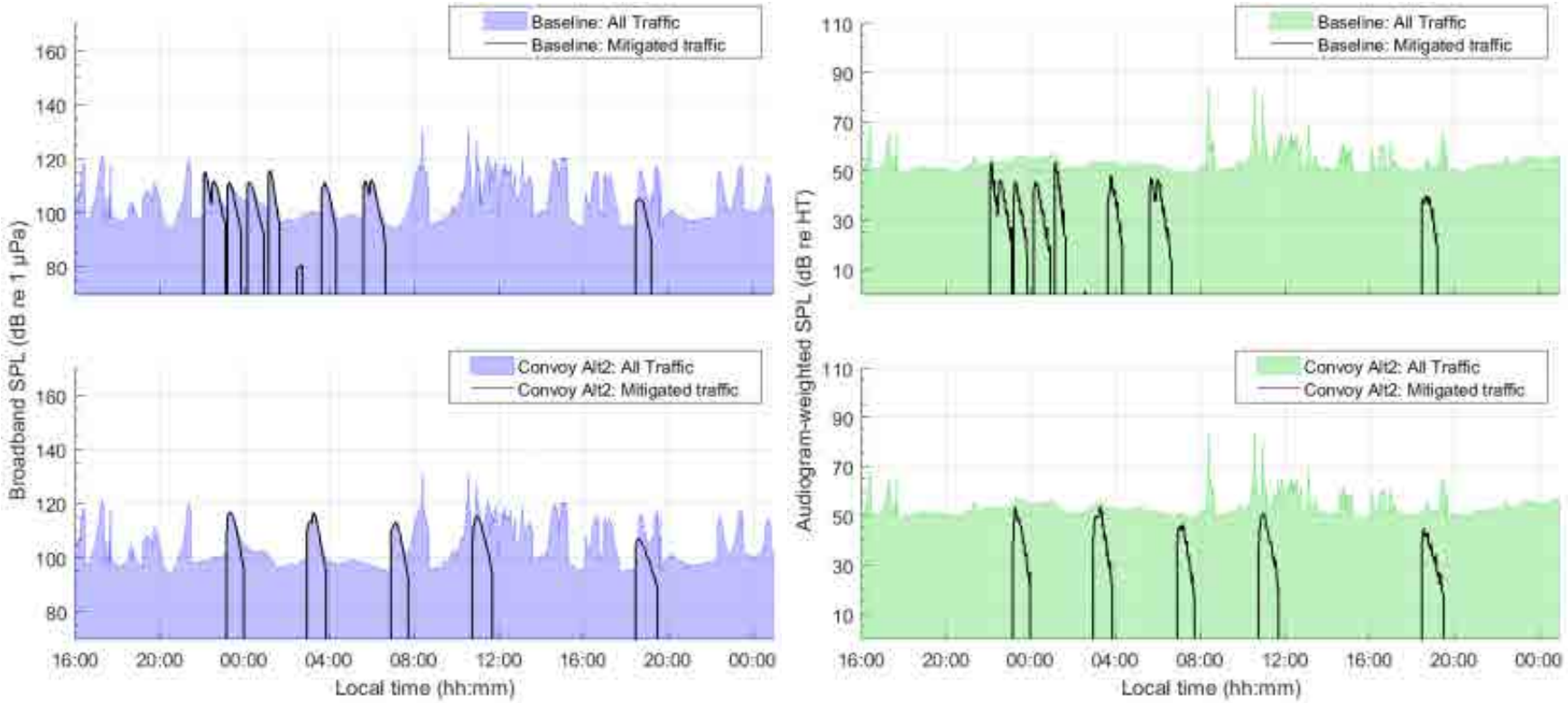

Figure 171. *Convoy Alternative 2, Haro Strait, Sample location 3*: Temporal variability of unweighted (left) and audiogram-weighted (right) received levels for (top) baseline (no convoy) and (bottom) convoy scenarios. The blue and green lines above the shaded area show received levels caused by all traffic and ambient noise. The black lines show received levels caused by commercial traffic only. The receiver location is shown in Figure 6.

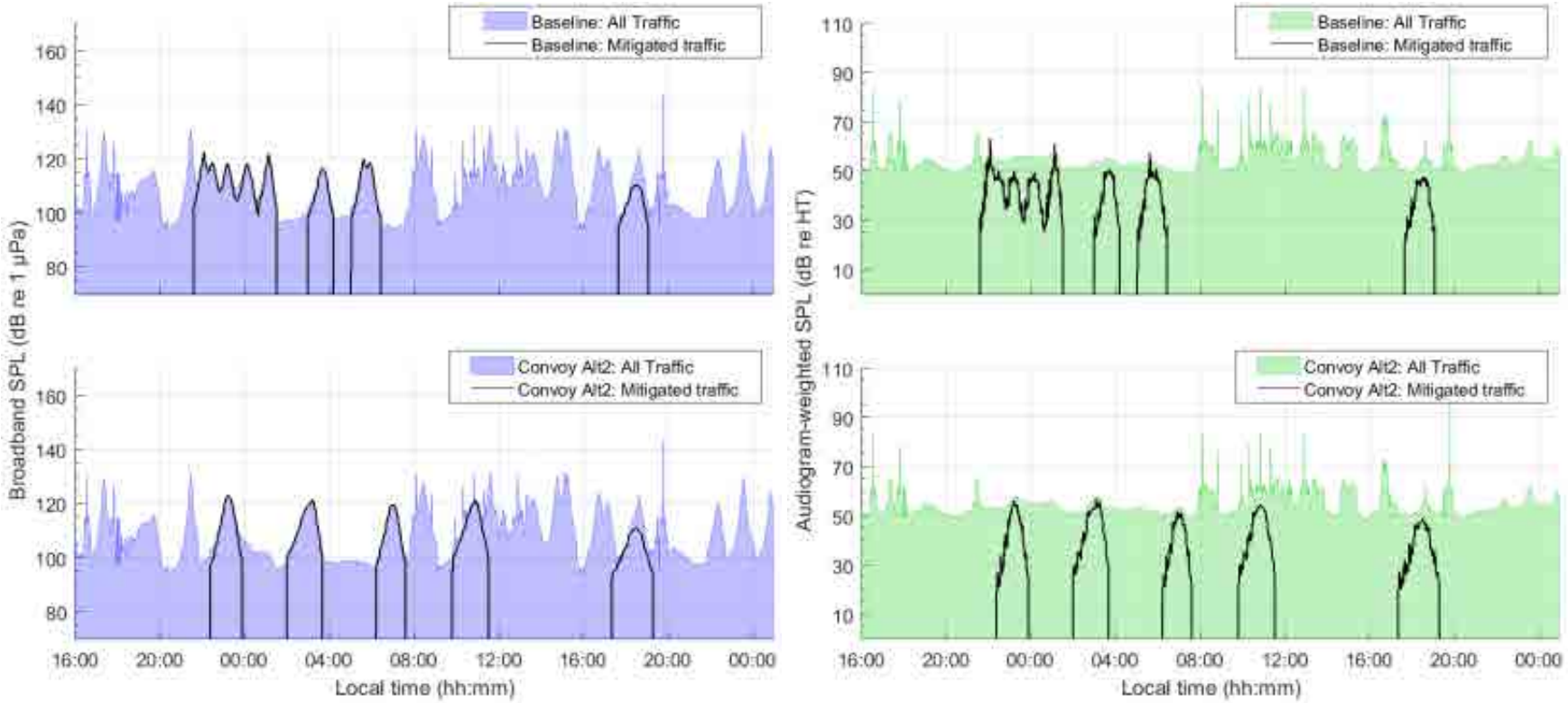

Figure 172. *Convoy Alternative 2, Haro Strait, Sample location 4*: Temporal variability of unweighted (left) and audiogram-weighted (right) received levels for (top) baseline (no convoy) and (bottom) convoy scenarios. The blue and green lines above the shaded area show received levels caused by all traffic and ambient noise. The black lines show received levels caused by commercial traffic only. The receiver location is shown in Figure 6.

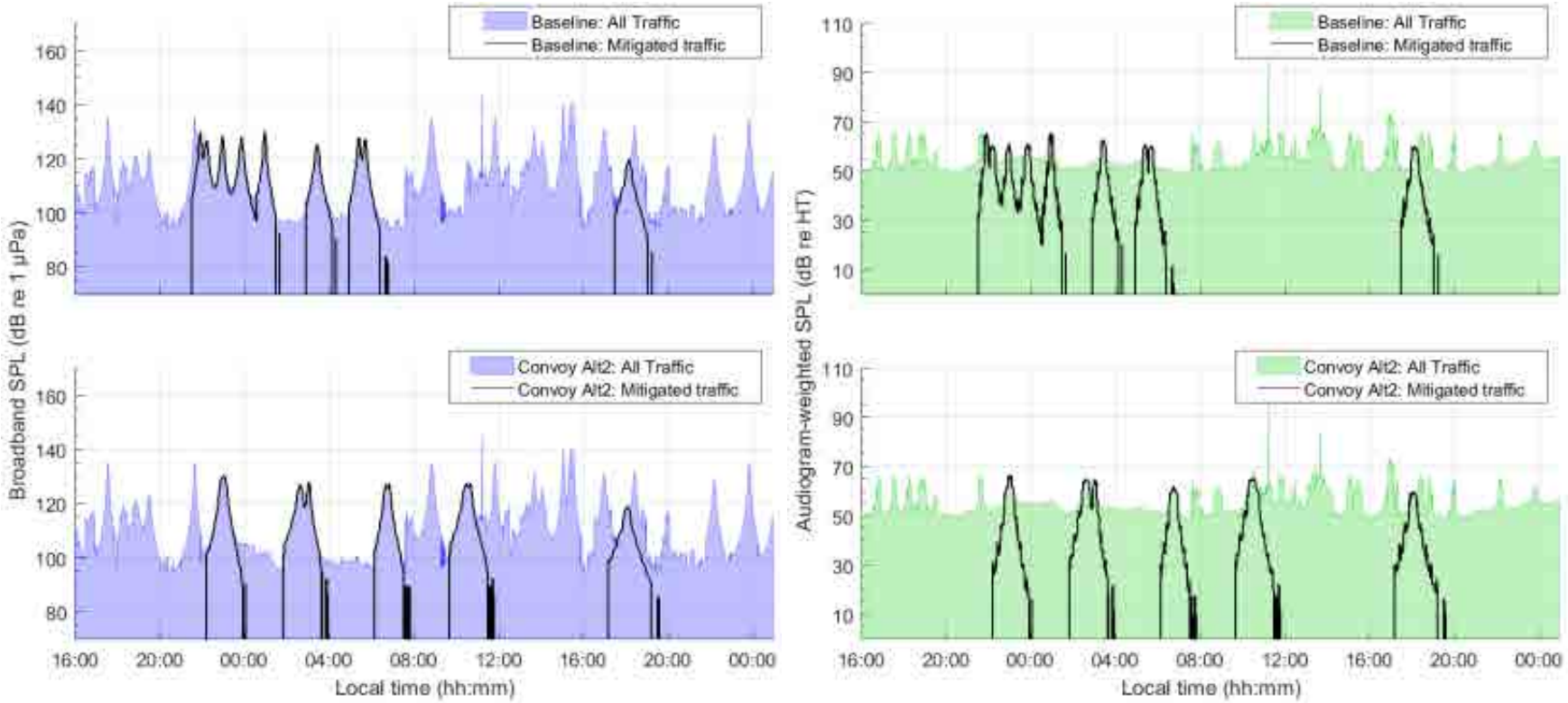

Figure 173. *Convoy Alternative 2, Haro Strait, Sample location 5*: Temporal variability of unweighted (left) and audiogram-weighted (right) received levels for (top) baseline (no convoy) and (bottom) convoy scenarios. The blue and green lines above the shaded area show received levels caused by all traffic and ambient noise. The black lines show received levels caused by commercial traffic only. The receiver location is shown in Figure 6.

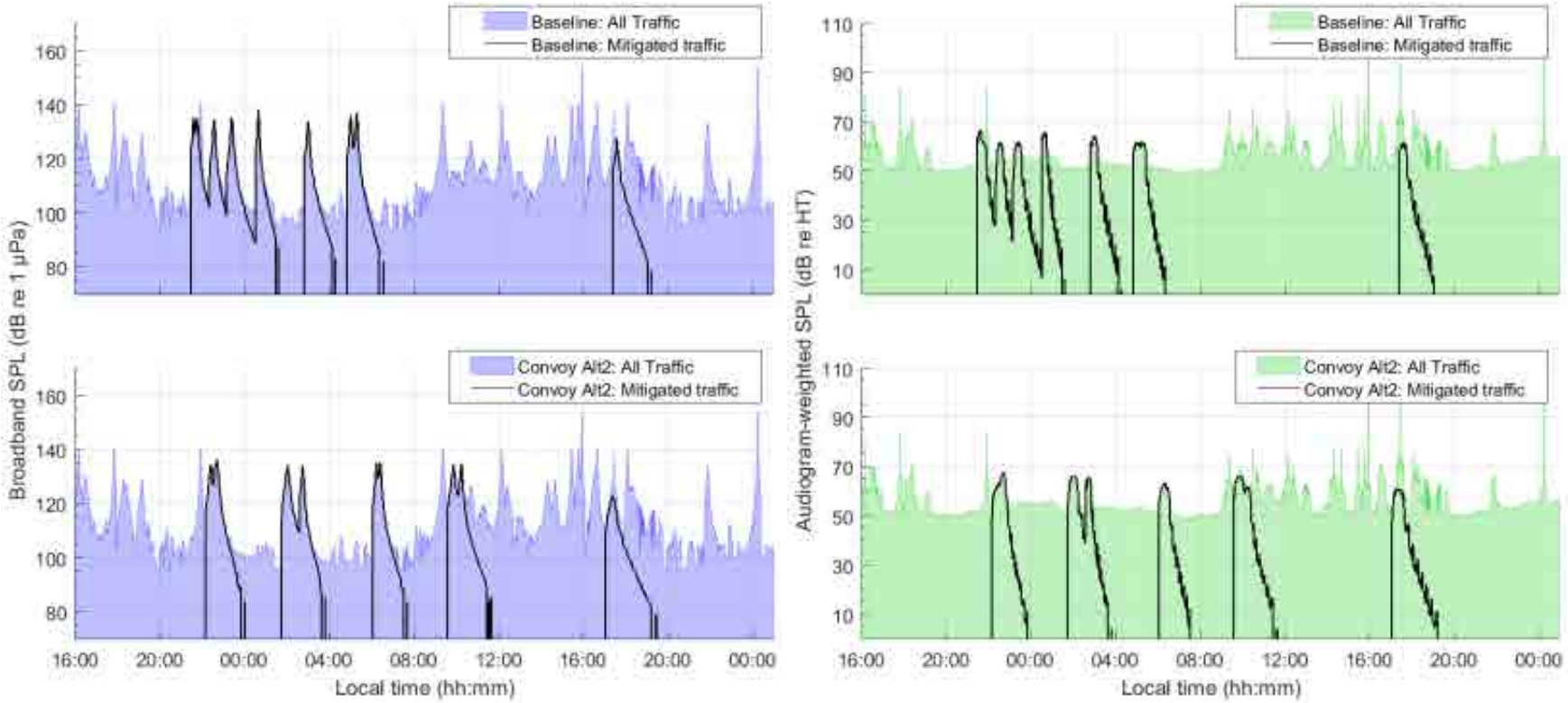

Figure 174. *Convoy Alternative 2, Haro Strait, Sample location 6*: Temporal variability of unweighted (left) and audiogram-weighted (right) received levels for (top) baseline (no convoy) and (bottom) convoy scenarios. The blue and green lines above the shaded area show received levels caused by all traffic and ambient noise. The black lines show received levels caused by commercial traffic only. The receiver location is shown in Figure 6.

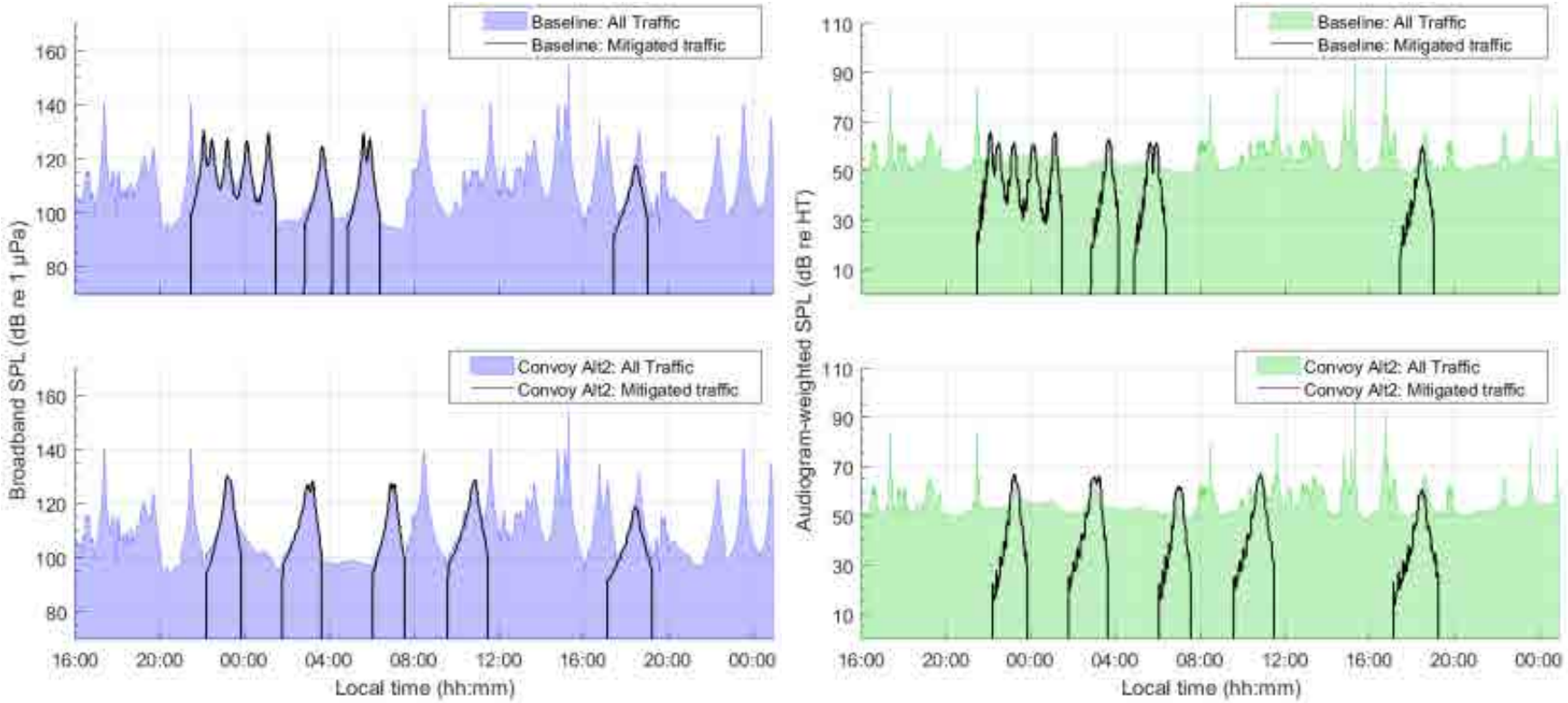

Figure 175. *Convoy Alternative 2, Haro Strait, Sample location 7*: Temporal variability of unweighted (left) and audiogram-weighted (right) received levels for (top) baseline (no convoy) and (bottom) convoy scenarios. The blue and green lines above the shaded area show received levels caused by all traffic and ambient noise. The black lines show received levels caused by commercial traffic only. The receiver location is shown in Figure 6.

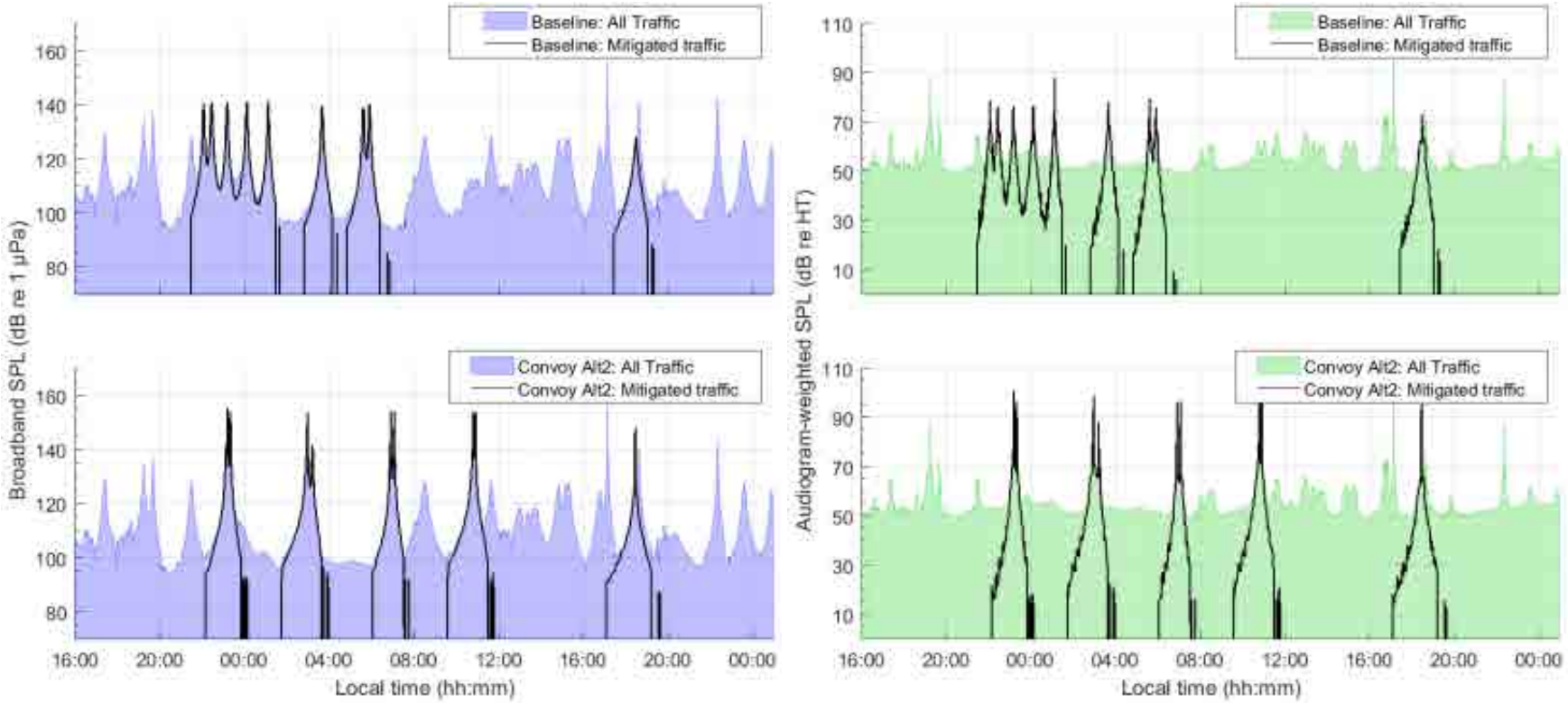

Figure 176. *Convoy Alternative 2, Haro Strait, Sample location 8*: Temporal variability of unweighted (left) and audiogram-weighted (right) received levels for (top) baseline (no convoy) and (bottom) convoy scenarios. The blue and green lines above the shaded area show received levels caused by all traffic and ambient noise. The black lines show received levels caused by commercial traffic only. The receiver location is shown in Figure 6.

Table 65. *Convoy Alternative 2, Haro Strait:* Temporal analysis of unweighted received noise levels (dB re 1 µPa), difference in received noise levels (dB), and difference acoustic intensity (%). The values indicate the percentile or mean calculated over a 33-hour period without (Baseline) and with mitigation (Convoy), at the sample locations within the SRKW critical habitat shown in Figure 6.

Sample location	Scenario	Temporal analysis of noise level (dB re 1 µPa), difference in noise levels (dB), and difference in acoustic intensity (%)			
		5th	50th	95th	Mean
1	Baseline	96.2	103.0	110.4	103.2 ±4.7
	Convoy	96.7	102.9	110.4	103.2 ±4.7
	Difference	**+0.5 (+12.3%)**	**−0.1 (−3.1%)**	**0.0 (0.0%)**	**0.0 (0.0%)**
2	Baseline	96.0	102.4	113.5	103.2 ±5.5
	Convoy	96.3	101.6	113.5	103.1 ±5.6
	Difference	**+0.3 (+6.8%)**	**−0.8 (−17.1%)**	**0.0 (0.0%)**	**0.0 (0.0%)**
3	Baseline	95.5	102.4	117.7	104.4 ±7.2
	Convoy	95.8	101.5	117.9	104.2 ±7.4
	Difference	**+0.3 (+6.5%)**	**−1.0 (−19.8%)**	**+0.2 (+4.0%)**	**−0.2 (−5.3%)**
4	Baseline	95.6	108.7	124.2	108.8 ±9.0
	Convoy	96.8	107.4	124.2	108.7 ±9.0
	Difference	**+1.2 (+31.8%)**	**−1.3 (−26.7%)**	**0.0 (0.0%)**	**−0.2 (−3.5%)**
5	Baseline	96.1	109.7	128.1	110.0 ±10.3
	Convoy	96.9	109.4	128.3	110.3 ±10.2
	Difference	**+0.8 (+21.1%)**	**−0.3 (−5.8%)**	**+0.2 (+5.6%)**	**+0.3 (+6.0%)**
6	Baseline	96.6	110.5	132.8	112.0 ±11.2
	Convoy	97.5	110.3	133.0	112.3 ±11.2
	Difference	**+0.9 (+22.8%)**	**−0.1 (−3.3%)**	**+0.2 (+4.1%)**	**+0.3 (+7.1%)**
7	Baseline	96.0	109.5	128.3	110.4 ±10.3
	Convoy	97.5	108.1	128.6	110.3 ±10.2
	Difference	**+1.5 (+41.4%)**	**−1.4 (−26.8%)**	**+0.3 (+7.9%)**	**−0.1 (−2.1%)**
8	Baseline	96.0	108.7	128.6	110.1 ±10.4
	Convoy	97.5	107.9	129.8	110.2 ±10.7
	Difference	**+1.4 (+39.4%)**	**−0.8 (−16.2%)**	**+1.2 (+32.1%)**	**+0.1 (+2.5%)**

Table 66. *Convoy Alternative 2, Haro Strait*: Temporal analysis of SRKW audiogram-weighted received noise levels (dB re HT), difference in received noise levels (dB), and difference acoustic intensity (%). The values indicate the percentile or mean calculated over a 33-hour period without (Baseline) and with mitigation (Convoy), at the sample locations within the SRKW critical habitat shown in Figure 6.

Sample location	Scenario	Temporal analysis of noise level (dB re HT), difference in noise levels (dB), and difference in acoustic intensity (%)			
		5th	50th	95th	Mean
1	Baseline	49.7	52.5	56.6	52.9 ±3.0
	Convoy	49.7	52.5	56.6	52.9 ±3.0
	Difference	**0.0 (0.0%)**	**0.0 (0.0%)**	**0.0 (0.0%)**	**0.0 (0.0%)**
2	Baseline	49.6	52.4	59.5	53.1 ±3.5
	Convoy	49.6	52.4	59.5	53.1 ±3.5
	Difference	**0.0 (0.0%)**	**0.0 (0.0%)**	**0.0 (0.0%)**	**0.0 (0.0%)**
3	Baseline	49.6	52.7	61.6	53.6 ±3.8
	Convoy	49.8	52.6	61.6	53.6 ±3.8
	Difference	**+0.1 (+3.2%)**	**0.0 (0.0%)**	**0.0 (0.0%)**	**0.0 (0.0%)**
4	Baseline	49.8	53.5	63.5	54.8 ±4.8
	Convoy	50.0	53.4	63.5	54.8 ±4.8
	Difference	**+0.2 (+5.2%)**	**−0.2 (−3.5%)**	**0.0 (0.0%)**	**0.0 (0.0%)**
5	Baseline	49.8	53.6	65.2	55.4 ±5.1
	Convoy	49.9	53.6	65.4	55.6 ±5.2
	Difference	**+0.1 (+2.5%)**	**0.0 (0.0%)**	**+0.2 (+5.6%)**	**+0.2 (+4.4%)**
6	Baseline	50.0	54.6	66.7	56.4 ±6.0
	Convoy	50.0	55.0	67.3	56.6 ±6.1
	Difference	**0.0 (0.0%)**	**+0.4 (+8.6%)**	**+0.7 (+17.3%)**	**+0.2 (+5.6%)**
7	Baseline	49.8	53.9	64.8	55.6 ±5.3
	Convoy	50.1	53.6	65.4	55.6 ±5.4
	Difference	**+0.3 (+7.3%)**	**−0.2 (−5.3%)**	**+0.6 (+14.4%)**	**0.0 (0.0%)**
8	Baseline	49.9	53.7	66.3	55.4 ±5.5
	Convoy	50.3	53.5	67.8	55.7 ±6.4
	Difference	**+0.4 (+8.5%)**	**−0.1 (−3.3%)**	**+1.5 (+41.4%)**	**+0.3 (+7.1%)**

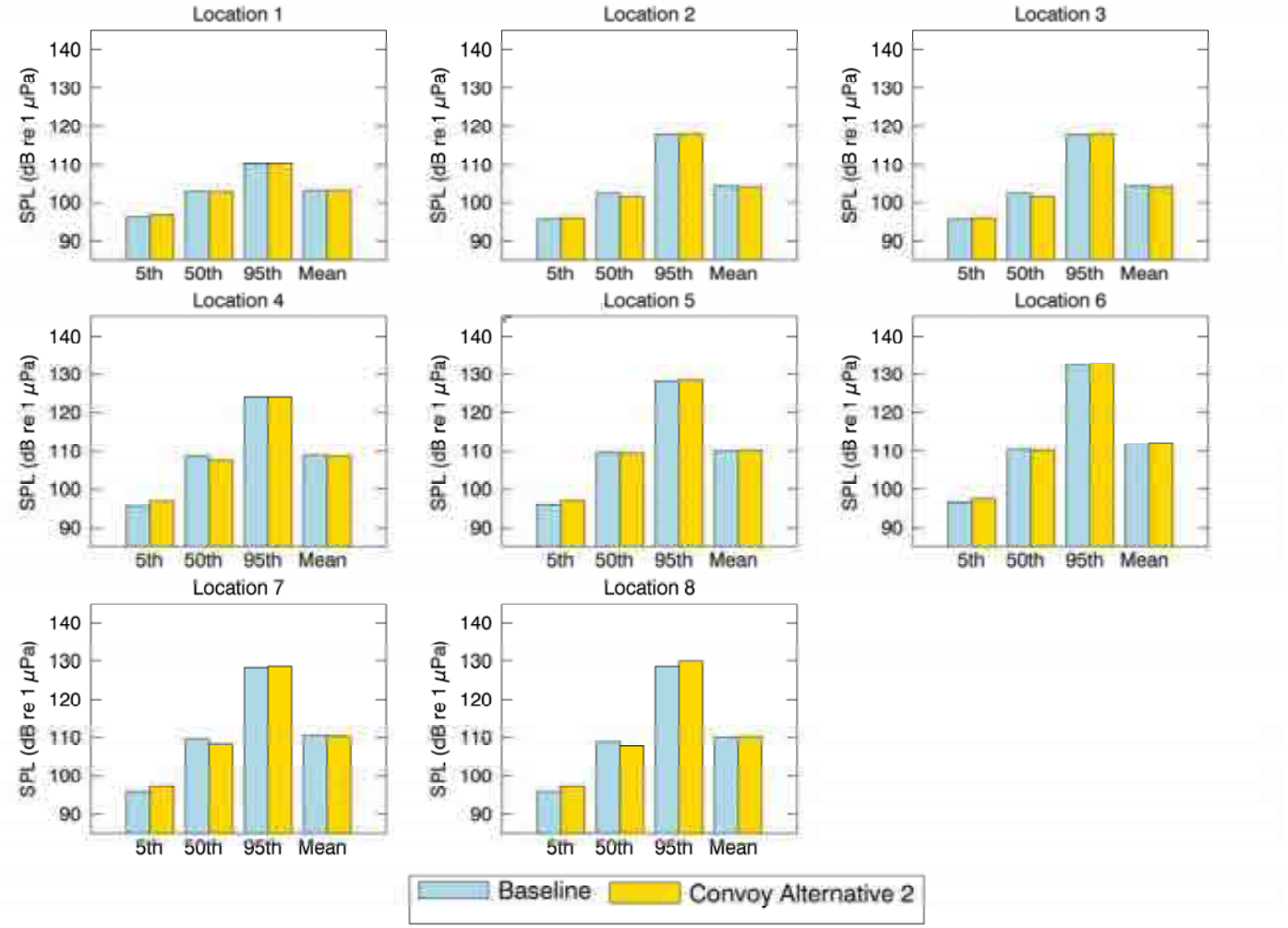

Figure 177. *Convoy Alternative 2, Haro Strait*: Histogram representation of the temporal analysis of unweighted received noise levels (dB re 1 µPa). The vertical bars indicate the percentile or mean calculated over a 33-hour period without (baseline) and with mitigation, at the sample locations within the SRKW critical habitat shown in Figure 6.

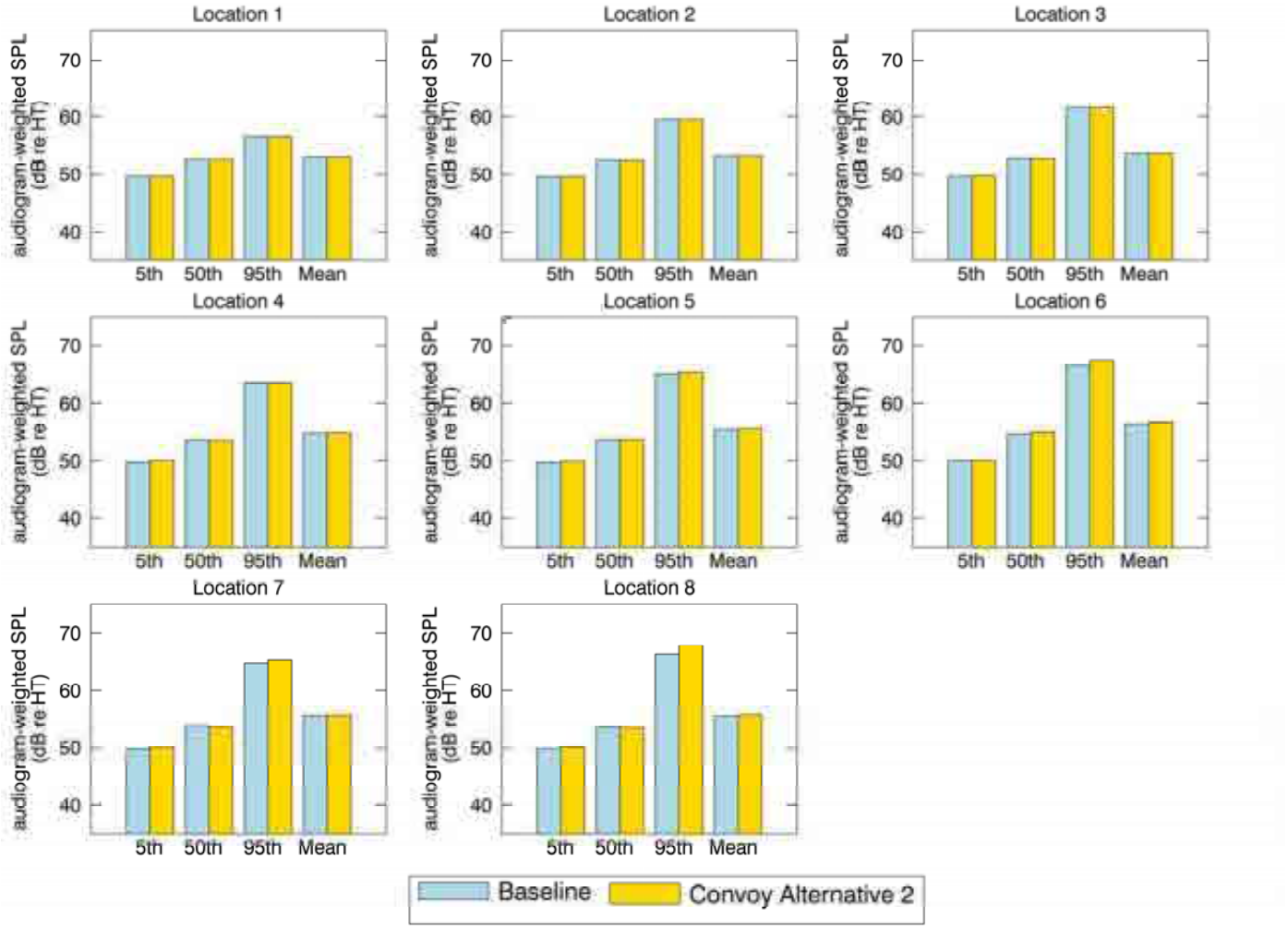

Figure 178. *Convoy Alternative 2, Haro Strait*: Histogram representation of the temporal analysis of SRKW audiogram-weighted received noise levels (dB re HT). The vertical bars indicate the percentile or mean calculated over a 33-hour period without (baseline) and with mitigation, at the sample locations within the SRKW critical habitat shown in Figure 6.

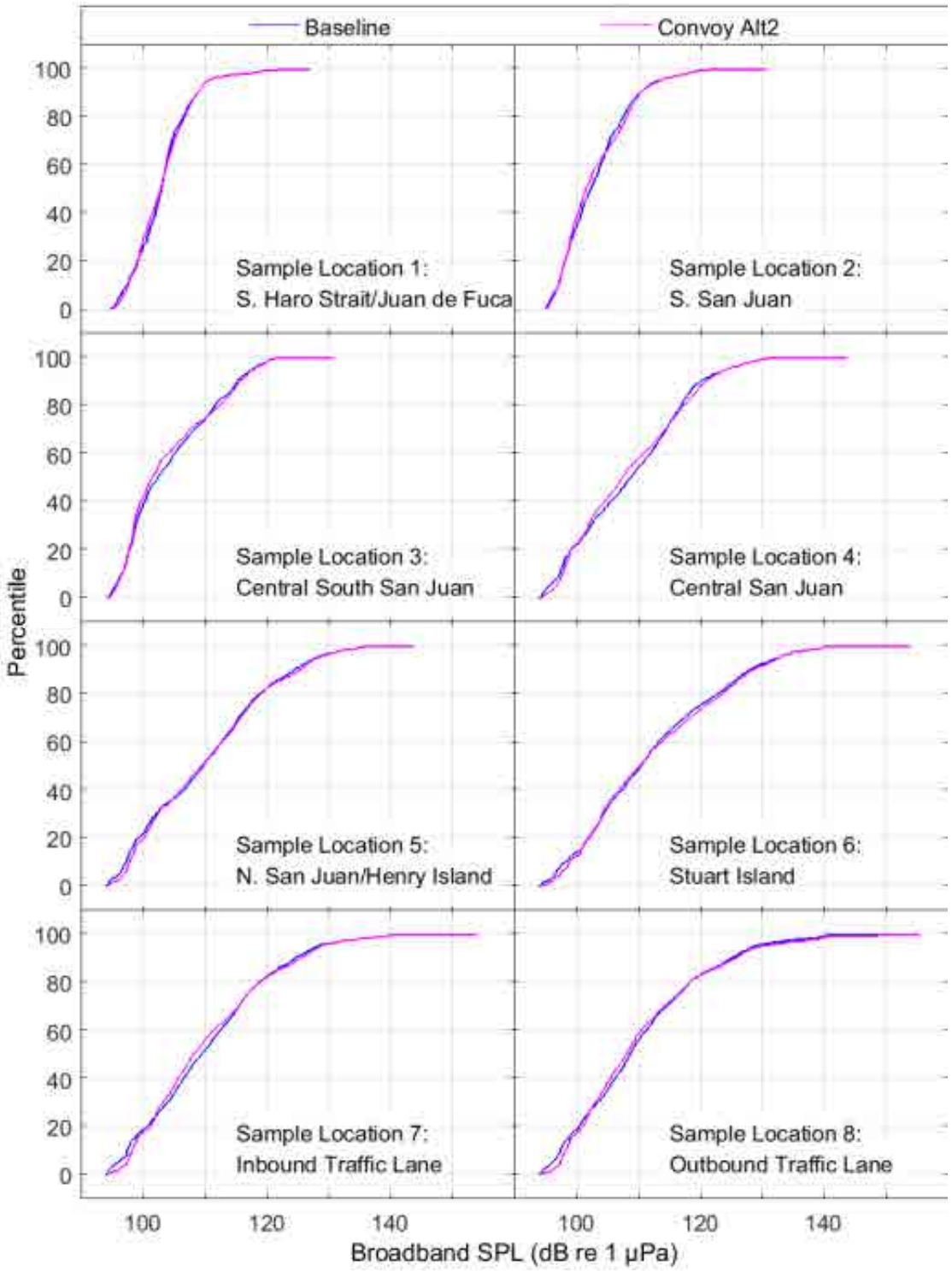

Figure 179. *Convoy Alternative 2, Haro Strait*: CDF curves of time-dependent unweighted SPL for baseline and mitigated scenarios at the sample locations shown in Figure 6.

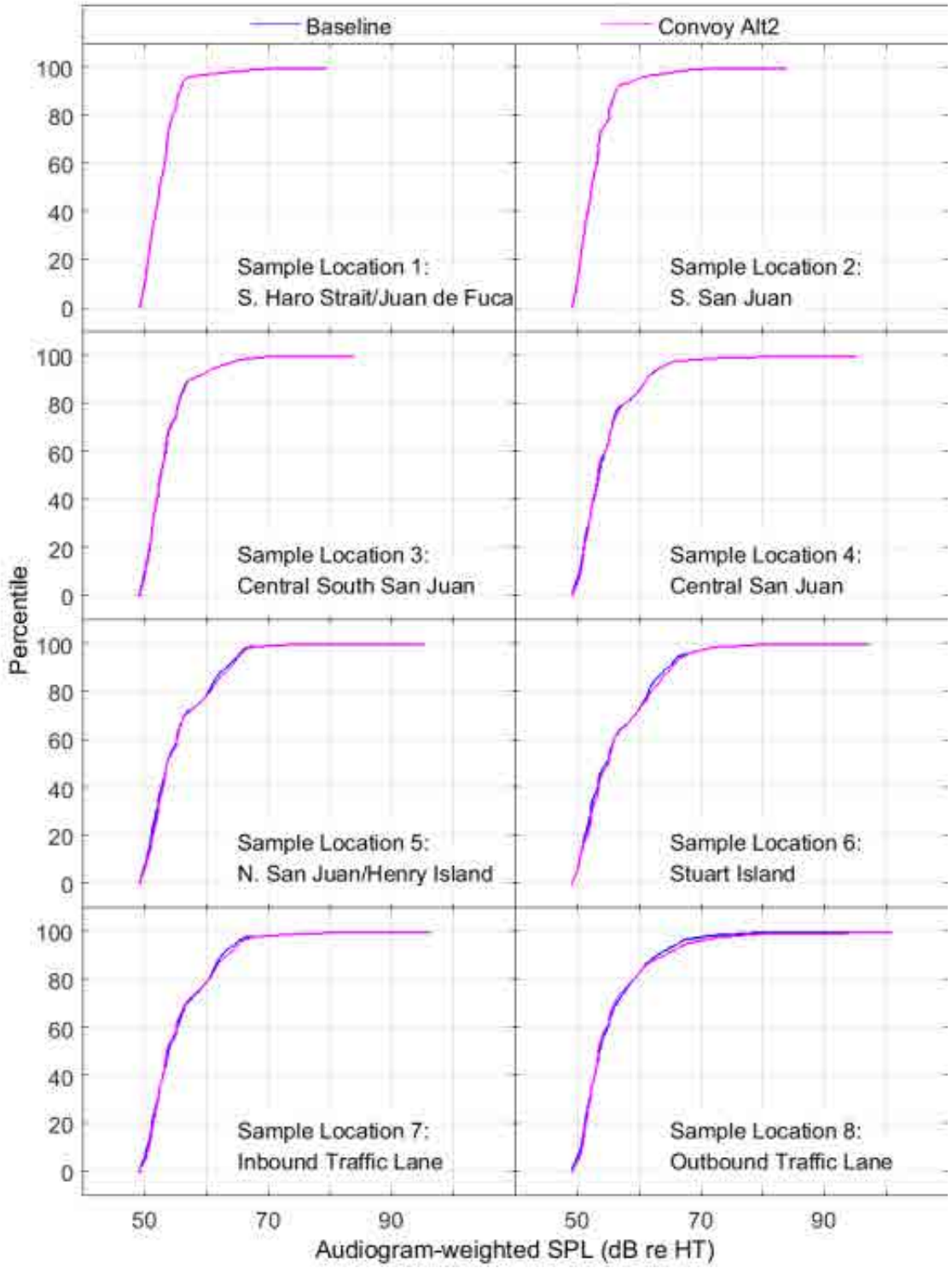

Figure 180. *Convoy Alternative 2, Haro Strait*: CDF curves of time-dependent audiogram-weighted SPL for baseline and mitigated scenarios at the sample locations shown in Figure 6.

3.8.2.3. Juan de Fuca Strait

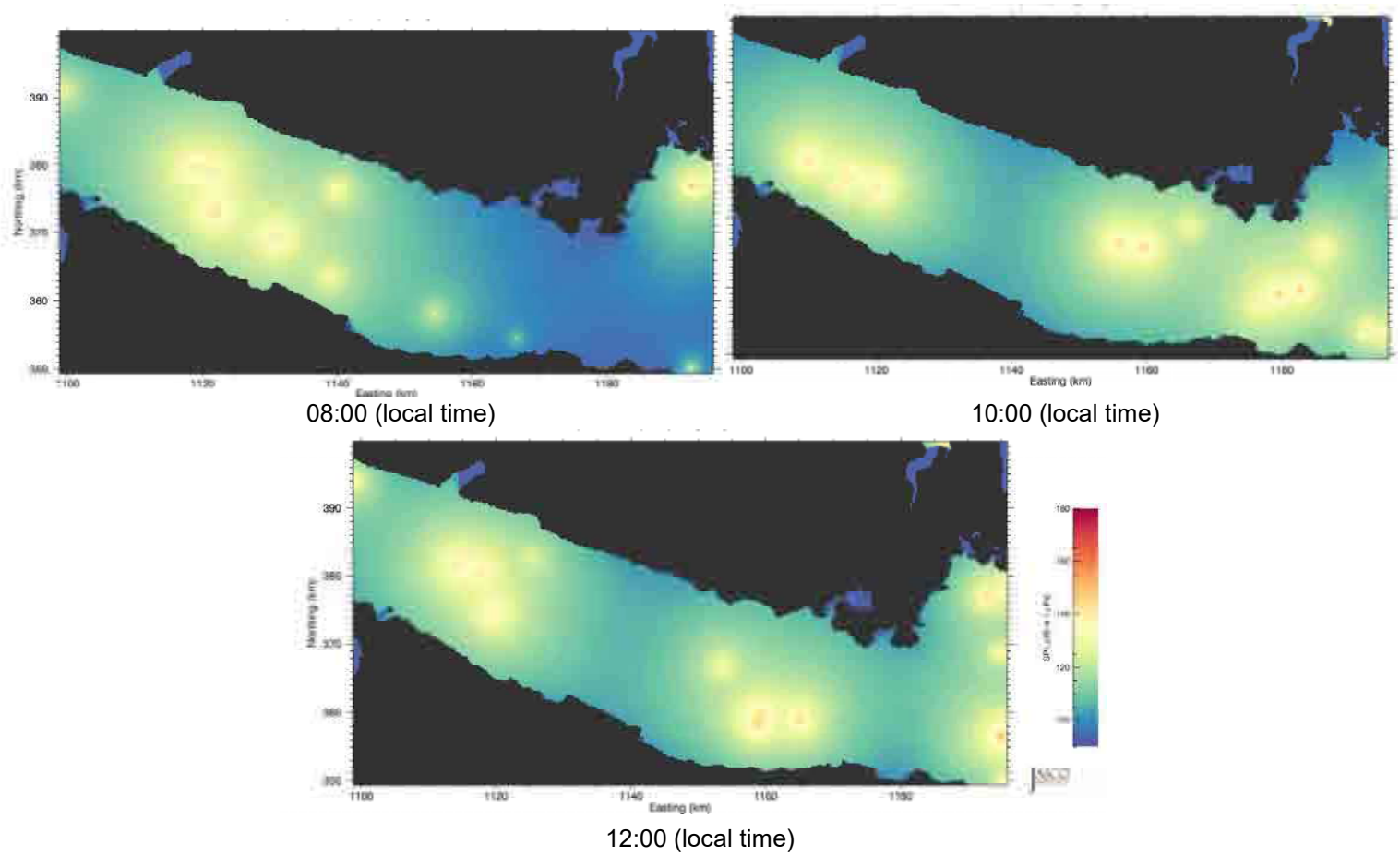

Figure 181. *Convoy Alternative 2, Juan de Fuca Strait:* Example time snapshots of future mitigated SPL (unweighted with ambient, 10 Hz to 50 kHz) from 08:00 to 12:00 (local time) in 2-hour increments. Easting and northing are BC Albers projected coordinates.

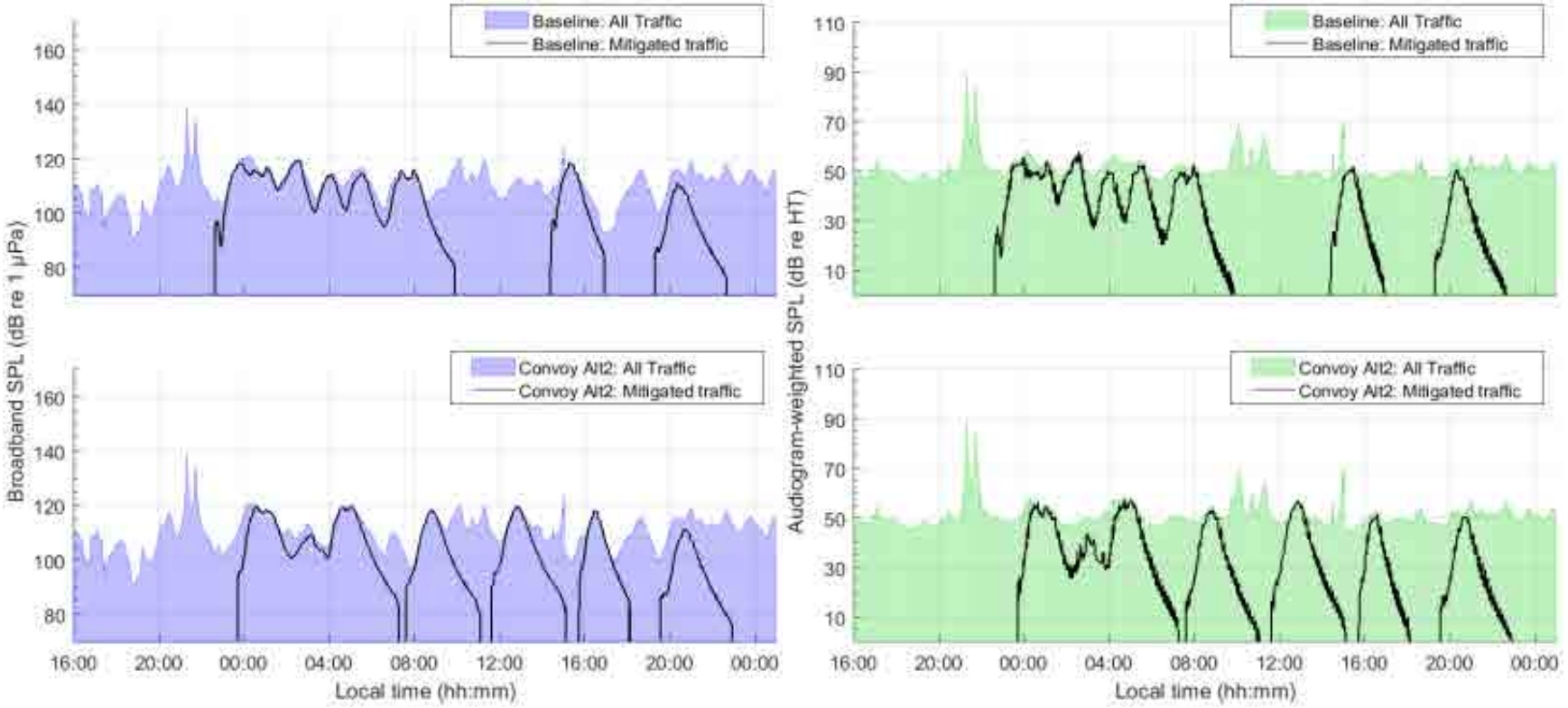

Figure 182. *Convoy Alternative 2, Juan de Fuca Strait, Sample location 1*: Temporal variability of unweighted (left) and audiogram-weighted (right) received levels for (top) baseline (no convoy) and (bottom) convoy scenarios. The blue and green lines above the shaded area show received levels caused by all traffic and ambient noise. The black lines show received levels caused by commercial traffic only. The receiver location is shown in Figure 7.

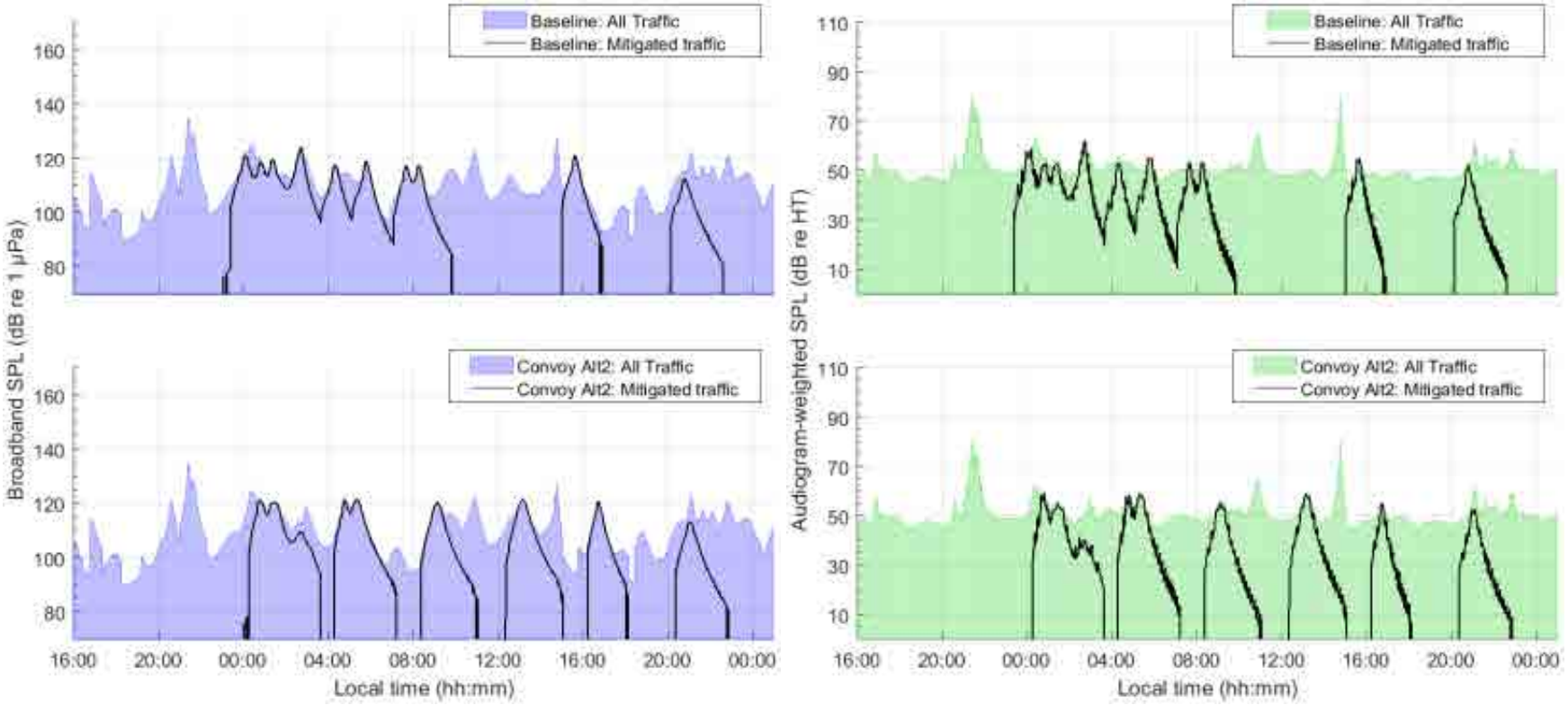

Figure 183. *Convoy Alternative 2, Juan de Fuca Strait, Sample location 2*: Temporal variability of unweighted (left) and audiogram-weighted (right) received levels for (top) baseline (no convoy) and (bottom) convoy scenarios. The blue and green lines above the shaded area show received levels caused by all traffic and ambient noise. The black lines show received levels caused by commercial traffic only. The receiver location is shown in Figure 7.

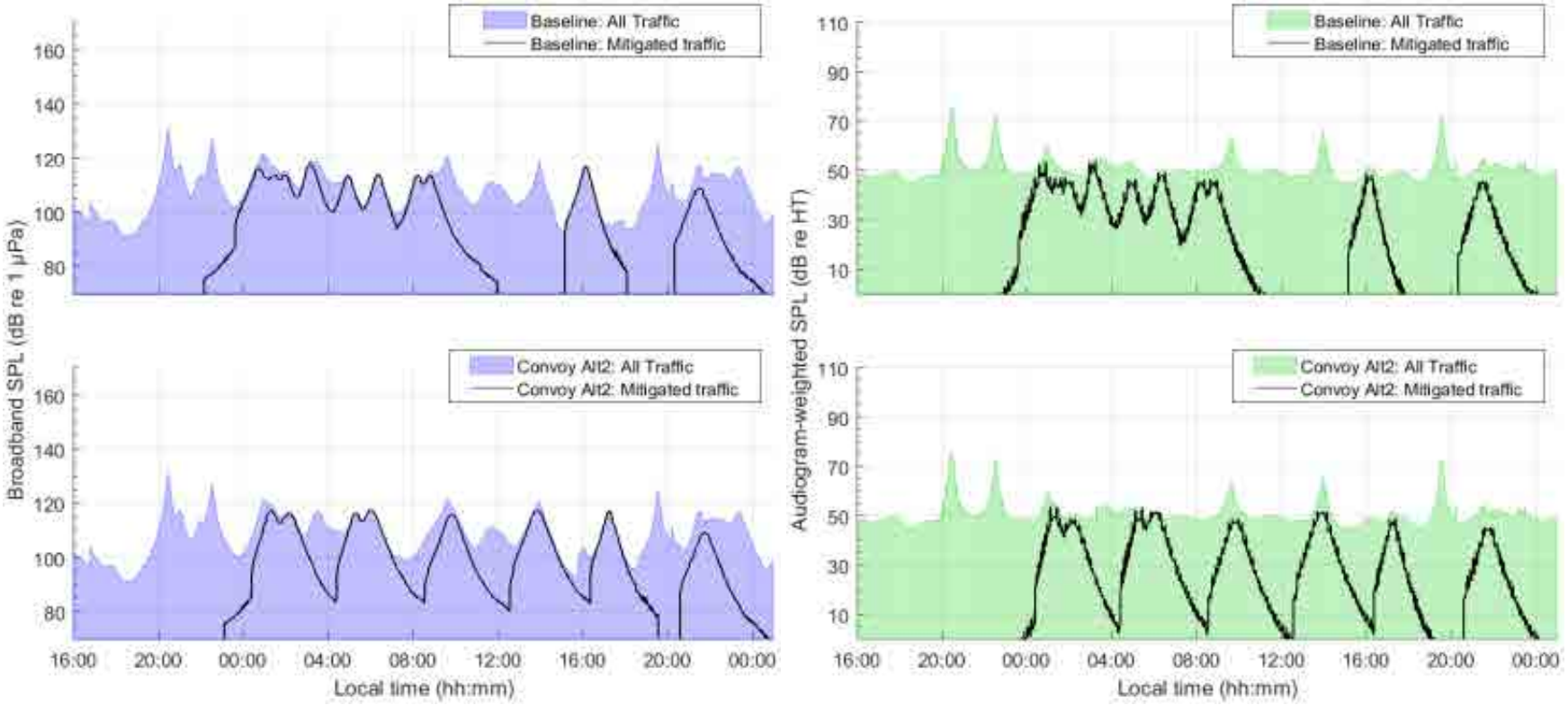

Figure 184. *Convoy Alternative 2, Juan de Fuca Strait, Sample location 3*: Temporal variability of unweighted (left) and audiogram-weighted (right) received levels for (top) baseline (no convoy) and (bottom) convoy scenarios. The blue and green lines above the shaded area show received levels caused by all traffic and ambient noise. The black lines show received levels caused by commercial traffic only. The receiver location is shown in Figure 7.

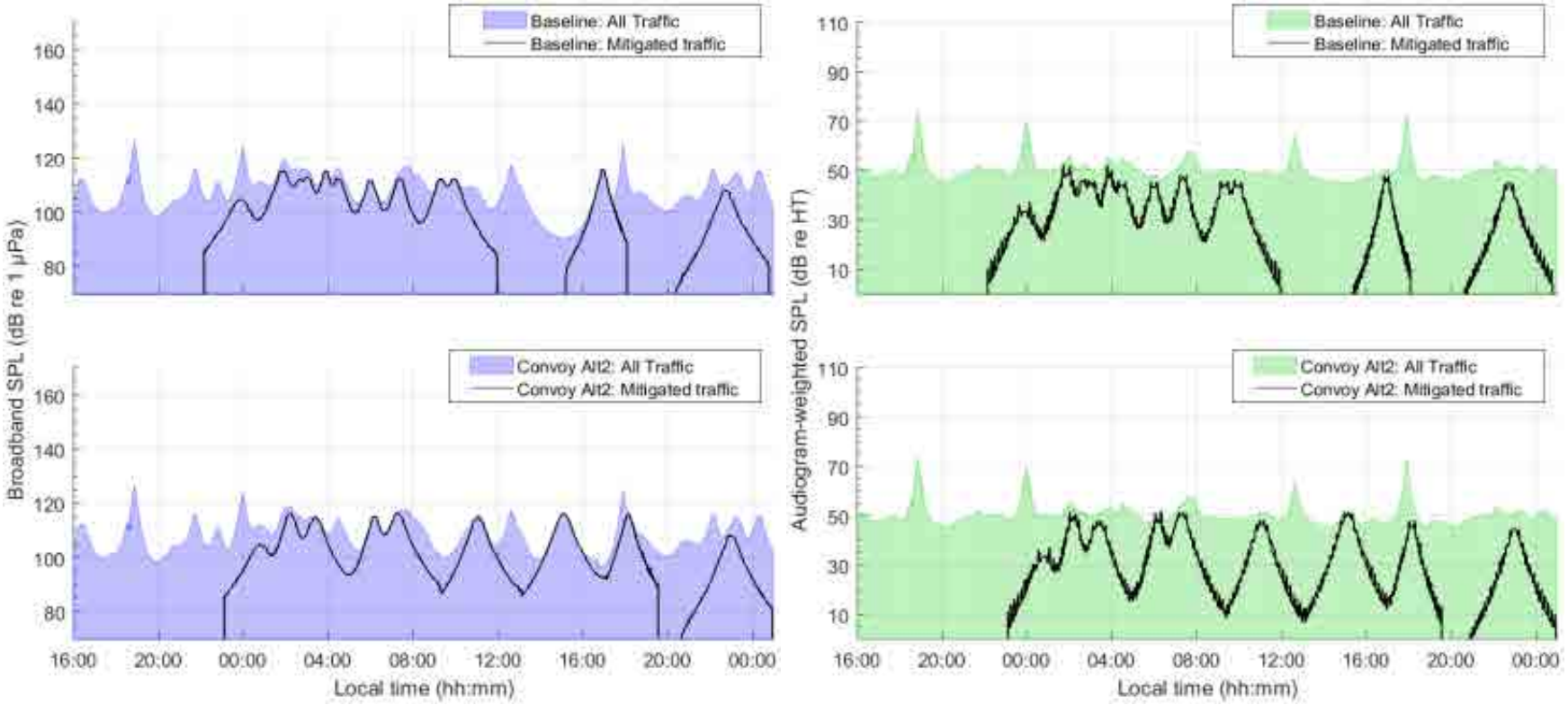

Figure 185. *Convoy Alternative 2, Juan de Fuca Strait, Sample location 4*: Temporal variability of unweighted (left) and audiogram-weighted (right) received levels for (top) baseline (no convoy) and (bottom) convoy scenarios. The blue and green lines above the shaded area show received levels caused by all traffic and ambient noise. The black lines show received levels caused by commercial traffic only. The receiver location is shown in Figure 7.

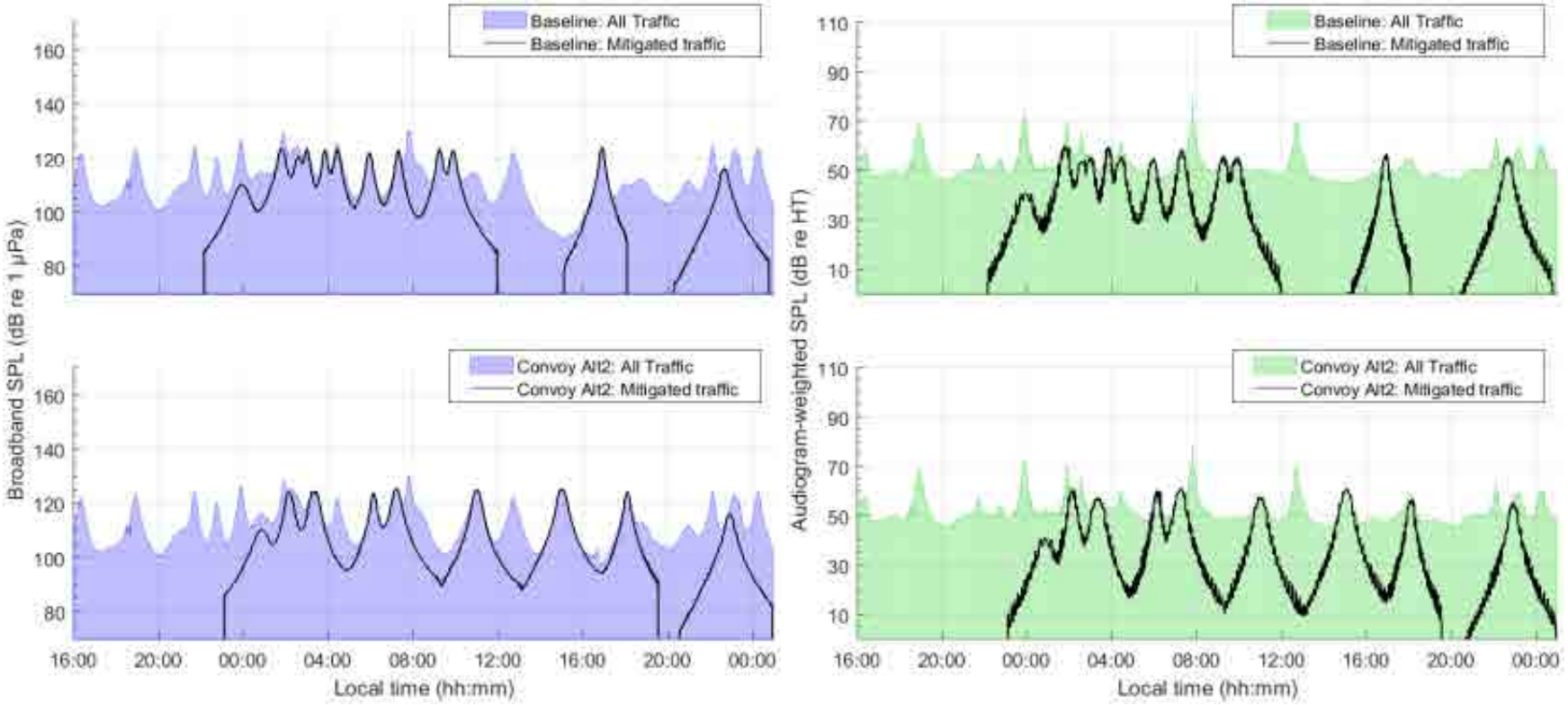

Figure 186. *Convoy Alternative 2, Juan de Fuca Strait, Sample location 5*: Temporal variability of unweighted (left) and audiogram-weighted (right) received levels for (top) baseline (no convoy) and (bottom) convoy scenarios. The blue and green lines above the shaded area show received levels caused by all traffic and ambient noise. The black lines show received levels caused by commercial traffic only. The receiver location is shown in Figure 7.

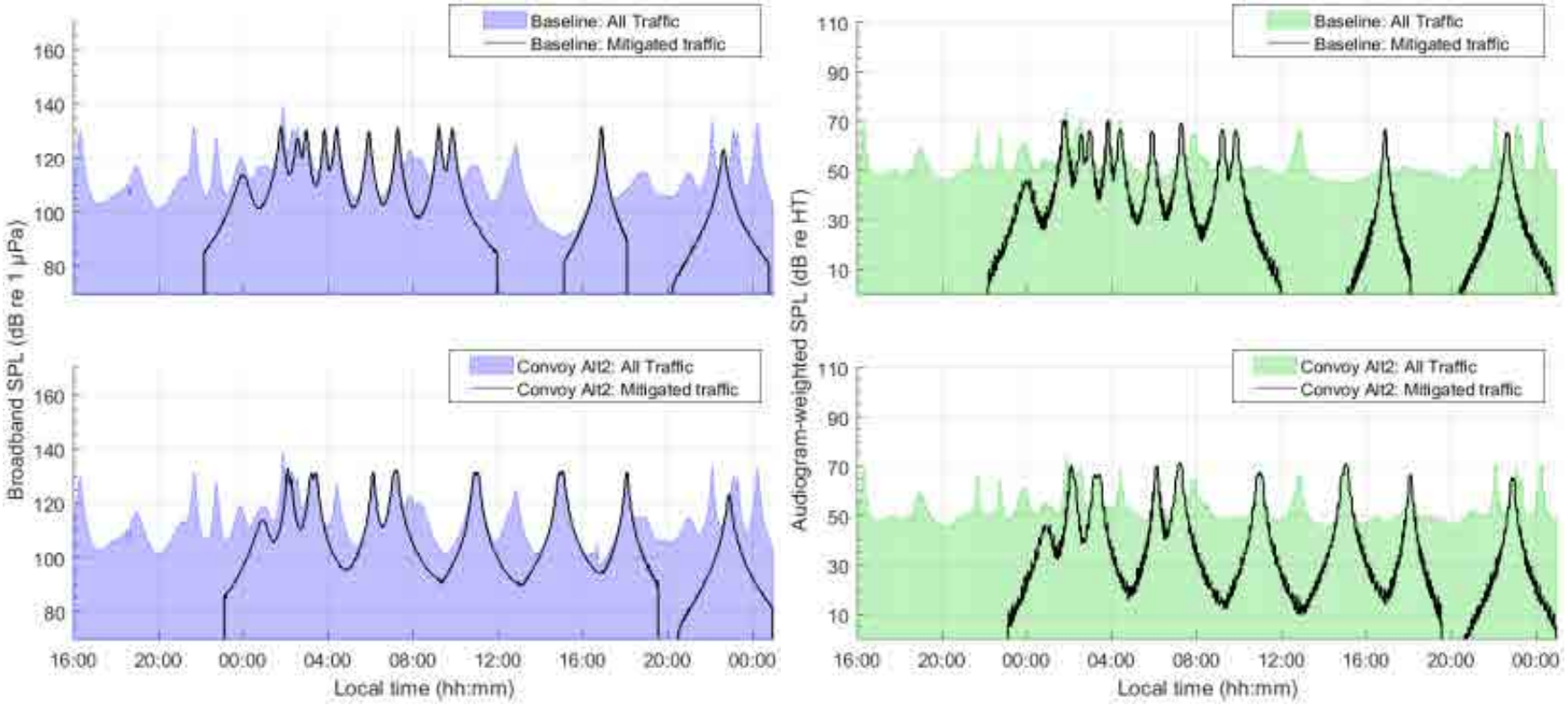

Figure 187. *Convoy Alternative 2, Juan de Fuca Strait, Sample location 6*: Temporal variability of unweighted (left) and audiogram-weighted (right) received levels for (top) baseline (no convoy) and (bottom) convoy scenarios. The blue and green lines above the shaded area show received levels caused by all traffic and ambient noise. The black lines show received levels caused by commercial traffic only. The receiver location is shown in Figure 7.

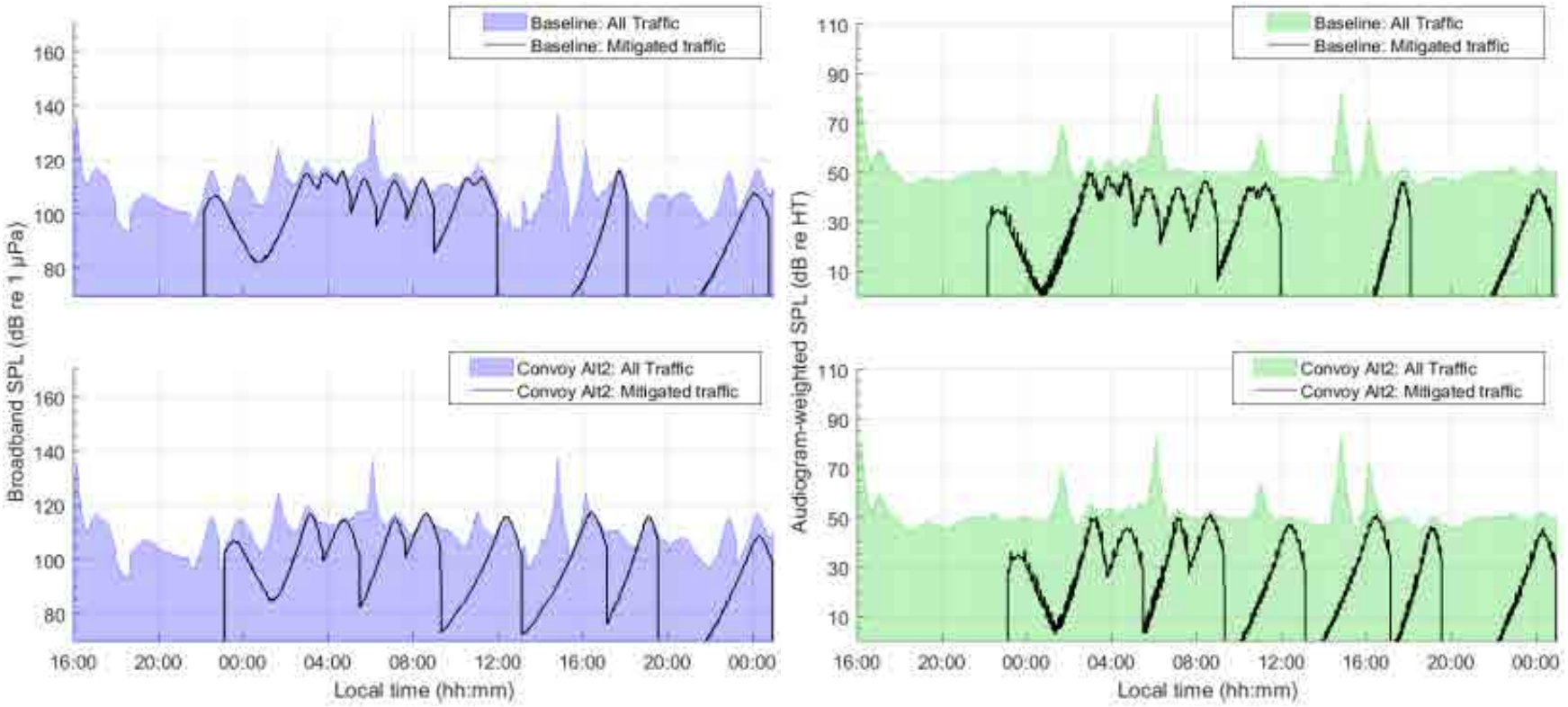

Figure 188. *Convoy Alternative 2, Juan de Fuca Strait, Sample location 7*: Temporal variability of unweighted (left) and audiogram-weighted (right) received levels for (top) baseline (no convoy) and (bottom) convoy scenarios. The blue and green lines above the shaded area show received levels caused by all traffic and ambient noise. The black lines show received levels caused by commercial traffic only. The receiver location is shown in Figure 7.

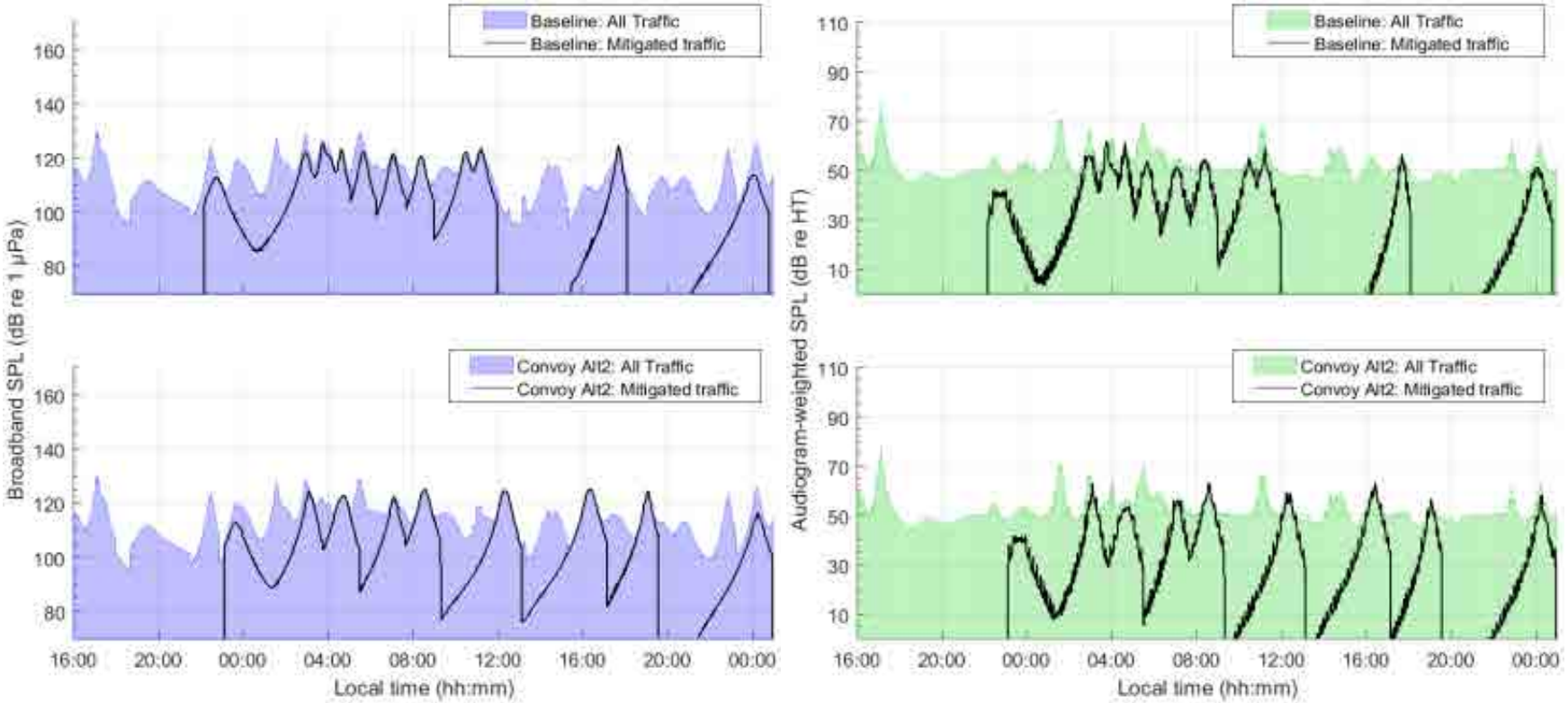

Figure 189. *Convoy Alternative 2, Juan de Fuca Strait, Sample location 8*: Temporal variability of unweighted (left) and audiogram-weighted (right) received levels for (top) baseline (no convoy) and (bottom) convoy scenarios. The blue and green lines above the shaded area show received levels caused by all traffic and ambient noise. The black lines show received levels caused by commercial traffic only. The receiver location is shown in Figure 7.

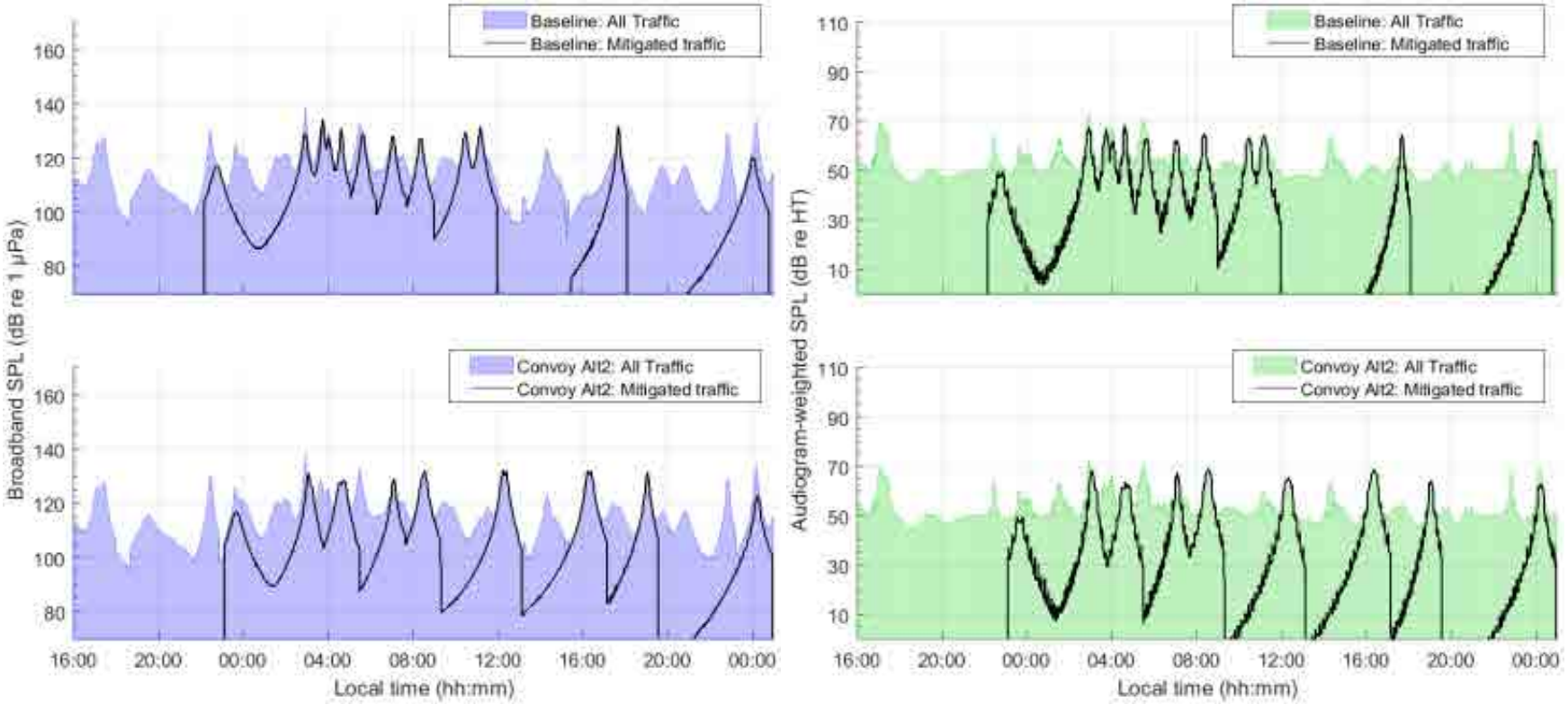

Figure 190. *Convoy Alternative 2, Juan de Fuca Strait, Sample location 9*: Temporal variability of unweighted (left) and audiogram-weighted (right) received levels for (top) baseline (no convoy) and (bottom) convoy scenarios. The blue and green lines above the shaded area show received levels caused by all traffic and ambient noise. The black lines show received levels caused by commercial traffic only. The receiver location is shown in Figure 7.

Table 67. *Convoy Alternative 2, Juan de Fuca Strait:* Temporal analysis of unweighted received noise levels (dB re 1 µPa), difference in received noise levels (dB), and difference acoustic intensity (%). The values indicate the percentile or mean calculated over a 33-hour period without (Baseline) and with mitigation (Convoy), at the sample locations within the SRKW critical habitat shown in Figure 7.

Sample location	Scenario	Temporal analysis of noise level (dB re 1 µPa), difference in noise levels (dB), and difference in acoustic intensity (%)			
		5th	50th	95th	Mean
1	Baseline	98.9	111.6	119.3	110.6 ±6.4
	Convoy	99.5	111.0	119.8	110.6 ±6.5
	Difference	**+0.6 (+14.7%)**	**−0.6 (−12.9%)**	**+0.5 (+12.6%)**	**0.0 (0.0%)**
2	Baseline	93.8	110.5	121.6	109.2 ±8.2
	Convoy	94.8	109.8	121.6	109.1 ±8.5
	Difference	**+1.0 (+25.9%)**	**−0.6 (−13.7%)**	**0.0 (0.0%)**	**−0.2 (−3.7%)**
3	Baseline	94.6	108.7	118.9	107.8 ±7.9
	Convoy	95.2	109.1	120.0	108.2 ±7.8
	Difference	**+0.6 (+16.0%)**	**+0.4 (+8.7%)**	**+1.1 (+28.0%)**	**+0.4 (+9.6%)**
4	Baseline	93.8	108.6	116.9	107.9 ±6.7
	Convoy	99.8	108.7	117.6	108.6 ±5.9
	Difference	**+5.9 (+291.6%)**	**+0.2 (+3.7%)**	**+0.6 (+15.6%)**	**+0.7 (+18.4%)**
5	Baseline	94.9	111.8	123.7	111.5 ±8.1
	Convoy	101.7	111.9	124.7	112.4 ±7.3
	Difference	**+6.8 (+381.1%)**	**+0.1 (+2.5%)**	**+1.0 (+26.1%)**	**+0.8 (+20.6%)**
6	Baseline	95.1	113.0	129.6	113.0 ±9.2
	Convoy	102.0	112.8	130.7	113.8 ±8.6
	Difference	**+6.9 (+386.3%)**	**−0.2 (−5.4%)**	**+1.1 (+28.1%)**	**+0.8 (+20.3%)**
7	Baseline	97.0	109.7	119.6	109.3 ±7.4
	Convoy	98.3	110.8	119.8	110.2 ±6.9
	Difference	**+1.4 (+37.0%)**	**+1.0 (+27.0%)**	**+0.2 (+3.8%)**	**+0.9 (+23.4%)**
8	Baseline	98.8	112.8	124.2	112.3 ±7.7
	Convoy	100.5	114.2	124.6	113.5 ±7.1
	Difference	**+1.7 (+49.5%)**	**+1.4 (+38.6%)**	**+0.4 (+8.8%)**	**+1.2 (+32.7%)**
9	Baseline	99.4	114.0	128.5	113.7 ±8.7
	Convoy	100.8	115.2	129.3	115.1 ±8.1
	Difference	**+1.4 (+39.4%)**	**+1.2 (+30.4%)**	**+0.8 (+20.4%)**	**+1.4 (+37.1%)**

Table 68. *Convoy Alternative 2, Juan de Fuca Strait:* Temporal analysis of SRKW audiogram-weighted received noise levels (dB re HT), difference in received noise levels (dB), and difference acoustic intensity (%). The values indicate the percentile or mean calculated over a 33-hour period without (Baseline) and with mitigation (Convoy), at the sample locations within the SRKW critical habitat shown in Figure 7.

Sample location	Scenario	Temporal analysis of noise level (dB re HT), difference in noise levels (dB), and difference in acoustic intensity (%)			
		5th	50th	95th	Mean
1	Baseline	47.1	50.2	58.7	51.4 ±4.6
	Convoy	46.6	50.1	58.7	51.4 ±4.8
	Difference	**−0.5 (−11.1%)**	**0.0 (0.0%)**	**0.0 (0.0%)**	**0.0 (0.0%)**
2	Baseline	46.4	49.7	60.1	51.2 ±4.9
	Convoy	46.1	49.7	59.6	51.2 ±5.0
	Difference	**−0.4 (−7.7%)**	**0.0 (0.0%)**	**−0.5 (−10.9%)**	**0.0 (0.0%)**
3	Baseline	45.9	49.6	60.1	50.8 ±4.7
	Convoy	45.9	49.7	60.3	50.9 ±4.7
	Difference	**0.0 (0.0%)**	**0.0 (0.0%)**	**+0.2 (+4.4%)**	**0.0 (0.0%)**
4	Baseline	46.1	49.8	58.4	50.6 ±4.2
	Convoy	46.5	49.8	58.4	50.7 ±4.1
	Difference	**+0.5 (+11.2%)**	**0.0 (0.0%)**	**0.0 (0.0%)**	**+0.2 (+4.0%)**
5	Baseline	46.1	50.5	62.3	52.1 ±5.1
	Convoy	46.7	50.6	61.9	52.4 ±5.1
	Difference	**+0.6 (+14.5%)**	**+0.1 (+2.8%)**	**−0.4 (−9.6%)**	**+0.3 (+8.2%)**
6	Baseline	46.1	50.9	66.8	53.1 ±6.3
	Convoy	46.9	50.9	68.0	53.6 ±6.6
	Difference	**+0.8 (+19.7%)**	**0.0 (0.0%)**	**+1.2 (+31.8%)**	**+0.5 (+11.5%)**
7	Baseline	46.3	49.9	64.5	51.6 ±6.0
	Convoy	46.4	50.1	64.5	51.7 ±5.9
	Difference	**0.0 (0.0%)**	**+0.2 (+4.5%)**	**0.0 (0.0%)**	**+0.1 (+3.1%)**
8	Baseline	46.5	50.6	62.9	52.1 ±5.0
	Convoy	46.6	50.8	63.1	52.5 ±5.1
	Difference	**+0.1 (+2.8%)**	**+0.3 (+6.2%)**	**+0.2 (+4.7%)**	**+0.4 (+9.2%)**
9	Baseline	46.7	51.1	65.7	53.0 ±5.7
	Convoy	47.1	51.7	66.7	53.6 ±5.9
	Difference	**+0.4 (+8.8%)**	**+0.6 (+14.0%)**	**+0.9 (+24.0%)**	**+0.6 (+15.6%)**

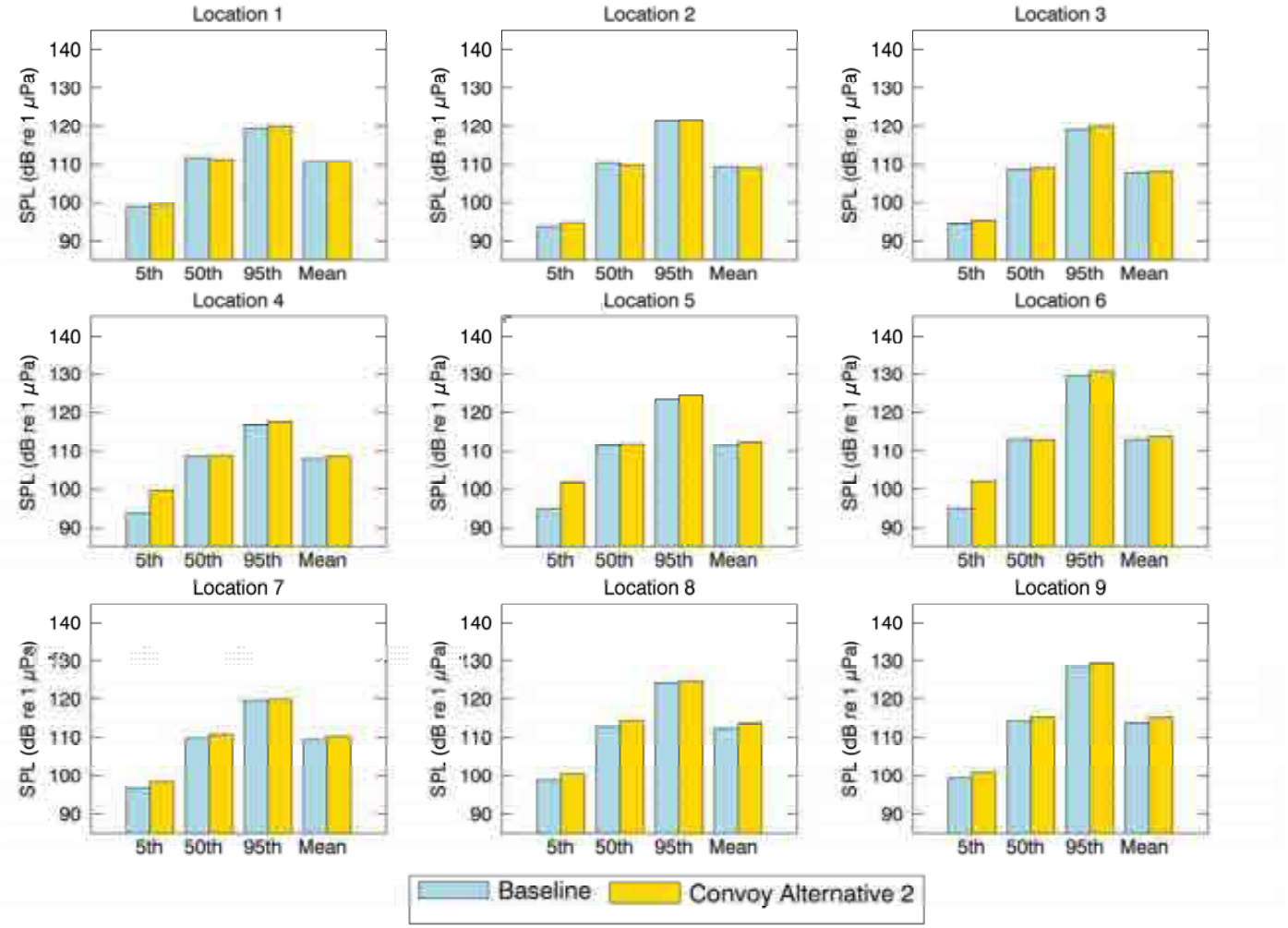

Figure 191. *Convoy Alternative 2, Juan de Fuca Strait*: Histogram representation of the temporal analysis of unweighted received noise levels (dB re 1 µPa). The vertical bars indicate the percentile or mean calculated over a 33-hour period without (baseline) and with mitigation, at the sample locations within the SRKW critical habitat shown in Figure 7.

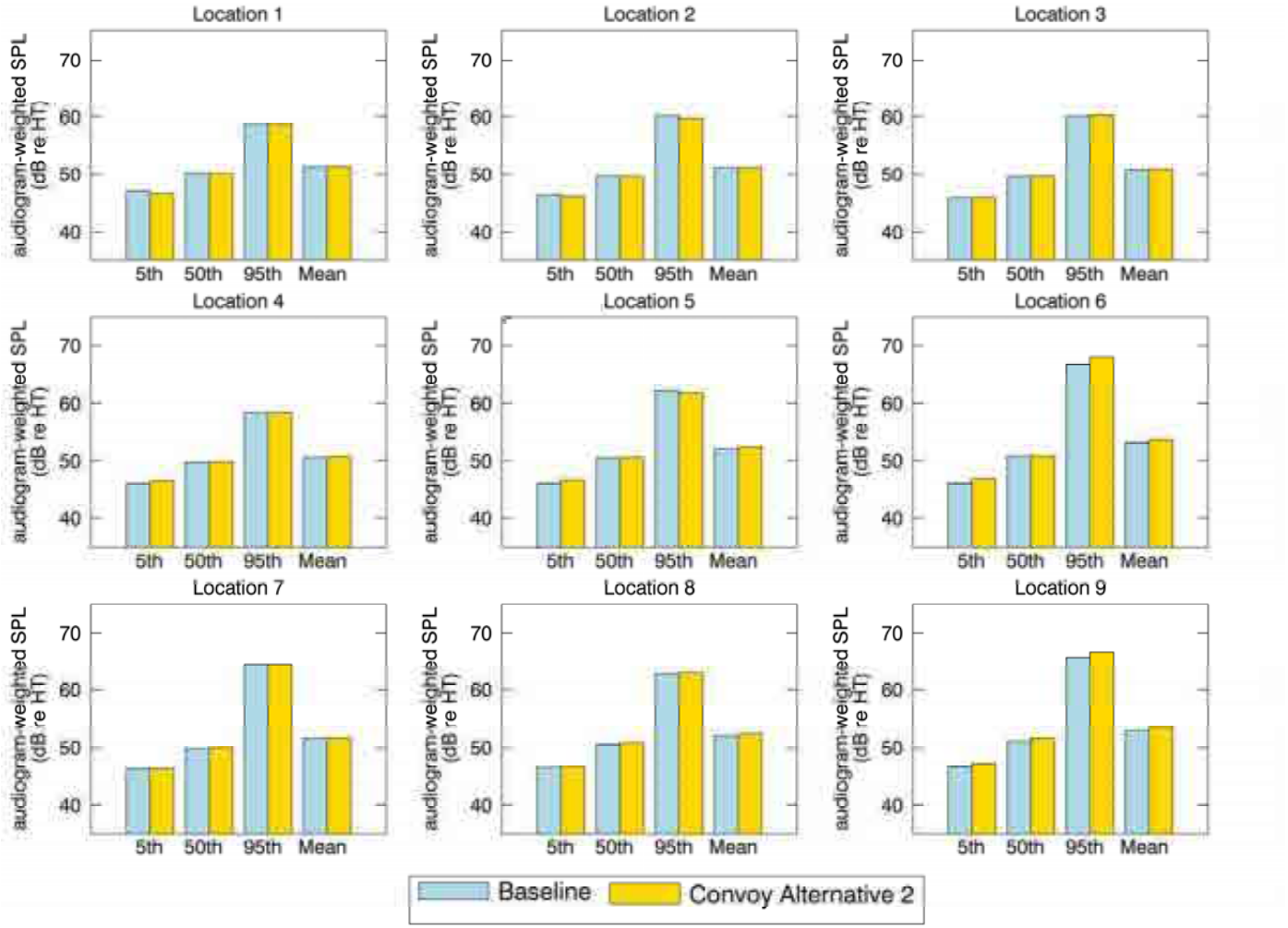

Figure 192. *Convoy Alternative 2, Juan de Fuca Strait*: Histogram representation of the temporal analysis of SRKW audiogram-weighted received noise levels (dB re HT). The vertical bars indicate the percentile or mean calculated over a 33-hour period without (baseline) and with mitigation, at the sample locations within the SRKW critical habitat shown in Figure 7.

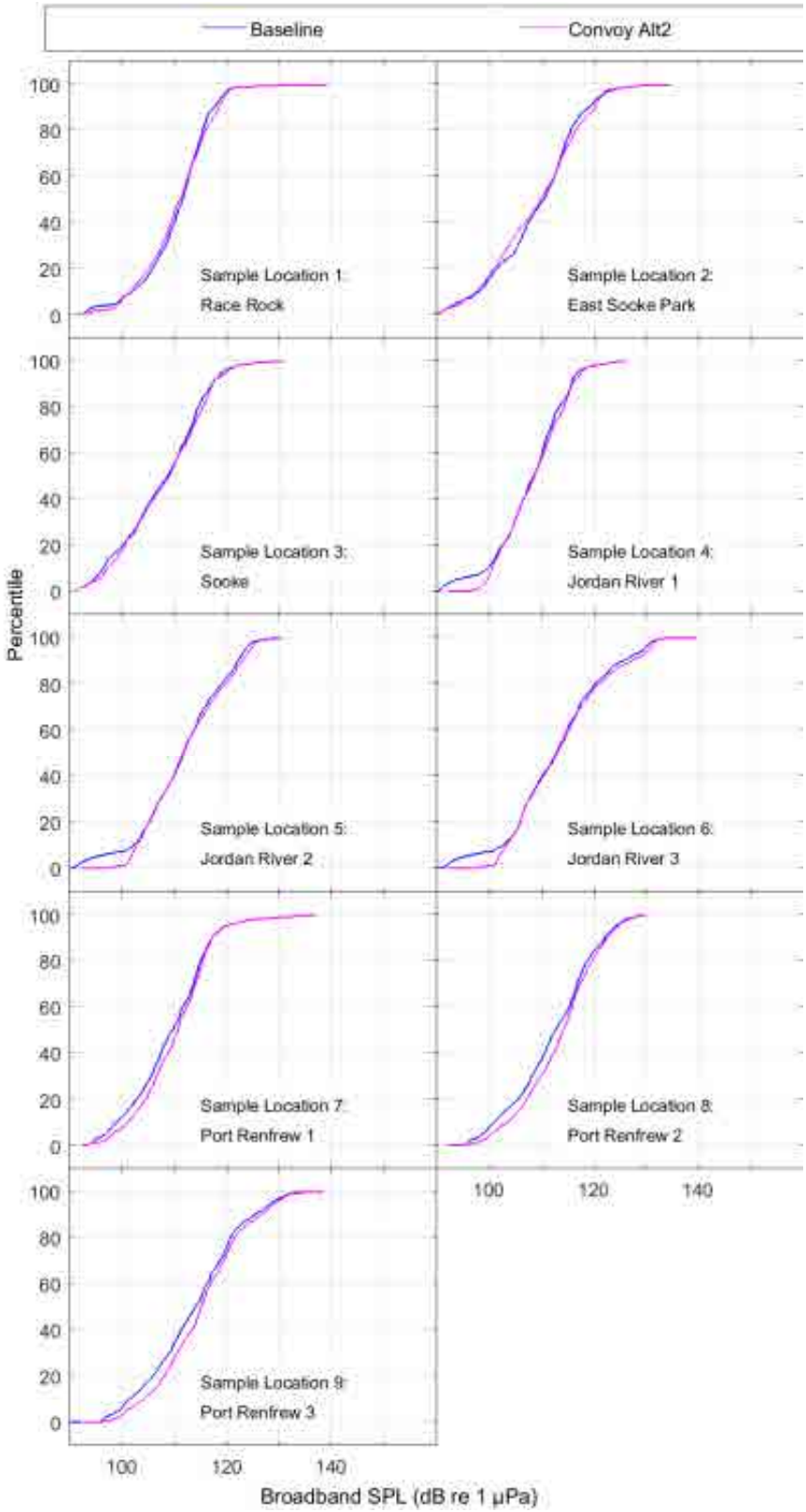

Figure 193. *Convoy Alternative 2, Juan de Fuca Strait*: CDF curves of time-dependent unweighted SPL for baseline and mitigated scenarios at the sample locations shown in Figure 7.

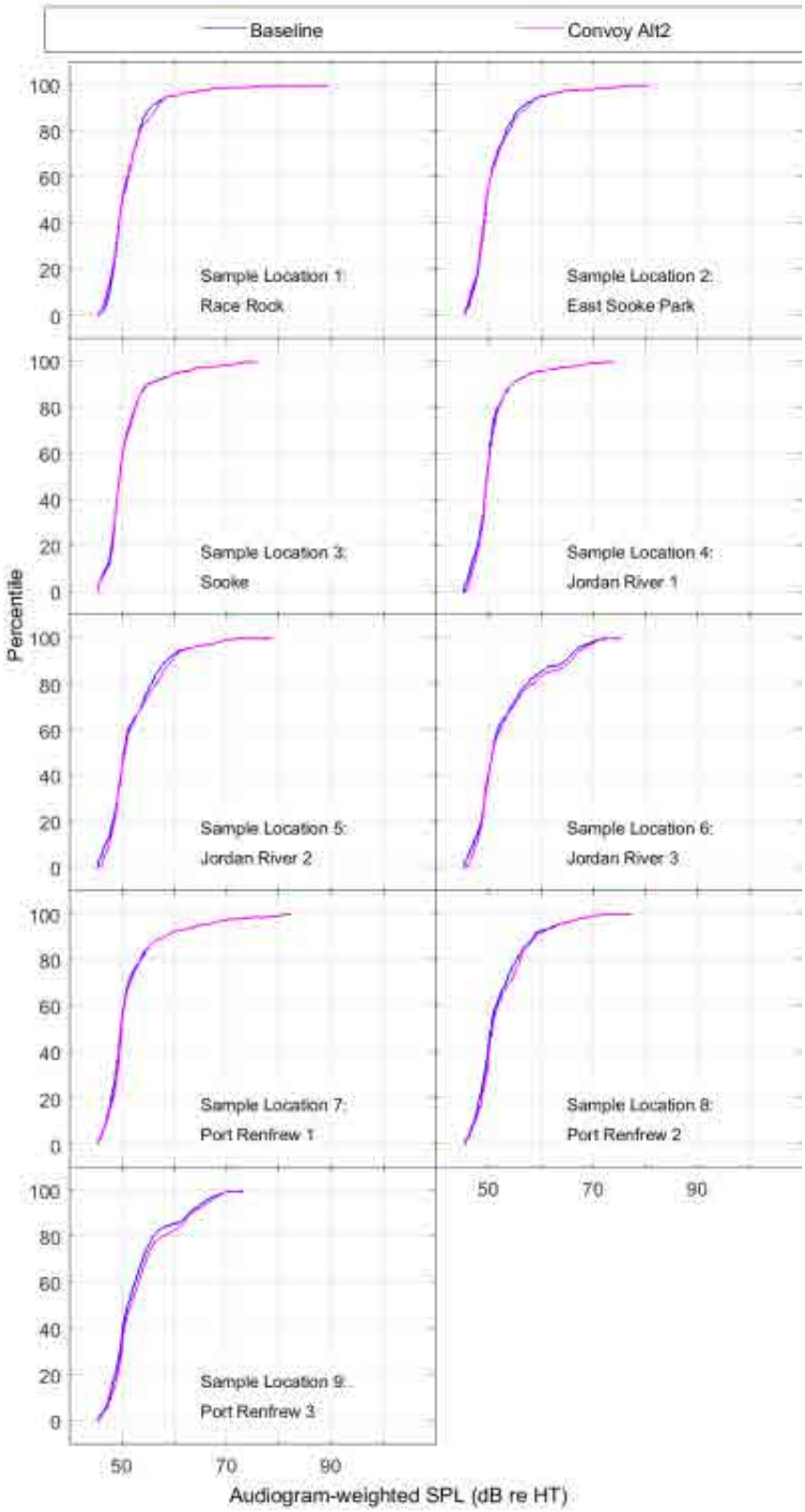

Figure 194. *Convoy Alternative 2, Juan de Fuca Strait*: CDF curves of time-dependent audiogram-weighted SPL for baseline and mitigated scenarios at the sample locations shown in Figure 7.

3.8.2.4. Swiftsure Bank

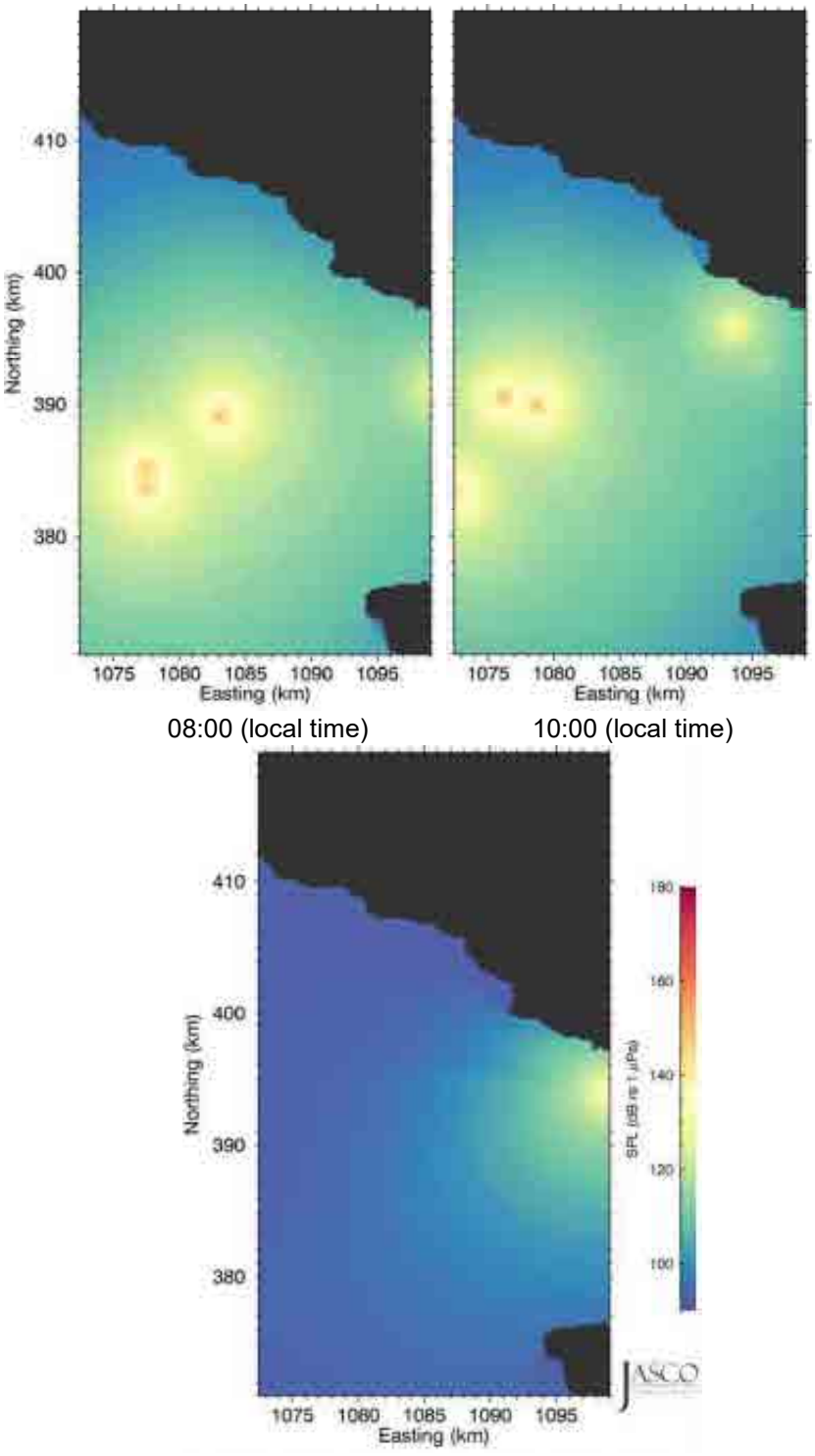

Figure 195. *Convoy Alternative 2, Swiftsure Bank:* Example time snapshots of future mitigated SPL (unweighted with ambient, 10 Hz to 50 kHz) from 08:00 to 12:00 (local time) in 2-hour increments. Easting and northing are BC Albers projected coordinates.

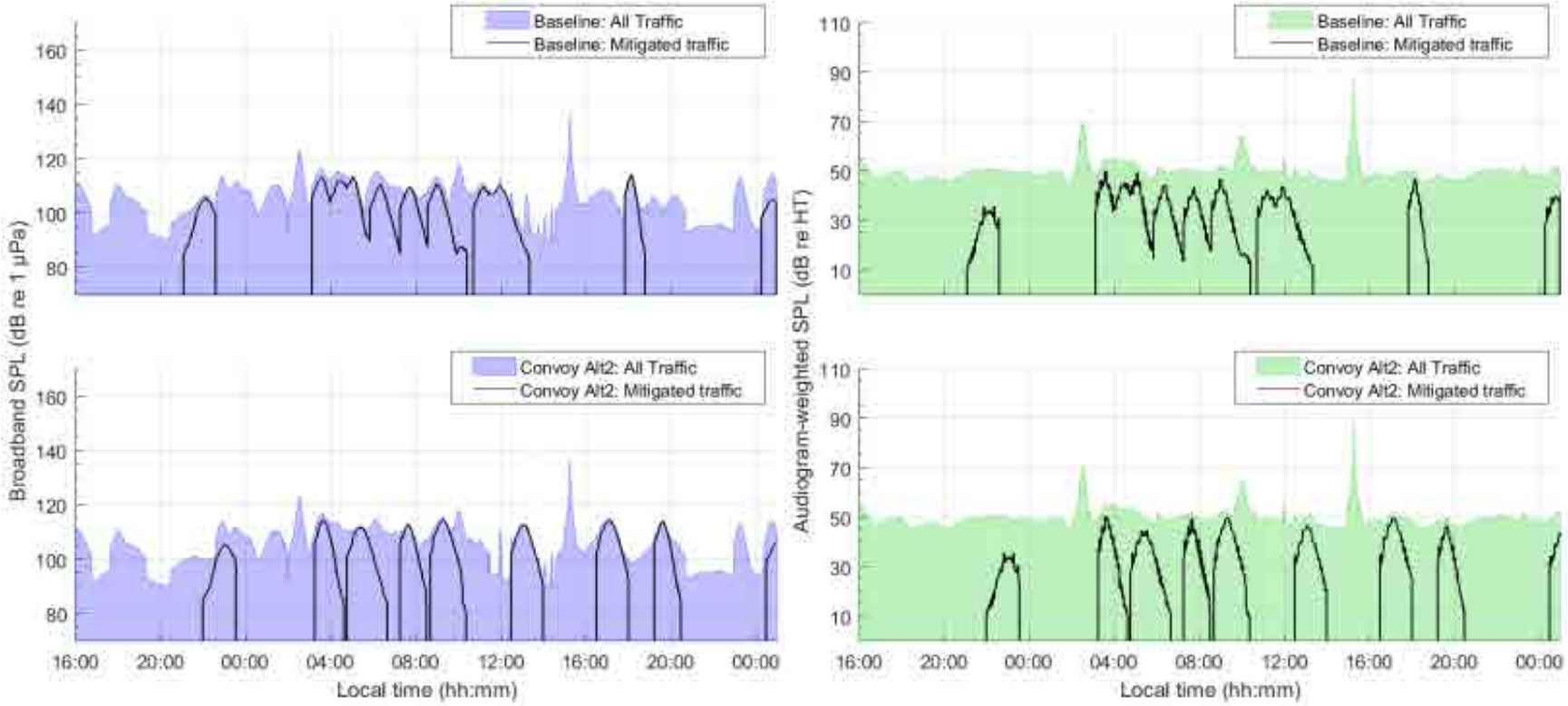

Figure 196. *Convoy Alternative 2, Swiftsure Bank, Sample location 1*: Temporal variability of unweighted (left) and audiogram-weighted (right) received levels for (top) baseline (no convoy) and (bottom) convoy scenarios. The blue and green lines above the shaded area show received levels caused by all traffic and ambient noise. The black lines show received levels caused by commercial traffic only. The receiver location is shown in Figure 8.

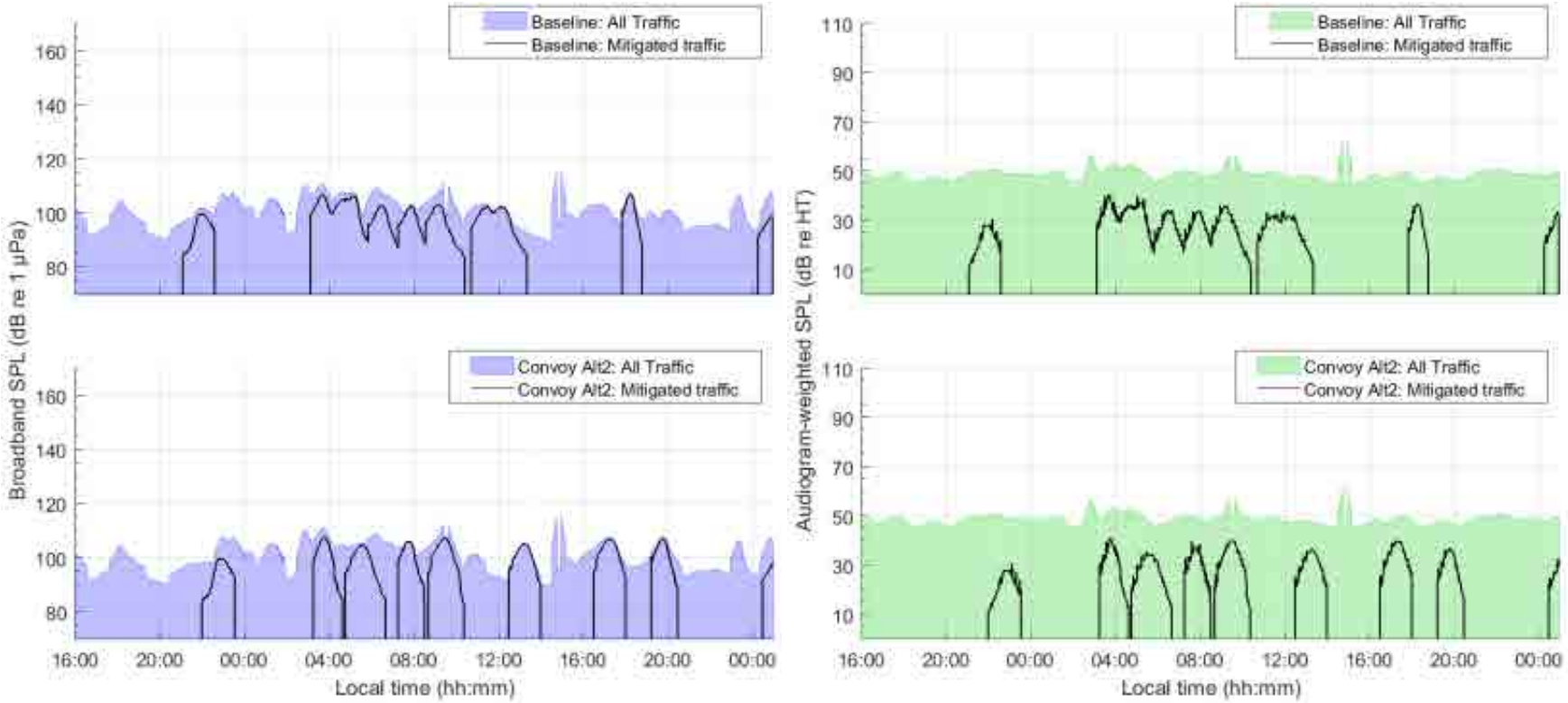

Figure 197. *Convoy Alternative 2, Swiftsure Bank, Sample location 2*: Temporal variability of unweighted (left) and audiogram-weighted (right) received levels for (top) baseline (no convoy) and (bottom) convoy scenarios. The blue and green lines above the shaded area show received levels caused by all traffic and ambient noise. The black lines show received levels caused by commercial traffic only. The receiver location is shown in Figure 8.

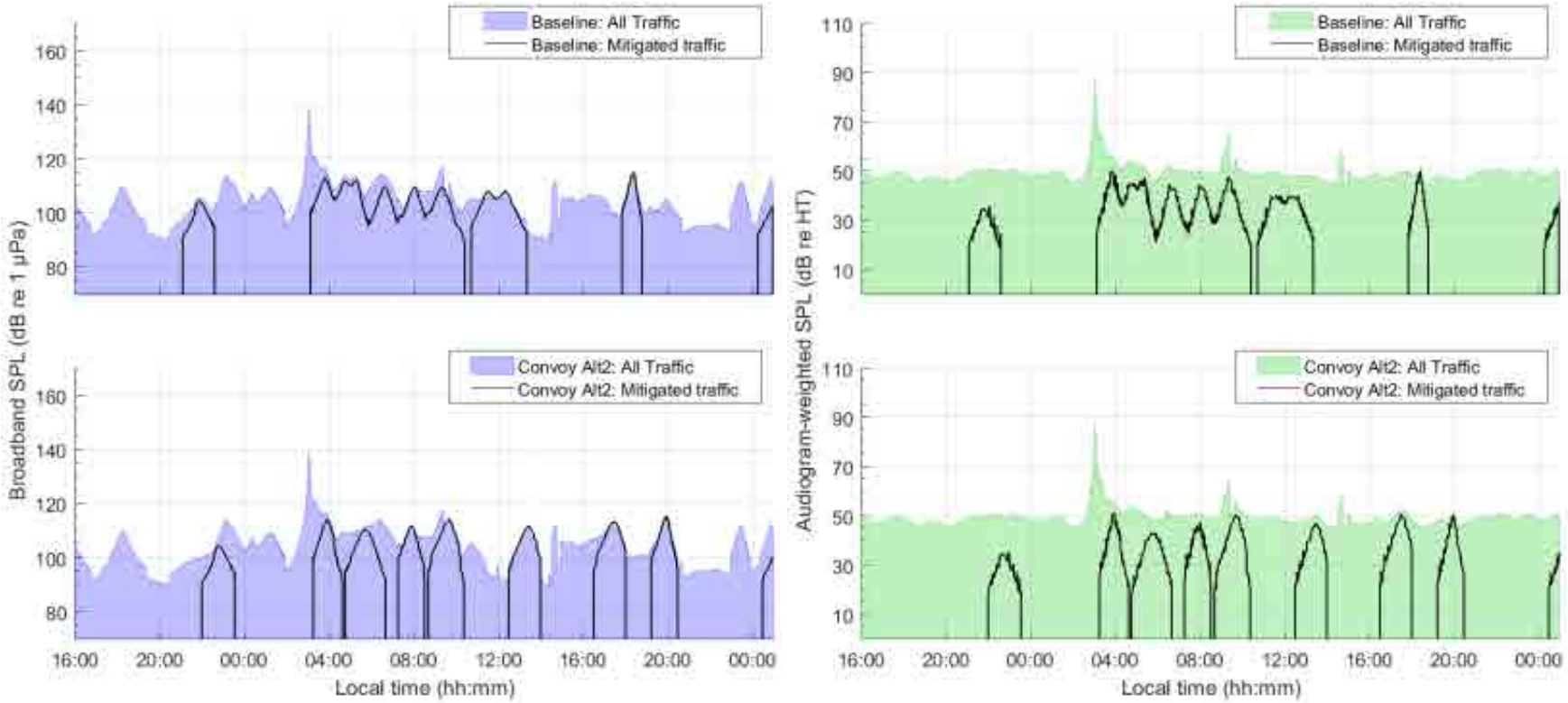

Figure 198. *Convoy Alternative 2, Swiftsure Bank, Sample location 3*: Temporal variability of unweighted (left) and audiogram-weighted (right) received levels for (top) baseline (no convoy) and (bottom) convoy scenarios. The blue and green lines above the shaded area show received levels caused by all traffic and ambient noise. The black lines show received levels caused by commercial traffic only. The receiver location is shown in Figure 8.

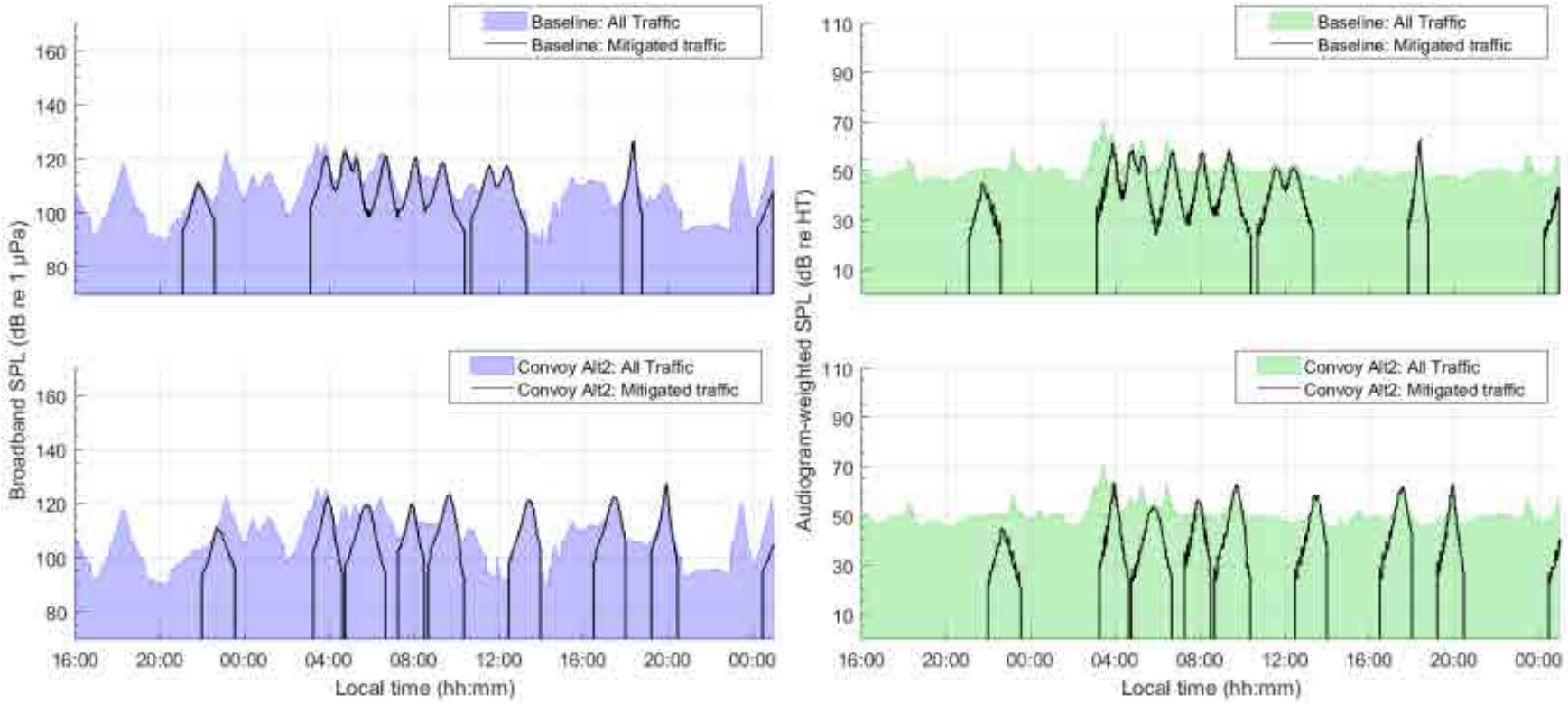

Figure 199. *Convoy Alternative 2, Swiftsure Bank, Sample location 4*: Temporal variability of unweighted (left) and audiogram-weighted (right) received levels for (top) baseline (no convoy) and (bottom) convoy scenarios. The blue and green lines above the shaded area show received levels caused by all traffic and ambient noise. The black lines show received levels caused by commercial traffic only. The receiver location is shown in Figure 8.

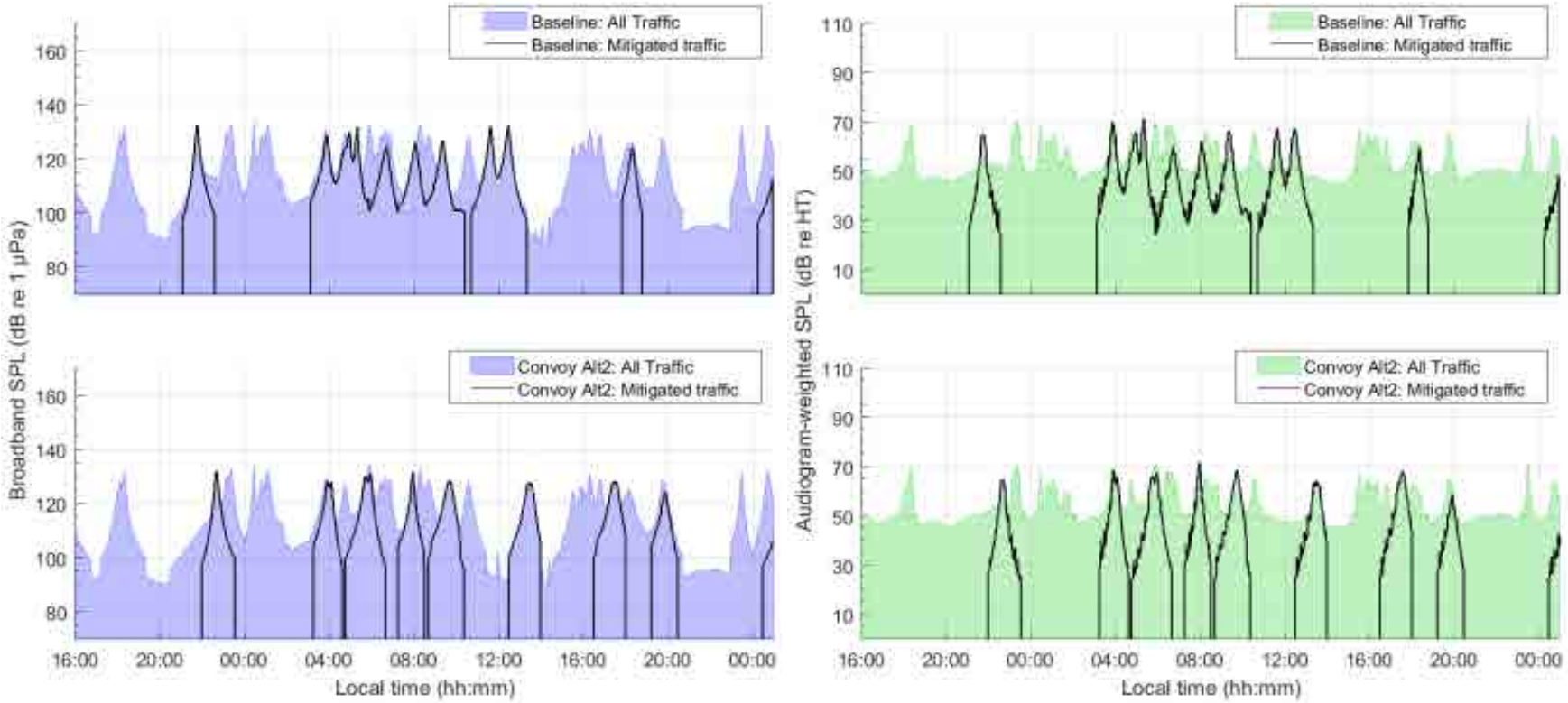

Figure 200. *Convoy Alternative 2, Swiftsure Bank, Sample location 5*: Temporal variability of unweighted (left) and audiogram-weighted (right) received levels for (top) baseline (no convoy) and (bottom) convoy scenarios. The blue and green lines above the shaded area show received levels caused by all traffic and ambient noise. The black lines show received levels caused by commercial traffic only. The receiver location is shown in Figure 8.

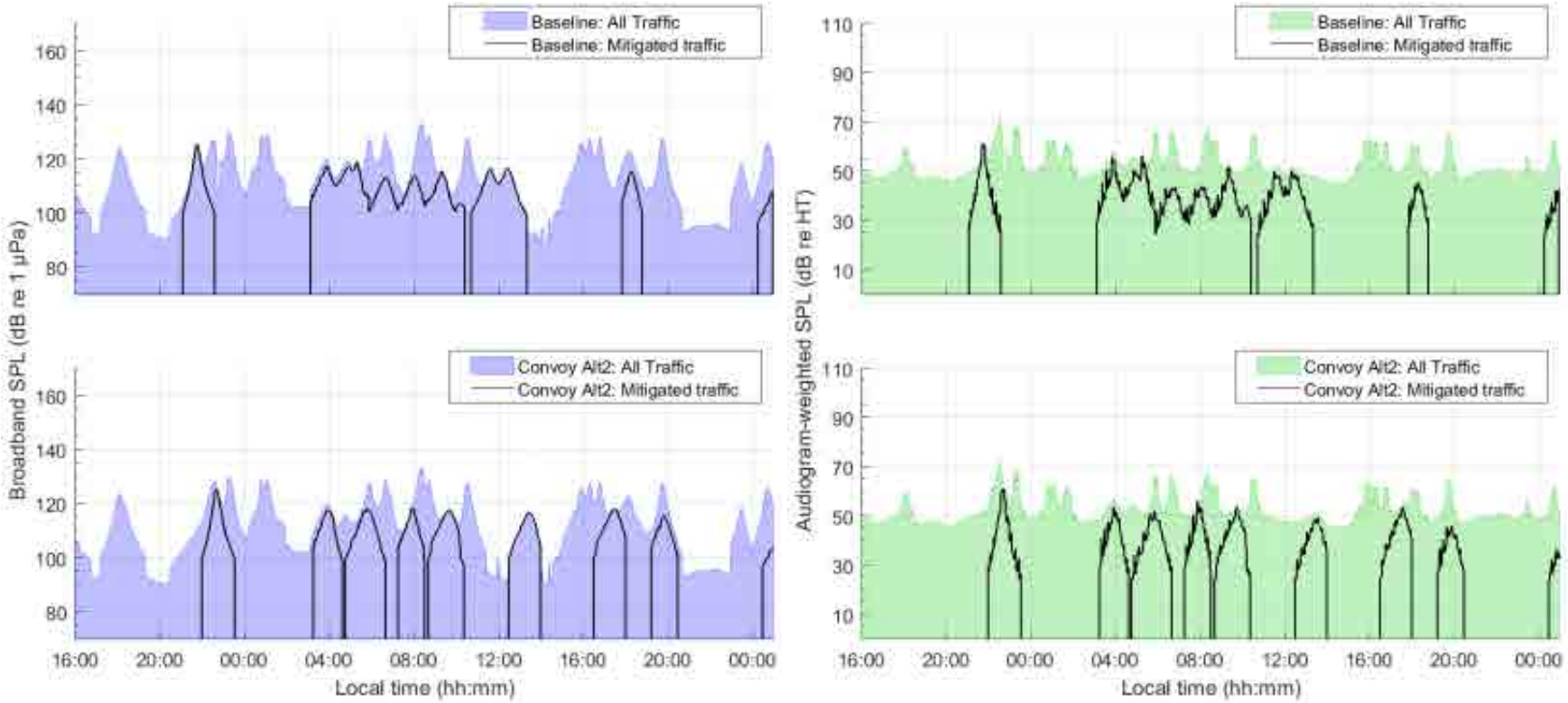

Figure 201. *Convoy Alternative 2, Swiftsure Bank, Sample location 6*: Temporal variability of unweighted (left) and audiogram-weighted (right) received levels for (top) baseline (no convoy) and (bottom) convoy scenarios. The blue and green lines above the shaded area show received levels caused by all traffic and ambient noise. The black lines show received levels caused by commercial traffic only. The receiver location is shown in Figure 8.

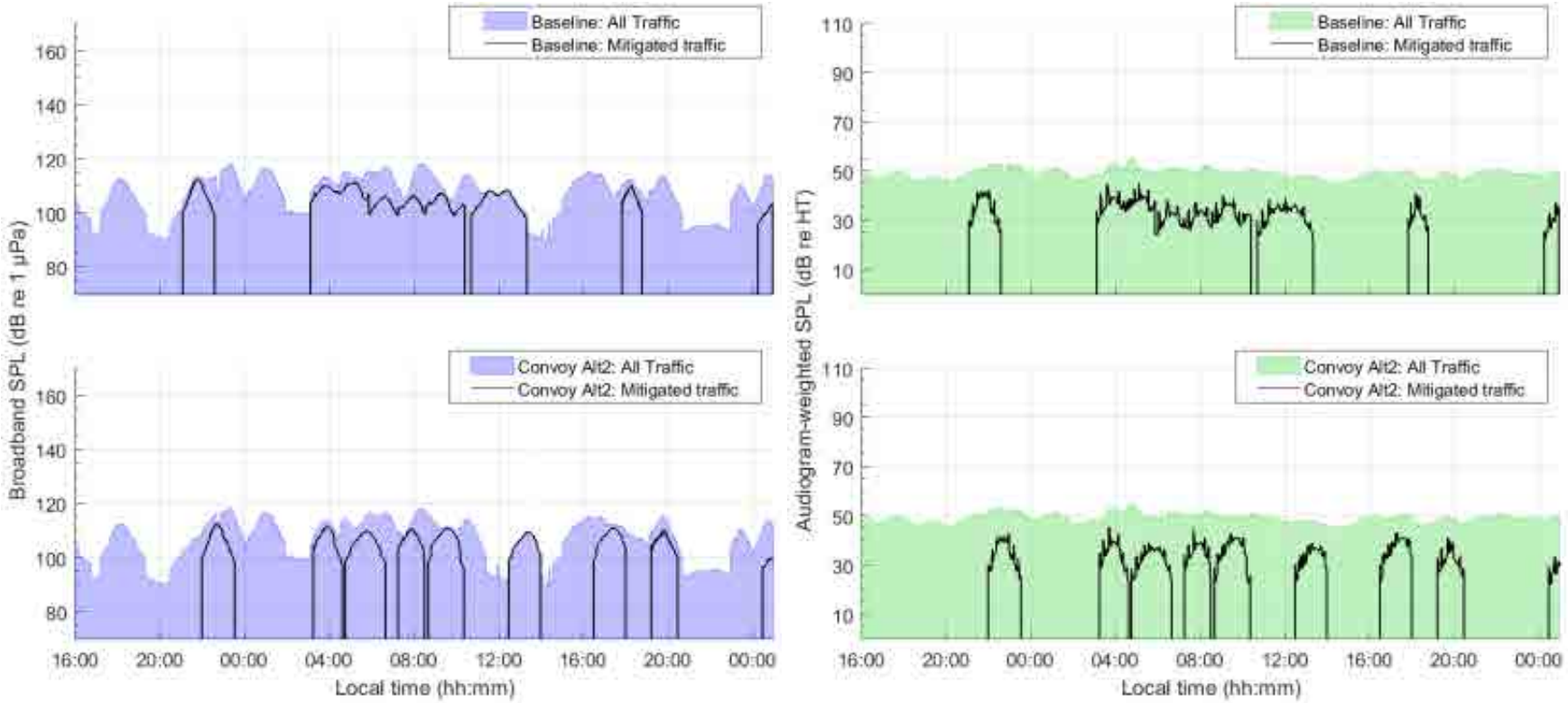

Figure 202. *Convoy Alternative 2, Swiftsure Bank, Sample location 7*: Temporal variability of unweighted (left) and audiogram-weighted (right) received levels for (top) baseline (no convoy) and (bottom) convoy scenarios. The blue and green lines above the shaded area show received levels caused by all traffic and ambient noise. The black lines show received levels caused by commercial traffic only. The receiver location is shown in Figure 8.

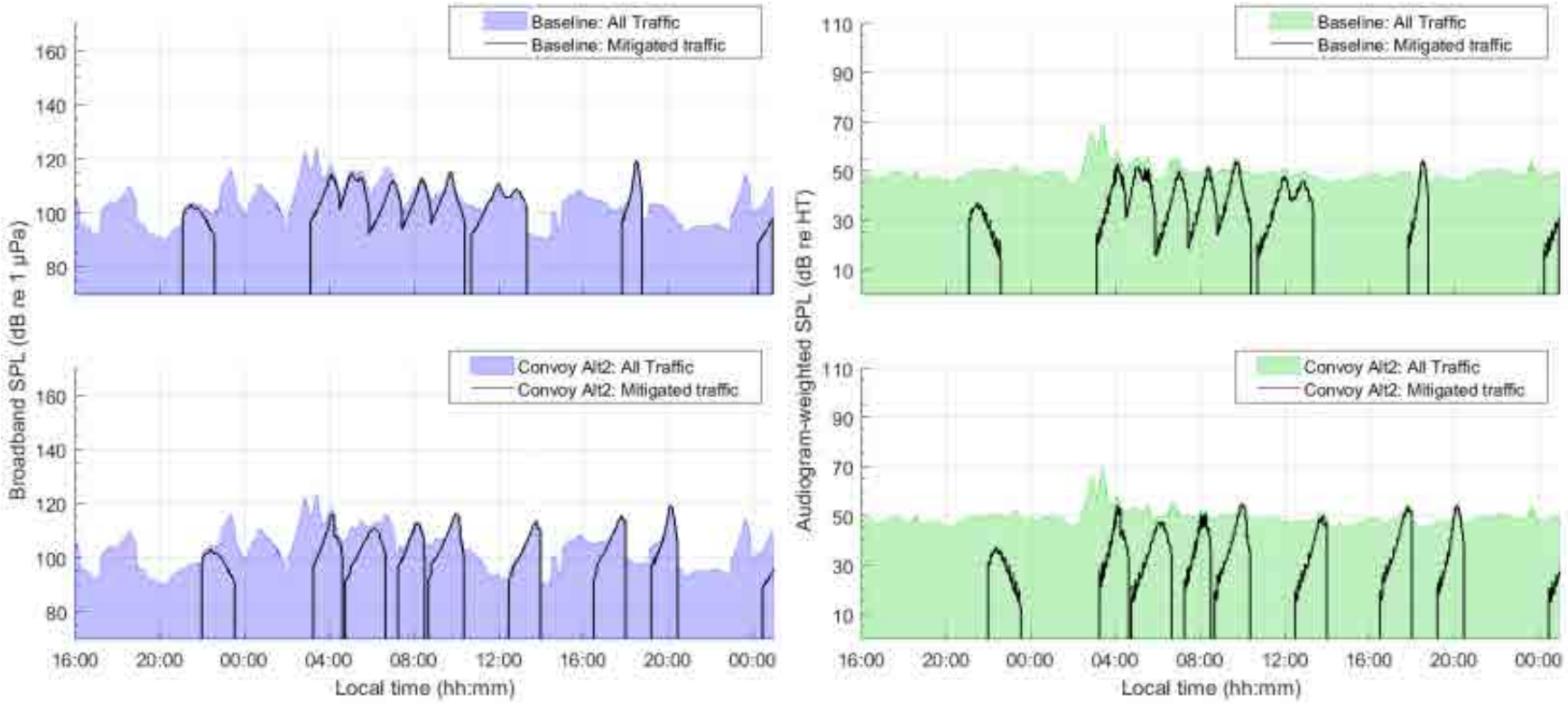

Figure 203. *Convoy Alternative 2, Swiftsure Bank, Sample location 8*: Temporal variability of unweighted (left) and audiogram-weighted (right) received levels for (top) baseline (no convoy) and (bottom) convoy scenarios. The blue and green lines above the shaded area show received levels caused by all traffic and ambient noise. The black lines show received levels caused by commercial traffic only. The receiver location is shown in Figure 8.

Table 69. *Convoy Alternative 2, Swiftsure Bank:* Temporal analysis of unweighted received noise levels (dB re 1 µPa), difference in received noise levels (dB), and difference acoustic intensity (%). The values indicate the percentile or mean calculated over a 33-hour period without (Baseline) and with mitigation (Convoy), at the sample locations within the SRKW critical habitat shown in Figure 8.

Sample location	Scenario	Temporal analysis of noise level (dB re 1 µPa), difference in noise levels (dB), and difference in acoustic intensity (%)			
		5th	50th	95th	Mean
1	Baseline	92.2	106.1	115.0	105.1 ±7.2
	Convoy	92.5	106.4	115.0	105.3 ±7.4
	Difference	**+0.3 (+7.3%)**	**+0.3 (+6.5%)**	**0.0 (0.0%)**	**+0.2 (+5.1%)**
2	Baseline	91.8	100.9	108.5	100.5 ±5.2
	Convoy	92.1	100.9	108.6	100.7 ±5.4
	Difference	**+0.3 (+7.7%)**	**0.0 (0.0%)**	**+0.1 (+2.8%)**	**+0.2 (+5.0%)**
3	Baseline	92.0	104.7	114.3	103.8 ±7.1
	Convoy	92.3	105.0	114.6	104.1 ±7.3
	Difference	**+0.3 (+7.6%)**	**+0.3 (+7.2%)**	**+0.3 (+8.3%)**	**+0.3 (+6.2%)**
4	Baseline	92.1	108.4	121.5	107.4 ±8.7
	Convoy	92.4	108.5	121.5	107.7 ±9.0
	Difference	**+0.3 (+7.4%)**	**+0.1 (+3.4%)**	**0.0 (0.0%)**	**+0.3 (+7.2%)**
5	Baseline	92.1	113.3	129.6	112.6 ±11.9
	Convoy	92.5	113.6	129.2	112.6 ±12.1
	Difference	**+0.3 (+8.0%)**	**+0.2 (+5.8%)**	**−0.4 (−8.8%)**	**0.0 (0.0%)**
6	Baseline	92.1	112.5	127.1	111.1 ±10.6
	Convoy	92.4	112.9	127.4	111.0 ±10.8
	Difference	**+0.3 (+7.0%)**	**+0.4 (+9.1%)**	**+0.2 (+5.0%)**	**−0.1 (−3.3%)**
7	Baseline	92.0	108.4	116.4	106.8 ±7.6
	Convoy	92.3	108.9	116.4	106.8 ±7.7
	Difference	**+0.3 (+7.3%)**	**+0.4 (+9.9%)**	**0.0 (0.0%)**	**0.0 (0.0%)**
8	Baseline	91.8	104.0	116.0	104.0 ±7.3
	Convoy	92.2	104.5	116.0	103.9 ±7.6
	Difference	**+0.4 (+10.3%)**	**+0.5 (+11.4%)**	**0.0 (0.0%)**	**−0.1 (−2.5%)**

Table 70. *Convoy Alternative 2, Swiftsure Bank:* Temporal analysis of SRKW audiogram-weighted received noise levels (dB re HT), difference in received noise levels (dB), and difference acoustic intensity (%). The values indicate the percentile or mean calculated over a 33-hour period without (Baseline) and with mitigation (Convoy), at the sample locations within the SRKW critical habitat shown in Figure 8.

Sample location	Scenario	Temporal analysis of noise level (dB re HT), difference in noise levels (dB), and difference in acoustic intensity (%)			
		5th	50th	95th	Mean
1	Baseline	46.0	49.3	55.0	49.9 ±3.8
	Convoy	46.0	49.4	55.0	50.0 ±3.8
	Difference	**0.0 (0.0%)**	**0.0 (0.0%)**	**0.0 (0.0%)**	**+0.1 (+2.2%)**
2	Baseline	45.8	48.9	52.7	48.9 ±2.1
	Convoy	45.8	48.9	52.7	48.9 ±2.1
	Difference	**0.0 (0.0%)**	**0.0 (0.0%)**	**0.0 (0.0%)**	**0.0 (0.0%)**
3	Baseline	46.1	49.0	55.0	49.6 ±3.7
	Convoy	46.0	49.1	55.5	49.7 ±3.7
	Difference	**0.0 (0.0%)**	**0.0 (0.0%)**	**+0.5 (+12.9%)**	**+0.1 (+2.3%)**
4	Baseline	46.4	49.8	59.5	50.6 ±3.9
	Convoy	46.3	49.9	60.2	51.0 ±4.1
	Difference	**0.0 (0.0%)**	**+0.1 (+3.0%)**	**+0.7 (+18.7%)**	**+0.3 (+7.4%)**
5	Baseline	46.4	51.0	66.2	53.9 ±6.5
	Convoy	46.5	51.1	66.8	54.1 ±6.6
	Difference	**+0.1 (+2.4%)**	**+0.1 (+3.4%)**	**+0.6 (+13.5%)**	**+0.2 (+5.4%)**
6	Baseline	46.4	50.5	63.6	52.4 ±5.3
	Convoy	46.4	50.6	63.7	52.4 ±5.3
	Difference	**0.0 (0.0%)**	**+0.1 (+2.4%)**	**+0.1 (+3.3%)**	**0.0 (0.0%)**
7	Baseline	46.2	49.3	52.5	49.2 ±1.8
	Convoy	46.2	49.3	52.5	49.2 ±1.8
	Difference	**0.0 (0.0%)**	**0.0 (0.0%)**	**0.0 (0.0%)**	**0.0 (0.0%)**
8	Baseline	46.2	49.2	55.3	49.8 ±3.3
	Convoy	46.0	49.2	55.1	49.8 ±3.2
	Difference	**−0.1 (−3.3%)**	**0.0 (0.0%)**	**−0.2 (−5.0%)**	**0.0 (0.0%)**

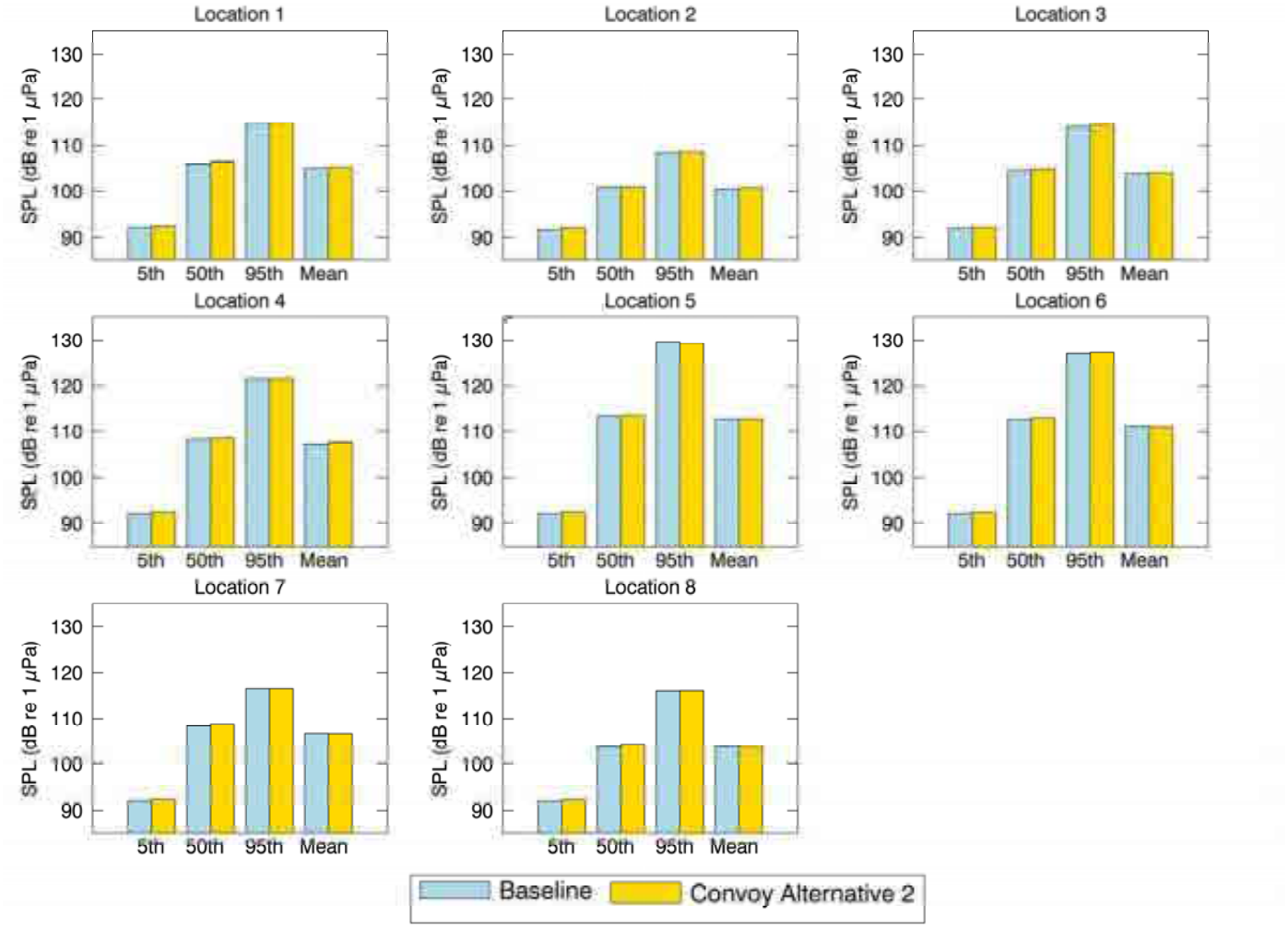

Figure 204. *Convoy Alternative 2, Swiftsure Bank*: Histogram representation of the temporal analysis of unweighted received noise levels (dB re 1 µPa). The vertical bars indicate the percentile or mean calculated over a 33-hour period without (baseline) and with mitigation, at the sample locations within the SRKW critical habitat shown in Figure 8.

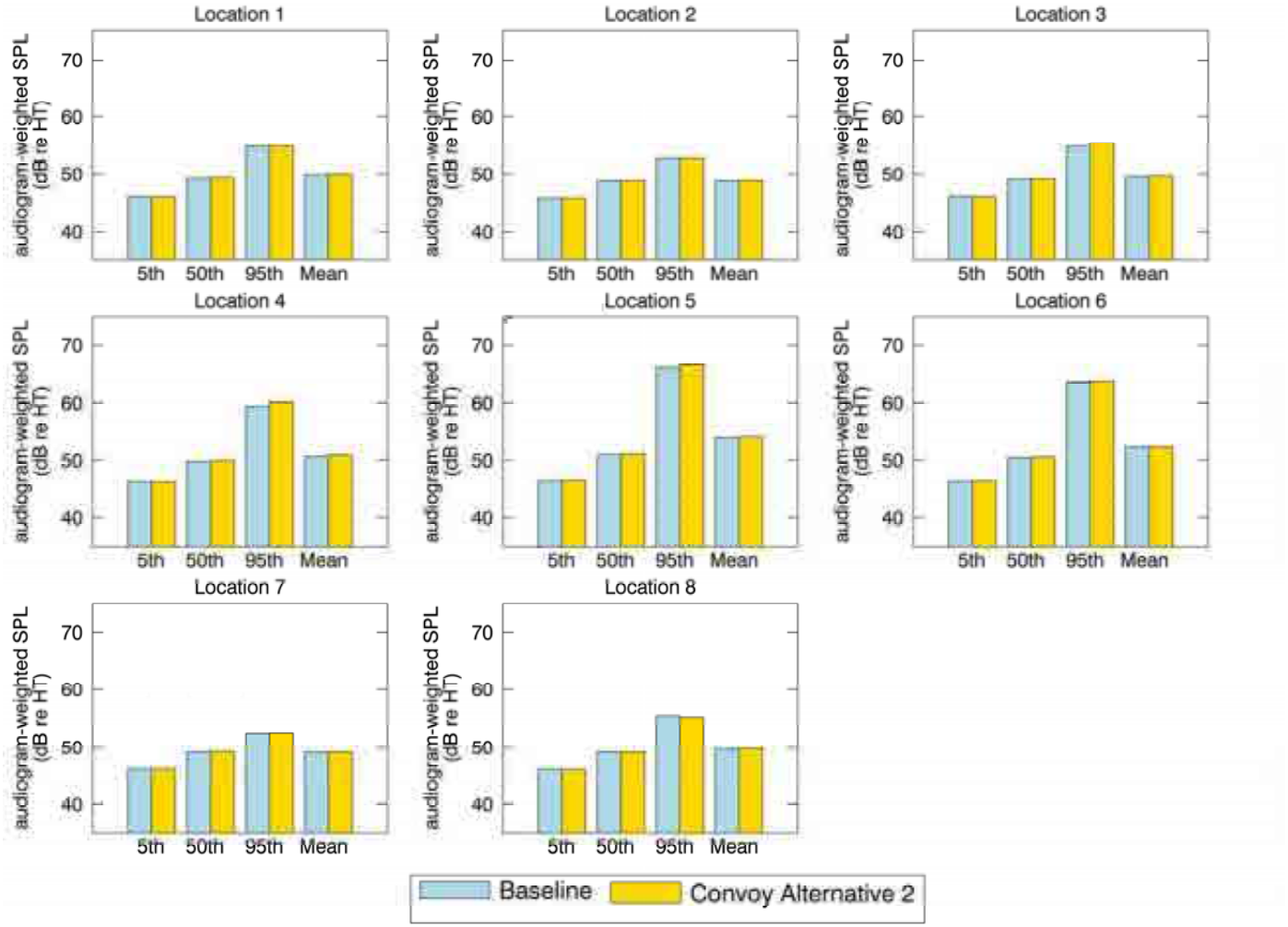

Figure 205. *Convoy Alternative 2, Swiftsure Bank*: Histogram representation of the temporal analysis of SRKW audiogram-weighted received noise levels (dB re HT). The vertical bars indicate the percentile or mean calculated over a 33-hour period without (baseline) and with mitigation, at the sample locations within the SRKW critical habitat shown in Figure 8.

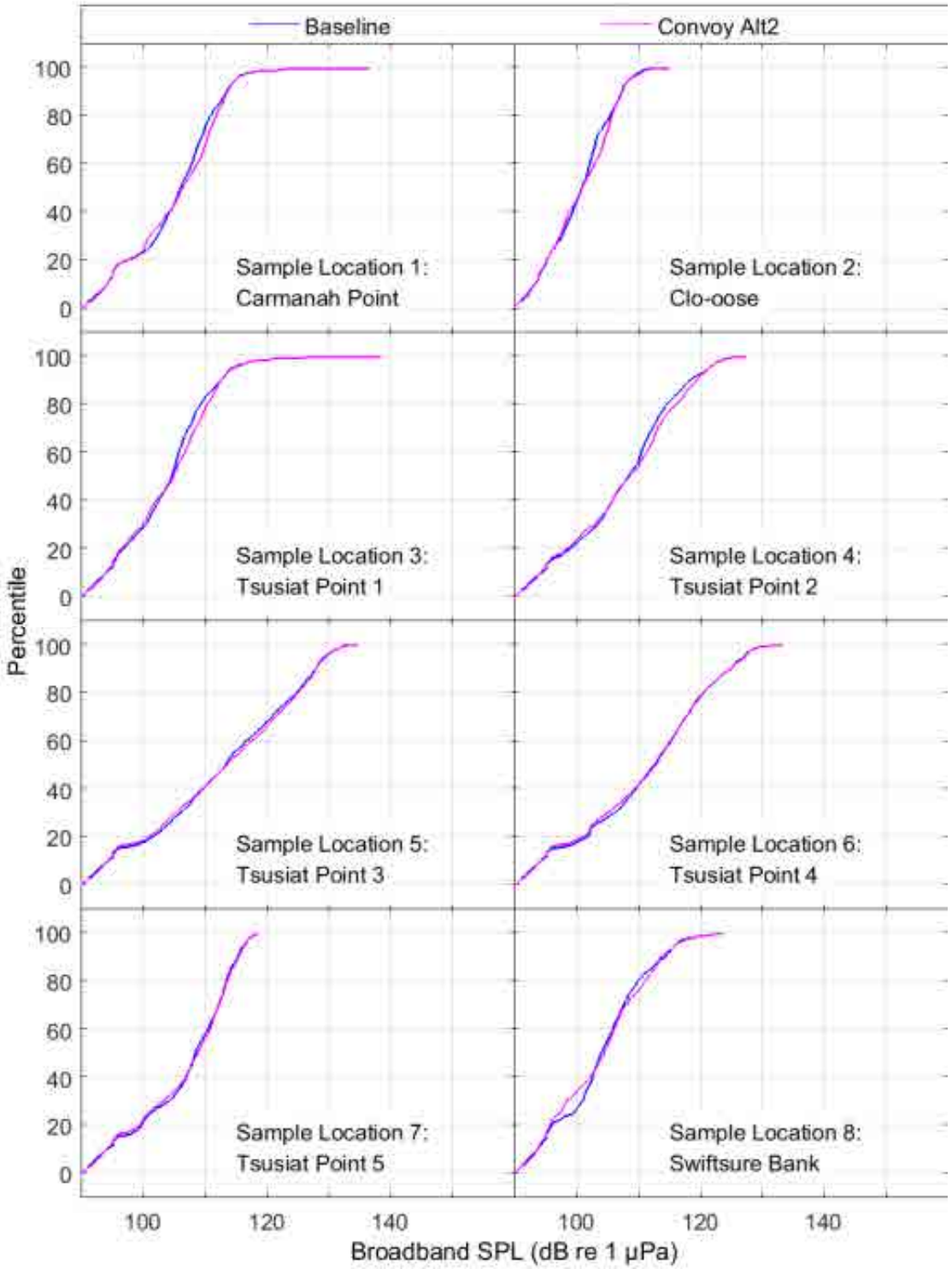

Figure 206. *Convoy Alternative 2, Swiftsure Bank*: CDF curves of time-dependent unweighted SPL for baseline and mitigated scenarios at the sample locations shown in Figure 8.

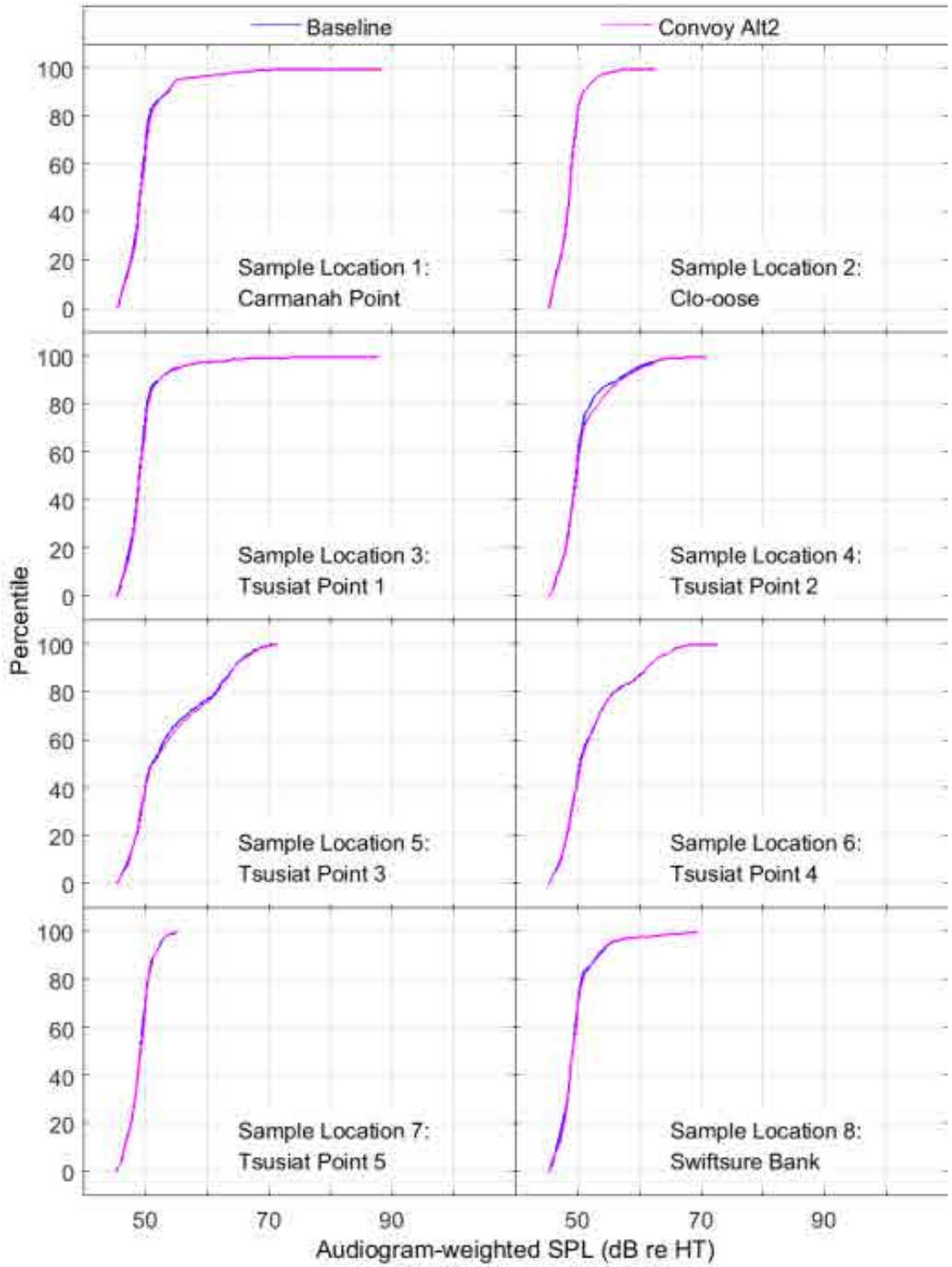

Figure 207. *Convoy Alternative 2, Swiftsure Bank*: CDF curves of time-dependent audiogram-weighted SPL for baseline and mitigated scenarios at the sample locations shown in Figure 8.

3.9. Retrofitting Ships

Commercial ships are generally designed with little consideration for underwater noise emissions. Most noise control is currently associated with minimizing noise exposures to vessel crews and passengers. While those controls often provide some corresponding reduction in underwater noise emissions, they are usually not highly effective for that purpose. This section provides a summary of the current technologies commonly available for retrofitting ships to improve hydrodynamics and decrease noise propagation, as well as the expected reduction in broadband noise emission levels, if available.

3.9.1. Cavitation Noise Control

The term cavitation refers to streams of vapour bubbles that form on the surface of marine propellers when a vessel is moving quickly. More information on cavitation noise is provided in Appendix A.3.1. The onset of cavitation is usually delayed by increasing the cavitation inception speed (Spence and Fischer 2017). This is primarily achieved by using propeller shapes that are less susceptible to cavitation and by optimizing hydrodynamic flow around the propellers. Circumferential variations (i.e., non-uniformities) in the wake inflow of the propeller are a major cause of cavitation. Cavitation creates mechanical wear on propellers, thrusters, and other hull components. It also affects propulsion efficiency. Reducing cavitation, therefore, has many other direct benefits besides reducing underwater noise emissions.

3.9.1.1. Reduced Cavitation Propeller Designs

Different design techniques are currently available for reducing cavitation from propeller and rudder systems and thrusters. For a given propeller blade design, a greater blade area can produce a given thrust with a smaller difference in pressure between the face (pressure side) and the back (suction side) of the blade. The current trend is toward manufacturing large-diameter, slow-turning propellers, which cause in less cavitation, since large propellers generate more thrust at lower turning rates.

Flow-optimized blade shapes also reduce cavitation. For example, forward-skew propellers have blades with the leading edge curved toward the rotation direction. They may have better cavitation performance than conventional propellers. Kappel propellers are designed with modified blade tips smoothly curved to the suction side of the blade, increasing efficiency. The end plate on Contracted and Loaded Tip propellers reduces the tip vortices, thereby enabling the radial load distribution to be more heavily loaded at the tip than with conventional propellers (optimum propeller diameter is smaller, and cavitation may be reduced). New Blade Section propellers are smaller and lighter. This might provide higher efficiency and reduce cavitation.

Another design technique is to add more propeller blades so the thrust on individual blades is reduced. Reduced-cavitation propeller designs are becoming more widespread in commercial shipping. Manufacturing and replacement costs are higher than for conventional propeller designs. The benefit of these designs is that they increase propeller life due to decreasing wear from cavitation.

The likely noise reduction from reduced cavitation propeller design is 3–20 dB (Spence et al. 2007, Andersen et al. 2009).

3.9.1.2. Reduced Hub Vortex Cavitation

Cavitation also occurs near the centre of the propeller, as seen in Figure 208(a). This central portion of the propeller is known as the hub, and its cover is referred to as the boss cap. Properly designed boss caps can reduce the hub vortex cavitation[4], thus decreasing the hydroacoustic noise and improving propeller efficiency. This is particularly important for controllable pitch propellers, for which the size and design of the hub and cap influence the reliability of the system (Wind 1978, Ghassemi et al. 2012).

Propeller cap turbines are comprised of many hydrofoil-shaped blades integrally cast into the hub cap. Propeller Boss Cap Fins, as seen in Figure 208b, are small fins attached to the propeller hub cap. Both systems reduce the magnitude of the hub vortices and propeller vibrations.

The effect on noise reduction from propeller cap turbines is unknown. Conversely, the Propeller Boss Cap Fins reduces cavitation, and it is claimed to reduce the sound pressure level by 3 to 6 dB (Ouchi et al. 1991, Abdel-Maksoud et al. 2004, Mewis and Hollenbach 2006).

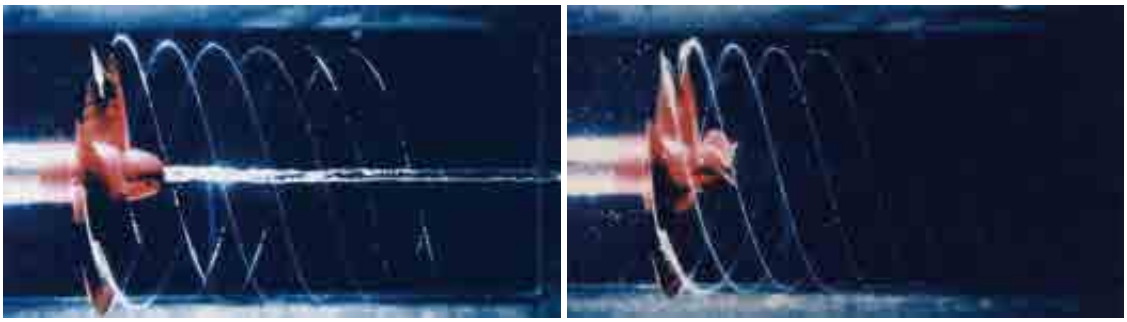

(a) (b)

Figure 208. Vortex cavitation around a propeller (a) without and (b) with boss cap fins. Pictures reproduced with the permission of MOL Techno-Trade, Ltd. http://www.mol.co.jp/en/pr/2015/15033.html

3.9.1.3. Ducted Propulsion

Ducted propellers are affixed with a stationary, ring-like nozzle around the propeller to improve hydrodynamic flow over the blades. The improved character of the flow field, which becomes more uniform when guided by a nozzle, can reduce propeller cavitation. The nozzle itself may also provide acoustic shielding at higher frequencies. Kort nozzles are widely-used ducted propulsion for tugs. The Mewis Duct and Schneekluth's Wake Equalizing Duct are fore-propeller appendages based on the essential science of the Kort nozzle but adapted for larger scale commercial vessels. Ducted propulsion is currently in widespread use in marine vessels. Ducted propellers improve the wake, increase propulsion efficiency, and decrease propeller wear.

The likely noise reduction from this design is not currently well understood.

[4] Hub vortex cavitation occurs when the lift is heavy on inward sections of the propeller blades.

3.9.1.4. Wake Inflow Optimization

Cavitation performance can be greatly improved by placing propellers along the hull where hydrodynamic flow is more uniform. The hull shape and the presence of nearby appendages is important in determining flow characteristics. Furthermore, it is essential to have adequate clearance between propeller tips and the hull to avoid boundary layer turbulence. Computational fluid dynamics simulations are widely used in predicting flow around vessel hulls, and they can be used to design vessel hulls and optimize propeller placement. Wake inflow optimization improves propeller efficiency and decreases propeller wear.

Other means to improve wake flow include:

- A simplified compensative nozzle (a nozzle that has a more vertical or cylindrical shape instead of being circular), which improves the uniformity of wake flow into the propeller,
- Grothues spoilers, a small series of curved fins attached to the hull just ahead of the propeller, and
- Pre-swirl stators, or Vortex generators, as added appendages.

Pre-swirl stators are especially suitable for the larger hull forms (container and tanker vessels for example).

The likely noise reduction from these design options is currently unknown.

3.9.1.5. Propeller/Rudder Interaction

Various concepts have been developed to increase the efficiency of propeller and rudder systems, including a twisted rudder (to account for the swirling flow from the propeller), rudder fins (the propeller recovers some of the rotational energy), and Costa Propulsion Bulb (the propeller is integrated hydrodynamically with the rudder by fitting a bulb to the rudder in line with the propeller shaft). Changes to propeller/rudder interaction increase propulsive efficiency.

The Costa Propulsion Bulb is claimed to reduce the hydroacoustic radiated noise levels by 5 dB (Ligtelijn 2007); the likely noise reduction from other options is currently unknown.

3.9.1.6. Air Injection to Propeller, Thruster, and Bubble Curtain

Bubbles can be produced in a deliberate arrangement to act as a barrier/curtain to break or reduce the sound propagating from the propulsion system or the hull. Air injection can also minimize the cavitation erosion in propeller ducts.

The likely noise reduction from this design varies according to how it is used:

- Bubble emission in a propeller and rudder system reduces the noise by at least 10 dB for frequencies above 500 Hz, but it increases the noise (0–10 dB) for frequencies between 20–80 Hz (Spence et al. 2007),
- Bubble emission in thrusters reduces the noise by 0–20 dB for frequencies above 100 Hz, but it possibly increases the noise for frequencies below 100 Hz (Spence et al. 2007), and
- An air bubble masker applied along a vessel hull reduces the noise by at least 10 dB for frequencies above 500 Hz, but it increases the noise (0–10 dB) for frequencies between 20–80 Hz (Spence et al. 2007).

3.9.2. Alternative Propulsion Designs

Alternatives to conventional direct-drive propulsion (i.e., propeller and rudder systems) can decrease noise. These technologies benefit from improved flow characteristics (i.e., less cavitation) and from reduced mechanical coupling of drive components to the hull. Another advantage is that they eliminate the need for conventional bow thrusters, which can be significant noise sources on direct-drive vessels.

3.9.2.1. Azimuth Propulsion

These systems (for example Z-drive and L-drive thruster systems), feature a conventional propeller mounted on the base of a 360° rotating pod affixed to the bottom of the vessel. Their main benefit is that they improve flow by separating the hull and the propeller. Azimuth thrusters offer greater flexibility in terms of hull placement than direct-drive propulsion. Azimuth propulsion also benefits from the cavitation control treatments described in the Section 3.9.1. Azimuth propulsion is currently in widespread use.

The likely noise reduction from this design is 5–10 dB (Spence et al. 2007).

3.9.2.2. Voith-Schneider Propulsion

Voith-Schneider propulsion is a unique technology that generates thrust using a rotating arrangement of vertical blades that protrude from a base mounted near the bottom of the hull. The blades have a lower turn rate than conventional propellers, and they may, therefore, be less susceptible to cavitation. Voith-Schneider propulsion also offers greater flexibility in terms of hull placement, similar to that of azimuth propulsion systems. This system is currently employed in many tug designs; however, it is more costly than conventional propulsion, and may be unsuitable for operations in very shallow water.

The likely noise reduction from this design is not currently know.

3.9.3. Machinery Noise Control

The main goal of machinery noise control is to decouple equipment vibrations from the structure of the vessel, which reduces airborne noise emissions from equipment. Noise from coupled equipment vibrations also radiates underwater. It substantially reduces structure-borne noise and vibration in vessel compartments, improving the comfort and longer-term well-being of crews. It also reduces mechanical fatigue on the vessel itself, thus reducing maintenance costs. While the primary goal is to benefit occupational health and vessel maintenance, this technique also reduces underwater noise.

3.9.3.1. Resilient Mounting

Resilient mountings are stiff, elastic, or elastomeric couplings that isolate equipment vibrations from the surfaces they are affixed to. They are most effective at reducing noise transmission at frequencies above 100 Hz. Resilient mountings are a mature and highly effective vibration isolation technology. For deck-mounted equipment, improved noise isolation can be achieved if the deck itself is resiliently mounted. If they are improperly installed or poorly maintained, however, they can worsen vibration problems. Resilient mountings are currently in widespread use. They are low cost, reduce maintenance, and improve crew comfort.

The likely noise reduction from this design is 0–25 dB (Spence et al. 2007).

3.9.3.2. Damping Layers

Applying a layer of damping material to surfaces before mounting equipment isolates vibration. Typically, decoupling cladding or constrained layers of viscoelastic material is used, with constrained layers being generally most effective. The greatest benefit is achieved when damping layers are used in combination with resilient mountings. Dampening layers can be costly to install and may increase vessel weight. They do, however, reduce maintenance and improve crew comfort.

The likely noise reduction from this design is 0–10 dB (Spence et al. 2007).

3.9.3.3. Low-noise Equipment

Different models of the same equipment often generate quite different noise and vibration levels; therefore, selecting inherently low-noise equipment will result in reduced underwater noise emissions. Diesel-electric engines may be quieter and more efficient than geared diesel engines, and they are ordinarily better suited to vibration isolation. Most manufacturers provide information regarding the noise emissions of their equipment. Low-noise equipment may be more expensive. One benefit of this equipment is that it improves crew comfort.

The likely noise reduction from this design is variable, but 5 dB is common (Spence et al. 2007).

3.9.3.4. Equipment Placement

Machinery generates more underwater noise when it is located in compartments adjacent to the hull. Noise transmission is generally reduced when equipment is situated toward the centerline of the vessel, away from the hull. The location of the engine room is an important consideration, since this compartment usually contains the largest and loudest vessel machinery. Replacing equipment may require large-scale modification of a ship's structure and thereby necessitate a complete refit, unless considered at the design stage.

The likely noise reduction from this design is unknown.

3.9.3.5. Acoustic Enclosures

Radiated noise can be mitigated by surrounding loud machinery in a sound-dampening enclosure. Acoustic enclosures are large, costly, and make equipment maintenance difficult. Situating noisy equipment inside a well-isolated engine room is usually a better option, and it provides similar advantages. One benefit of this equipment is that it improves crew comfort.

The likely noise reduction from this design is 10–20 dB (Spence et al. 2007).

3.10. Replacing Trans Mountain Tugs with Specialized Tugs

As discussed in Section 2.6, shipboard machinery is the main source of underwater noise produced by ship at speeds lower than the cavitation inception speed. Most large vessels or tugs in service today use diesel-powered internal combustion engines. However, alternatives, in the form of electric and hybrid-electric engines, now exist that provide some noise reduction benefits. Beyond the cavitation inception speed, as discussed in Appendix A.3.1, the gain from machinery noise mitigation measures is usually shadowed by cavitation noise.

3.10.1. Electric Tugs

Electric tugs use an electric motor driven by a battery pack. This system reduces the shipboard machinery components of the propulsion system, thus eliminating engine noise. Because the battery bank needs to be charged through onshore connection, electric tugs are best suited to smaller, short-range, low-speed operations, such as harbour-assist operations.

Electric engines are used on ferries and pleasure craft, but they are only recently started being used on tugs. Retro-fitting older tugs might be difficult since they might not have the space available for the required battery banks. The limitation in transit range may make this type of tug unpractical for use as escort tug based on the expected Trans Mountain shipping requirements. The benefits for electric tugs are that they eliminate fossil fuel consumption (unless a generator is used for off-grid charging), eliminate gas emissions, and improve crew comfort.

The amount of noise reduction would depend on the tug's speed. If the tug was moving below cavitation speed, then substantial noise savings could be achieved, as noise generation is limited to flow interaction with hull features.

3.10.2. Hybrid-electric Tugs

A marine hybrid-electric system includes an internal combustion engine, a generator, an electric storage unit, and an electric motor. These tugs can use the internal combustion engine and electric motor separately or together, depending on their operational mode. This allows tugs to maximize each system's efficiency, to reduce fuel consumption and gas emissions, and to minimize their acoustic footprint. They are more versatile than all-electric tugs. Their noise reduction characteristics depend on the operational mode (namely if and how the internal combustion engine is running), but they are generally noisier than all-electric tugs.

The amount of noise reduction depends on their speed and operational mode. If the tug is moving below cavitation speed and using only its electric system, noise is mainly created by flow interaction with hull features.

Hybrid-electric tugs are used in Europe and the United States. They are becoming more popular as harbour managers consider ways to reduce environmental footprints. The noise signature of hybrid electric vessels (gas engine running electric generator, powering electric drive motors) has been measured at the ULS (JASCO, unpublished data). Once publicly available, these measurements could provide insight into the potential benefits of equipping tugs with hybrid-electric engines.

Diesel-electric (a form of hybrid-electric) propulsion systems are used in cruise ships (Kipple 2002). At low speed (e.g., ~10 knots), noise levels produced by cruise ships equipped with these systems are generally higher than cruise ships with conventional propulsion systems. However, hybrid vessels showed less noise dependency to speed, making them substantially quieter at greater speeds (e.g., 15 and 19 knots; Kipple 2002).

3.11. Changing Ship Designs

A recent study estimated that the cost of engineering and mechanical work to reduce noise by propeller design for a new vessel could be from 1–5% of the total cost of the commercial vessel (Spence and Fischer 2017). Similarly, the total cost for machinery noise control devices would be ~1–5% of the cost of the vessel. In both cases, retrofitting with a quiet propeller or installing treatments (for machinery noise) will be more costly than including these options at the design phase (Spence and Fischer 2017).

The two critical components influencing cavitation performance are the propeller design itself and how the wake is managed. The wake is influenced by the shape of the hull. Careful propeller and hull designs are essential for improving the cavitation performance. For new ships, the wake flow can be improved by more careful design, which requires an increased design effort, including careful model testing and computational fluid dynamic analysis.

Predicting noise for newly built ships could be valuable in ensuring that they are as quiet as possible. Kellett et al. (2013) reported that waiting until the ship is fully designed and built before taking measurements leaves little room for alteration and improvement. They suggested building a numerical noise prediction model to predict the noise of a newly built vessel. Such models would be of increasing value if validated by empirical full-scale measurements.

3.11.1. Propellers

The first aspect to consider is whether the propeller has been designed for the actual operating conditions. In many cases, propellers are optimized for the service speed and full load condition in calm water. In practice, a ship often operates at a reduced speed and draught, and in less than ideal sea conditions.

For a given ship fitted with a fixed pitch propeller, reducing the speed decreases the overall noise (Kipple 2002). Ships with controllable pitch propellers or with thrusters are unlikely to exhibit the same reduction in noise with speed. In many cases, the noise from those ships may actually increase when they operate at reduced speed due to face cavitation, unless they are fitted with new propellers designed for the lower speed.

3.11.2. Changes to the Hull Form

Numerical methods, such as computational fluid dynamics tools used in early design stages, could optimize hull forms for noise reduction. A well-designed hull form requires less power for a given speed, which likely results in less underwater noise. Moreover, a well-designed hull form provides a more uniform inflow to the propeller, thereby increasing the propeller efficiency and reducing noise and vibration caused by an uneven wake flow.

3.12. Changing Ship Maintenance

The ship maintenance procedures that reduce or control noise primarily involve regularly cleaning and maintaining the propeller, engines, and hull (Baudin et al. 2015, Audoly et al. 2016).

McKenna et al. (2013) suggested that tonal components of ship sounds may be related to propeller damage, and these sounds contribute greatly to the radiated underwater noise of ships. Regularly inspecting and repairing propellers increases the inception speed of cavitation (Spence and Fischer 2017) and reduces noise resulting from the propeller and propeller shaft or thruster movements.

Regularly cleaning and maintaining the hull reduces friction noise from water flow (Hollenbach and Friesch 2007). Combined with regularly cleaning and maintaining the propeller, hull maintenance increases fuel efficiency and reduces noise output (Baudin and Mumm 2015). Cleaning and polishing has been shown to smooth the hull and propeller surface, which controls noise. Routinely applying anti-fouling agents or coatings maintains smoothness longer, thereby maintaining lower noise emission (Southall 2005, Baudin and Mumm 2015).

Engine vibration is another source of noise that can be reduced by regular maintenance (Spence et al. 2007).

In general, ships following a regular cleaning and repair routine can run at higher speeds with lower fuel consumption and lower noise emission than ships with irregular or few maintenance periods (Baudin and Mumm 2015). Overall, regular ship maintenance is expected to reduce noise output between 0.5 to 3.5 dB (Baudin and Mumm 2015).

3.13. Changing Operator Behaviour

While operator behaviour is intuitively an important component of ship noise mitigation, given that operators are controlling vessel operations, there is little mention of specific behaviours that can reduce noise in the reviewed literature. Using vague terms, such as ‘optimized ship handling’, Audoly et al. (2017) referred to operational changes as beneficial for noise mitigation; however, the authors did not explain what is involved in optimization.

Operational factors that seem to be important are the load and speed. The load of a vessel appears to affect the noise output: partially loaded vessels (i.e., in ballast condition) have higher noise outputs due to lower hydrostatic pressures acting on the propeller higher in the water column causing more cavitation (André et al. 2011). In addition, propeller efficiency is optimized for vessels with full loads travelling in calm seas. Therefore, engine noise potentially increases when travelling the same speed without a full load (Renilson et al. 2013). These ideal conditions hardly ever exist in the real world, and vessel operators could be trained to operate their vessels optimally by varying speed based on environmental conditions and percentage of load, for the purpose of reducing noise emissions. This could include operating their vessels just below cavitation inception speed whenever possible, especially when in critical habitat (Spence and Fischer 2017). The actual inception speed can be increased with frequent propeller and hull maintenance regimes, as mentioned in Section 3.12. Another technique involves using air injectors near the propellers, which may reduce noise output when air is injected if a vessel is not fully loaded (IMO 2014).

Quick acceleration above optimal cruising speed is also a potential source for increased noise levels (Audoly et al. 2016), and so is selecting the optimal trim for sea conditions and speed (Hollenbach and Friesch 2007, IMO 2014, Baudin and Mumm 2015). Operators should pay special attention to trim conditions and when and how to speed up. If possible, ships should be equipped with a trim optimization aid (Baudin and Mumm 2015). Vessels equipped with a controllable pitch propeller do not reduce noise output linearly with reduced propeller speed. To minimize noise emission, it is important for vessels with controllable pitch propeller to operate with the optimal shaft speed for design propeller pitch (Baudin and Mumm 2015).

Within the narrower waterways of the Salish Sea, it may also be useful to have a Marine Mammal Observer (MMO) on the bridge, in addition to the coast pilot responsible for safe navigating. An MMO familiar with the area could keep in contact with whale watch operators and others with knowledge of SRKW presence. The MMO could alert the pilot of whales nearby.

3.14. Changing Shipping Practices

Planning the spatial arrangement and timing of commercial vessel traffic might reduce noise. Other changes in shipping practices, including changes related to vessel load, speed reductions, temporal closures, and convoying, are presented individually elsewhere in this report; they will only be addressed here in combination with marine traffic planning.

Marine traffic planners make recommendations to ship traffic regulators to arrange port arrival and departure times of vessels. They can make recommendations to manage traffic composition to minimize noise presence in sensitive habitat areas (Audoly et al. 2017). Specific measures resulting from spatial and temporal traffic management could result in grouping vessels with lower underwater noise emission and spacing vessels with higher noise emission farther apart (Baudin and Mumm 2015, Williams et al. 2015, McKenna et al. 2017).

Other regulatory mechanisms to impose changes in shipping practices and reduce noise include forbidding vessels with a certain gross tonnage and a noise level above a set threshold from entering sensitive areas (Redfern et al. 2017), and applying temporal area closures for all motorized vessels (McKenna et al. 2017). These measures are unlikely to affect the majority of commercial vessels travelling in shipping lanes, but may require vessels, such as cruise ships travelling into sensitive areas, to either re-route or slow down (McKenna et al. 2017). This measure would improve noise conditions in localized areas and could increase sound levels in other areas due to re-routing. Such regulations may, however, lead to an increase in retro-fitting vessels with quieting measures (Hatch et al. 2008). Similarly, speed reductions in sensitive areas where vessels travel often (i.e., several times daily such as along ferry routes) could immediately reduce the overall noise level in those areas.

The effects of speed reductions in choke points (i.e., slow-down in areas with high densities of ships and animals) are modelled in Section 3.3. An alternative approach to slow-down zones is to apply temporal changes in speed limits between locations with changes in animal occurrence, such as discussed in Section 3.15. In addition to the notification method described in Section 3.15, a traffic control system (flashing lights warning ships of animal presence) could be installed in choke points (e.g., Haro Strait, Boundary Pass, and Active Pass for SRKW). The traffic control system could be used to regulate the speed of commercial vessels, but it could also limit access of other vessel classes to sensitive habitats.

3.15. Applying Real-time Mitigation in Hot Spots

In many cases, measures referred to as “real-time mitigation” do not focus on mitigating noise, but on mitigating the risk of vessels striking marine animals (Ward-Geiger et al. 2005, Silber et al. 2012). Underwater acoustic observatories can perform real-time detection of vocalizing marine mammals to identify their presence near shipping lanes. Those detections could be used to establish temporary speed or navigation mitigations that would have less effect on shipping industry than full-time limits. Some observatories, such as the Port of Vancouver ECHO program’s ULS, can also measure noise emission levels of vessels that arrive at the port. This is potentially useful for programs that provide incentives to quieter vessels. Systems like this are promising tools for real-time noise mitigation in some coastal areas (Simard et al. 2006, Zaugg et al. 2010, André et al. 2011, Moloney et al. 2014).

Data collection and automated analysis technology may allow real-time mitigation of noise exposure of animals around underwater listening stations, by using automated ship/pilot notification of animal presence. These notifications could initiate appropriate vessel operation around the animals and in areas of expected presence, and, therefore, reduce noise output. This type of alert system is already used in whale strike reduction management tools at several locations.

Currently, whale presence notifications are sent to ships travelling through a sensitive whale area via specialized communications systems, such as satellite internet or telex or via Automated Identification Systems (AIS). The alert systems are part of the Mandatory Ship Reporting System (MSRS) in the right whale critical habitat off Massachusetts and Florida (Ward-Geiger et al. 2005). The MSRS, an IMO sanctioned management tool to reduce whale strikes, requires ships entering a whale-sensitive area to report the vessel name, call sign, course, speed, location, destination, and route (waypoints). In return, the system automatically sends whale locations established via acoustic monitoring and appropriate vessel operations including speed limits to reduce strike risk.

There is a relationship between the relative distance of vessels and noise levels received by the animal, which can be deduced based on propagation loss and the animal’s hearing ability (Hatch et al. 2008). Similar to the ship strike alerts system, a noise mitigation alert system would alert ships with regularly updated information on animal presence, anticipated travel direction based on modelling of typical animal behaviour, and guidance on vessel operating procedures within sensitive habitat areas. Speed limits are a common management tool for reducing ship strikes in areas with a high density of whales (Russell et al. 2001, Ward-Geiger et al. 2005). Speed limits could also be used to reduce noise exposure in sensitive areas (Baudin et al. 2015). The resulting noise reductions would be proportional to the reduction in source level due to lower speed, minus the increase in exposure due to the increase in the time it takes for a vessel to clear the sensitive area.

Real-time mitigation using acoustic monitoring systems is limited by the system’s detection accuracy. All automated acoustic animal detection algorithms produce some errors in the form of false positive (animals are detected but not present) and false negative (animals are present but not detected) detections (Mouy et al. 2009). The error rate usually increases with higher ambient noise levels, which would limit the distance where animals can be detected with high accuracy in areas and times with high ambient sound levels, such as areas with dense ship traffic. Accuracy also differs with environmental conditions because rain, wind, and sea state affect ambient noise levels, and those conditions differ by season. The ambient noise level affects signals with different spectral composition differently. For example, detecting high-frequency echolocation clicks may not be affected as strongly by low-frequency than high-frequency ambient noise. These limitations are important for SRKW because many areas within their critical habitat are characterized by high ambient sound levels. While SRKW signals contain spectral components that differ from most ambient sounds, their detection distance is mostly affected by the travel distance of the lower-frequency component of the signal (Miller 2006), where ambient sound is loudest.

Another limitation dependents on an animal's acoustic behaviour and behaviour state. Whales and other marine mammals are often silent and, therefore, undetectable by acoustic monitoring. Acoustic signalling rates vary greatly, depending on the activity that the animals engage in (e.g., foraging/travelling versus socializing versus resting). For example, the SRKW vocalization rate is high in social contexts, when foraging, and sometimes when travelling. The rate is much lower when the animals travel slowly, and SRKW may be completely silent when resting (e.g., Ford 1989). The vocalization rate may not always be a good indicator of possible disturbance, however, since whales may be most easily disturbed when resting. The vocalization rate is also affected by group size, which is lower in single pod encounters versus multi-pod encounters. Single pod encounters are much more common in late fall, winter, and early spring, when ambient noise is generally higher than in summer.

Visual observers may therefore be needed to augment acoustic animal detections in sensitive areas and hotspots. A project to improve the detection of non-vocal SRKW and small vessels was conducted by researchers from the University of Victoria as part of the Noise Exposure to the Marine Environment from Ships (NEMES) project funded by the Marine Environmental Observation, Prediction and Response Network (MEOPAR). It uses camera images taken at regular intervals at underwater listening stations, to assess detection accuracy of whales and to report the presence of small vessels. The study is ongoing and initial results are encouraging in that the method may allow ground-truthing of acoustic detections (L. McWhinnie, pers comm. August 2017).

3.16. Adjusting Traffic Lanes

This section presents a qualitative analysis of possible changes in noise levels due to shifting traffic lanes in areas other than Haro Strait, Juan de Fuca Strait, and Swiftsure Bank. This analysis is based on a literature review and on modelled results from the shifting of vessel traffic presented in Section 3.7.

In 2014, the IMO released non-mandatory guidelines asking owners, operators, and regulatory bodies of their member states to mitigate commercial ship noise. Even before the guidelines were released, studies on the impact of noise on whales suggested that certain ship strike mitigation methods may also reduce noise exposure (e.g., Hatch et al. 2008). Researchers, conservation managers, and the IMO have considered ships striking whales a serious problem for many years (Jensen et al. 2004). Attempts to mitigate ship strikes lead to several specifically mandated actions (Silber et al. 2012). Among those actions was geographically moving traffic lanes to account for marine spatial planning for whales.

The goal of adjusting traffic lanes is to increase the separation between vessel traffic and animals. Shipping lane adjustments, which include moving shipping lanes geographically, have been primarily discussed as a regulatory measure to avoid collisions between animals and ships or to lower the potential risk of ship strikes in areas of high animal density (Russell et al. 2001, Vanderlaan et al. 2008, Abramson et al. 2009, Silber et al. 2009, Silber et al. 2012, Wiley et al. 2016). Noise exposure reduction can be a another effect of moving shipping lanes, with benefits such as reducing high noise level concentration in sensitive areas (e.g., foraging or breeding areas; Haren 2007, Hatch et al. 2008, Baudin and Mumm 2015, McKenna et al. 2017) and/or decreasing cumulated noise levels in the soundscape of a larger area and thereby improving the acoustic quality of a habitat (Chion et al. 2017, Redfern et al. 2017).

Shipping lane adjustments have been implemented in a few locations around the world, but the direct effects in sound exposure to marine life have not been fully studied. For example, to reduce the risk of collisions between ships and North Atlantic right whales, the shipping lanes leading traffic into Boston Harbour that traverse through a Marine Protected Area (Stellwagen Bank Marine National Sanctuary) were moved based on whale distribution and oceanographic factors, as seen in Figure 209. Moving the shipping lane to an area with lower expected whale density also increased the average distance of most whales from the ship noise sources, thereby potentially reducing noise exposure for whales in the Sanctuary. This reduction is inferred from the spatial distribution pattern of whales, but the difference in received levels before and after the change in shipping lanes has not been measured. Hatch et al. (2008) reported that the median received levels over the most important shipping noise bandwidth (10–1000 Hz) varied by 3 dB between quietest and loudest locations in the Sanctuary, and the loudest locations were closest to the Boston shipping lanes. Since other noise mitigation measures, such as reducing vessel speed in the Sanctuary, were implemented at the same time, the direct effect of the change in shipping lanes cannot be established. Nevertheless, the experience gathered from studying acoustic impact of shipping lanes on the soundscape of North Atlantic right whales has been used to consider changes in shipping lanes in other areas, such as the entry in the San Francisco Bay, to reduce both ship strike risk and noise impact on blue and fin whales (Joint Working Group on Vessel Strikes and Acoustic Impacts 2012).

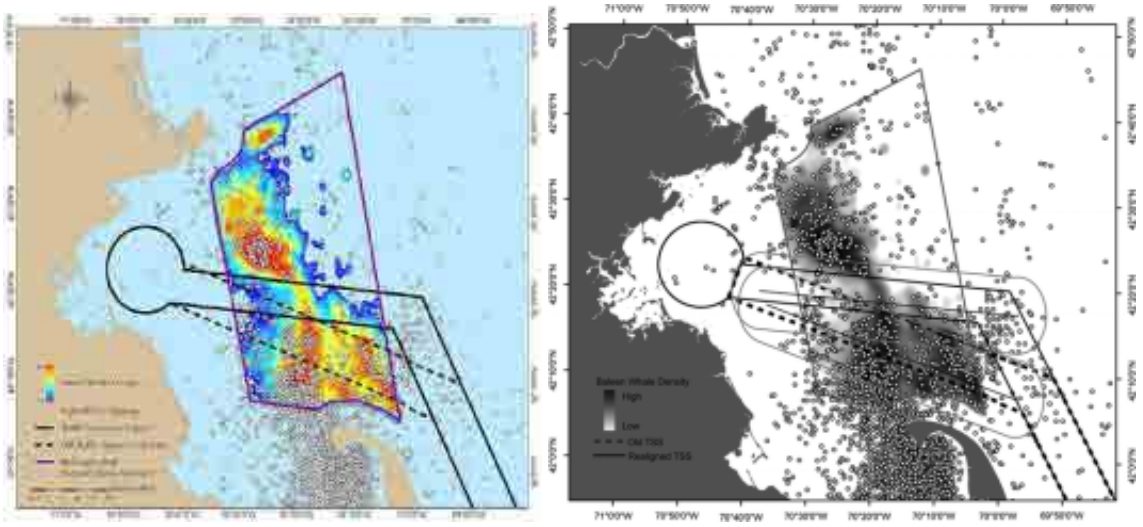

Figure 209. (Left) Traffic Separation Scheme change through Stellwagen Bank National Marine Sanctuary (map from Wiley et al. 2006, courtesy of NOAA). (Right) Change in ensonified areas above 120 dB re 1 µPa (rectangular shapes with rounded short sides) based on a simple propagation loss calculated from the centre by Hatch et al. (2008).

The first steps in developing ship traffic management regulations to reduce impact on whales are to identify temporal and spatial overlaps between animal occurrence and shipping routes and to establish a spatial or temporal profile for the animals' habitat preference in an area that overlaps with shipping routes (Berman-Kowalewski et al. 2010, Hazen et al. 2016).

If research establishes that:

- The area is characterized by a high animal density at certain times of the year or year-round, and/or
- Oceanographic and biological data support a high expectancy of animal presence in the area (Hazen et al. 2016),

then a high risk of mortality due to ship strikes is likely, and so is a high risk of disturbance due to noise exposure from ships (Hildebrand 2005).

A detailed analysis of resident key species density and habitat quality in both areas (current and proposed traffic lane locations) is necessary for assessing if there are sufficient benefits from moving and/or separating shipping lanes. Acoustic monitoring may allow rough density estimates of key species that are present during a recording (Ford 1991).

Based on the results for shifting vessel traffic in Haro Strait, Juan de Fuca Strait, and Swiftsure Bank, presented in Section 3.7, it is expected that moving traffic lanes would result in little to no decrease in noise levels over the entire studied area. This is because the same amount of traffic would continue to pass through the region, but along a different path. However, the changes in noise levels would be localized. A decrease would be expected along the old shipping lane location; similarly, there would be an increase in sound levels at the new shipping lane location. The amount by which the noise level increases or decreases is highly dependant on the environment and the amount of traffic removed/added to an area.

3.17. Using Larger Vessels

Length is a proxy for a vessel's gross tonnage and, therefore, the amount of cargo a vessel transports (i.e., longer vessels can move greater amounts of goods). Generally, larger vessels (longer, greater gross tonnage, and deeper draft) have higher noise outputs than smaller ones, especially at frequencies below 1 kHz (Richardson et al. 1995). A possible increase in noise level could be compensated for, however, by reducing the number of transits required to move the same amount of goods.

The relationship between vessel length and broadband noise level is complex and varies between vessel classes. Propeller cavitation and hull vibration due to internal machinery are the main sources of vessel noise. Since vessels of the same length and class can have different hull designs, propeller type and size, and internal components, their broadband noise levels can also be different. For example, Kipple and Gabriele (2007) estimated noise emission from vessels entering Glacier Bay, AK. Generally, ships longer than ~183 m (600 ft) were large cruise ships, while ships between 30 and 76 m (100 and 250 ft) were mostly tour boats entering the Bay daily. Estimated source levels from large cruise ships (indicated as "more than 600 ft" in Figure 210) were lower than for tour boats (indicated as "100 to 250 ft" in Figure 210) transiting at the same speed. The broadband source levels for each vessel length class also varied by at least 10 dB.

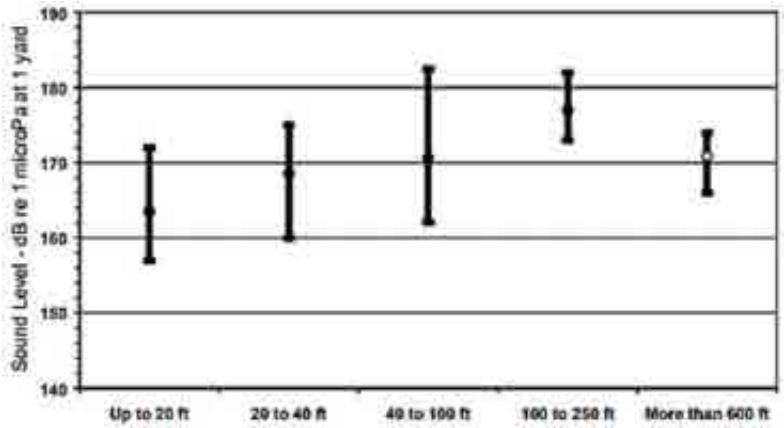

Figure 210. Estimated sound source levels of vessels entering in Glacier Bay, AK, at speed of 10 knots (figure from Kipple and Gabriele 2007).

McKenna et al. (2013) investigated the relationship between ship length, gross tonnage, horse power, service speed (the speed the ship was designed to travel with max efficiency), actual speed, draft, and oceanographic conditions. Their work supports earlier suggestions of a positive relationship between speed (service and actual) and length with broadband noise levels. Although variation in actual speed explained most noise level variations in all estimated frequency bands, vessel length was the second most important parameter. The authors presented positive relationships between vessel length, gross tonnage, and draft. Therefore, length can be considered as a proxy for the amount of cargo a vessel can transport. The study also showed considerable variation in source levels among ships of the same size and between measurements of the same ship. Thus, factors other than size, such as speed and the year a vessel was of built, are also correlated to noise levels. These results match findings made by JASCO (unpublished results) from an underwater listening station in the Strait of Georgia.

Multivariate statistical analysis on a large number of vessels, for multiple commercial classes, is required to estimate the relationship between vessel size (i.e., length) and source level spectra. An increase in the proportion of larger container vessels could reduce the number of transits, which could mean an overall reduction in average noise levels. Such analysis could be used to determine the number and size of vessels required to reduce noise level over a large area. The vessel size may, however, be limited because of the available water space along the commercial route and/or the port's facilities.

4. DISCUSSION

Section 4.1 discusses the overall effectiveness of each mitigation approach. Section 4.2 discusses the regional effectiveness of each approach.

4.1. Summary of Mitigation Effectiveness

The results for each assessed mitigation approach are summarized below. Tables 71 and 72 present a spatial analysis of the differences between one-month average baseline levels and one-month average levels for each mitigation approach. The percentiles and mean changes in noise levels (dB) and acoustic intensity (%) were calculated over all grid cells for each Local Study Area. These values may be used to assess the spatial effectiveness of the mitigation approaches over a large area.

Table 71. *Unweighted*: Spatial analysis of the differences in one-month average noise level (dB) and acoustic intensity (%) for each mitigation approach. The values indicate the percentile or mean of the differences over all grid cells in each Local Study Area.

Scenario		Area	Spatial changes in noise level (dB) and acoustic intensity (%)			
			5th	50th	95th	Mean
Future unmitigated		Strait of Georgia	0.00 (0.0%)	0.00 (0.0%)	+0.65 (+16.2%)	+0.13 (+3.1%)
		Haro Strait	0.00 (0.0%)	+0.38 (+9.1%)	+0.86 (+21.9%)	+0.38 (+9.1%)
		Juan de Fuca Strait	+0.29 (+6.9%)	+0.53 (+13.0%)	+0.71 (+17.7%)	+0.52 (+12.7%)
		Swiftsure Bank	+0.07 (+1.6%)	+0.43 (+10.3%)	+0.68 (+16.9%)	+0.4 (+9.8%)
Slow-down	11 knots	Strait of Georgia	−0.87 (−18.1%)	0.00 (0.0%)	0.00 (0.0%)	−0.14 (−3.1%)
		Haro Strait	−2.44 (−43.0%)	−0.34 (−7.5%)	0.00 (0.0%)	−0.76 (−16.1%)
		Juan de Fuca Strait	−2.22 (−40.0%)	−0.53 (−11.5%)	+0.51 (+12.4%)	−0.57 (−12.4%)
		Swiftsure Bank	−2.30 (−41.1%)	−0.23 (−5.2%)	+0.36 (+8.6%)	−0.54 (−11.7%)
	10 knots	Haro Strait	−3.26 (−52.8%)	−0.50 (−10.9%)	0.00 (0.0%)	−1.04 (−21.3%)
	7 knots	Haro Strait	−6.03 (−75.1%)	−1.01 (−20.7%)	−0.01 (−0.2%)	−1.90 (−35.4%)
	11 and 15 knots	Strait of Georgia	−0.48 (−10.4%)	0.00 (0.0%)	+0.02 (+0.5%)	−0.06 (−1.3%)
		Juan de Fuca Strait	−1.24 (−24.9%)	−0.22 (−5.0%)	+0.54 (+13.3%)	−0.19 (−4.4%)
		Swiftsure Bank	−1.27 (−25.3%)	−0.09 (−2.1%)	+0.41 (+9.9%)	−0.19 (−4.3%)
No-go*	Restricted period (midnight to 04:00)	Haro Strait	−19.57 (−98.9%)	−11.40 (−92.8%)	−2.59 (−44.9%)	−11.13 (−92.3%)
	Unrestricted period (04:00 to midnight)	Haro Strait	+0.13 (+3.0%)	+1.03 (+26.8%)	+1.70 (+47.9%)	+0.98 (+25.3%)
Replacing 10%	Vessels ranked by unweighted source level	Strait of Georgia	−1.43 (−28.0%)	−0.61 (−13.0%)	−0.03 (−0.6%)	−0.64 (−13.6%)
		Haro Strait	−1.19 (−24.0%)	−0.39 (−8.6%)	−0.01 (−0.1%)	−0.47 (−10.2%)
		Juan de Fuca Strait	−1.41 (−27.8%)	−0.64 (−13.7%)	−0.02 (−0.4%)	−0.64 (−13.8%)
		Swiftsure Bank	−1.42 (−27.8%)	−0.56 (−12.2%)	−0.03 (−0.8%)	−0.63 (−13.5%)
	Vessels ranked by weighted source level	Strait of Georgia	−0.64 (−13.7%)	−0.19 (−4.2%)	+0.18 (+4.1%)	−0.22 (−5.0%)
		Haro Strait	−0.38 (−8.4%)	−0.06 (−1.4%)	+0.35 (+8.4%)	−0.06 (−1.3%)
		Juan de Fuca Strait	−0.23 (−5.2%)	−0.01 (−0.1%)	+0.26 (+6.3%)	+0.02 (+0.5%)
		Swiftsure Bank	−0.41 (−9.1%)	−0.11 (−2.4%)	+0.24 (+5.7%)	−0.09 (−2.1%)
Reducing source level by 3 dB		Strait of Georgia	−2.83 (−47.8%)	−1.64 (−31.4%)	−0.07 (−1.5%)	−1.48 (−29.0%)
		Haro Strait	−2.39 (−42.3%)	−1.57 (−30.3%)	−0.21 (−4.8%)	−1.48 (−28.9%)
		Juan de Fuca Strait	−2.44 (−43.0%)	−2.23 (−40.1%)	−0.96 (−19.8%)	−2.00 (−37.0%)
		Swiftsure Bank	−2.56 (−44.5%)	−2.21 (−39.9%)	−0.85 (−17.7%)	−1.99 (−36.7%)
Reducing source level by 6 dB		Strait of Georgia	−5.54 (−72.1%)	−2.96 (−49.4%)	−0.10 (−2.3%)	−2.83 (−47.8%)
		Haro Strait	−5.22 (−69.9%)	−3.03 (−50.3%)	−0.34 (−7.6%)	−3.03 (−50.2%)
		Juan de Fuca Strait	−5.33 (−70.7%)	−4.92 (−67.8%)	−1.77 (−33.4%)	−4.30 (−62.9%)
		Swiftsure Bank	−5.42 (−71.3%)	−4.66 (−65.8%)	−1.48 (−28.9%)	−4.12 (−61.3%)
Shifting vessel traffic		Haro Strait	−3.37 (−54.0%)	+0.06 (+1.4%)	+3.64 (+131.2%)	+0.11 (+2.6%)
		Juan de Fuca Strait	−2.60 (−45.0%)	+0.53 (+13.0%)	+3.33 (+115.4%)	+0.22 (+5.1%)
		Swiftsure Bank	−3.43 (−54.6%)	+0.12 (+2.9%)	+2.34 (+71.5%)	+0.04 (+1.0%)

* Results compared to Baseline scenario calculated over the same period (midnight to 04:00 or 04:00 to midnight).

Table 72. *Audiogram-weighted*: Spatial analysis of the differences in one-month average noise level (dB) and acoustic intensity (%), for each mitigation approach. The values indicate the percentile or mean of the differences over all grid cells in each Local Study Area.

Scenario		Area	Spatial changes in noise level (dB) and acoustic intensity (%)			
			5th	50th	95th	Mean
Future unmitigated		Strait of Georgia	0.00 (0.0%)	0.00 (0.0%)	+0.60 (+14.8%)	0.00 (0.0%)
		Haro Strait	0.00 (0.0%)	+0.07 (+1.6%)	+1.11 (+29.1%)	+0.30 (+7.2%)
		Juan de Fuca Strait	+0.02 (+0.5%)	+0.33 (+7.9%)	+1.06 (+27.5%)	+0.44 (+10.7%)
		Swiftsure Bank	0.00 (0.0%)	+0.12 (+2.9%)	+1.12 (+29.6%)	+0.32 (+7.6%)
Slow-down	11 knots	Strait of Georgia	−0.24 (−5.5%)	0.00 (0.0%)	+0.08 (+2.0%)	−0.10 (−2.2%)
		Haro Strait	−1.21 (−24.3%)	−0.01 (−0.2%)	+0.25 (+5.9%)	−0.17 (−3.8%)
		Juan de Fuca Strait	−1.29 (−25.7%)	−0.01 (−0.3%)	+0.82 (+20.8%)	−0.04 (−0.9%)
		Swiftsure Bank	−1.22 (−24.5%)	0.00 (0.0%)	+0.69 (+17.3%)	−0.06 (−1.3%)
	10 knots	Haro Strait	−1.60 (−30.8%)	−0.01 (−0.2%)	+0.15 (+3.5%)	−0.26 (−5.8%)
	7 knots	Haro Strait	−2.69 (−46.2%)	−0.05 (−1.1%)	0.00 (0.0%)	−0.52 (−11.3%)
	11 and 15 knots	Strait of Georgia	−0.08 (−1.7%)	0.00 (0.0%)	+0.21 (+5.0%)	−0.06 (−1.4%)
		Juan de Fuca Strait	−0.52 (−11.3%)	+0.01 (+0.2%)	+0.89 (+22.7%)	+0.14 (+3.2%)
		Swiftsure Bank	−0.59 (−12.7%)	0.00 (0.0%)	+0.81 (+20.5%)	+0.08 (+2.0%)
No-go*	Restricted period (midnight to 04:00)	Haro Strait	−9.99 (−90.0%)	−3.90 (−59.3%)	−0.17 (−3.8%)	−4.35 (−63.3%)
	Unrestricted period (04:00 to midnight)	Haro Strait	+0.01 (+0.2%)	+0.37 (+8.9%)	+1.82 (+52.1%)	+0.62 (+15.3%)
Replacing 10%	Vessels ranked by unweighted Source Level	Strait of Georgia	−0.05 (−1.0%)	+0.04 (+0.9%)	+0.38 (+9.2%)	0.00 (0.0%)
		Haro Strait	−0.01 (−0.3%)	+0.04 (+1.0%)	+0.73 (+18.3%)	+0.17 (+3.9%)
		Juan de Fuca Strait	+0.01 (+0.2%)	+0.15 (+3.6%)	+0.66 (+16.4%)	+0.25 (+6.0%)
		Swiftsure Bank	−0.12 (−2.7%)	+0.06 (+1.3%)	+0.70 (+17.6%)	+0.15 (+3.6%)
	Vessels ranked by weighted Source Level	Strait of Georgia	−1.98 (−36.7%)	−0.77 (−16.3%)	0.00 (0.0%)	−0.94 (−19.4%)
		Haro Strait	−1.63 (−31.3%)	−0.42 (−9.3%)	−0.01 (−0.3%)	−0.56 (−12.1%)
		Juan de Fuca Strait	−1.84 (−34.5%)	−1.18 (−23.8%)	−0.05 (−1.1%)	−1.01 (−20.7%)
		Swiftsure Bank	−2.00 (−36.9%)	−0.98 (−20.2%)	−0.05 (−1.1%)	−0.97 (−20.0%)
Reducing Source Level by 3 dB		Strait of Georgia	−2.72 (−46.6%)	−1.00 (−20.6%)	0.00 (0.0%)	−1.22 (−24.5%)
		Haro Strait	−1.66 (−31.8%)	−0.52 (−11.2%)	−0.02 (−0.4%)	−0.63 (−13.5%)
		Juan de Fuca Strait	−2.20 (−39.8%)	−1.48 (−28.8%)	−0.06 (−1.5%)	−1.24 (−24.9%)
		Swiftsure Bank	−2.42 (−42.7%)	−1.26 (−25.2%)	−0.07 (−1.6%)	−1.21 (−24.3%)
Reducing Source Level by 6 dB		Strait of Georgia	−5.25 (−70.2%)	−1.74 (−33.1%)	−0.01 (0.0%)	−2.16 (−39.1%)
		Haro Strait	−3.55 (−55.9%)	−0.93 (−19.4%)	−0.03 (−0.6%)	−1.29 (−25.7%)
		Juan de Fuca Strait	−4.58 (−65.2%)	−3.12 (−51.2%)	−0.11 (−2.5%)	−2.61 (−45.2%)
		Swiftsure Bank	−4.89 (−67.6%)	−2.50 (−43.8%)	−0.11 (−2.5%)	−2.44 (−43.0%)
Shifting vessel traffic		Haro Strait	−2.80 (−47.5%)	0.00 (0.0%)	+3.99 (+150.6%)	+0.28 (+6.7%)
		Juan de Fuca Strait	−2.56 (−44.5%)	+0.12 (+2.7%)	+2.94 (+96.9%)	+0.22 (+5.2%)
		Swiftsure Bank	−2.71 (−46.4%)	0.00 (0.0%)	+2.37 (+72.6%)	+0.14 (+3.4%)

* Results compared to Baseline scenario calculated over the same period (midnight to 04:00 or 04:00 to midnight).

4.1.1. Slowing Down Vessels

This modelled mitigation approach applied a slow-down zone along a portion of the traffic lanes in each Local Study Area. The slow-down zones where commercial vessels would be required to limit their speed are shown in Figure 10. Different alternatives were studied: vessel density and speed data from the future unmitigated scenario were modified to simulate traffic slowing down to a maximum speed of 11, 10, and 7 knots through Haro Strait, vessels through the other Local Study Areas were simulated at a maximum speed of 11 knots, and class-dependent speeds of 11 and 15 knots.

This mitigation approach would result in a general decrease in noise from the baseline levels along the traffic lanes within the slow-down and transition zones. For example, at Sample location 7 in Haro Strait, located in the inbound traffic lane, unweighted levels would decrease by 2.4–6.3 dB below baseline levels and audiogram-weighted levels by 1.9–4.0 dB below baseline levels, depending on the speed limit. Figures 46–51 show that the same increase in noise levels as for the future unmitigated scenario was estimated along the traffic lanes outside the studied slow-down zones. This increase is due to the additional traffic associated with the Trans Mountain project. The large decrease in noise levels in the northern region of the Haro Strait slow-down zone (e.g., dark blue region seen in Figures 46–51) was caused by the slowing of ferry traffic from Anacortes, WA, to Sidney, BC. These ferries participated in the slow-down trial organized by the Port of Vancouver in 2017 (Port of Vancouver 2018); they are expected to adhere to a slow-down limit.

Generally, these results indicate that, even with the increased tanker and tug traffic proposed by the Trans Mountain project, future unmitigated monthly-averaged noise levels in and near the slow-down zone could be lower than current noise levels.

This effect is not as important, however, when SRKW audiogram-weighting is applied. Since future tankers and tugs are expected to be tethered in the outbound transit, their expected maximum speed was limited to 10 knots. Thus, they would be unaffected by the 11 and 10 knot limits in the slow-down zone. While these classes of vessels are not as loud as others at low frequencies, they are louder than most at high frequencies. Thus, they have a larger influence on the audiogram-weighted than the unweighted sound field, as discussed in Sections 2.2.3.3 and 2.5. Consequently, the mitigated results show an increase in audiogram-weighted sound levels along the traffic lanes relative to baseline levels, within the slow-down zone.

The time-dependent results, applying a speed limit of 11 knots in each Local Study Area, are easiest to understand using the bar plots presented in Figures 42–43, 61–62, 79–80, and 96–97. They show that noise levels were reduced only at the sample locations closest to the slow-down zones. An increase in the 5th percentile can be seen at many sample locations, such as in Figure 61 showing this increase at all sample locations in Haro Strait. This indicates that the lower noise levels (i.e., levels close to current ambient levels) will be perceived less often than they currently are, which is related to the fact that vessels spend more time in the area due to their slower speed. A decrease in the 50th percentile indicates that half of the time, future mitigated levels will be lower than the baseline levels. This decrease is seen at most sample locations, in all regions.

Although it is known that changing a vessel's speed changes its noise level, the exact frequency-dependent relationship for various vessel classes is difficult to establish. In this study, source levels from vessels at slower speeds were simulated by reducing the levels by a fixed amount at all frequencies, as described in Appendix C. With more available data, a frequency dependence in the relation between vessel source level and speed may be established. This relationship might change the audiogram-weighted results for the slow-down mitigation approach.

4.1.2. Implementing a No-go Period

This modelled mitigation approach assessed restricting commercial vessels from transiting in Haro Strait from midnight to 04:00 (no-go period). This would provide “quiet hours’ for marine animals that are otherwise subjected to vessel traffic noise for almost 24 hours each day. This scenario assumed that the commercial traffic from the 4-hour no-go period was redistributed into the unrestricted 20 hours of the day. It also assumed that non-commercial traffic would be unrestricted at all times and that the traffic densities in the assessed periods would be equal to the current densities, as listed in Table 4. The AIS dataset shows that the density of non-commercial traffic is, however, very low at night.

The mitigated results for the restricted and unrestricted period can be compared to baseline results calculated over the same averaging period (i.e., top right maps versus top left maps in Figures 100–103). The traffic density of most vessel classes decreases in the restricted period but increases in the unrestricted period. Thus, the results show a significant decrease in noise levels from midnight and 04:00, with a mean decrease over the entire Haro Strait Local Study Area of 11.13 dB (unweighted) and 4.35 dB (audiogram-weighted), and an increase in noise levels from 04:00 to midnight, with a mean of 0.98 dB (unweighted) and 0.62 dB (audiogram-weighted).

Although the decrease in noise levels during restricted hours seems much larger (numerically) than during non-restricted hours, it must be taken into consideration that the changes are calculated in units of decibels, i.e. on a logarithmic scale as explained in Figure A-1, and over different periods (4 versus 20 hours). Thus, the same change in energy leads to a larger decrease than increase, in units of decibels. Still, the most important reason for the difference in changes in noise levels between the two periods is that commercial vessels represent the majority of noise contributors at night. Implementing a restricted night-time period therefore could create a very low-noise situation for a few hours.

4.1.3. Replacing 10% of Noisiest Ships

This modelled mitigation approach assessed replacing the top 10% of noisiest commercial vessels by the quietest 10% of vessels in the same class, in each Local Study Area. Two criteria for selecting the noisiest vessels were examined: vessels were first ranked based on their unweighted broadband source level and then ranked based on their audiogram-weighted broadband source level. For each criterion, the unweighted and audiogram-weighted mitigated levels were compared to baseline levels.

By selecting the noisiest vessels based on unweighted source levels, the mitigation approach significantly reduced unweighted sound levels throughout the Local Study Areas. The mitigation approach had no benefit, however, with respect to SRKW’s perceived loudness of mean noise levels. This can be seen by comparing Figures 104 and 105 in the Strait of Georgia, Figures 108 and 109 in Haro Strait, Figures 112 and 113 in Juan de Fuca Strait, and Figures 116 and 117 in Swiftsure Bank.

On the other hand, selecting the noisiest vessels based on SRKW audiogram-weighted source levels produced unweighted sound levels slightly lower than the future unmitigated levels away from the traffic lanes and higher than baseline levels along the traffic lanes. However, it produced significantly reduced audiogram-weighted levels throughout the model area. This can be seen by comparing Figures 106 and 107 in the Strait of Georgia, Figures 110 and 111 in Haro Strait, Figures 114 and 115 in Juan de Fuca Strait, and Figures 118 and 119 in Swiftsure Bank. Thus, in implementing this type of mitigation, it is important to consider the hearing of the key species in the area. For mid-frequency hearing species such as SRKW, assessing vessels based on their unweighted broadband source level is likely inappropriate. Criteria other than SRKW audiograms that also include biological causality could be considered for selecting the noisiest vessels. For example, vessel spectra could be filtered to emphasize frequencies used in a species’ communication signals or echolocation signals. The Vancouver Fraser Port Authority’s ECHO

program implements a vessel noise emissions measurement system that calculates both unweighted and audiogram-weighted vessel source levels.

4.1.4. Reducing Noise Emissions of Classes of Concern

This mitigation approach assessed reducing source levels by 3 and 6 dB equally at all frequencies, for these classes of concern: Containers, Cruise ship, Merchant, Tankers, Tugs, and Vehicle carriers. For both source level reductions, this mitigation approach produced net decreases from baseline in both unweighted and audiogram-weighted levels throughout the Local Study Areas. This can be seen in Tables 47–48 and Figures 120–123 for the Strait of Georgia, Tables 49–50 and Figures 124–127 for Haro Strait, Tables 51–52 and Figures 128–131 for Juan de Fuca Strait, and Tables 53 and 54 and Figures 132–135 for Swiftsure Bank. The decrease in source levels was not equal to the reduction in noise levels experienced by marine animals: the amount received levels were reduced was less than the specified reduction to commercial vessels, because non-commercial vessels also contribute to the soundscape.

Although this mitigation approach seems the most efficient, its feasibility may be questionable. Presently, there are no known methods for reducing the source levels of commercial vessels at all frequencies by a specific amount.

4.1.5. Shifting Vessel Traffic

This mitigation approach assessed the impact of shifting the shipping lanes or the main traffic density away from key locations in the SRKW critical habitat in Haro Strait, Juan de Fuca Strait, and Swiftsure Bank.

In Haro Strait, the outbound (west) lane was narrowed and shifted farther west by up to 500 m. The inbound lane was rerouted to the west side of the shoals northeast of Discovery Island where the outbound lane is currently located, and narrowed north of that point. As expected, there was no significant net decrease in noise levels relative to baseline when considering the full Haro Strait Boundary region. That is because all traffic continued to pass through this region, but along different routes. Consequently, the mean change in noise level was positive and attributed to the additional future Trans Mountain traffic. The largest changes, both positive and negative, in noise levels were localized near the traffic lanes, as seen in Figures 136 and 137. The largest decreases in mean monthly noise levels occurred along the southern portion of the current inbound traffic lane, because shifting the lane moved traffic away from these locations. For example, a 5.8 dB (unweighted) and 7.0 dB (audiogram-weighted) decrease is estimated at Sample location 7, which lies in the current lane.

In Haro Strait, the maps of changes in noise levels between the baseline and adjusted route scenarios, seen in Figures 136 and 137, show some local decreases in noise levels in the traffic lanes north of the adjusted lanes through Haro Strait, despite adding projected Trans Mountain tankers and tugs in the mitigation scenario. That is a modelling artifact, caused by the randomization width in the simulated vessel tracks being larger than that of the actual baseline traffic.

This mitigation approach also assessed the impact of condensing the commercial traffic within the outbound traffic lane through the Juan de Fuca Strait and Swiftsure Bank, therefore shifting traffic away from key locations in the SRKW critical habitat, north of the lanes. Outbound commercial vessels with higher speeds, generally navigating at the centre of the outbound lane (i.e., Container, Cruise ship, Merchant, Tanker, and Vessel carrier) were simulated as following the south boundary of the outbound lane. Outbound commercial vessels with slower speeds, generally navigating north of the outbound lane (i.e., Tug) were simulated as navigating at the centre of the outbound lane. The inbound traffic was not modified for this mitigation scenario.

As in Haro Strait, there was no significant net decrease in noise levels relative to baseline when considering the full Juan de Fuca Strait and Swiftsure Bank Local Study Areas. The largest

changes, both positive and negative, in noise levels were localized near the outbound traffic lane, as seen in Figures 138–141. A relatively small decrease in noise was seen north of the outbound lane, where mainly tug traffic was removed. For example, a 1.5 dB (unweighted) and 0.5 dB (audiogram-weighted) decrease was estimated at Sample location 6 in Juan de Fuca Strait, which lies 2 km north of the current lane.

4.1.6. Implementing Vessel Convoys

This modelled scenario assessed the temporal variations in noise levels (over approximately one day) due to implementing commercial vessel convoys for passage through Haro Strait (Alternative 1) and Juan de Fuca Strait (Alternative 2). Similar to the no-go scenario discussed in Section 4.1.2, the goal of this mitigation approach was to provide periods of lower noise levels throughout the day, between convoys. Two convoy intervals (2 and 4 hours) in Haro Strait and one convoy interval (4 hours) in Juan de Fuca Strait were assessed and compared to baseline levels (i.e., without convoying).

4.1.6.1. Alternative 1–Convoying Through Haro Strait

Results of SPL as a function of time for Alternative 1 (convoying through Haro Strait), seen in Figures 143–150, show the black line much lower than shaded area at Sample locations 1 and 2, meaning that non-commercial traffic is the largest contributor of noise at the two locations farthest from the traffic lanes. Thus, at these locations, there is little to no difference in noise levels between baseline and mitigated scenarios, which can be seen in the bar plots for the two sample locations in Figures 151 and 152. The black lines are higher relative to the shaded area at the other Haro Strait locations, meaning that commercial traffic is a larger noise contributor. Thus, applying mitigation management to commercial traffic would have a larger effect at these locations. At all locations, the black lines are higher relative to the shaded area for unweighted levels than for audiogram-weighted levels. Thus, while looking at unweighted results, commercial traffic dominated the sound field, especially at night (midnight to 08:00, and 20:00 to midnight) at Sample locations 3–8. With respect to SRKW perceived loudness, however, commercial traffic only dominated the sound field at the locations closest to the traffic lanes (Sample locations 5–8).

The 2-hour convoy scenario in Haro Strait does not appear to be an effective approach. It increased the mean noise level relative to baseline (mean level up to 3.8 dB higher than baseline mean level; as seen in Tables 61 and 62 at all sample locations and in the bar plots in Figures 151 and 152). This increase is due, in part, to the additional traffic associated with the Trans Mountain expansion (two tankers and two tugs were added over the course of one day, relative to baseline), and to commercial vessels slowing down to 10 knots in the convoy corridor, which increased the time spent close to the sample locations. Figures 143–150 show that the 2-hour interval between convoys (middle graph) decreased the period of low received levels relative to baseline (top graph), especially at night (after 20:00 hours and before 08:00). This is also seen in the CDF plots in Figures 153 and 154, for Sample locations 3–8, which show that received levels between 100 and 130 dB re 1 µPa (or 55 to 65 dB re HT) are the least present (lowest percentile) for the 2-hour convoy scenario.

The 4-hour convoy interval in Haro Strait, on the other hand, resulted in unweighted mean noise levels lower than baseline (up to 0.8 dB lower than baseline) over the 24-hour period, with the largest difference seen in the traffic lanes (Sample locations 7 and 8). This effect is not as clear in the audiogram-weighted results, where mean levels increased only slightly (up to 0.7 dB higher than baseline). Figures 143–150 show that the 4-hour interval between convoys (black line) increases the period of low received levels (at or slightly above ambient level), especially at night (after 20:00 hours and before 08:00). This is also seen in the bar plots, in Figures 151 and 152, and in CDF plots, in Figures 153 and 154, which show that lower received levels are present more often for the 4-hour convoy scenario (i.e., the CDF line for the 4-hour convoy scenario (green line) is generally higher than that for the other scenarios). Therefore, the 4-hour interval is possibly long enough to compensate for the increase in traffic associated with the

Trans Mountain expansion and due to the relatively slow speed of the convoy in the corridor. Even so, a longer convoy interval may be needed to more effectively lower noise levels, with respect to SRKW perceived loudness.

4.1.6.2. Alternative 2–Convoying Through Juan de Fuca Strait

Alternative 2 (convoying through Juan de Fuca Strait), was studied in all four Local Study Areas. Results of SPL as a function of time in the Strait of Georgia, seen in Figures 156–163, show that the mitigated commercial traffic (i.e., the outbound commercial traffic from Westridge terminal, Nanaimo, and Roberts Bank, en route to Juan de Fuca Strait) had a limited contribution to the overall noise levels at most sample locations in the Strait of Georgia. Thus, at most locations, there was little to no difference in noise levels between baseline and mitigated scenarios. This can be seen in the bar plots in Figures 164 and 165.

Sample location 7 in the Strait of Georgia is closest to the outbound traffic lane joining the Strait of Georgia and Haro Strait, as seen in Figure 7. Therefore, the mitigated vessels were important noise contributors at this location. The convoying of vessels in Juan de Fuca Strait changed the time at which the mitigated vessels transited by Sample location 7, slightly decreasing the duration of the quiet periods early in the morning, between 04:00 and 09:00 (local time), as seen in Figure 162. But in general, this mitigation alternative has little influence on the noise levels in the Strait of Georgia.

Results for Alternative 2 in Haro Strait, seen in Figures 169–176, show that the noise from mitigated vessels is lower than that from non-mitigated traffic at Sample location 1. The noise contribution from the mitigated vessels is higher at all the other locations within Haro Strait. In Haro Strait, daytime noise levels are higher than nighttime levels, largely due to the presence of non-commercial vessels. Thus, the additional daytime outbound traffic had little influence on the overall daytime noise levels. The reduction of nighttime outbound traffic slightly increased the duration of quiet nighttime periods. In general, this mitigation alternative reduced the median (50th percentile) broadband noise levels (by up to 1.4 dB, as shown in Table 65 and Figure 177) at all sample locations in Haro Strait. With respect to SRKW perceived loudness, commercial traffic only dominated the sound field at the locations closest to the traffic lanes (Sample locations 5–8). The differences in median noise levels are smaller than for unweighted levels (-0.2 to 0 dB at all but one location), but represent a decrease relative to baseline median noise levels even with the addition of the Trans Mountain traffic, as shown in Table 66 and Figure 178.

Results in Juan de Fuca Strait, shown in Figures 182–194 and 67–68, indicate that the mitigated outbound commercial vessels are important noise contributors in this area, accounting for approximately half of the noise peaks at most sample locations. However, traffic originating from the U.S. accounts for similar noise levels, and this traffic was not included in convoys. The convoy scenario considered here increases median noise levels at most sample locations relative to baseline. This result is apparent in the tabulated results in Tables 67 and 68 and the associated bar plots in Figures 191 and 192, which show increased median noise levels up to 1.4 dB for unweighted levels, and between 0 and 0.6 dB for audiogram-weighted levels. The decrease in quiet periods is apparent in the CDF plots of Figures 193 and 194 (especially for Sample locations 7–9), where the pink curve (convoy scenario) indicates lower percentiles than the blue curve (baseline scenario) for a given SPL. This means that the lower received levels (less than ~115 dB re 1 µPa and ~60 dB re HT) occur more often in the baseline scenario than in the mitigated scenario.

The increase in median level in Juan de Fuca Strait is partly due to the increase in traffic from the Trans Mountain project, and to the spreading of the outbound commercial traffic over the period when convoying was applied (i.e., midnight to midnight, local time). In the baseline scenario, the outbound traffic transited the Strait more often at night and in the morning, leaving some relatively quiet periods during the afternoon and evening.

Results in Swiftsure Bank, seen in Figures 196–207 and Tables 69–70, indicate that at many sample locations the mitigated outbound commercial vessels were not as important noise

contributors as they were in Juan de Fuca Strait. Figure 8 shows the sample locations in this area; Sample locations 5–7 are located south of the outbound traffic lane. The received noise levels at these locations are mainly influenced by non-mitigated commercial traffic transiting inbound. As with Juan de Fuca Strait, the overall effect of this mitigation approach is a slight increase (up to 0.5 dB in median levels).

4.1.7. Other Mitigation Options

The literature review on the effectiveness of additional mitigation approaches found several ways to reduce noise levels, including:

- Technical solutions involving changing ship designs and retrofitting vessels;
- Operational changes at the vessel level, involving operator behaviour and regular ship maintenance schedules planned by ship owners;
- Operational changes at the shipping industry level, involving loading plans and timing; and
- Operational changes at the traffic management level, involving dynamic speed limits, temporal and spatial area closures in response to real-time monitoring of whale presence, etc.

Carefully planning ship designs with noise output in mind and retrofitting older ships with quieting technology has been suggested as a very effective means to reduce noise in the long term (Audoly et al. 2017). The noise reduction due to these technical upgrades is estimated as high as 15 dB, which is the current spread between the quietest and loudest ships in similar ship classes (Baudin and Mumm 2015).

The most effective technical solutions involve reducing: a) cavitation and b) engine and other machinery noise travelling through the hull into the water (Renilson et al. 2013, Wittekind and Schuster 2016). The cavitation inception speed of propellers can be increased by increasing the size of propellers (Baudin and Mumm 2015), changing blade design (Spence and Fischer 2017), and equipping vessels with blade bubble injectors and propeller guards (Southall and Scholik-Schlomer 2008). Noise output from engines can be reduced by changing engine type (Baudin and Mumm 2015), applying dampening material to the inside of the hull to reduce airborne noise transmission from inside the vessel into the water (Spence and Fischer 2017), and placing the engines on isolation mounts to reduce transmission of vibration into the water (Spence and Fischer 2017). Possible improvements to hull design including using bulbuous bows, special hull paints, as well as overall optimized hull design to reduce wind and sea state impact, also reduce noise (Hollenbach and Friesch 2007, Baudin et al. 2015).

Ship design changes and vessel retrofitting should be long term goals to reduce noise in SRKW habitats. They would also benefit other oceanic habitats and results in a long lasting change of underwater noise levels everywhere. These changes can be achieved through better education and incentives for shipping companies and by setting maximum noise thresholds for access to sensitive habitats.

Regular ship maintenance is expected to reduce noise output by up to 3.5 dB (Baudin et al. 2015). Regular maintenance schedules increase cavitation inception speed and lower fuel consumption. This should be an incentive for vessel operators. Operating costs are associated with fuel costs; if fuel costs are lower than maintenance costs, the likelihood for implementing regular maintenance schedules through voluntary compliance, however, are low. Ship noise measurements when travelling, combined with hull inspections at port, could be used to incentivize ship maintenance via port fees imposed on vessels with low maintenance conditions.

Operator behaviour changes include avoiding sudden vessel accelerations, maintaining speed limits within critical habitats, and reducing speed to maintain appropriate distances to other vessels and animals. These changes can be achieved either through voluntary compliance or by regulations within a critical habitat. Adding marine mammal observers to piloted ships as a

requirement to accessing critical habitats would likely further increase compliance with regulations. The effectiveness of these measures would need to be tested before implementation.

Shipping companies would need to voluntarily make operational changes at the industry level. Within the Salish Sea, the port authorities could use incentives to improve the behaviour of shipping companies. For example, port authorities could report the noise level of vessels arriving at and leaving the port over the course of a year (via ULS measurements, for example) combined with loading information, and offer monetary incentives to vessels below a certain noise level threshold.

Plans and regulations for commercial traffic within the SRKW habitat, such as seasonal and/or dynamic speed limits, and temporal and spatial area closures for some or all marine traffic, may be the quickest most effective means to implement noise reduction. An added benefit is that regulations can be tailored to vessel type, time of day or year, as well as small- or large-scale areas. The noise reduction and, more importantly, improvement in the acoustic quality of the SRKW habitat will need to be assessed scientifically during implementation trials. While noise reduction is a mitigation goal, improved habitat quality leading to increased foraging and better habitat use by SRKW is the ultimate goal of any mitigation procedure.

4.2. Summary of Regional Effectiveness

This section discusses the expected change in noise levels from the future addition of tankers and tugs from the Trans Mountain project and the effectiveness of mitigation approaches at the individual sample locations defined in Section 2.1. Results are summarized in tables of mean expected levels (dB re 1 µPa and dB re HT) and changes (%) in acoustic intensity relative to Baseline (July) at these sample locations in each Local Study Area.

4.2.1. Strait of Georgia Local Study Area

Commercial traffic in the Strait of Georgia Local Study Area is concentrated along well-defined traffic lanes and ferry routes, in the central and southern region of the modelled area, resulting in localized zones of high and low noise levels. This can be seen in Figure 17, which maps the one-month average baseline equivalent continuous noise levels (L_{eq}) in this region. The traffic in the northern region is more spread out and less dominated by large commercial traffic, resulting in noise levels that are uniform in this region.

The monthly-averaged results in the Strait of Georgia are summarized in Tables 73 and 74, which show unweighted and audiogram-weighted noise levels at the eight sample locations presented in Figure 5 and Table 1. The associated change in acoustic intensity relative to baseline levels for July is shown as a percentage in parentheses.

The distribution of traffic influences the changes in future unmitigated noise levels at different sample locations. These changes are mapped in Figures 21 and 22. For sample locations in the northern region (i.e., Sample locations 1 and 3 in Tables 73 and 74), there is little effect from the addition of tankers and tugs from the Trans Mountain project (i.e., the future unmitigated levels are the same as baseline levels). Applying a mitigation approach that influences traffic along the shipping lanes (e.g., slowing down traffic, mapped in Figures 29–32) also has no effect on the levels at these two northern sample locations. The application of a mitigation approach that influences all commercial traffic through the region (e.g., replacing 10% of the noisiest vessels or reducing noise emission by a fix amount, mapped in Figures 104–107), however, greatly decreases the levels below baseline at those two sample locations.

There is also no increase due to future Trans Mountain traffic at Sample locations 4, 6, and 8. Sample location 4 is located close to the traffic entering and leaving the commercial port in Roberts Bank (south of Vancouver), and in shallower water than the traffic lanes. Since the future Trans Mountain traffic will be associate with the Westridge Terminal (in Vancouver), it has little influence compared to the Roberts Bank traffic on expected levels at Sample location 4. An important portion of the sound energy from the vessels in the main traffic lanes is also cut off by the slope in the seabed between the lanes and Sample location 4.

Sample locations 6 and 8 are located away from the main traffic lanes that will be used by the future Trans Mountain traffic; few vessels other than ferries, tugs, government and recreational vessels navigate in this region. Thus, there are no increases due to future Trans Mountain traffic at these locations. Because of the large amount of unmitigated vessel classes in this region, the mitigation approaches result in a smaller reduction in levels at these sample locations than at locations along the shipping lanes.

In contrast, Sample location 7 is centred between the inbound and outbound traffic lanes where most commercial traffic navigates. It sees the greatest increase in received levels due to future Trans Mountain traffic, and a relatively large decrease for the various mitigation approaches.

Table 73. *Strait of Georgia – Unweighted*: Mean expected levels (dB re 1 µPa) and changes (%) in acoustic intensity relative to Baseline (July) for each time-averaged (one month) scenario at sample locations in the SRKW critical habitat and current traffic lanes. SL: Source Level.

Scenario		Sample location							
		1	2	3	4	5	6	7	8
Baseline		113.0	118.2	106.4	113.0	107.8	129.8	125.3	130.9
Future unmitigated		113.0 (0.0%)	118.2 (0.0%)	106.4 (0.0%)	113.0 (0.0%)	107.9 (+2.3%)	129.8 (0.0%)	125.7 (+9.6%)	130.9 (0.0%)
Slow-down	11 knots	113.0 (0.0%)	117.5 (−14.9%)	106.4 (0.0%)	113.0 (0.0%)	106.9 (−18.7%)	129.8 (0.0%)	125.7 (+9.6%)	130.9 (0.0%)
	11 and 15 knots	113.0 (0.0%)	117.9 (−6.7%)	106.4 (0.0%)	113.0 (0.0%)	107.5 (−6.7%)	129.8 (0.0%)	125.7 (+9.6%)	130.9 (0.0%)
Replacing 10%	Vessels ranked by unweighted SL	111.9 (−22.4%)	117.0 (−24.1%)	104.2 (−39.7%)	112.5 (−10.9%)	107.0 (−16.8%)	129.7 (−2.3%)	123.9 (−27.6%)	130.8 (−2.3%)
	Vessels ranked by weighted SL	112.4 (−12.9%)	117.9 (−6.7%)	106.1 (−6.7%)	112.8 (−4.5%)	107.5 (−6.7%)	129.8 (0.0%)	125.3 (0.0%)	130.9 (0.0%)
Reducing SL by 3 dB		110.2 (−47.5%)	116.4 (−33.9%)	104.4 (−36.9%)	112.2 (−16.8%)	106.2 (−30.8%)	129.7 (−2.3%)	122.7 (−45.0%)	130.8 (−2.3%)
Reducing SL by 6 dB		107.4 (−72.5%)	115.0 (−52.1%)	102.9 (−55.3%)	111.7 (−25.9%)	105.1 (−46.3%)	129.7 (−2.3%)	119.8 (−71.8%)	130.8 (−2.3%)

Table 74. *Strait of Georgia – Audiogram-weighted*: Mean expected levels (dB re HT) and changes (%) in acoustic intensity relative to Baseline (July) for each time-averaged (monthly) scenario at sample locations in the SRKW critical habitat and current traffic lanes. SL: Source Level.

Scenario		Sample location							
		1	2	3	4	5	6	7	8
Baseline		59.5	63.5	53.9	64.7	53.8	74.9	66.0	72.9
Future unmitigated		59.5 (0.0%)	63.5 (0.0%)	53.9 (0.0%)	64.7 (0.0%)	53.9 (+2.3%)	74.9 (0.0%)	66.4 (+9.6%)	72.9 (0.0%)
Slow-down	11 knots	59.5 (0.0%)	63.3 (−4.5%)	53.9 (0.0%)	64.7 (0.0%)	53.7 (−2.3%)	74.9 (0.0%)	66.4 (+9.6%)	72.9 (0.0%)
	11 and 15 knots	59.5 (0.0%)	63.4 (−2.3%)	53.9 (0.0%)	64.7 (0.0%)	53.8 (0.0%)	74.9 (0.0%)	66.4 (+9.6%)	72.9 (0.0%)
Replacing 10%	Vessels ranked by unweighted SL	59.6 (+2.3%)	63.5 (0.0%)	53.9 (0.0%)	64.7 (0.0%)	53.8 (0.0%)	74.9 (0.0%)	65.8 (−4.5%)	72.9 (0.0%)
	Vessels ranked by weighted SL	57.6 (−35.4%)	62.5 (−20.6%)	53.7 (−4.5%)	64.6 (−2.3%)	53.5 (−6.7%)	74.8 (−2.3%)	63.5 (−43.8%)	72.8 (−2.3%)
Reducing SL by 3 dB		56.9 (−45.0%)	62.1 (−27.6%)	53.7 (−4.5%)	64.5 (−4.5%)	53.5 (−6.7%)	74.8 (−2.3%)	63.6 (−42.5%)	72.8 (−2.3%)
Reducing SL by 6 dB		54.5 (−68.4%)	61.2 (−41.1%)	53.6 (−6.7%)	64.4 (−6.7%)	53.3 (−10.9%)	74.7 (−4.5%)	60.9 (−69.1%)	72.7 (−4.5%)

4.2.2. Haro Strait Local Study Area

Commercial traffic in the Haro Strait Local Study Area is concentrated along well-defined traffic lanes, in the main central channel. This can be seen in Figure 18, which maps the one-month average baseline equivalent continuous noise levels (L_{eq}) in this region. The line of high noise levels perpendicular to traffic lanes, in the northern region of Haro Strait, is due to frequent ferry transits between Anacortes, WA, and Sidney, BC.

The monthly-averaged results in Haro Strait are summarized in Tables 75 and 76, which show unweighted and audiogram-weighted noise levels at the eight sample locations presented in Figure 6 and Table 1. The associated change in acoustic intensity relative to baseline levels for July are shown as a percentage in parentheses.

In this region, unweighted noise levels at all sample locations increase with the addition of future Trans Mountain traffic; audiogram-weighted noise levels increase at all locations except Sample locations 1 and 2, the sample locations farthest from the traffic lanes. The increase from baseline noise levels is highest along the traffic lanes since all additional traffic is simulated along this route. This can be seen in Figures 23 and 24. The largest difference in noise levels is expected to occur in the southern section of the Haro Strait Boundary, where traffic would decrease speed before turning almost 90 degrees by Discovery Island. While only a slight increase in SRKW audiogram-weighted levels is expected, this increase in levels would likely reduce SRKW communication distances and decrease the travel distance of echolocation clicks used for detecting prey.

Table 75. *Haro Strait – Unweighted*: Mean expected levels (dB re 1 µPa) and changes (%) in acoustic intensity relative to Baseline (July) for each time-averaged (one month) scenario at sample locations in the SRKW critical habitat and current traffic lanes. SL: Source Level.

Scenario		Sample location							
		1	2	3	4	5	6	7	8
Baseline		109.2	103.9	106.5	114.3	119	123.4	122.9	123.5
Future unmitigated		109.3 (+2.3%)	104.1 (+4.7%)	107.1 (+14.8%)	114.9 (+14.8%)	119.6 (+14.8%)	124.1 (+17.5%)	123.5 (+14.8%)	124.0 (+12.2%)
Slow-down	11 knots	109.2 (0.0%)	103.5 (−8.8%)	105.1 (−27.6%)	112.5 (−33.9%)	117.0 (−36.9%)	122.8 (−12.9%)	120.5 (−42.5%)	121.0 (−43.8%)
	10 knots	109.2 (0.0%)	103.3 (−12.9%)	104.7 (−33.9%)	111.9 (−42.5%)	116.3 (−46.3%)	122.4 (−20.6%)	119.6 (−53.2%)	120.3 (−52.1%)
	7 knots	109.2 (0.0%)	103.0 (−18.7%)	103.5 (−49.9%)	110.0 (−62.8%)	114.0 (−68.4%)	121.1 (−41.1%)	116.6 (−76.6%)	117.6 (−74.3%)
No-go*	Restricted period (midnight to 04:00)	93.8 (−97.0%)	92.0 (−88.8%)	93.1 (−95.4%)	98.6 (−97.3%)	106.3 (−94.9%)	106.4 (−98.1%)	103.5 (−98.9%)	105.5 (−98.5%)
	Unrestricted period (04:00 to midnight)	110.0 (+17.5%)	104.9 (+17.5%)	107.8 (+34.9%)	115.6 (+38.0%)	120.3 (+38.0%)	124.9 (+41.3%)	124.3 (+38.0%)	124.8 (+34.9%)
Replacing 10%	Vessels ranked by unweighted SL	108.5 (−14.9%)	103.8 (−2.3%)	106.1 (−8.8%)	113.5 (−16.8%)	117.9 (−22.4%)	122.4 (−20.6%)	121.8 (−22.4%)	122.4 (−22.4%)
	Vessels ranked by weighted SL	108.8 (−8.8%)	103.8 (−2.3%)	106.4 (−2.3%)	114.3 (0.0%)	119.2 (+4.7%)	123.7 (+7.2%)	123.0 (+2.3%)	123.5 (0.0%)
Reducing SL by 3 dB		107.3 (−35.4%)	103.0 (−18.7%)	104.6 (−35.4%)	112.2 (−38.3%)	116.9 (−38.3%)	121.3 (−38.3%)	120.6 (−41.1%)	121.1 (−42.5%)
Reducing SL by 6 dB		105.9 (−53.2%)	102.3 (−30.8%)	102.5 (−60.2%)	109.9 (−63.7%)	114.4 (−65.3%)	118.5 (−67.6%)	117.7 (−69.8%)	118.3 (−69.8%)
Shifting vessel traffic		107.5 (−32.4%)	103.5 (−8.8%)	105.0 (−29.2%)	111.6 (−46.3%)	117.4 (−30.8%)	122.8 (−12.9%)	117.1 (−73.7%)	123.0 (−10.9%)

* Results compared to Baseline scenario calculated over the same period (midnight to 04:00 or 04:00 to midnight).

Table 76. *Haro Strait – Audiogram-weighted*: Mean expected levels (dB re HT) and changes (%) in acoustic intensity relative to Baseline (July) for each time-averaged (monthly) scenario at sample locations in the SRKW critical habitat and current traffic lanes. SL: Source Level.

Scenario		Sample location							
		1	2	3	4	5	6	7	8
Baseline		56.2	51.6	46.9	56.3	60.8	64.6	65.2	66.2
Future unmitigated		56.2 (0.0%)	51.6 (0.0%)	47.1 (+4.7%)	56.5 (+4.7%)	60.9 (+2.3%)	65.7 (+28.8%)	65.8 (+14.8%)	66.8 (+14.8%)
Slow-down	11 knots	56.2 (0.0%)	51.6 (0.0%)	46.7 (−4.5%)	56.1 (−4.5%)	60.7 (−2.3%)	65.0 (+9.6%)	63.3 (−35.4%)	64.9 (−25.9%)
	10 knots	56.2 (0.0%)	51.6 (0.0%)	46.6 (−6.7%)	56.0 (−6.7%)	60.6 (−4.5%)	64.8 (+4.7%)	62.8 (−42.5%)	64.6 (−30.8%)
	7 knots	56.2 (0.0%)	51.5 (−2.3%)	46.5 (−8.8%)	55.9 (−8.8%)	60.5 (−6.7%)	64.2 (−8.8%)	61.2 (−60.2%)	63.6 (−45.0%)
No-go*	Restricted period (midnight to 04:00)	42.0 (−94.8%)	43.3 (−20.6%)	37.8 (−76.0%)	47.6 (−67.6%)	58.2 (−24.1%)	58.1 (−77.6%)	55.2 (−90.5%)	58.1 (−84.5%)
	Unrestricted period (04:00 to midnight)	57.0 (+12.2%)	52.3 (+2.3%)	47.8 (+12.2%)	57.2 (+9.6%)	61.3 (+7.2%)	66.4 (+51.4%)	66.5 (+38.0%)	67.5 (+34.9%)
Replacing 10%	Vessels ranked by unweighted SL	56.3 (+2.3%)	51.6 (0.0%)	47.0 (+2.3%)	56.4 (+2.3%)	60.9 (+2.3%)	65.5 (+23.0%)	65.1 (−2.3%)	66.3 (+2.3%)
	Vessels ranked by weighted SL	55.3 (−18.7%)	51.5 (−2.3%)	46.4 (−10.9%)	55.9 (−8.8%)	60.5 (−6.7%)	63.7 (−18.7%)	63.2 (−36.9%)	64.7 (−29.2%)
Reducing SL by 3 dB		55.0 (−24.1%)	51.5 (−2.3%)	46.3 (−12.9%)	55.9 (−8.8%)	60.5 (−6.7%)	63.7 (−18.7%)	63.3 (−35.4%)	64.7 (−29.2%)
Reducing SL by 6 dB		54.1 (−38.3%)	51.5 (−2.3%)	45.8 (−22.4%)	55.5 (−16.8%)	60.3 (−10.9%)	62.1 (−43.8%)	61.2 (−60.2%)	63.0 (−52.1%)
Shifting vessel traffic		54.3 (−35.4%)	51.5 (−2.3%)	46.2 (−14.9%)	55.8 (−10.9%)	60.8 (0.0%)	63.6 (−20.6%)	58.2 (−80.0%)	63.7 (−43.8%)

* Results compared to Baseline scenario calculated over the same period (midnight to 04:00 or 04:00 to midnight).

4.2.3. Juan de Fuca Strait Local Study Area

Most vessel traffic in the Juan de Fuca Strait Local Study Area is concentrated along well-defined traffic lanes. However slower traffic (e.g., tugs, fishing vessels, and whale watching boats) usually navigate outside the lane, closer to the coast. This can be seen in Figure 19, which maps the one-month average baseline equivalent continuous noise levels (L_{eq}) in this region. Relatively high noise levels are expected throughout this area, compared to the localized zones of high noise levels in the Strait of Georgia and Haro Strait.

The monthly-averaged results in Juan de Fuca Strait are summarized in Tables 77 and 78, which show unweighted and audiogram-weighted noise levels at the nine sample locations presented in Figure 7 and Table 1. The associated change in acoustic intensity relative to baseline levels for July are shown as a percentage in parentheses.

The increase in noise levels due to future Trans Mountain traffic, although higher along the traffic lanes, is seen throughout the Local Study Area. Within this relatively narrow Strait, a significant noise contribution from commercial traffic in the lanes is received at the coast when considering unweighted noise levels. The increase in noise levels is not as wide spread when considering SRKW audiogram-weighted noise levels. This can be seen in Figures 25 and 26 and in Tables 77 and 78.

In this region, slowing-down vessels and shifting vessel traffic were only applied to vessels in the outbound lane. Nevertheless, these options resulted in a decrease of noise levels compared to baseline levels at all sampling locations. The other approaches also resulted in a decrease of

noise levels compared to baseline levels, except for SRKW audiogram-weighted levels when replacing 10% of vessels ranked by unweighted broadband emission level.

Table 77. *Juan de Fuca Strait – Unweighted*: Mean expected levels (dB re 1 µPa) and changes (%) in acoustic intensity relative to Baseline (July) for each time-averaged (one month) scenario at sample locations in the SRKW critical habitat and current traffic lanes. SL: Source Level.

Scenario		Sample location								
		1	2	3	4	5	6	7	8	9
Baseline		111.4	111.6	110.2	109.9	113.8	117.5	109.6	114.0	117.5
Future unmitigated		111.5 (+2.3%)	111.9 (+7.2%)	110.5 (+7.2%)	110.2 (+7.2%)	114.3 (+12.2%)	118.2 (+17.5%)	110.0 (+9.6%)	114.5 (+12.2%)	118.1 (+14.8%)
Slow-down	11 knots	111.4 (−4.5%)	111.0 (−12.9%)	109.6 (−12.9%)	109.4 (−10.9%)	112.8 (−20.6%)	115.7 (−33.9%)	109.1 (−10.9%)	112.8 (−24.1%)	115.7 (−33.9%)
	11 and 15 knots	111.3 (−2.3%)	111.3 (−6.7%)	109.9 (−6.7%)	109.7 (−4.5%)	113.3 (−10.9%)	116.6 (−18.7%)	109.4 (−4.5%)	113.4 (−12.9%)	116.6 (−18.7%)
Replacing 10%	Vessels ranked by unweighted SL	111.1 (−6.7%)	111.4 (−4.5%)	110.1 (−2.3%)	109.8 (−2.3%)	113.3 (−10.9%)	116.7 (−16.8%)	109.6 (0.0%)	113.5 (−10.9%)	116.7 (−16.8%)
	Vessels ranked by weighted SL	111.2 (−4.5%)	111.5 (−2.3%)	110.1 (−2.3%)	109.8 (−2.3%)	113.8 (0.0%)	117.7 (+4.7%)	109.6 (0.0%)	114.0 (0.0%)	117.6 (+2.3%)
Reducing SL by 3 dB		110.3 (−22.4%)	110.4 (−24.1%)	109.2 (−20.6%)	109.0 (−18.7%)	111.9 (−35.4%)	115.4 (−38.3%)	108.7 (−18.7%)	112.1 (−35.4%)	115.3 (−39.7%)
Reducing SL by 6 dB		109.6 (−33.9%)	109.4 (−39.7%)	108.3 (−35.4%)	108.3 (−30.8%)	109.9 (−59.3%)	112.7 (−66.9%)	107.8 (−33.9%)	110.1 (−59.3%)	112.7 (−66.9%)
Shifting vessel traffic		110.3 (−22.4%)	110.9 (−14.9%)	109.8 (−8.8%)	109.8 (−2.3%)	112.7 (−22.4%)	116.0 (−29.2%)	109.5 (−2.3%)	113.0 (−20.6%)	116.1 (−27.6%)

Table 78. *Juan de Fuca Strait – Audiogram-weighted*: Mean expected levels (dB re HT) and changes (%) in acoustic intensity relative to Baseline (July) for each time-averaged (monthly) scenario at sample locations in the SRKW critical habitat and current traffic lanes. SL: Source Level.

Scenario		Sample location								
		1	2	3	4	5	6	7	8	9
Baseline		59.1	56.9	55.4	56.6	55.6	56.3	55.0	55.9	55.9
Future unmitigated		59.1 (0.0%)	57.0 (+2.3%)	55.4 (0.0%)	56.6 (0.0%)	55.7 (+2.3%)	57.0 (+17.5%)	55.0 (0.0%)	56.1 (+4.7%)	56.4 (+12.2%)
Slow-down	11 knots	59.1 (0.0%)	56.9 (0.0%)	55.4 (0.0%)	56.6 (0.0%)	55.5 (−2.3%)	55.6 (−14.9%)	55.0 (0.0%)	55.8 (−2.3%)	55.4 (−10.9%)
	11 and 15 knots	59.1 (0.0%)	56.9 (0.0%)	55.4 (0.0%)	56.6 (0.0%)	55.5 (−2.3%)	56.1 (−4.5%)	55.0 (0.0%)	55.9 (0.0%)	55.8 (−2.3%)
Replacing 10%	Vessels ranked by unweighted SL	59.1 (0.0%)	57.0 (+2.3%)	55.4 (0.0%)	56.6 (0.0%)	55.7 (+2.3%)	56.7 (+9.6%)	55.0 (0.0%)	56.0 (+2.3%)	56.2 (+7.2%)
	Vessels ranked by weighted SL	58.8 (−6.7%)	56.8 (−2.3%)	55.3 (−2.3%)	56.6 (0.0%)	54.8 (−16.8%)	55.2 (−22.4%)	54.9 (−2.3%)	55.4 (−10.9%)	54.6 (−25.9%)
Reducing SL by 3 dB		58.7 (−8.8%)	56.8 (−2.3%)	55.3 (−2.3%)	56.6 (0.0%)	54.5 (−22.4%)	55.0 (−25.9%)	54.9 (−2.3%)	55.2 (−14.9%)	54.3 (−30.8%)
Reducing SL by 6 dB		58.5 (−12.9%)	56.7 (−4.5%)	55.2 (−4.5%)	56.5 (−2.3%)	53.7 (−35.4%)	53.6 (−46.3%)	54.9 (−2.3%)	54.7 (−24.1%)	52.6 (−53.2%)
Shifting vessel traffic		58.4 (−14.9%)	56.7 (−4.5%)	55.3 (−2.3%)	56.6 (0.0%)	53.7 (−35.4%)	55.8 (−10.9%)	54.9 (−2.3%)	54.7 (−24.1%)	54.2 (−32.4%)

4.2.4. Swiftsure Bank Local Study Area

Similar to Juan de Fuca Strait, most traffic in the Swiftsure Bank Local Study Area is concentrated along well-defined traffic lanes, and little non-commercial traffic is found throughout the area. Slower traffic (e.g., tugs and fishing vessels) usually navigate outside the lane, closer to the coast. Some commercial traffic also diverges from the outbound traffic lane at the turn in the lane, in the eastern portion of the Local Study Area, to make their transit northward. This can be seen in Figure 20, which maps the one-month average baseline equivalent continuous noise levels (L_{eq}) in this region. Relatively high noise levels are expected throughout this area, compared to the localized zones of high noise levels in the Strait of Georgia and Haro Strait.

The monthly-averaged results in Swiftsure Bank are summarized in Tables 79 and 80, which show unweighted and audiogram-weighted noise levels at the eight sample locations presented in Figure 8 and Table 1. The associated change in acoustic intensity relative to baseline levels for July is shown as a percentage in parentheses.

The increase in noise levels due to future Trans Mountain traffic, although higher along the traffic lanes, is seen throughout the region. Within the Strait's relatively narrow opening, a significant noise contribution from commercial traffic in the lanes is received at the coast when considering unweighted noise levels. The increase in noise levels is not as wide spread when considering SRKW audiogram-weighted noise levels. This can be seen in Figures 27 and 28 and Tables 79 and 80.

In this region, slowing-down vessels and shifting vessel traffic were only applied to vessels in the outbound lane. Nevertheless, these options resulted in a decrease of noise levels compared to baseline levels at all sampling locations except Sample locations 5–7, located south of the outbound lane. Thus, applying these mitigation approaches only to the outbound traffic is not enough to compensate for the increase in noise levels south of the lanes due to the modelled increase in inbound traffic.

The other time-independent approaches were applied to all commercial traffic throughout the region. They resulted in a decrease of noise levels compared to baseline levels at all sample locations, except for SRKW audiogram-weighted levels when replacing 10% of vessels ranked by unweighted broadband emission levels at Sample locations 5–7 (south of the outbound lane), as can be seen in Figure 118.

Table 79. *Swiftsure Bank – Unweighted*: Mean expected levels (dB re 1 µPa) and changes (%) in acoustic intensity relative to Baseline (July) for each time-averaged (one month) scenario at sample locations in the SRKW critical habitat and current traffic lanes. SL: Source Level.

Scenario		Sample location							
		1	2	3	4	5	6	7	8
Baseline		105.9	99.1	107.4	114.3	118.3	114.8	106.8	112
Future unmitigated		106.3 (+9.6%)	99.6 (+12.2%)	107.7 (+7.2%)	114.5 (+4.7%)	118.8 (+12.2%)	115.3 (+12.2%)	107.4 (+14.8%)	112.1 (+2.3%)
Slow-down	11 knots	105.3 (−12.9%)	98.4 (−14.9%)	106.9 (−10.9%)	111.0 (−53.2%)	117.8 (−10.9%)	115.1 (+7.2%)	106.9 (+2.3%)	109.9 (−38.3%)
	11 and 15 knots	105.6 (−6.7%)	98.8 (−6.7%)	107.2 (−4.5%)	112.4 (−35.4%)	118.1 (−4.5%)	115.2 (+9.6%)	107.0 (+4.7%)	111.0 (−20.6%)
Replacing 10%	Vessels ranked by unweighted SL	105.9 (0.0%)	99.1 (0.0%)	107.1 (−6.7%)	113.1 (−24.1%)	117.3 (−20.6%)	114.0 (−16.8%)	106.5 (−6.7%)	110.5 (−29.2%)
	Vessels ranked by weighted SL	105.9 (0.0%)	99.0 (−2.3%)	107.2 (−4.5%)	114.1 (−4.5%)	118.3 (0.0%)	114.8 (0.0%)	106.7 (−2.3%)	111.7 (−6.7%)
Reducing SL by 3 dB		104.8 (−22.4%)	97.6 (−29.2%)	105.9 (−29.2%)	111.9 (−42.5%)	115.9 (−42.5%)	112.4 (−42.5%)	104.6 (−39.7%)	109.4 (−45.0%)
Reducing SL by 6 dB		103.8 (−38.3%)	96.1 (−49.9%)	104.7 (−46.3%)	109.6 (−66.1%)	113.0 (−70.5%)	109.6 (−69.8%)	102.0 (−66.9%)	107.0 (−68.4%)
Shifting vessel traffic		106.0 (+2.3%)	99.3 (+4.7%)	107.4 (0.0%)	114.0 (−6.7%)	122.3 (+151.2%)	115.6 (+20.2%)	107.6 (+20.2%)	111.9 (−2.3%)

Table 80. *Swiftsure Bank – Audiogram-weighted*: Mean expected levels (dB re HT) and changes (%) in acoustic intensity relative to Baseline (July) for each time-averaged (monthly) scenario at sample locations in the SRKW critical habitat and current traffic lanes. SL: Source Level.

Scenario		Sample location							
		1	2	3	4	5	6	7	8
Baseline		52.3	43.1	52.3	55.8	55.2	52.3	41.4	53.2
Future unmitigated		52.3 (0.0%)	43.1 (0.0%)	52.3 (0.0%)	55.9 (+2.3%)	56.1 (+23.0%)	52.9 (+14.8%)	41.7 (+7.2%)	53.3 (+2.3%)
Slow-down	11 knots	52.2 (−2.3%)	43.1 (0.0%)	52.3 (0.0%)	54.3 (−29.2%)	55.1 (−2.3%)	52.8 (+12.2%)	41.6 (+4.7%)	52.3 (−18.7%)
	11 and 15 knots	52.2 (−2.3%)	43.1 (0.0%)	52.3 (0.0%)	54.9 (−18.7%)	55.4 (+4.7%)	52.9 (+14.8%)	41.6 (+4.7%)	52.8 (−8.8%)
Replacing 10%	Vessels ranked by unweighted SL	52.3 (0.0%)	43.1 (0.0%)	52.3 (0.0%)	55.6 (−4.5%)	55.6 (+9.6%)	52.6 (+7.2%)	41.5 (+2.3%)	53.1 (−2.3%)
	Vessels ranked by weighted SL	52.2 (−2.3%)	43.0 (−2.3%)	51.8 (−10.9%)	54.8 (−20.6%)	53.6 (−30.8%)	50.7 (−30.8%)	40.3 (−22.4%)	52.3 (−18.7%)
Reducing SL by 3 dB		52.2 (−2.3%)	43.0 (−2.3%)	51.7 (−12.9%)	54.5 (−25.9%)	53.4 (−33.9%)	50.2 (−38.3%)	39.8 (−30.8%)	51.9 (−25.9%)
Reducing SL by 6 dB		52.2 (−2.3%)	43.0 (−2.3%)	51.3 (−20.6%)	53.6 (−39.7%)	50.9 (−62.8%)	47.6 (−66.1%)	38.4 (−49.9%)	51.0 (−39.7%)
Shifting vessel traffic		52.2 (−2.3%)	43.1 (0.0%)	52.3 (0.0%)	55.7 (−2.3%)	58.1 (+95.0%)	53.0 (+17.5%)	41.9 (+12.2%)	53.2 (0.0%)

REFERENCES

[DFO] Fisheries and Oceans Canada. 2011. *Recovery Strategy for the Northern and Southern Resident Killer Whales (Orcinus orca) in Canada*. Species at Risk Act Recovery Strategy Series. Fisheries & Oceans Canada, Ottawa. 80 pp. http://www.sararegistry.gc.ca/virtual_sara/files/plans/rs_epaulard_killer_whale_1011_eng.pdf.

[IMO] International Maritime Organisation. 2014. *Noise from commercial shipping and its adverse impacts on marine life, MEPC 66/17*. http://ocr.org/ocr/pdfs/policy/2014_Shipping_Noise_Guidelines_IMO.pdf.

[ISO] International Organization for Standardization. 2006. *ISO 80000-3:2006. Quantities and units -- Part 3: Space and time*. https://www.iso.org/standard/31888.html.

[ISO] International Organization for Standardization. 2017. *ISO/DIS 18405.2:2017. Underwater acoustics—Terminology*. Geneva. https://www.iso.org/standard/62406.html.

[NEB] National Energy Board. 2016. *Trans Mountian Expension Project*. Document Number OH-001-2014.

[NGDC] National Geophysical Data Center. 2013. High resolution NOAA digital elevation model. *U.S. Coastal Relief Model (CRM)*. National Oceanic and Atmospheric Administration, U.S. Department of Commerce. http://www.ngdc.noaa.gov/dem/squareCellGrid/download/655.

[NOAA] National Oceanic and Atmospheric Administration. 2018. National Data Buoy Center. Department of Commerce, National Oceanic and Atmospheric Administration, National Weather Service. http://www.ndbc.noaa.gov/ (Accessed 14 Feb 2017).

[NOAA] National Oceanic and Atmospheric Administration (US), [NOS] National Ocean Service, and [CO-OPS] Center for Operational Oceanographic Products and Services. 2017. NOAA Tide Predictions. Center for Operational Oceanographic Products and Services, National Oceanic and Atmospheric Administration, US Department of Commerce. https://tidesandcurrents.noaa.gov/noaatidepredictions.html?id=9457261&legacy=1 (Accessed 4 Jun 2017).

[NRC] National Research Council. 2003. *Ocean Noise and Marine Mammals*. National Research Council (U.S.), Ocean Studies Board, Committee on Potential Impacts of Ambient Noise in the Ocean on Marine Mammals. The National Academies Press, Washington, DC. http://www.nap.edu/openbook.php?record_id=10564.

[ONC] Ocean Networks Canada and [UVic] University of Victoria. 2017. *Ocean Networks Canada Data Archive* (webpage). http://www.oceannetworks.ca.

[SARA] Species at Risk Act. 2002. *Species at Risk Act*. *In*: Government of Canada (ed.). *S.C. 2002, c. 29*. Government of Canada. http://laws-lois.justice.gc.ca/eng/acts/S-15.3/page-1.html.

Abdel-Maksoud, M., K. Hellwig, and J. Blaurock. 2004. *Numerical and experimental investigation of the hub vortex flow of a marine propeller*. *Proceedings of the 25th Symposium on Naval Hydrodynamics*, St. John's, Newfoundland, Canada.

Abramson, L.M., S. Polefka, S. Hastings, and K. Bor. 2009. *Reducing the Threat of Ship Strikes on Large Cetaceans in the Santa Barbara Channel Region and Channel Islands National*

Marine Sanctuary: Recommendations and Case Studies. US Department of Commerce, National Oceanic and Atmospheric Administration, National Ocean Service, Office of Ocean and Coastal Resource Management, Office of National Marine Sanctuaries. www.channelislands.noaa.gov.

Andersen, P., J.J. Kappel, and E. Spangenberg. 2009. *Aspects of Propeller Developments for a Submarine*. *First International Symposium on Marine Propulsors*, June 2009, Trondheim, Norway.

André, M., M. Van Der Schaar, S. Zaugg, L. Houégnigan, A. Sánchez, and J. Castell. 2011. Listening to the deep: live monitoring of ocean noise and cetacean acoustic signals. *Marine Pollution Bulletin* 63(1): 18-26.

ANSI S1.1-1994. R2004. *American National Standard Acoustical Terminology*. American National Standards Institute, New York.

ANSI/ASA S1.13-2005. R2010. *American National Standard Measurement of Sound Pressure Levels in Air*. American National Standards Institute and Acoustical Society of America, New York.

ANSI/ASA S12.64/Part 1. 2009. *American National Standard Quantities and Procedures for Description and Measurement of Underwater Sound from Ships Part 1: General Requirements*. American National Standards Institute and Acoustical Society of America, New York.

Arveson, P.T. and D.J. Vendittis. 2000. Radiated noise characteristics of a modern cargo ship. *Journal of the Acoustical Society of America* 107(1): 118-129. https://doi.org/10.1121/1.428344.

Au, W.W.L., J.K.B. Ford, J.K. Horne, and K.A.N. Allman. 2004. Echolocation signals of free-ranging killer whales (*Orcinus orca*) and modeling of foraging for chinook salmon (*Oncorhynchus tshawytscha*). *Journal of the Acoustical Society of America* 115(2): 901-909. https://doi.org/10.1121/1.1642628.

Audoly, C., C. Rousset, E. Baudin, and T. Folegot. 2016. *AQUO project-Research on solutions for the mitigation of shipping noise and its impact on marine fauna–Synthesis of guidelines*. *Proceedings of the 23rd International Congress on Sound and Vibration*.

Audoly, C., T. Gaggero, E. Baudin, T. Folegot, E. Rizzuto, R.S. Mullor, M. André, C. Rousset, and P. Kellett. 2017. Mitigation of Underwater Radiated Noise Related to Shipping and Its Impact on Marine Life: A Practical Approach Developed in the Scope of AQUO Project. *IEEE Journal of Oceanic Engineering* 42(2): 373-387.

Baudin, E. and H. Mumm. 2015. *Guidelines for Regulation on UW Noise from Commercial Shipping*. Prepared by Bureau Veritas, DNV GL for SONIC. Revision 4.3. http://www.aquo.eu/downloads/AQUO-SONIC%20Guidelines_v4.3.pdf.

Baudin, E., C. Rousset, C. Audoly, and T. Folegot. 2015. *Guidelines to Reduce Ship Noise Footprint - Synthesis of Recommendations: The Practial Guide*. *In*: Achieve Quieter Oceans - AQUO (ed.). Achieve QUieter Oceans by shipping noise footprint reduction.

Berman-Kowalewski, M., F.M. Gulland, S. Wilkin, J. Calambokidis, B. Mate, J. Cordaro, D. Rotstein, J. St Leger, P. Collins, et al. 2010. Association between blue whale (Balaenoptera musculus) mortality and ship strikes along the California coast. *Aquatic Mammals* 36(1): 59.

Branstetter, B.K., J. St. Leger, D. Acton, J. Stewart, D. Houser, J.J. Finneran, and K. Jenkins. 2017. Killer whale (*Orcinus orca*) behavioral audiograms. *Journal of the Acoustical Society of America* 141(4): 2387-2398. https://doi.org/10.1121/1.4979116.

Cato, D.H. 2008. Ocean ambient noise: Its measurement and its significance to marine animals. *Proceedings of the Institute of Acoustics* 30(5): 1-9.

Chion, C., D. Lagrois, J. Dupras, S. Turgeon, I.H. McQuinn, R. Michaud, N. Ménard, and L. Parrott. 2017. Underwater acoustic impacts of shipping management measures: Results from a social-ecological model of boat and whale movements in the St. Lawrence River Estuary (Canada). *Ecological Modelling* 354: 72-87. http://dx.doi.org/10.1016/j.ecolmodel.2017.03.014.

Collins, M.D. 1993. A split-step Padé solution for the parabolic equation method. *Journal of the Acoustical Society of America* 93: 1736-1742.

Collins, M.D., R.J. Cederberg, D.B. King, and S. Chin-Bing. 1996. Comparison of algorithms for solving parabolic wave equations. *Journal of the Acoustical Society of America* 100(1): 178-182.

Erbe, C., A. MacGillivray, and R. Williams. 2012. Mapping cumulative noise from shipping to inform marine spatial planning. *Journal of the Acoustical Society of America* 132(5): EL423-EL428. https://doi.org/10.1121/1.4758779

Ford, J.K. 1989. Acoustic behaviour of resident killer whales (Orcinus orca) off Vancouver Island, British Columbia. *Canadian Journal of Zoology* 67(3): 727-745.

Ford, J.K. 1991. Vocal traditions among resident killer whales (Orcinus orca) in coastal waters of British Columbia. *Canadian Journal of Zoology* 69(6): 1454-1483.

Ford, J.K.B., J.F. Pilkington, A. Reira, M. Otsuki, B. Gisborne, R.M. Abernethy, E.H. Stredulinsky, J.R. Towers, and G.M. Ellis. 2017. *Habitats of Special Importance to Resident Killer Whales (Orcinus orca) off the West Coast of Canada*. DFO Can. Sci. Advis. Sec. Res. Doc. 2017/035. viii + 57 p.

François, R.E. and G.R. Garrison. 1982a. Sound absorption based on ocean measurements: Part II: Boric acid contribution and equation for total absorption. *Journal of the Acoustical Society of America* 72(6): 1879-1890.

François, R.E. and G.R. Garrison. 1982b. Sound absorption based on ocean measurements: Part I: Pure water and magnesium sulfate contributions. *Journal of the Acoustical Society of America* 72(3): 896-907.

Ghassemi, H., A. Mardan, and A. Ardeshir. 2012. Numerical Analysis of Hub Effect on Hydrodynamic Performance of Propellers with Inclusion of PBCF to Equalize the Induced Velocity. *Polish Maritime Reseach* 19: 17-24.

Hamilton, E.L. 1980. Geoacoustic modeling of the sea floor. *Journal of the Acoustical Society of America* 68(5): 1313-1340.

Hanson, M.B., R.W. Baird, J.K.B. Ford, J. Hempelmann-Halos, D.M. Van Doornik, J.R. Candy, C.K. Emmons, G.S. Schorr, B. Gisborne, et al. 2010. Species and stock identification of prey consumed by endangered southern resident killer whales in their summer range. *Endangered Species Research* 11(1): 69-82. https://doi.org/10.3354/esr00263.

Haren, A.M. 2007. Reducing Noise Pollution from Commercial Shipping in the Channel Islands National Marine Sanctuary: A Case Study in Marine Protected Area Management of Underwater Noise. *Journal of International Wildlife Law and Policy* 10(2): 153-173. https://doi.org/10.1080/13880290701347432.

Hatch, L., C. Clark, R. Merrick, S. Van Parijs, D. Ponirakis, K. Schwehr, M. Thompson, and D. Wiley. 2008. Characterizing the relative contributions of large vessels to total ocean noise fields: A case study using the Gerry E. Studds Stellwagen Bank National Marine Sanctuary. *Environmental Management* 42(5): 735-752. https://doi.org/10.1007/s00267-008-9169-4.

Hauser, D.D., M.G. Logsdon, E.E. Holmes, G.R. VanBlaricom, and R.W. Osborne. 2007. Summer distribution patterns of southern resident killer whales *Orcinus orca*: Core areas and spatial segregation of social groups. *Marine Ecology Progress Series* 351: 301-310. http://www.int-res.com/articles/meps2007/351/m351p301.pdf.

Hazen, E.L., D.M. Palacios, K.A. Forney, E.A. Howell, E. Becker, A.L. Hoover, L. Irvine, M. DeAngelis, S.J. Bograd, et al. 2016. WhaleWatch: A dynamic management tool for predicting blue whale density in the California Current. *Journal of Applied Ecology* 54: 1415–1428. http://dx.doi.org/10.1111/1365-2664.12820.

Hemmera Envirochem Inc. and SMRU Canada Ltd. 2014. *Roberts Bank Terminal 2 Technical Data Report: Marine Mammal Habitat Use Studies: Parts 1, 2, and 3*. Document Number 302-042-02. Prepared for Port Metro Vancouver. http://www.robertsbankterminal2.com/wp-content/uploads/RBT2-Marine-Mammals-Habitat-Use-Studies-TDR.pdf.

Hildebrand, J.A. 2005. Impacts of anthropogenic sound. *Marine mammal research: conservation beyond crisis*: 101-124.

Hollenbach, U. and J. Friesch. 2007. *Efficient hull forms–What can be gained*. *1st International Conference on Ship Efficiency*, 8-9 Oct 2007, Hamburg. https://www.ship-efficiency.org/onTEAM/pdf/HOLLENBACH_FRIESCH.pdf.

JASCO. 2015. *Underwater Acoustic Measurements in Haro Strait and Strait of Georgia: Transmission Loss, Vessel Source Levels, and Ambient Measurements. Appendix A in Hemmera and SMRU. Roberts Bank Terminal 2 Technical Data Report: Ship Sound Signature Analysis Study*. Prepared for Port Metro Vancouver, Vancouver, BC.

Jensen, A.S., G.K. Silber, and J. Calambokidis. 2004. *Large whale ship strike database*. US Department of Commerce, National Oceanic and Atmospheric Administration Washington, DC.

Joint Working Group on Vessel Strikes and Acoustic Impacts. 2012. *Vessel Strikes and Acoustic Impacts*. Report of a Joint Working Group of Gulf of the Farallones and Cordell Bank National Marine Sanctuaries Advisory Councils., San Francisco, CA 43 pp.

Kellett, P., O. Turan, and A. Incecik. 2013. A study of numerical ship underwater noise prediction. *Ocean Engineering* 66: 113-120. http://dx.doi.org/10.1016/j.oceaneng.2013.04.006.

Kipple, B. 2002. *Southeast Alaska Cruise Ship Underwater Acoustic Noise*. Document Number NSWCCD-71-TR-2002/574. Prepared by Naval Surface Warfare Center, Detachment Bremerton, for Glacier Bay National Park and Preserve. https://www.nps.gov/glba/learn/nature/upload/CruiseShipSoundSignaturesSEAFAC.pdf.

Kipple, B. and C. Gabriele. 2007. *Underwater noise from skiffs to ships*. *Fourth Glacier Bay Science Symposium*. Volume U.S. Geological Survey Investigation Report(2007-5047). U.S. Geological Survey 2007-5047, pp. 172-175.

Leaper, R.C. and M.R. Renilson. 2012. A review of practical methods for reducing underwater noise pollution from large commercial vessels. *International Journal of Maritime Engineering* 154: A79-A88.

Ligtelijn, J.T. 2007. *Advantages of different propellers for minimising noise generation*. *Proceedings of the 3rd International Ship Noise and Vibration Conference*, London, UK.

MacGillivray, A.O., Z. Li, G. Warner, and C. O'Neill. 2014. Regional Commercial Vessel Traffic Underwater Noise Exposure Study. *In Roberts Bank Terminal 2 Project Environmental Impact Statement*. Volume 2, Appendix 9.8-B. Canadian Environmental Assessment Agency Registry Reference Number 80054. http://www.ceaa-acee.gc.ca/050/documents/p80054/101367E.pdf.

MarineTraffic. 2017. *MarineTraffic: Historical AIS data* (webpage). https://www.marinetraffic.com/en/p/ais-historical-data.

Marquardt, T., J. Hensel, D. Mrowinski, and G. Scholz. 2007. Low-frequency characteristics of human and guinea pig cochleae. *Journal of the Acoustical Society of America* 121(6): 3628-3638. http://dx.doi.org/10.1121/1.2722506.

McCauley, R.D., D.H. Cato, and A.F. Jeffery. 1996. *A study of the impacts of vessel noise on humpback whales in Hervey Bay*. James Cook University, Department of Marine Biology, Townsville, Queensland, Australia. 137 pp.

McFarlane, G., D. Ware, R. Thomson, D. Mackas, and C. Robinson. 1997. Physical, biological and fisheries oceanography of a large ecosystem (west coast of Vancouver Island) and implications for management. *Oceanologica Acta* 20(1): 191-200.

McKenna, M.F., S.M. Wiggins, and J.A. Hildebrand. 2013. Relationship between container ship underwater noise levels and ship design, operational and oceanographic conditions. *Scientific Reports* 3: 1760. http://dx.doi.org/10.1038/srep01760.

McKenna, M.F., C. Gabriele, and B. Kipple. 2017. Effects of marine vessel management on the underwater acoustic environment of Glacier Bay National Park, AK. *Ocean & Coastal Management* 139: 102-112. http://dx.doi.org/10.1016/j.ocecoaman.2017.01.015.

Mewis, F. and U. Hollenbach. 2006. Special measures for improving propulsive efficiency. *HSVA NewsWave* 1: 1-4.

Miller, P.J. 2006. Diversity in sound pressure levels and estimated active space of resident killer whale vocalizations. *Journal of Comparative Physiology A* 192(5): 449.

Moloney, J., C. Hillis, X. Mouy, I. Urazghildiiev, and T. Dakin. 2014. *Autonomous Multichannel Acoustic Recorders on the VENUS Ocean Observatory*. *Oceans-St. John's, 2014*. IEEE, pp. 1-6.

Mouy, X., M. Bahoura, and Y. Simard. 2009. Automatic recognition of fin and blue whale calls for real-time monitoring in the St. Lawrence. *The Journal of the Acoustical Society of America* 126(6): 2918-2928.

Nedwell, J.R. and A.W. Turnpenny. 1998. The use of a generic frequency weighting scale in estimating environmental effect. *Workshop on Seismics and Marine Mammals*. 23–25th June 1998, London, U.K.

Nedwell, J.R., A.W.H. Turnpenny, J. Lovell, S.J. Parvin, R. Workman, and J.A.L. Spinks. 2007. *A validation of the dB_{ht} as a measure of the behavioural and auditory effects of underwater noise*. Report No. 534R1231 prepared by Subacoustech Ltd. for the UK Department of Business, Enterprise and Regulatory Reform under Project No. RDCZ/011/0004. www.subacoustech.com/information/downloads/reports/534R1231.pdf.

Osborne, R.W. 1999. *A historical ecology of Salish Sea resident killer whales (Orcinus orca): With implications for management*. Ph.D. Thesis. University of Victoria, Victoria, BC.

Ouchi, K., M. Tamashima, and K. Arai. 1991. Reduction of propeller cavitation noise by PBCF (propeller boss cap fins). *Journal of the Kansai Society of Naval Architects* 216: 9.

Port of Vancouver. 2018. *Vessel Slowdown Trial in Haro Strait* (webpage). © 2018 Vancouver Fraser Port Authority. https://www.portvancouver.com/environment/water-land-wildlife/marine-mammals/echo-program/vessel-slowdown-trial-in-haro-strait/.

Redfern, J.V., L.T. Hatch, C. Caldow, M.L. DeAngelis, J. Gedamke, S. Hastings, L. Henderson, M.F. McKenna, T.J. Moore, et al. 2017. Assessing the risk of chronic shipping noise to baleen whales off Southern California, USA. *Endangered Species Research* 32: 153-167. https://doi.org/10.3354/esr00797.

Renilson, M., R. Leaper, and O. Boisseau. 2013. Hydro-acoustic noise from merchant ships – impacts and practical mitigation techniques *Third International Symposium on Marine Propulsors* Launceston, Tasmania, Australia. pp 201-208.

Renilson, M.R., R.C. Leaper, and O. Boisseau. 2012. *Practical techniques for reducing the underwater noise pollution generated by commercial ships*. *Proceedings of the International Conference on the Environmentally Friendly Ship*, February 2012. Royal Institution of Naval Architects, pp. 28-29.

Richardson, W.J., C.R. Greene, Jr., C.I. Malme, and D.H. Thomson. 1995. *Marine Mammals and Noise*. Academic Press, San Diego, California. 576 pp.

Ross, D. 1976. *Mechanics of Underwater Noise*. Pergamon Press, New York.

Russell, B.A., A. Knowlton, and B. Zoodsma. 2001. Recommended measures to reduce ship strikes of North Atlantic right whales. *Contract report to NMFS. 37pp*.

Silber, G.K., S. Bettridge, and D. Cottingham. 2009. Report of a workshop to identify and assess technologies to reduce ship strikes of large whales. *US Department of Commerce, NOAA Technical Memorandum NMFS-OPR-42*.

Silber, G.K., A.S. Vanderlaan, A.T. Arceredillo, L. Johnson, C.T. Taggart, M.W. Brown, S. Bettridge, and R. Sagarminaga. 2012. The role of the International Maritime Organization in reducing vessel threat to whales: process, options, action and effectiveness. *Marine Policy* 36(6): 1221-1233.

Simard, Y., M. Bahoura, C. Park, J. Rouat, M. Sirois, X. Mouy, D. Seebaruth, N. Roy, and R. Lepage. 2006. *Development and experimentation of a satellite buoy network for real-time acoustic localization of whales in the St. Lawrence*. *OCEANS 2006*. IEEE, pp. 1-6.

Southall, B.L. 2005. *Shipping noise and marine mammals: a forum for science, management, and technology*. *Final report of the National and Atmospheric Administration (NOAA) International Symposium*.

Southall, B.L. and A. Scholik-Schlomer. 2008. Final Report of the National Oceanic and Atmospheric Administration (NOAA) International Symposium: Potential Application of Vessel-Quieting Technology on Large Commercial Vessels, 1-2 May 2007, Silver Spring, MD.

Spence, J., R. Fischer, M. Bahtiarian, L. Boroditsky, N. Jones, and R. Dempsey. 2007. *Review of Existing and Future Potential Treatments for Reducing Underwater Sound from Oil and Gas Industry Activities*. Report Number NCE REPORT 07-001. Report prepared by Noise Control Engineering, Inc., for Joint Industry Programme on E&P Sound and Marine Life.

Spence, J.H. and R.W. Fischer. 2017. Requirements for reducing underwater noise from ships. *IEEE Journal of Oceanic Engineering* 42(2): 388-398.

Szymanski, M.D., D.E. Bain, K. Kiehl, S. Pennington, S. Wong, and K.R. Henry. 1999. Killer whale (*Orcinus orca*) hearing: Auditory brainstem response and behavioral audiograms. *Journal of the Acoustical Society of America* 106(2): 1134-1141.

Urick, R.J. 1983. *Principles of Underwater Sound*. 3rd edition. McGraw-Hill, New York, London. 423 pp.

Vanderlaan, A.S., C.T. Taggart, A.R. Serdynska, R.D. Kenney, and M.W. Brown. 2008. Reducing the risk of lethal encounters: vessels and right whales in the Bay of Fundy and on the Scotian Shelf. *Endangered Species Research*.

Veirs, S., V. Veirs, and J.D. Wood. 2016. Ship noise extends to frequencies used for echolocation by endangered killer whales. *PeerJ* 4(e1657). https://doi.org/10.7717/peerj.1657.

Ward-Geiger, L.I., G.K. Silber, R.D. Baumstark, and T.L. Pulfer. 2005. Characterization of ship traffic in right whale critical habitat. *Coastal Management* 33(3): 263-278.

Wenz, G.M. 1962. Acoustic Ambient Noise in the Ocean: Spectra and Sources. *Journal of the Acoustical Society of America* 34(12): 1936-1956. https://doi.org/10.1121/1.1909155.

Wiles, G.J. 2004. *Washington State status report for the killer whale*. Washington Department of Fish and Wildlife, Olympia. 106 pp.

Wiley, D.N., M.A. Thompson, and R. Merrick. 2006. Realigning the boston traffic separation scheme to reduce the risk of ship strike to right and other baleen whales. *In* Börner, K. and E.F. Hardy (eds.). *5th Iteration (2009): Science Maps for Science Policy-Makers*. Courtesy of the National Oceanic and Atmospheric Administration. Places & Spaces: Mapping Science. http://www.scimaps.org/detailMap/index/realigning_the_bosto_88.

Wiley, D.N., C.A. Mayo, E.M. Maloney, and M.J. Moore. 2016. Vessel strike mitigation lessons from direct observations involving two collisions between noncommercial vessels and North Atlantic right whales (*Eubalaena glacialis*). *Marine Mammal Science* 32(4): 1501-1509. http://dx.doi.org/10.1111/mms.12326.

Williams, R., C. Erbe, E. Ashe, A. Beerman, and J. Smith. 2014. Severity of killer whale behavioral responses to ship noise: A dose–response study. *Marine Pollution Bulletin* 79(1-2): 254-260. https://doi.org/10.1016/j.marpolbul.2013.12.004.

Williams, R., C. Erbe, E. Ashe, and C.W. Clark. 2015. Quiet (er) marine protected areas. *Marine pollution bulletin* 100(1): 154-161.

Wind, J. 1978. Hub size selection criteria for controllable pitch propellers as a means to ensure system integrity. *Naval Engineers Journal* 90(4): 49-61.

Wittekind, D. and M. Schuster. 2016. Propeller cavitation noise and background noise in the sea. *Ocean Engineering* 120: 116-121.

Zaugg, S., M. van der Schaar, L. Houégnigan, C. Gervaise, and M. André. 2010. Real-time acoustic classification of sperm whale clicks and shipping impulses from deep-sea observatories. *Applied Acoustics* 71(11): 1011-1019. http://www.sciencedirect.com/science/article/pii/S0003682X1000112X.

Zhang, Y. and C. Tindle. 1995. Improved equivalent fluid approximations for a low shear speed ocean bottom. *Journal of the Acoustical Society of America* 98(6): 3391-3396. https://doi.org/10.1121/1.413789.

APPENDIX A. UNDERWATER ACOUSTICS

APPENDIX A. UNDERWATER ACOUSTICS

A.1. Acoustic Metrics

Underwater sound pressure amplitude is measured in decibels (dB) relative to a fixed reference pressure of p_0 = 1 µPa. Because the perceived loudness of sound, especially pulsed noise such as from seismic airguns, pile driving, and sonar, is not generally proportional to the instantaneous acoustic pressure, several sound level metrics are commonly used to evaluate noise and its effects on marine life. Specific definitions of relevant metrics used in the accompanying report are provided. Where possible the American National Standard Institute (ANSI) and International Organization for Standardization (ISO) definitions and symbols for underwater sound metrics are followed, but these standards are not always consistent.

The sound pressure level (SPL; dB re 1 µPa; symbol L_p) is the root-mean-square (rms) pressure level, $p(t)$, in a stated frequency band over a specified time window (T; s) containing the acoustic event of interest. It is important to note that SPL always refers to an rms pressure level and therefore not instantaneous pressure:

$$L_p = 10\log_{10}\left(\frac{1}{T}\int_T p^2(t)dt \Big/ p_0^2\right). \quad \text{(A-1)}$$

The SPL represents a nominal effective continuous sound over the duration of an acoustic event, such as the emission of one acoustic pulse, a marine mammal vocalization, the passage of a vessel, or over a fixed duration. Because the window length, T, is the divisor, events with similar sound exposure level (SEL), but more spread out in time have a lower SPL.

The sound exposure level (SEL, dB re 1 µPa^2·s; symbol L_E) is a measure related to the acoustic energy contained in one or more acoustic events (N). The SEL for a single event is computed from the time-integral of the squared pressure over the full event duration (T):

$$L_E = 10\log_{10}\left(\int_T p^2(t)dt \Big/ T_0 p_0^2\right), \quad \text{(A-2)}$$

where T_0 is a reference time interval of 1 s. The SEL continues to increase with time when non-zero pressure signals are present. It therefore can be construed as a dose-type measurement, so the integration time used must be carefully considered in terms of relevance for impact to the exposed recipients.

SEL can be calculated over periods with multiple acoustic events or over a fixed duration. For a fixed duration, the square pressure is integrated over the duration of interest. For multiple events, the SEL can be computed by summing (in linear units) the SEL of the N individual events:

$$L_{E,N} = 10\log_{10}\left(\sum_{i=1}^{N} 10^{\frac{L_{E,i}}{10}}\right). \quad \text{(A-3)}$$

Energy equivalent SPL (L_{eq}; dB re 1 µPa) denotes the SPL of a stationary (constant amplitude) sound that generates the same SEL as the signal being examined, $p(t)$, over the same period of time, T:

$$L_{eq} = 10\log_{10}\left(\frac{1}{T}\int_T p^2(t)dt \Big/ p_0^2\right). \quad \text{(A-4)}$$

The equations for SPL and the energy-equivalent SPL are numerically identical; conceptually, the difference between the two metrics is that the former is typically computed over short periods (typically of one second or less) and tracks the fluctuations of a non-steady acoustic signal, whereas the latter reflects the average SPL of an acoustic signal over times typically of one minute to several hours.

Audiogram-weighted SPL, or SPL above hearing threshold, is calculated by subtracting species-unique audiograms from the received 1/3octave-band sound pressure level. Audiogram-weighted levels are expressed in units of dB above hearing threshold (dB_{ht}(species)). If applied, the frequency weighting of an acoustic event should be specified, as in the case of auditory-weighted SPL ($L_{p,ht}$).

A.2. One-Third-Octave-Band Analysis

The distribution of a sound's power with frequency is described by the sound's spectrum. The sound spectrum can be split into a series of adjacent frequency bands. Splitting a spectrum into 1 Hz wide bands, called passbands, yields the power spectral density of the sound. This splitting of the spectrum into passbands of a constant width of 1 Hz, however, does not represent how animals perceive sound.

Because animals perceive exponential increases in frequency rather than linear increases, analyzing a sound spectrum with passbands that increase exponentially in size better approximates real-world scenarios. In underwater acoustics, a spectrum is commonly split into 1/3-octave bands, which are approximately one-then of an octave (base 10) wide (referred as decidecade-bands). Each octave represents a doubling in sound frequency. The centre frequency of the ith band, $f_c(i)$, is defined as:

$$f_c(i) = 10^{i/10}, \tag{A-5}$$

and the low (f_{lo}) and high (f_{hi}) frequency limits of the ith band are defined as:

$$f_{lo} = 10^{-1/20} f_c(i) \text{ and } f_{hi} = 10^{1/20} f_c(i) . \tag{A-6}$$

The 1/3-octave bands become wider with increasing frequency, but on a logarithmic scale the bands appear equally spaced. This is illustrated in Figure A-1.

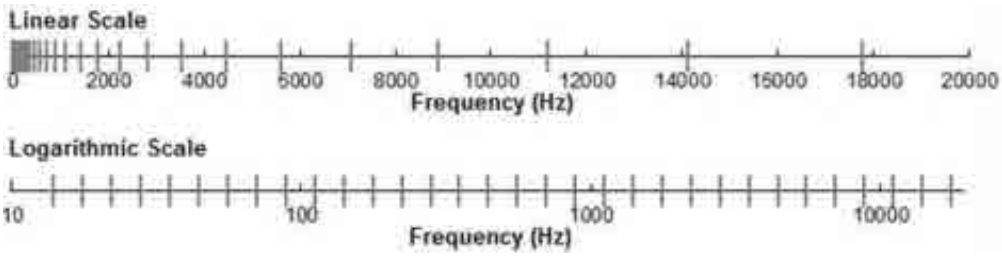

Figure A-1. One-third-bands shown on a linear frequency scale and on a logarithmic scale.

The sound pressure level in the ith band ($L_b^{(i)}$; where the subscript b refers to a 1/3-octave band) is computed from the power spectrum $S(f)$ between f_{lo} and f_{hi}:

$$L_b^{(i)} = 10\log_{10}\left(\int_{f_{lo}}^{f_{hi}} S(f)df\right) . \tag{A-7}$$

Summing the sound pressure level of all the bands yields the broadband sound pressure level:

$$\text{Broadband SPL} = 10 \log_{10} \sum_i 10^{L_b^{(i)}/10} \quad . \tag{A-8}$$

Figure A-2 shows an example of how the 1/3-octave-band sound pressure levels compare to the power spectrum of an ambient noise signal. Because the 1/3-octave-bands are wider with increasing frequency, the 1/3-octave-band SPL is higher than the power spectrum, especially at higher frequencies. Acoustic modelling of 1/3-octave-bands require less computation time than 1 Hz bands and still resolves the frequency-dependence of the sound source and the propagation environment.

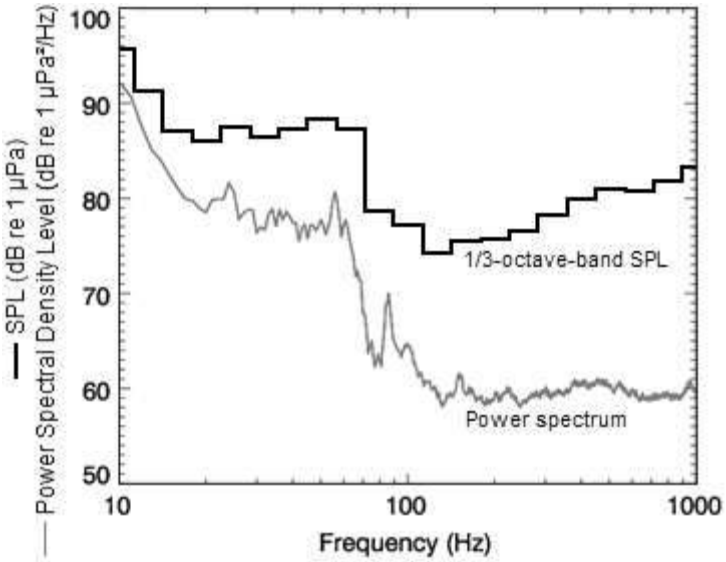

Figure A-2. A power spectrum and the corresponding 1/3-octave-band sound pressure levels of example ambient noise shown on a logarithmic frequency scale.

A.3. Vessels Sounds

Underwater sound that radiates from vessels is produced mainly by propeller cavitation, with a smaller fraction of noise produced by sound transmitted through the hull, such as by engines, gearing, and other mechanical systems. Sound levels tend to be the highest when thrusters are used to position the vessel (e.g., at a pier or for keeping station using dynamic positioning systems) and when the vessel is transiting at high speeds. A vessel's sound signature depends on the vessel's size, power output, propulsion system (e.g., conventional propeller-shaft configuration vs. azimuthal thruster or Voith Schneider propulsion system), and the design characteristics of the given system (e.g., blade shape and size). A vessel produces broadband acoustic energy with most of the energy emitted below a few kilohertz. Sound from onboard machinery, particularly sound below 200 Hz, dominates the sound spectrum before cavitation begins, around 8–12 knots for many commercial vessels (Spence et al. 2007). Noise from vessels typically raises the background sound level by tenfold or more (Arveson and Vendittis 2000).

A.3.1. Cavitation Noise

The term cavitation refers to streams of vapour bubbles that form on the surface of marine propellers as they rotate . Cavitation bubbles make a lot of underwater noise when they collapse in the vessel's wake. Cavitation occurs when the propeller tip speed exceeds a certain onset threshold, which depends on the propeller design and wake field. Generally, the onset of cavitation is between 8–12 knots, although it may occur at even lower vessel speeds for heavily loaded propellers (Spence et al. 2007). The lowest speed at which cavitation occurs is known as the cavitation inception speed.

Cavitation noise is very broadband (5 Hz to 100 kHz) and may, therefore, be important when considering effects on killer whales, who hear best at frequencies above 10 kHz. The spectrum of cavitation noise typically has a peak between 40−300 Hz and a steady −6 dB/decade roll off at higher frequencies (Ross 1976). Cavitation noise increases rapidly with vessel speed: the difference between cavitation onset and full cavitation may be up to 30 dB (Spence et al. 2007). Cavitation also results in the phenomenon of blade-rate tonals, which are strong, low-frequency tones appearing at harmonics of the blade-passing frequency (Arveson and Vendittis 2000). Most control treatments for propulsion noise are therefore concerned with delaying the onset of cavitation.

Another source of propulsion noise is vibration induced by unsteady flow around the propellers. Oscillating fluid forces, created by turbulence, can cause the propeller blades and hull to vibrate, thereby radiating low-frequency underwater noise. Usually, this type of vibration noise is quieter than cavitation noise.

A.3.2. Mechanical Noise

Because machinery noise is primarily structure-borne, most noise control treatments are concerned with isolating machine vibrations from the structure of the vessel. In general, main and auxiliary machinery are the dominant sources of radiated noise at speeds lower than the cavitation inception speed. The most important transmission path for shipboard machinery noise is via structure-borne vibration. Mechanical vibration is coupled through the vessel structure to the hull, where it radiates as underwater noise. Airborne sound transmission is of secondary importance to structure-borne underwater sounds. The main engines and electric generators are usually the greatest sources of mechanical vibration. Machinery noise is predominantly concentrated at mid-to-low frequencies (10–1000 Hz), and it is dominated by strong low-

frequency tones at harmonics of the piston firing rate. Thus, machinery noise may be less audible to SRKW than cavitation noise.

A literature review was carried out to identify the best available underwater noise control technologies currently available for ships; results are presented in Sections 3.9–3.12.

A.3.3. Vessel Source Levels

Since September 2015, an Underwater Listening Station (ULS) has been measuring vessel noise emissions (i.e., source levels) in the Strait of Georgia. This ULS is situated in the inbound shipping lane, on the VENUS East Node seen in Figure A-3. It captures noise emissions from commercial vessels bound for the Port of Vancouver, as well as ferry traffic along several passenger and cargo routes. Automated processing of vessel source levels is performed by JASCO's ShipSound software, which uses AIS data to detect when vessels transit through the measurement funnel of the ULS. Valid vessel tracks, as selected by the automated system, are used for the vessel source level analysis, which conforms approximately to the ANSI standard for ship sound measurements (ANSI/ASA S12.64/Part 1 2009). As of April 2017, the ShipSound system had collected over 2700 valid source level measurements.

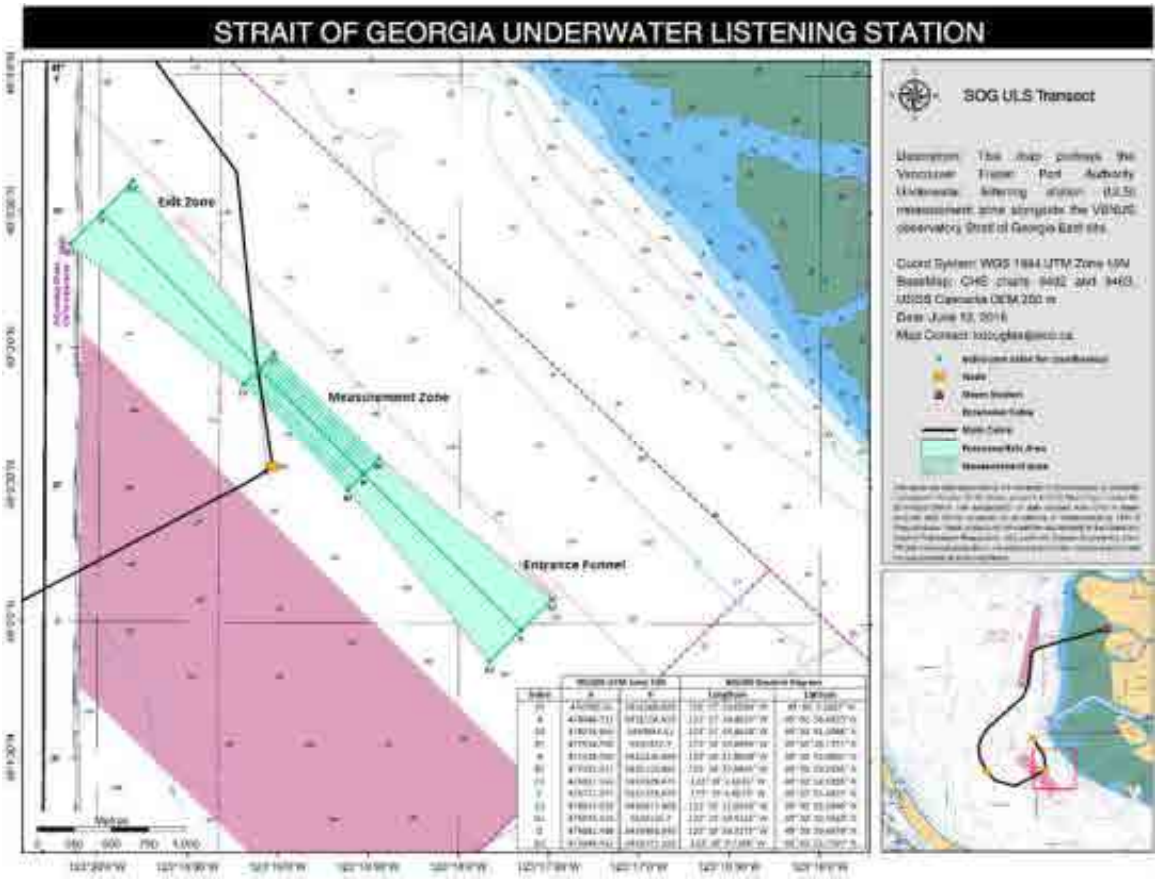

Figure A-3. The Underwater Listening Station (ULS) location (yellow circle) at the VENUS East Node in Strait of Georgia. Pilots use the measurement funnel (cyan) to ensure vessel source level measurements are accurate.

For this study, source level measurements from the ULS were assigned to ten different classes, according to vessel class information embedded in the AIS logs. The classes are listed in Table A-1. Average frequency-dependent source levels were calculated for each vessel class. These source levels were used to represent noise emissions of corresponding vessels in the cumulative noise model. Source levels for four additional vessel classes were not covered by the ULS data (Passenger (<100 m); Clipper Ferry[5]; Recreational, and Other[6]) and were obtained from other sources. For each vessel class, average monopole source levels (MSL) were compiled in 1/3-octave-bands from 10 Hz to 63.1 kHz; the spectra are shown in Figure 16. This is the frequency range where noise emissions from vessels overlap the hearing sensitivity of marine mammals and fish inside the Local Study Areas.

Table A-1. The number of measurements used to calculate mean (power average) monopole source levels for each vessel class represented in the Underwater Listening Station (ULS) data. The Merchant category includes both Bulk Carriers and General Cargo. The Government category includes Navy (Royal Canadian Navy or others) and Research Vessels. Ferries measurements are grouped before averaging to properly account for repeat vessel passes.

Category	Measurements	Unique vessels
Container	233	118
Ferry (Ro-ro Passenger)	1505	8
Ferry (Ro-ro Cargo)	134	3
Fishing	23	20
Government	6	5
Merchant	464	445
Cruise ship	17	11
Tanker	86	50
Tug	206	67
Vehicle carrier	31	28
Total	**2705**	**755**

[5] Clipper Ferry jet catamarans source levels were based on passenger vessel source levels from Veirs et al. (2016).
[6] Recreational and Other source levels were based on a prior review of published vessel measurements carried out for the Roberts Bank Terminal 2 cumulative modelling assessment (MacGillivray et al. 2014).

A.4. Environmental Parameters

In temperate zones, the temperature and salinity profile of oceans greatly change over the seasons. These changes affect the speed that sound travels through the water. Water column sound speed profiles for January and July were computed from historical temperature and salinity data in the southern region of the Salish Sea (ONC and U Vic 2017). These monthly-averaged sound speed profiles are most variable in the upper 80 m of the water column, as seen in Figure A-4. Solar heating in summer increases the surface water temperature, which increases the sound speed at the top of the water column and, therefore, redirects sound toward the seafloor. Wind-driven mixing in winter combined with atmospheric cooling results in lower surface water temperatures, which decrease the sound speed at the top of the water column and redirect sounds toward the surface. The mean sound speed profiles for January and July, the two months when the difference in sound speed in the upper 80 m of water is greatest, were used to represent the acoustic properties of the water column in the model. Analysis of the sound speed profiles showed no strong geographical variations in the data; therefore, a single sound speed profile was assumed for each month throughout the Regional Study Area, as shown in Figure 2, for each month.

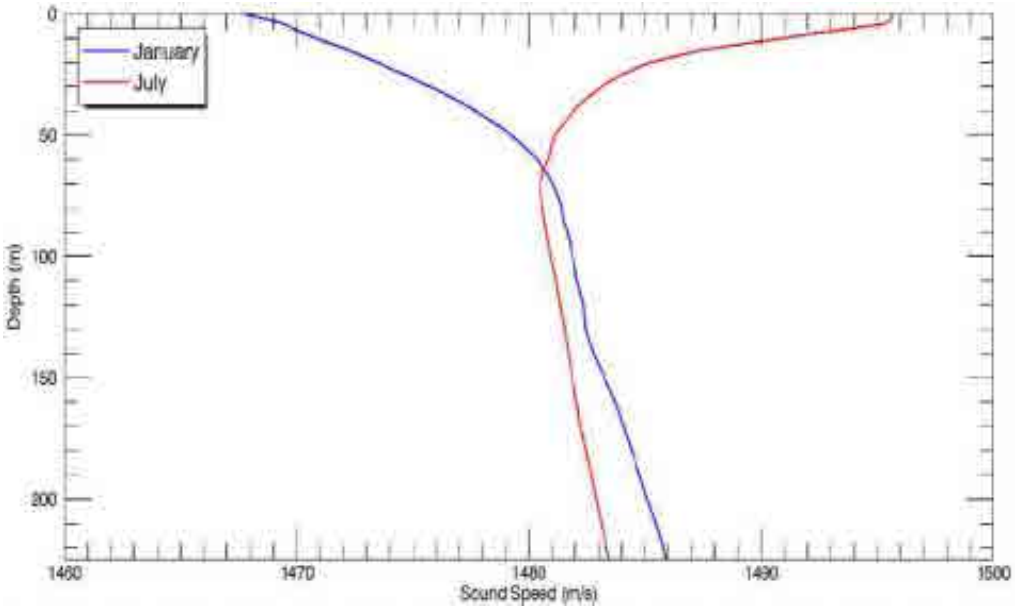

Figure A-4. Mean sound speed profiles for the Regional Study Area, based on historical ocean temperature and salinity profiles for January and July.

The bathymetry (depth contours) inside the Regional Study Area was modelled on a 20 m resolution BC Albers grid. It was compiled from the following sources:

1. NOAA digital elevation model (NGDC 2013) for data south of latitude 49°N.
2. Canadian Hydrographic Service digital elevation map from Nautical Data International Inc. for data north of latitude 49°N.

The water depths in the region range from 0 to 870 m.

The geoacoustic properties of the seabed strongly influence how sound travels through the water. Reflection and absorption of sound energy at the seabed is the dominant mechanism by which sound is attenuated in shallow (less than ~200 m) water (Urick 1983). The seabed geoacoustic properties for the Regional Study Area were obtained by combining geoacoustic inversion results from acoustic measurements (JASCO 2015) and reviewing scientific literature (Hamilton 1980, Erbe et al. 2012). To account for geographic variation inside the Regional Study

Area, it was divided into four geoacoustic regions with similar bottom types: Strait of Georgia, Haro Strait, eastern Juan de Fuca Strait, and western Juan de Fuca Strait, as seen in Figure A-5. A different set of geoacoustic properties, listed in Table A-2, was used to represent each region.

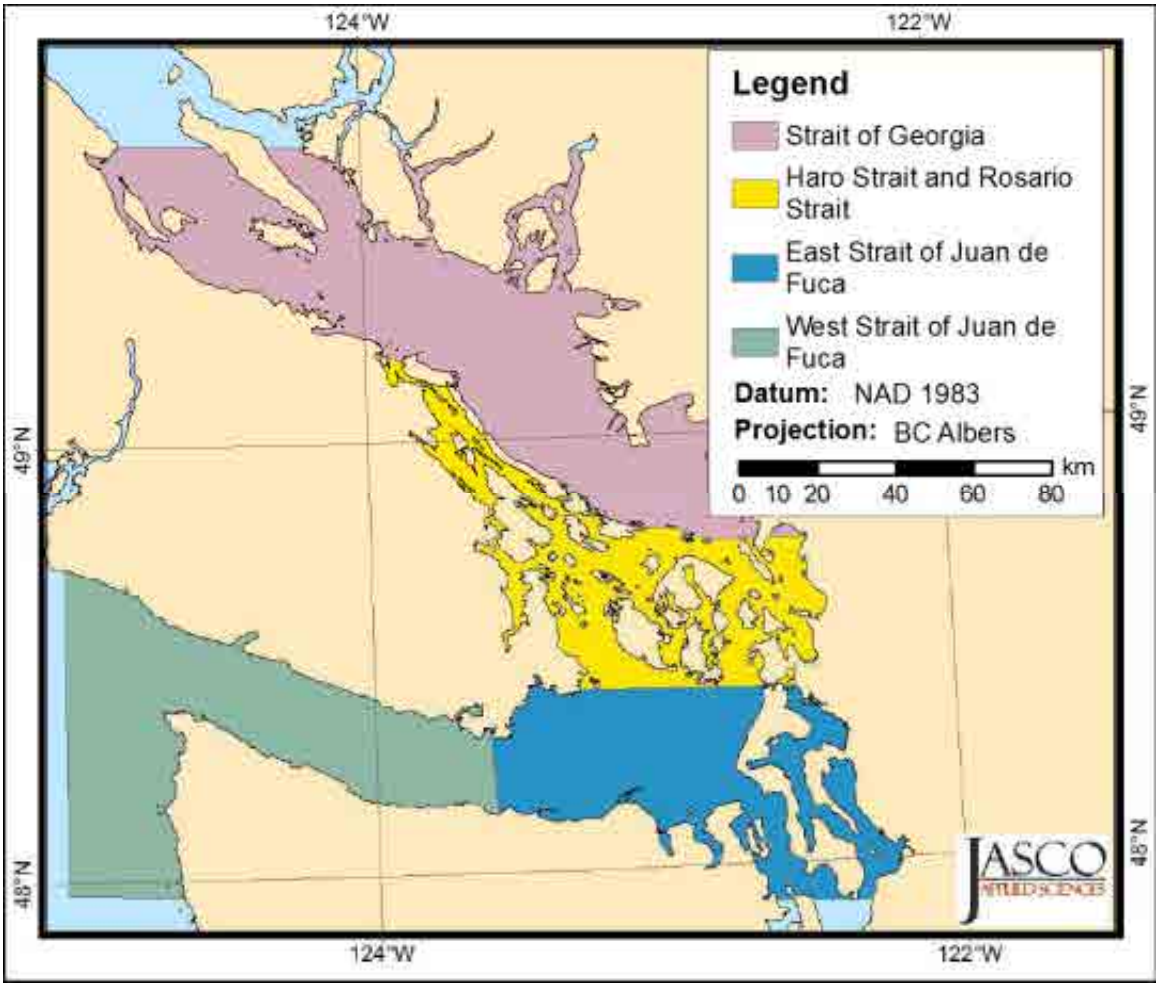

Figure A-5. Map of geoacoustic regions for defining sound propagation in the model. Pink for Strait of Georgia, yellow for Haro Strait and Rosario Strait, blue for eastern Juan de Fuca Strait, and green for western Juan de Fuca Strait.

Table A-2. Seabed profiles for the four geoacoustic regions.

Depth below seafloor (m)	Sediment type	Compressional speed (m/s)	Density (g/cm^3)	Compressional attenuation (dB per wavelength)	Shear speed (m/s)	Shear attenuation (dB per wavelength)
Strait of Georgia						
0–100	Clayey-silt	1502–1602	1.54	0.61	125.0	2.2
> 100	Bedrock	2275	1.90	0.10		
Haro Strait and Rosario Strait						
0–50	Sand-silt-clay	1541–1591	1.80	0.72	250	1.2
> 50	Bedrock	2275	1.90	0.10		
Eastern Juan de Fuca Strait						
0–50	Silt	1558–1608	1.64	0.83	250	3.4
> 50	Bedrock	2275	1.90	0.10		
Western Juan de Fuca Strait						
0–50	Sand	1713–1763	1.94	0.90	500	3.4
> 50	Bedrock	2275	2.20	0.10		

Wind-driven ambient noise was included in the time-dependent version of the cumulative noise model, based on historical wind speed data in Swiftsure Bank[7] and Haro Strait[8], for a 24-hour period in July (NOAA 2018). The simulated wind speeds for the Local Study Areas shown in Figure A-6. Time-dependent wind-driven ambient noise was calculated in 1/3-octave-bands, based on published curves of ambient noise versus frequency and wind speed, as presented in Figure A-7. Aggregate sound levels in all map grid cells were computed from the sum of the vessel noise plus the wind-driven ambient noise, for each time step in the model.

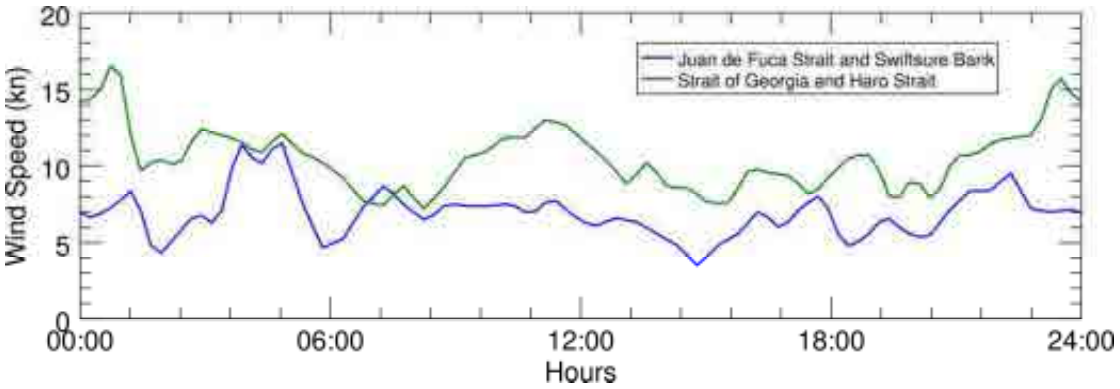

Figure A-6. Simulated wind speed in the Local Study Areas during a 24-hour period in July. Wind speeds were based on historical data from the NOAA National Buoy Data Centre in July 2015. Mean wind speeds on the selected day (6.9 knots in Juan de Fuca Strait and Swiftsure Bank; 10.5 knots in Strait of Georgia and Haro Strait) were closest to the average value for the month.

[7] Station 46087 Neah Bay Traffic Separation Lighted Buoy: http://www.ndbc.noaa.gov/station_history.php?station=46087
[8] Station 46088 New Dungeness NOAA Environmental Lighted Buoy: http://www.ndbc.noaa.gov/station_history.php?station=46088

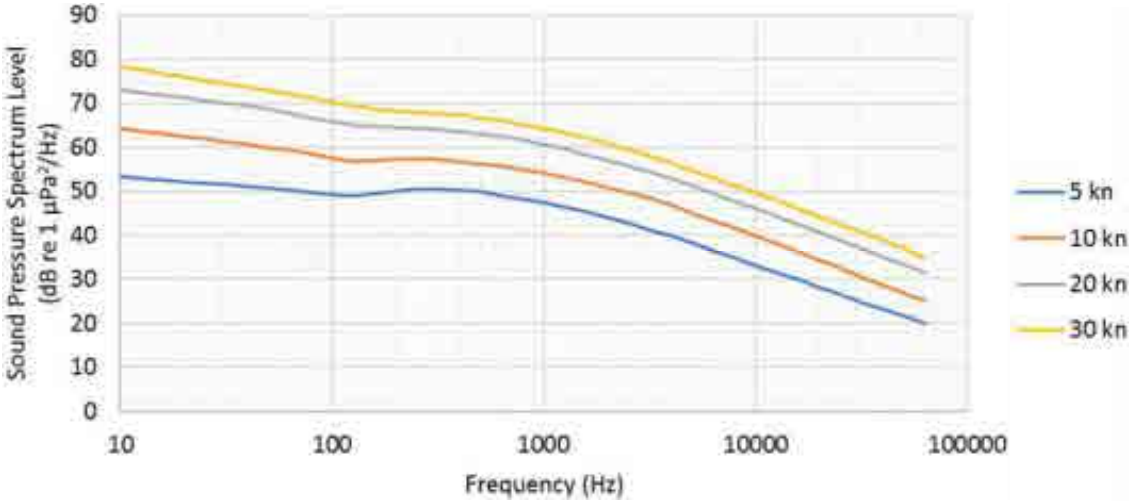

Figure A-7. Wind-driven ambient noise level as a function of frequency, for wind speeds ranging from 5 to 30 knots (Cato 2008).

A.5. Sound Propagation Models

A.5.1. Propagation Loss Model

The propagation of sound through the environment was modelled by predicting the acoustic propagation loss (hereafter referred as transmission loss)—a measure, in decibels, of the decrease in sound level between a source and a receiver some distance away. Geometric spreading of acoustic waves is the predominant way by which transmission loss occurs. Transmission loss also happens when the sound is absorbed and scattered by the seawater, and absorbed scattered, and reflected at the water surface and within the seabed. Transmission loss depends on the acoustic properties of the ocean and seabed; its value changes with frequency.

If the acoustic source level (SL), expressed in dB re 1 µPa m, and transmission loss (TL), in units of dB, at a given frequency are known, then the received level (RL) at a receiver location can be calculated in dB re 1 µPa m by:

$$RL = SL - TL. \quad \text{(A-9)}$$

Transmission loss was calculated using JASCO's Marine Operations Noise Model (MONM). MONM computes acoustic propagation via a wide-angle parabolic equation solution to the acoustic wave equation (Collins 1993) based on a version of the U.S. Naval Research Laboratory's Range-dependent Acoustic Model (RAM), which has been modified to account for elastic seabed properties (Zhang and Tindle 1995). The parabolic equation method has been extensively benchmarked and is widely employed in the underwater acoustics community (Collins et al. 1996). MONM incorporates the following site-specific environmental properties: a bathymetric grid of the model area; underwater sound speed as a function of depth; and a geoacoustic profile based on the overall stratified composition of the seafloor. Past measurements obtained during a dedicated transmission loss study (JASCO 2015) were used to validate MONM predictions for the Regional Study Area.

The Regional Study Area was divided into 20 zones, as seen in Figure A-8, based on the four unique geoacoustic regions shown in Figure A-5, and the five water depth ranges listed in Table A-3. MONM was used to compute curves of transmission loss compared to range for each zone in 1/3-octave-bands between 10 Hz and 5 kHz, out to a maximum distance of 75 km from the source. Transmission loss for each zone was modelled assuming uniform bathymetry (i.e., range-independent water depth) for a receiver depth of 10 m. Transmission loss was averaged

over five frequencies inside each 1/3-octave-band, and the transmission loss compared to range curves were smoothed inside a 200 m window to remove fine-scale interference effects. At high frequencies, mean transmission loss computed by MONM is expected to converge to a high frequency (i.e., ray-theoretical) limit; therefore, transmission loss values for bands above 5 kHz were approximated by adjusting transmission loss at 5 kHz to account for frequency-dependent absorption at higher frequencies (François and Garrison 1982a, 1982b). For each of the 20 zones, transmission loss was modelled using two different sound speed profiles, representing July and January conditions, and six source depths (1 to 6 m, in 1 m step), representing the nominal acoustic emission centres of small and large draft vessels. Figure A-9 presents plots that help visualize how the modelled transmission loss varies with distance from the source and frequency, as well as with zones and seasons.

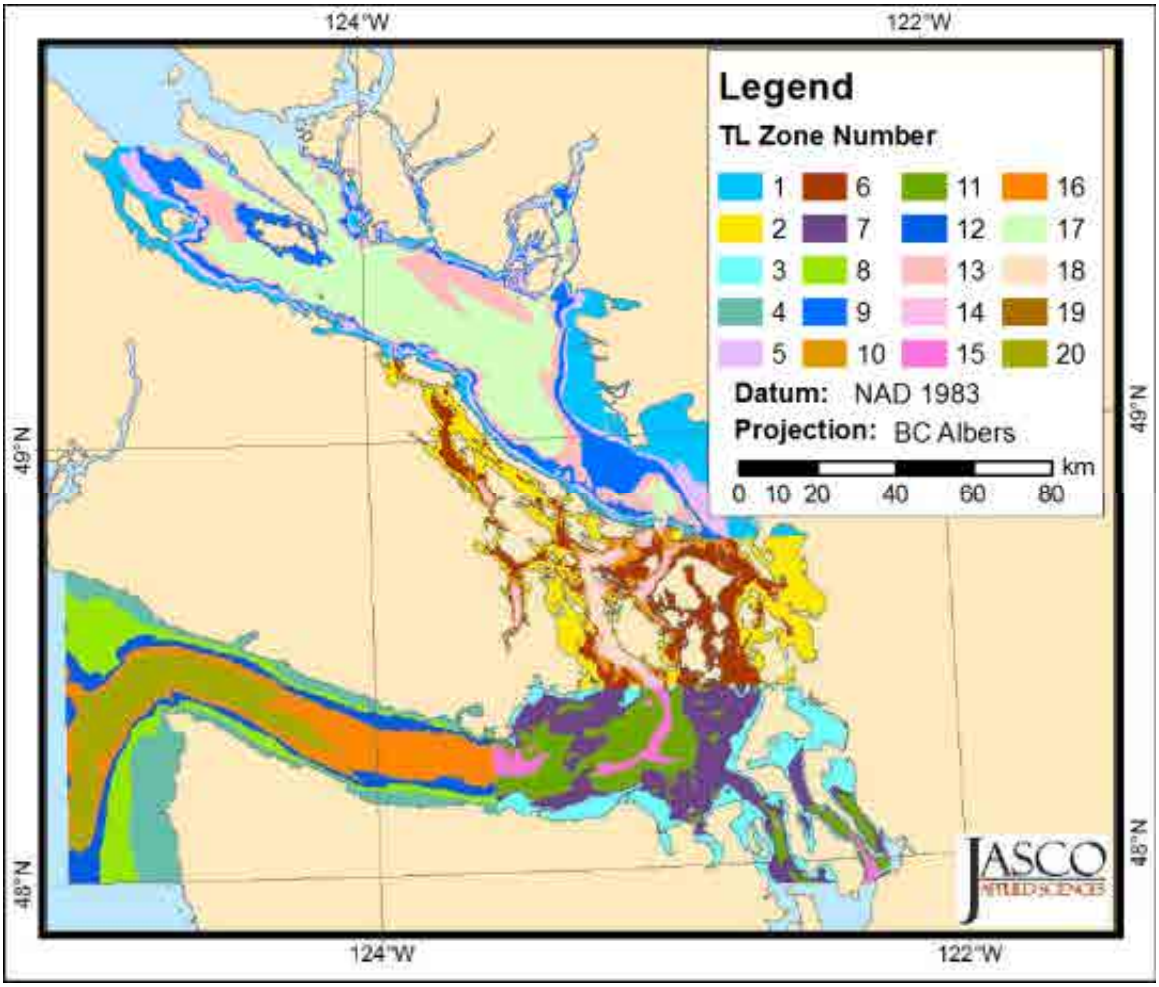

Figure A-8. Map of transmission loss (TL) zones 1–20 used for modelling sound propagation in the Regional Study Area.

Table A-3. Zone numbers, corresponding geoacoustics, and water depths. Geoacoustic properties of each region are listed in Table A-2.

Zone	Water depth range (m)	Modelled water depth (m)	Geoacoustic region
1	0–50	25	Strait of Georgia
2	0–50	25	Haro Strait and Rosario Strait
3	0–50	25	East Juan de Fuca Strait
4	0–50	25	West Juan de Fuca Strait
5	50–100	75	Strait of Georgia
6	50–100	75	Haro Strait and Rosario Strait
7	50–100	75	East Juan de Fuca Strait
8	50–100	75	West Juan de Fuca Strait
9	100–150	125	Strait of Georgia
10	100–150	125	Haro Strait and Rosario Strait
11	100–150	125	East Juan de Fuca Strait
12	100–150	125	West Juan de Fuca Strait
13	150–200	175	Strait of Georgia
14	150–200	175	Haro Strait and Rosario Strait
15	150–200	175	East Juan de Fuca Strait
16	150–200	175	West Juan de Fuca Strait
17	>200	225	Strait of Georgia
18	>200	225	Haro Strait and Rosario Strait
19	>200	225	East Juan de Fuca Strait
20	>200	225	West Juan de Fuca Strait

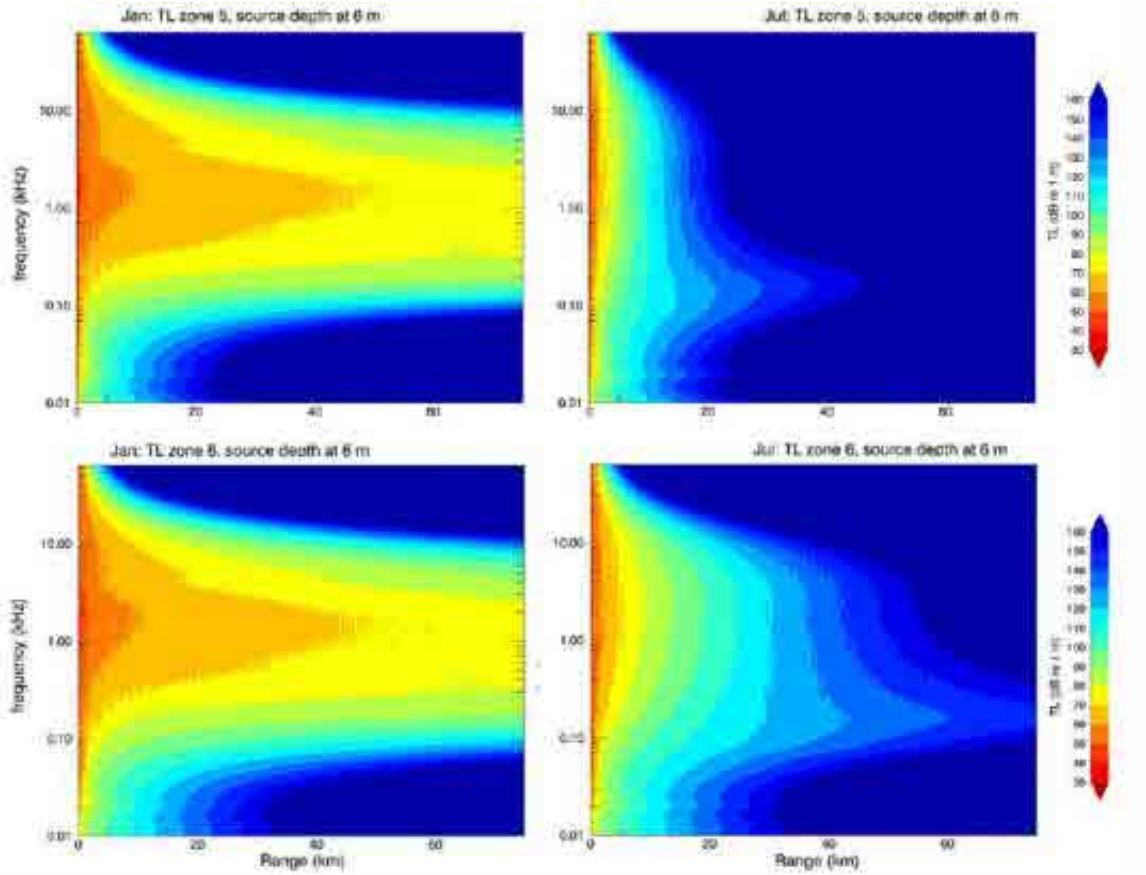

Figure A-9. Example plots of modelled transmission loss as a function of distance from the source and frequency. This example represents the transmission loss in Zone 5 (top) and Zone 6 (bottom) seen in Figure A-8, for January (left) and July (right). Source depth was 6 m, and receiver depth was 10 m.

A.5.2. Cumulative Noise Model

Maps of cumulative monthly commercial vessel traffic noise were modelled for several vessel traffic scenarios based on the vessel source level data described in Section 2.3.3, the vessel density data described in Section 2.3.2, and the tabulated transmission loss compared to range curves described in Section 2.3.1 and Appendix A.5.1. For the scenarios modelled over the Regional Study Area, the study area represented a 208 × 184 km BC Albers grid, where acoustic sources and receivers were assumed to be at the centre of each 800 × 800 m map grid cell. For the scenarios modelled over the Local Study Areas, each study area represented a higher resolution BC Albers grid, where acoustic sources and receivers were assumed to be at the centre of each 200 × 200 m map grid cell. The area covered varied between 27 × 50 km for Swiftsure Bank and 86 × 82 km for the Strait of Georgia. The 1/3-octave-band SEL in each map cell was computed as the total vessel noise energy originating from all adjacent map cells within a 75 km radius for the Regional Study Area and 30 km for the Local Study Areas. The maximum propagation range from the sources was limited for computational efficiency, but the range was long enough to cover the width of channels where vessels transited. SEL is a measure of the total acoustic energy received at a location over a specific time duration, and it is the standard metric for quantifying the total sound exposure of marine organisms.

To compute transmission loss between pairs of cells, geometric rays were projected from each cell where the density of a given vessel class was non-zero (the source cell) to all nearby cells (the receiver cells) not blocked by land within maximum propagation range. The 1/3-octave-band transmission loss between source and receiver cells was then interpolated from the tabulated

transmission loss compared to range curves, based on the midpoint separation of the cells and on the transmission loss zone traversed by the ray. For the range-dependent case, where the ray between a source cell *i* and a receiver cell *j* traverses more than one zone, the transmission loss was computed as the weighted-average value:

$$TL_{ij} = -10\log_{10}\sum_{n} 10^{-TL^{(n)}(r_{ij})/10} \times d_n / r_{ij} \quad . \tag{A-10}$$

In the above equation, r_{ij} is the source-receiver separation, $TL^{(n)}$ is the tabulated transmission loss in zone *n*, and d_n is the distance traversed by the ray in zone *n*. For the special case where the source and receiver cell are identical, transmission loss, TL_{ii}, was estimated by assuming that the sound power radiated by all sources in a cell is distributed evenly over the cell's area, resulting in a horizontally uniform sound field. For a square cell of size *D*, this assumption results in the following expression:

$$TL_{ii} = 10\log_{10}(4\pi / D^2) = 20\log_{10} D - 11 \quad . \tag{A-11}$$

For an 800 m square cell, the corresponding TL_{ii} value is 47.1 dB.

The total ship noise energy, E_{ij}, transmitted from each source cell *i* to receiver cell *j*, was computed using the source level and corresponding cell-to-cell transmission loss values summed over all vessel classes and adjusted for individual vessel speeds and the cumulative vessel class time in each source cell:

$$E_{ij} = \sum_{k} 10^{\left(SL_k - TL_{ij}\right)/10} \times \left(\frac{v_k}{v_{ref}}\right)^{C_{v,k}} \times T_k \quad . \tag{A-12}$$

In the above equation, the source level for each vessel class *k* is computed by adjusting the reference source level SL_k for speed v_k according to the power-law model (Ross 1976), where v_{ref} is the reference speed of the class *k*. The power of the ratio of speeds, $C_{v,k}$, depends on the modelled vessel class. The source energy is then computed by multiplying the source power by the cumulative time T_k that vessels from class *k* occupied the source cell. The total SEL in the receiver cell *j* was then computed as the sum of the sound energy transmitted from all cells with vessels within maximum propagation range:

$$SEL_j = 10\log_{10}\left(\sum_{j} E_j\right) \quad . \tag{A-13}$$

The mean monthly equivalent continuous noise level (L_{eq}) in the receiver cell *j* was equal to the total noise energy in all 1/3-octave-bands, divided by the number of seconds in the month, T_{mon}, that is:

$$L_{eq\,j} = SEL_j - 10\log_{10}(T_{\mathrm{mon}}) \, . \tag{A-14}$$

A.5.3. Time-Dependent Noise Model

Time-dependent SPL over 24–33 hours were modelled for the slow-down and convoy scenarios based on the vessel source level data described in Section 2.3.3, the vessel traffic distribution described in Section 2.3.2, and the tabulated transmission loss compared to range curves described in Section 2.3.1 and Appendix A.5.1. SPL in 1/3-octave-bands were modelled on a BC Albers grid covering the Local Study Area (between 27 × 50 km for Swiftsure Bank and 86 × 82 km for the Strait of Georgia), where acoustic sources and receivers were assumed to be at the centre of each 200 × 200 m map grid cell. For every time increment of the simulation, vessels were assigned to map grid cells based on their interpolated coordinates from the track data. For each source cell, a fan of geometric rays was projected to all receiver cells not blocked by land within 75 km range. Along each ray, the 1/3-octave-band transmission loss between source and receiver cells was computed from the tabulated transmission loss versus range curves, based on the transmission loss zones traversed by the ray. To accommodate range-dependent transitions between zones, a composite transmission loss curve was created for each ray, based on a recursive sum of the range-dependent transmission loss curve at each range step along the ray:

$$\mathrm{TL}(n\Delta r) = \mathrm{TL}((n-1)\Delta r) + (\mathrm{TL}'[n;k] - \mathrm{TL}'[n-1;k]) \quad , \qquad \text{(A-15)}$$

where Δr is the range increment, n is the range step (an integer), k is the zone number corresponding to step n along the current ray, and $\mathrm{TL}'[n;k]$ denotes the tabulated TL value at step n for zone k. For the special case where the source and receiver cells are identical, TL was calculated by assuming that the radiated sound power in a cell is distributed evenly over the cell's area, resulting in a horizontally uniform sound field. This assumption gives an in-cell TL value of $20\times\log D - 11$, where D is the edge-length of a cell.

The contribution of wind-driven ambient noise was also included in the model. Tabulated curves of 1/3-octave-band ambient noise versus wind speed were obtained from Wenz (1962) and Cato (2008). Hourly mean wind speed data were obtained from NOAA weather stations 46087 and 46088, located at Neat Bay (~ 6 nm north of Cape Flattery, WA) and New Dungeness (~7 nm northeast of Port Angeles, WA) (NOAA 2017, NOAA 2018). Wind-driven noise SPL for the study area were interpolated from the Wenz and Cato curves according to the recorded wind speed versus time data from the weather stations. Aggregate SPL in all map grid cells were computed from the cumulative sound field of all vessels in the simulation, plus the wind-driven ambient contribution, for each time step in the model.

A.6. Marine Mammal Frequency Weighting

The potential for noise to affect animals depends on how well the animals can hear it. Noises are less likely to disturb or injure an animal if they are at frequencies that the animal cannot hear well. An exception occurs when the sound pressure is so high that it can physically injure an animal by non-auditory means (i.e., barotrauma). For sound levels below such extremes, the importance of sound components at particular frequencies can be scaled by frequency weighting that is relevant to an animal's sensitivity to those frequencies (Nedwell and Turnpenny 1998, Nedwell et al. 2007).

A.6.1. SRKW Audiogram-Weighting

Audiograms represent the hearing threshold for tonal sounds (i.e., single-frequency sinusoidal signals) as a function of the tone frequency. These species-unique sensitivity curves are generally U-shaped, with higher hearing thresholds at low and high frequencies. Noise levels above hearing threshold are calculated by subtracting species-unique audiograms from the received 1/3-octave-band noise levels. The audiogram-weighted 1/3-octave-band levels are summed to yield broadband noise levels relative to each species' hearing threshold. Audiogram-weighted levels are expressed in units of dB re HT, which is the decibel (dB) level of sound above hearing threshold (HT). Sound levels less than 0 dB re HT are below the typical hearing threshold for a species and are likely inaudible to those animals.

SRKW use sound actively when foraging to echolocate their prey. The echolocation signals range in frequency from 15 and 100 kHz (Au et al. 2004). SRKW also produce communication calls when foraging. Groups can spread out over several kilometres while foraging, but the area they cover is limited by the distance where they can detect calls. Calls typically range in frequency from 500 Hz to 40 kHz (Miller 2006). Although substantially louder below 1 kHz, ship noise reaches above 60 kHz. Thus, shipping noise may determine the distance between SRKW while foraging.

The SRKW audiogram used in this study is presented in Figure A-10. Based on values from Szymanski et al. (1999) and Branstetter et al. (2017), it was extrapolated from the lowest measured frequency down to 10 Hz using a 12 dB/octave slope, which represents the hearing roll-off toward the infrasound range for mammals (Marquardt et al. 2007). Although the validity of the extrapolation for marine mammals is not physiologically confirmed, it is likely that these animals have a higher hearing threshold at frequencies outside their hearing range than the terminal trend of their audiogram predicts.

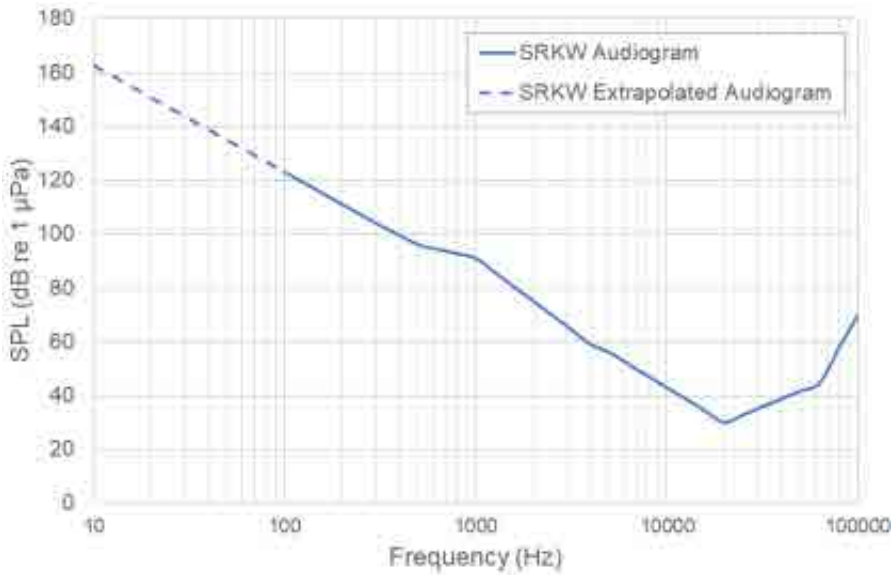

Figure A-10. Southern Resident Killer Whale (SRKW) audiogram used for this study, based on Szymanski et al. (1999) and Branstetter et al. (2017). The dashed curve is extrapolated low-frequency threshold.

APPENDIX B. AUTOMATIC IDENTIFICATION SYSTEM (AIS) VESSEL CATEGORY ASSIGNMENTS

APPENDIX B. AUTOMATIC IDENTIFICATION SYSTEM (AIS) VESSEL CATEGORY ASSIGNMENTS

B.1. AIS Vessel Category Assignments

Table B-1 shows the assignment of vessel type codes from the Marine Traffic AIS dataset (Vessel type) to vessel categories in the cumulative noise model (Model class). Clipper Line vessels travelling a Victoria-Seattle route and roll-on/roll-off vessels in the Seaspan Ferries fleet were manually assigned to the Ferry category. Sailing vessels were excluded from the Recreational vessel category, and they were excluded from the model (i.e., they were assumed not to be under power).

Table B-1. Vessel types from the Marine Traffic AIS dataset and their vessel class for modelling.

Model class	Vessel type
Container	Cargo/container ship
	Container ship
Cruise ship	Passenger (greater than 100 m in length)
	Passenger ship (greater than 100 m in length)
Ferry	Ro-Ro/Passenger ship
Fishing	Factory trawler
	Fish carrier
	Fish factory
	Fishing
	Fishing vessel
	Trawler
Government	Buoy-laying vessel
	Fishery patrol vessel
	Fishery research vessel
	Law enforcement
	Logistics naval vessel
	Military ops
	Patrol vessel
	Replenishment vessel
	Research/survey vessel
Merchant	Bulk carrier
	Cargo
	Cargo - Hazard A (major)
	Chemical tanker
	General cargo
	LPG tanker
	Rail/vehicle carrier
	Reefer
	Ro-Ro cargo
	Ro-Ro/Container carrier
	Self-discharging bulk carrier
	Timber carrier
	Vehicle carrier
	Wood chip carrier

Model class	Vessel type
Miscellaneous	Anti-pollution
	Cable layer
	Dive vessel
	Drill ship
	Heavy lift vessel
	High speed craft
	Hopper dredger
	Local vessel
	Other
	Pilot vessel
	Port tender
	Reserved
	SAR
	Tender
	Unspecified
	Wing In Grnd
Passenger (less than 100 m in length)	Passenger (less than 100 m in length)
	Passenger ship (less than 100 m in length)
Recreational	Pleasure craft
	Yacht
Tanker	Crude oil tanker
	Oil product tanker
	Oil/Chemical tanker
	Tanker
Tug	Anchor handling vessel
	Fire fighting vessel
	Multi-purpose offshore vessel
	Offshore supply ship
	Pollution control vessel
	Pusher tug
	Towing vessel
	Tug

APPENDIX C. MULTIPLE LINEAR REGRESSION MODELS–PREDICTING MONOPOLE SOURCE LEVEL (MSL) FROM THREE PARAMETERS

APPENDIX C. MULTIPLE LINEAR REGRESSION MODELS–PREDICTING MONOPOLE SOURCE LEVEL (MSL) FROM THREE PARAMETERS

C.1. Multiple Regression Model

Vessel noise emissions generally increase with speed through water, due to speed-related increases in machinery vibration and propeller cavitation. A multivariate analysis was applied to the Underwater Listening Station (ULS) source level data to determine an appropriate speed scaling parameter for each category of vessel in the model. To control for the effect of parameters other than speed on the measurements, multiple regression was used to fit monopole source levels (MLS; 20–31,600 Hz) to the following equation for each category:

$$MSL = C_v \times 10\log_{10}\left(\frac{v}{v_{ref}}\right) + C_l \times 10\log_{10}\left(\frac{l}{l_{ref}}\right) + \beta \times d + MSL_{ref}\ . \quad \text{(C-1)}$$

The terms in this equation are:

- MSL = monopole source level (dB re 1 µPa m),
- C_v = speed power law coefficient (dimensionless),
- v = speed over water (kn),
- v_{ref} = reference speed (1 kn),
- C_l = length power law coefficient (dimensionless),
- l = length overall (m),
- l_{ref} = reference length (1 m),
- β = closest point of approach (CPA) correction slope (dB/m),
- d = vessel CPA (m), and
- MSL_{ref} = intercept term (MSL at v_{ref}, l_{ref}, and d = 0).

Table C-1 shows the best-fit MSL scaling parameters from the multiple-regression analysis. Categories that are missing or insufficiently represented in the ULS data were assumed to have a default scaling coefficient of C_v = 6, per the original Ross power-law model (Ross 1976).

Table C-1. Terms of the monopole source level (MSL) linear regression model for vessel classes based on speed, length, and closest point of approach (CPA). The r^2 value is the percent of the total data variance explained by the multiple regression model. Length and speed were strongly correlated for fishing vessels, so length was not included as an independent parameter for this category.

Vessel class	C_v	C_l	β	r^2 (%)
Container	3.384	−0.604	0.00346	34
Cruise ship	5.069	−2.283	0.00358	46
Ferry (Ro-ro passenger and Ro-ro cargo)	8.061	−4.878	0.00067	50
Fishing	3.634	NA	0.00305	52
Merchant	4.544	0.725	0.00320	20
Miscellaneous	4.070	0.240	0.00126	43
Tanker	2.999	0.845	0.00582	16
Tug	0.949	1.055	0.00564	28
Vehicle carrier	3.312	−0.335	−0.00041	41

C.2. Partial Residual Plots

For each vessel class, the plots below show the trend of MSL with speed, length, and CPA derived from the multivariate analysis (red lines), along with the partial residuals (black dots) of the MSL data for each parameter. These plots show the relationship between a given independent variable (speed, length, or CPA) and the MSL of the vessel class. A steep slope in the multivariate analysis (red lines) translates to the strong relation between the variable and the MSL.

For fishing vessels, the speed and vessel length are highly correlated. Thus, the partial residual plots for this vessel class are only shown for the independent variables used in the linear regression: speed and CPA.

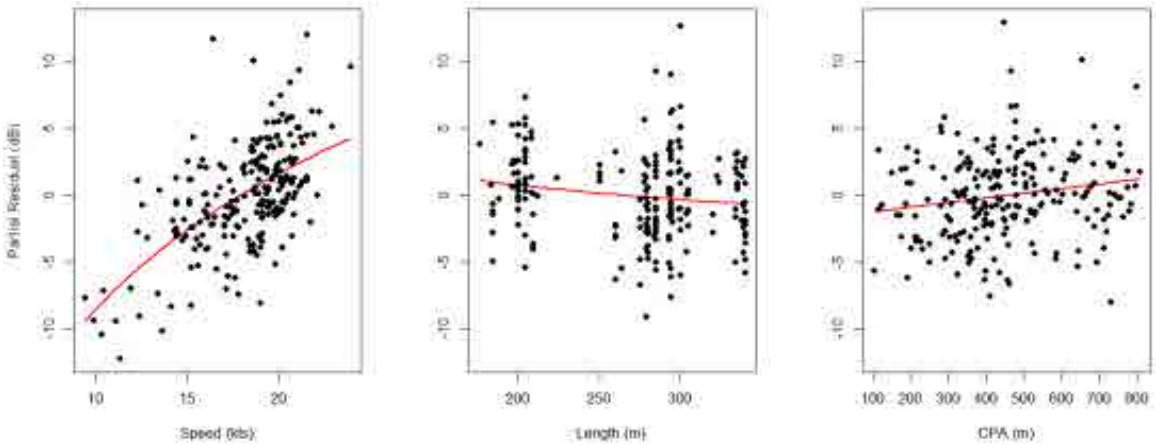

Figure C-1. *Container*: Partial residual plots for speed (left), length (centre), and closest point of approach (CPA) (right) derived from the multivariate analysis (red line), along with the partial residuals (black dots) of the monopole source level (MSL) data.

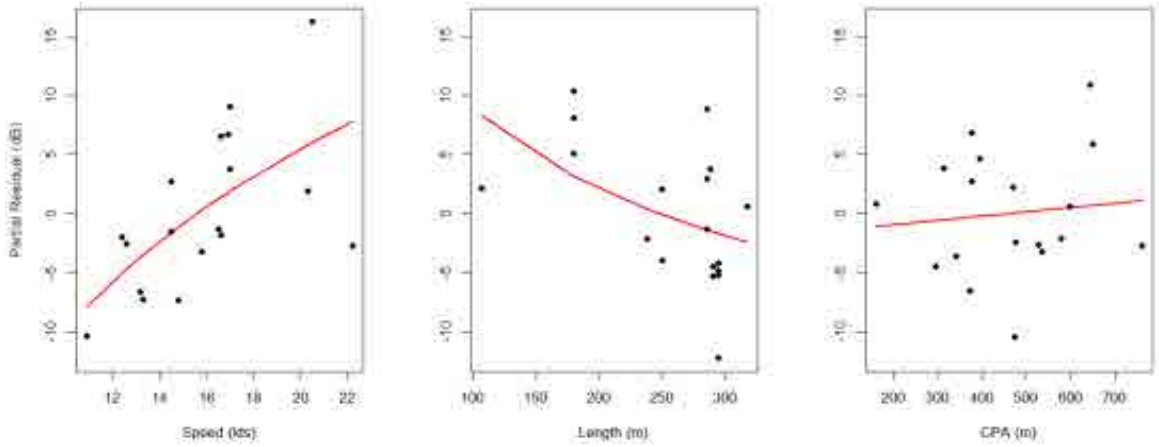

Figure C-2. *Cruise ship:* Partial residual plots for speed (left), length (centre), and closest point of approach (CPA) (right) derived from the multivariate analysis (red line), along with the partial residuals (black dots) of the monopole source level (MSL) data.

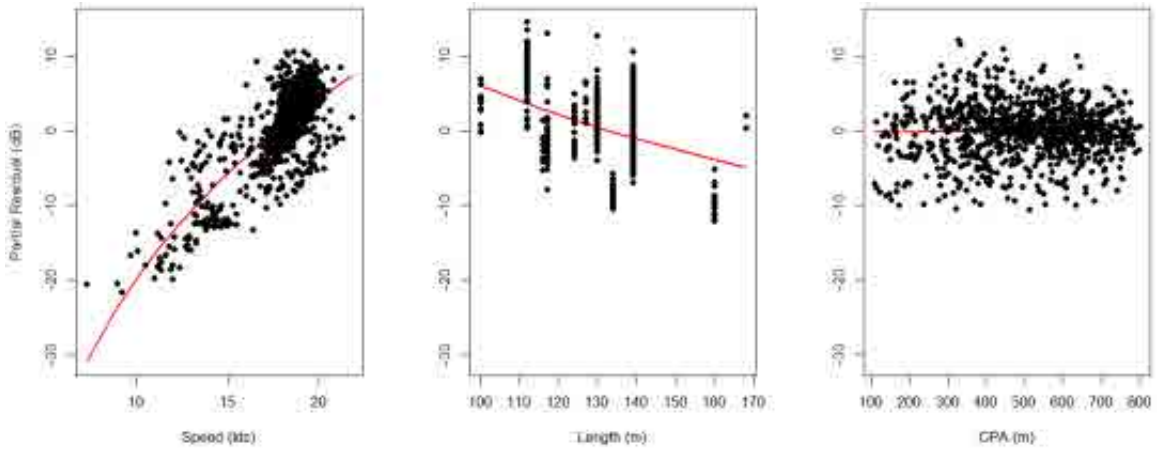

Figure C-3. *Ferry*: Partial residual plots for speed (left), length (centre), and closest point of approach (CPA) (right) derived from the multivariate analysis (red line), along with the partial residuals (black dots) of the monopole source level (MSL) data.

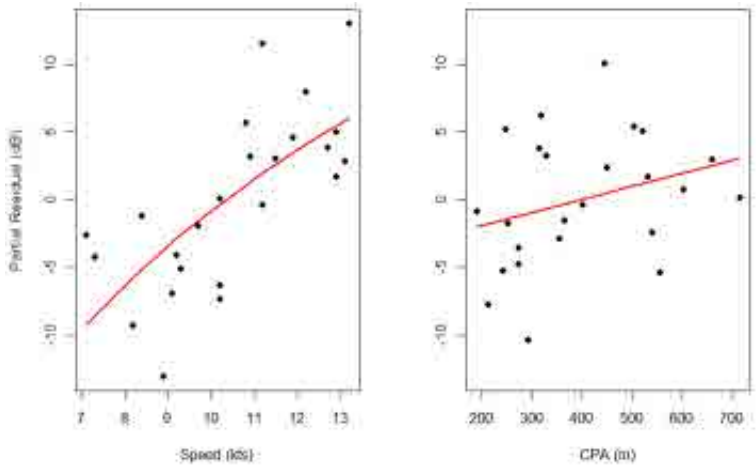

Figure C-4. *Fishing vessel*: Partial residual plots for speed (left), length (centre), and closest point of approach (CPA) (right) derived from the multivariate analysis (red line), along with the partial residuals (black dots) of the monopole source level (MSL) data.

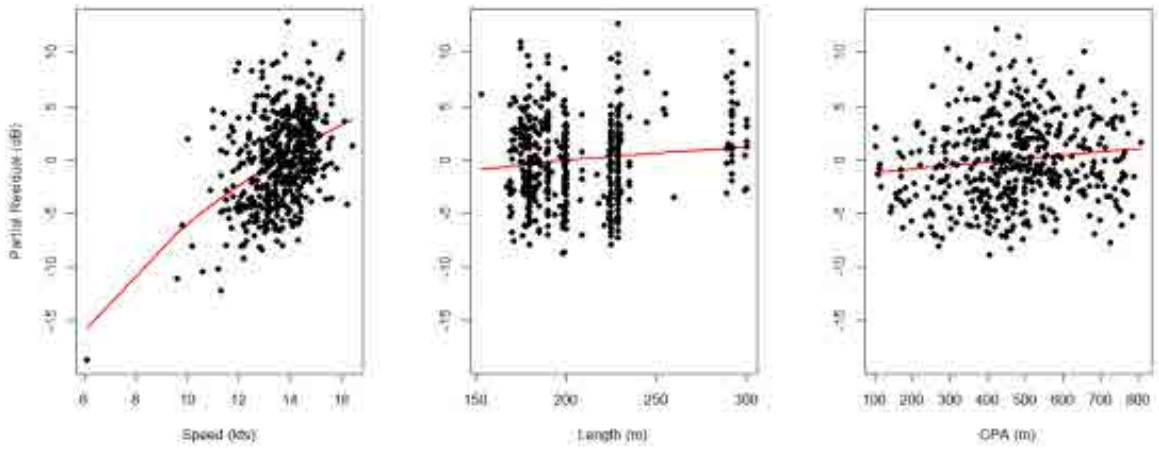

Figure C-5. *Merchant*: Partial residual plots for speed (left), length (centre), and closest point of approach (CPA) (right) derived from the multivariate analysis (red line), along with the partial residuals (black dots) of the monopole source level (MSL) data.

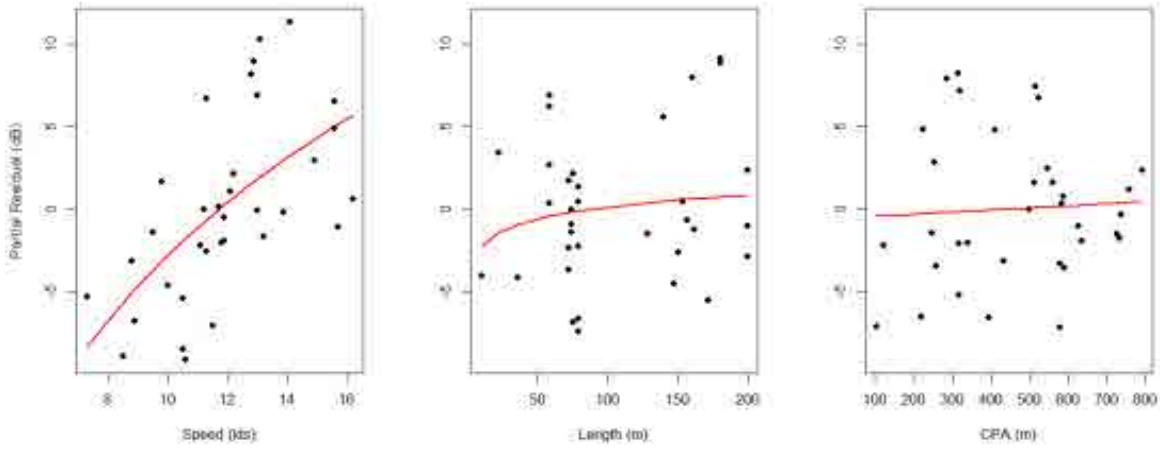

Figure C-6. *Miscellaneous*: Partial residual plots for speed (left), length (centre), and closest point of approach (CPA) (right) derived from the multivariate analysis (red line), along with the partial residuals (black dots) of the monopole source level (MSL) data.

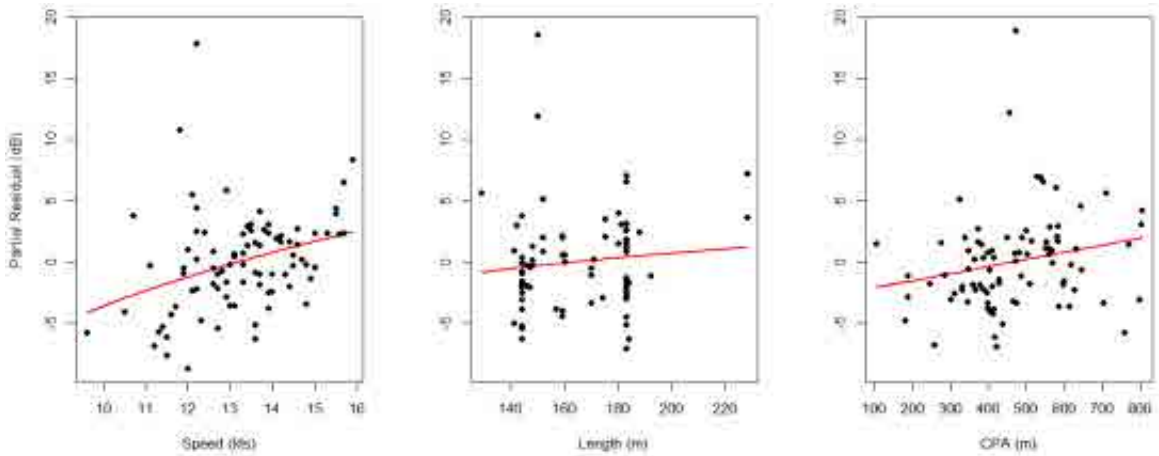

Figure C-7. *Tanker*: Partial residual plots for speed (left), length (centre), and closest point of approach (CPA) (right) derived from the multivariate analysis (red line), along with the partial residuals (black dots) of the monopole source level (MSL) data.

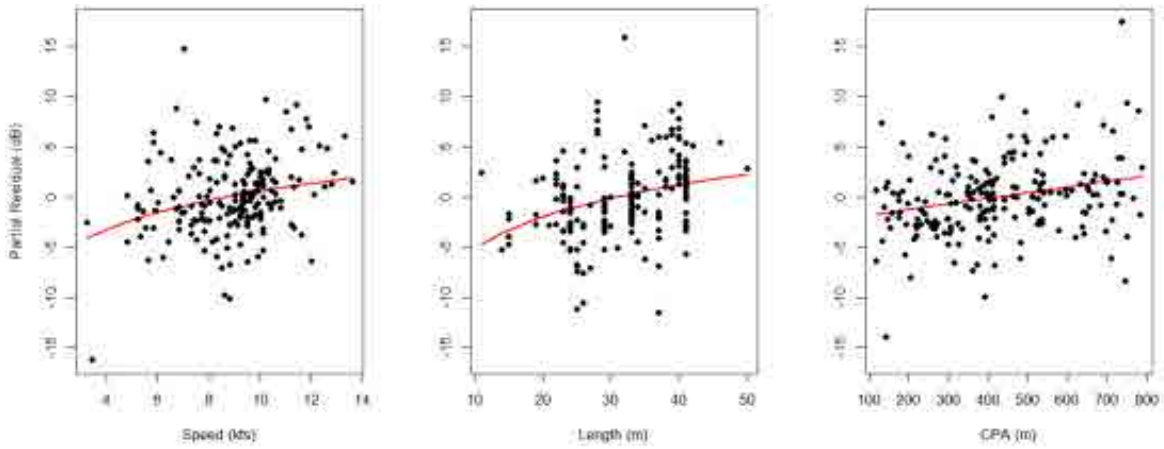

Figure C-8. *Tug*: Partial residual plots for speed (left), length (centre), and closest point of approach (CPA) (right) derived from the multivariate analysis (red line), along with the partial residuals (black dots) of the monopole source level (MSL) data.

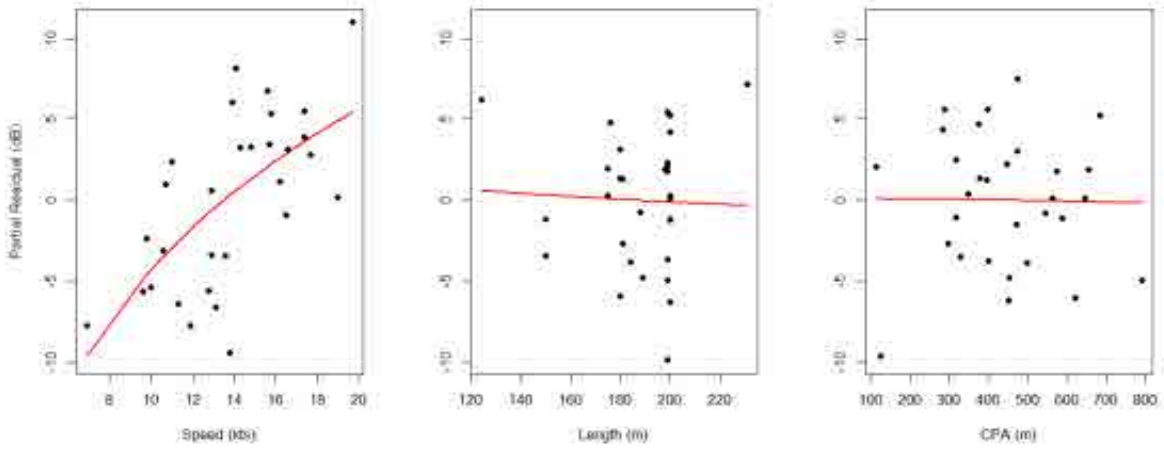

Figure C-9. *Vehicle carrier*: Partial residual plots for speed (left), length (centre), and closest point of approach (CPA) (right) derived from the multivariate analysis (red line), along with the partial residuals (black dots) of the monopole source level (MSL) data.

APPENDIX D. REPLACING 10% OF NOISIEST SHIPS

APPENDIX D. REPLACING 10% OF NOISIEST SHIPS

What constitutes a “noisy ship” can be defined in many ways. It can be based on the vessel’s noise emissions (i.e., source levels) at one frequency, over a small frequency band, or over the entire frequency range from low to high frequencies (i.e., broadband source levels). It can also be defined for source levels with or without frequency weighting applied. In this study, vessels within each commercial class were ranked according to their unweighted and audiogram-weighted broadband source level. The audiogram used is presented in Figure A-10

Vessel noise emissions are generally much higher at frequencies below 1 kHz than above. Also, vessels with the highest low-frequency levels may or may not have the highest levels at frequencies above 1 kHz. Since SRKW hearing is better at frequencies above 1 kHz, applying audiogram-weighting results in a different ranking for noisiest vessel then when no frequency-weighting is applied. The left-hand images in Figures D-1 to D-6 show the measured spectra for each class of commercial vessels, highlighting the noisiest 10% and quietest 10% of vessels according to their unweighted broadband source levels. The right-hand images present the same information, according to the SRKW audiogram-weighted source levels.

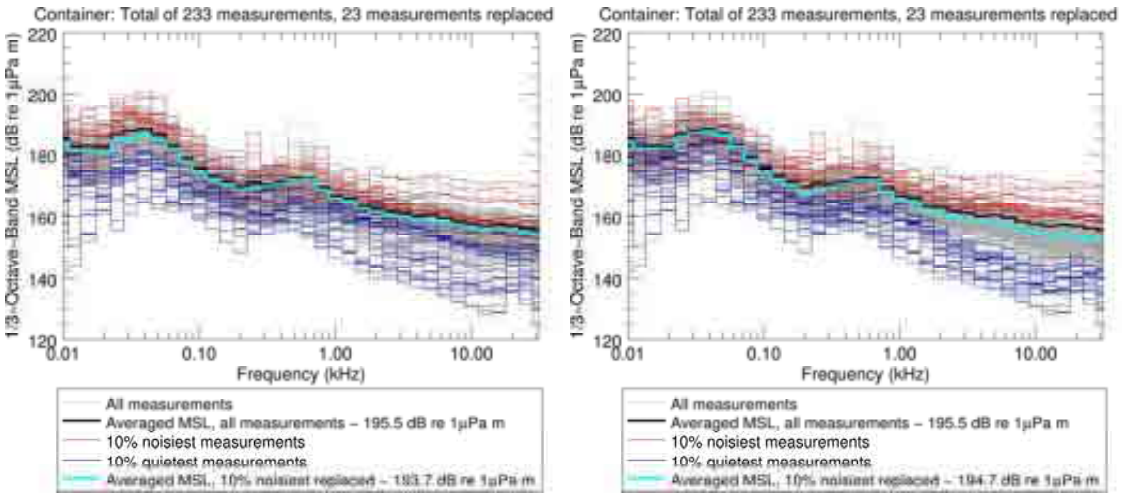

Figure D-1. *Container ships*: 1/3-octave-band source level spectra for all measured vessels in the class. The spectra are ranked according to their (left) unweighted and (right) audiogram-weighted broadband level. The 10% of spectra with the highest broadband levels are red, and the 10% of spectra with the lower broadband level are blue. The averaged spectra for all measurements is black, and the average spectra after replacing the highest 10% by the lowest 10% is cyan.

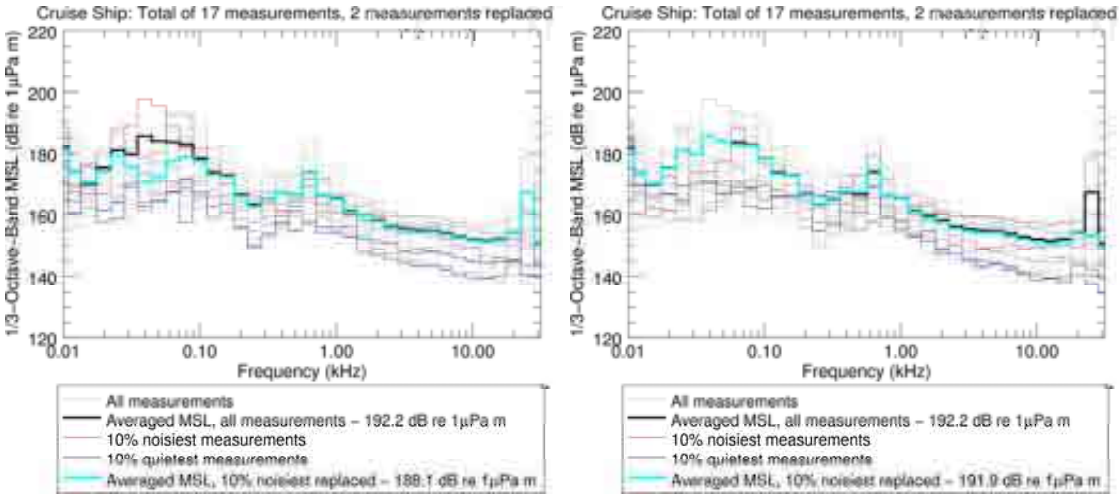

Figure D-2. *Cruise ship:* 1/3-octave-band source level spectra for all measured vessels in the . The spectra are ranked according to their (left) unweighted and (right) audiogram-weighted broadband level. The 10% of spectra with the highest broadband levels are red, and the 10% of spectra with the lower broadband level are blue. The averaged spectra for all measurements is black, and the average spectra after replacing the highest 10% by the lowest 10% is cyan.

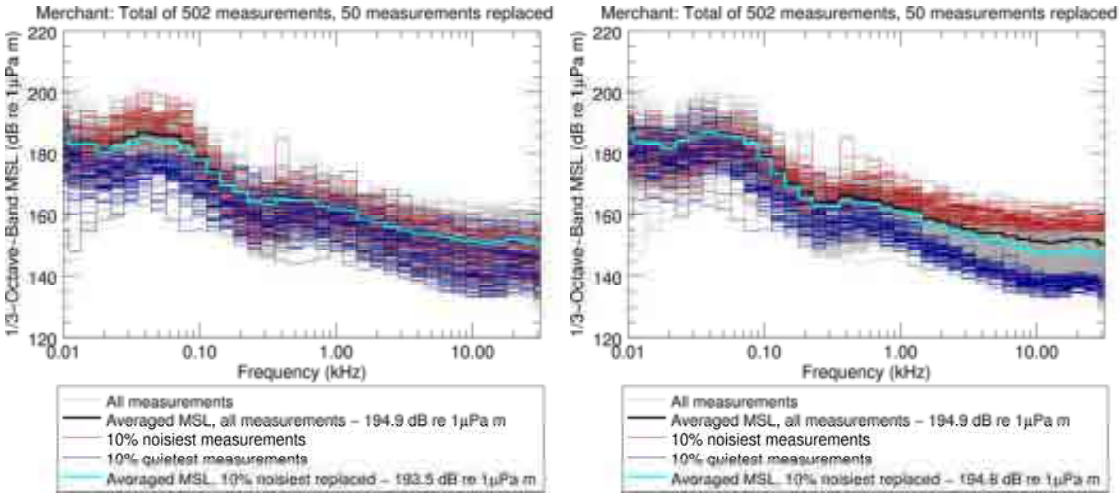

Figure D-3. *Merchant*: 1/3-octave-band source level spectra for all measured vessels in the . The spectra are ranked according to their (left) unweighted and (right) audiogram-weighted broadband level. The 10% of spectra with the highest broadband levels are red, and the 10% of spectra with the lower broadband level are blue. The averaged spectra for all measurements is black, and the average spectra after replacing the highest 10% by the lowest 10% is cyan.

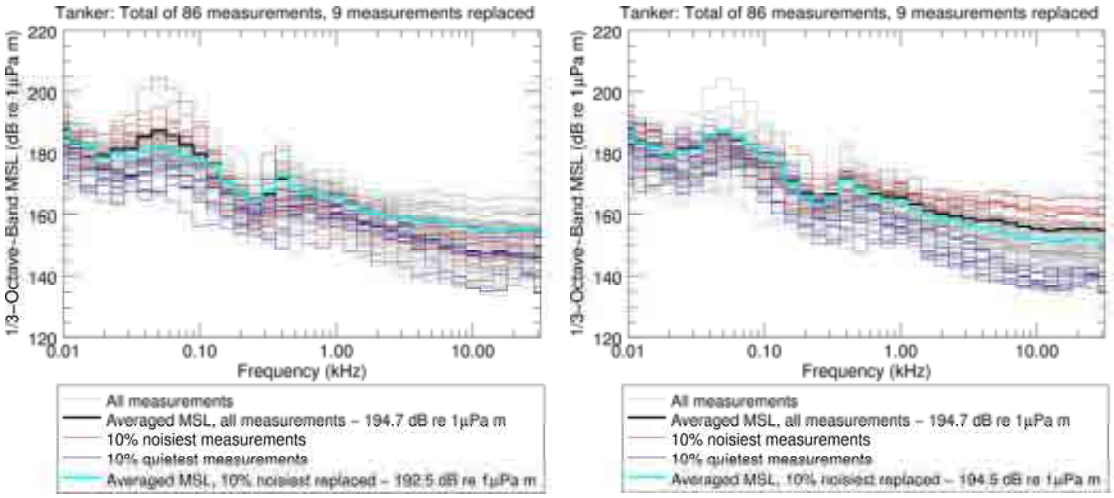

Figure D-4. *Tanker:* 1/3-octave-band source level spectra for all measured vessels in the . The spectra are ranked according to their (left) unweighted and (right) audiogram-weighted broadband level. The 10% of spectra with the highest broadband levels are red, and the 10% of spectra with the lower broadband level are blue. The averaged spectra for all measurements is black, and the average spectra after replacing the highest 10% by the lowest 10% is cyan.

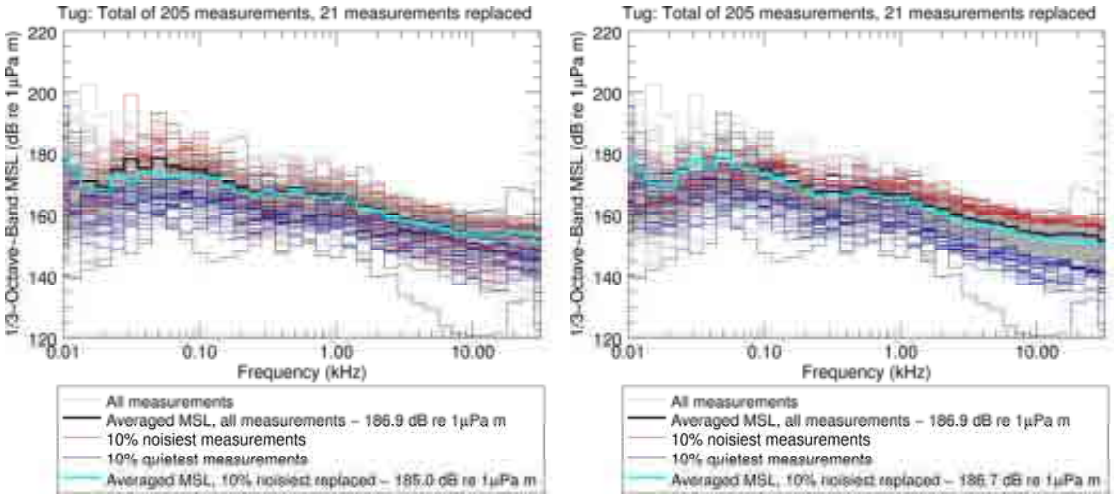

Figure D-5. *Tug:* 1/3-octave-band source level spectra for all measured vessels in the . The spectra are ranked according to their (left) unweighted and (right) audiogram-weighted broadband level. The 10% of spectra with the highest broadband levels are red, and the 10% of spectra with the lower broadband level are blue. The averaged spectra for all measurements is black, and the average spectra after replacing the highest 10% by the lowest 10% is cyan.

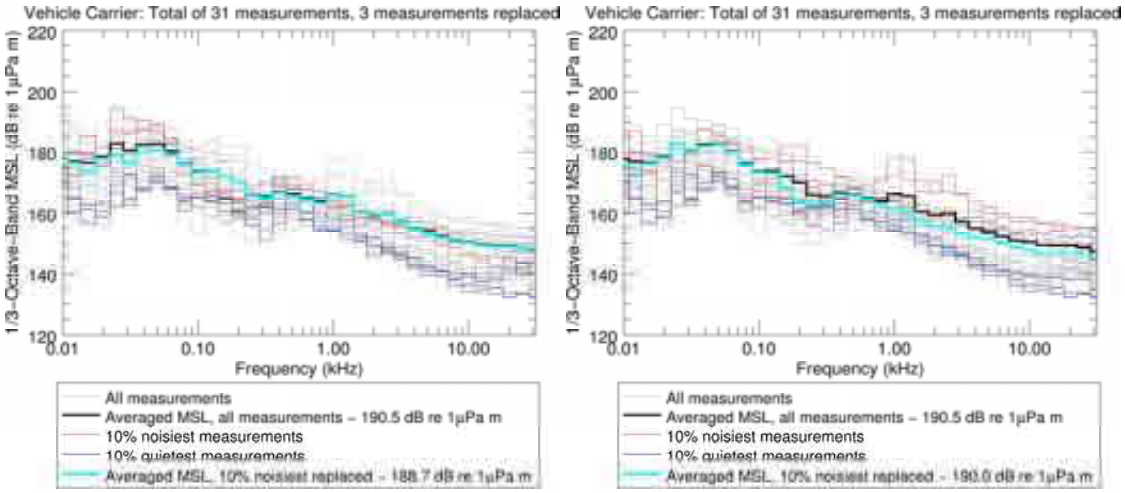

Figure D-6. *Vehicle carrier:* 1/3-octave-band source level spectra for all measured vessels in the . The spectra are ranked according to their (left) unweighted and (right) audiogram-weighted broadband level. The 10% of spectra with the highest broadband levels are red, and the 10% of spectra with the lower broadband level are blue. The averaged spectra for all measurements is black, and the average spectra after replacing the highest 10% by the lowest 10% is cyan.

APPENDIX E. LOWER RESOLUTION MODEL FOR THE REGIONAL STUDY AREA

APPENDIX E. LOWER RESOLUTION MODEL FOR THE REGIONAL STUDY AREA

E.1. Regional Study Area Results

In this section, all results are present with and without SRKW audiogram-weighting applied. The two types of results are easily identified by the different colour scale used in mapping equivalent continuous noise levels (L_{eq}).

Maps of L_{eq} for the baseline scenarios are presented in Figure E-1 in Section E.1.1. Maps of L_{eq} and changes in L_{eq} relative to the baseline are then presented for each time-averaged modelled scenario (i.e., future monthly-averaged unmitigated and mitigation scenarios, as seen in Figures E-2 to E-11 in Sections E.1.2–E.1.4). Baseline levels include noise from all vessels in the July 2015 AIS data. Future unmitigated and mitigated levels include noise from vessels associated with the Trans Mountain Project expansion as described in Section 2.2.2, in addition to that from all vessels in the 2015 AIS data.

E.1.1. Baseline Noise Levels

Figure E-1 shows maps of unweighted and audiogram-weighted equivalent noise levels for January and July 2015. The maps represent winter and summer baseline levels over the large-scale (800 × 800 m map grid cell resolution) Regional Study Area.

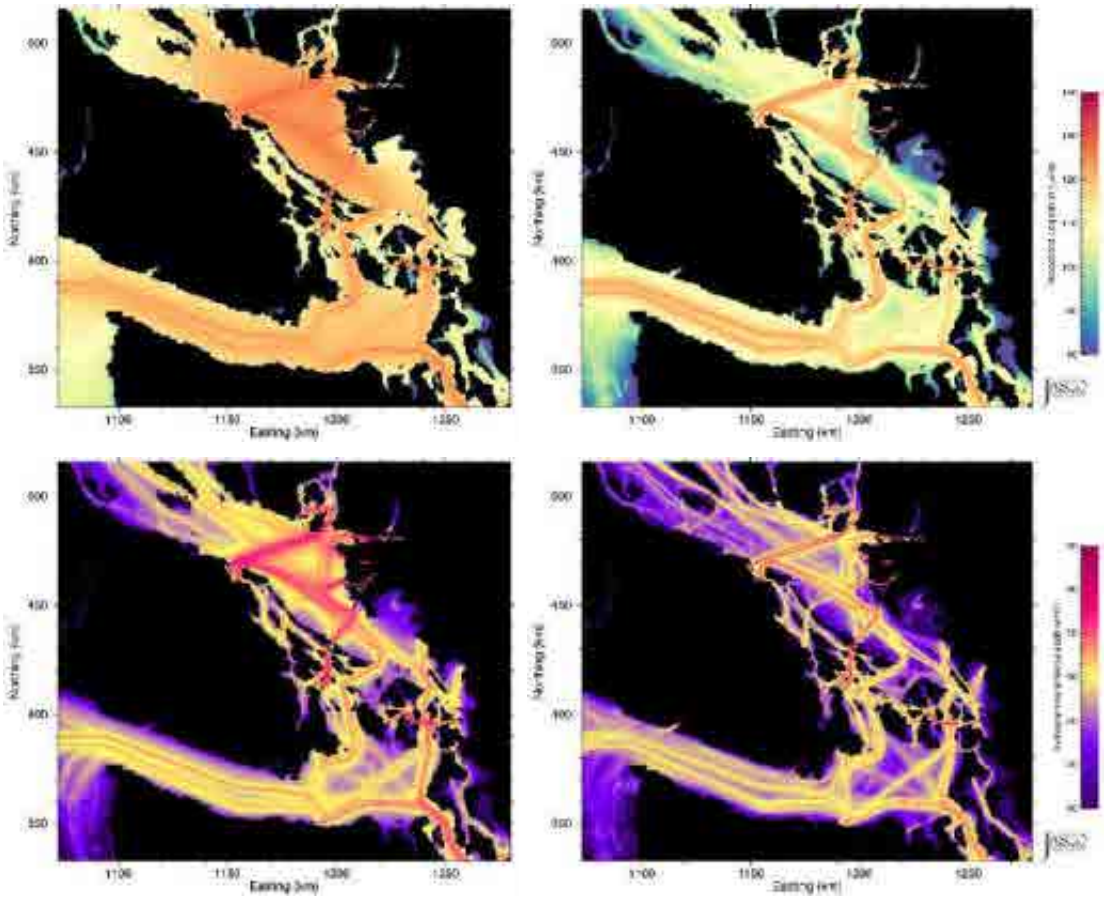

Figure E-1. *Baseline, January (left) and July (right) 2015*: Unweighted (top) and audiogram-weighted (bottom) equivalent continuous noise levels (L_{eq}) over the Regional Study Area. Grid resolution is 800 × 800 m.

E.1.2. Future Unmitigated Noise Levels

Figures E-2 and E-3 (left) present maps of future unmitigated equivalent noise levels (unweighted and audiogram-weighted, respectively) for July 2020. The maps represent the projected (i.e., future) noise levels due to expected increase in vessel traffic associated with the Trans Mountain requirements over the Regional Study Area. Figures E-2 and E-3 (right) present maps of the increase in equivalent noise levels (unweighted and audiogram-weighted, respectively) relative to the 2015 baseline levels over the same area.

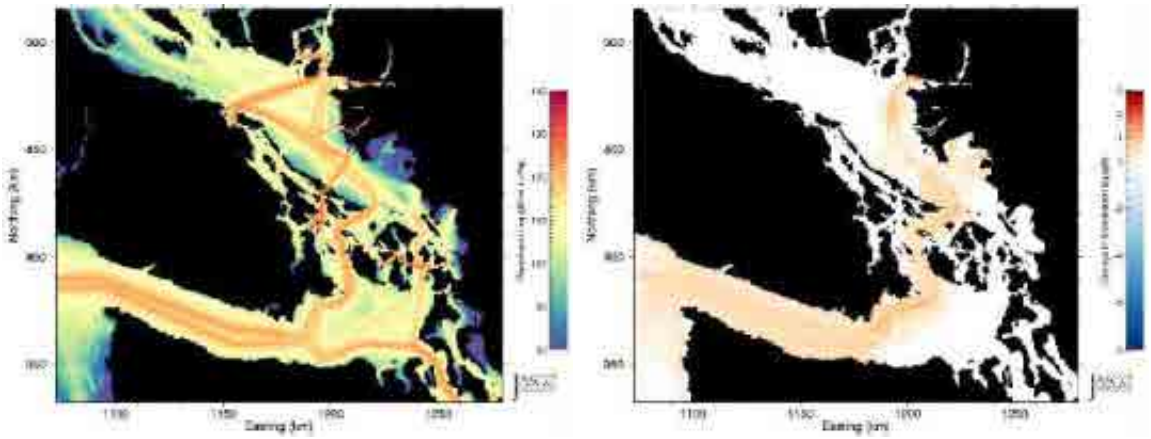

Figure E-2. *Future unmitigated, July 2020*: Unweighted equivalent continuous noise levels (L_{eq}; left), and changes in L_{eq} (dB; right) relative to July 2015 baseline levels in the Regional Study Area. Grid resolution is 800 × 800 m.

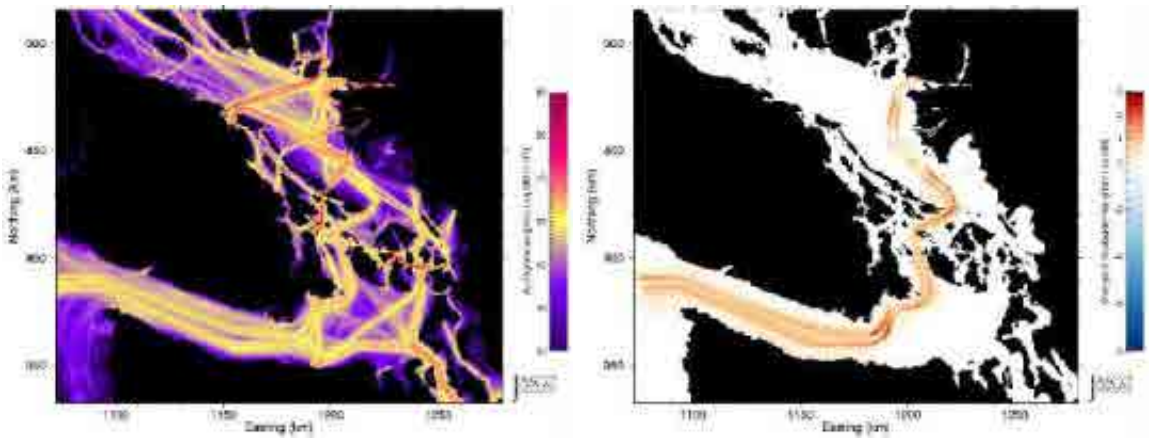

Figure E-3. *Future unmitigated, July 2020*: Audiogram-weighted equivalent continuous noise levels (*Leq*; left), and changes in *Leq* (dB; right) relative to July 2015 baseline levels in the Regional Study Area. Grid resolution is 800 × 800 m.

E.1.3. Replacing 10% of Noisiest Ships

This section presents equivalent noise levels (L_{eq}, unweighted and audiogram-weighted) for July 2020 over the Regional Study Area. The mitigated results represent the expected increase in vessel traffic associated with the Trans Mountain requirements and replacing 10% of the noisiest vessels by the same amount of the least noisy vessels of that class, as described in Section 2.2.3.3. Two sets of results are present:

- 10% of noisiest vessels selected based on unweighted broadband source levels, and
- 10% of noisiest vessels selected based on audiogram-weighted broadband source levels.

Figures E-4 to E-7 present maps of (left) L_{eq} and (right) change in L_{eq} with respect to baseline levels for July, seen in Figure E-1 (right).

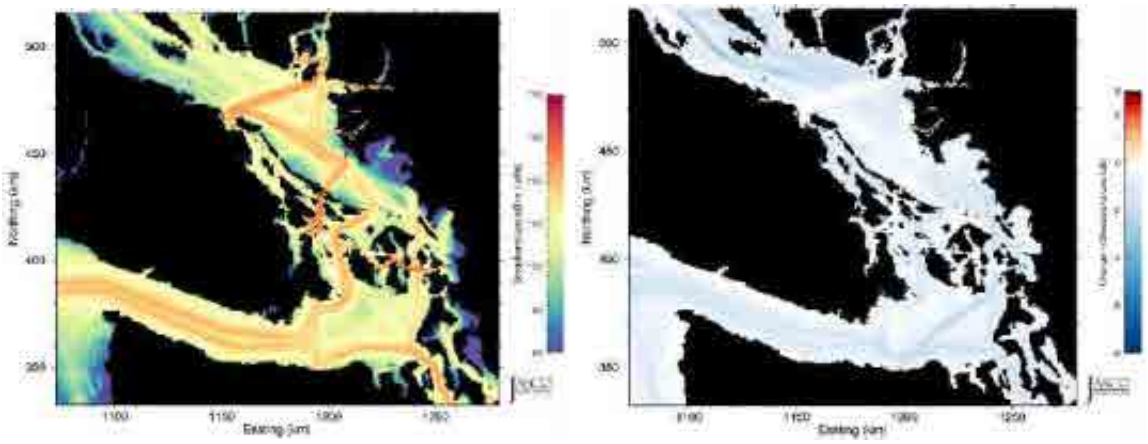

Figure E-4. *Replacing 10% of ships with highest unweighted broadband source levels, July 2020*: Unweighted equivalent continuous noise levels (*Leq*; left), and changes in *Leq* (dB; right) relative to July 2015 baseline levels in the Regional Study Area. Grid resolution is 800 × 800 m. Sample locations are omitted in figures since, at this scale, they would have obscured the results in Haro Strait.

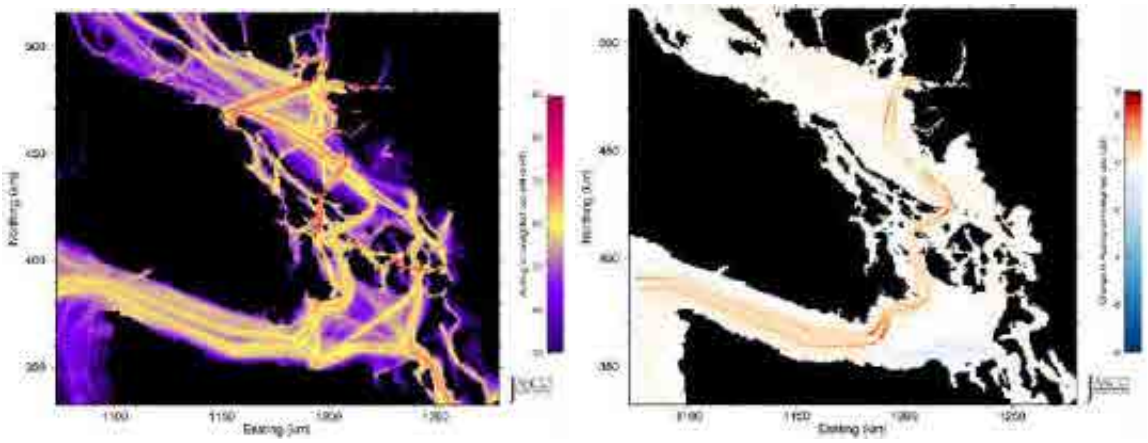

Figure E-5. *Replacing 10% of ships with highest unweighted broadband source levels, July 2020*: Audiogram-weighted equivalent continuous noise levels (*Leq*; left), and changes in *Leq* (dB; right) relative to July 2015 baseline levels in the Regional Study Area. Grid resolution is 800 × 800 m. Sample locations are omitted in figures since, at this scale, they would have obscured the results in Haro Strait.

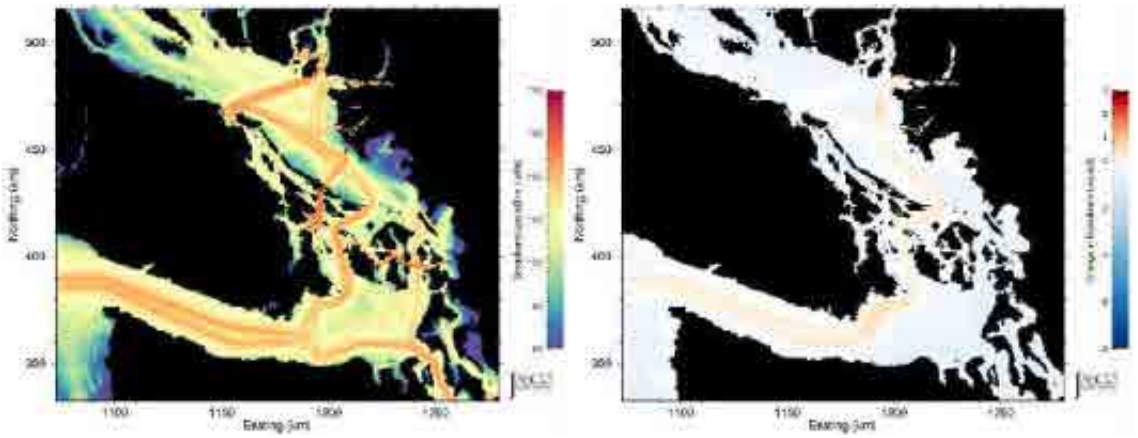

Figure E-6. *Replacing 10% of ships with highest audiogram-weighted broadband source levels, July 2020*: Unweighted equivalent continuous noise levels (*Leq*; left), and changes in *Leq* (dB; right) relative to July 2015 baseline levels in the Regional Study Area. Grid resolution is 800 × 800 m. Sample locations are omitted in figures since, at this scale, they would have obscured the results in Haro Strait.

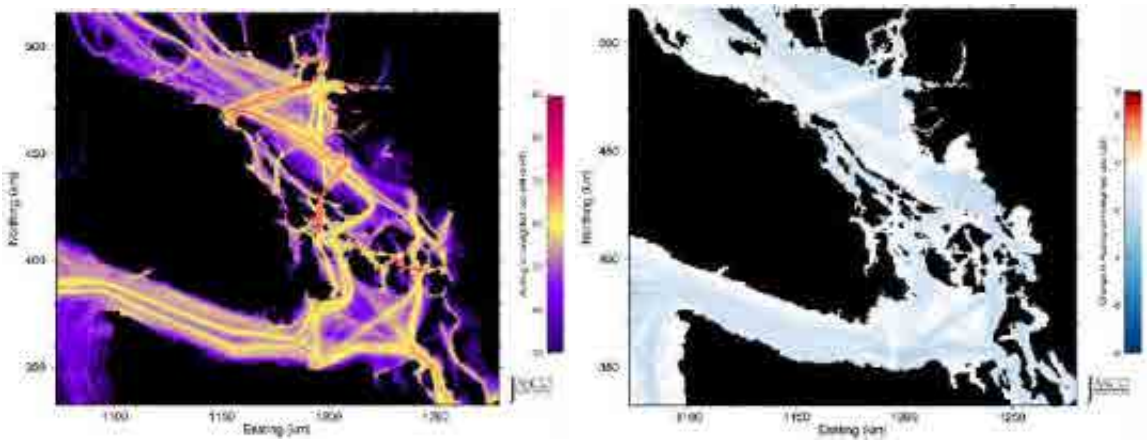

Figure E-7. *Replacing 10% of ships with highest audiogram-weighted broadband source levels, July 2020*: Audiogram-weighted equivalent continuous noise levels (*Leq*; left), and changes in *Leq* (dB; right) relative to July 2015 baseline levels in the Regional Study Area. Grid resolution is 800 × 800 m. Sample locations are omitted in figures since, at this scale, they would have obscured the results in Haro Strait.

E.1.4. Reducing Source Levels for Classes of Concern

This section presents equivalent noise levels (L_{eq}, unweighted and audiogram-weighted) for July 2020 over the Regional Study Area. The mitigated results represent the expected increase in vessel traffic associated with the Trans Mountain requirements and reducing the source levels of classes of concern by 3 and 6 dB, as described in Section 2.2.3.4. In Figure E-8 to Figure E-11, the maps on the left present the L_{eq} and the maps on the right present the change in L_{eq} with respect to baseline levels for July, shown in Figure E-1. Figures E-8 and E-9 show the mitigated levels with a source level reduction of 3 dB. Figures E-10 and E-11 show the mitigated levels with a source level reduction of 6 dB.

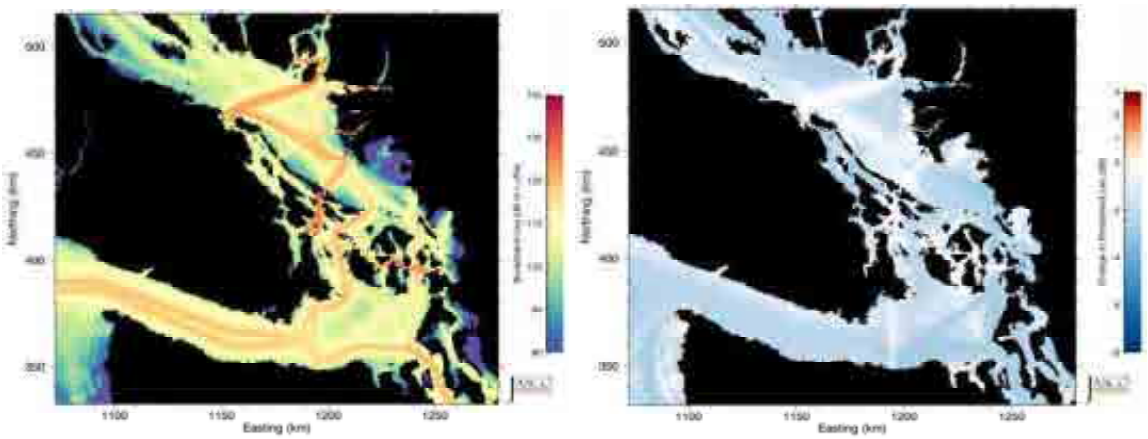

Figure E-8. *Reducing spectral source levels by 3 dB, July 2020*: Unweighted equivalent continuous noise levels (*Leq*; left), and changes in *Leq* (dB; right) relative to July 2015 baseline levels in the Regional Study Area. Grid resolution is 800 × 800 m. Sample locations are omitted in figures since, at this scale, they would have obscured the results in Haro Strait.

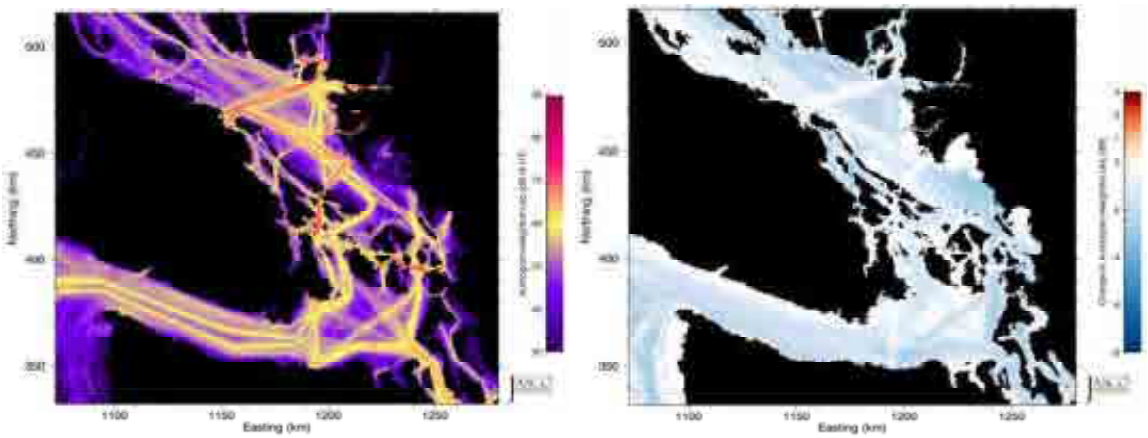

Figure E-9. *Reducing spectral source levels by 3 dB, July 2020*: Audiogram-weighted equivalent continuous noise levels (*Leq*; left), and changes in *Leq* (dB; right) relative to July 2015 baseline levels in the Regional Study Area. Grid resolution is 800 × 800 m. Sample locations are omitted in figures since, at this scale, they would have obscured the results in Haro Strait.

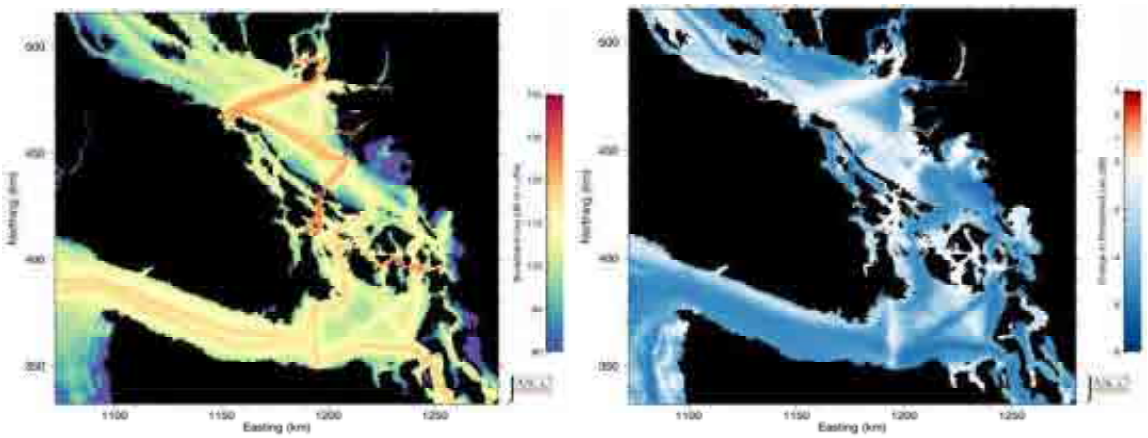

Figure E-10. *Reducing spectral source levels by 6 dB, July 2020*: Unweighted equivalent continuous noise levels (*Leq*; left), and changes in *Leq* (dB; right) relative to July 2015 baseline levels in the Regional Study Area. Grid resolution is 800 × 800 m. Sample locations are omitted in figures since, at this scale, they would have obscured the results in Haro Strait.

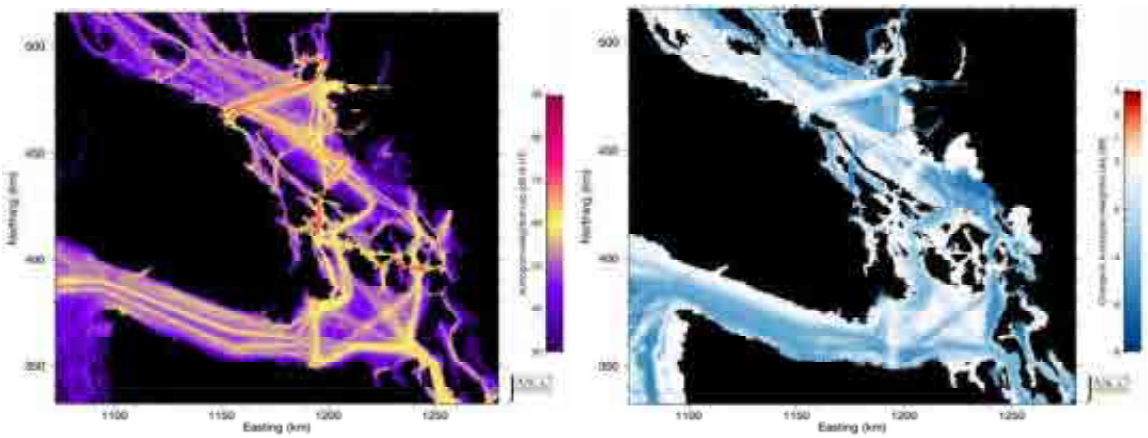

Figure E-11. *Reducing spectral source levels by 6 dB, July 2020*: Audiogram-weighted equivalent continuous noise levels (*Leq*; left), and changes in *Leq* (dB; right) relative to July 2015 baseline levels in the Regional Study Area. Grid resolution is 800 × 800 m. Sample locations are omitted in figures since, at this scale, they would have obscured the results in Haro Strait.

E.2. Regional Study Area Discussion

The monthly-averaged results are summarized in Tables E-1 and E-2, which present the spatial average (percentiles and mean) in received noise levels and in the difference in acoustic intensity relative to July baseline levels. The statistical values are calculated from unweighted and audiogram-weighted levels over each grid cell in the Regional Study Area (marked by the dash purple line in Figure 2). The percentage, shown in parentheses, represents the associated change in acoustic intensity relative to July baseline levels. These values may be used to assess the effectiveness of the mitigation approaches over the entire region (from the Strait to Georgia to Swiftsure Bank).

Table E-1. *Unweighted*: Spatial analysis of the one-month average noise level (dB re 1 µPa) and differences in acoustic intensity (%), for each mitigation approach. The values indicate the percentile or mean of the received noise levels over all grid cells in the Regional Study Area, and the difference in acoustic intensity relative to baseline levels in July.

Scenario		Spatial percentile and mean noise level (dB re 1 µPa) and changes in acoustic intensity (%)			
		5th	50th	95th	Mean
Baseline	July	85.0	108.0	121.6	106.5±11.5
	January	103.1 (+6356%)	118.2 (+947%)	125.0 (+119%)	116.2±7.7 (+833%)
Future unmitigated		85.1 (+2.3%)	108.1 (+2.3%)	122.0 (+9.6%)	106.7±11.6 (+4.7%)
Replacing 10%	Vessels ranked by unweighted source level	84.7 (−6.7%)	107.2 (−16.8%)	120.5 (−22.4%)	105.8±11.4 (−14.9%)
	Vessels ranked by weighted source level	84.7 (−6.7%)	107.6 (−8.8%)	121.6 (0.0%)	106.3±11.6 (−4.5%)
Reducing source level by 3 dB		83.7 (−24.6%)	106.0 (−36.1%)	119.7 (−35.0%)	104.7±11.4 (−33.4%)
Reducing source level by 6 dB		82.5 (−43.3%)	104.2 (−57.6%)	117.6 (−59.8%)	103.0±11.2 (−54.5%)

Table E-2. *Audiogram-weighted*: Spatial analysis of the one-month average noise level (dB re HT) and differences in acoustic intensity (%), for each mitigation approach. The values indicate the percentile or mean of the received noise levels over all grid cells in the Regional Study Area, and the difference in acoustic intensity relative to baseline levels in July.

Scenario		Spatial percentile and mean noise level (dB re HT) and changes in acoustic intensity (%)			
		5th	50th	95th	Mean
Baseline	July	30.5	53.3	64.0	51.1±10.5
	January	37.5 (+401%)	57.1 (+140%)	68.5 (+182%)	55.8±9.4 (+195%)
Future unmitigated		31.0 (+12.2%)	53.4 (+2.3%)	64.4 (+9.6%)	51.3±10.3 (+4.7%)
Replacing 10%	Vessels ranked by unweighted source level	30.4 (−2.3%)	53.4 (+2.3%)	64.1 (+2.3%)	51.2±10.6 (+2.3%)
	Vessels ranked by weighted source level	30.1 (−8.8%)	52.4 (−18.7%)	63.1 (−18.7%)	50.2±10.3 (−18.7%)
Reducing source level by 3 dB		29.9 (−12.5%)	52.1 (−23.6%)	62.8 (−24.2%)	49.9±10.3 (−23.4%)
Reducing source level by 6 dB		29.4 (−22.6%)	51.1 (−40.3%)	62.0 (−37.1%)	48.9±10.1 (−39.6%)

E.2.1. Baseline Noise Levels

This modelled scenario represents vessel traffic conditions in 2015 as determined by the AIS dataset over the Regional Study Area (MarineTraffic 2017). A small percentage of commercial vessels may have been absent from this dataset due to a lack of broadcast compliance and the lack of AIS coverage over the full area. Also, most small vessels (less than 20 m in length) are not required to broadcast AIS. Therefore, the results in this report likely do not contain contributions from a large fraction of recreational vessels and small commercial vessels. Those vessels were similarly absent from the future case scenarios, described in the following sections, so the comparisons with the baseline case are unaffected.

Baseline results are presented for two one-month periods, January and July 2015. These months represent environmental conditions that are respectively the most and least favourable to long-range sound propagation in the upper water column, at depths above the thermocline. These months also represent contrasting probabilities of SRKW presence in the area; this population has historically had a higher presence in the Salish Sea in summer than in winter.

Shipping noise caused the monthly L_{eq} levels near the sea surface to be higher in January than July throughout the Regional Study Area. L_{eq} for other months are expected to fall between these two extremes. SRKW are most common in the area in July. Thus, our study limited analysis of mitigation options to July.

E.2.2. Future Unmitigated Noise Levels

Future unmitigated monthly L_{eq}, tentatively representing vessel traffic of the year 2020, were computed by adding tanker and tug traffic associated with the Trans Mountain shipping requirements, as defined in NEB (2016), to baseline traffic. For this scenario, 29 additional tankers and 29 additional tugs were modelled in July, transiting along the inbound and outbound traffic lanes between Swiftsure Bank and Burrard Inlet (Vancouver), passing through Haro Strait. This scenario did not account for other possible increases in commercial traffic, as traffic has been relatively constant between 2015 and early 2017. However, the Vancouver Fraser Port Authority recently (August 15, 2017) reported an overall shipping increase of 4% for the first half of 2017 relative to 2016. It is therefore important to note the assumptions made here with regard to projected traffic; interpretations should account for differences in true future shipping rates as forecasts are updated.

Under the above assumptions for future commercial vessel traffic, the mean increase in unweighted noise levels over the Regional Study Area is estimated at 0.25 dB, with a 95th percentile increase of 0.71 dB over all map grid cells. With respect to SRKW's perceived loudness, the increase in traffic results in a mean increase in audiogram-weighted noise levels of 0.25 dB with a 95th percentile of 1.12 dB over the Regional Study Area

The increase from baseline to future unmitigated noise levels is concentrated along the traffic lanes, since all additional traffic was simulated along this route. This can be seen in Figures E-2 and E-3. The audiogram-weighted source levels for the tankers and tugs is higher than that of the other classes, while the opposite is true when comparing unweighted source levels. Thus, the additional tankers and tugs have a greater influence on the audiogram-weighted sound field then unweighted sound field. This results in a higher maximum change in L_{eq} over the modelled areas.

The largest difference in noise levels is expected to occur south of Haro Strait, near the Brotchie Pilot Station, where traffic would increase/decrease speed when transitioning in/out of Haro Strait piloted area. While it is expected these levels to only slightly increase SRKW's perceived loudness, the increase in levels (no more than 3.09 dB re HT) would likely reduce their communication distance and decrease the travel distance of echolocation clicks used for detecting prey.

E.2.3. Replacing 10% of Noisiest Ships

This modelled mitigation approach assessed replacing the top 10% of noisiest commercial vessels by the quietest 10% of vessels of the same class. Two criteria for selecting the noisiest vessels were examined: vessels were first ranked based on their unweighted broadband source level, and then ranked based on their audiogram-weighted broadband source level. For each criterion, the unweighted and audiogram-weighted mitigated levels were compared to baseline levels.

By selecting the noisiest vessels based on unweighted source levels, the mitigation approach significantly reduces unweighted sound levels throughout the Regional Study Area. The mitigation approach has almost no benefit, however, with respect to SRKW's perceived loudness of mean noise levels. This can be seen by comparing Figures E-4 and E-5. On the other hand, selecting the noisiest vessels based on SRKW audiogram-weighted source levels produces unweighted sound levels slightly lower than the future unmitigated levels and significantly reduces audiogram-weighted levels, as seen by comparing Figures E-6 and E-7. Thus, in implementing this type of mitigation, it is important to consider the hearing of the key species in the area. For mid-frequency hearing species such as SRKW, assessing vessels based on their unweighted broadband source level is likely inappropriate. Other criteria that include biological causality could be considered for selecting the noisiest vessels. For example, vessel spectra could be filtered to emphasize frequencies used in a species' communication signals or echolocation signals. Note that the Vancouver Fraser Port Authority's ECHO program implements a vessel noise emissions measurement system that calculates both unweighted and audiogram-weighted vessel source levels.

E.2.4. Reducing Source Levels for Classes of Concern

This mitigation approach assessed reducing source levels by 3 and 6 dB for classes of concern: Container, Cruise ship, Merchant, Tanker, Tug, and Vehicle carrier. For both source level reductions, this mitigation approach produced net decreases from baseline in both unweighted and audiogram-weighted levels throughout the Regional Study Area, as seen in Tables E-1 to E-2 and in Figures E-8 to E-11. Note that the decrease in shipping source levels is not equal to the reduction in noise levels experienced by marine animals: the amount received levels are reduced by is less than the specified reduction to commercial vessels, because non-commercial vessels also contribute to the soundscape.

Although this mitigation approach seems the most efficient, its feasibility may be questionable. Presently, there are no known methods for reducing the source levels of commercial vessels at all frequencies by a specific amount.